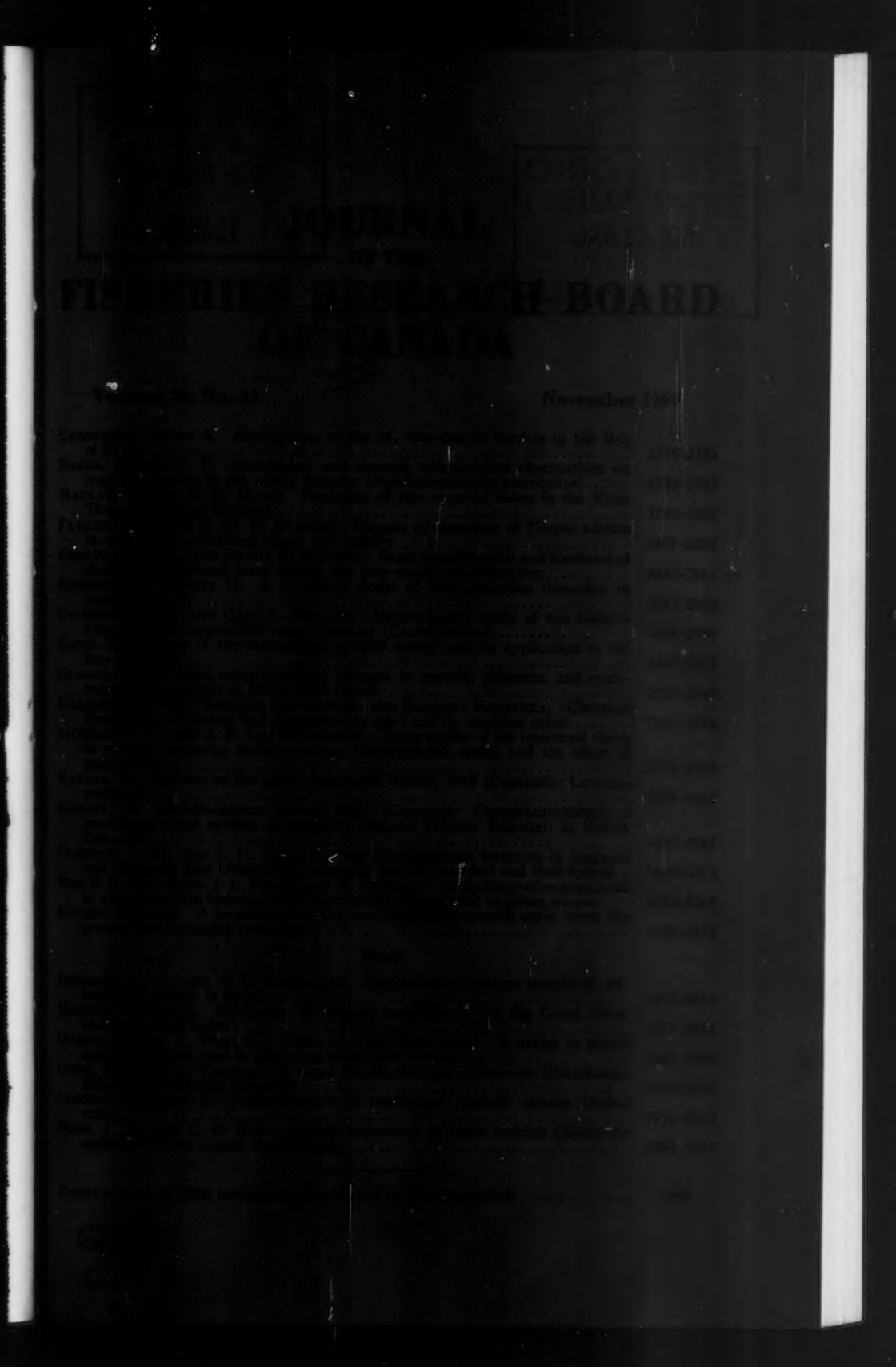

JOURNAL OF THE FISHERIES RESEARCH BOARD OF CANADA

This *Journal* of the Fisheries Research Board of Canada is devoted to original research papers and shorter contributions pertaining to problems or environments relevant to Canada. Review articles are also published; they should be timely, critical appraisals of the state of knowledge in broad areas of research. Submissions in either English or French are accepted without distinction as to origin, but must not have been published elsewhere or copyrighted.

Guides to authors and typists are given in each issue of the *Journal*.

The *Journal*, or part or some of its predecessors, has been published continuously since 1901. Its predecessor series were *Contributions to Canadian Biology*, 1901–1921; *Contributions to Canadian Biology and Fisheries*, 1922–1936; and *Journal of the Biological Board of Canada*, 1937–1937.

The *Journal* is published in annual volumes of twelve numbers. This number (Vol. 26, No. 11) was issued on December 15, 1969.

Editor:

J. C. STEVENSON, PH.D.

Associate Editor: L. W. BRANNEMAN, PH.D.
Assistant Editor: R. H. WOMBOLT, M.SC.

Production: E. L. MacIntyre, Marilyn Campbell, B.A.

Fisheries Research Board of Canada
Office of the Editor
(1) Lisgar Street
Ottawa 4, Ont., Canada

Manuscripts for publication should be addressed to the Editor

---

All Fisheries Research Board of Canada publications are for sale by the Queen's Printer, Ottawa. Remittances must be in advance, payable in Canadian funds to the order of the Receiver General of Canada. Subscription rates to the *Journal* are: Canada, United States, Mexico, $5.00; single copy $1.00; to other countries, $6.00 and $1.25. The Fisheries Research Board of Canada also publishes a Translation series (limited circulation) and several types of miscellaneous publications. All publications may be purchased at Book Distributions Limited in Ottawa, Montreal and Vancouver, at the University Bookstore in Toronto, at Les Presses de l'Université Laval in Quebec, at Archambault's in Montreal, and at Hunting's in Halifax and Saint John, N.B.; Edmonton, Alta.; and St. John's, Nfld.

Modification of the M_2 Tide due to Barriers in the Bay of Fundy

DAVID A. GREENBERG

Marine Sciences Branch
Department of Energy, Mines and Resources, Ottawa, Ont.

GREENBERG, DAVID A. 1969. Modification of the M_2 tide due to barriers in the Bay of Fundy. J. Fish. Res. Bd. Canada 26: 2775–2783.

The one-dimensional channel equations with linear bottom friction are integrated numerically to determine the modification of the M_2 tide for several cases of barriers in the bay. The barriers are treated as "complete barriers" in the sense that no flow is permitted through them.

Received March 19, 1969

INTRODUCTION

THE PROBLEM OF the effect of barriers on the tidal regime in the Bay of Fundy is examined here. The interest in this problem arises from the proposals of building dams at certain points in the Bay of Fundy to trap the enormous tidal power and harness it for practical purposes.

Some preliminary studies have already been made to investigate the reduction in tidal amplitudes on account of the barriers — namely those of J. R. Rossiter (personal communication), Yuen (MS, 1967), and G. F. D. Duff (personal communication). In all these investigations the barrier is treated as a complete barrier in the sense that no transport of mass is permitted through it. This effectively means that the Bay of Fundy is artificially terminated at the site of the barrier.

Rossiter, in one case, represented the bay by five frictionless rectangular channels; in another, a dynamical model with friction, he divided the bay into 10 channels, each of length 15.5 nautical miles. He calculated the reduction of the M_2 tidal amplification for the case of a barrier located at Cape Split. Yuen's study of this problem is a more elaborate one. He considered both one- and two-dimensional dynamical models of the bay with quadratic friction. In addition, Yuen considered the cases of several barriers and the modification in the tidal regimes of several tidal components. Yuen, however, took the mouth of the bay along a line passing just north of the Grand Manan Island. It is felt that a significant difference may arise if the mouth of the bay is taken further south (see Fig. 1B). Duff has indeed done this. To show the effect of considering a longer bay, he extended the bay to about 100 miles south of where Yuen has taken it. Duff calculated the reduction in the M_2 tide for the case of a barrier at Cape Chignecto using a frictionless one-dimensional model.

Printed in Canada (J1420)

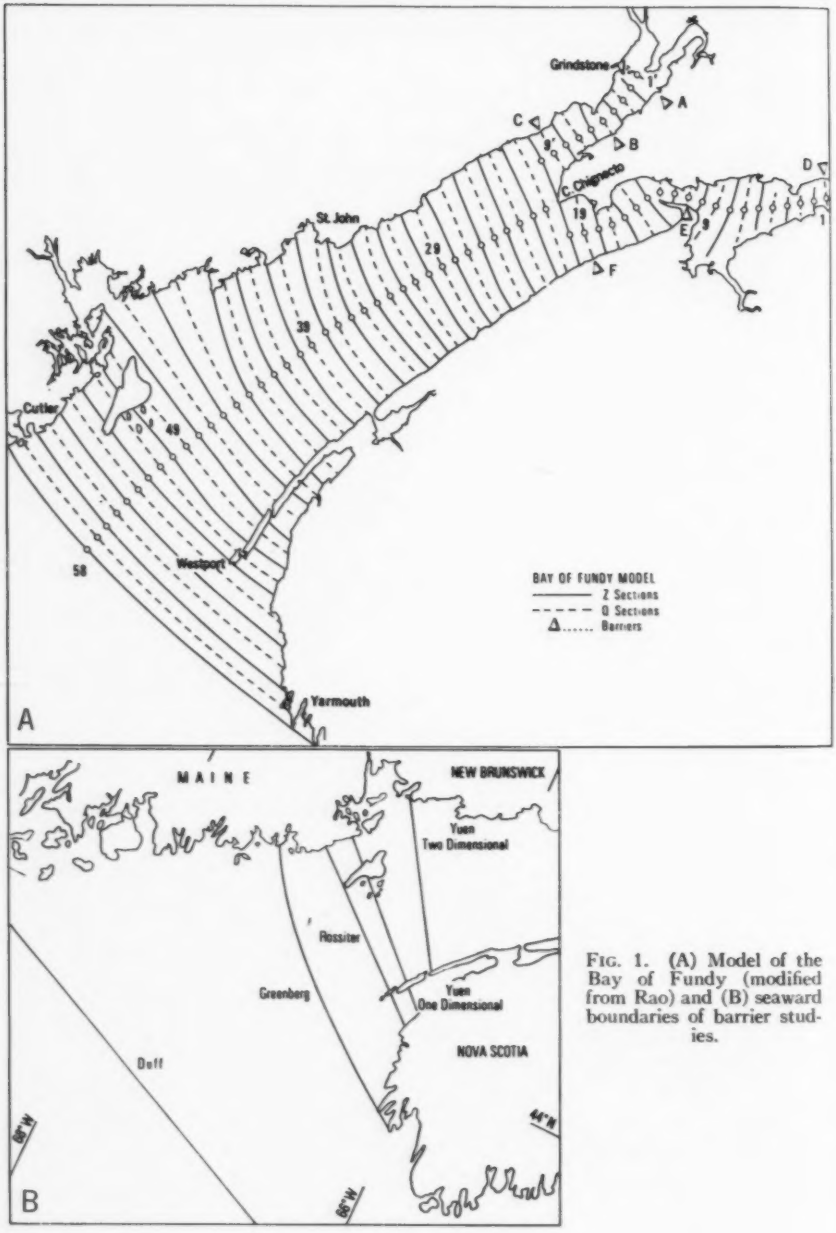

FIG. 1. (A) Model of the Bay of Fundy (modified from Rao) and (B) seaward boundaries of barrier studies.

In the present analysis the mouth of the bay is taken along a line joining Machias (Maine) and Chebogue Point (Nova Scotia). This places the mouth at about 35 miles south of the position of Yuen's model. Further south of this position, we enter the Gulf of Maine and this seems to establish the present position as a logical choice for the mouth of the bay. All the calculations done so far are to be interpreted in the sense that the observed tidal amplitude at the mouth is not significantly altered by the presence of dam(s) in the upper reaches of the bay.

The barrier cases considered in this study are listed in Table 1 and the amplification per unit amplitude at the mouth of the bay was calculated at proposed barrier sites for each of the cases listed.

TABLE 1. Summary of the barrier cases (see Fig. 1).

Case	Barrier location		Section no.
1	A	D (No barriers)	1′– 1
2	A	E	1′–11
3	A	F	1′–19
4	B	D	5′– 1
5	B	E	5′–11
6	B	F	5′–19
7	C	D	9′– 1
8	C	E	9′–11
9	C	F	9′–19

METHOD OF INTEGRATION

The Channel equations are

$$\frac{\partial \hat{Q}}{\partial t} = -gS \frac{\partial \hat{Z}}{\partial x} - \frac{kub}{S} \hat{Q} \tag{1a}$$

$$\frac{\partial \hat{Z}}{\partial t} = -\frac{1}{b} \frac{\partial \hat{Q}}{\partial x} \tag{1b}$$

in which we assume

$$\hat{Q}(x,t) = Q(x)\ e^{i\sigma t}$$
$$\hat{Z}(x,t) = Z(x)\ e^{i\sigma t}. \tag{2}$$

The symbols employed in equations 1 and 2 are: Q = volume transport; Z = height above mean water level; σ = frequency of oscillation; t = time; S = cross-sectional area; b = width of a section; k = frictional coefficient; u = velocity; g = gravitational acceleration 32.16 ft/sec^2; and x = distance along bay (head to mouth).

S and b were calculated for Q and Z sections, respectively, using maps 4010 and 4011 published by the Canadian Hydrographic Service (see Fig. 2).

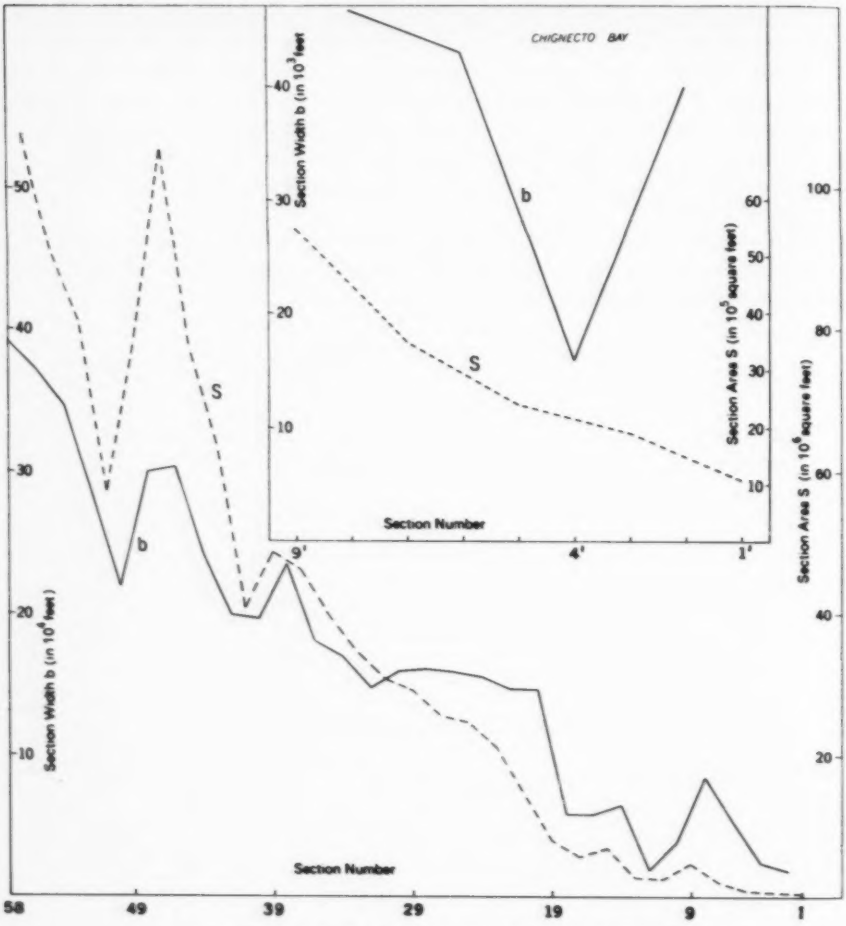

FIG. 2. Graphs of S, cross-sectional area, and b, breadth.

Substituting equation 2 in equation 1 and replacing the resulting ordinary differential equation by central differences

$$Q_{j+1} = Q_{j-1} - i\sigma b_j \Delta x Z_j, \; j \text{ — even} \tag{3a}$$

$$Z^{j+1} = Z_{j-1} - \frac{i\sigma \Delta x Q_j}{gS_j} - \frac{\Delta x k u b_j Q_j}{gS^2_j}, \; j \text{ — odd} \tag{3b}$$

Δx is the interval between two successive Z or Q sections. It is taken equal to 6.3 statute miles. In this calculation we shall consider the co-oscillating response due to the M_2 tidal component for which $\sigma = 2\pi/(12.42 \times 3600)$ sec^{-1}. We begin the integration at the head of the Minas

Basin (or at the barrier sight, depending on the case under consideration) by setting $Q_B = 0$, which is the appropriate boundary condition. Setting $Z_{B+1} = 1$ and using equations 3*a* and 3*b* we then proceed with the integration until we get Z_{20}.

At Section 20, Chignecto Bay and the Minas Channel join the main branch of the Bay of Fundy. Before we can proceed with our integration into the main channel, we have to solve for $Q_{9'}$ (see Fig. 1). (All quantities with primes on indices refer to Chignecto Bay.) At this stage we can consider the oscillation in Chignecto Bay as a co-oscillation imposed at its mouth (Section $j = 10'$) with an amplitude $Z_{19'} = Z_{20}$ and the frequency of the M_2. Using the condition that $Q_{B'} = 0$, it is possible to explicitly relate $Q_{9'}$ to $Z_{10'}$ from equation 3:

$$Q_{9'} = \alpha_{9'} Z_{10'}$$

where

$$\alpha_{9'} = \left(- \frac{i\sigma\Delta x}{gS_{9'}} - \frac{ku\Delta x b_{9'}}{gS^2_{9'}} + \alpha_8 \right)^{-1}.$$

$\alpha_{8'}$ is obtained from the general statement:

$$\alpha_{B+j'} = \left(- \frac{i\sigma\Delta x}{gS_{B+j'}} - \frac{ku\Delta x b_{B+j'}}{gS^2_{B+j'}} + \alpha_{B+j'-1} \right)^{-1}$$

with the final value of α being given by

$$\alpha_{B+1'} = (-i\sigma\Delta x b_{B+1'})^{-1}.$$

If the barrier is located at section 9′ then $Q_{9'} = 0$ and we effectively eliminate the presence of Chignecto Bay altogether. Knowing $Q_{9'}$ we can calculate $Q_{21} = Q_{9'} + Q_{1'9'} - i\sigma b_{20}\Delta x Z_{20}$ and continue the integration to the mouth of the bay.

In equation 1*a* friction is represented by the term $\frac{kub}{S}Q$ in which k is frictional constant and u is some constant velocity, specified this way to keep the equations linear. Values of ku = 0, .00125, .0025, and .00416 ft/sec were tried. The tidal amplification was calculated using each value and compared to the observed values; $ku = .00416$ gave the best agreement when χ^2 type calculations were made. The comparisons of the calculated and observed tidal amplification and phase are shown in Fig. 3 and 4. It is seen that there is good agreement as far as tidal amplification is concerned. However, the agreement is not good for the phase-angle. This might be explained partly as the result of considering average phase along an entire cross section. Also, it should be pointed out that those observations that disagree most were taken from around Grand Manan Island, which was considered not as an obstacle, but just as zero depth in the procedure for finding cross-sectional area.

DISCUSSION OF THE RESULTS

Amplification per unit amplitude at the mouth is taken at the sections Z_{B+1} (or $Z_{B'+1'}$) where all j = B or B′ indicate the locations of all barriers considered. No flow is considered to pass through the barriers so no amplification is shown at positions beyond the barriers considered in each case. The amplifications for the various cases are given in Table 2.

The percentage decrease in amplification due to the presence of the barriers is given in Table 3.

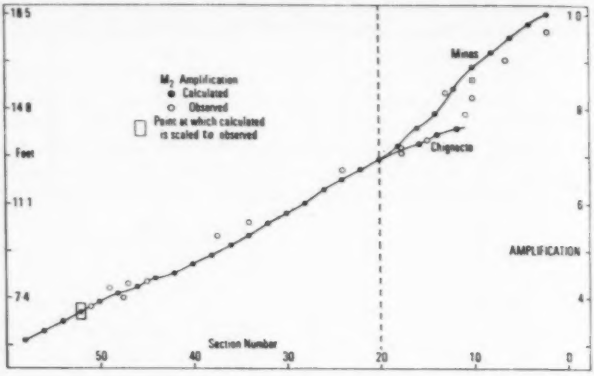

FIG. 3. Comparison of observed and calculated M_2 tidal amplification.

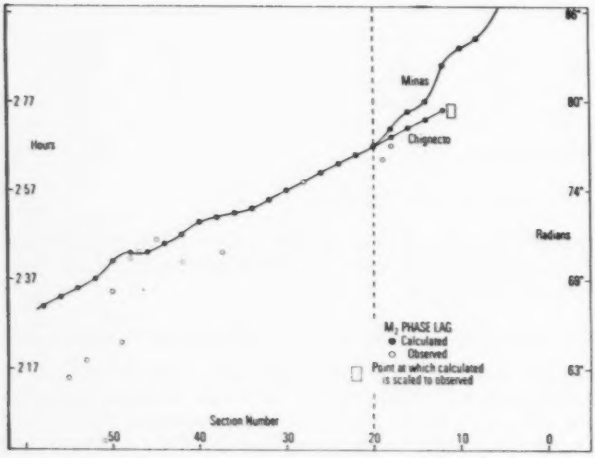

FIG. 4. Comparison of observed and calculated phase lags for M_2 tide.

TABLE 2. Amplification factors for each barrier case.

Case	Amplification at				
	A	B	C–F	D	E
1	2.36	2.28	2.18	3.15	2.65
2	2.03	1.96	1.87	–	1.97
3	1.84	1.77	1.70	–	–
4	–	2.13	2.09	3.02	2.53
5	–	1.84	1.80	–	1.89
6	–	1.67	1.64	–	–
7	–	–	1.99	2.87	2.41
8	–	–	1.73	–	1.82
9	–	–	1.58	–	–

TABLE 3. Percentage decrease in tidal amplification due to barriers.

Case	Decrease at A	B	C–F	D	E
1	0	0	0	0	0
2	14	14	14	–	26
3	22	22	22	–	–
4	–	6	4	4	4
5	–	20	18	–	28
6	–	27	25	–	–
7	–	–	9	9	9
8	–	–	21	–	32
9	–	–	28	–	–

Figure 5 shows the tidal amplification as a function of distance in the bay for the barrier cases 1, 5, and 9.

The reason for the changes in the tidal amplification in the bay when barriers are present is the change in the free period of the fundamental mode of the bay. The free periods are now calculated with friction for each one of the cases following the same method as Rao (1968), who made the calculation without friction and gave a correction to the period when friction is included:

Case	1	2	3	4	5	6	7	8	9
Period (*hr*)	9.05	7.82	7.22	8.88	7.56	6.94	8.69	7.30	6.68

The period of the natural bay with friction is 9.05 hr, as compared to 9.047 without friction as found by Rao. It is easy to see for which cases the greatest reduction in tidal amplification of the M_2 tide would occur. These, of course, are the cases for which the free period with barriers is farthest removed from the natural period. That this is indeed so may be verified by looking at the results of Table 3. With the inclusion of friction, one has a

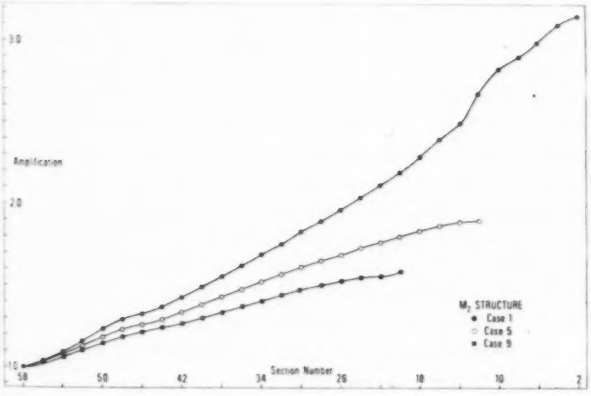

FIG. 5. Structure of the M_2 tide in the bay for barrier cases 1 (no barriers), 5 (barriers part way up Minas Basin and Chignecto Bay), and 9 (barrier at Cape Chignecto).

system with damped oscillations. However, the rate of damping for the chosen value of the friction coefficient is very small and is not of interest here.

Next we shall compare our results with those of Rossiter, Yuen, and Duff. This comparison is summarized in Table 4 in terms of percent decrease in amplification. It should be noted that the barriers are not exactly in the same positions for the cases compared.

TABLE 4. Comparison of results for appropriate cases.

	Case 2		
Position	A	C–F	E
Greenberg	14	14	26
Rossiter (5 channels)	16	16	26
Rossiter (10 channels)	10	–	20
Yuen (1-dimensional)	2	11	22
Yuen (2-dimensional)	7	–	15
	Case 4		
Position	B	D	
Greenberg	7	4	
Yuen (2-dimensional)	13	6	
	Case 5		
Position	B		E
Greenberg	18		28
Yuen (2-dimensional)	20		21
	Case 9		
Position		C–F	
Greenberg		28	
Yuen (2-dimensional)		21–27	
Duff		36	

In comparing this work to Yuen's, it must be noted that he did only a single one-dimensional calculation, so the pertinent cases had to be compared to his two-dimensional quadratic friction models in which he estimated an upper bound for percentage decreases of amplification. In most cases, though not all, the percentage reduction of amplification is greater than in Yuen's work. Duff gets the greatest amplification decrease of all for the case studied by him, which corresponds to case 9. Of course, the further out the bay is extended, the greater the amplification. But in using one-dimensional equations there is the assumption of no significant transverse motions. This effect will certainly become important once we go further south into the Gulf of Maine and indeed may be significant at section 58 of Fig. 1A. In the framework of the linear equations, which were shown to be adequate for representing the tidal regime in the bay, the present results give an indication of the probable reduction in tidal amplification due to barriers.

CONCLUSIONS

The barriers affected the tidal flow even as far down as Sections 47, 50, and 52 where the seaward end of Yuen's two-dimensional model, Yuen's one-dimensional model, and Rossiter's model are located (Fig. 5). Beyond Section 58 (seaward boundary of this model) the appropriateness of one-dimensional equations is suspect. The one-dimensional model incorporating linear friction accurately reproduced the M_2 amplification and is felt to be accurate for the purpose of measuring the effect of barriers on the tide in the bay.

ACKNOWLEDGMENTS

I would like to thank Dr D. B. Rao for giving me the opportunity to work on this project and for putting in so much time working on it with me. I also should mention Mr J. Koval who helped devise the method of finding relative accuracies of the frictional models and Maurice Isabelle who prepared the diagrams.

REFERENCES

RAO, DESIRAJU B. 1968. Natural oscillations of the Bay of Fundy. J. Fish. Res. Bd. Canada 25: 1097–1114.

YUEN, KENNETH B. MS, 1967. Effects of tidal barriers upon the M_2 tide in the Bay of Fundy. Marine Sci. Branch, Dept. Energy, Mines Resources Canada, MS Rept. 5.

Histological and Electron Microscopical Observations on Copper Poisoning in the Winter Flounder (*Pseudopleuronectes americanus*)

JEREMY T. P. BAKER

Marine Sciences Centre
McGill University, Montreal, Que.

BAKER, JEREMY T. P. 1969. Histological and electron microscopical observations on copper poisoning in the winter flounder (*Pseudopleuronectes americanus*). J. Fish. Res. Bd. Canada 26: 2785–2793.

Effects of high, medium, and low levels of copper on the morphology of winter flounder were investigated using routine histological techniques and electron microscope analyses.

High and medium levels of copper resulted in fatty metamorphosis in the liver, necrosis in the kidney, destruction of the hemopoetic tissue, and gross changes in gill architecture. Seven other structures and organs were examined for copper-induced morphological changes but none were found.

Light microscope studies showed that low levels of copper caused an extracted appearance in gill lamellae; the epithelial layer appeared vacuolated; the basi-lamellar region was reduced in thickness. Lamellar mucus cells were few compared with control specimens and chloride cells appeared in their stead.

Electron microscope study of gill lamella from fish exposed to low levels of copper confirmed vacuolation in the epithelial layer. Also found were myelinlike figures, various membrane-bound vesicles, and apical homogeneous layers of reduced thickness. Increased amounts of particulate matter adhering to the external surface of the epithelial cells were apparent. Chloride cells were found instead of mucus cells.

Received June 5, 1969

INTRODUCTION

A SMALL AMOUNT OF COPPER, 3–20 μg/liter, normally appears in the marine environment. Increased amounts appear in the sea from rivers contaminated by base-metal mines and by algicide spraying. Some of the effects on freshwater vertebrates of increases in copper above trace amounts have been documented (Sprague, 1964, and Sprague and Ramsay, 1965). Invertebrate response to copper has been studied by Hubschmann (1967).

This study has a twofold purpose: to determine the histological and ultrastructural effects of varying concentrations of copper on a representative marine vertebrate, and to relate these findings to medical knowledge of copper metabolism.

The winter flounder, *Pseudopleuronectes americanus*, was chosen as the experimental animal because it is a commercially important species and, since it is found in a coastal and estuarine environment, is more likely to be exposed to pollutants such as copper.

Printed in Canada (J1497)

MATERIALS AND METHODS

Medium and High Levels of Copper

In this experiment, winter flounder were collected by otter trawl from Passamaquoddy Bay, N.B., in May 1967 and held in running sea water for 2 weeks at 9.4 C. The fish were 3 years old, as determined from otolith annulations. Five fish were placed in each of four tanks containing 25 liters of sea water under a constant flow rate of 1 liter per min. Copper was supplied as copper sulphate; concentrations of 3200 μg/liter Cu^{++}, 1000 μg/liter Cu^{++}, and 560 μg/liter Cu^{++} were maintained by dripping a solution into three tanks continuously at a predetermined rate from stock copper sulphate solutions, agitated with magnetic stirrers. The fourth tank, kept free of exogenous copper, acted as control. All tanks were aerated. *p*H throughout the experiment remained at 8.0 ± 0.1. Copper concentration, measured by the diethyldithiocarbonate method, similar to that found in Standard Methods (APHA, 1960), was 3 μg/liter in normal sea water.

The fish were fed frozen clams daily. Since only the control animals were feeding well, a fifth tank was set up as a starved control (Fig. 19).

Tissues for histological examination were taken from fish killed by decapitation just before death. Death was deemed imminent when the fish presented typical neuromuscular disabilities; when these were ignored, the fish died and were considered unusable for microscopic examination. In this experiment, one fish in each of the three tanks with copper died before being killed (these fish are notated by a crossed circle in Fig. 19). None of the control fish exhibited such symptoms throughout the 700-hr experiment and none died. The tissues taken for histological examination were: somatic muscle, gills, heart, stomach, duodenum, intestine, kidney, liver, eyes, spleen, and brain. All were routinely fixed in Bouin's fluid, embedded in 56 C wax, sectioned at 6–8 μ, and stained with hematoxylin and eosin.

Low Level of Copper

In this experiment, 2-year-old fish were used and were collected by handlining. Four 60-liter tanks were used, two with 180 μg/liter Cu^{++} and two as control. Fresh, live clams were used as food and all fish were seen to feed well. (See Fig. 19; circles with a cross represent fish that died and were not examined histologically.) The temperature of the tanks was maintained at 10 C.

Tissue taken for histology was treated as in the previous experiment. Gill tissue for electron microscope examination was fixed in 2% phosphate-buffered glutaraldehyde at 10 C for 2 hr, rinsed in phosphate buffer for 15 min, then post-fixed in osmium tetroxide. Tissues were dehydrated by graded ethanol baths and embedded in Epon 812. The thin sections were examined in an RCA 3E and a Phillips 200 electron microscope after staining with lead (Reynolds).

RESULTS

Effects of Medium and High Levels of Copper on Liver, Kidney, and Gills

LIVER

In the normal liver (Fig. 1) the central vein was prominent, with cords of hepatic cells leading to it. Nucleated red blood cells filled the sinusoids that separated the columns of hepatic cells. There seemed to be no appreciable effect from 560 μg/liter of copper, but at 1000 μg/liter and 3200 μg/liter there was fat in the cells around the central vein (Fig. 2)

KIDNEY

The teleostean kidney was characterized by tubules surrounded by hemopoetic tissue. Normally the tubular cells were well formed with little cellular debris within the tubule lumen (Fig. 3). Immature red blood cells were found

about the tubules. The kidneys from fish exposed to 560 μg/liter were not noticeably different from the normal; kidneys of fish from the tanks containing 1000 μg/liter and 3200 μg/liter, however, show considerable change (Fig. 4). The hemopoetic tissue was necrotic and very much reduced in volume and the tubule cells themselves were vacuolated and reduced in size. The apical portion of the tubule cells seemed to disintegrate and the lumen of the tubules contained much dense material.

GILL LAMELLAE

Control (see Fig. 5) — The structure of the flounder gill was similar to that of other species described (Newstead, 1967). Each lamella was composed of central pillar cells having arms that stretch out to touch those of adjacent pillar cells. The space between pillar cells formed lacunae through which blood cells flowed. A basement membrane lay between the pillar cells and the epithelial cells. At the tip of the lamella was an expanded lacuna in which there were many blood cells. In the basilamellar region, situated on the filament, were chloride cells and at intervals along the layer of epithelial cells there were numerous mucus cells (Fig. 7). In normal epithelium there were very few chloride cells among the epithelial cells of the lamellae.

560 μg/liter Cu^{++} — At this level, the epithelial layer of lamellar cells was reduced in size, but there was no detachment from the basement membrane. Mucus cells were larger than in control specimens. Chloride cells made their appearance along the epithelial layer. They were in few or large numbers; in some instances the epithelial layer was made up entirely of chloride cells.

1000 μg/liter Cu^{++} — The epithelial layer was divorced from the remaining parts of the lamella. Chloride cells were greatly enlarged, as were the mucus cells. In some instances it appeared that the lifting off of the epithelium was really a greatly expanded chloride cell, since the typical eosinophilic content of chloride cells was contained in the bubbles caused by epithelial detachment. Lamellae fuse in some instances, whereas others became swollen with red blood cells, presumably due to the pillar cells losing their supporting properties. Epithelial cells often became so disintegrated that there was little observable cellular detail.

3200 μg/liter Cu^{++} (see Fig. 6) — There was complete cell destruction with some fusion of adjacent lamellae. Apart from red blood cells, only chloride cells were still recognizable. The remains of the epithelial layer became completely detached from the more central portion of each lamella.

Effect of Low Level of Copper on Gills

LIGHT MICROSCOPE OBSERVATIONS

Control — (see Fig. 5 and 7 and first section of results).

180 μg/liter Cu^{++} (see Fig. 8 and 9) — There were very few mucus cells along the epithelial lining of each lamella but several chloride cells appeared to have taken their place. The epithelial cells themselves were vacuolated and were not as tall as in the control.

ELECTRON MICROSCOPE OBSERVATIONS

Control — The ultrastructure of normal gill lamellae of several other species has been described in some detail (Newstead, 1967). Each lamella has a semi-lunar shape with one end taller than the other with the taller end facing the incurrent of water. The relationship of the water flow direction on the outside of the gill and blood flow on the inside is of the counter-current type. Since all sections were made across the lamellae, the blood cells were either moving into or out of the electron micrographs. Around the blood cells were the pillar cells, the structural support of the lamella (Fig. 10); together they formed lacunae or spaces within which the blood cells moved. External to the pillar cells was the basement membrane, on which stood a thin layer of cells. External to this layer lay the epithelial cells and mucus cells. Frequently, there was another lacuna between the single layer and the epithelial layer; within this second lacuna, isolated cells were seen. External to the second lacunal system was the epithelial layer, one or two cells thick. Beneath the external membrane of epithelial cell was a homogeneous layer of cytoplasm (Fig. 11).

The pillar cell has four "arms" and a centrally located nucleus. Its homogeneous cytoplasm contains a few mitochondria, but there are few free ribosomes and little rough endoplasmic reticulum. The two arms on each side of the cell extend to those from an adjacent cell to form a space that is a blood lacuna. The basement membrane is about 300 Å in thickness and is continuous. It is intimately related to the pillar cells (Hughes and Grimstone, 1965). The single layer of cells external to the basement membrane is very thin, usually of less thickness than the membrane itself; the cytoplasm of these cells contains a little endoplasmic reticulum and scattered mitochondria.

The second lacunal space (Fig. 12) contained a clear fluid in which were free cells, membrane-bounded vesicles, and myelinlike bodies.

The epithelial cells (Fig. 12) were long and flat and had prominent nuclei. There was extensive endoplasmic reticulum and the Golgi apparatus was large. The junction of one epithelial cell with another was complex, with many inter-foldings of adjacent cell membranes.

Located in a similar position to the epithelial cells are the mucus cells (Fig. 11). The mucus cell opens to the exterior by a small aperture. Overlaying the mucus cell and surrounding the aperture are extensions of neighbouring epithelial cells. The mucus cell consists of membrane-bounded vesicles of mucus, each vesicle having a fine granular appearance. The nucleus is in a basal position. At the periphery of the cell there was extensive rough endoplasmic reticulum. There were numerous free ribosomes in the cytoplasm and a few mitochondria. Found at the base of the cell was the Golgi apparatus from which the mucus vesicles appeared to originate. There was no apparent membrane separating the cell contents from the outside at the apical aperture.

180 μg/liter Cu++ — The most obvious change was in the relationship of mucus cells to chloride cells; very few mucus cells were found, whereas chloride cells were common (Fig. 13 — note the extensive smooth endoplasmic reticulum

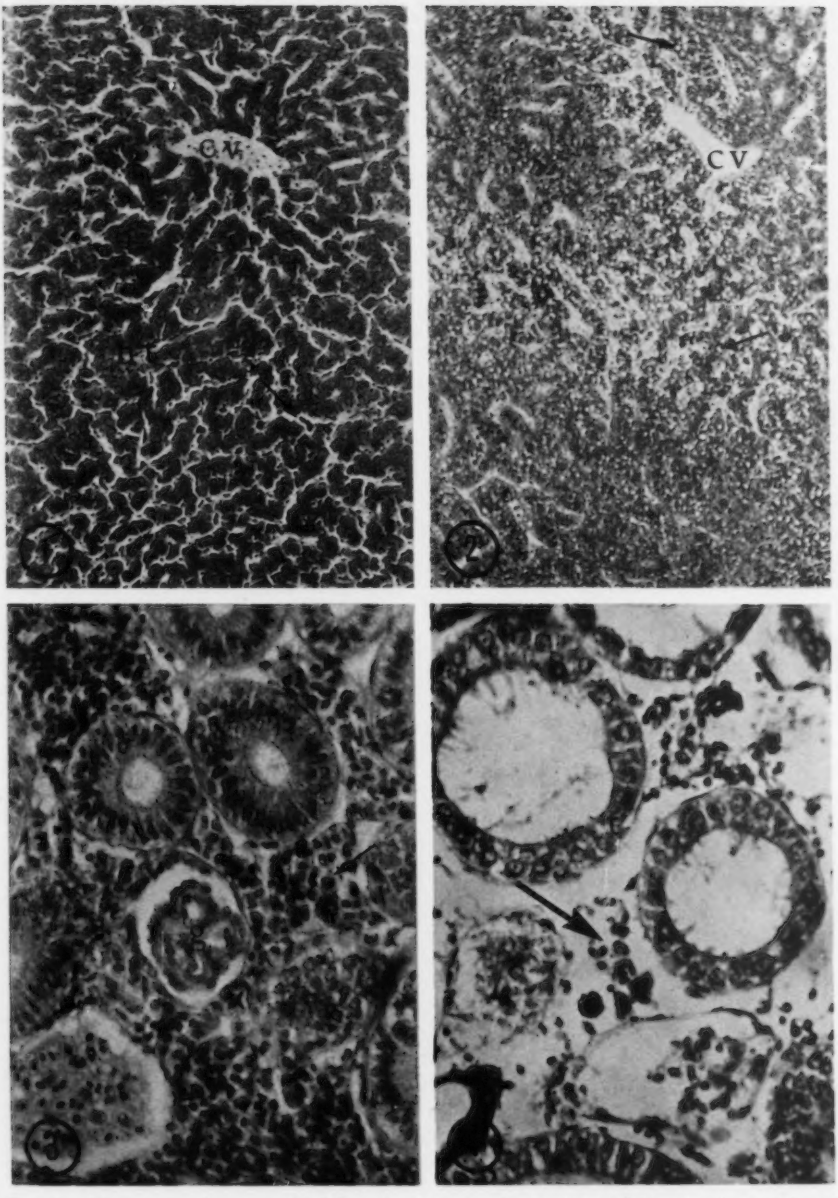

FIG. 1. Liver tissue from control fish; note the central vein (*cv*) and hepatic tissue (*ht*) and sinusoids (*s*) and red blood cells (arrow) contained within them between the strands of hepatic tissue. 280×.

FIG. 2. Liver tissue from fish subjected to 1000 μg/liter Cu++. Cells surrounding central vein are characterized by deposition of large droplets of fat indicated by clear areas (arrows). 280×.

FIG. 3. All the tissue between tubules (*t*) and glomerulus (*g*) is hemopoetic; note nucleated red blood cell (arrow). 1100×.

FIG. 4. Kidney tissue from flounder exposed to 3200 μg/liter Cu++ shows tubule cells shrunken and with vacuolated cytoplasm. The few remaining peri-tubular hemopoetic cells have a necrotic appearance (arrow). 1100×.

Baker — J. Fish. Res. Bd. Canada

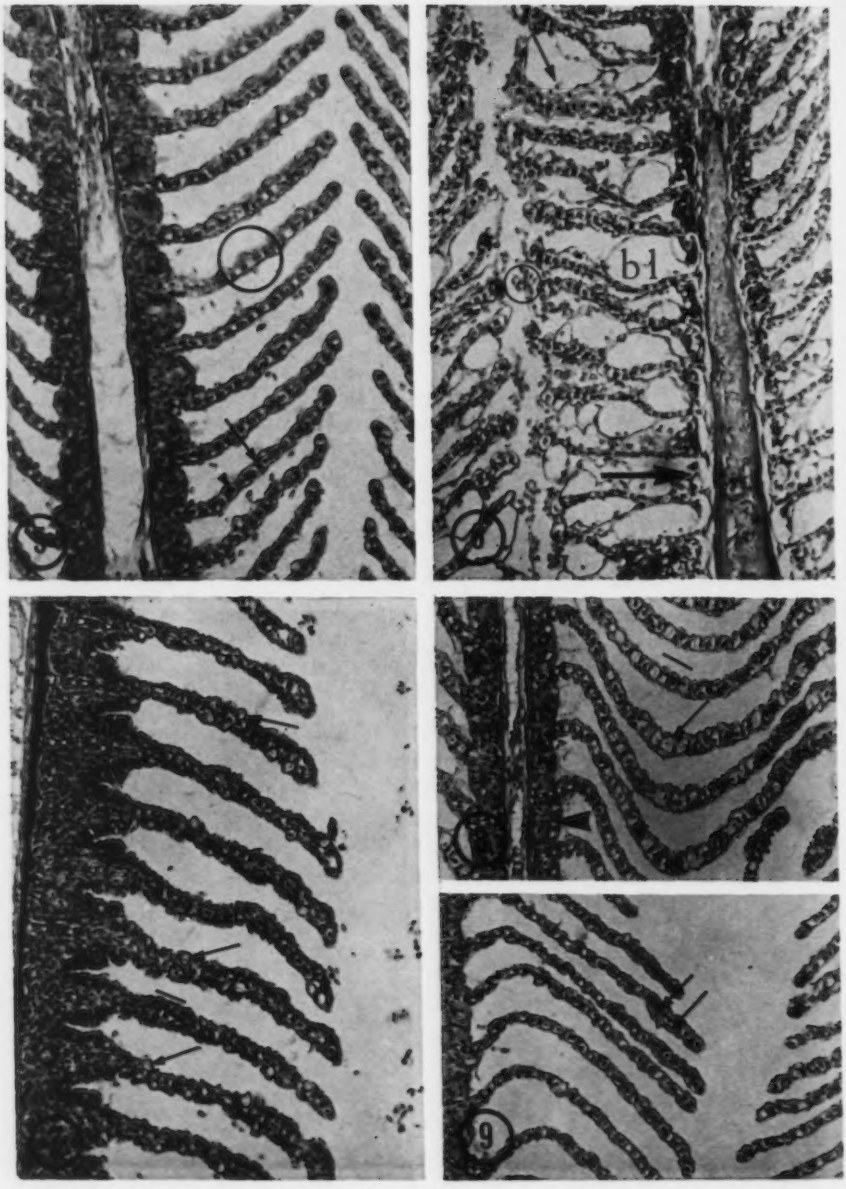

FIG. 5. Cross-sectioned gill filament; lamellae (*l*) originate on either side of filament. Lamellae consist of centrally located pillar cells (arrow) that support the epithelial layer and delimit blood lacunae. See Fig. 10 for electron microscope examination of circled area. 450×.

FIG. 6. Gill lamellae from flounder exposed to 3200 μg/liter Cu^{++}. Epithelium, which has a balloonlike appearance (*bl*), contains dense material (arrow) and does not adhere to pillar cell substructure. Basi-lamellar region has disintegrated (heavy arrow). Nucleated red blood cells outside lamellae (circle). 380×.

FIG. 7. Normal gill lamellae showing a number of mucus cells (arrows). Compare appearance of epithelial layer between parallel lines with same area in Fig. 8. 725×.

FIG. 8. Lamellae from gills of flounder subjected to 180 μg/liter Cu^{++}. Numerous cells are vacuolated (e.g., between parallel lines). Blood lacunae appear empty (arrow) and basi-lamellar region is reduced in thickness (arrow head). 725×.

FIG. 9. Lamellae from flounder subjected to 180 μg/liter Cu^{++} showing two chloride cells (arrows). 725×.

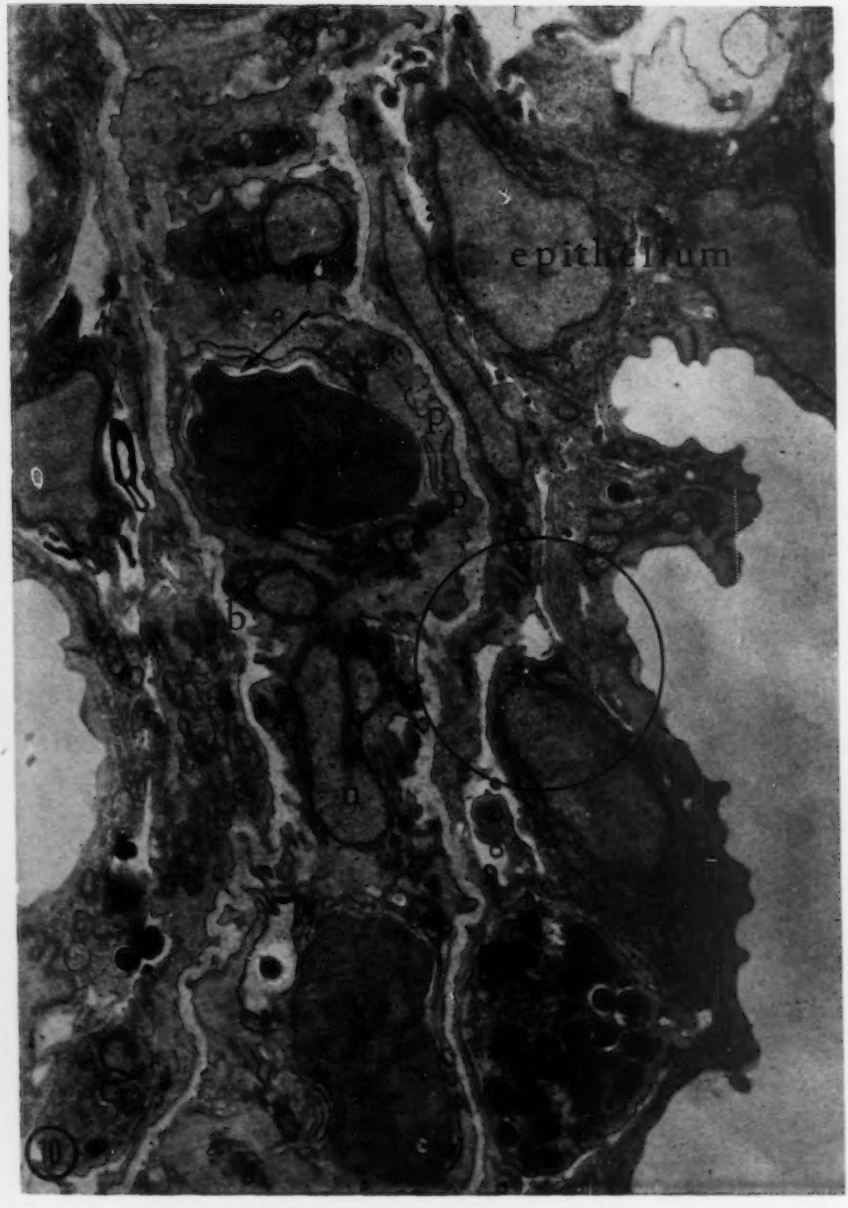

FIG. 10. Normal gill lamella area circled in Fig. 5, showing two red blood cells (*rbc*) within the lacuna (arrow) limited by the pillar cell "arms" (*p*). Nucleus of pillar cell (*n*). Basement membrane (*b*) lies under epithelium. Dark cell at bottom is within second lacunal space. See remaining plates for detail of circled area. 5500×.

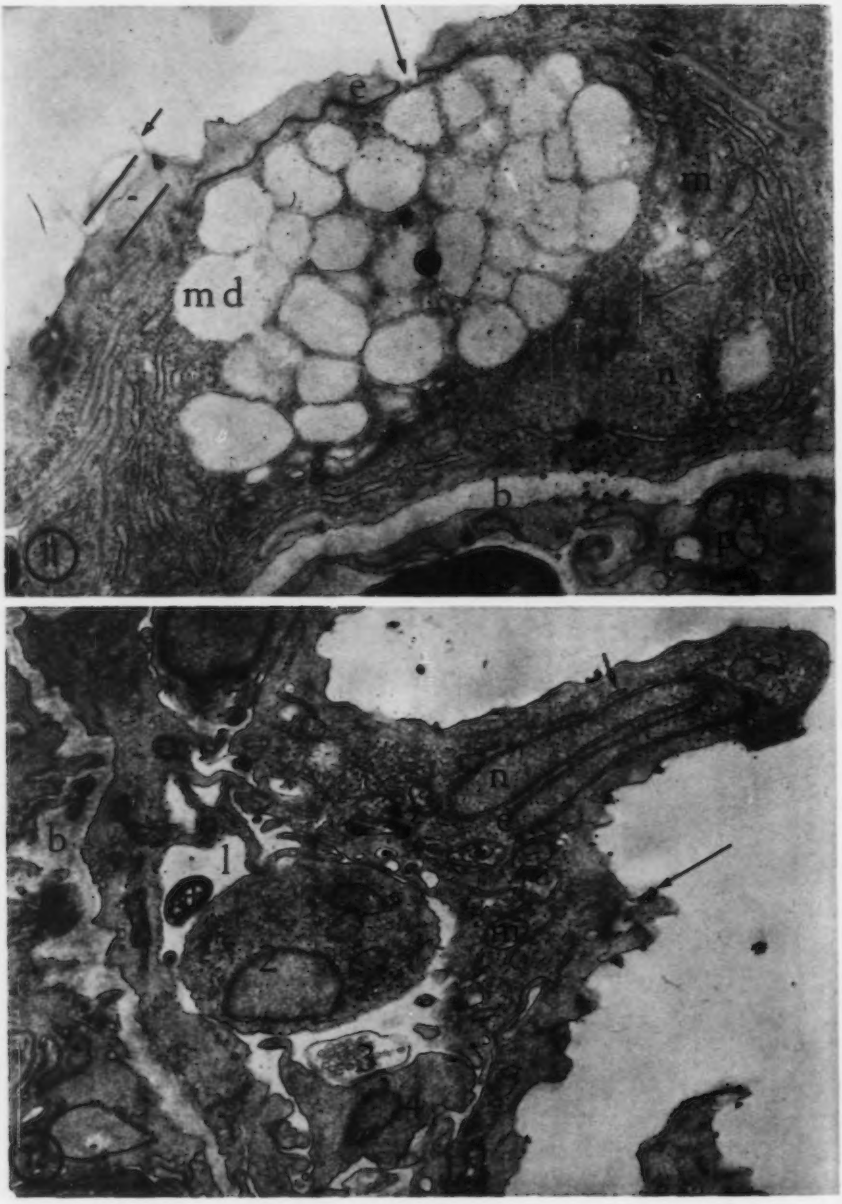

FIG. 11. Mucus cell from control fish showing apical aperture (arrow) surrounded by overlying extension of epithelial cells (*e*) and basal nucleus (*n*) with extensive endoplasmic reticulum (*er*). Mucus droplets (*md*) appear to originate from the Golgi apparatus (*g*). A few mitochondria (*m*) in the cytoplasm. Hairlike extension (arrow) of apical homogeneous layer (parallel lines). 10,500×.

FIG. 12. Secondary lacunal space (*l*) showing four different cell forms (1, 2, 3, 4). Dense particles (arrow) adhere to surface of epithelial cell containing some mitochondria (*m*), prominent nucleus (*n*), and little endoplasmic reticulum (small arrow). 10,000×.

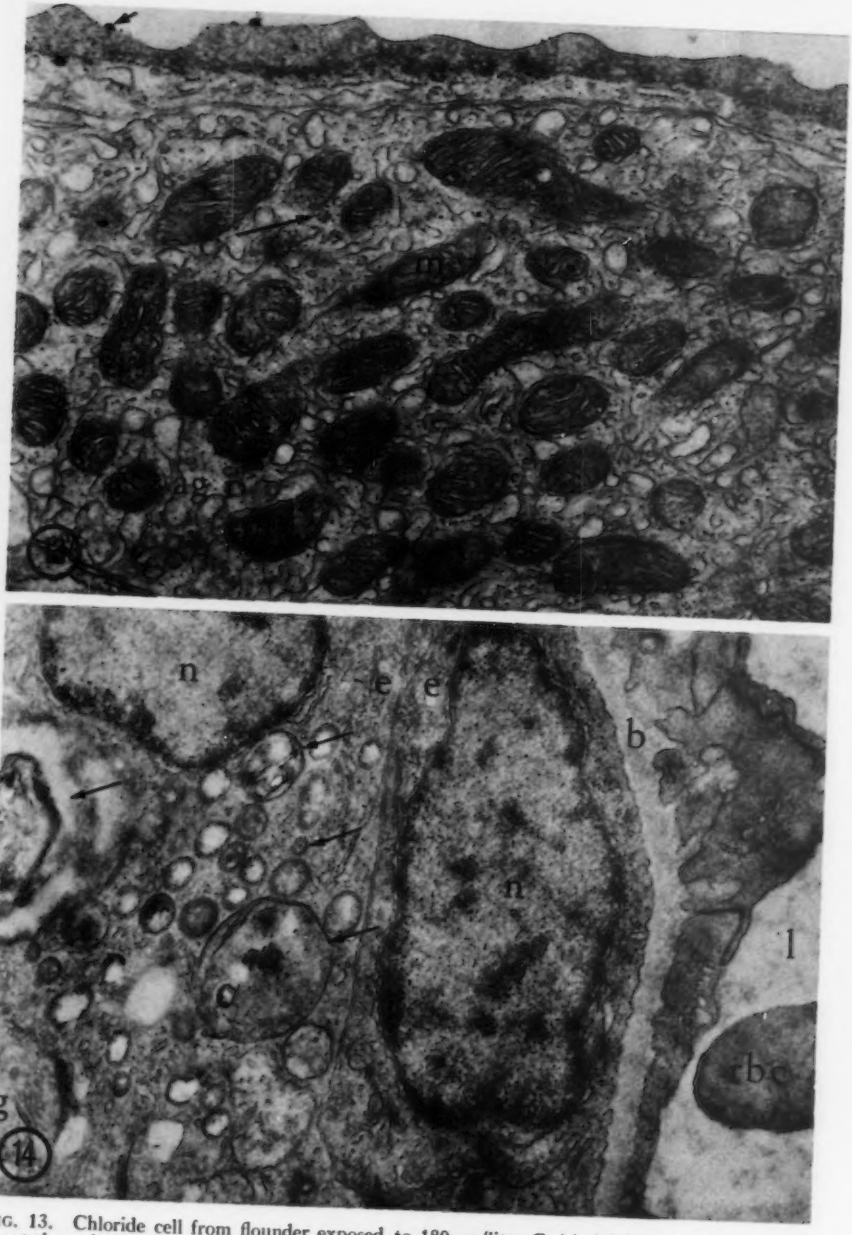

FIG. 13. Chloride cell from flounder exposed to 180 μg/liter Cu++ (cf. Fig. 9). Since section is not through the aperture, overlying epithelial cell (*e*) appears to completely occlude the chloride cell. Numerous mitochondria (*m*) and extensive agranular reticulum (*ag r*). A few free ribosomes (arrow). Dark granules on external membrane of epithelial cell are similar to those within mitochondria (arrow heads). 29,500×.

FIG. 14. Portions of two epithelial cells (*ee*) of fish exposed to 180 μg/liter Cu++ with outermost cell full of myelinlike bodies in various stages of development (arrows). 20,000×.

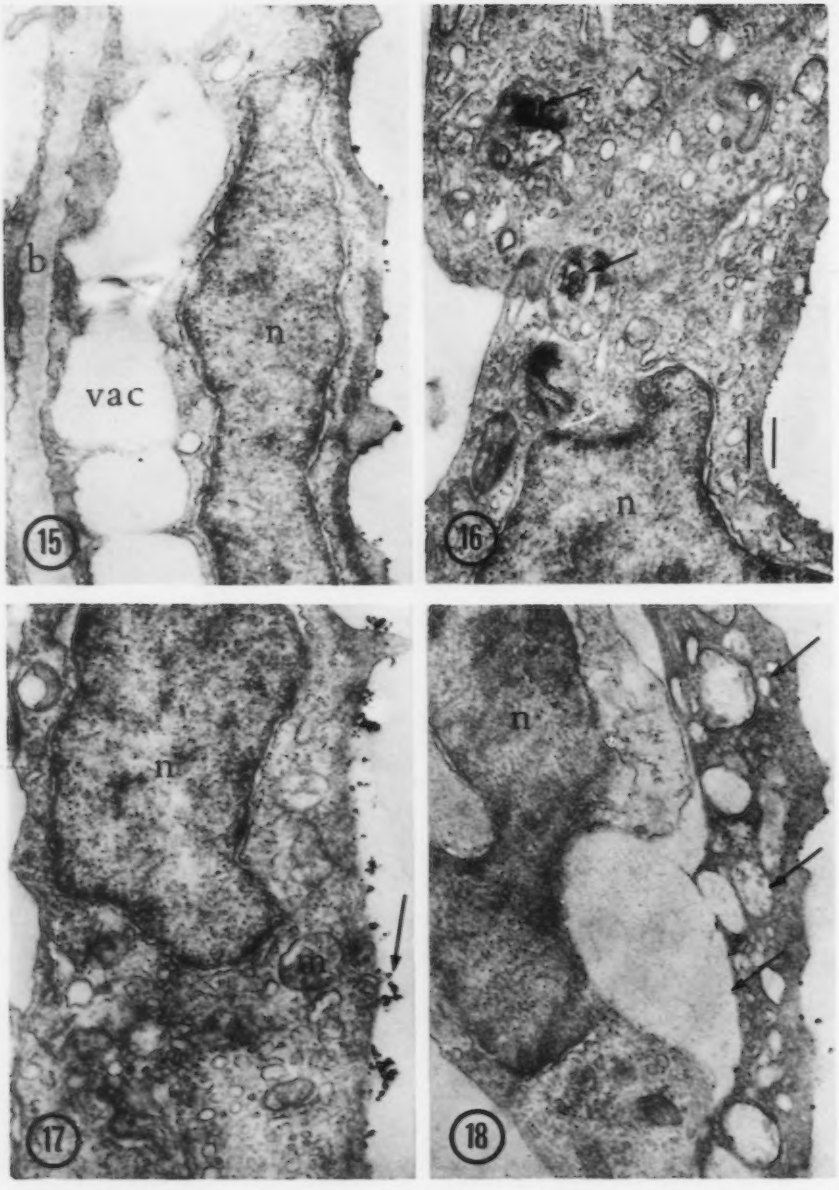

FIG. 15. Note large cytoplasmic vacuoles (*vac*) within epithelial cells of fish exposed to 180 μg/liter Cu++. 21,500×.

FIG. 16. Membrane-bound vesicles formed within cell of fish exposed to 180 μg/liter Cu++ contain elements of endoplasmic reticulum (arrows). Compare apical homogeneous layer (parallel lines) with Fig. 11. 21,500×.

FIG. 17. Note the increase in particulate matter adhering to epithelial cell of fish exposed to 180 μg/liter Cu++ (arrow) compared with Fig. 12. 21,500×.

FIG. 18. Vesicular system (arrows) in apical region of epithelial cell of fish exposed to 180 μg/liter Cu++. 21,500×.

and the large number of mitochondria). The granules that were present within the mitochondria seemed similar to those just outside the cell. Occasionally there were large clumps of dense particulate material adhering to the outer cell membrane (Fig. 17), and numerous myelinlike bodies within the cell (Fig. 14).

Large vacuoles were found within the cytoplasm of epithelial cells (Fig. 15); these vacuoles were either empty, or filled with a fibrillar material. Near the surface of the epithelial cell were numerous vesicles (Fig. 18); these vesicles were bounded by a double membrane and some contained smaller vesicles. The apical homogeneous layer (Fig. 16) was found to be reduced in thickness when compared with the control (Fig. 11).

The epithelial cells also contained bodies that appeared to be autophagosomes, since the vesicular content was partially formed of rough endoplasmic reticulum (Fig. 16). Other cellular vesicles were uniformly bounded by double membranes; they were either empty or contained a homogeneous, moderately dense material.

DISCUSSION

The use of histopathological techniques to investigate pollution effects is increasing. Some pollution scientists, following the lead of medical pathologists who have used these techniques for a much longer time and have accumulated much data on cellular response to various toxicants, are beginning to relate the amount of cell damage in organisms to the concentration of a pollutant, or the synergistic effect of more than one toxicant, or both (Brown et al., 1968; Crandell and Goodnight, 1963).

A toxic agent may be exogenous or produced by the organism itself as a result of deficient metabolic cycles. It is possible that the data accumulated by medical practitioners on pathological metabolism may be relevant to pollution studies of the histopathological type that concern only exogenous toxicants. Copper, as most heavy metals, is an essential part of every animal's intake, since it too is involved in the complex molecular structure of enzymes, but in larger than trace amounts it is a poison. Therefore, before discussing copper as a specific pollutant in this study of winter flounder, a review of the medical knowledge of copper metabolism will be useful.

In normal mammalian physiology, copper, found in greatest amounts in the liver, brain, kidney, and hemopoetic tissue, is evident in many processes. Dietary copper is absorbed from the upper portion of the small intestine and bound in the liver to an α-globulin producing a complex called ceruloplasmin; it is excreted in the feces, urine, and bile; it is intimately involved in normal hematopoesis since it is essential for the absorbtion of iron from the intestines and so controls the amount of iron available for hemoglobin synthesis (Goodman and Gilman, 1956).

Both excess and deficiency of copper cause pathological results. Sheep that graze on copper-deficient pasture have poor hemoglobin levels and are

anaemic (Comar and Bromer, 1962). The chronic effects of excess copper have been studied within the framework of Wilson's disease (Peisach et al., 1967). The behaviour of fish exposed to medium and high levels of copper, i.e. jerky, uncoordinated, spontaneous movement, was similar to symptoms of Wilson's disease described below. It seems possible that the symptoms shown by flounders in this study could be the result of copper acting on their central nervous systems even though there were no brain lesions present as is typical in Wilson's disease (possibly because maximum exposure of flounders in this study was only 700 hr).

Wilson's disease is the result of an inborn error of metabolism, inherited in a recessive manner, that causes a toxic increase in body copper levels resulting in hepatic necrosis, hemolytic anaemia, and deposition of copper within the cornea in the form of a "Kayser-Fleischer" ring. Symptoms arising from neurological disorders include jerky, spontaneous movements and possibly schizophrenia. (Ansel et al., 1957) reported that copper levels are high in schizophrenic patients, but there is some controversy over this finding (Comar and Bromer, 1962).)

High levels of copper, even though exogenous, produce similar results in a variety of subjects. Peters (1967) reported that application of copper to the brain of pigeons produced serious convulsions. Vogel (1959) has shown that goldfish subjected to 1000 μg/liter doses of copper present severe neurotoxic and nephrotoxic effects.

Wilson's disease itself results in chronic excess of copper not because of increased intake but because the liver fails to bind the cupric ion to the α-globulin producing the main clinical indication of the disease, a resulting drop in ceruloplasmin level. Thus, the copper is not excreted and is free to be carried about the body. This excess copper accumulates in the brain, liver, kidney, hemopoetic tissue, and cornea.

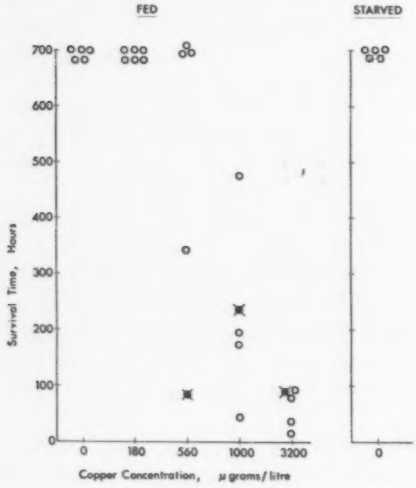

FIG. 19. Survival time of fish, in hours, is plotted against various concentrations of copper. Circles with an × represent animals that died and were not examined for pathological changes.

Enzyme systems then become involved, especially membrane ATPase (Peters, 1967) and the lipoic-acid pyruvate system, resulting in cirrhosis of the liver, death of brain neurones, necrosis of kidney tubules, and the formation of Kayser-Fleischer rings. Copper interference with membrane ATPase also results in uncoordinated limb action and jerky, spontaneous movements. Copper attacks various renal enzymes that mediate the resorbtion of several compounds. Hemolysis, a distinctive facet of Wilson's disease, could be the result of membrane ATPase — copper interaction resulting in a breakdown of the sodium pump.

An attempt is made in this paper to define the histopathological effects of levels of copper that exist in nature as a result of man's activities by experimentally exposing a representative animal to levels of a pollutant that are sublethal (sublethal pollution being far more widespread and much less obvious than lethal pollution). Copper is found normally in sea water at very low levels in the order of 3–20 μg/liter (Atkins, 1954; Chow and Thompson, 1952, 1954). In copper-polluted sea water the concentration may reach over 300 μg/liter (Fujiya, 1960).

Much of the research accomplished to date on effects of heavy metals on aquatic organisms is biased towards determining lethal limits for a particular toxicant. Little work has been done to determine the effects of low doses and little is known about the physiological responses of fish to such concentrations: Hubschmann (1967) has discussed the inhibitory effects of copper on the respiratory enzymes of crayfish; copper has been shown to cause hemolytic anaemia by inhibiting erythrocytic glycolysis, denaturing hemoglobin, and oxidizing glutathione (Fairbanks, 1967); Verity et al. (1967) have shown that copper induces increased specific activity of three lysosomal hydrolases and several mitochondrial enzymes.

The suggestion in this paper that copper induces hemolytic anaemia as the initial lesion is supported by the fact that the hemopoetic tissue in the kidney undergoes necrosis. Fatty metamorphosis of the liver and renal necrosis are assumed to be secondary lesions due to the probable anoxic state of the organism. No Kayser-Fleischer ring was found due to, probably, the relatively short time the flounders were exposed to copper; patients suffering from Wilson's disease are not examined clinically until several years after the onset of the disease, giving the copper a much longer time to accumulate within the cornea.

Whether the changes in gill lamellae observed under light and electron microscopes are secondary or primary effects is difficult to tell. Copper may be absorbed by the gill epithelium and act primarily on the cell enzymes resulting in the formation of lysosomes, vacuoles, and vesicles. The apical homogeneous layer of the epithelial cells may be a protective device and the reduction observed by electron microscope may enable copper to enter these cells via this route instead of, or as well as, via the blood. The particulate matter that is normally present on the epithelial cell surface (Fig. 12) occurs more extensively in animals that have been exposed to low levels of copper (Fig. 17); perhaps the copper acts as a coagulant on the mucus secreted by cells within

the epithelial layer. It is not known whether increased particulate matter affects oxygen/carbon dioxide exchange through the epithelial cells.

Normal chloride cells have been studied by Kessel and Beams (1962) and Philpott and Copeland (1963) and are similar to those that appear in the gill lamellae of fish exposed to low doses of copper. It was suggested by Munshi (1964) that mucus cells can either secrete mucus or chloride ions and that mucus cells of freshwater fish can become functionally chloride-excreting cells when the fish are exposed to hypertonic salt solutions.

Chloride cells in the winter flounder are normally found only in the basilamellar region and mucus cells mainly on the lamellae. After exposure to a low dose of copper the number of mucus cells was reduced and chloride cells found instead. If the copper-induced chloride cells were originally mucus cells, as seems to be the case, how and why do these transformations occur? Do these chloride cells possibly excrete copper ions instead of chloride ions? Are there latent ion-excreting cells within the epithelium that only come into action when the outside medium requires it? These are only a few of the questions that arise from the results of this study.

ACKNOWLEDGMENTS

I thank Dr J. B. Sprague of the Fisheries Research Board of Canada, Biological Station, St. Andrews, N.B., for suggesting the initial project and for providing the many facilities. Dr H. Sheldon of the Pathological Institute, McGill University, Montreal, Que., gave valuable encouragement and advice during the preparation of the manuscript. Dr M. Burt of the Biology Department, University of New Brunswick, Moncton, N.B., kindly allowed me the use of his Phillips 200 Electron Microscope.

REFERENCES

American Public Health Association. 1960. Standard methods. APHA, Washington.

Ansel, C., B. E. Leach, S. Martens, M. Cohen, and R. G. Heath. 1957. Serum oxidation tests in schizophrenic and normal subjects. A.M.A. Arch. Neurol. Psychiat. 78: 500–504.

Atkins, W. R. G. 1963. The seasonal variation in the copper content of sea water. J. Marine Biol. Assoc. U.K. 31: 493–502.

Brown, V. M., V. V. Mitrovic, and G. T. C. Stark. 1968. Effects of chronic exposure to zinc on toxicity of a mixture of detergent and zinc. Water Res. 2: 255–264.

Chow, T. J., and T. G. Thompson. 1952. The determination and distribution of copper in sea water. Part I, The spectrophotometric determination of copper in sea water. J. Marine Res. 11: 124–138.

1954. Seasonal variation in the concentration of copper in the surface waters of San Juan Channel, Washington. J. Marine Res. 13: 233–244.

Comar, C. L., and F. Bromer. 1962. Mineral metabolism. Vol. 2. Academic Press, Inc., Washington, D.C. p. 371.

Crandall, C. A., and C. J. Goodnight. 1963. The effects of sublethal concentrations of several toxicants to the common guppy, *Lebistes reticulates*. Trans. Am. Microscop. Soc. 82: 59–73.

Fairbanks, U. F. 1967. Copper sulphate — induced hemolytic anemia. Arch. Intern. Med. 120: 428–432.

Fujiya, M. 1960. Effects of copper dissolved in sea water on oysters. Bull. Japan. Soc. Sci. Fish. 26: 462–468.

GOODMAN, A. G., AND F. GILMAN. 1956. The pharmacological basis of therapeutics. Macmillan Co., New York.

HUBSCHMANN, J. H. 1967. Effects of copper on the crayfish *Orconectes rusticus* (Girard). II. Mode of toxic action. Crustaceana 12: 141–151.

HUGHES, G. M., AND A. V. GRIMSTONE. 1965. The fine structure of the secondary lamellae of the gill of *Gadus pollachius*. Quart. J. Microscop. Sci. 106: 343–353.

KESSEL, R. G., AND H. W. BEAMS. 1962. Electron microscope studies on the gill filaments of *Fundulus heteroclitus* from sea water and fresh water with special reference to the ultrastructural organization of the chloride cell. J. Ultrastruct. Res. 6: 77–88.

MUNSHI, J. S. 1964. Chloride cells in the gills of fresh water teleosts. Quart. J. Microscop. Sci. 105: 79–90.

NEWSTEAD, J. D. 1967. Fine structure of the respiratory lamellae of teleostean gills. Z. Zuckerind. 79: 396–428.

PEISACH, J., P. AISEN, AND W. E. BLUMBERG [ed.]. 1967. The biochemistry of copper. Academic Press, Inc., New York. p. 475–503.

PETERS, J. 1967. Effects of copper on pigeon brain, p. 175–183. *In* Peisach et al. [ed.] The biochemistry of copper. Academic Press, Inc., New York.

PHILPOTT, H. C. W., AND D. E. COPELAND. 1963. Fine structure of chloride cells from three species of *Fundulus*. J. Cell Biol. 18: 389–401.

REYNOLDS, E. S. 1963. The use of lead citrate at high *p*H as an electron opaque stain in electron microscopy. J. Cell Biol. 17: 208–210.

SCHEINBERG, I. H., AND I. STEMLEIB. 1960. Copper metabolism. Pharmacol. Rev. 12: 355–373.

SPRAGUE, J. B. 1964. Lethal concentrations of copper and zinc for young Atlantic salmon. J. Fish. Res. Bd. Canada 21: 17–26.

SPRAGUE, J. B., AND B. A. RAMSAY. 1965. Lethal levels of mixed copper–zinc solutions for juvenile salmon. J. Fish. Res. Bd. Canada 22: 425–432.

VERITY, M. A., L. K. GAMBELL, A. R. REITH, AND W. J. BROWN. 1967. Subcellular distribution and enzyme changes following subacute copper intoxication. Lab. Invest. 16: 580–990.

VOGEL, F. S. 1959. The deposition of exogenous copper under experimental conditions with observations on its neurotoxic and nephrotoxic properties in relation to Wilson's disease. J. Exptl. Med. 110: 801–809.

Fecundity of Two Cyprinid Fishes in the River Thames, Reading, England[1]

I. MACKAY[2] AND K. H. MANN[3]

Department of Zoology
The University, Reading, England

MACKAY, I., AND K. H. MANN. 1969. Fecundity of two cyprinid fishes in the River Thames, Reading, England. J. Fish. Res. Bd. Canada 26: 2795–2805.

Egg production by two cyprinids in the River Thames at Reading, England, was studied quantitatively from January to June 1966. Roach (*Rutilus rutilus*) had a short spawning period, shedding all their eggs in one batch, whereas bleak (*Alburnus alburnus*) had a protracted spawning period and produced two or three batches of eggs. The relationship between egg numbers (Y) and age (X) for roach was given by $\log Y = 0.0840X + 3.2085$; the estimated fecundity of a 6-year-old fish was 5157 with 95% confidence limits at 4725 and 5631. For bleak the relationship was $\log Y = 0.0564X + 3.5221$, and the estimated fecundity of a 5-year-old fish was 6356 with 95% confidence limits at 5987 and 6776. Combining previously obtained data on population density with new data on sex ratio and percentage breeding in each age class, the population fecundity for roach was about 600 eggs/m² and for bleak about 3000 eggs/m².

The roach population had lower fecundity than roach populations in other studies and there was some evidence that a proportion of females ceased egg production during the period of the study. The possibility that low fecundity was a response to food shortage is discussed.

Received October 6, 1967

INTRODUCTION

DURING A STUDY of energy transformations in the River Thames at Reading, England (Mann, 1965), an estimate was made of the energy value of the annual gonad production but not of the number of eggs produced. It was also found that some of the fish of the appropriate age-groups failed to breed and it seemed likely that this was one of the factors affecting population density, and hence population production. Moreover, it has been commonly found that a very large proportion of population production is attributable to fish in the early stages of their life history. Thus, Allen (1951) found that for trout having a life span of over 12 years, 95% of the total production of a year-class had been completed by the end of the 2nd year, and Greze (1965) showed that although round goby grow to about 50 g, 75% of population production is attributable to fish under 10 g. To obtain a complete picture of population

[1]Bedford Institute Contribution No. 169.

[2]Present address: Department of Biology, the University of Waterloo, Waterloo, Ont.

[3]Present address: Fisheries Research Board of Canada, Marine Ecology Laboratory, Bedford Institute, Dartmouth, N.S.

Printed in Canada (J916)

production it is, therefore, necessary to discover as much as possible about egg production and growth and survival of the young stages. This paper reports on the first of these parameters for the two most abundant species in the population, roach (*Rutilus rutilus* L.) and bleak (*Alburnus alburnus* L.).

GENERAL METHODS

Samples of the fish populations were taken in experimental seines at frequent intervals from January to June 1966. Age, determined by scale readings, and length were recorded for each fish, and the sex and condition of the gonads noted. Two types of gonad could be recognized: (i) Inactive: gonads that were not producing mature germ cells. This type could be found either in fish that had not reached sexual maturity or in fish that for some other reason were failing to breed; (ii) Active: gonads that were producing maturing germ cells.

The numbers of eggs in selected ovaries were determined by weighing the whole ovary and then a segment in which the eggs were subsequently counted. Size-frequency curves for egg samples were prepared by measuring the diameter of the eggs under a microscope with an eyepiece micrometer (1 division = 0.037 mm).

Although fecundity is most likely to be proportional to body weight in sexually mature fish, and often shows a linear relationship with log length (Raitt, 1932; Ricker, 1932; Bagenal, 1957), it was desired to match the fecundity data of the Thames fish to data on the abundance of the various year-classes to obtain approximate figures for population fecundity. Accordingly, a multivariate examination of fecundity on both length and age was carried out, to see whether a valid relationship of fecundity to age could be established.

ROACH

Two categories of eggs (Fig. 1) could be recognized in active ovaries at all times up to the beginning of spawning: (i) recruitment eggs; transparent, with nuclei visible, and having a diameter of less than 10 eyepiece units; (ii) yolky eggs of diameter more than 10 eyepiece units.

Only the yolky eggs were counted for fecundity estimates. An analysis of the number of eggs per gram of ovary, for fish of different sizes on various

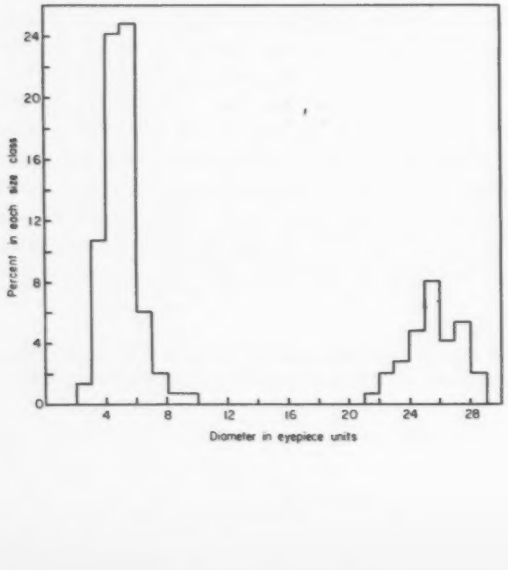

FIG. 1. Size frequency distribution of 401 eggs from an ovary of roach in March. One eyepiece unit = 0.037 mm. The smaller eggs were transparent, the larger eggs were yolky.

dates (Fig. 2) showed that the eggs increased in size steadily from January to May, and on any given date larger fish had larger eggs. May 10 was the last date on which ripe females were caught. From that time onwards the ovaries contained only recruitment eggs. Figure 2 may be interpreted as showing either that larger fish produce larger eggs, or alternatively that on any given date the larger fish were more advanced in egg development. The facts that the trend was visible just prior to spawning and that all fish spawned in a relatively short period suggests that the first explanation is the correct one. Early in the season the variation between individual fish was large, but by the time most of the fish were ready to spawn individual variation was not

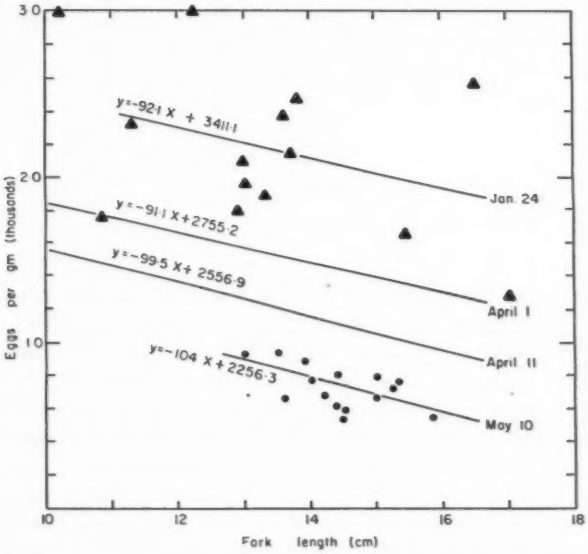

FIG. 2. Relationship between number of opaque eggs per gram of ovary and length of roach at different times. Each plotted point represents one fish. The points for April 1 and April 11 are omitted for clarity.

very great, as the points show. At this time an egg of a 16-cm fish was about 50% larger than that of a 13-cm fish.

A preliminary plot of log fecundity against length on each sampling date (Fig. 3) gave a series of lines that were very close and intersected near the middle of the size range. Accordingly a multiple regression analysis of length and age on fecundity was carried out on the combined data. The simple correlation coefficients were all high: between fecundity and length $r = 0.8888$, between fecundity and age $r = 0.8400$ and between length and age $r = 0.9437$. The partial correlation coefficient for fecundity on length, independent of age, was 0.5597, whereas the corresponding figure for fecundity on age, in-

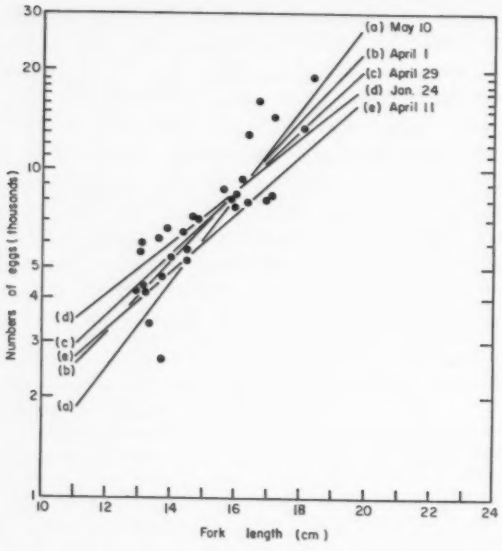

FIG. 3. Relationship between the total number of opaque eggs and length of roach at different times. Each plotted point represents one fish. Only the points for April 29 are plotted.

dependent of length was very small, 0.0079. The multiple correlation coefficient was 0.8888. From these results we see that the closest correlation is between fecundity and length, and that a consideration of age adds little to the predictive value of the relationship. However, there is a good correlation between age and length, so that a regression of fecundity on age is nearly as good for predictive purposes as the regression on length. Since the regression on age could be combined with existing population parameters, it was preferred. As a further check on the differences in fecundity between sampling dates, sums of squares of products and sums of errors of estimates were calculated for the separate sampling dates and used to test the difference in fecundity adjusted to average length and weight. The variation attributable to date of sampling was not found to be significant ($F = 1.45$, 4 and 81 df).

The line relating log fecundity to age is given by: log egg numbers = (0.0840 × age in years) + 3.2085. From Fig. 4 we see that the estimate of the number of eggs produced by a 6-year-old fish, for example, is 5157 with 95% confidence limits at 4725 and 5631.

A proportion of the males matured at age 2+, but the youngest maturing females seen were age 3+ (Table 1). Although the sample sizes are too low for statistical analysis it seems likely that as the season progressed a smaller and smaller percentage of roach had active gonads. For example, nearly one-quarter of the 3+ females in January had active gonads, but there were no egg-producing females in the April sample. Similarly, among 3+ males the percentage with active gonads declined from 94% in January to 50% at the end of April.

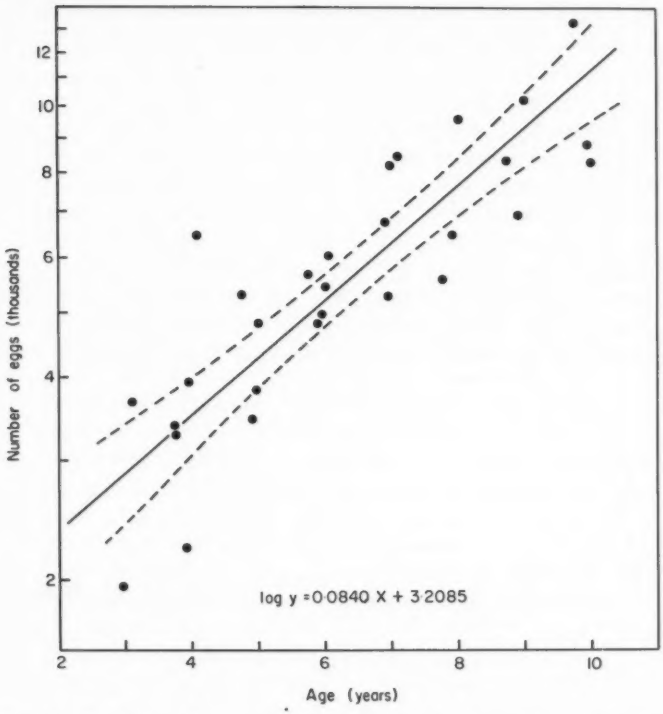

FIG. 4. Regression of mean numbers of eggs on age for each sampling date, for roach. Broken lines represent 95% confidence limits for the estimates.

TABLE 1. Percentages of roach with active gonads in samples taken at various dates. Numbers in parentheses indicate sample sizes.

Age-group	Females			Males		
	Jan. 24	Apr. 1	Apr. 29	Jan. 24	Apr. 1	Apr. 29
1	–	–	–	0(2)	–	–
2	0(23)	0(23)	–	44(18)	25(20)	–
3	23(13)	6(31)	0(7)	94(16)	65(20)	50(2)
4	50(4)	28(14)	–	100(5)	91(11)	66(3)
5	100(6)	67(6)	71(14)	100(4)	100(5)	100(5)
6	–	100(6)	66(12)	100(1)	100(1)	100(2)
7	100(1)	100(1)	75(4)	–	–	100(1)
8	100(1)	100(2)	100(4)	–	–	–
9	100(1)	100(1)	80(5)	100(1)	–	–
10			100(2)		100(1)	
11						100(1)
Total	49	84	48	47	58	14

BLEAK

Interpretation of the breeding cycle of bleak is made more difficult than for the roach by the appearance of three kinds of eggs in the ovaries (Fig. 5). These were: (i) transparent recruitment eggs of less than 10 units diameter; (ii) white, opaque eggs usually of diameter 9–25 units; and (iii) golden yolky eggs occupying part of the range 18–35 units in diameter. Not all fish were at the same stage of development at one time, but the histograms in Fig. 5 have been selected to show a representative sequence of events. In January the ovaries showed a large number of recruitment eggs and a smaller number of white opaque eggs. On March 7 the number of white opaque eggs had increased and showed signs of bimodality, with a more advanced group in the size range 17–25 units and another group in the size range 9–16 units. On April 1 a proportion of the ovaries had large golden yolky eggs in the size range

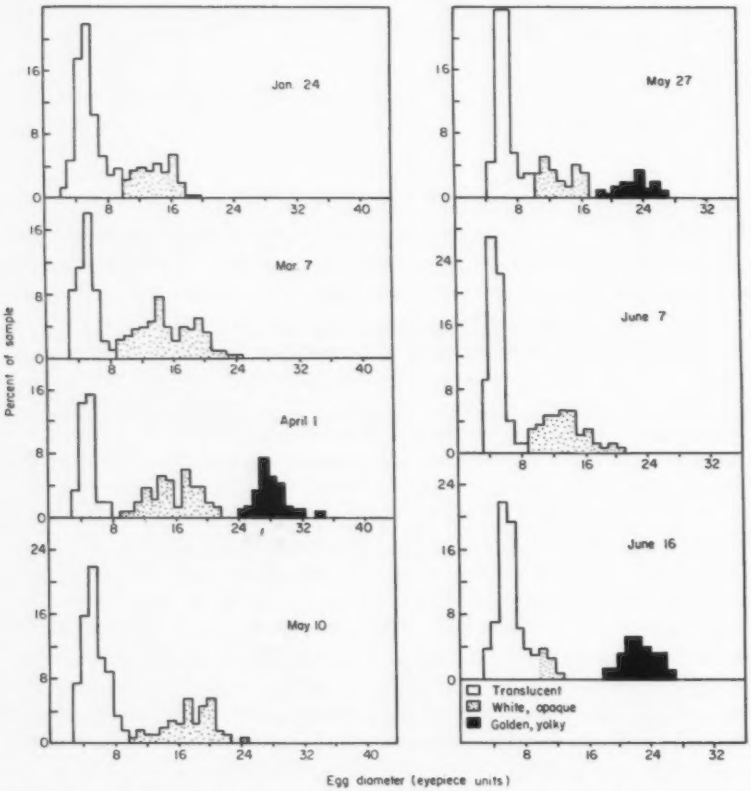

FIG. 5. Size-frequency histograms for samples of eggs from ovaries of bleak at different dates. One eyepiece unit = 0.037 mm. Sample sizes, January–June, 298, 182, 214, 217, 197, 173, and 158, respectively.

24–35 units. By April 29 all the gonads in a sample of 28 mature females were in this condition. On May 10 a proportion of the fish were lacking the yolky eggs, and by May 20 the majority lacked them, presumably because they had spawned. In late May the majority in the sample were again carrying yolky eggs. In the first half of June the proportion having yolky eggs declined and then increased again and on June 16 some fish were still carrying yolky eggs, but 70% of a sample of 43 fish were spent. It therefore appears from the samples that the population shed a batch of eggs in early May, and that there was one, possibly two peaks of spawning activity during June.

In view of this pattern of breeding activity, fecundity was calculated from the total numbers of white opaque and golden yolky eggs in the ovaries in the samples taken before spawning began, i.e., up to the end of April. The egg numbers in individual fish were much more variable in bleak than in roach, presumably on account of the complex pattern of spawning. Hence the simple correlation coefficients were lower: between fecundity and length $r = 0.2551$, between fecundity and age $r = 0.5312$, and between length and age $r = 0.3453$. The partial correlation coefficient for fecundity on length, independent of age, was very low, only 0.0902, whereas the partial coefficient for fecundity on age, independent of length, was 0.4883. Hence, in contrast to the roach, the fecundity was much better correlated with age than with length. An analysis of variance again showed that there was no significant difference in fecundity on the different sampling dates, after adjustment to average length and weight ($F = 2.43$, 4 and 97 df).

In Fig. 6 is shown the mean number of eggs (white opaque plus golden yolky) for each age-group on all dates of sampling up to the end of April, when spawning began. The regression of log egg numbers on age is given by: log egg numbers = (0.0564 × age in years) + 3.5221. For example the mean egg production of 5-year-old fish is 6356 with 95% confidence limits at 5987 and 6776.

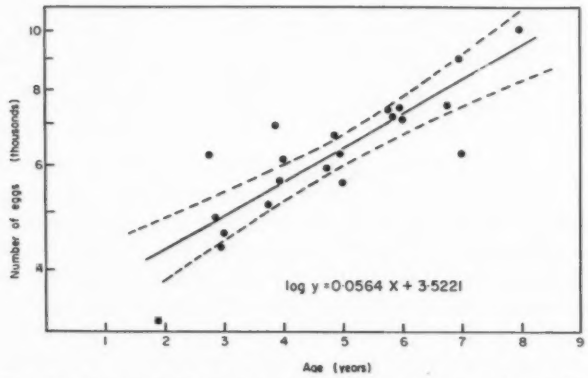

FIG. 6. Regression of mean numbers of eggs on age at each sampling date, for bleak. Broken lines represent 95% confidence limits for the estimates.

POPULATION FECUNDITY

It is now possible to estimate at least the order of magnitude of population fecundity for the two species, using the population parameters in Mann (1965) together with estimates of the sex ratio, the percentage spawning, and the mean egg production for each age-group. The distribution of sexes with age in a sample of 296 roach is as follows:

Age:	2+	3+	4+	5+	6+	7+	8+	9+	10+	Total
No. of fish	84	89	37	40	22	7	7	8	2	296
% females	54	57	48	65	81	85	100	87	100	

Females tended to predominate in the older age-groups. As the season progressed there was a reduction in the proportion of mature fish in the 3+ and 4+ year groups (Table 1), and the estimate of population fecundity is based on the assumption that only fish of 5 years and over were breeding. The calculation suggests a population fecundity of approximately 600 eggs per m^2 of river (Table 2).

Data on the sex ratio of bleak are as follows:

Age:	1+	2+	3+	4+	5+	6+	7+	Total
No. of fish	30	48	82	94	47	12	1	314
% females	53	45	42	44	42	75	100	

TABLE 2. Rough estimates of population fecundity.

Age	Total no. of fish per 100 m^2,[a]	No. of females per 100 m^2	% mature Apr. 29	Avg no. eggs per female	Total egg production per 100 m^2
		Roach			
5+	8	5.20	71	4,251	15,695
6+	6	4.86	66	5,185	16,631
7+	2	1.70	75	6,259	7,980
8+	1	1.00	100	7,597	7,597
9+	<1	<0.87	80	9,234	<6,427
10+	<1	<1.00	100	11,180	<11,180
					<65,510
		Bleak			
2+	167	75.1	50	4,314	161,990
3+	84	35.3	83	4,912	143,916
4+	12	5.3	91	5,593	26,975
5+	1	0.42	80	6,396	2,149
6+	<1	<0.75	67	7,252	<3,644
7+	<1	<1.00	100	8,258	<8,258
					<346,932

[a]Based on Mann (1965). The best estimate for fish of 5+ about to spawn is the figure for age-6 fish, and so on.

A good proportion of the bleak from age 2 upwards produced eggs, so that the population fecundity is of the order of 3000 eggs per m^2, about five times that of roach (Table 2).

DISCUSSION

Titova (1965) compared the fecundities of two populations of roach and found that in a population feeding mainly on animal material the average fecundity per fish was 25,560 whereas in those eating mainly plant material it was 2318. This is further evidence for the view (Mann, 1967) that roach eat animal material by preference and plant material only when forced to do so by shortage of preferred food. The average figure for Thames roach is about 5000 or 6000 eggs per fish, which is at the lower end of the range quoted by Titova.

Nikolskii (1962) analyzed the data of Chugunova (1951) to show that in 1946 the fecundity of Caspian semi-migratory roach lay in the range 34,000–51,000, whereas in the following year it had fallen to 19,000 to 41,000. Making comparisons between fish of comparable sizes, one finds that a Caspian roach of 17 cm produced 34,000 eggs in 1 year and 20,000 in the other, whereas Thames roach in 1966 produced about 10,000 eggs. Nikolskii emphasized the importance of fecundity changes in matching the size of the population to its resources.

Although Table 1 is not conclusive, it suggests that the proportion of roach in the population having maturing eggs in the ovaries declined steadily as the season progressed. If this effect was real, it is possible that it was produced by follicular atresia as reported by Scott (1962) or by higher mortality of fish with large, active gonads. However, no dead fish were seen at this time.

In general, it has been found that the roach population in the river at Reading is very dense and slow growing (Williams 1965, 1967), and the fish fill their guts with organic debris in winter and early spring, presumably because more nutritious food is scarce (R. H. Britton, unpublished data). Moreover, Williams (1967) found that at age 5 the roach grew large enough to eat the large gastropod *Viviparus* and that this was associated with an improvement in growth rate. We see that at age 5 the proportion of reproducing females also increased.

All this evidence suggests that the roach population is severely limited by food shortage so that its fecundity is low and that possibly a proportion of the fish maturing eggs in January are forced to resorb them before spawning time. A similar but less marked reduction was seen in the porportion of males with mature and active gonads. There are two possible reasons why the phenomenon should be less marked in males. One is that the strain on the physiology of the fish caused by maturing a testis is probably less than that caused by maturing an ovary. (In a previous study an ovary was found to average 13.87% of the body weight whereas a testis averaged 6.40% (Mann, 1965).) Conversely, the advantage gained from resorbing the germ cells is less for a male.

In bleak, decrease in the proportion of sexually active fish was less marked, but at the end of April, 7 out of 36 females examined were not in breeding condition, although a higher proportion of the population had been maturing in the first 3 months of the year. Williams (1965) found that the bleak population had a growth rate that was not below average, although R. H. Britton (unpublished data) has found that they feed mainly on detritus for several months of the year. Bleak feed on plankton and surface drift, whereas roach are mainly benthic feeders, so there is little inter-specific competition. Allochthonous drifting material is reasonably abundant at certain times of the year in this part of the river, which is downstream of the town.

The data available suggest that fish populations that have expanded to the limit of their food resources respond by reducing fecundity as well as growth rate. Williams' (1967) data indicate that Thames roach of age 8 were about 60% as long as fish of the same age in highly favourable habitats. Taking weight as proportional to (length)^3, their weight would be about 23% of that of the fast growers. Titova's (1965) figures indicate that the fecundity of the Thames fish also lies in the range 20–25% of the fecundity of the carnivorous fish, whereas Nikolskii's (1962) paper suggests that some varieties of roach may have fecundities six to eight times as great as the Thames fish. In general it seems that the reduction in fecundity is in about the same proportion as the reduction in growth in weight, and that there is no evidence of a mechanism tending to change the balance between somatic and germinal production. However, Scott (1962) has shown that starvation results in follicular atresia, and there is a suggestion of a similar phenomenon in roach. In this instance, the demand for resources of the somatic tissue clearly takes precedence over that of the gonads.

ACKNOWLEDGMENTS

The work was supported by a grant from the Science Research Council, later transferred to the Natural Environmental Research Council. The authors are indebted to Professor A. Graham, the University of Reading, for the facilities of his Department and for advice and encouragement; to Dr T. B. Bagenal for helpful discussions; and to Messrs R. H. Britton and I. McDonald who assisted with the sampling. Most of the analysis of the data was carried out while the authors were at their Canadian addresses, and Dr L. M. Dickie, Director of the Marine Ecology Laboratory Dartmouth, N.S., gave valuable assistance and criticism.

REFERENCES

ALLEN, K. R. 1951. The Horokiwi stream. Bull. Marine Dept. New Zealand Fish. No. 10. 238 p.

BAGENAL, T. B. 1957. The breeding and fecundity of the long rough dab, *Hippoglossoides platessoides* (Fabr.), and the associated cycle in condition. J. Marine Biol. Assoc. U.K. 36: 339–375.

CHUGUNOVA, N. I. 1951. Relation of the growth and maturity of the Caspian roach in the northern Caspian to food conditions. Trans. Inst. Marine Fish. U.S.S.R. 18: 153–170.

GREZE, V. N. 1965. [Growth rate and production potential of fish populations.] Gidrobiol. Zh. 1: 35–42. (In Russian.) (Fish. Res. Bd. Canada Transl. 897.)

MANN, K. H. 1965. Energy transformations by a population of fish in the River Thames. J. Animal Ecol. 34: 253–275.

1967. The cropping of the food supply. *In* S. D. Gerking [ed.] The biological basis of freshwater fish production. Blackwell Scientific Publications, Oxford and Edinburgh. 495 p.

NIKOLSKII, G. V. 1962. On some adaptions to the regulations of population density in fish species with different types of stock structure. *In* E. D. LeCren and M. W. Holdgate [ed.] The exploitation of natural animal populations. Blackwell Scientific Publications, Oxford and Edinburgh. 399 p.

RAITT, D. S. 1932. Fecundity of the haddock. Fish. Scotland, Sci. Invest. 1: 1–42.

RICKER, W. E. 1932. Studies of speckled trout (*Salvelinus fontinalis*) in Ontario. Publ. Ont. Fish. Res. Lab. 44: 67–110.

SCOTT, D. P. 1962. Effect of food quantity on fecundity of rainbow trout, *Salmo gairdneri*. J. Fish. Res. Bd. Canada 19: 715–731.

TITOVA, K. N. 1965. [Contributions to the biology of roach (*Rutilus rutilus* L.) of southern and northern U.S.S.R.] Nauchn. Dokl. Vysshei Shkoly Biol. Nauki 2: 27–31. (In Russian.)

WILLIAMS, W. P. 1965. The population density of four species of freshwater fish, roach (*Rutilus rutilus* L.), bleak (*Alburnus alburnus* L.), dace (*Leuciscus leuciscus* (L.)) and perch (*Perca fluviatilis* L.) in the River Thames at Reading. J. Animal Ecol. 34: 173–185.

1967. The growth and mortality of four species of fish in the River Thames at Reading. J. Animal Ecol. 36: 695–720.

Oxygen Consumption of *Tilapia nilotica* in Relation to Swimming Speed and Salinity

G. J. Farmer and F. W. H. Beamish

Department of Zoology
University of Guelph, Guelph, Ont.

Farmer, G. J., and F. W. H. Beamish. 1969. Oxygen consumption of *Tilapia nilotica* in relation to swimming speed and salinity. J. Fish. Res. Bd. Canada 26: 2807–2821.

Oxygen consumption of *Tilapia nilotica* (L.) at 25 C was measured for various swimming speeds at salinities of 0, 7.5, 11.6, 22.5, and 30‰.

Oxygen consumption for a given swimming speed and salinity increased linearly with weight when expressed on a double logarithmic grid. Slopes of regression lines relating oxygen consumption and weight were less than unity, ranging from 0.5117 to 0.9887.

Generally, oxygen consumption at 0, 7.5, and 22.5‰ was approximately equal; values at 11.6‰ were lowest and those at 30‰ highest. Presumably, energy required for osmoregulation was least in the absence of an osmotic gradient (11.6‰) and greatest when the osmotic gradient was highest (30‰). Assuming energy required for osmoregulation was zero at the isosmotic salinity (11.6‰), it was estimated that approximately 29% of the total oxygen consumption was required for osmoregulation at 30‰ and 19% at 0, 7.5, and 22.5‰.

Plasma osmotic concentration was used as an index of capacity for osmotic regulation. Concentrations for unexercised fish remained about the same at 0, 15, and 30‰. At no salinity were plasma osmotic concentrations for exercised and unexercised fish statistically different at $P < 0.05$. However, there was a trend for concentrations for exercised fish to decrease from the unexercised level at 0‰ and to increase from the unexercised level at 30‰. Only at 15‰ were concentrations similar for exercised and unexercised fish. Of the salinities tested, fish were able to osmoregulate most efficiently at 15‰, the salinity closest to the isosmotic salinity.

Received June 19, 1969

INTRODUCTION

Fish commonly inhabit waters varying in salinity from approximately 0.1 part per thousand (‰) referred to as fresh water to about 35‰ in the surface waters of oceans. However, instances of fish living in salinities twice that of the oceans have been observed (Parry, 1966).

Some species of fish tolerate a wide range of salinity and are termed euryhaline. Others, referred to as stenohaline, survive only within a comparatively narrow range of salinities. Some euryhaline species withstand changes in body fluids in response to changes in salinity but most are able to maintain homeostasis. In migrating adult Atlantic salmon, *Salmo salar*, internal osmotic concentration changed only about 5% between fresh and sea water (Parry, 1961). Stenohaline fish, beyond a narrow range of salinities, are unable to control water and salt balance.

Printed in Canada (J1509)

Salt concentration in the blood of fish is less than that of sea water, the notable exception being the myxinoid cyclostomes. Thus, in a marine environment, water is lost at the gills and other body surfaces (Black, 1957). Conversely, freshwater homeostasis is dependent on the elimination of absorbed water, the concentration of the body fluids being greater than that of the environment (Black, 1957). Whatever the mechanism, fish must expend energy for osmotic regulation.

Oxygen consumption is often taken as a measure of metabolic expenditure and includes energy dissipated in locomotion, osmotic regulation, and other activities necessary for the well being of an animal. Oxygen consumption has been determined in relation to many parameters (Beamish and Dickie, 1967) but salinity and sustained swimming have received little attention, the recent research of Rao (1968) being a notable exception. To increase information on the influence of salinity and sustained swimming on oxygen uptake, a study was made on the euryhaline fish *Tilapia nilotica* (L.).

MATERIALS AND METHODS

Specimens of *T. nilotica* were obtained in June of 1967 from the Stral Company in Greensboro, Alabama, where they were cultured in freshwater ponds.

In the laboratory, fish were held in 450-liter holding tanks. A photoperiod of approximately 15 hr, from 0800 to 2300 E.S.T., was maintained throughout the study. Fish were fed a commercial fish food in pellet form once daily.

Water in the holding tanks was maintained at 25 C throughout the experiment. A chemical analysis of the tap water used during the study is presented in Table 1.

Fish were acclimated to fresh water (0‰) and to salinities of 7.5, 11.6, 22.5, and 30‰. For acclimation to various salinities, 1‰ of "New" Tropic-Marin artificial marine salt was added to the holding tanks every other day until the desired salinity was reached. Fish were allowed at least 2 weeks at the final salinity before being exercised. Salinities were regularly checked with a Beckman electrodeless induction salinometer.

Prophylactic treatments were not given to the fish as disease was apparent at no time during the study.

The respiration chamber was designed as a recirculating water tunnel (Fig. 1). A centrifugal pump was used to recirculate water in the chamber. The drive unit consisted of a 2-hp electric motor coupled to a variable speed hydraulic gear. Water velocity through the chamber was regulated by the hydraulic gear, which was coupled to the centrifugal pump. From the pump outlet, water passed through the tunnel portion of the chamber and was then diverted 180° to enter the expansion chamber. From the expansion chamber water passed through the reduction cone and into the swimming chamber. Thereafter, water was diverted 90° to enter the centrifugal pump and was again recirculated. The respiration chamber was constructed of acrylic tubing. The tunnel portion of the respirometer and the swimming chamber had an inner diameter of 9.6 cm. The chamber available to a fish was 36 cm long. The expansion chamber had an inner diameter of 26 cm and a length of 44 cm. Five turbulence grids were mounted in the expansion chamber. The swimming chamber contained an opening for introduction of the fish. A lid, machined to fit the curvature of the tunnel, was clamped over the opening to prevent water leakage.

In the portion of the respirometer in which fish swam, the velocity profile was constant over the range of velocities used. This was achieved by the use of a diffuser section consisting of the expansion cone and turbulence grids. Macroturbulent flow produced in the pump was straightened after passing through the grids in the expansion chamber and reduced to microturbulent flow in the reduction cone. The flow pattern was observed by the use of small particles of dried

Table 1. Variations in characteristics of laboratory tap water. Temperature ranged from 10.0 to 14.5 C and *p*H from 7.1 to 7.5.

	Range (*mg/liter*)
Carbon dioxide	16.0–28.0
Chlorine	0
Hardness (*a*) Calcium	60.0–80.0
(*b*) Total	90.0–120.0
(*c*) Magnesium	25.0–40.0
Iron	0
Nitrate nitrogen	0.17–0.33
Nitrite nitrogen	0
Ammonia nitrogen	0.0–0.25
Turbidity	0

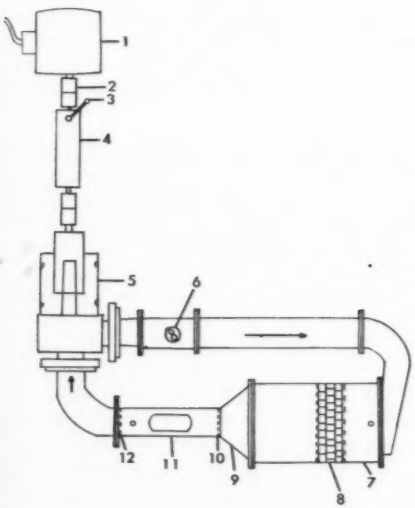

FIG. 1. Diagram of the respirometer. Arrows indicate the direction of water flow. (1) Electric motor; (2) coupling; (3) lever for control of water velocity; (4) variable speed hydraulic gear; (5) centrifugal pump; (6) openings for oxygen electrode and temperature probe; (7) expansion chamber; (8) turbulence grids; (9) reduction cone; (10, 12) nylon mesh; (11) swimming chamber with opening.

aluminum paint coated with a detergent. Water velocity was measured with a small current meter. Maximum velocity was 130 cm/sec.

Movement of fish was confined by nylon mesh at each end of the swimming chamber. The volume of the respiration chamber was 37 liters. Generally, fish of 40–120 g were used. This allowed space for free swimming without sacrificing sensitivity to oxygen change by involving too large a volume of water. The maximum cross-sectional area of an average fish was about 10% of the cross-sectional area of the swimming chamber. Hence no correction for error in swimming speed was made.

An oxygen electrode and temperature probe, mounted into a portion of the respirometer, were used to measure ambient oxygen concentrations and temperature. The oxygen electrode was standardized daily by the sodium azide modification of the Winkler method (American Public Health Association, 1955).

The experimental procedure followed was identical for all fish. After fish were put into the respirometer, water velocity was gradually increased to 30 cm/sec. Oxygen concentration and temperature were determined at 10-min intervals. Fish were exercised at 30 cm/sec until oxygen consumption was constant for three consecutive 10-min periods. The swimming speed was then increased to 40 cm/sec and the same procedure followed. Oxygen consumption was thus determined for swimming speeds of 30, 40, 50, and 60 cm/sec. A swimming speed of 30 cm/sec was the slowest swimming speed at which *T. nilotica* swam continually; 60 cm/sec was the greatest swimming speed they were able to maintain for a period long enough to record accurately oxygen consumption. Fish were exercised in the respirometer only at the salinity to which they were acclimated.

Dissolved oxygen in the respirometer was not allowed to fall below 6 mg/liter. Oxygen consumption of *T. nilotica* was dependent on the ambient oxygen concentration only below 4.2 mg/liter regardless of salinity. When the oxygen concentration approached 6 mg/liter, water in the respirometer was exchanged for water saturated with oxygen and held in a reservoir above the respirometer. Similarly, water temperature in the respirometer was maintained at 25 ± 0.5 C by recirculation.

Before the final experiments were run, it was found necessary to train the fish. Fish were exercised at 40 cm/sec on alternate days to investigate the effects of training (Table 2). All fish were given at least four trials in the respirometer and exercised until oxygen consumption remained constant. Oxygen consumption during the second trial was lower than during the first for most fish. Oxygen consumption did not decline on trials after the third. Thus, it was decided to train fish by subjecting them to three trials in the respirometer at a swimming speed of 40 cm/sec. Final experiments were run on the second day after the third trial period. A blank was run daily

TABLE 2. Influence of training on the oxygen consumption of *Tilapia nilotica* at a swimming speed of 40 cm/sec.

Salinity (‰)	Wt (g)	Trial	Oxygen consumption (*mg*) for consecutive 20-min periods						
			1	2	3	4	5	6	7
0	105	1	13.32	12.65	14.58	13.25	11.99		
		2	11.06	8.44	9.81	9.55	11.51	[a]	
		3	9.44	7.59	7.55	8.84	8.88	9.32	
		4	8.28	7.36	8.62	7.70	8.07	8.84	
		5	8.36	7.81	7.92	7.62	6.40	9.66	
0	109	1	12.10	11.47	11.77	8.95	9.92		
		2	11.77	8.70	8.25	8.25	8.10	8.40	
		3	9.84	8.92	8.03	8.33	7.99		
		4	9.95	7.77	9.29	8.07	9.62	[a]	
0	67	1	7.99	7.70	6.73[a]				
		2	6.11	5.51	7.03	7.20	7.36	5.77	6.44
		3	7.84	5.03	6.96	6.29	7.29	5.70	6.70
		4	7.73	6.77	7.14	7.14	7.10	7.84	
		5	5.03	6.99	5.37	6.59	6.33	6.92	
30	40	1	8.62	6.25	6.22	6.81	6.25	5.25	6.25
		2	8.25	5.92	5.92	4.11	5.62	4.66	4.81
		3	9.88	6.48	4.48	5.22	5.33	5.70	4.59
		4	8.58	6.48	5.37	4.74	5.33	4.70	5.07

[a]Failed to continue swimming.

for a 1-hr period to determine oxygen consumption not attributable to fish. Oxygen consumption of fish was then calculated.

Oxygen consumption of three trained fish, unfed for 24 hr, was measured at the four swimming speeds and compared with that for the same three fish after deprivation of food for 72 hr. Appreciable differences were not observed at any of the swimming speeds. Thereafter food was withheld for 24 hr prior to an experiment.

Standard metabolism was estimated by extrapolation of the relation between oxygen consumption and swimming speed to zero activity as described by Brett (1965).

Freezing point depression of plasma was determined for exercised and unexercised fish acclimated to salinities of 0, 15, and 30‰. The procedure for exercising fish was the same as that followed for oxygen consumption determinations. Blood was taken from the caudal artery with a glass syringe and immediately introduced into heparinized capillary tubes and centrifuged for 10 min. Freezing point depressions of plasma were determined with a Clifton nanoliter osmometer, which is essentially a thermoelectric cooling module mounted on the stage of a stereo microscope. Plasma samples were frozen then gradually thawed. The thawing process was observed through the stereo microscope. The freezing point depression for each sample was taken as the temperature at which the last ice crystal that it contained neither shrank nor swelled.

The plasma freezing point depression for *T. nilotica* was calculated by averaging all values for unexercised fish at the three salinities. From the formulae: freezing point depression $= -0.0966\ Cl - 0.0000052\ Cl^3$ (Thompson and Robinson, 1932), and salinity $= 0.03 + 1.805 \cdot$chlorinity (Knudsen, 1901), a straight line relationship was established between salinity and freezing point depression. A vertical line was erected from the plasma freezing point for *T. nilotica* to the line relating salinity and freezing point depression to determine the salinity isosmotic to the blood of *T. nilotica*.

Regression lines for the relation between oxygen consumption and weight were fitted according to the principle of least squares (Alder and Roessler, 1964). Correlation coefficients (Alder and Roessler, 1964) and 95% confidence intervals of slopes (Steel and Torrie, 1960) were calculated for all regression lines. Differences in oxygen consumption for fish acclimated to different salinities but at the same swimming speed were tested for significance by analysis of covariance (Steel and Torrie, 1960). To compare plasma freezing point depression for exercised and unexercised fish at a given salinity the standard error of difference between means and the significance of the difference between means was calculated (Alder and Roessler, 1964).

RESULTS

Oxygen consumption for a given swimming speed and salinity increased linearly with weight when expressed on a double logarithmic grid. Number of fish used, weights, regression equations, and 95% confidence intervals of slopes are listed in Table 3.

Slopes of all regression lines were less than unity. In fresh water (0‰) the proportionate change in oxygen consumption in relation to swimming speed was independent of size, the regression lines being approximately parallel. However, at other salinities slopes increased with swimming speed. At 7.5‰ (Fig. 2) the slope at 30 cm/sec was 0.8136 and increased to 0.9605 at 60 cm/sec. Similarly at 22.5‰, slopes increased from 0.7106 to 0.8665. In contrast, slopes at 11.6‰ increased from 0.5117 at 30 cm/sec to 0.7060 at 60 cm/sec and slopes at 30‰ increased from 0.5354 to 0.7791. Slopes were significantly lower at 11.6 and 30‰ than at 0, 7.5, and 22.5‰ for a given swimming speed. At 11.6 and 30‰, slopes of the regression lines were not significantly different among the various swimming speeds ($P < 0.05$). Generally, slopes at 0, 7.5, and 22.5‰ were not different at $P < 0.05$ for a given swimming speed.

TABLE 3. Relation between oxygen consumption and weight at each salinity and swimming speed for *Tilapia nilotica* at 25 C. Differences in oxygen consumption for fish acclimated to different salinities but at the same swimming speed were accepted as significant at $P < 0.05$.

Salinity (‰)	Swimming speed (*cm/sec*)	Date	No. fish	Wt range (*g*)	Mean wt (*g*)	Regression equation $\log y = a + b \log x$	Oxygen consumption for an 80-g fish (*mg/hr*)	95% confidence interval of slope
0	30	July 21–	15	47–137	77.10	$\log y = -0.2881 + 0.8058 \log x$	17.60	.0755
	40	Aug. 29,	15	47–137	75.15	$\log y = -0.2672 + 0.8397 \log x$	21.42	.0816
	50	1967	15	47–137	75.15	$\log y = -0.2129 + 0.8537 \log x$	25.81	.0735
	60		15	47–137	70.44	$\log y = -0.0631 + 0.8549 \log x$	36.64	.0568
7.5	30	Sept. 10–	15	41–138	88.84	$\log y = -0.3046 + 0.8136 \log x$	17.53	.0280
	40	Oct. 3,	15	41–138	88.84	$\log y = -0.5323 + 0.9887 \log x$	22.36	.0540
	50	1967	15	41–138	88.84	$\log y = -0.3769 + 0.9492 \log x$	26.87	.0421
	60		15	41–138	88.84	$\log y = -0.2592 + 0.9605 \log x$	37.03	.0441
11.6	30	July 15–	15	46–142	83.89	$\log y = 0.1672 + 0.5117 \log x$	13.84	.0687
	40	Aug. 3,	15	46–142	83.89	$\log y = 0.1838 + 0.5510 \log x$	17.08	.0693
	50	1968	15	46–142	83.89	$\log y = 0.0029 + 0.7049 \log x$	22.10	.0603
	60		15	46–142	83.89	$\log y = 0.1364 + 0.7060 \log x$	30.20	.0637
22.5	30	Nov. 29–	15	27–143	82.66	$\log y = -0.1504 + 0.7106 \log x$	15.92	.0690
	40	Jan. 3,	15	27–143	82.66	$\log y = 0.0031 + 0.6981 \log x$	21.46	.0633
	50	1968	15	27–143	82.66	$\log y = -0.2703 + 0.8939 \log x$	26.98	.0632
	60		15	27–143	87.52	$\log y = -0.1252 + 0.8665 \log x$	33.40	.0765
30.	30	Jan. 19–	15	29–165	80.42	$\log y = 0.2771 + 0.5354 \log x$	19.77	.0546
	40	Feb. 16,	15	29–165	80.42	$\log y = 0.2953 + 0.5743 \log x$	24.45	.0828
	50	1968	15	29–165	80.42	$\log y = 0.2679 + 0.6382 \log x$	30.38	.0565
	60		15	41.5–165	94.01	$\log y = 0.0800 + 0.7791 \log x$	36.54	.0533

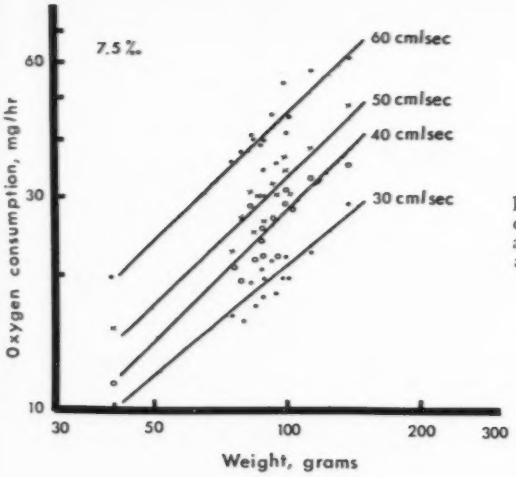

FIG. 2. Relation between logarithm of oxygen consumption and logarithm of weight of *Tilapia nilotica* at different swimming speeds for a salinity of 7.5‰.

Oxygen consumption at each salinity and swimming speed was calculated for an 80-g fish from the regression equations relating oxygen consumption and weight (Table 3).

The pattern of the relation between oxygen consumption and salinity was the same for each swimming speed and the estimated standard rates (Fig. 3). Oxygen consumption remained about the same at 0 and 7.5‰ but decreased at 11.6‰. At 22.5‰, oxygen consumption increased from that at 11.6‰ and continued to increase at 30‰. For example at a swimming speed of 50 cm/sec oxygen consumption in fresh water was 25.81 mg/hr and about the same, 26.87 mg/hr, at 7.5‰. At 11.6‰, oxygen consumption was 22.10 mg/hr, less than in 0 or 7.5‰. Oxygen consumption increased to 26.98 mg/hr at 22.5‰ and continued to increase to 30.38 mg/hr at 30‰.

Generally oxygen consumption for a given swimming speed was higher at 30‰ than at all other salinities. Differences, however, were not significant in all cases at $P < 0.05$. The one exception occurred at the highest sustained swimming speed used, 60 cm/sec. Here, oxygen consumption at 30‰, 36.54 mg/hr, was about the same as that at 7.5‰, 37.03 mg/hr, and 0‰, 36.64 mg/hr.

Oxygen consumption at 11.6‰ was significantly lower than at any other salinity for a given swimming speed.

At no swimming speed was oxygen consumption at 0 and 7.5‰ statistically different at $P < 0.05$. Generally, oxygen consumption at 22.5‰ was lower than at 7.5‰ but not lower than at 0‰ ($P < 0.05$) for a given swimming speed.

Plasma freezing point depressions remained about the same at 0, 15, and 30‰ for unexercised fish (Table 4). The average value was −0.621° C. Plasma freezing points for exercised fish decreased from −0.588° C at 0‰ to

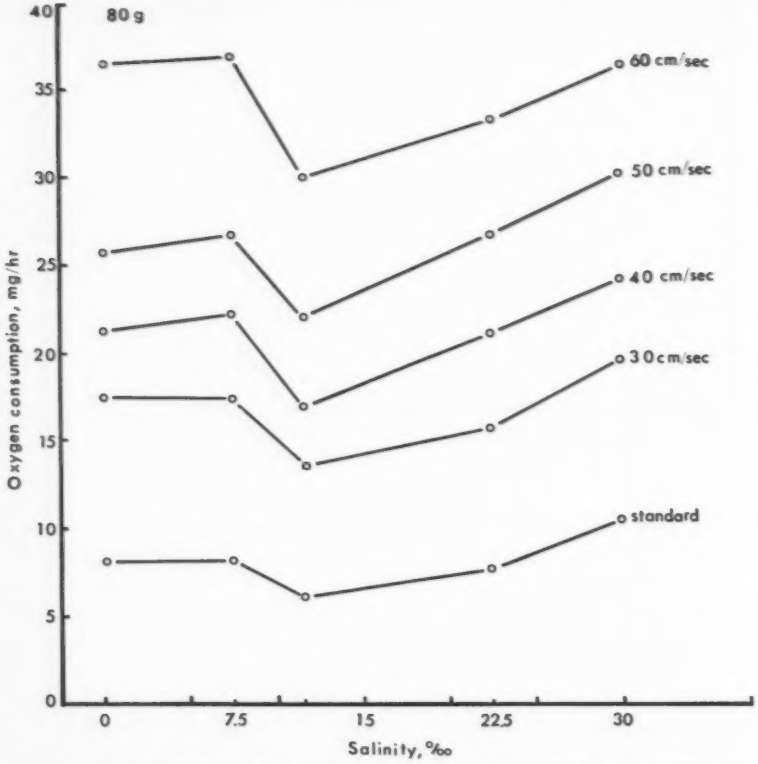

FIG. 3. Oxygen consumption of *Tilapia nilotica* in relation to swimming speed and salinity. All values were corrected to correspond to that for an 80-g fish. An estimate of standard oxygen consumption is shown.

−0.6138 C at 15‰ and continued to decrease to −0.6500 C at 30‰. Plasma freezing points were similar for exercised and unexercised fish only at 15‰, the test salinity nearest the isosmotic salinity. The salinity isosmotic to the blood of *T. nilotica* was calculated to be 11.6‰.

At no salinity were values for exercised and unexercised fish statistically different at $P < 0.05$. Plasma freezing points for exercised fish at the three salinities were different at $P < 0.05$. Differences between plasma freezing points of unexercised fish at the three salinities were not significant.

DISCUSSION

Generally, oxygen consumption of *T. nilotica* during the 1st hr of exercise was greater than during the 2nd hr. Presumably the higher rate of oxygen consumption during the 1st hr of exercise was associated with excitability. Smit (1965) demonstrated differences in oxygen consumption between short-

TABLE 4. Plasma freezing point depressions of fish acclimated to different salinities. Figures within parentheses show number of fish used.

Salinity (‰)	Unexercised			Exercised			
	Mean wt (g)	Freezing point (C)	SE	Mean wt (g)	Freezing point (C)	SE	t
0	267.4	−0.6176(5)	0.0187	142.0	−0.5882(5)	0.0052	1.5139[a]
15	170.0	−0.6220(5)	0.0043	150.0	−0.6138(5)	0.0079	0.9083[a]
30	157.6	−0.6226(5)	0.0078	141.6	−0.6500(5)	0.0090	2.2967[a]

[a]No significant difference at $P < 0.05$.

and long-term exercise of goldfish, *Carassius auratus*, for a given swimming speed. Goldfish exercised for several hours at a given swimming speed displayed decreasing oxygen consumption with time. He attributed the decline in oxygen consumption to the subsidence of excitement.

With training, *T. nilotica* appeared to swim with less effort and to be less excited. MacLeod (1967) observed that the maximum swimming speed of largemouth bass fingerlings, *Micropterus salmoides*, increased from 18 to 30 cm/sec with training. Brett et al. (1958) found that underyearling coho salmon, *Oncorhynchus kisutch*, reared in tanks with a water velocity of 24 cm/sec showed a higher cruising speed and less susceptability to fatigue than salmon reared in tanks with lower current velocity.

In addition to improved swimming performance oxygen consumption of *T. nilotica* was lowered with training. Hochachka (1961) suggests physiological changes occur with training. He found rainbow trout, *Salmo gairdneri*, trained in a current for 6 months had more hemoglobin in their blood and relatively larger hearts than untrained trout.

Little information is available on the relation between weight and oxygen consumption for fish at sustained swimming speeds. For *T. nilotica*, slopes of the linear relation between weight and oxygen consumption increased with swimming speed at each salinity except 0‰. In accord, slopes were found to increase with swimming speed for rainbow trout (Rao, 1968) and sockeye salmon, *Oncorhynchus nerka* (Brett, 1965). Both Rao and Brett found regression coefficients of approximately 1.0 at the maximum sustained swimming speed for each species. Only at 7.5‰ did slope approach 1.0 for *T. nilotica* at the maximum swimming speed applied, 60 cm/sec.

Slopes of regression lines increased with swimming speed at all salinities except 0‰. Thus, except at 0‰, if regression lines are extended below the weight range used, oxygen consumption for small fish is less at high swimming speeds than at low swimming speeds. For example, at 30‰ a 1-g fish would consume 0.08 mg O_2/hr at 60 cm/sec and 0.28 mg O_2/hr at 30 cm/sec. This may suggest that at the high swimming speeds small fish do not osmoregulate so well as at the lower swimming speeds.

Rao (1968) found an increase in slope with swimming speed for rainbow trout at all salinities tested. The increase was particularly marked at 30‰. Rao attributed this to a decrease in the relative level of metabolism of small fish at 30‰ because of a failure in osmotic regulation.

Similarly if regression lines for *T. nilotica* at the isosmotic salinity, 11.6‰, are extended below the weight range used, oxygen consumption for small fish is less at high than low swimming speeds. Here it is unlikely that differences result entirely from failure in osmotic regulation at the higher swimming speeds. It is possible that the range of weights used may not have been sufficient to describe the relation with oxygen consumption. Further, small fish are unable to swim at the speeds maintained by the larger fish. Hence extrapolation of the relation between weight and oxygen consumption far below the weight range tested is unwise.

Generally slopes of regression lines relating oxygen consumption and weight were significantly lower at 30 and 11.6‰ than at other salinities for a given swimming speed. Low slopes at 30‰ may indicate the expenditure for osmoregulation per unit weight is higher for small than large fish. In accord, Parry (1960) found for young Atlantic salmon, *S. salar*, survival and osmotic regulation after transfer from fresh water to dilutions of sea water were dependent on size and age, the more important being size. She attributed this to the ratio of surface area to volume of fish, a larger fish being subjected to a lower osmotic stress. Conte et al. (1966) found survival of juvenile coho salmon, *O. kisutch*, in sea water was a function of size not chronological age. Hence observations for *T. nilotica* at 30‰ are consistent with those for other species. However at 11.6‰, slopes were similar to those at 30‰. This is in contrast to the suggestion that energy required for osmoregulation is minimal at 11.6‰. Possibly the weight range used at 11.6‰ may not have been sufficient to describe the relation with oxygen consumption. Moreover, correlation coefficients at 11.6‰, although significant, were less than at other salinities, suggesting slope values at the isosmotic concentration may not be so precise as at the other salinities.

Oxygen consumption for a given swimming speed was lowest at 11.6‰ and highest at 30‰. Oxygen consumption at 0, 7.5, and 22.5‰ was intermediate. Presumably energy expenditure associated with osmoregulation is highest at 30‰ and least at 11.6‰. As 11.6‰ is isosmotic with the blood of *T. nilotica*, energy required to maintain homeostasis is minimal. When the osmotic gradient was greatest (30‰) oxygen consumption was highest. Oxygen consumption of fish at salinities osmotically equidistant (0 and 22.5‰) from the isosmotic salinity was approximately equal. Hence the magnitude and not the direction of the osmotic gradient is important in the energy requirements for osmoregulation. Concordant with observations on *T. nilotica*, Rao (1968) found lowest oxygen consumption for rainbow trout at 7.5‰, a salinity about isosmotic with their blood. Moreover at 0 and 15‰, salinities osmotically equidistant from the isosmotic salinity, oxygen consumption was about the same for a given swimming speed.

Hickman (1959) estimated standard oxygen consumption of the starry flounder, *Platichthys stellatus*, and concluded that in high salinity a large proportion of the animals minimum energy requirements must be devoted to maintaining homoiosmoticity. He stated that the different metabolic rates at 0 and 25‰ were related to the metabolic demands for transportation of electrolytes and water in the principal organs of exchange, the gills, kidney, and gut.

Generally oxygen consumption of *T. nilotica* at 30‰ was higher than at the other salinities for a given swimming speed. However, at 60 cm/sec the highest sustained swimming speed used, oxygen consumption was about the same at 30‰ as that at 0 and 7.5‰. Further, oxygen consumption at 60 cm/sec was higher than at any other swimming speeds for a given salinity. Hence it is possible that failure to increase oxygen consumption at 30‰ may reflect

a limitation of the respiratory system. Total metabolic expenditure at the highest sustained speed applied and, particularly at a salinity of 30‰, may not have been met by the oxygen consumed. Thus, additional energy may have been released anaerobically. In accord, Beamish (1968) found evidence of anaerobic metabolism in Atlantic cod, *Gadus morhua*, only at the higher swimming speeds. Brett (1964) found that oxygen consumption of sockeye salmon swimming at maximum sustained speeds could be elevated 50% by increasing ambient oxygen concentration above air saturation. Similarly, Saunders (1962) suggests for various species that at high swimming speeds they may be unable to extract sufficient oxygen from the water for metabolic demands.

Oxygen required for osmotic regulation at each salinity and swimming speed can be calculated by assuming energy for osmotic regulation is zero at the isosmotic salinity (Rao, 1968). Further, oxygen consumption for swimming and osmoregulation at a given swimming speed and salinity can be calculated by subtraction of the estimated standard rate for that salinity from the total oxygen consumption (Table 5). Oxygen required for swimming can then be obtained by subtracting the uptake of oxygen for osmotic regulation from that for swimming and osmotic regulation. Estimates of oxygen consumption for swimming were lowest at 30‰ and approximately equal at 0, 7.5, and 22.5‰ for all swimming speeds. If density of the medium were to exert an effect, oxygen required for swimming would be highest at 30‰ because of increased surface drag on fish. However, estimates of the oxygen required for swimming suggest it is independent of salinity. Similarly Rao (1968) showed that the energy expenditure associated with swimming was independent of salinity for rainbow trout. Differences in oxygen consumption at various salinities for *T. nilotica* can thus be ascribed to energy expenditure associated with osmoregulation.

Energy required for osmoregulation was calculated as a percentage of the total oxygen consumption at each salinity and swimming speed. Much of the total oxygen consumption was utilized for osmoregulation, the expenditure being greatest at 30‰. For swimming speeds of 30, 40, and 50 cm/sec approximately 29% of the total oxygen uptake was required for osmoregulation at 30‰, and 19% was required at 0, 7.5, and 22.5‰. Rao (1968) found that 27% of the total oxygen consumption was required for osmoregulation at 30‰ and 20% at 0‰ for active rainbow trout.

Energy required for osmoregulation was about the same at salinities of 0, 7.5, and 22.5‰. In accord, fish at 0 and 22.5‰ were osmotically equidistant from the isosmotic salinity. Rao (1968) found that energy required for osmoregulation was equal for rainbow trout osmotically equidistant (0‰ and 15‰) from the isosmotic salinity. However, energy required for osmoregulation by *T. nilotica* at 0 and 22.5‰ was comparable to that required by fish at 7.5‰, the osmotic gradient being least at 7.5‰.

Plasma osmotic concentrations (plasma freezing point depressions) of exercised and unexercised fish at salinities of 0, 15, and 30‰ provide a useful index on capacity for osmotic regulation. Plasma osmotic concentrations of

TABLE 5. Total oxygen consumption and that required for osmotic regulation of *Tilapia nilotica* in relation to salinity and swimming speed.

Speed (*cm/sec*)	Salinity (‰)				
	0	7.5	11.6	22.5	30
0	8.35[a](2.16)[b]	8.39(2.20)	6.19	7.82(1.63)	10.71(4.52)
	(9.25)[c]	(9.14)	(7.65)	(8.10)	(9.06)
30	17.60(3.76)	17.53(3.69)	13.84	15.92(2.08)	19.77(5.93)
	(13.07)	(13.97)	(10.89)	(13.64)	(13.74)
40	21.42(4.34)	22.36(5.28)	17.08	21.46(4.38)	24.45(7.37)
	(17.46)	(18.48)	(15.91)	(19.16)	(19.67)
50	25.81(3.71)	26.87(4.77)	22.10	26.98(4.88)	30.38(8.28)
	(28.29)	(28.64)	(24.01)	(25.58)	(25.83)
60	36.64(6.44)	37.03(6.83)	30.20	33.40(3.20)	36.54(6.34)

[a]Total oxygen consumption corrected to correspond to that for an 80-g fish.
[b]Total oxygen consumption at a given salinity minus total oxygen consumption at the isosmotic salinity, 11.6‰.
[c]Total oxygen consumption at a given swimming speed and salinity minus standard oxygen consumption at that salinity.

exercised fish acclimated to 0‰ decreased from the unexercised level, and plasma osmotic concentrations of exercised fish acclimated to 30‰ increased from the unexercised level. Only at 15‰ were plasma osmotic concentrations similar for exercised and unexercised fish. Of the three salinities tested, *T. nilotica* was able to osmoregulate most efficiently at 15‰, the salinity closest to the isosmotic salinity. Apparently, at 0‰ exercised fish were unable to control the osmotic influx of water so efficiently as unexercised fish. Similarly at 30‰ exercised fish were unable to control salt balance so well as unexercised fish. Thus, strenuously exercised fish are unable to meet energy demands for osmoregulation at the salinity extremes.

Similar observations have been made for Atlantic salmon, *S. salar*, in relation to exercise (Byrne, MS, 1969). Osmoregulatory ability of salmon was better at 15‰ than at either 0 or 30‰, the osmotic gradient being least at 15‰. Plasma chloride concentration was least at 0 and highest at 30‰. However, Rao (1969) observed that plasma osmotic concentration of rainbow trout increased with exercise at all salinities between 0 and 30‰. He suggested that the increase may result from other inorganic ions or organic compounds such as amino acids or both.

Beamish (1968) observed that Atlantic cod, when exercised at moderate swimming speeds, exhibited comparatively small amounts of muscle and blood lactic acid. At higher swimming speeds fish accumulate larger quantities of lactic acid in the muscle and blood. During recovery after strenuous swimming muscle and blood lactic acid increased precipitously.

Although accumulation of metabolites may have increased plasma osmotic concentration of *T. nilotica* swimming at 30‰, the increase probably resulted largely from the inability of exercised fish to completely remove excess salt. Similarly if the accumulation of metabolites by exercised fish had significantly altered plasma osmotic concentration at 0‰, the difference between exercised and unexercised fish may not have been evident.

ACKNOWLEDGMENTS

We are grateful to the following, all from the University of Guelph. Drs K. Ronald, H. R. MacCrimmon, E. D. Bailey, and W. Dall of the Department of Zoology offered suggestions for improvement of the manuscript. Dr R. W. Shuel, Department of Apiculture, assisted in statistical analysis of the data. We are particularly grateful to J. Underwood of the Department of Agricultural Engineering for his help in designing the respirometer.

Financial support was given by the National Research Council of Canada.

REFERENCES

ALDER, H. L., AND E. B. ROESSLER. 1964. Introduction to probability and statistics. 3rd ed. W. H. Freeman and Company, San Francisco and London. 313 p.

AMERICAN PUBLIC HEALTH ASSOCIATION. 1955. Standard methods for the examination of water sewage and industrial wastes. 10th ed. American Public Health Association, New York. 626 p.

BEAMISH, F. W. H. 1968. Glycogen and lactic acid concentrations in Atlantic cod (*Gadus morhua*) in relation to exercise. J. Fish. Res. Bd. Canada 25: 837–851.

BEAMISH, F. W. H., AND L. M. DICKIE. 1967. Metabolism and biological production in fish, p. 215–242. *In* S. D. Gerking [ed.] The biological basis of fresh water fish production. Blackwell Scientific Publications, Oxford and Edinburgh.

BLACK, V. S. 1957. Excretion and osmoregulation. Chap. IV, p. 163–205. *In* M. E. Brown [ed.] The physiology of fishes. Vol. I. Academic Press, Inc., New York.

BRETT, J. R. 1964. The respiratory metabolism and swimming performance of young sockeye salmon. J. Fish. Res. Bd. Canada 21: 1183–1226.

1965. The relation of size to rate of oxygen consumption and sustained swimming speed of sockeye salmon (*Oncorhynchus nerka*). J. Fish. Res. Bd. Canada 22: 1491–1501.

BRETT, J. R., M. HOLLANDS, AND D. R. ALDERDICE. 1958. The effect of temperature on the cruising speed of young sockeye and coho salmon. J. Fish. Res. Bd. Canada 15: 587–605.

BYRNE, J. M. MS, 1969. Osmoregulation of Atlantic salmon, *Salmo salar* L. in relation to salinity, temperature and exercise. M.Sc. Thesis. Univ. Guelph, Guelph, Ont. 85 p.

CONTE, F. P., H. H. WAGNER, J. FESSLER, AND C. GNOSE. 1966. Development of osmotic and ionic regulation in juvenile coho salmon, *Oncorhynchus kisutch*. Comp. Biochem. Physiol. 18: 1–15.

HICKMAN, C. P., JR. 1959. The osmoregulatory role of the thyroid gland in the starry flounder, *Platichthys stellatus*. Canadian J. Zool. 37: 997–1060.

HOCHACHKA, P. W. 1961. The effect of physical training on oxygen debt and glycogen reserves in trout. Canadian J. Zool. 39: 769–776.

KNUDSEN, M. 1901. Hydrographical tables. Hydrographical Laboratory, Copenhagen. 63 p.

MACLEOD, J. C. 1967. A new apparatus for measuring maximum swimming speeds of small fish. J. Fish. Res. Bd. Canada 24: 1241–1252.

PARRY, G. 1960. The development of salinity tolerance in the salmon, *Salmo salar* L. and some related species. J. Exptl. Biol. 37: 425–434.

1961. Osmotic and ionic changes in the blood and muscle of migrating salmonids. J. Exptl. Biol. 38: 411–427.

1966. Osmotic adaptation in fishes. Biol. Rev. 41: 392–444.

RAO, G. M. M. 1968. Oxygen consumption of rainbow trout (*Salmo gairdneri*) in relation to activity and salinity. Canadian J. Zool. 46: 781–785.

1969. Effect of activity, salinity and temperature on plasma concentrations of rainbow trout. Canadian J. Zool. 47: 131–134.

SAUNDERS, R. L. 1962. The irrigation of the gills in fishes. II. Efficiency of oxygen uptake in relation to respiratory flow, activity and concentrations of oxygen and carbon dioxide. Canadian J. Zool. 40: 817–862.

SMIT, H. 1965. Some experiments on the oxygen consumption of goldfish (*Carassius auratus* L.) in relation to swimming speed. Canadian J. Zool. 43: 623–633.

STEEL, G. D., AND J. H. TORRIE. 1960. Principles and procedures of statistics. McGraw-Hill Book Company Inc., New York. 481 p.

THOMPSON, T. G., AND R. ROBINSON. 1932. Chemistry of the sea. Physics of the earth. Vol. 5. Oceanography. Natl. Res. Council Bull. 85. Washington, D.C. p. 95–203.

Some Morphological and Biochemical Changes in Steelhead Trout During the Parr–Smolt Transformation

JAMES L. FESSLER AND HARRY H. WAGNER

Oregon State Game Commission, Research Division
Oregon State University, Corvallis, Oreg. 97331, USA

FESSLER, JAMES L., AND HARRY H. WAGNER. 1969. Some morphological and biochemical changes in steelhead trout during the parr–smolt transformation. J. Fish. Res. Bd. Canada 26: 2823–2841.

This study was initiated to determine changes in chemical composition, coefficient of condition, and body morphology for juvenile steelhead trout from premigratory through postmigratory periods, January through July. Winter-run steelhead trout, originating from Big Creek and the Sandy River, in Oregon, were used as experimental animals.

A discriminant analysis indicated that coefficient of condition and fork length were nearly as powerful in separating smolts from parr as were 10 morphological measurements.

The parr–smolt transformation in winter steelhead is size-dependent and characterized by a marked decrease in body depth and coefficient of condition. Changes in depth measurements and coefficient of condition provided the most meaningful measure of morphological change at the time of parr–smolt transformation.

During the migratory period, lipid content was substantially lower than in the premigratory period for migrant-sized fish ($\geq$160 mm) but remained relatively constant in nonmigrants ($\leq$159 mm) throughout all periods. Seasonal changes in moisture and protein levels occurred in the larger fish, although moisture and protein content for the smaller fish remained relatively constant. The amount of ash did not change within a size group.

The coefficient of condition of migrant-sized fish declined continuously from February through May but increased in June and July. The mean coefficient of condition for nonmigrants declined from December through February, but remained relatively stable from March through June, with an upward trend in July.

Received June 16, 1969

INTRODUCTION

AN INTERESTING ASPECT of the biology of steelhead trout, *Salmo gairdneri*, is the parr–smolt transformation or metamorphosis. In many anadromous salmonids the process of smolting includes profound changes in morphology, physiology, and behavior that precede seaward migration. Such changes transform the cryptic-colored, bottom-dwelling fish (parr) into a silvery pelagic animal (smolt) adapted to the marine environment (Hoar, 1963). In steelhead the parr–smolt transformation is markedly size-dependent and seasonal in occurrence (Wagner, 1968). Morphological and physiological changes taking place during the parr–smolt transformation are of interest in understanding early stages of development. The changes also are of direct importance to biologists concerned with the recognition of potential steelhead migrants.

Printed in Canada (J1507)

Morphological and chemical changes occurring in steelhead trout during the parr–smolt transformation have not been previously described. The objective of this study was to determine changes in chemical composition, coefficient of condition, and body morphology for juvenile steelhead trout from premigratory through the postmigratory period, January through July.

Morphological data have been used extensively in systematic, racial, and relative-growth studies of fish (Milne, MS, 1948; Martin, 1949; Marr, 1955). Evropeitseva (1957) found that Atlantic salmon (*Salmo salar*) smolts differed from parr in having longer and thinner caudal peduncles, less depth to the body, and relatively shorter pectoral and ventral fins. Holding Atlantic salmon in fresh water after smolting resulted in a complete loss of the silvery coloration, reduction in relative caudal peduncle length, and an increase in body and caudal peduncle depths (Evropeitseva, 1962). A decrease in the coefficient of condition at the time of parr–smolt transformation has been described for Atlantic salmon by several fishery scientists (Hoar, 1939; Evropeitseva, 1957; Houston and Threadgold, 1963).

Differences in chemical composition have been noted between parr and smolts of juvenile sockeye salmon (*Oncorhynchus nerka*) by Kizevetter (1948) and Akulin (1966), in Atlantic salmon by Malikova (1957), and in coho salmon (*Oncorhynchus kisutch*) by Vanstone and Markert (1968). Qualitative changes in chemical constituents were observed by Lovern (1934) in fatty acids and by Malikova (1957) in amino acids. A decrease in hepatic glycogen has been noted in smolting Atlantic salmon (Fontaine and Hatey, 1950).

METHODS

General

Winter-run steelhead trout originating from Big Creek and the Sandy River in Oregon were used as experimental animals. Big Creek enters the Columbia River about 10 miles from the ocean; the Sandy River enters the Columbia 80 miles from the ocean.

The eggs were incubated and the two stocks of fish reared under identical conditions at Gnat Creek Hatchery. The hatchery is located on the lower Columbia River, about 15 miles from the ocean, and is operated by the Oregon State Game Commission. The fish were fed a commercially prepared diet (J. R. Clark Co., Salt Lake City, Utah) at a rate based on fish size and water temperature. Seasonal water temperature ranged from 5 to 13 C during the sampling period.

Big Creek steelhead were reared in a single raceway; the larger number of Sandy River fish were reared in two raceways. For the study, the two groups of Sandy River fish were treated as a single population.

Sampling Technique

Fish in the hatchery, and migrating hatchery fish, were routinely sampled for length and weight. In addition, the size of native downstream migrants in the Sandy River was determined. Specimens were collected for chemical and morphological measurements concurrently with the monthly length–weight samples. Individual fish were anesthetized in M.S. 222 (tricane methanesulfonate), weighed to the nearest 0.1 g, and measured to the nearest millimeter (fork length = FL). Fish collected for morphological measurements were fixed in 10% formalin for 10 days and stored in 70% alcohol. Prior to sampling, fish in the hatchery were starved for 24–36 hr. A sample of fish in the rearing pond was obtained after lowering the water level and crowding the fish.

On May 11–13, 1964, about 82,000 juvenile steelhead of Sandy River stock were released about 8 miles above Marmot Dam on the upper Sandy River. A total of 39,000 juvenile steelhead from Big Creek stock was released at the same location on May 11, 1964. Some of the hatchery fish migrating downstream were captured and sampled at the Marmot Dam trapping facility.

Chemical Analysis

Juvenile steelhead from the two stocks were examined for changes in chemical composition. Each month fish were selected for analysis from two categories, those of migrant size (160 mm and 190 mm in FL), and those not so (130 mm in FL). The size categories for the migrant groups were based on length distribution of downstream migrants captured on the Sandy River in the spring of 1963. Three or more fish (minimum combined weight of 100 g) were blotted dry and then placed in a plastic bag that was collapsed by submersion in water and then sealed. The process was repeated with a second bag and the sample was frozen. Three samples were taken for each of the size groups used in the study, and the results of the three analyses were averaged.

The analyses were carried out at the Department of Agricultural Chemistry, Oregon State University, according to approved methods (Association of Official Agricultural Chemists, 1960). The frozen fish samples were thawed and autoclaved in sealed jars for 45 min at 15 lb pressure to soften the bone before reduction to a homogeneous paste with mortar and pestle. Samples were analyzed from 1 to 2 months after freezing.

Difficulties arise in detecting chemical changes in body composition when the data are in the form of percentage of total weight (Parker and Vanstone, 1966). To circumvent the difficulty, actual weights of each body component were estimated. Because the mean length of fish in a specific size group making up the samples varied slightly from month to month, the weight of each component was estimated for a fish of a common length, assuming no difference in relative weight or shape. The common length in a specific size group was selected as the most frequent mean length occurring in monthly samples.

The allometric equation $W = aL^b$, where W = weight, L = length, and a and b are unknowns, was used to standardize samples to a common length. The exponent b is identified as the slope of the regression of log W on log L and log a is the intercept or height of the regression line where it crosses the ordinate. The equation (log adjusted length − log actual length)3 + log actual weight = log adjusted weight was used to standardize all samples to the common length.

Morphological Measurements

The Sandy River and Big Creek stocks were examined each month for changes in coefficient of condition (K_{FL}) at the hatchery. The mean coefficient of condition ($\bar{K}_{FL}$) was calculated by using the equation

$$\bar{K}_{FL} = \frac{\Sigma \frac{100\ W}{L^3}}{N}$$

where W = weight in grams, L = fork length in centimeters, and N = sample size. The population was divided into two size groups for the computation of mean K_{FL}. The first group (nonmigrants) included fish from 70 to 139 mm in length and the second group (potential migrants) ranged from 140 to 209 mm in length. Fish from 140 to 159 mm appeared to be intermediate with respect to the occurrence of smolting, but for purposes of presentation they have been included in the potential migrant group.

The study of relative growth of certain external body parts was based on specimens from Big Creek stock collected from February through July 1964. Monthly collections consisted of 5–10 fish from each available 10-mm size group. The coefficient of condition was computed from FL, and weight, taken prior to fixation. The following measurements were made on each preserved specimen for the relative growth of certain body parts:

Fork length = tip of snout to fork of caudal fin
Standard length = tip of snout to end of hypural plate
Head length = tip of snout to terminal edge of opercle

Trunk length = terminal edge of opercle to insertion of anal fin
Caudal peduncle length = insertion of anal fin to end of hypural plate
Caudal fin length = end of hypural plate to tip of caudal fin
Dorsal fin length = origin of dorsal fin to insertion of dorsal fin
Body depth = maximum depth anterior to origin of dorsal fin
Caudal peduncle depth = minimum depth of caudal peduncle

All morphological measurements were made to the nearest millimeter. Linear body measurements were obtained with a measuring board constructed with an adjustable pointer on a sliding arm for individual projected measurements. Measurements of the dorsal fin and of depth were made with dial calipers.

The relationship of body part to standard length is best represented by a curve line that is conveniently rectified to form a straight line by use of logarithmic coordinates (Huxley, 1932; Milne, MS, 1948). When K = 1, growth rate of the body part and standard length are equal and the relationship is called isometric growth. The mean values of each morphological measurement were plotted on logarithmic coordinates to show monthly changes with respect to isometric growth (K = 1) for fish of different size. Actual K values were not calculated for each month. The percentage of standard length was calculated for the five most important morphological characters, selected to illustrate changes in overall body form taking place during the sampling period.

Discriminant Analysis

The major objective of the linear discriminant analysis was to distinguish a parr from a smolt. An attempt at cluster analysis using the technique of principle components failed because of the evolutionary nature of the parr–smolt transformation. The cluster analysis did reveal that FL and K_{FL} were the two variables containing most of the information. Retrospectively, we concluded that the only way to solve the problem was to obtain a sample of fish representing parr and another sample representing smolts and conduct a linear discriminant function. The smolt group was made up of Sandy River native migrants and hatchery migrants of Big Creek stock. The nonmigrant or parr group included fish from the hatchery during the premigratory period (January, February, and March).

Two linear discriminant analyses were made on migrants and nonmigrants, one using K_{FL} and nine relative growth measurements, and the other K_{FL} and FL. A discriminant function approach combines the values of several variables to derive a statistical partition between two or more groups. It is based on a statistical procedure originally developed by Fisher (1936). Analyses were made with the BMD05M program, as modified for the CDC 3300 computer (Yates, MS, 1967).

RESULTS

Chemical Composition

There were significant changes in the chemical composition of the larger fish. In February, Big Creek steelhead in the 167- and 191-mm groups weighed more than fish of comparable length in May. The lower weight in May was the result of a lesser amount of moisture, protein, and lipid. Approximately 50% of the total weight loss was a result of less moisture whereas lipid and protein accounted for approximately 35% and 15% respectively. Fish in the 134-mm size group had similar weights throughout the sampling period. However, the most dramatic change occurred in the amount of lipid where a 72–78% decrease was observed. There was a decrease of 10–11% in protein and 8–9% in moisture content.

Lipid content showed the greatest change in the 191- and 167-mm groups and the least change in the 134-mm group. Lipid constituted 2.47 g of the total adjusted body weight for fish in the 167-mm size group in February; during May the mean weight of lipid was 0.54 g. In July lipid again made up 2.41 g of the total adjusted weight in the 167-mm size group. Big Creek steelhead in the 191-mm group showed a similar pattern of variation in the amount of lipid except for the month of July when no increase was noted.

Lipid content was similar for the 167-mm size groups of Big Creek and Sandy River fish during the premigratory period. At the time of release, fish of Sandy River origin in the 167-mm size group had a higher lipid content (1.25 g) than Big Creek fish of similar size (0.54 g). Hatchery fish from both stocks captured while they were migrating downstream shortly after release (May 12–18) were similar in chemical composition.

Hatchery migrants of Sandy River origin, captured while they were migrating downstream were similar in chemical composition to the native stock in the Sandy River shortly after release. Hatchery migrants in the 167-mm group had a lipid content of 0.58 g in mid-May, decreasing to 0.32 by mid-June. Lipid content of native migrants in the 167-mm size group increased from 0.65 g in May to 0.70 g in June.

Seasonal changes in protein levels occurred in the 167- and 191-mm groups (Fig. 1). Here protein decreased from February through March and then increased in June and July. The pattern was similar to that seen for lipid. Protein content for the 134-mm group remained relatively constant throughout the sampling period.

The amount of moisture decreased from 34.38 g in February to 31.34 g in May in the 167-mm group of Big Creek steelhead. Fish in the 191-mm group showed a similar pattern of variation in the amount of moisture. Sandy River steelhead in the 167-mm group were comparable to Big Creek steelhead in moisture content.

The amount of ash remained relatively constant for each size group (Fig. 1). The Big Creek and Sandy River fish in the 167-mm group contained a similar amount of ash.

Coefficient of Condition

Changes in $\overline{K}_{FL}$ (Fig. 2) were similar to changes in body depth (Fig. 6). The mean coefficient of condition for the larger fish (140–209 mm) from the Sandy River stock paralleled that of the smaller fish initially but was lower in April and May (Fig. 2). Fish condition in both groups increased in July. Condition of fish in the larger size group originating from Big Creek stock declined continuously from February through May and then increased in June and July. The $\overline{K}_{FL}$ for small fish (nonmigrants) held at the hatchery declined during the December–February period for stocks from both rivers. The initial decline was followed by a more or less stable $\overline{K}_{FL}$ during the March–June period, with an upward trend noted in July.

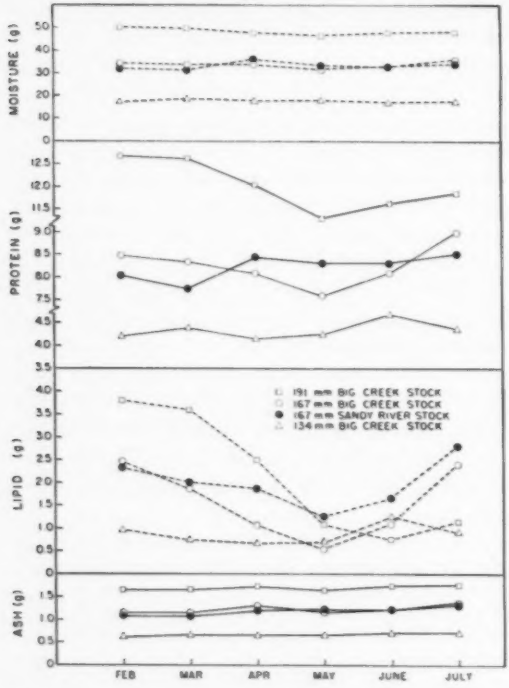

FIG. 1. Body composition of Big Creek and Sandy River hatchery-reared steelhead from February through July 1964.

Juvenile steelhead captured while they were migrating downstream within the first few days after stocking had a lower $\bar{K}_{FL}$ than the population at release (Fig. 2). Big Creek fish released on May 11, 1964, had a $\bar{K}_{FL}$ of 0.896. Here the $\bar{K}_{FL}$ for fish with a typical silvery smolt appearance was 0.876 (n = 819) as contrasted with 0.963 (n = 127) for fish resembling parr. Big Creek fish trapped 8 miles below the release site from May 12–15 had a $\bar{K}_{FL}$ of 0.859 (Fig. 2). Condition of migrants captured during the ensuing days and weeks continued to decline until the latter part of June, but increased in July (Fig. 2).

Steelhead of Sandy River origin released May 11–13, 1964, had a $\bar{K}_{FL}$ of 0.943. Fish with the silvery smolt appearance had a $\bar{K}_{FL}$ of 0.907 (n = 495), whereas $\bar{K}_{FL}$ for those with a parr appearance was 0.970 (n = 515). The $\bar{K}_{FL}$ for migrants captured from May 12–15 was 0.869, considerably lower than observed at time of release (Fig. 2). The condition of fish captured while they were moving downstream continued to decline through June and increased rapidly in the first weeks of July, as it had done for the Big Creek stock. The condition of the native migrants remained relatively constant during the March to May period (Fig. 2).

Length–frequency distributions of Sandy River steelhead differed markedly for fish in the hatchery and for hatchery migrants (Fig. 3). The Sandy River

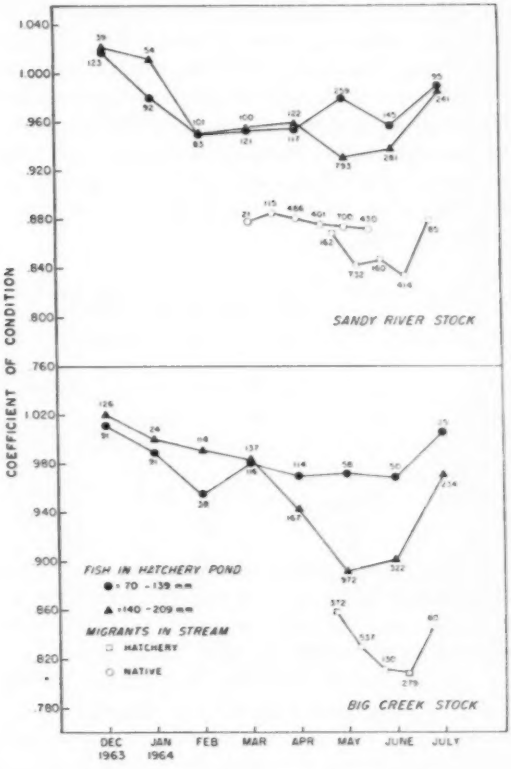

FIG. 2. Mean coefficient of condition ($\bar{K}_{FL}$) for Big Creek and Sandy River juvenile steelhead trout in the hatchery and for native and hatchery migrants. Sample sizes are noted at each point.

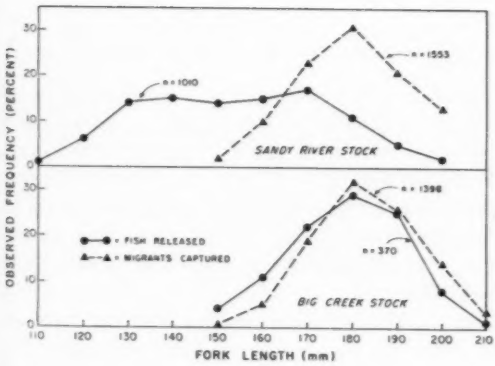

FIG. 3. Length–frequency distribution for Big Creek and Sandy River steelhead for fish released from the hatchery and for migrants captured while moving downstream. The Sandy River release group was composed of fish from two ponds that had a later and wider range of hatching dates than did the Big Creek stock.

fish ranged from 110 to 200 mm at the time of release, whereas the range of FL for migrants captured was 150–200 mm. From an analysis of length frequencies, assuming little or no growth during the period, we estimated that 40–50% of the Sandy River fish that were stocked did not migrate downstream. In contrast, the length–frequency distributions for fish released and migrants captured were almost identical for the Big Creek stock, suggesting that a large percentage of the animals had smolted and migrated downstream. At the time of release, Big Creek steelhead were larger than the Sandy River fish (Table 1), because of a longer rearing period resulting from earlier fertilization and hatching dates.

TABLE 1. Growth (weight in grams) of Big Creek and Sandy River steelhead during the experimental period, January through July 1964.

	Month						
Stock	Jan.	Feb.	Mar.	Apr.	May	June	July
Big Cr.	36.6	45.5	47.0	49.6	54.9	61.5	79.5
Sandy R.	24.2	31.0	29.5	38.5	39.2	49.7	57.2

The length–weight relationships of Big Creek steelhead in the hatchery approached a line with a slope of 3.0 (Fig. 4). Native migrants approached the same line. Hatchery migrants followed a line with a slope near 3.0 but fell into another growth stanza.

Coefficient of condition was similar for the Sandy River and Big Creek steelhead migrants regardless of length. The frequency distributions of K_{FL} for the Big Creek fish at the time of release and for migrants captured (Fig. 5) are almost identical, except for a downward shift for the migrants. The shift was greater for Sandy River fish and again reflects the larger number of parr present in the population at time of release.

RELATIVE GROWTH RATES AND PROPORTIONATE SIZE OF BODY PARTS

Seasonal changes in depth measurements provided the most meaningful index of morphological change (Fig. 6). Maximum body depth approached a line with $K = 1$ for all fish regardless of length during January, February, and March and for fish with a standard length up to 120 mm (Fig. 7) during April, May, and June. Fish larger than 120 mm standard length decreased in body depth ($K < 1$) during the migratory period (April, May, and June). Body depth decreased from 22.8% of standard length to 20.4% from the premigratory to migratory periods (Fig. 6).

Caudal peduncle depth followed a growth pattern similar to body depth (Fig. 6) but changes were not so great. Caudal peduncle depth approached a line with $K = 1$ for January, February, March, and April fish, but $K < 1$ for May, June, and July fish regardless of length (Fig. 7).

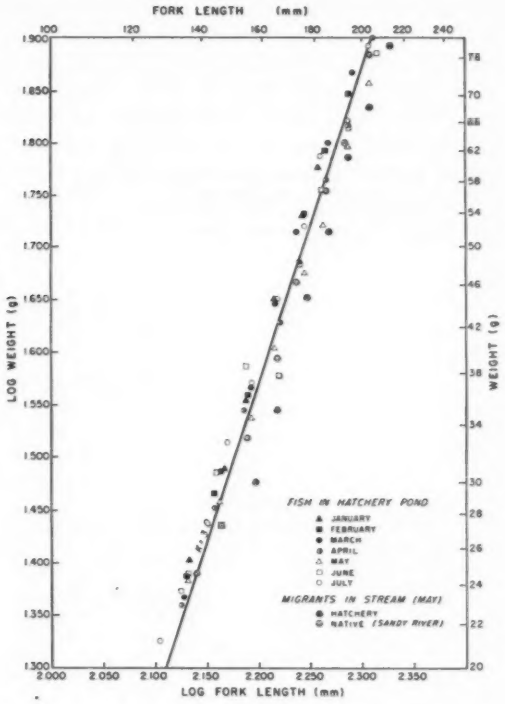

FIG. 4. Relation of weight to fork length for Big Creek steelhead in the hatchery and for native and hatchery migrants.

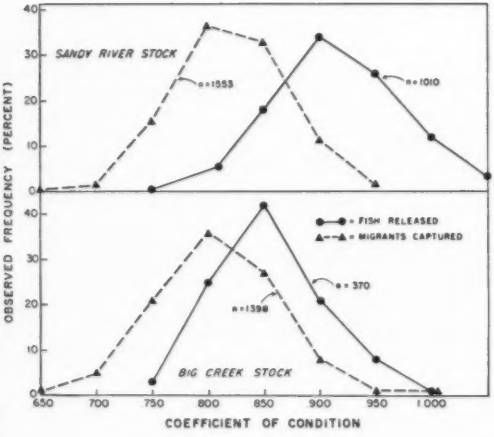

FIG. 5. Frequency distribution of the coefficient of condition (K_{FL}) for Big Creek and Sandy River steelhead released from the hatchery and migrants captured while moving downstream.

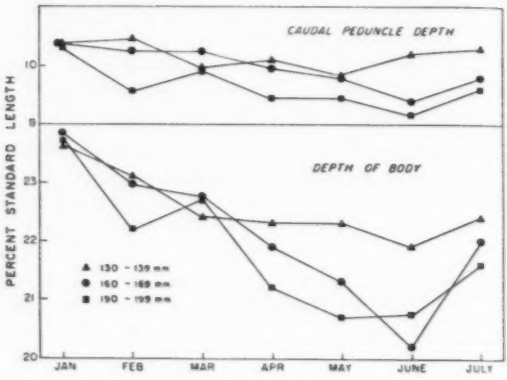

FIG. 6. Body and caudal peduncle depth as a percentage of standard length for Big Creek juvenile steelhead from January through July 1964.

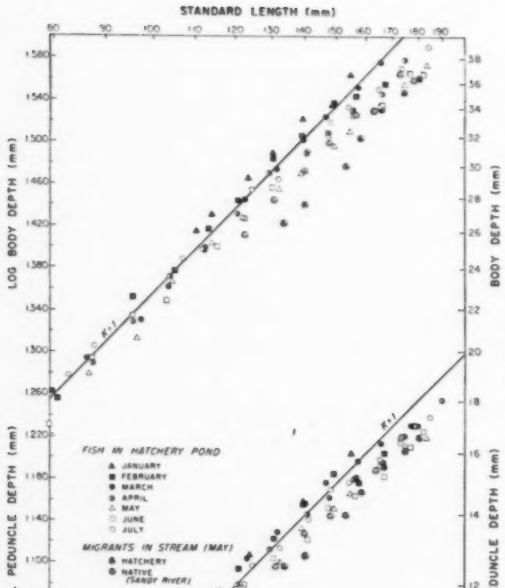

FIG. 7. Relation of caudal peduncle and body depth to standard length for Big Creek juvenile steelhead in the hatchery and for migrants in the stream.

Head length approximated a line with K = 1 for animals up to 100 mm standard length; head length approximated a line with K < 1 for animals greater than 100 mm (Fig. 8). From January through July the 130-mm group showed a gradual increase in head length, from 21.8 to 22.8% of standard length, indicating that slower-growing animals had larger heads (Fig. 9). This is consistent with the observations by White (1936) on Atlantic salmon with respect to head length for fast- and slow-growing juveniles. Head length for the 160-mm group was more variable and inconsistent throughout the experimental period. Animals in the 190-mm group had shorter heads than the 130- and 160-mm fish.

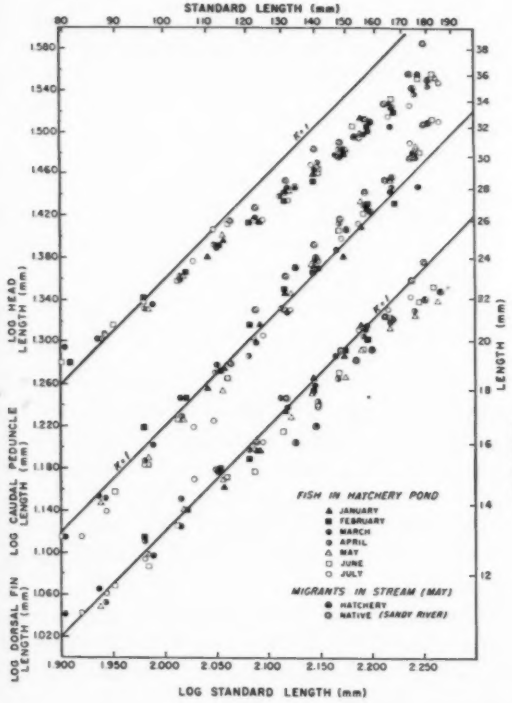

FIG. 8. Relation of dorsal fin, caudal peduncle, and head length to standard length for Big Creek juvenile steelhead in the hatchery and for migrants in the stream.

Caudal peduncle length approximated a line with K = 1 for all groups, with a slight increase (K > 1) as the fish approached 120 mm standard length (Fig. 8). Caudal peduncle length remained constant throughout the experimental period for the 160- and 190-mm groups, but decreased in the 130-mm group from 16.6% of standard length in April to 15.0% in July (Fig. 9).

The length of the base of the dorsal fin approached a line with K = 1 for most of the groups up to a standard length of 120 mm (Fig. 8). For fish ≥120 mm, the growth pattern was characterized by K < 1.

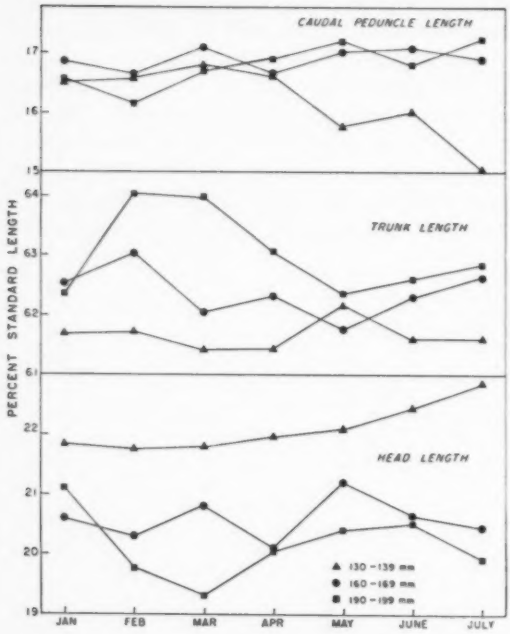

FIG. 9. Head, trunk, and caudal peduncle length as a percentage of standard length for Big Creek juvenile steelhead from January through July 1964.

Trunk length approximated a line with K = 1 for all groups sampled (Fig. 10). As a percentage of standard length, it remained relatively constant for the 130- and 160-mm size groups (Fig. 9). Measurements for 190-mm groups increased from 62.3% of standard length to 65% during the premigratory period, with a decrease to 62.4% during the migratory period (Fig. 9).

Caudal fin length was difficult to determine because of fin erosion, which resulted in increased variability (Fig. 10). The growth pattern of the caudal fin was similar to that of the head.

No distinct pattern or trend between sexes could be detected for changes in any of the morphological characters. We concluded that no morphological difference existed between juvenile male and female steelhead before, during, and immediately after the migration period.

DISCRIMINANT ANALYSIS

A preliminary cluster analysis, using the technique of principal components, showed that FL and K_{FL} were the two most important variables. No other pair combination of variables was used in the discriminant analysis.

A linear discriminant function was computed for a sample of fish representing parr and another sample of fish representing smolts. A summary of the discriminant analysis (Table 2) between smolts and parr indicates that

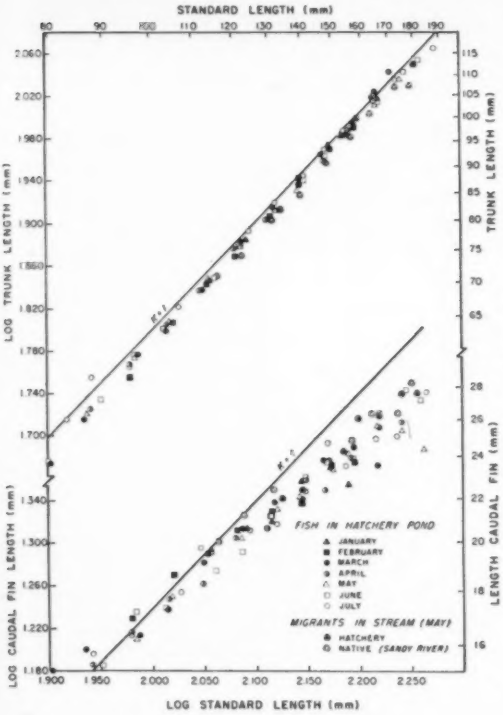

FIG. 10. Relation of caudal fin and trunk length to standard length for Big Creek juvenile steelhead in the hatchery and for migrants in the stream.

TABLE 2. Summary of discriminant analysis between smolts and parr.

		Classification matrix				
	Group	Smolt	Parr	Total	D^2	df
10 variables	Smolt	158	4	162	1490.0[a]	10
	Parr	2	218	220		
	Total	160	222	382		
2 variables	Smolt	143	19	162	773.4[a]	2
	Parr	5	215	220		
	Total	148	234	382		

[a]Significant at .001 level.

the classification matrix using 10 variables was similar to the matrix resulting from K_{FL} and FL.

With K_{FL} and FL as the two variables, the equation

$$u = X_2 - .002191\ X_1$$

represents the discriminant line separating smolts and parr. In this equation X_2 and X_1 are K_{FL} and FL, respectively. If $u > 0.55428$, the fish is classified

as a parr and if $u < 0.55428$, the fish is classified as a smolt (Fig. 11). The misclassified fish in Table 2 were very close to the discriminant line. If the fish are close to the discriminant line (Fig. 11), the equation should be used for classification.

In the months of January, February, and March the two discriminants classified practically all of the fish into the parr group (Table 3). The number of smolts and parr does not reflect percentages of each in the population because the samples were not random. In the premigratory and postmigratory periods, an attempt was made to sample 5–10 fish from each available 10-mm size group.

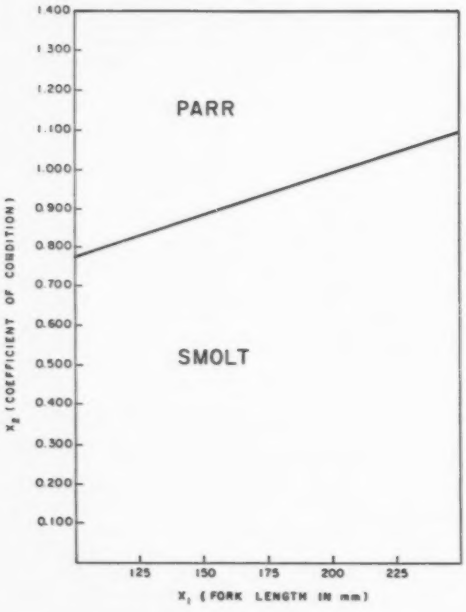

FIG. 11. A discriminant function for steelhead trout, separating parr from smolts. The equation $u = X_2 - .002191\ X_1$ represents the discriminant line separating smolts and parr. If $u > 0.55428$, the fish is classified as a parr; if $u < 0.55428$, the fish is classified as a smolt.

The number of smolts increased in April, peaked in May, then decreased in June. The mean FL ranged from 129 to 156 mm for parr for all samples. The $\overline{K}_{FL}$ ranged from 0.946 to 1.010 for all monthly samples of fish in the parr classification. The monthly $\overline{K}_{FL}$ for fish classified as smolts was lower than the $\overline{K}_{FL}$ for fish classified as parr.

The most important information gained by the discriminant analysis was that the first discriminant, which was calculated using 10 variables, was similar to the second discriminant, calculated from FL and K_{FL} alone. The similarity indicates that FL and K_{FL} were a good index of smolting in this sample of steelhead trout. The single exception might be the second discriminant as used for native migrants. One would expect a high percentage of the fish sampled to be smolts but the second discriminant classified 69 fish as smolts and

TABLE 3. Number, mean fork length, and mean K_{FL} of Big Creek smolts and parr in the hatchery and migrants in the stream as separated by two linear discriminant functions.

Month	Discriminant	No.		Mean FL[a] (*mm*)		Mean K_{FL}	
		Smolt	Parr	Smolt	Parr	Smolt	Parr
Jan.	1	0	53	0	156	0	0.996
	2	0	53	0	156	0	0.996
Feb.	1	1	68	177	151	0.959	0.983
	2	3	66	186	150	0.943	0.984
Mar.	1	1	97	172	142	0.951	0.977
	2	2	96	197	142	0.963	0.977
Apr.	1	26	85	188	133	0.898	0.963
	2	32	79	188	129	0.901	0.966
May	1	70	64	183	132	0.861	0.955
	2	72	62	183	131	0.859	0.961
June	1	26	34	188	137	0.876	0.985
	2	26	34	190	135	0.873	0.988
July	1	13	43	197	146	0.887	1.010
	2	11	45	201	147	0.869	1.009
Hatchery	1	73	1	192	190	0.812	0.963
Migrants	2	74	0	192	0	0.814	0
Native	1	85	3	177	179	0.884	0.956
Migrants	2	69	19	180	166	0.870	0.946

[a]FL = Fork length.

19 as parr. The 19 migrant fish classified as parr had a higher K_{FL} than fish classified as smolts, and their FL ranged from 140 to 191 mm. A combination of the two factors was probably responsible for classifying these fish as parr.

DISCUSSION

The parr–smolt transformation in winter steelhead is characterized by a marked reduction in lipid, and a lesser reduction in protein and moisture. At the termination of downstream migration, lipid, protein, and moisture return to premigratory levels. The decline in lipid, protein, and moisture results in gross changes in K_{FL} and body depth for migrant-sized fish ($\geq$160 mm FL). A decrease in K_{FL} at the time of the parr–smolt transformation might be the result of the individual fish remaining the same length but losing weight in the form of lipid, protein, and moisture, or the individual fish growing in length, but not proportionately in weight. The design for this study and the resulting data do not distinguish between the two events.

There are some unpublished data on growth from our laboratory for winter steelhead trout that might provide some insight into the question of changes in K_{FL}. Fish were reared under seasonal photoperiod and water temperature cycles from the fry stage through the following spring when they smolted as yearlings. Three distinct growth stanzas were observed for weight

and two for length. The first inflection on the growth curves occurred in mid-October when the instantaneous growth rates (Ricker, 1958) decreased from 0.021 (on a daily basis) to 0.004 for weight (in grams) and from 0.007 to 0.002 for FL (in centimeters). There was no substantial change in rate of length increase after the initial inflection.

A second inflection occurred in the growth curve for weight in early June when the fish reverted to a nonmigratory form. The new stanza had an increased growth rate of 0.009 for weight. In early May when the nadir of the K_{FL} curve was observed, a weight loss occurred from the previous sampling period (mid-April). The data indicate that the decline in K_{FL} during the winter was a result of a proportionately greater reduction in the rate of growth in weight than in length. An actual weight loss during the parr–smolt transformation contributed further to the decline in K_{FL} in the spring. Thus, both hypothesized events could have occurred in the fish in the present study.

The linear discriminant analysis showed that K_{FL} and FL were nearly as effective as all 10 variables in distinguishing a smolt from a parr. The length–frequency distribution (Fig. 3) for fish released and migrants captured reveals that few fish under 150 mm migrated downstream. The size-dependency of the smolting phenomenon has been demonstrated in earlier studies of migration (Gudjonsson, MS, 1946; Shapovalov and Taft, 1954; Wagner et al., 1963).

The condition of Atlantic salmon, as studied through comparisons of length–weight relationships, was found to vary considerably from place to place, from year to year, and from time to time during the same year (Hoar, 1939). There are several variables that could affect the value of K_{FL} (Kesteven, 1947). Among these variables that are applicable to fish in the present study are a genetic capacity for growth, seasonal variations in the physical and biological environments as related directly or indirectly to growth, and seasonal physiological changes such as occur in sexual maturation or the parr–smolt transformation.

Seasonal variations in the availability of food were of minor importance in the study because the fish were fed a commercially prepared diet on a systematic feeding regime while in the hatchery. The nutritional requirements of smolting salmonids have not been investigated and the diet at this time might not be adequate for normal growth processes. No decrease in intensity of feeding activity has been observed during the parr–smolt transformation. In captivity Atlantic salmon smolts feed as avidly as parr (Hoar, 1942).

The effects of seasonal changes in water temperature and photoperiod on metabolism have been discussed by Brown (1957) and Gross et al. (1965). In the present study the initial decline in K_{FL}, October through February, in steelhead of migrant and nonmigrant size is probably a result of the direct effect on metabolism of the above two factors. After the initial decline, K_{FL} remained relatively constant for the nonmigrants, whereas it showed a continued sharp decline in the larger fish of migrant size.

The parr–smolt transformation probably requires an expenditure of energy, or results in an expenditure of energy, or both. A 30% increase in

oxygen consumption (routine) for Atlantic salmon smolts has been observed by Baraduc and Fontaine (1956). The method employed by the above authors was not stated and the increase might have resulted totally or partially from an increase in spontaneous activity. Fish undergoing the parr–smolt transformation have been observed to exhibit increased activity and alertness to stimuli (Hoar et al., 1957; Pinhorn and Andrews, 1965). Juvenile steelhead reared under natural photoperiods exhibited a bimodal activity pattern with peaks occurring in the general migratory period (April through June) and late fall months (Lichtenheld, MS, 1966). The high rate of activity displayed by steelhead trout in the spring could increase the metabolic rate. Therefore, the amount of food consumed might not be sufficient to meet the increased metabolic demands and additional energy could be obtained from lipid reserves.

At the time of release, Sandy River fish had a higher mean K_{FL} and lipid content than the Big Creek steelhead. The higher K_{FL} and lipid content in the Sandy River fish might have been a result of the larger porportion of nonmigrants in that population or of the Sandy River fish being inherently heavier. A higher proportion of nonmigrants is possible because migrants from both stocks arriving at the trapping facility 1–5 days after release were similar in chemical composition and K_{FL}. The chemical composition and K_{FL} of hatchery fish that migrated were similar to those of native migrants. Later hatchery migrants from both release groups had a lower K_{FL} and lipid content than did early migrants. The continued decline of lipid levels in later migrants might be attributed to reduced food consumption accompanied by increased energy demands for physical activity, growth, and completion of the transformation.

Migrants captured in late June and July had a higher K_{FL} than migrants captured in late May and early June. At the same time, an increase in K_{FL} was noted for fish retained in the hatchery. A possible explanation for the increase in K_{FL} in hatchery fish is that fish were reverting to the nonmigratory form and energy reserves were being rebuilt. For fish in the stream, an interpretation is more difficult. Food was possibly becoming more available or the fish were adapting to the stream environment. It is possible that the fish were reverting to a nonmigratory form.

Chemical composition and K_{FL} of the native migrants remained relatively constant from April through June. A slight upward trend in lipid content was noted for later native and hatchery migrants. The findings differ from those established for coho salmon by Vanstone and Markert (1968), who observed a decrease in lipid in laboratory-reared fish but an increase in the total lipid in wild fish during the period of downstream migration.

Both stocks of fish in the present study reverted to premigratory conditions of body morphology and chemical composition when they were held in the hatchery beyond the normal period of migration. The findings concur with those of Malikova (1957) and Evropeitseva (1962) for Atlantic salmon. The increase in the relative growth rates in head and caudal peduncle length noted for smolting Atlantic salmon by Evropeitseva (1957) was not apparent in smolting steelhead trout.

Changes in K_{FL} for fish larger than 140 mm appear to be a good criterion of smolting for juvenile steelhead trout reared under normal photoperiod and temperature cycles. Further research is needed on food consumption, activity, growth, and routine metabolism in order to identify the major causes of lipid turnover during the parr–smolt transformation.

ACKNOWLEDGMENTS

The authors wish to express their appreciation to Drs James D. Hall, C. E. Bond, and W. S. Overton for their constructive criticisms of the manuscript. Dr Overton was responsible for the discriminant analysis. We are also grateful to the late Arne Shannon, the late Ray Wood, as well as other personnel at Gnat Creek Hatchery for their interest and assistance. We wish to thank Louise Hogan for her help with the chemical analyses and Mrs C. D. Young for drawing the figures.

This study was financed in part by funds received from the United States Fish and Wildlife Service, Bureau of Commercial Fisheries, through the Columbia Fisheries Program Office.

REFERENCES

AKULIN, V. N. 1966. Izmeneniya zhirnosti molodi krosnoi i svyaz' ikh so skatom. [Change in fatness of young sockeye as related to their downstream migration.] Rybn. Khozy. 42(8): 11–12. (FRB Transl. Ser. 431.)

ASSOCIATION OF OFFICIAL AGRICULTURAL CHEMISTS. 1960. Official methods of analysis. 9th ed. AOAC, Washington, D.C. 832 p.

BARADUC, M. M., AND M. FONTAINE. 1956. Etude comparée du métabolisme respiratoire du jeune Saumon sédentarire (parr) et migrateur (smolt). Compt. Rend. Soc. Biol. Paris 149: 1327–1329.

BROWN, M. E. 1957. Experimental studies on growth, p. 361–400. *In* M. E. Brown [ed.] The physiology of fishes. Academic Press, Inc., New York.

EVROPEITSEVA, N. V. 1957. Perekhod v pokatnoe sostoianie i skat molodi lososei. [Transformation to smolt stage and downstream migration of young salmon.] Uch. Zap. Leningr. Gos. Univ. Ser. Biol. Nauk 44(228 of main Ser.): 117–154. (FRB Transl. Ser. 234.)

1962. Sravnitelnyi analiz protessa desmoltifikatsii u molodi raznykh ekologicheskikh form Atlanticheskogo lososia. [Comparative analysis of the desmoltification process among the young of different ecological forms of Atlantic salmon.] Uch. Zap. Leningr. Gos. Univ. 311: 46–73. (FRB Transl. Ser. 431.)

FISHER, R. A. 1936. The use of multiple measurements in taxonomic problems. Ann. Eugenics 7: 179–188.

FONTAINE, M., AND J. HATEY. 1950. Variations de la teneur du foie en glycogéne chez le jeune saumon (*Salmo salar* L.) au cours de la "smoltification." Compt. Rend. Soc. Biol. Paris 144: 953–955.

GROSS, W. L., E. W. ROELOFS, AND P. O. FROMM. 1965. Influence of photoperiod on growth of green sunfish, *Lepomis cyanellus*. J. Fish. Res. Bd. Canada 22: 1379–1386.

GUDJONSSON, T. W. MS, 1946. Age and body length at the time of seaward migration of immature steelhead trout (*Salmo gairdneri* Richardson) in Minter Creek, Washington. M.S. Thesis. Univ. Washington, Seattle, Wash. 52 p.

HOAR, W. S. 1939. The weight-length relationship of the Atlantic salmon. J. Fish. Res. Bd. Canada 4: 441–460.

1942. Diurnal variation in feeding activity of young salmon and trout. J. Fish. Res. Bd. Canada 6: 90–101.

1963. The endocrine regulation of migratory behaviour in anadromous teleosts. Proc. XVI Intern. Congr. Zool. 3: 14–20.

HOAR, W. S., M. H. A. KEENLEYSIDE, AND R. G. GOODALL. 1957. Reactions of juvenile Pacific salmon to light. J. Fish. Res. Bd. Canada 14: 815–830.

HOUSTON, A. H., AND L. T. THREADGOLD. 1963. Body fluid regulation in smolting Atlantic salmon. J. Fish. Res. Bd. Canada 20: 1355–1356.

HUXLEY, J. S. 1932. Problems of relative growth. Methuen, London. 276 p.

KESTEVEN, G. L. 1947. On the ponderal index or condition factor, as employed in fisheries biology. Ecology 28: 78–80.

KIZEVETTER, I. V. 1948. Ob zmeneniyakh khimicheskogo sostava tela krasnoi (nerki). [Changes in chemical composition of the body of red (sockeye) salmon.] Izv. Tikhookeans. Nauchn. Issled. Inst. Rybn. Khoz. i Okeanogr. 27: 29–42. (*Transl. in* Pacific salmon. Office Tech. Serv. 60–51139, U.S. Dept. Commerce, Washington, D.C. p. 86–100.)

LICHTENHELD, R. W. MS, 1966. Effect of light, temperature and gamma radiation on the locomotor activity of juvenile steelhead trout (*Salmo gairdneri*). Ph.D. Thesis. Univ. Washington, Seattle, Wash. 237 p.

LOVERN, V. A. 1934. CCLVI. Fat metabolism in fishes. V. The fat of the salmon in its young freshwater stages. Biochemistry 28: 1961–1963.

MALIKOVA, E. M. 1957. Biokhimicheskaia otsenka molodi lososia pri perekhodi v sostoianie, blizkoe k pokatnomu, i pri zodershke serebianok v presnoi vode. [Biochemical analysis of young salmon at the time of their transformation to a condition close to the smolt stage, and during retention of smolts in freshwater.] Tr. Latv. Otd. VNIRO 2: 241–255.

MARR, J. C. 1955. The use of morphometric data in systematic, racial and relative growth studies in fishes. Copeia 1955: 23–30.

MARTIN, W. R. 1949. The mechanics of environmental control of body form in fishes. Univ. Toronto Studies, Biol. Ser. 58, Publ. Ont. Fish. Res. Lab. 70: 1–91.

MILNE, D. J. MS, 1948. The growth, morphology, and relationship of the species of Pacific salmon and the steelhead trout. Ph.D. Thesis. McGill Univ., Montreal, Que. 101 p.

PARKER, R. R., AND W. E. VANSTONE. 1966. Changes in chemical composition of Central British Columbia pink salmon during early sea life. J. Fish. Res. Bd. Canada 23: 1353–1384.

PINHORN, A. T., AND C. W. ANDREWS. 1965. Effect of photoperiods on the behavior of juvenile Atlantic salmon (*Salmo salar* L.) in vertical and horizontal light gradients. J. Fish. Res. Bd. Canada 22: 369–383.

RICKER, W. E. 1958. Handbook of computations for biological statistics of fish populations. Bull. Fish. Res. Bd. Canada 119: 300 p.

SHAPOVALOV, L., AND A. C. TAFT. 1954. The life histories of the steelhead rainbow trout (*Salmo gairdneri gairdneri*) and silver salmon (*Oncorhynchus kisutch*) with special reference to Waddell Creek, California and recommendations regarding their management. Calif. Dept. Fish. Game, Fish. Bull. 98: 375.

VANSTONE, W. E., AND J. R. MARKERT. 1968. Some morphological and biochemical changes in coho salmon *Oncorhynchus kisutch*, during parr–smolt transformation. J. Fish. Res. Bd. Canada 25: 2403–2418.

WAGNER, H. H. 1968. Effect of stocking time on survival of steelhead trout, *Salmo gairdnerii*, in Oregon. Trans. Am. Fish. Soc. 97: 374–379.

WAGNER, H. H., R. L. WALLACE, AND H. J. CAMPBELL. 1963. The seaward migration and return of hatchery-reared steelhead trout (*Salmo gairdneri* Richardson). Trans. Am. Fish. Soc. 92: 202–210.

WHITE, H. C. 1936. Age determinations of salmon parr by effect of rate of growth on body proportions. J. Biol. Bd. Canada 2: 379–382.

YATES, T. L. [ed.] MS, 1967. Oregon State University statistical analysis program library. Oregon State University, Statistics Dept., Corvallis, Oreg. Various paging.

A Stochastic Model of Interpopulation Dynamics in Marine Ecology

ROBERT H. RIFFENBURGH[1]

Scripps Institution of Oceanography
University of California, La Jolla, Calif., USA

RIFFENBURGH, ROBERT H. 1969. A stochastic model of interpopulation dynamics in marine ecology. J. Fish. Res. Bd. Canada 26: 2843–2880.

A nonstationary Markov chain was developed to analyze and model the passage of energy through an ecological system composed of the Pacific sardine, the northern anchovy, their competitors, their predators, and their prey; then to carry the model forward through time projecting the biomasses of the relevant species if anchovy or hake fisheries, or both, are begun. The model seemed to agree adequately with observed data.

The hypothesis of some earlier work of the author that the abundances of populations could be completely controlled by fishing intensities was rejected. Although no measure was made of the robustness of the ecosystem, it was concluded to be relatively impervious to artificial pressures, although there was seen a measurable boundary beyond which the ecological interactions became unstable and the system collapsed.

Specifically, based on 1950–59 data, the sardine catch was projected to stabilize in the vicinity of 20 metric kilotons per year. Overfishing did not seem to have been a cause of the sardine "disappearance." To maximize sardine catch, the introduction of anchovy and hake fisheries with annual catches limited to certain percentages (depending on the maximizing criterion) of abundances would double or triple sardine catch and stabilize the fishing industry, but sardines could *not* be reinstated as the most abundant species as a result of selective fishing. To maximize the combined catch of the three fisheries, annual catches of 30% and 20% (for all criteria) of abundances of anchovy and hake, respectively, would yield nearly 1800 metric kilotons of fish, although most of it would be of less commercial interest than the sardine.

Received January 21, 1969

INTRODUCTION

A PROBLEM OF MAJOR CONCERN to marine ecologists is how to analyze the patterns of passage of energy or biomass among fishes and trophic levels in the marine environment. This analysis may allow a prediction of relative and possibly absolute abundances. An important application of such a prediction method would be to experimentally vary fishing intensities and study the implications on relative and absolute abundances.

Fishes' interactions with their environments have been modelled before. Royce et al. (1963) considered four species of salmon simultaneously in a computer simulation without documenting the model, assumptions, or equation derivation. Larkin and Hourston (1964), Paulik and Greenough (1966), and

[1]Present address: Naval Undersea Research and Development Center, San Diego, Calif., USA, and University of Connecticut, Storrs, Conn., USA.

Printed in Canada (J1339)

Silliman (1967) wrote models that were sophisticated in the environment's relationships to the fish, but all of these studies were restricted to a single fish. There is one paper that considers an inter-fish, inter-trophic level model, viz. Riffenburgh (1960 or 1961). In that paper, the format of the model and the major steps in the mathematics were given, but it was not applied to data.

The application of the author's inter-fish, inter-trophic level model is undertaken in the present paper. It concerns the interactions of two cohabiting commercial fishes, the Pacific sardine (*Sardinops sagax* (Janyns)) and the northern anchovy (*Engraulis mordax*), with their ecological subsystem off the Pacific Coast of North America. The sardine–anchovy ecosubsystem was studied in an attempt to answer the following questions:

1. Can a model of the sardine–anchovy population dynamics be made to fit reality reasonably well?
2. If so, how good is such a fit?
3. If the fit is adequate, what are the extrapolations for sardine abundances and catches, and abundances of competitors (principally anchovies) and predators of sardines?
4. If an anchovy fishery had been begun in 1950, could we have affected the sardines beneficially? If so, what would have been the optimum effect attainable and what fishing efforts would have yielded this optimum effect?
5. If a hake fishery had been begun in 1950, could we have affected the sardines beneficially? If so, what would have been the optimum effect attainable and what fishing efforts would have yielded this optimum effect?
6. If both anchovy and hake fisheries had been begun in 1950, what would have been the mix of fishing efforts in the three fisheries that would have, without upsetting the ecological balance, optimized (*a*) the sardine catch and (*b*) the combined catches from the three fisheries?
7. For the mixes of fishing effort for question 6, what are the projected catches of sardines, anchovies, and hake?
8. Can we affect population abundances generally by the control of fishing intensities?
9. If so, how delicate must this control be? That is, can we optimize catch while maintaining ecological balance or are we likely to upset the ecological balance at the slightest change in fishing intensity?
10. What recommendations does the study suggest for the fishing industry? Can control of fishing intensities "bring back the sardine"?

In several questions, the word "optimum" or "optimize" was used. Either word is meaningful only against some criterion. Of the many possible criteria, five are considered in this paper:

(*a*) Maximizing the average sardine catch.

(*b*) Maximizing the average combined catch for the three fishes: sardines, anchovies, and hake.

(*c*) Maximizing the average of a linear function of the catches of the three fishes. For example,

$$\frac{1}{\text{no. years}} \sum_{\text{years}} \sum_{3 \text{ fishes}} \frac{(\$ \text{ price per kiloton})(\text{kilotons of catch})}{(\$ \text{ cost to catch a kiloton})}$$

might be used.

(*d*) Maximizing the minimum sardine catch over the years considered.

(*e*) Maximizing the minimum combined catch for the three fishes over the years considered.

The first three criteria are called "maxiav" for short and the last two "maximin."

The development of the model in this paper will draw criticism from some biologists because the data are not adequately estimated. This weakness is well recognized. However, the paper is intended to be largely methodological. The presentation of the methodology even without adequately sophisticated data may stimulate gathering of the right sorts of data for future analysis and the development of novel modes of analysis. Yet the study may yield considerable biological information.

There are many advantages of system-level models (Riffenburgh, 1969), although they are too seldom utilized in the biological sciences. The particular advantages of the model used here include (i) coordination and quality assessment of univariate models; (ii) estimation (or refinement of estimates) per se; (iii) identification of the most relevant or important elements in a system; (iv) experimentation (in the cybernetic sense) in situations where data are infrequent or uncontrollable, or both; (v) experimentation (in the cybernetic sense) with new patterns of subsystems abstracted from their constraining physical orientations; and (vi) prediction of the future behavior of systems either with or without control.

The germane aspects of the ecosubsystem may be described as follows. Sardine larvae (SL) and anchovy larvae (AL) hatch and are preyed upon by sardine adults (SA), by anchovy adults (AA), and by competitors of these adults (e.g., the jack mackerel), which we shall class together as competitors (Co). The sardine larvae grow into an intermediate stage in which they are too large to be preyed upon by their adults but too small to be recruited into the adult population; in this stage they are still preyed upon by Co. All species pass through such a stage, of course, but maturation in the sardine is sufficiently slow that this stage must be considered as a separate population here. Eventually the juvenile sardines and anchovies are recruited into the adult population. Also, a set of predators (e.g., hake and barracuda), which are climax for the ecosubsystem, prey upon sardine adults, anchovy adults, and Co during the whole process. Let us denote these climax predators by CP. Competing with the CP for sardine adults only (except for a negligible amount during the years represented in this study) is man's fishing effort, which we shall denote by Fy (see Fig. 1). A symbol list follows, which brings together all symbols and their definitions for reference.

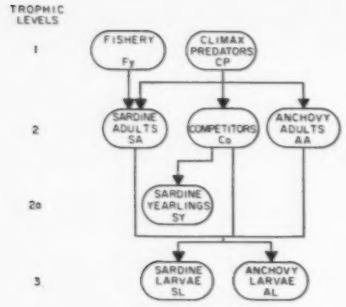

FIG. 1. A diagram of predator–prey relationships for the animals and trophic levels utilized in the model, with the arrow pointing toward the prey.

LIST OF ABBREVIATIONS

Maxiav = a criterion for optimizing fishing effort consisting of maximizing the average catch per year.

Maximin = a criterion for optimizing fishing effort consisting of maximizing the smallest of yearly catches over a time period.

Ecological categories	Symbol	Category index (i or sometimes j)
Sardine larvae	SL	1
Anchovy larvae	AL	2
Sardine yearlings	SY	3
Sardine adults	SA	4
Anchovy adults	AA	5
Competitors (to SA and AA)	Co	6
Climax predators (for this system)	CP	7
Fishery	Fy	8
Biomass lost from system	—	9

TY = "transition year," June 1 to May 31 where TY 1 is June 1950 through May 1951.

r = year index, 0, 1, . . ., 9 for TY 0 through TY 9 respectively.

$n_i^{(0)}$ = biomass in metric kilotons of ith ecological category at start of TY 0.

$\mathbf{N}_0$ = row vector of $n_i^{(0)}$. See format in App. 1.

$\mathbf{N}_r, r > 0$ = N-vectors computed from Markov chain, i.e., $\mathbf{N}_r = \mathbf{N}_0 \prod_{r=0}^{k-1} (\mathbf{T}_r + \mathbf{A}_r)$. Format as in App. 1.

$\mathbf{M}_r, r > 0$ = N-vectors for TY 1, . . ., 9 computed from data (as was $\mathbf{N}_0$) instead of from Markov chain. Use for comparison with Markov predictors. Format same as $\mathbf{N}_r$ in App. 1.

$t_{ij}^{(r)}$ = probability that a weight unit randomly chosen at the beginning of TY r from category i will end the year in category j.

$\mathbf{T}_r$ = matrix of $t_{ij}^{(r)}$. See App. 2.

$\mathbf{T}_j^{(r)}$ = column j of $\mathbf{T}_r$.

$a_{ij}^{(r)}$ = proportion of biomass of category i at beginning of TY r that is added by growth or spawning to the biomass of category j during the year.

$\mathbf{A}_r$ = matrix of $a_{ij}^{(r)}$. See App. 3.

$\mathbf{G}_r$ = $\mathbf{T}_r + \mathbf{A}_r$, i.e., proportions of influx to categories from transition plus growth.

M = instantaneous mortality rate due to natural causes.

F = instantaneous mortality rate due to fishing.

E = exploitation rate. Rate per year for sardines is t_{48} in this paper.

$R_l^{(r)}$ = number ($\times 10^{-6}$) of sardines recruited into the lth year-class during TY r.

Φ_i = abundance of category i (relative to category 6) in localized spawning region at hatching of a category specified in text.

d_r = difference between the Markov predictor $n_i^{(r)}$ and the data-computed value $m_i^{(r)}$ for some category i as specified in the text.

b_r = "observed value," i.e., m value, for category as in d_r.

METHOD: THE MODE OF SOLUTION

A More Exact Statement of the Problem

Let us place in a one-to-one correspondence with the first nine positive integers respectively the names of the eight groups above plus energy loss: SL (1), AL (2), SY (for sardine yearlings) (3), SA (4), AA (5), Co (6), CP (7), Fy (8), and energy lost from the system (9). Let us denote by n_i the biomass (in thousands of metric tons) of the ith group, $i = 1, 2, \ldots, 9$, in the pelagic region under consideration (absolute abundance). Let us denote by t_{ij} the probability that some weight of a randomly chosen animal of the ith group will pass by some means into the jth group during a certain time period (here 1 year) ($i, j = 1, \ldots, 9$). If $i = j$, this implies that the randomly chosen individual of the ith group remains in this group for the time period. When $i \neq j$, this implies that the ith individual's weight passes into the jth group by its growing large enough to become a member of the jth group, by its being eaten by a member of the jth group, or by its being fished out of the ith group, as is appropriate in the individual case. For example, t_{13} represents the proportion of sardine larvae that survive to become sardine yearlings, t_{15} represents the proportion of sardine larvae eaten by anchovy adults during the year, and t_{48} represents the proportion of adult sardines removed from the fishery by fishing efforts during the year.

Since both the n_i and the t_{ij} may change from year to year, let us assign a superscript to denote the year involved in each instance. Let us think of a "transition year," or TY, from June 1 through May 31 where TY 1 starts in June 1950. Let us define by $n_i^{(r)}$ the value of n_i at the start of the rth year, i.e., TY r, and by $t_{ij}^{(r)}$ the value of t_{ij} for TY r ($r = 0, 1, \ldots, k$). Let us further use the convenience of matrix algebra to attain compact notation such that $\mathbf{N}_r$ is the row vector of the $n_i^{(r)}$ in order of ascending i and such that $\mathbf{T}_r$ is the square 9×9 matrix of $t_{ij}^{(r)}$ where $t_{ij}^{(r)}$ is the element appearing at the intersection of the ith row and jth column. Diagrams of $\mathbf{N}_r$ and $\mathbf{T}_r$ appear as App. 1 and 2, respectively. Let us further denote by $\mathbf{T}_j^{(r)}$ the jth column of $\mathbf{T}_r$ as a vector.

We may now express our problem as: (1) to refine the general method (Riffenburgh, 1960) to the special case of the sardine–anchovy ecosubsystem; (2) to test the efficacy of the method by comparing the predicted $\mathbf{N}_r$ with observed $\mathbf{N}_r$ for several r; (3) to use the technique to predict $\mathbf{N}_r$; (4) to ascertain if control of $\mathbf{T}_8^{(r)}$ will control (or strongly influence) $\mathbf{N}_{r+1}$ and/or $\mathbf{N}_{r+2}$ and/or ...; (5) if (4) is successful, to estimate what values of $\mathbf{T}_8^{(r)}$ will enlarge $n_4^{(r)}$

for various r associated with future years (i.e., what fishing efforts are desirable to increase the biomass and therefore the catch of sardine adults).

Use of Nonstationary Markov Chains for Solution

Markov chains will be defined only conceptually here. The reader is referred to standard texts on linear algebra and stochastic processes for theory and rules of manipulation.

The vector $\mathbf{N}_r$ is a vector of biomass measures of the several categories of animals entering into the system at the beginning of TY r and may therefore be referred to as the input vector. The matrix $\mathbf{T}_r$ is composed of the probabilities of transition of weight of a randomly chosen animal from one category into another category during TY r and therefore may be referred to as a transition matrix. Since all weight of a species goes somewhere with probability 1, i.e., doesn't disappear, each row of $\mathbf{T}_r$ sums to 1. The product of the input vector times the transition matrix results in an output vector, $\mathbf{N}_{r+1}$, of the biomass measures of the various classes of animals at the end of TY r, or

$$\mathbf{N}_{r+1} = \mathbf{N}_r\mathbf{T}_r. \tag{1}$$

Thus, if we know $\mathbf{N}_r$ and $\mathbf{T}_r$, we may obtain $\mathbf{N}_{r+1}$; more realistically if, we estimate $\mathbf{N}_r$ and $\mathbf{T}_r$, we may predict $\mathbf{N}_{r+1}$. Because the state at any discrete point in time of a Markov process depends by definition only upon the state of the process at the immediately preceding discrete point in time, if we are able to estimate $\mathbf{T}_{r+1}$ we may then solve for $\mathbf{N}_{r+2} = \mathbf{N}_{r+1}\,\mathbf{T}_{r+1} = \mathbf{N}_r\,\mathbf{T}_r\,\mathbf{T}_{r+1}$. Iterating the process and generalizing slightly, we see that, given initial biomass estimates and a method for estimating transition probabilities, we may predict the biomass distribution of the various categories in $\mathbf{N}$ k time periods after the initial information, or

$$\mathbf{N}_k = \mathbf{N}_0 \prod_{r=0}^{k-1} \mathbf{T}_r. \tag{2}$$

The change in the elements of the transition matrix from one time period to another accounts for the name "nonstationary" as opposed to a "stationary" Markov chain in which the transition matrix remains constant throughout the entire process. In the stationary case, equation 2 becomes $\mathbf{N}_k = \mathbf{N}_0\,\mathbf{T}^k$.

Spawning and Growth

The chain presented in the preceding section permits exit of biomass from the animal system, but no entry. Since some categories (at least categories 8 and 9) are absorbing states, and since the states are in general ergodic, the animal system will disappear without incoming biomass. In the greatest generality in which all energy sources and transpositions would be represented, we would have a closed system and no modification would be necessary. However,

the effort to keep the magnitude of the problem small for this special case dictates an adjustment.

The larvae that enter a new category by growth are replaced by new larvae; also the animals remaining in their present category gain in biomass by growth. Let us then introduce a new matrix, $\mathbf{A}_r = \{a_{ij}^{(r)}\}_{k\times k}$, where $a_{ij}^{(r)}$ represents the proportion of $n_i^{(r)}$ that is introduced into $n_j^{(r+1)}$ as new biomass. A diagram of $\mathbf{A}_r$ appears as App. 3. It follows in the same way that $\mathbf{N}_r \mathbf{T}_r$ represents the distribution of previously present biomass during TY r, that $\mathbf{N}_r \mathbf{A}_r$ represents the amounts and distribution of new biomass added during TY r. Thus, the biomass at the end of TY r must be the sum of these figures, and equation 1 alters to

$$\mathbf{N}_{r+1} = \mathbf{N}_r \mathbf{T}_r + \mathbf{N}_r \mathbf{A}_r = \mathbf{N}_r (\mathbf{T}_r + \mathbf{A}_r). \tag{3}$$

Let us define

$$\mathbf{G}_r \equiv \mathbf{T}_r + \mathbf{A}_r. \tag{4}$$

Then equation 3 becomes again of the form of 1, viz. the recursion formula $\mathbf{N}_{r+1} = \mathbf{N}_r \mathbf{G}_r$, but $\mathbf{G}_r$ is no longer a stochastic matrix. For this reason, and because the unit row sum constraint assists estimation, we will maintain the identity of $\mathbf{T}_r$ while using $\mathbf{G}_r$ for the actual matrix multiplication. It can be easily derived that, analogous to equation 2,

$$\mathbf{N}_k = \mathbf{N}_0 \prod_{r=0}^{k-1} \mathbf{G}_r = \mathbf{N}_0 \prod_{r=0}^{k-1} (\mathbf{T}_r + \mathbf{A}_r). \tag{5}$$

Again similarly, if the $\mathbf{G}_r$ are the same for all years (say $\mathbf{G}$), then $\mathbf{N}_k = \mathbf{N}_0 \mathbf{G}^k$.

METHOD: THE BIOLOGICAL IMPLEMENTATION

Initial Data

Although the Markov chain method requires initial information only for the first year, we wish to compare the performance of the method with empirical data for later years, so we shall list initial data for several years. The years for which data were obtainable at the outset of this study (1963) and the associated data appear as Table 1.

Estimating $\mathbf{N}_0$

The method behaves as if we got a glimpse of the system and measured its states in a July at the end of the spawning season, and then the system went black until the next glimpse exactly 1 year later.

The fourth element of $\mathbf{N}_0$, $n_4^{(0)}$, was estimated by

$$n_4^{(0)} = n_8^{(0)} / l_{48}^{(0)}. \tag{6}$$

From equation 6

$$n_5^{(0)} = (\mathrm{A/S})^{(0)}\, n_4^{(0)}. \tag{7}$$

TABLE 1. Data for model input as obtainable at the outset of the study (1963).

Transition year r	Recorded sardine catch (*metric kilotons*)[a] n_8	Relative abundance anchovy to sardine adults[b] A/S	Proportion of sardine adults taken by the fishery[c] t_{48}	Recruitment no. $\times 10^{-6}$ of 2-year-old sardines[d] $R_2(r)$
1949	307.5		0.3539	
1950=0	320.3	1.32	0.3627	4.151
1951=1	131.8	2.7	0.2549	2.205
1952=2	13.5	2.6	0.0269	2.494
1953=3	17.1	6.9	0.0266	3.380
1954=4	73.4	6.2	0.1211	3.011
1955=5	71.4	9.9	0.1855	0.935
1956=6	42.9	8.7	0.1613	0.695
1957=7	29.2	14.9	0.1521	1.216
1958=8	114.6	18.0	0.4494	2.490
1959=9	53.2	38.8	0.3093	1.327

[a]Computed from Murphy (1966, p. 5, table 1).

[b]Estimated from ratios for larvae and eggs in areas sampled systematically by plankton tows (Anon., 1950, 1951, 1959).

[c]t_{48} may also be written as E, the exploitation rate. If M denotes the instantaneous mortality rate due to natural causes, and F that due to fishing, $E = F(1 - e^{-f-m})(F + M)$, where $F = Z - M$, Z is estimated from the age composition of the catch, and M is estimated from the Silliman (1943) method. E was computed for 2-year-olds and separately for older fish, and the two E's were combined in computing t_{48}.

[d]Given in Murphy (1966, p. 41, table 14, column 2).

The biomass spawned, $n_1^{(0)}$, was assumed to be a proportion of the adult population, $n_4^{(0)}$. The volume of an egg times its specific gravity times the average adult's fecundity times a measure scale correction gives an approximate proportion, assuming all eggs hatch. Using an approximate egg radius of 0.062 cm from Clark (1934), assuming the specific gravity of the egg to be unity, and computing a fecundity of 365 eggs per gram weight (assuming 50% females in the spawning stock) from some data of Clark (1934), the proportion was estimated by

$$\frac{4}{3}\,\pi\, r^3 \text{ (sp gr) (fecundity)} =$$

$$(0.000998 \text{ cc/egg})\ (1 \text{ g/cc})\ (365 \text{ eggs/g}) = 0.36. \tag{8}$$

Thus,

$$n_1^{(0)} = 0.36\ n_4^{(0)}. \tag{9}$$

Also

$$n_2^{(0)} = 0.36\ n_5^{(0)} \tag{10}$$

by the same logic and values, except for the information that anchovy eggs are half the size (volume) but twice the number, according to a 1965 personal communication from John S. MacGregor, Pelagic Resources Laboratory, U.S. Bureau of Commercial Fisheries, La Jolla, Calif.

Under the assumption that 51 g is the average weight of a 2-year-old sardine being recruited into adult population (Phillips (1948) gives an age-to-length conversion relationship and Clark (1928) gives a length-to-weight conversion relationship),

$$n_3^{(0)} = (R_2^{(1)})\ (51)\ (10^{-3})\ (e^M), \tag{11}$$

where 10^{-3} is a factor in the conversion of grams to metric tons and e^M is a survival factor with $M = 0.8$ (Silliman, 1943). Inspection of equation 11 will show that, with both sides multiplied by e^{-M} and transformed from weight to numbers, it says: the number of 1-year-old sardines at the beginning of some year times the proportion that survive during that year equals the number of 2-year-old sardines at the end of that year.

Since n_6 is a combination of all other animals in the trophic level, e.g. jack mackerel, Pacific mackerel, short-lived invertebrates, et al., it is more difficult to estimate. Let us attempt to estimate from CalCOFI station data the amount of food available to support the trophic level represented by $n_4 + n_5 + n_6$ and extend it to that part of the California current system that supports sardines and anchovies. From basic carbon fixation estimates, let us estimate the phytoplankton that could be supported. From this we can estimate the amount of zooplankton that could be supported, and, combining these two estimates, the size of the $n_4 + n_5 + n_6$ trophic level that could be supported. One such computation yields 8×10^6 metric tons. Many will seriously disagree with this poorly justified estimate, but the very lack of objective evidence seems to leave it much to opinion; some estimate had to be made. If the ratio of an estimate of anchovy plankton consumption to total plankton biomass is assumed approximately equal to the ratio of an estimate of the anchovy biomass to the trophic level's biomass, an estimate of similar magnitude of the trophic level's biomass results, according to 1965 personal communication with Garth I. Murphy, then of the California Academy of Sciences and Scripps Institution of Oceanography, La Jolla, Calif. This trophic level contains many species that have very short life cycles and that cannot compete effectively with sardines and anchovies due to inefficient predation and escape capabilities. These species would quickly fill gaps left by reducing biomasses of sardines or anchovies and similarly would reduce themselves very quickly due to any pressure from increasing biomass of sardines or anchovies. Thus, it was assumed that

$$n_6^{(0)} = 8 \times 10^6 - n_4^{(0)} - n_5^{(0)}. \tag{12}$$

$n_7^{(0)}$ was also very roughly estimated due to the absence of relevant data. Let us assume that a biomass's predators cannot be sustained in excess of 15% of the biomass. Further, let us assume that half of the predation by the n_7 trophic level is on the sardine-anchovy trophic level. Then

$$n_7^{(0)} = 2(0.15)\ (n_4^{(0)} + n_5^{(0)} + n_6^{(0)}) = 2.4 \times 10^6, \tag{13}$$

which agrees with intuition.

$n_8^{(0)}$ is given in the initial data and $n_9^{(0)} = 0$; there is no biomass lost from the system at the beginning of the system.

Although only $\mathbf{N}_0$ (biomass distribution for 1950) was used in the Markov chain model (as initial inputs), it was necessary to compare the results with some set of biomass distributions for subsequent years obtained independently of the model. Thus, in addition to $\mathbf{N}_0$, similar vectors were computed for the years 1951 through 1959 for comparison; let us denote this set of vectors by $\mathbf{M}_r$ (Table 2).

TABLE 2. Biomass estimates by categories and years, i.e., $\mathbf{N}_0$ and $\mathbf{M}_r$ for $r = 1, 2, \ldots, 9$.

Vector & year designation	Categories							
	Sardine larvae 1	Anchovy larvae 2	Sardine yearlings 3	Sardine adults 4	Anchovy adults 5	Competitors 6	Climax predators 7	Sardine fishery 8
$\mathbf{N}_0$	317.88	279.72	250.27	883	1165.0	6340.0	2400	307.5
$\mathbf{M}_1$	186.12	502.52	283.07	517	1395.9	6087.1	2400	320.3
$\mathbf{M}_2$	180.72	469.87	383.63	502	1305.2	6192.8	2400	131.8
$\mathbf{M}_3$	231.48	1597.21	341.75	643	4436.7	2920.3	2400	13.5
$\mathbf{M}_4$	218.16	1352.59	106.12	606	3757.2	3636.8	2400	17.1
$\mathbf{M}_5$	138.60	1372.14	78.88	385	3811.5	3803.5	2400	73.4
$\mathbf{M}_6$	95.76	833.11	138.02	266	2314.2	5419.8	2400	71.4
$\mathbf{M}_7$	69.12	1029.89	282.62	192	2860.8	4947.2	2400	42.9
$\mathbf{M}_8$	91.80	1652.40	150.62	255	4590.0	3155.0	2400	29.2
$\mathbf{M}_9$	61.92	2352.96		172	6536.0	1292.0	2400	114.6

ESTIMATING $\mathbf{T}_0$

Let us consider $\mathbf{T}_0$ row by row. Recall that $t_{ij}^{(0)}$ is the probability that a randomly selected gram (say) of biomass existing in category i at time 0 will by one means or another come to lie in category j at time 1. Let us also recall that $\mathbf{T}_0$ is a stochastic matrix and by definition the sum of elements of any row is unity.

Let us consider row 1. Sardine larvae cannot remain sardine larvae; they either are eaten or mature to yearlings. Sardine larvae biomass can in no way become or enter anchovy larvae biomass. The CP's are too large to prey upon the SL and there is no fishing effort on SL. Thus,

$$t_{11}^{(0)} = t_{12}^{(0)} = t_{17}^{(0)} = t_{18}^{(0)} = 0. \tag{14}$$

Consider $R_2^{(r)}$ of our original data. If we assume the natural mortality coefficient, M, to be the same (0.8) for sardines in their second year as in later years, we may estimate the "recruitment" of sardine yearlings into their second year as

$$R_1^{(1)} = R_2^{(2)} e^M, \tag{15}$$

and, with $R_0^{(0)}$ defined as $n_1^{(0)}$/weight per egg (from 8),

$$t_{13}^{(0)} = R_1^{(1)}/R_0^{(0)}. \tag{16}$$

$t_{13}^{(0)}$ is the only nonzero element of the first row in which entrance occurs by means other than predation. Since all elements add to unity,

$$t_{14}^{(0)} + t_{15}^{(0)} + t_{16}^{(0)} + t_{19}^{(0)} = 1 - t_{13}^{(0)}.$$

Consider the metabolic efficiency of predation, i.e., a conversion of a calorie of food to a calorie of weight gain. This factor must obviously be taken into account to achieve any realistic model of interpopulation dynamics. Data on calorie conversion in fish populations appear to be lacking. It was grossly assumed that 1 g is gained for each 6 g of food consumed for all species, with adjustment if necessary to insure that the model agrees with observed outcomes. This has the additional benefit of providing a rough estimate (having few desirable statistical properties, but better than nothing) of such a conversion ratio. The model agreed reasonably without adjusting the $\frac{1}{6}$ efficiency estimate, so it was left unchanged.

If conversion efficiency is $\frac{1}{6}$, $\frac{5}{6}$ of the weight of the elements involved in predation is lost from the system so that

$$t_{19}^{(0)} = \frac{5}{6}(1 - t_{13}^{(0)}). \tag{17}$$

It directly follows that

$$\sum_{j=4}^{6} t_{ij}^{(0)} = (1 - t_{13}^{(0)})/6. \tag{18}$$

From reasoning set forth in Brock and Riffenburgh (1960), random predation encounters for predators of equal predatory efficiency should be equal in probability. Thus, if categories 4, 5, and 6 were distributed randomly relative to their prey and were equally efficient predators, the transition probabilities for each would be proportional to their respective population sizes. However, these conditions are not quite true, so that an adjusted proportion statement would assume the general form

$$t_{14}^{(0)} : t_{15}^{(0)} : t_{16}^{(0)} : : \varphi_4 n_4^{(0)} : \varphi_5 n_5^{(0)} : n_6^{(0)}, \tag{19}$$

$\varphi_4 > \varphi_5 > 1$. φ_4 and φ_5 are both larger than 1, since category 6 (Co) contains many predators, e.g., invertebrates, that are less efficient at predation than are sardines and anchovies. $\varphi_4 > \varphi_5$ since sardine adults are more likely to be in the vicinity of sardine larvae just hatching than are anchovy adults. Since data were totally lacking on these quantities, it was grossly assumed $\varphi_4 = 3$ and $\varphi_5 = 2$ for experimental purposes, with provision to adjust the values to permit the model to agree with observed data. However, again the agreement was adequate without adjustment and we may infer that either 3 and 2 are

not too unreal estimates or these elements are not very crucial in the Markov chain. (Since even a small error would tend to accrue into a large one through repeated multiplication of the matrix, the first interpretation is the more likely.) Thus, the specific form of equation 19 used was

$$t_{14}^{(0)} : t_{15}^{(0)} : t_{16}^{(0)} : : 3\ n_4^{(0)} : 2\ n_5^{(0)} : n_6^{(0)}. \tag{20}$$

The three independent conditions imposed by equations 18 and 20 yielded solutions for elements $t_{14}^{(0)}$, $t_{15}^{(0)}$, and $t_{16}^{(0)}$, which completed the estimation of the first row of $\mathbf{T}_0$.

Let us consider the second row of $\mathbf{T}_0$. By reasoning similar to that that led to equation 14,

$$t_{21}^{(0)} = t_{22}^{(0)} = t_{23}^{(0)} = t_{27}^{(0)} = t_{28}^{(0)} = 0. \tag{21}$$

$t_{25}^{(0)}$ presented a unique problem. Anchovy larvae contribute weight to the adult anchovy population through predation, but during the same year mature anchovy contribute weight to the adult anchovy population by recruitment. If we denote by t_{25}^{*} the part of $t_{25}^{(0)}$ due to predation and by t_{25}^{**} the part due to recruitment, then

$$t_{25}^{(0)} = t_{25}^{*} + t_{25}^{**}. \tag{22}$$

Following reasoning similar to that leading to equations 19 and 20, with the alteration that anchovy adults are more likely to be in the vicinity of just-hatched anchovy larvae than are sardine adults so that φ_4 and φ_5 switch positions in the equation 19 format, there followed

$$t_{24}^{(0)} : t_{25}^{*} : t_{26}^{(0)} : : 2\ n_4^{(0)} : 3\ n_5^{(0)} : n_6^{(0)}. \tag{23}$$

$t_{13}^{(0)}$ represents the proportion of sardine larvae that survive to become 1 year old; t_{25}^{**} represents the proportion of anchovy larvae that survive to become 1 year old, and are hence recruited into the adult population, which fact does not alter the survival rate. Thus, if we are willing to assume that the natural mortality coefficient of anchovy larvae is similar to that for sardine larvae, we may assume that

$$t_{25}^{**} = t_{13}^{(0)}. \tag{24}$$

From reasoning similar to that leading to equations 17 and 18,

$$t_{29}^{(0)} = \frac{5}{6}(1 - t_{25}^{**}) \tag{25}$$

and

$$t_{24}^{(0)} + t_{25}^{*} + t_{26}^{(0)} = (1 - t_{25}^{**})/6. \tag{26}$$

The three independent conditions imposed by equations 23 and 26 yielded estimates for elements $t_{24}^{(0)}$ and $t_{26}^{(0)}$ and component t_{25}^{*}. Solutions for equations 23, 24, and 26 were put into 22 to obtain an estimate for $t_{25}^{(0)}$.

The third row was simpler to estimate. Accepting 0.8 for the sardine mortality coefficient, M, as before, the surviving proportion is the complement of the proportion lost to natural mortality, or

$$t_{34}^{(0)} = e^{-0.8} = 0.4449329, \tag{27}$$

since the sardine yearlings that survive are recruited into the adult population. Since sardine yearlings do not stay as such (they mature or are consumed), since there is no fishery for yearlings, and since there is no predation upon yearlings by sardine larvae, anchovy larvae, sardine adults, anchovy adults, or anchovy–sardine competitors,

$$t_{31}^{(0)} = t_{32}^{(0)} = t_{33}^{(0)} = t_{35}^{(0)} = t_{36}^{(0)} = 0. \tag{28}$$

Remaining was only loss by natural mortality. Using the $\frac{1}{6}$ metabolic efficiency ratio as before,

$$t_{37}^{(0)} = \frac{1}{6}(1 - t_{34}^{(0)}) \tag{29}$$

and

$$t_{39}^{(0)} = \frac{5}{6}(1 - t_{34}^{(0)}). \tag{30}$$

Let us consider the row initiating as sardine adults. There is no direct way during 1 year in which sardine adults may contribute to the weight of anchovy larvae, sardine yearlings, anchovy adults, or sardine–anchovy competitors, so that

$$t_{42}^{(0)} = t_{43}^{(0)} = t_{45}^{(0)} = t_{46}^{(0)} = 0. \tag{31a}$$

Sardine adults contribute the weight of sardine larvae, but this represents an introduction of biomass into the system rather than a loss of adults from their population, so was considered in the estimation of $\mathbf{A}_r$. For the purpose of estimating $\mathbf{T}_0$,

$$t_{41}^{(0)} = 0. \tag{31b}$$

$t_{48}^{(0)}$ was given in the initial data. The estimation of $t_{44}^{(0)}$ follows that leading to equation 27, with the additional complication of fishing mortality. Thus,

$$t_{44}^{(0)} = e^{-M-F}, \tag{32}$$

where M = 0.8 as before and F, the coefficient of fishing mortality, was obtained from a solution of

$$t_{48}^{(0)} = \frac{F}{F + M}(1 - e^{-M-F}). \tag{33}$$

By subtraction and the metabolic efficiency ratio,

$$t_{47}^{(0)} = (1 - t_{44}^{(0)} - t_{48}^{(0)})/6 \tag{34}$$

and

$$t_{49}^{(0)} = 5\ t_{47}^{(0)}. \tag{35}$$

The fifth row of $\mathbf{T}_0$ follows the reasoning of the third row, except that $t_{52}^{(0)}$ follows the reasoning for $t_{41}^{(0)}$. However, there was needed a figure for M for anchovies, say M_a. No data were found from which to estimate such a figure. It was intuitively felt that anchovies should have a natural mortality coefficient similar to or slightly larger than that for sardines; they are smaller animals that may have a faster metabolic rate and shorter lives. $M_a = 1$ was assumed rather arbitrarily with the understanding that it could be adjusted downward as far as 0.8 to permit the model to fit observed data; again, no adjustment was necessary to obtain an adequate fit. Inspection of the magnitude of $\mathbf{T}_0$ will show that the influence of $t_{55}^{(0)}$ is substantial, implying that $M_a = 1.0$ is a rough estimate rather than the result of being inconsequential in the model. Thus, the estimates for the fifth row were

$$t_{51}^{(0)} = t_{52}^{(0)} = t_{53}^{(0)} = t_{54}^{(0)} = t_{56}^{(0)} = t_{58}^{(0)} = 0, \tag{36}$$

$$t_{55}^{(0)} = e^{-1.0} = 0.367879, \tag{37}$$

$$t_{57}^{(0)} = (1 - t_{55}^{(0)})/6, \tag{38}$$

and

$$t_{59}^{(0)} = 5\ t_{57}^{(0)}. \tag{39}$$

The sixth, or Co, row followed the reasoning of the fifth. For want of any data for an average M for this collective class of animals, the sardine's $M = 0.8$ was assumed, and again no adjustment appeared necessary. The estimates for the sixth row were

$$t_{61}^{(0)} = t_{62}^{(0)} = t_{63}^{(0)} = t_{64}^{(0)} = t_{65}^{(0)} = t_{68}^{(0)} = 0, \tag{40}$$

$$t_{66}^{(0)} = e^{-0.8} = 0.449329, \tag{41}$$

$$t_{67}^{(0)} = (1 - t_{66}^{(0)})/6, \tag{42}$$

$$t_{69}^{(0)} = 5\ t_{67}^{(0)}. \tag{43}$$

Before the addition of a hake fishery, in the seventh row (for CP) $t_{77}^{(0)}$ and $t_{79}^{(0)}$ are the only elements that can be other than 0, since CP does not contribute to any other category in the ecosubsystem. Since climax predators appear to be more efficient at surviving than the smaller animals, their mortality coefficient, say M_h (for hake), should be lower. For lack of data, $M_h = 0.6$ was assumed. Then

$$t_{77}^{(0)} = e^{-0.6} = 0.548812, \tag{44}$$

$$t_{79}^{(0)} = 1 - t_{77}^{(0)}, \tag{45}$$

$$t_{7j}^{(0)} = 0,\ j = 1, 2, 3, 4, 5, 6, 8. \tag{46}$$

The fishery (row 8) and the amount of weight lost from the ecosubsystem (row 9) represent absorbing states; all weight entering these categories remain there and do not directly reenter the ecosubsystem. Since $\mathbf{T}_0$ is a stochastic matrix and states 8 and 9 are absorbing states,

$$t_{88}^{(0)} = 1, \tag{47}$$

$$t_{8j}^{(0)} = 0, j = 1, 2, 3, 4, 5, 6, 7, 9, \tag{48}$$

$$t_{99}^{(0)} = 1, \tag{49}$$

and

$$t_{9j}^{(0)} = 0, j = 1, 2, 3, 4, 5, 6, 7, 8. \tag{50}$$

Estimating $\mathbf{A}_0$ and $\mathbf{G}_0$

If $\mathbf{T}$ represented an instantaneous transition, equation 2 could represent the model of our system dynamics. However, the input to $\mathbf{T}$ is measured at the beginning of a year and the output at the end, and during the interval many of the categories of animals have had time for growth or introduction by other means of weight coming from outside the ecosubsystem. Hence, $\mathbf{A}$ was introduced and equation 4 used. Let us consider the estimation of $\mathbf{A}_0$, which automatically completes the estimation of $\mathbf{G}_0$, since $\mathbf{G}_0 = \mathbf{T}_0 + \mathbf{A}_0$.

Since $\mathbf{A}_0$ represents growth, only those elements representing the survival of a portion of a category's biomass may have an associated nonzero element of $\mathbf{A}_0$, since animals that do not survive do not increase in weight. Thus, the nonzero elements of $\mathbf{A}_0$ are $a_{13}^{(0)}$, $a_{25}^{(0)}$, $a_{34}^{(0)}$, $a_{44}^{(0)}$, $a_{55}^{(0)}$, $a_{66}^{(0)}$ and $a_{77}^{(0)}$.

$$\begin{aligned}
a_{1j}^{(0)} &= 0, j = 1, 2, 4, 5, 6, 7, 8, 9 \\
a_{2j}^{(0)} &= 0, j = 1, 2, 3, 4, 6, 7, 8, 9 \\
a_{3j}^{(0)} &= 0, j = 1, 2, 3, 5, 6, 7, 8, 9, \\
a_{4j}^{(0)} &= 0, j = 1, 2, 3, 5, 6, 7, 8, 9, \\
a_{5j}^{(0)} &= 0, j = 1, 2, 3, 4, 6, 7, 8, 9 \\
a_{6j}^{(0)} &= 0, j = 1, 2, 3, 4, 5, 7, 8, 9 \\
a_{7j}^{(0)} &= 0, j = 1, 2, 3, 4, 5, 6, 8, 9 \\
a_{8j}^{(0)} &= 0, j = 1, 2, 3, 4, 5, 6, 7, 8, 9 \\
a_{9j}^{(0)} &= 0, j = 1, 2, 3, 4, 5, 6, 7, 8, 9
\end{aligned} \tag{51}$$

Note that, from equations 47 and 48 and the last two entries of 51, n_8 and n_9 will accumulate with no source of reductions. This is proper. If we wished to constrain either, we could have used a negative $\mathbf{A}$ element. For example, to constrain n_9 to the weight loss from the system for that particular year, we could have required $a_{i9} = -t_{i9}$, $i = 1, 2, \ldots, 9$.

$t_{13}^{(0)}$ represents the proportion of the number of SL that survive to become SY. However, each animal during the transition from a larva to a yearling has increased many times its weight. The sardine larva at hatching (weighing almost the same as an egg at laying) was taken as 0.000998 g as computed

for equation 8; the sardine yearling was taken as 19 g, following procedures as for 11. Thus, the total weight at the end of the year is the proportion surviving times the growth multiple, or

$$g_{13}^{(0)} = \frac{19}{0.000998}\, t_{13}^{(0)} = 19038\, t_{13}^{(0)}, \tag{52}$$

and, from equation 4,

$$a_{13}^{(0)} = g_{13}^{(0)} - t_{13}^{(0)}. \tag{53}$$

$t_{34}^{(0)}$ represents the proportion of SY, starting the year at 19 g, that survive to become SA. As in equation 11, sardines being recruited into adulthood will be assumed to weight 51 g. Then, by reasoning as in equations 52 and 53,

$$g_{34}^{(0)} = \frac{51}{19}\, t_{34}^{(0)} = 2.6842\, t_{34}^{(0)} \tag{54}$$

and

$$a_{34}^{(0)} = g_{34}^{(0)} - t_{34}^{(0)}. \tag{55}$$

If anchovies are half the weight of sardines from eggs to yearlings, as in equation 10, then the growth increment is identical, i.e., 19038. The total weight at the end of the period, $g_{25}^{(0)}$, is the proportion that survive multiplied by their growth increment, plus the weight added by cannibalism, or

$$g_{25}^{(0)} = 19038\, t_{25}^{**} + t_{25}^{*}. \tag{56}$$

$$a_{25}^{(0)} = g_{25}^{(0)} - t_{25}^{(0)}. \tag{57}$$

The estimate of $a_{44}^{(0)}$ is more involved. The adult sardines continue to grow, but more slowly as they age, so that the growth factor should be of the form

$$\sum_{i=3}^{8} \left[\begin{array}{c}\text{proportion of SA}\\ \text{in } i\text{th year}\end{array}\right] \times \left[\begin{array}{c}\text{average proportion weight gain}\\ \text{for a SA in its } i\text{th year}\end{array}\right], \tag{58}$$

where 8 should be taken to represent "8 or more"; the proportion of SA older than 8 is negligible. The figures necessary are shown in Table 3. Equation 58 is the sum of products of elements of the second times fifth columns, or 0.2920. Then

$$a_{44}^{(0)} = 0.2920\, t_{44}^{(0)} \tag{59}$$

and

$$g_{44}^{(0)} = 1.2920\, t_{44}^{(0)}. \tag{60}$$

Data were not so complete for anchovies. In considering AA, the only data the author could obtain were from Clark and Phillips (1952). Some computations on their results yielded an estimated average proportional

TABLE 3. Estimated sardine weight gain by year-class.

Growth year	Proportion of SA[a]	Estimated avg wt at end of this year (g)[a]	Growth during this year (g)	Proportion wt gain
2		51		
3	0.5553	86	35	0.4070
4	0.2493	103	17	0.1650
5	0.1122	120	17	0.1417
6	0.0505	137	17	0.1241
7	0.0228	150	13	0.0867
8	0.0100	162	12	0.0741

[a]An extention of information and method given in Clark (1928) done in 1965 by Garth I. Murphy, then of California Academy of Sciences and Scripps Institution of Oceanography.

weight gain of 2.8873 for the second year and 0.7805 thereafter, and an estimated 41% of the adult population to be yearlings. Thus,

$$a_{55}^{(0)} = [0.41(2.8873) \times 0.59(0.7805)]\, t_{55}^{(0)} = 1.6443\, t_{55}^{(0)} \tag{61}$$

and

$$g_{55}^{(0)} = 2.6443\, t_{55}^{(0)}, \tag{62}$$

upon following the same logic as in equation 58.

The growth proportions for Co and CP posed a particular problem; they represent growth proportions averaged over agglomerations of rather diverse animals, for many of which no data at all are available. Thus, the only solution appeared to be to make bald, undocumented assumptions. The Co contain many short-lived invertebrates that grow rapidly, so that the assumption of a growth factor much larger than for sardines is reasonable. On the other hand, CP are mostly larger fishes and might be expected to have a growth rate of the order of SA or perhaps slightly less. Thus, growth factors of 1 for Co and 0.25 for CP were assumed with the understanding that they would be adjusted if necessary to permit the model to conform to observed data. Such adjustment was unnecessary. This assumption yielded

$$a_{66}^{(0)} = t_{66}^{(0)}, \tag{63}$$

$$g_{66}^{(0)} = 2\, t_{66}^{(0)}, \tag{64}$$

$$g_{77}^{(0)} = 0.25\, t_{77}^{(0)}, \tag{65}$$

and

$$g_{77}^{(0)} = 1.25\, t_{77}^{(0)}. \tag{66}$$

ESTIMATING $\mathbf{G}_r$

So far we have considered $\mathbf{N}_0$ and $\mathbf{G}_0$; $\mathbf{N}_0\mathbf{G}_0 = \mathbf{N}_1$, but to find $\mathbf{N}_2, \ldots, \mathbf{N}_k$, we must have $\mathbf{G}_1, \ldots, \mathbf{G}_{k-1}$. In general, given $\mathbf{G}_{r-1}$ and $\mathbf{N}_r$, let us establish formulae for obtaining $\mathbf{G}_r$.

First, consider $\mathbf{T}_r$. The logic that yielded zero elements in $\mathbf{T}_0$ continues, so that a replacement of 0 by r is valid in equations 14, 21, 28, 31, 36, 40, 46, 48, and 50 for the first through ninth rows, respectively, of $\mathbf{T}_r$. For $t_{13}^{(r)}$, the logic of equation 15 yields a Ricker (1954) type equation

$$R_1^{(r+1)} = R_2^{(r+2)}\, e^{M_s^{(r)}}, \tag{67}$$

where $R_2^{(r+2)}$ comes from Table 1, and

$$R_0^{(r)} = n_1^{(r)}/\text{wt per egg}, \tag{68}$$

so that

$$t_{13}^{(r)} = R_1^{(r+1)}/R_0^{(r)}. \tag{69}$$

The only change is in equation 67, where $M_s^{(r)}$ denotes the natural mortality rate for sardines for the rth year. ($M_a^{(r)}$ would denote anchovies.) It is recognized that the mortality rate will be affected by the abundance of predators, but the author has found no estimates of how much. Roughly guessing at $\frac{3}{4}$ of the mortality being attributable to the predation of CP and the remainder to other causes, e.g., disease, and assuming that the predation effort is proportional to the absolute abundance of CP, we obtain an estimate:

$$M_s^{(r)} = \frac{1}{4}\left(1 + 3\frac{n_7^{(r)}}{n_7^{(r-1)}}\right)M_s^{(r-1)} \tag{70}$$

The $\frac{1}{6}$ metabolic efficiency factor was retained throughout. Following the same reasoning as in equations 17 through 20, r may replace 0 in these displays to yield estimates for $t_{14}^{(r)}$, $t_{15}^{(r)}$, $t_{16}^{(r)}$, and $t_{19}^{(r)}$.

For the second and third rows of $\mathbf{T}_r$, the reasoning of $\mathbf{T}_0$ holds with 0 replaced by r and an implicit r associated with t_{25}^{*} and t_{25}^{**} in equations 22–26, 29, and 30, and with 27 replaced by

$$t_{34}^{(r)} = e^{-M_s^{(r)}}. \tag{71}$$

In the fourth row, $t_{48}^{(r)}$ is given in Table 1. For $r > 9$, $t_{48}^{(r)}$ was taken as $\frac{1}{5}\sum_{r=5}^{9} t_{48}^{(r)}$. As in equation 32, $t_{44}^{(r)}$ was estimated by e^{-M-F}, where M was given in 70 and F was calculated as in 33 with r for 0. The remainder are obtained by replacing 0 by r in equations 34 and 35.

Following the reasoning of equation 70, the mortality coefficient for anchovies was estimated by

$$M_a^{(r)} = \frac{1}{4}\left(1 + 3\frac{n_7^{(r)}}{n_7^{(r-1)}}\right)M_a^{(r-1)}, \tag{72}$$

from which

$$t_{55}^{(r)} = e^{-M_a^{(r)}}. \tag{73}$$

Replacing 0 by r in equations 38 and 39 yields the remainder of row five.

The sixth row is obtained by replacing 0 by r in equations 41, 42, and 43.

In the seventh row, the mortality coefficient, say M_h (for hake), was allowed to vary as in equation 70, such that

$$M_h^{(r)} = \frac{1}{4}(1 + 3\frac{n_7^{(r)}}{n_7^{(r-1)}})M_h^{(r-1)}. \tag{74}$$

Then

$$l_{77}^{(r)} = e^{-M_h^{(r)}} \tag{75}$$

and

$$l_{79}^{(r)} = 1 - l_{77}^{(r)}.$$

States 8 and 9 remain absorbing states, so that $\mathbf{T}_r$ is completed by

$$l_{88}^{(r)} = l_{99}^{(r)} = 1. \tag{76}$$

For $\mathbf{A}_r$ and $\mathbf{G}_r$, the zero elements of the equations 51 all remain with the replacement of 0 by r, except for $a_{41}^{(r)}$ and $a_{52}^{(r)}$. The logic leading to equation 8 remains so that 9 and 10 hold with r replacing 0. The invariance of matrix multiplication under column transposition permits $n_4^{(r+1)}$ to be computed before $n_1^{(r+1)}$ and $n_5^{(r+1)}$ before $n_2^{(r+1)}$, in the computer program only, requiring no conceptual change. Thus,

$$a_{41}^{(r)} = g_{41}^{(r)} = 0.36\,\frac{n_4^{(r+1)}}{n_4^{(r)}} \tag{77}$$

and

$$a_{52}^{(r)} = g_{52}^{(r)} = 0.36\,\frac{n_5^{(r+1)}}{n_5^{(r)}}. \tag{78}$$

The remainder of $\mathbf{G}_r$ and $\mathbf{A}_r$ may be taken from equations 52 through 67 by letting r replace 0.

One further restriction became necessary. AA steadily increased in the model, as it has in fact. It certainly cannot increase without bound, but since such a bound was not reached during the period of available data, the bound was unknown. Extending the logic of equation 12 from 0 to r and rewriting,

$$n_5^{(r)} = 8 \times 10^6 - n_4^{(r)} - n_6^{(r)}. \tag{79}$$

Now $n_4^{(r)}$ is reducing to a negligible amount and we have assumed that Co are rapidly adaptable to population pressures and are competitively less efficient than AA, so that they become negligible as AA increases. Thus, the upper bound on AA was taken as 8×10^6 metric tons. If the computed $n_5^{(r)}$ exceeded 8×10^6, it was replaced by 8×10^6.

Extrapolation, Introducing Anchovy and Hake Fisheries, and Limiting the Sardine Fishery

When adequate agreement between the model and observed data was obtained, the following steps were of prime interest: (i) Extrapolate the model to later years, observing the absolute and relative abundances of the several animal classes and their interactions, noting the temporal sequence of biomasses as stable, cyclic, or steadily changing, and recording the estimated sardine catches for future years. (ii) Introduce an anchovy fishery, a hake fishery, and both combined, in various levels of anchovy and hake biomass removal, to examine the effects of such fisheries in regard to maximizing sardine relative abundance. (iii) Introduce a limit on the amount of sardine catch to estimate the role played by the sardine fishery in the reduction of sardine biomass.

For step i, the estimation of $\mathbf{N}_r$, already considered from $r = 0$ (1950) through $r = 9$ (1959), was continued until $r = 19$ (1968).

For step ii, $\mathbf{N}_r$, already computed for $(t_{58}^{(r)}, t_{78}^{(r)}) = (0, 0)$ for all 20 years, was computed for the sequence of pairs $(t_{58}^{(r)}, t_{78}^{(r)})$: (0, 0.10), (0, 0.20), (0, 0.30), (0.10, 0), (0.10, 0.10), (0.10, 0.20), (0.10, 0.30), (0.20, 0), (0.20, 0.10), (0.20, 0.20), (0.20, 0.30), (0.30, 0), (0.30, 0.10), (0.30, 0.20), and (0.30, 0.30).

For step iii, the entire runs of steps i and ii were repeated with $t_{48}^{(r)} \leqslant 0.10$; i.e., the recorded $t_{48}^{(r)}$ was used whenever it was 0.10 or less, but was replaced by 0.10 if it exceeded 0.10. This had the effect of limiting the sardine catch to 10% of the adult biomass in any one year.

For years after those for which values of $R_2^{(r)}$ were available, $R_2^{(r)}$ was taken as the arithmetic mean of the last five values available.

PRESENTATION AND EVALUATION

Mode of Presentation and Evaluation

The output of the model was a computer printout of more than 100 $14\frac{3}{4} \times 11$ sheets. Summaries were calculated from these output data and are presented in 21 graphs.

The best evaluation of the methodology used in this paper would be to compare the results (abundances, catches) predicted by this method with the actual abundances and catches. We cannot, of course, observe the actual abundances, but we can construct a new model for each year for which data are observed. Let us, then, for the moment give the name "observed" results to results from a model based on directly observed data and fresh assumptions, as opposed to data and assumptions carried over from a previous time period. Recall that we begin by building a model of the biosystem based on data and assumptions, then allow the "initial state" to progress through a sequence of time periods, predicting abundances and catches for each time period, without the introduction of any additional data (except recruitment values) or assumptions. Let us, then, for the moment name this set of results the "predicted"

results. To evaluate the efficacy of the Markov chain predictions, the best we can do within the limitations of the data and form of model is to compare these "predicted" against "observed" results. The observed results were given in Table 2.

We may think of the predicted results as being exactly composed of the observed results plus the difference between observed and predicted results. Let us denote by p the predicted results, by b the observed results, and by d their difference; then we may write the above relationship as

$$p \equiv b + d. \tag{80}$$

If our Markov chain model agrees with the directly constructed model exactly except for random fluctuations that average to zero, $\mathrm{E}(d) = 0$ and

$$\mathrm{E}(p) = \mathrm{E}(b), \tag{81}$$

where E is the mathematical expectation operator. Also, for our Markov chain model to be of value, the random fluctuations about the expectation of the observed results should not exceed a small quantity, say q. Symbolically,

$$d_r \leq q, \text{ where } r = 1, 2, \ldots, 9. \tag{82}$$

Thus, if equations 81 and 82 are satisfied, the predicted results are satisfactorily close to the observed results and the model may be accepted as adequate. Ideally, we should consider equations 81 and 82 as hypotheses and test them statistically; in this instance, we could measure the probability that these hypotheses do not deviate from fact by more than a measured amount. However, even the most primitive assumptions underlying statistical tests are violated. (For example, the observations are not independent, the probability distribution(s) is (are) not known nor even known to be symmetric, and the variance is apparently not uniform.) There exists at this time no statistical test that may honestly be used in assessing how well equations 81 and 82 are satisfied. Therefore, the decision as to whether or not the model is adequate must rest in the intuitive judgment of the reader. The best that can be done is to present the results in such a way that the pattern of behavior of the predicted against the observed results will be clear to the reader and amenable to his intuitive consideration.

Equation 82 says d_r should be small. A "small" deviation when dealing with an anchovy abundance of 4000 metric ktons might be a large deviation when dealing with a sardine catch of 50 metric ktons. Thus, let us include b_r as a factor of q, or, dividing both sides of 82, consider the statistic

$$|d_r/b_r|, \tag{83}$$

the magnitude of the ratio of the deviation to the observed value. The statistic $|d_r/b_r|$ will be graphed for $r = 0, 1, \ldots, 9$, along with plus or minus the average $|d_r/b_r|$ over the several r. If $|d_r/b_r|$ is sufficiently small — and "small" must be up to the judgment of the reader — equation 82 will be satisfied. However,

$|d_r/b_r|$ could be small but consistently biased, in which case equation 81 would not be satisfied. Let us consider another statistic

$$\sum_{i=0}^{r} d_i/b_i, \text{ where } r = 0, 1, 2, \ldots, 9, \tag{84}$$

the accumulating sum of d_r/b_r. If equation 81 is true, 84 will oscillate about 0; if 81 is not true, 84 will accumulate (either positively or negatively) and will deviate further and further from 0 as r progresses. Thus, if $|d_r/b_r|$ is small and if $\Sigma\ d_i/b_i$ oscillates about 0, we will consider our model as fitting the "observed" model adequately.

Agreement of the Predictive Model with Observed Model

The recorded catch of sardines ($n_8^{(r)}$) represents both the most accurate of the data used as inputs and the most significant process in the implications of this study. Thus, the agreement of predicted catch with observed catch was considered the most stringent criterion; the Markov chain model was refined continuously until the agreement appeared adequate (Fig. 2). The mean magnitude of proportion error, for $n_8^{(r)}$, i.e., the statistic $|d_r/b_r|$, is just over $\frac{1}{4}$ and no error exceeds about $\frac{3}{4}$ (Fig. 3). The statistic $\Sigma d_i/b_i$ for $n_8^{(r)}$ oscillates

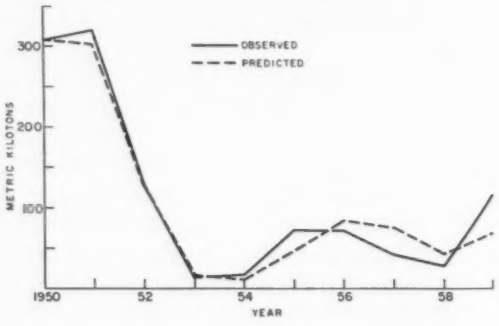

FIG. 2. Sardine catches ($n_8^{(r)}$) for 1950–59 as recorded and as extrapolated from 1950 data by the model.

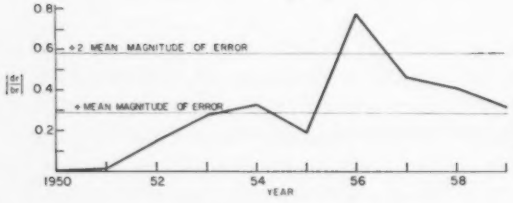

FIG. 3. Proportion error $[|d_r/b_r|]$ for sardine catch ($n_8^{(r)}$), i.e., the unsigned magnitude of the difference between catches as recorded and as extrapolated by the model from 1950 data divided by the recorded catch.

about zero rather than consistently growing farther away from zero (Fig. 4). On the basis of these three figures, the adequacy of the model's prediction of sardine catch may be inferred.

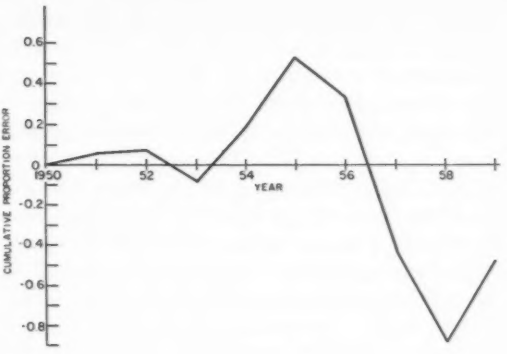

FIG. 4. Cumulative proportion error $\left[\sum_{i=0}^{r} d_i/b_i\right]$ for sardine catch ($n_3(r)$), i.e., the sum from 1950 through year r of the signed difference between catches as recorded and as extrapolated by the model from 1950 data divided by the recorded catch.

The sardine adult absolute abundances as predicted by the Markov chain model and as computed from observed data are better perceived through their average behaviors, which are less influenced by random fluctuations. Moving averages of four superimposed upon the actual results suggest that the two curves behave in much the same fashion (Fig. 5). Max $|d_r/b_r|$ and mean $|d_r/b_r|$ for sardine abundance are approximately the same as for the sardine catch (Fig. 6). Similarly, the accumulating sum of d_r/b_r returns to zero consistently

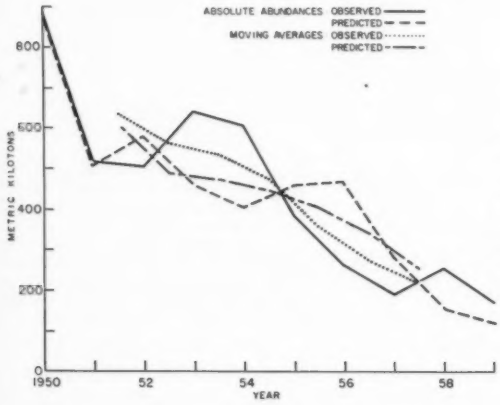

FIG. 5. Absolute abundances of sardine adults ($n_4(r)$) with superimposed four-term moving averages for observed results (i.e., results from a model based on directly observed data and fresh assumptions) and predicted results (i.e., results extrapolated by the model from 1950 data).

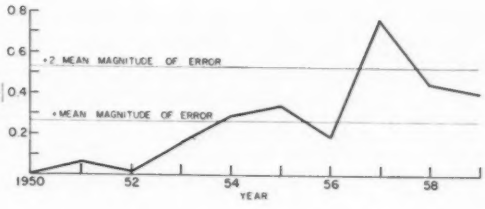

FIG. 6. Proportion error $[|d_r/b_r|]$ for absolute abundance of sardine adults ($n_4(r)$), i.e., the unsigned difference between observed (in the Fig. 5 sense) and predicted (in the Fig. 5 sense) results divided by the observed results.

(Fig. 7). It may be inferred that the expectation of the predicted sardine abundance is approximately the same as the expectation of the observed sardine abundance and the errors about the expectation are not large.

The observed anchovy abundance seems to vary quixotically whereas the predicted abundance seems to plod steadily toward its goal (Fig. 8). However, the moving averages appear to represent a compromise between the actual output and identical curves, which implies that the two methods will show the same overall process. The proportion error for the anchovy abundance is less than that for the sardine (Fig. 9); mean $|d_r/b_r|$ is considerably less than $\frac{1}{4}$ and maximum $|d_r/b_r|$ is just over $\frac{1}{2}$. The accumulating sum of proportion error oscillates about zero, although its return to zero is more lethargic than

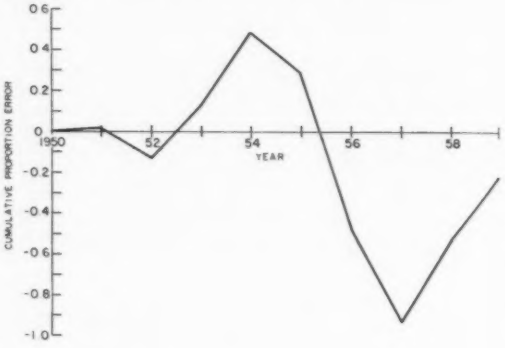

FIG. 7. Cumulative proportion error $\left[\sum_{i=0}^{r} \frac{di}{bi}\right]$ for absolute abundances of sardine adults ($n_4^{(r)}$), i.e., the sum from 1950 through year r of the signed difference between observed (in the Fig. 5 sense) and predicted (in the Fig. 5 sense) results divided by the observed results.

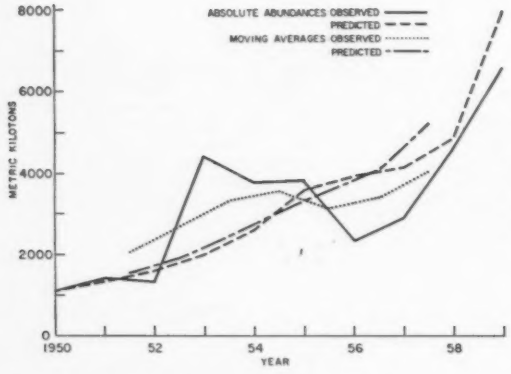

FIG. 8. Absolute abundances of anchovy adults ($n_5^{(r)}$) with superimposed four-term moving averages for observed results (i.e., results from a model based on directly observed data and fresh assumptions) and predicted results (i.e., results extrapolated by the model from 1950 data).

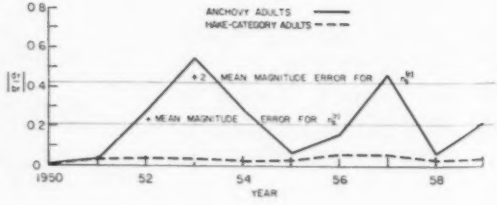

FIG. 9. Proportion error $[|d_r/b_r|]$ for absolute abundances of anchovy adults ($n_5^{(r)}$) and for absolute abundances of hake-category adults ($n_7^{(r)}$), i.e., the unsigned difference between observed (in the Fig. 8 sense) and predicted (in the Fig. 8 sense) results divided by the observed results. (Mean magnitude error for $n_7^{(r)} = 0.0349$).

in the case of the sardine (Fig. 10). This last result illustrates the statistical dependence among the observations in the random time series, although the autocorrelation function damps to zero with time. In other words, when the dynamics of a population experiences a significant but small and temporary change, the resulting effect on the population lasts for a while and then dies out gradually.

The predicted values of $n_7^{(r)}$, the category including hake, appear to be close to the observed values and not to vary remarkably, but they are consistently larger (Fig. 11). Since the observed results, i.e., the results of the model using newly observed data when available and new assumptions each year, gave this category as a constant 2400 metric ktons, both the observed and the moving average of four of these observed values lie on the straight line segment 2400. Thus, we would expect the proportion

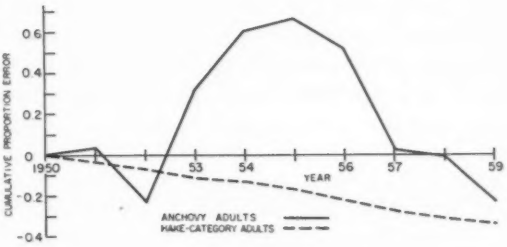

FIG. 10. Cumulative proportion error $\left[\sum_{i=0}^{r} \frac{d_i}{b_i}\right]$ for absolute abundances of anchovy adults ($n_3^{(r)}$) and of hake-category adults ($n_7^{(r)}$), i.e., the sum from 1950 through year r of the signed difference between observed (in the Fig. 8 sense) and predicted (in the Fig. 8 sense) results divided by the observed results.

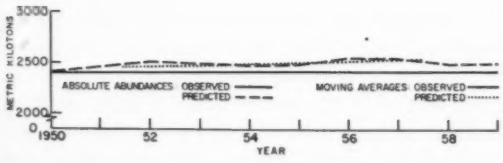

FIG. 11. Absolute abundances of hake-category adults ($n_7^{(r)}$) with superimposed four-term moving averages for observed results (i.e., results from a model based on directly observed data and fresh assumptions) and predicted results (i.e., results extrapolated by the model from 1950 data).

error to be small but the accumulating sum of the proportion error to grow larger consistently. The statistic $|d_r/b_r|$ may be seen to have a maximum of less than 0.06; it averages 0.0349 (Fig. 9). However, the statistic 4.5 grows larger (negatively) consistently and does not oscillate about zero, implying the expectation of the predicted $n_7^{(r)}$ abundance is biased by a small positive amount (Fig. 10). Although certainly an undesirable property of the modelling process, the amount of bias is too small in this particular case to be debilitating. If the modelling process is used further in the future, the source of this bias should be uncovered and eliminated.

Although $|d_r/b_r|$ is a useful statistic in comparing predictions with the supposedly more accurate "observations," the contrasting statistic

$$|d_r/p_r|, \tag{85}$$

i.e., the magnitude of the ratio of observed minus predicted to *predicted* results,

has more meaning in considering the adequacy of projections into the future. The statistic 85 and also its accumulating sum were computed for all years for the four abundances and in all instances were found to be not very different from their analogous statistics 83 and 84. For example, statistic 85 was 0.31 for $n_4^{(r)}$, 0.29 for $n_5^{(r)}$, 0.02 for $n_7^{(r)}$, and 0.33 for $n_8^{(r)}$.

This section attempts to answer question 1 and 2 posed in the beginning. How adequately the Markov chain model fits our best attempt at reality cannot be evaluated probabilistically and must be left to the judgment of the reader. However, the analyses of this section shows agreement that, in view of the paucity of data and plethora of assumptions, the author judges to be eminently reasonable. Further, on the basis of these analyses, projections of future abundances and catches would be expected to be in error of not more than 20–30%. On scores of early computer runs, the results "blew up" into nonsense. The model was improved by adding or altering assumptions after each, and another run attempted. The author had the intuitive feeling, when the model finally "behaved" and rendered sensible results, that it must be a reasonable approximation. With so many interlocking relationships, a serious departure from reality in one item would magnify upon carrying the model through time.

PROJECTIONS AND SIMULATIONS

Projections of Catch and Abundances for 1960 through 1968

Consider extrapolations through 1968 of the absolute abundances of the several categories. They are legitimate extrapolations, but must be approached with reservations if they are to be interpreted as predictions. Implicit in the prediction concept is the assumption that the model continues to accurately represent the true ecosubsystems. This assumption implies subsidiary assumptions, such as that growth, recruitment, and mortality rates remain constant despite changes in relative abundances, age compositions, fishing intensities, and food availability. We may extrapolate freely, but we must interpret with care.

Consider projections through 1968 of sardine adult absolute abundance ($n_4^{(r)}$) and sardine catch ($n_8^{(r)}$) (question 3). Such "projections" are in the sense of extrapolations from the 1950 input data. They have been compared with sardine catch records to 1959, but they cannot be compared with catches to date since the sardine fishing effort has been limited in recent years and since the recent records include Mexican catches as well. A stabilization of both $n_4^{(r)}$ and $n_8^{(r)}$ is projected (Fig. 12). The sardine adult absolute abundance is projected to stabilize in the vicinity of 110 metric ktons; catch in the vicinity of 20 metric ktons. There is no indication of a "return" of the Pacific sardine in the sense of a revival of the abundances of two and three decades ago, but there is indication of a stable, slight increase.

$n_5^{(r)}$ is the abundance of the primary portion of the sardine competitors and $n_7^{(r)}$ is the abundance of a large portion, or at least an indicator, of the sardine's predators. $n_5^{(r)}$ continues to oscillate rather extensively, ending on

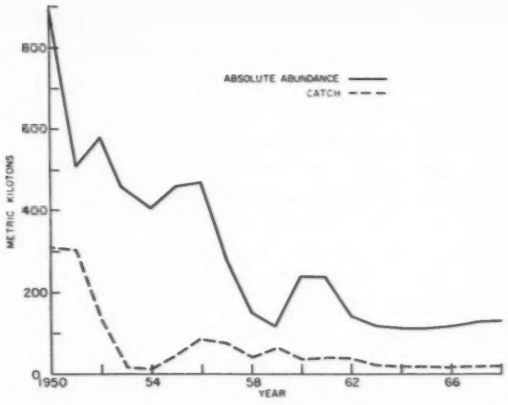

FIG. 12. Absolute abundances ($n_4^{(r)}$) of sardine adults and catches ($n_9^{(r)}$) extrapolated by the Markov chain model through 1968 from 1950 data.

a rapidly increasing path (Fig. 13). The projection indicates that anchovies will remain the major influence and, cyclically, will represent the major part of the biomass in that trophic level. $n_7^{(r)}$ is seen to become less stable with time, probably reflecting the gross anchovy abundance oscillation, but not deviating radically enough from past performance to represent a major influence on the sardine–anchovy's trophic level as differing from past history. This class, including hake, retains a projected absolute abundance of between 2000 and 3000 metric ktons.

The pattern of continued paucity of the sardine and high abundance of the anchovy for a decade is hardly surprising — rather might be expected — in light of recent work by Soutar (1967). Distributions of scale frequencies for the Pacific sardine and northern anchovy in bottom cores show that the anchovy has been the most abundant species for most of the time during the past 1000 years, with the sardine becoming the most abundant only occasionally and for only a few decades at a time.

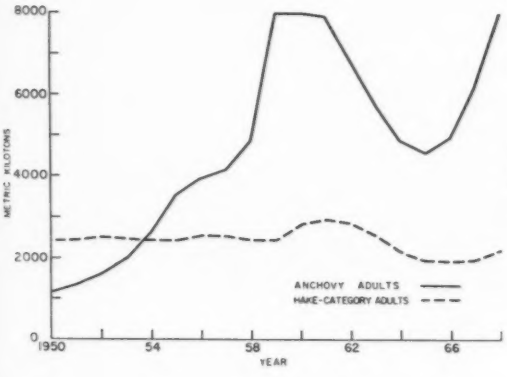

FIG. 13. Absolute abundances of anchovy adults ($n_5^{(r)}$) and of hake-category adults ($n_7^{(r)}$) extrapolated by the Markov chain model through 1968 from 1950 data.

Effect on Catches of Initiating an Anchovy Fishery

Consider the effects of various simulated catches from an anchovy fishery (begun 1950) on the abundances of sardines, anchovies, and the hake category (Fig. 14, 15, and 16 respectively). At the outset, the sardine population is diminishing, the anchovies are "taking over," and the hake category is stable. By initiating an anchovy fishery, the sardine population is negatively affected at first, positively eventually. The effect is gradual improvement

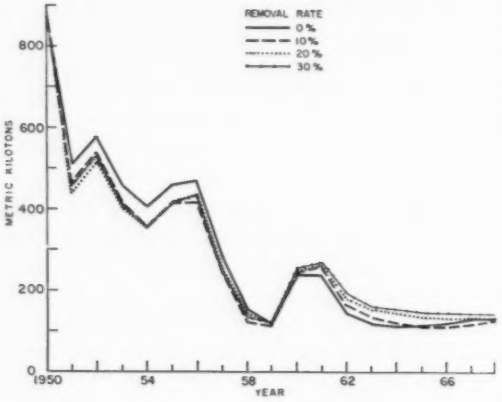

Fig. 14. Effects on sardine abundances of initiating anchovy fisheries in 1950 at four rates of removal of annual anchovy biomass.

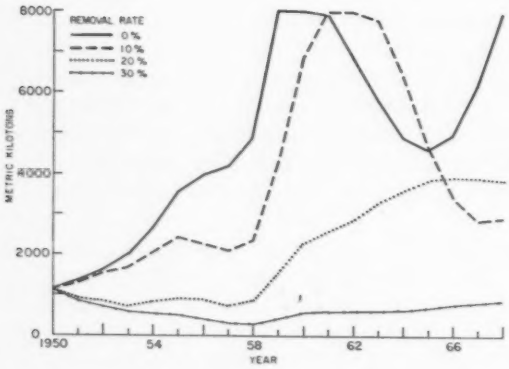

Fig. 15. Effects on anchovy abundances of initiating anchovy fisheries in 1950 at four rates of removal of annual anchovy biomass.

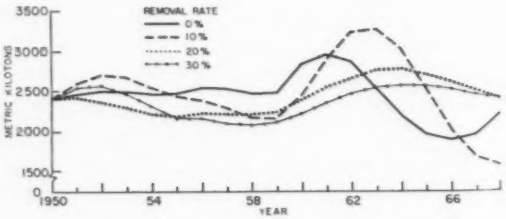

Fig. 16. Effects on hake-category abundances of initiating anchovy fisheries in 1950 at four rates of removal of annual anchovy biomass.

as more and more anchovies are taken, but the effect is not striking and the sardine abundance continues to diminish in the same pattern (not quantities) as without an anchovy fishery. The maximum increase in sardine abundance is about a third, but it is not maintained. It is clear that the model does not predict a "return of the sardine" as a result of initiating an anchovy fishery.

The effect on anchovy abundance of initiating an anchovy fishery is more striking. As the catch increases, the anchovy population growth diminishes. At 20% (of anchovy abundance) catch, the maximum tonnage catch of anchovies appears. The total catch of all animals is, in fact, 20–40 *times* the sardine catch at this level. The anchovy population is still slowly growing, and will probably survive and continue to yield an impressive catch. At 30%, the anchovy population begins to diminish and appears unable to overcome the loss. The total catch of all animals is about one-third of the tonnage at the 20% rate, due to the diminished population of anchovies.

The hake-category abundance is not greatly affected by initiating an anchovy fishery. Its oscillation continues, somewhat lagging, at the 10% catch level, but damps to yield a more stable abundance at the 20 and 30% levels.

Effect on Catches of Initiating a Hake Fishery

Consider the effects of various simulated catches from a hake fishery (begun in 1950) on the abundances of sardines, anchovies, and the hake category (Fig. 17, 18, and 19 respectively). At the outset, the sardine population is diminishing, the anchovies are "taking over," and the hake category is stable. Let us consider the effects on the three abundances of each catch percent in turn.

At the catch rate of 10% of abundance, the sardine abundance is diminished at first, then increases considerably from the 0% catch rate abundance, but still follows the same decline pattern. In the last half of the period, the increase

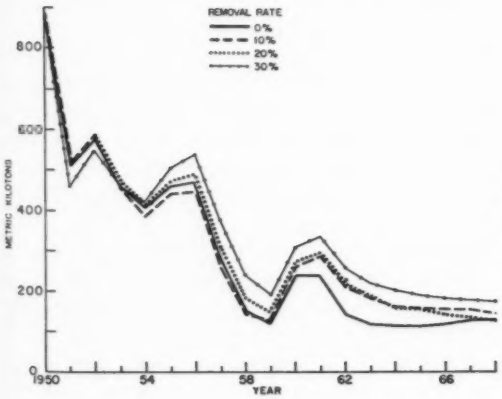

FIG. 17. Effects on sardine abundances of initiating hake fisheries in 1950 at four rates of removal of annual biomass of the hake category.

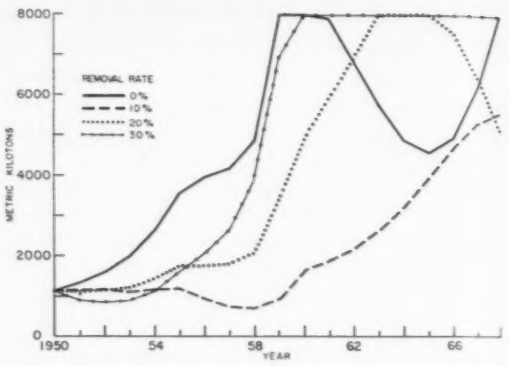

FIG. 18. Effects on anchovy abundances of initiating hake fisheries in 1950 at four rates of removal of annual biomass of the hake category.

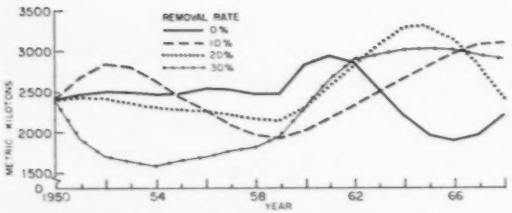

FIG. 19. Effects on hake-category abundance of initiating hake fisheries in 1950 at four rates of removal of annual biomass of the hake category.

in the sardine abundance is variously 25–75 metric ktons above the 0% catch rate abundance. The anchovy abundance increases much more slowly, getting very close to stabilization until the sardines are well reduced, apparently because the increased competition affects the anchovies negatively much more than the predator reduction affects positively. The hake-category abundance retains its same pattern of oscillation, but the coefficients of periodicity are altered. The total catch of all animals is from 10 times at first to 20 times eventually the catch of all animals for the 0% hake fishery catch rate.

At the catch rate of 20% of abundance, the sardine population is larger than at the 0% rate throughout the period, but still follows the same pattern of decline. The anchovy abundance drops at first, but recovers to enter the same oscillatory pattern, somewhat lagging. Apparently the increased competition approximately balances the predator reduction effect. The hake-category abundance again follows a pattern of oscillation, but with altered coefficients of periodicity. The total catch of all animals is from 20 times at first to 30 times eventually the catch of all animals for the 0% hake fishery catch rate.

At the catch rate of 30% of abundance, the sardine population is clearly better off than at the 0% rate, showing signs of stabilizing in the vicinity of 150–175 metric ktons, about one-third again its 0% catch rate. However, the same decline pattern appears. In contrast, the anchovy abundance rises quickly to the maximum the environment will tolerate and remains there; clearly the predator reduction has far outbalanced the competition increase and the

anchovy population goes out of control. Due to the maximum anchovy population, the total catch of all animals is about 45 times that at the 0% catch rate.

Question 4 was answered during the discussion of "Effect on Catches of Initiating an Anchovy Fishery." In answer to 5, the sardine abundance could be affected beneficially, but not raised to the level of two or three decades ago. The best result attainable appears to be an increase of 25–60 metric ktons in absolute abundance, from about a 10% catch rate in the hake category. (A greater sardine abundance increase would result from a 30%-catch-rate level, but would institute rapid and extreme changes in the ecological "balance" or pattern.)

Effect on Catches of Initiating both Anchovy and Hake Fisheries

Consider the effects of various simulated catches from both anchovy and hake fisheries (begun in 1950) on the abundances of sardines, anchovies, and the hake category, starting with the average per year sardine catch (Fig. 20).

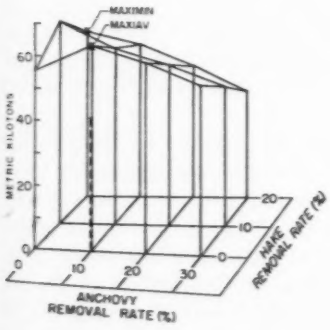

Fig. 20. Average yearly sardine catches for various mixes of fishing intensities. Broken line represents average yearly sardine catch for controlled (≤10%/year) removal of sardine biomass.

The maximum sardine catch, i.e., the optimum catch according to the maxiav criterion, occurs for an anchovy fishery at the 10% rate and no hake fishery. The predicted average sardine catch for the years 1951 through 1968 under this fishing strategy (i.e., mix of fishing intensities; "strategy" as used in game theory) is about 64.5 metric ktons. The strategy yielding the largest minimum catch, i.e., the maximin criterion or maximizing the "worst year's" catch, occurs for a hake fishery at the 20% rate but no anchovy fishery. The predicted average sardine catch for the 18 years under this strategy is about 51.9 metric ktons. The same entire simulation was conducted with an additional constraint on the fishing strategy: the sardine catch was limited to 10% of the sardine abundance, in order to consider the question of whether or not "overfishing" contributed to the sardine decline. Overfishing did *not* appear to be a cause; at the maxiav strategy of a 10% rate at maximum for sardines, 10% rate for anchovies, and no hake fishery, the average sardine catch occurred at about 41.4 metric ktons. If the control of overfishing had permitted the sardine

population to grow to its prior size, the 10% constraint would have permitted a maxiav much larger than the 51.9 metric ktons resulting from uncontrolled sardine fishing.

Now let us consider $n_8^{(r)}$, in this instance the average annual combined catches of sardines, anchovies, and hake (Fig. 21). Both criteria fall at the

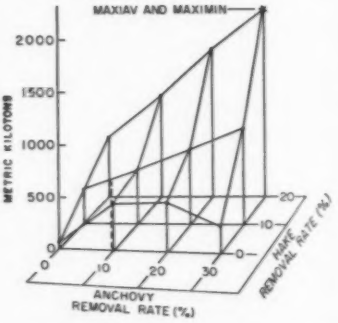

FIG. 21. Average yearly total catches ($n_8^{(r)}$) for various mixes of fishing intensities. Broken line represents average yearly total catch for controlled ($\leq$10%/year) removal of sardine biomass.

same point, viz. an anchovy fishery at the 30% rate and a hake fishery at the 20% rate. Whereas the predicted sardine catch averages only about 33.8 metric ktons at this strategy, the total catch for the three categories is about 1797.9 metric ktons!

Last, only as an illustration of the concept of maximizing the average catch or the minimum catch through a linear function of catches of the three populations, let weights be 10:3:1. In other words, suppose the profit per unit fishing effort for sardines is 10/3 that for anchovies and 10 times that for hake. Let us denote by C^* the linear function of catches with 10, 3, and 1 as coefficients. Interestingly, the maxiav and maximin criteria occur together again and at the same fishing strategy as for the last figure (which would represent a 1:1:1 weighting). In this instance, the catch in metric kilotons is about 33.8 for sardines, 1234.7 for anchovies, and 529.4 for hake (Fig. 22).

As a final note, we might observe that the maxima and minima of the oscillation of the hake population abundance lags behind those of the anchovy regularly about 2 years.

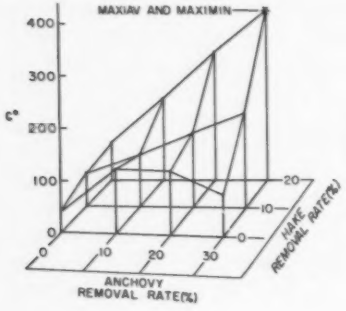

FIG. 22. Values of C^* (a linear function of catch assigning 10:3:1 "importance" or "value" ratios to sardine, anchovy, and hake catches, respectively) for various mixes of fishing intensities.

DISCUSSION AND IMPLICATIONS

Statistical

Despite the imposing appearance of the large mass of variables and data involved, the model is still simple statistically. The statistical problems lie in the possibility of missing data and in the evaluation of the model's outputs.

In the first problem, missing elements of a Markov chain are not always estimable, i.e., the problem is not always subject to solution. Riffenburgh and Sogliero (1964) have given an existence theorem for the solution and a method for the solution when it exists.

The second problem, that of evaluating the model's outputs, appears not to have been solved in a statistically acceptable way. System-level models usually have inputs of varied accuracy. The transducing of these inputs affects and is affected by such variable accuracy in an unknown way. Thus, the use of traditional statistical methods in evaluating such outputs, however much they may appear similar to, say, simple time series, would be seriously spurious. The whole problem of system-model accuracy is badly in need of some very sophisticated thinking. As a result of the uncertain statistical accuracy, we must be chary in interpretation of the model's extrapolations and keep the many assumptions starkly in mind.

Biological

In answer to question 8, we can affect the abundances of populations by the control of fishing effort. It is possible to seriously upset the ecological pattern. However, in answer to question 9, the system seems to be robust enough to survive moderate changes in fishing intensities if such changes are made under conditions of advance prediction and continued measurement to alert the controllers to the changing population dynamics. This result appears to reinforce empirically the theoretical statement by the author that model "structure is more stable than the unrelated agglomeration of information inputs and that the rigorous formation of structure based on logic and both repeated and varied sampling damps out perversions of knowledge" (Riffenburgh, 1966).

Fishery Biology and the Fishing Industry

From the results of this study and within the limitations of the model here presented, we may draw the following conclusions. To maximize sardine catch and stabilize the sardine fishing industry as closely as possible simultaneously, introduce *limited* (a maximum catch of 10% of abundance per year) anchovy and hake fisheries. Sardines will not be "brought back," but catch will run two to three times that predicted in the absence of hake or anchovy, or both, fisheries. It would not have improved catches in the long run to have limited sardine fishing efforts earlier.

To maximize and stabilize the small-fish commercial fishing industry off the Pacific coast as a whole, introduce large but controlled fisheries for anchovy (at about the 30% catch rate) and hake (at about the 20% rate). The sardine catch will be smaller than above, but will run half again the size of catch predicted in the absence of hake or anchovy, or both, fisheries.

If the different fishes are taken as being worth different amounts, value-weighted optimizing criteria may be used in this model to predict intermediate optimum strategies and results.

ACKNOWLEDGMENTS

Grateful acknowledgment is tendered to Professor Garth I. Murphy, University of Hawaii, who supplied data, suggestions, corrections, inspiration, and time; the mistakes that remain, however, must be claimed by the author. Further grateful acknowledgment is tendered to Vernon E. Brock, University of Hawaii, whose creative thought of a dozen years ago was responsible for the basic idea.

This work was supported (in part) by the Public Health Service Research Grant GM-11608 from the Institute of General Medical Sciences during 1963–66 to The University of Connecticut where the author is Professor of Statistics.

REFERENCES

ANON. 1950. Sardine eggs and larvae and other fish larvae, Pacific coast, 1950. Fish Wildlife Serv. Spec. Sci. Rept., Fish. Ser.

1951. Sardine eggs and larvae and other fish larvae, Pacific coast, 1951. Fish Wildlife Serv. Spec. Sci. Rept., Fish. Ser.

1959. Sardine eggs and larvae and other fish larvae, Pacific coast, 1959. Fish Wildlife Serv. Spec. Sci. Rept., Fish. Ser.

BROCK, V. E., AND R. H. RIFFENBURGH. 1960. Fish schooling: a possible factor in reducing predation. J. Conseil Conseil Perm. Intern. Exploration Mer 25: 307–317.

CLARK, F. N. 1928. The weight-length relationship of the California sardine (*Sardina caerulea*) at San Pedro. Calif. Div. Fish Game Fish. Bull. 12: 1–59.

1934. Maturity of California sardine determined by ova diameter measurements. Calif. Div. Fish Game Fish. Bull. 42: 1–49.

CLARK, F. N., AND J. B. PHILLIPS. 1952. The northern anchovy (*Engraulis mordax*). Calif. Div. Fish Game Fish. Bull. 38: 189–207.

LARKIN, P. A., AND A. S. HOURSTON. 1964. A model for the simulation of the population biology of Pacific salmon. J. Fish. Res. Bd. Canada 21: 1245–1265.

MURPHY, G. I. 1966. Population biology of the Pacific sardine (*Sardinops caerulea*). Proc. Calif. Acad. Sci. 34: 1–84.

PAULIK, G. J., AND J. W. GREENOUGH, JR. 1966. Management analysis for a salmon resource system, p. 215–252. *In* K. E. F. Watt [ed.] Systems analysis in ecology. Academic Press, Inc., New York.

PHILLIPS, J. B. 1948. Growth of the sardine, 1941–42 through 1946–47. Calif. Div. Fish Game Fish. Bull. 71: 1–33.

RICKER, W. E. 1954. Stock and recruitment. J. Fish. Res. Bd. Canada 11: 559–623.

RIFFENBURGH, R. H. 1960. Un analisis sistematico de la ecologia marina. Bol. Tecnicas Aplicaciones Muestreo 7: 43–53.

1961. A system analysis of the marine ecology. Bull. Inst. Intern. Statist. 33: 57–66.

1966. On problems of sampling and decision in exotic environments. Cybernética 2: 109–117.

1969. A speculative mathematical model of the psychophysiologic system. Ann. New York Acad. Sci. (In press.)

RIFFENBURGH, R. H., AND G. S. SOGLIERO. 1964. On the estimation of missing elements of a Markov chain. Statist. Dept. Univ. Conn. Res. Rept. 13: 1–19.

ROYCE, W. F., D. E. BEVAN, J. A. CRUTCHFIELD, G. J. PAULIK, AND R. L. FLETCHER. 1963. Salmon gear limitation in northern Washington waters. Univ. Wash. Publ. Fish. (N.S.) 2: 1–123.

SILLIMAN, R. P. 1943. Studies on the Pacific pilchard or sardine (*Sardinops caerulea*) 5. A method of computing mortalities and replacements. U.S. Fish Wildlife Serv. Spec. Sci. Rept. 24: 1–10.

1967. Analog computer models of fish populations. U.S. Fish Wildlife Serv. Fish. Bull. 66: 31–46.

SOUTAR, A. 1967. The accumulation of fish debris in certain coastal sediments. Calif. Coop. Oceanic Fish. Invest. Rept. 11: 136–139.

(APPENDICES 1–3 *follow*)

APPENDIX 1. Diagram of vector $\mathbf{N}_r$.

$\mathbf{N}_r$:	Biomass of sardine larvae at start of rth year	Biomass of anchovy larvae at start of rth year	Biomass of sardine yearlings at start of rth year	Biomass of sardine adults at start of rth year	Biomass of anchovy adults at start of rth year	Biomass of competitors of S and A at start of rth year	Biomass of climax predators at start of rth year	Biomass of fish taken by fishery up to start of rth year	Biomass exiting from the system up to start of rth year
	$n_1(r)$	$n_2(r)$	$n_3(r)$	$n_4(r)$	$n_5(r)$	$n_6(r)$	$n_7(r)$	$n_8(r)$	$n_9(r)$

APPENDIX 2. Diagram of matrix $\mathbf{T}_r$.

Prefix the contents of each square by the words: "The probability that a weight unit randomly chosen at the beginning of the rth year from".

APPENDIX 2. Diagram of matrix T_r.

Prefix the contents of each square by the words: "The probability that a weight unit randomly chosen at the beginning of the rth year from".

1st subscript: \ 2nd subscript:	1	2	3	4	5	6	7	8	9
1	SL will end the year as SL	SL will end the year as AL	SL will end the year as SY	SL will end the year as SA	SL will end the year as AA	SL will end the year as Co	SL will end the year as CP	SL will be taken during year by Fy	SL will exit system during year
	0	0	$t_{12}^{(r)}$	$t_{14}^{(r)}$	$t_{15}^{(r)}$	$t_{16}^{(r)}$	0	0	$t_{19}^{(r)}$
2	AL will end the year as SL	AL will end the year as AL	AL will end the year as SY	AL will end the year as SA	AL will end the year as AA	AL will end the year as Co	AL will end the year as CP	AL will be taken during year by Fy	AL will exit system during year
	0	0	0	$t_{24}^{(r)}$	$t_{25}^{(r)}$	$t_{26}^{(r)}$	0	0	$t_{29}^{(r)}$
3	SY will end the year as SL	SY will end the year as AL	SY will end the year as SY	SY will end the year as SA	SY will end the year as AA	SY will end the year as Co	SY will end the year as CP	SY will be taken during year by Fy	SY will exit system during year
	0	0	0	$t_{34}^{(r)}$	0	0	$t_{37}^{(r)}$	0	$t_{39}^{(r)}$
4	SA will end the year as SL	SA will end the year as AL	SA will end the year as SY	SA will end the year as SA	SA will end the year as AA	SA will end the year as Co	SA will end the year as CP	SA will be taken during year by Fy	SA will exit system during year
	0	0	0	$t_{44}^{(r)}$	0	0	$t_{47}^{(r)}$	$t_{48}^{(r)}$	$t_{49}^{(r)}$
T_r: 5	AA will end the year as SL	AA will end the year as AL	AA will end the year as SY	AA will end the year as SA	AA will end the year as AA	AA will end the year as Co	AA will end the year as CP	AA will be taken during year by Fy	AA will exit system during year
	0	0	0	0	$t_{55}^{(r)}$	0	$t_{57}^{(r)}$	$t_{58}^{(r)}$	$t_{59}^{(r)}$
6	Co will end the year as SL	Co will end the year as AL	Co will end the year as SY	Co will end the year as SA	Co will end the year as AA	Co will end the year as Co	Co will end the year as CP	Co will be taken during year by Fy	Co will exit system during year
	0	0	0	0	0	$t_{66}^{(r)}$	$t_{67}^{(r)}$	0	$t_{69}^{(r)}$
7	CP will end the year as SL	CP will end the year as AL	CP will end the year as SY	CP will end the year as SA	CP will end the year as AA	CP will end the year as Co	CP will end the year as CP	CP will be taken during year by Fy	CP will exit system during year
	0	0	0	0	0	0	$t_{77}^{(r)}$	$t_{78}^{(r)}$	$t_{79}^{(r)}$
8	Fy will end the year as SL	Fy will end the year as AL	Fy will end the year as SY	Fy will end the year as SA	Fy will end the year as AA	Fy will end the year as Co	Fy will end the year as CP	Fy will stay a fished-out unit	Fy will exit system during year
	0	0	0	0	0	0	0	1	0
9	Lost energy will end year as SL	Lost energy will end year as AL	Lost energy will end year as SY	Lost energy will end year as SA	Lost energy will end year as AA	Lost energy will end year as Co	Lost energy will end year as CP	Lost energy will be taken by Fy	Lost energy will remain lost
	0	0	0	0	0	0	0	0	1

The value of the probability is shown if always known and is indicated by t with subscripts if it lies between 0 and 1 and must be estimated.

APPENDIX 3. Diagram of matrix A_r.

The symbols "prop. $n_i^{(r)} \rightarrow n_j^{(r+1)}$" represent "proportion of biomass of category i at beginning of year r which is added to the biomass of category j during the year."

A_r:

1st subscript \ 2nd subscript:	1	2	3	4	5	6	7	8	9
1	prop. $n_1^{(r)} \rightarrow n_1^{(r+1)}$	prop. $n_1^{(r)} \rightarrow n_2^{(r+1)}$	prop. $n_1^{(r)} \rightarrow n_3^{(r+1)}$	prop. $n_1^{(r)} \rightarrow n_4^{(r+1)}$	prop. $n_1^{(r)} \rightarrow n_5^{(r+1)}$	prop. $n_1^{(r)} \rightarrow n_6^{(r+1)}$	prop. $n_1^{(r)} \rightarrow n_7^{(r+1)}$	prop. $n_1^{(r)} \rightarrow n_8^{(r+1)}$	prop. $n_1^{(r)} \rightarrow n_9^{(r+1)}$
	0	0	$a_{12}^{(r)}$	0	0	0	0	0	0
2	prop. $n_2^{(r)} \rightarrow n_1^{(r+1)}$	prop. $n_2^{(r)} \rightarrow n_2^{(r+1)}$	prop. $n_2^{(r)} \rightarrow n_3^{(r+1)}$	prop. $n_2^{(r)} \rightarrow n_4^{(r+1)}$	prop. $n_2^{(r)} \rightarrow n_5^{(r+1)}$	prop. $n_2^{(r)} \rightarrow n_6^{(r+1)}$	prop. $n_2^{(r)} \rightarrow n_7^{(r+1)}$	prop. $n_2^{(r)} \rightarrow n_8^{(r+1)}$	prop. $n_2^{(r)} \rightarrow n_9^{(r+1)}$
	0	0	0	0	$a_{25}^{(r)}$	0	0	0	0
3	prop. $n_3^{(r)} \rightarrow n_1^{(r+1)}$	prop. $n_3^{(r)} \rightarrow n_2^{(r+1)}$	prop. $n_3^{(r)} \rightarrow n_3^{(r+1)}$	prop. $n_3^{(r)} \rightarrow n_4^{(r+1)}$	prop. $n_3^{(r)} \rightarrow n_5^{(r+1)}$	prop. $n_3^{(r)} \rightarrow n_6^{(r+1)}$	prop. $n_3^{(r)} \rightarrow n_7^{(r+1)}$	prop. $n_3^{(r)} \rightarrow n_8^{(r+1)}$	prop. $n_3^{(r)} \rightarrow n_9^{(r+1)}$
	0	0	0	$a_{34}^{(r)}$	0	0	0	0	0
4	prop. $n_4^{(r)} \rightarrow n_1^{(r+1)}$	prop. $n_4^{(r)} \rightarrow n_2^{(r+1)}$	prop. $n_4^{(r)} \rightarrow n_3^{(r+1)}$	prop. $n_4^{(r)} \rightarrow n_4^{(r+1)}$	prop. $n_4^{(r)} \rightarrow n_5^{(r+1)}$	prop. $n_4^{(r)} \rightarrow n_6^{(r+1)}$	prop. $n_4^{(r)} \rightarrow n_7^{(r+1)}$	prop. $n_4^{(r)} \rightarrow n_8^{(r+1)}$	prop. $n_4^{(r)} \rightarrow n_9^{(r+1)}$
	$a_{41}^{(r)}$	0	0	$a_{44}^{(r)}$	0	0	0	0	0
5	prop. $n_5^{(r)} \rightarrow n_1^{(r+1)}$	prop. $n_5^{(r)} \rightarrow n_2^{(r+1)}$	prop. $n_5^{(r)} \rightarrow n_3^{(r+1)}$	prop. $n_5^{(r)} \rightarrow n_4^{(r+1)}$	prop. $n_5^{(r)} \rightarrow n_5^{(r+1)}$	prop. $n_5^{(r)} \rightarrow n_6^{(r+1)}$	prop. $n_5^{(r)} \rightarrow n_7^{(r+1)}$	prop. $n_5^{(r)} \rightarrow n_8^{(r+1)}$	prop. $n_5^{(r)} \rightarrow n_9^{(r+1)}$
	0	$a_{52}^{(r)}$	0	0	$a_{55}^{(r)}$	0	0	0	0
6	prop. $n_6^{(r)} \rightarrow n_1^{(r+1)}$	prop. $n_6^{(r)} \rightarrow n_2^{(r+1)}$	prop. $n_6^{(r)} \rightarrow n_3^{(r+1)}$	prop. $n_6^{(r)} \rightarrow n_4^{(r+1)}$	prop. $n_6^{(r)} \rightarrow n_5^{(r+1)}$	prop. $n_6^{(r)} \rightarrow n_6^{(r+1)}$	prop. $n_6^{(r)} \rightarrow n_7^{(r+1)}$	prop. $n_6^{(r)} \rightarrow n_8^{(r+1)}$	prop. $n_6^{(r)} \rightarrow n_9^{(r+1)}$
	0	0	0	0	0	$a_{66}^{(r)}$	0	0	0
7	prop. $n_7^{(r)} \rightarrow n_1^{(r+1)}$	prop. $n_7^{(r)} \rightarrow n_2^{(r+1)}$	prop. $n_7^{(r)} \rightarrow n_3^{(r+1)}$	prop. $n_7^{(r)} \rightarrow n_4^{(r+1)}$	prop. $n_7^{(r)} \rightarrow n_5^{(r+1)}$	prop. $n_7^{(r)} \rightarrow n_6^{(r+1)}$	prop. $n_7^{(r)} \rightarrow n_7^{(r+1)}$	prop. $n_7^{(r)} \rightarrow n_8^{(r+1)}$	prop. $n_7^{(r)} \rightarrow n_9^{(r+1)}$
	0	0	0	0	0	0	$a_{77}^{(r)}$	0	0
8	prop. $n_8^{(r)} \rightarrow n_1^{(r+1)}$	prop. $n_8^{(r)} \rightarrow n_2^{(r+1)}$	prop. $n_8^{(r)} \rightarrow n_3^{(r+1)}$	prop. $n_8^{(r)} \rightarrow n_4^{(r+1)}$	prop. $n_8^{(r)} \rightarrow n_5^{(r+1)}$	prop. $n_8^{(r)} \rightarrow n_6^{(r+1)}$	prop. $n_8^{(r)} \rightarrow n_7^{(r+1)}$	prop. $n_8^{(r)} \rightarrow n_8^{(r+1)}$	prop. $n_8^{(r)} \rightarrow n_9^{(r+1)}$
	0	0	0	0	0	0	0	0	0
9	prop. $n_9^{(r)} \rightarrow n_1^{(r+1)}$	prop. $n_9^{(r)} \rightarrow n_2^{(r+1)}$	prop. $n_9^{(r)} \rightarrow n_3^{(r+1)}$	prop. $n_9^{(r)} \rightarrow n_4^{(r+1)}$	prop. $n_9^{(r)} \rightarrow n_5^{(r+1)}$	prop. $n_9^{(r)} \rightarrow n_6^{(r+1)}$	prop. $n_9^{(r)} \rightarrow n_7^{(r+1)}$	prop. $n_9^{(r)} \rightarrow n_8^{(r+1)}$	prop. $n_9^{(r)} \rightarrow n_9^{(r+1)}$
	0	0	0	0	0	0	0	0	0

Hematological Study of Two Buffalofishes, *Ictiobus cyprinellus* and *I. bubalus* (Catostomidae)

ANNE CHLEBECK AND GARY L. PHILLIPS

Department of Zoology
University of Minnesota, Minneapolis, Minn. 55455, USA

CHLEBECK, ANNE, AND GARY L. PHILLIPS. 1969. Hematological study of two buffalofishes, *Ictiobus cyprinellus* and *I. bubalus* (Catostomidae). J. Fish. Res. Bd. Canada 26: 2881–2886.

A hematological study was made based on 10 specimens each of the buffalofishes *Ictiobus cyprinellus* and *I. bubalus* (Catostomidae). Average results of analyses of selected blood characteristics of *I. cyprinellus* and *I. bubalus*, respectively, were: hemoglobin content, 7.8 and 8.5 g/100 ml; erythrocyte count, 1.08 and 1.28 millions/mm³; hematocrit, 34.6 and 32.9%; mean corpuscular hemoglobin, 67 and 64 μμg; and leucocyte count, 23916 and 29004 cells/mm³. Types of leucocytes noted were lymphocytes, neutrophils, "secretory granulocytes," eosinophils, and thrombocytes. No basophils were found. The secretory granulocyte is apparently derived from the neutrophil series. The status of the secretory granulocyte in buffalofishes is discussed with reference to pertinent literature.

Received July 10, 1969

INTRODUCTION

A HEMATOLOGICAL STUDY of the bigmouth buffalofish, *Ictiobus cyprinellus* (Valenciennes), and the smallmouth buffalofish, *Ictiobus bubalus* (Rafinesque), of the family Catostomidae, was made to further the knowledge of the blood of these species and to investigate a "special" leucocyte in buffalofish blood (Jordan and Speidel, 1924; Jordan, 1938).

MATERIALS AND METHODS

The study was based chiefly on specimens collected in Lake St. Croix at Lakeland, Washington County, Minnesota, in 1968 and 1969. In 1969, specimens were also taken in Lake Tetonka, Waterville, LeSueur County, Minnesota, and from the Mississippi River, Bay City, Pierce County, Wisconsin.

Buffalofishes used in the present study were captured alive in commercial seines. Blood was drawn from all study specimens in the field. The study of general blood properties was based on 10 specimens each of *I. cyprinellus* and *I. bubalus* collected at Lakeland, Minnesota, from August 7 through September 25, 1968. Approximately 2 cc of blood was drawn from the dorsal aorta between the kidneys into a 3-cc disposable syringe coated with an anticoagulant solution of 10% ethylenediaminetetraacetate (EDTA). The blood was transferred immediately into 4-cc vacuum containers coated with 10% EDTA and transported to St. Joseph's Hospital, St. Paul, Minnesota, where laboratory analyses were performed.

Hemoglobin concentrations in grams/100 ml were determined by the standard cyanmethemoglobin method (Wintrobe, 1961; Larsen and Snieszko, 1961).

Printed in Canada (J1523)

Numbers of erythrocytes in millions/mm³ were determined using a Model F Coulter Counter. In order to ascertain how counts obtained through the Coulter Counter compared with counts obtained through the standard chamber erythrocyte count method (Wintrobe, 1961), erythrocytes of five *I. cyprinellus* were counted using both methods. Results agreed, on the absolute average, within 7.46% (extremes 5.47 and 10.48%). The Coulter Counter was used thenceforth because of its greater accuracy (Wintrobe, 1961).

Hematocrits (volume of packed erythrocytes expressed as per cent of volume of whole blood) were determined by filling 75-mm heparinized capillary tubes ⅔ full with whole blood, plugging the tubes with plastic clay, and centrifuging at 11,000 rpm for 20 min. Hematocrit readings were determined by use of a standard tube reader chart.

Mean corpuscular hemoglobins (average amount of hemoglobin per erythrocyte in $\mu\mu g$) were determined by the formula of Wintrobe (1961, p. 403).

Numbers of leucocytes per mm³ were determined by counting the number of leucocytes found per 7000 erythrocytes on blood smears stained with Wright's stain and applying the formula of McKnight (1966, p. 49).

All of the foregoing analyses were performed in duplicate on each specimen.

Blood smears, stained with Wright's stain, were made from buffalofishes taken at Lakeland in 1968 and 1969, and from specimens taken at Waterville and Bay City in 1969. Some slides were stained with Sudan Black B stain.

The nomenclature of blood cell types used herein is essentially that of Jakowska (1956) except that we do not differentiate between "large" and "small" lymphocytes, and we use the term "secretory granulocyte" (taken from Jordan, 1938) for a leucocyte to be discussed further.

RESULTS

The results of the analyses of selected blood characteristics of *I. cyprinellus* and *I. bubalus* are summarized in Table 1. Differences between the two species in these characteristics were analyzed by use of the standard Student's *t*-test (Dixon and Massey, 1957). Using standard length as a measure of fish size, specimens of *I. cyprinellus* in the sample were significantly larger than the *I. bubalus* tested at a 1% level of confidence ($t = 3.26$; df = 11;

TABLE 1. Results of analyses of selected blood characteristics of 10 specimens of the bigmouth buffalofish, *Ictiobus cyprinellus* ("BM") and the smallmouth buffalofish, *Ictiobus bubalus* ("SM").

	Species	Extremes	Mean ± 1 $SE_{\bar{x}}$	Coefficient of variation (%)
Standard length (*mm*)	BM	379–570	439±21.3	15.3
	SM	295–391	362±9.9	8.7
Hemoglobin (*g/100 ml*)	BM	5.4–9.8	7.8±0.6	22.2
	SM	7.2–9.6	8.5±0.3	9.9
RBC[a] (*millions/mm³*)	BM	.71–1.40	1.08±0.08	22.7
	SM	1.06–1.44	1.28±0.04	10.5
Hematocrit (%)	BM	20.0–44.0	34.6±2.76	25.3
	SM	23.5–44.0	32.9±2.19	21.1
Mean corpuscular hemoglobin ($\mu\mu g$)	BM	63–75	67±1.3	6.1
	SM	60–78	64±1.7	8.4
WBC[a] (*no./mm³*)	BM	8046–43259	23916±3310.6	43.8
	SM	12907–45369	29004±3332.1	36.3

[a]RBC = red blood cells; WBC = white blood cells.

$P < .01$). In order to determine if any of the blood properties studied varied with size of fish, graphs were constructed, for both species, in which individual data for each blood characteristic were plotted against standard length. Visual inspection of these charts revealed no obvious trends in variation of blood properties with length, so no corrections for differences in size between the two species were made preceding the statistical analyses. No sexual variation was noted in the blood characteristics examined.

Hemoglobin concentrations, hematocrits, mean corpuscular hemoglobins, and numbers of leucocytes per mm^3 did not differ significantly between the species. Numbers of erythrocytes per mm^3 were significantly higher in *I. bubalus* at a 5% confidence level but not at 2% ($t = 2.26$; df = 12; $.05 > P > .02$). Smith et al. (1952) noted an average of 1,332,000 erythrocytes per mm^3 and an average mean corpuscular hemoglobin content of 52.3 $\mu\mu g$ in four specimens of *I. bubalus* compared to an average of 1.28 million erythrocytes per mm^3 and an average mean corpuscular hemoglobin of 64 $\mu\mu g$ in this species in the present study.

Differential leucocyte counts were not done here. The leucocytes noted, in order of decreasing abundance, were lymphocytes, neutrophils (including advanced stages here termed "secretory granulocytes"), eosinophils, and thrombocytes. No basophils were noted.

Our study of the general blood properties of buffalofish blood was done in late summer. A study done in a different season might have yielded slightly different results, since blood characteristics of fish are known to vary with season and other external factors (see Gardner and Yevich, 1969, for review).

DEVELOPMENT OF THE "SECRETORY GRANULOCYTE"

Both species of buffalofish studied here possess a cell apparently like that noted in *I. bubalus* by Jordan and Speidel and called by them (1924, p. 533) "pseudo-eosinophil or special leucocyte." Jordan (1938, p. 743) apparently referred to the same cell type in describing a "secretory granulocyte" in *I. bubalus*. Jordan attributed the term "secretory granulocyte" to Downey (1909).

The present authors did not note the term "secretory granulocyte" in Downey's (1909) paper. Downey (1909, p. 430) noted seven types of "granular leucocytes" in the kidney of the paddlefish, *Polyodon spathula*. He documented the secretory activities of three of these leucocytes (his Series I, II, and III), and was convinced (p. 432) that three more types were also secretory cells. Because of the rarity of the seventh granular leucocyte, Downey could (p. 432) "say nothing about the origin or function" of its granules. Thus, of Downey's seven types of granular leucocytes, he considered six to definitely be "secretory" and called these "secretory leucocytes," as was correctly noted by Jordan and Speidel (1924, p. 542).

Jordan (1938), seemingly drawing from the discussion of Jordan and Speidel (1924, p. 542), traced the life history of the "secretory granulocyte."

With special reference to these cells in *I. bubalus*, Jordan stated (1938, p. 743):

"They are actively ameboid in earlier stages. These cells have at first a round or oval nucleus and the cytoplasm contains fine eosinophilic granules. Subsequently the nucleus becomes horseshoe shaped or polymorphous. The granules liquefy, swell and coalesce, converting the cells into a goblet-shaped structure, with pale flattened nucleus at the stem pole."

In the present study, various stages of the secretory granulocyte were found in both *I. bubalus* (Fig. 1–4) and *I. cyprinellus*. This cell has apparently not been reported previously in the latter species.

Judging from its morphology in the peripheral blood, the present authors feel that the leucocyte from which the secretory granulocyte develops is a neutrophil. When first seen in peripheral blood this cell has a polymorphous nucleus and cytoplasm containing minute, purple granules. The nucleus then moves toward one side of the cell and whitish vacuoles formed from the dissolving granules begin to appear in the cytoplasm. The granules at this stage resemble granules of Jordan's secretory granulocyte, which (1938, p. 743) "liquefy, swell and coalesce...." The nucleus of the neutrophil is pushed progressively toward the cell's periphery as the cytoplasm becomes filled with large, colorless vacuoles. Advanced stages of this secretory granulocyte resemble in appearance the mammalian lipocyte. To see if our secretory granulocytes did in fact contain fat droplets, some blood smears were stained with Sudan Black B stain. No fat was found in the vacuoles.

Saunders (1966, p. 447) described a "ring cell" from the blood of the balloonfish, *Diodon holacanthus*. She noted the similarity between this ring cell and the cell shown in Downey's (1909) fig. 56. She also noted ways (Saunders, 1966, p. 447–448) in which the ring cell resembles an erythrocyte. She accurately described Downey's fig. 56 as (Saunders, 1966, p. 447):

"...a round cell which, with Wright's stain, had a deep blue-staining, flattened nucleus pushed to one side against the blue-staining, thin cell wall. The rest of the cell's contents was a single featureless, roundish mass of material which stained a rather deep pink and which contained no granules."

In reading Saunders' account, it appears to us that she interprets Jordan's (1938) secretory granulocyte to be the same kind of cell as that shown in Downey's (1909) fig. 56. We do not feel that Jordan's statements are definite enough to establish a specific link between his secretory granulocyte and Downey's fig. 56.

Jordan's secretory granulocyte is, indeed, at some stage, apparently similar to the cell in Downey's fig. 56. Jordan and Speidel (1924, p. 549), upon whose observations Jordan's 1938 account of the secretory granulocyte in *I. bubalus* seems based, show in their fig. 24 a "special granulocyte," which is similar to Downey's fig. 56 but which possesses pale cytoplasmic granules instead of a homogeneous-appearing cytoplasmic mass. Jordan and Speidel (1924, p. 542) and Jordan (1938, p. 743) both state that the granules in their respective "secretory" leucocytes coalesce, an occurrence that would, judging from the

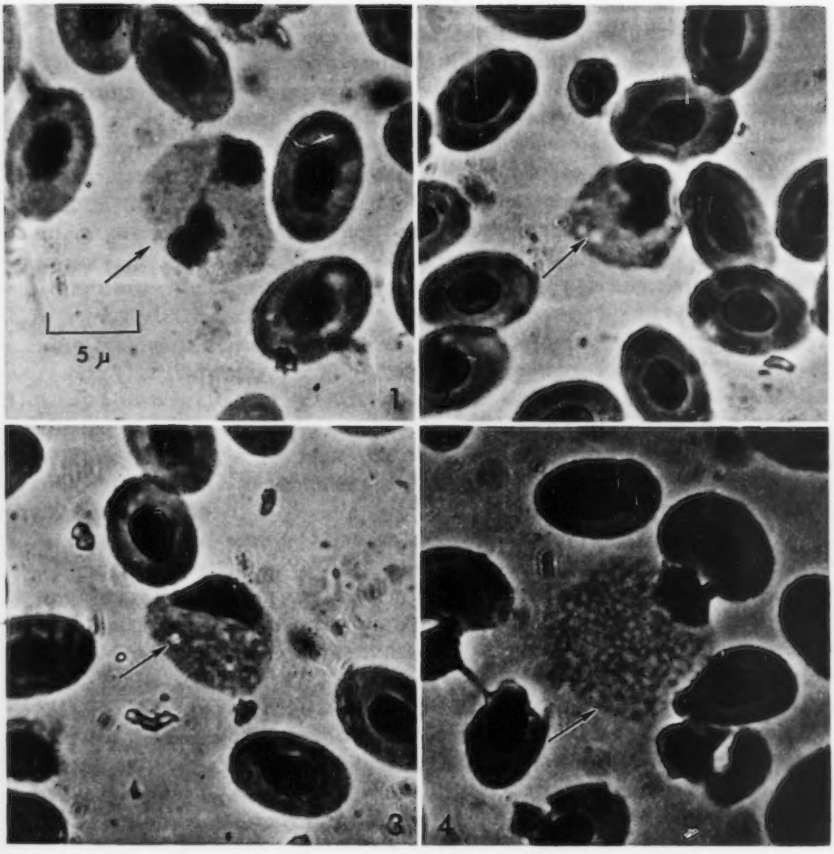

FIGURES 1–4. ***Ictiobus bubalus.***

Fig. 1: Neutrophil (arrow) from a stained blood film showing segmented nucleus and finely granulated cytoplasm; Fig. 2: Neutrophil with nucleus moving peripherally and granules coalescing to form vacuoles (arrow); Fig. 3: Nucleus being pushed further toward edge of cell as granules continue to coalesce (arrow); Fig. 4: Neutrophil (arrow) in advanced ("secretory granulocyte") stage, with nucleus at side and cytoplasm completely filled with vacuoles, which may contain undissolved particles of the coalesced granules.

Chlebeck and Phillips — J. Fish. Res. Bd. Canada

staining properties of the cell shown in Jordan and Speidel's (1924) fig. 24, result in a cell looking much like the one in Downey's fig. 56.

Because of the above considerations, the present authors acknowledge a possible relationship between Jordan's secretory granulocyte and the cell in Downey's fig. 56. However, we interpret Jordan's statements differently than did Saunders. We feel that in stating, "Especially in buffalofish [*I. bubalus*] there occurs the type of granulocyte so abundant in the ganoid, Polyodon, and designated 'secretory granulocytes' by Downey (1909)," Jordan (1938, p. 743) was referring not to any particular one of Downey's granular leucocytes, but was instead referring in a more general way to the series of granular leucocytes that Downey recognized. (We do not imply that Jordan intended to encompass Downey's entire series of granular leucocytes within the term "secretory granulocyte." We do feel, however, that Jordan's description is such that one cannot relate his secretory granulocyte to any particular one of Downey's granular leucocytes.)

As Saunders herself notes (1966, p. 447), Jordan's statement that his secretory granulocyte is "so abundant in the ganoid, Polyodon" contradicts Downey's own statement (Downey, 1909, p. 465) regarding his fig. 56 that "Cells like these are not frequent." The possibility that Jordan was referring broadly to Downey's granular leucocyte series in characterizing secretory granulocytes as "...so abundant..." is bolstered by Downey's statements (1909, p. 434, 436) that certain types of granular leucocytes are abundant in various parts of the *Polyodon* kidney.

Saunders also (1966, p. 447) points out discrepencies between Jordan's description of his secretory granulocyte and the cell shown in Downey's fig. 56. Thus it seems possible that Jordan did not intend that his description of the secretory granulocyte necessarily reflect the appearance of the cell in Downey's fig. 56. It also seems clear to us that the descriptions of Jordan and Speidel (1924, p. 542) and Jordan (1938, p. 743) of their respective "secretory" leucocytes were based on their own observations and did not rely on Downey's descriptions. (We are not certain that the version of Downey's paper read by us is the same as that read by Saunders. She (Saunders, 1966, p. 449) cited the pagination of Downey's article as 415–503 — the article with the same title read by us included pages 415–466, plus two unnumbered pages of figures. Thus, information occurring in the additional pages of Downey's article as read by Saunders was not obtained by us.)

Based on Saunders' (1966) description, it is agreed here that (*a*) the "ring cells" she noted in *Diodon holacanthus* resemble in appearance the cell in Downey's fig. 56, and that (*b*) her ring cells appear to have properties of an erythrocyte. Thus, in our opinion, Saunders established a link between the erythrocyte and the cell in Downey's fig. 56 (which Downey considered a leucocyte). But it is also felt here that the reader relying only upon Saunders' discussion might possibly also associate the secretory granulocyte of buffalofish discussed by Jordan (1938) with an erythrocyte because of Saunders' association of Jordan's secretory granulocyte with Downey's fig. 56, and her

statement (1966, p. 447) that Downey's fig. 56 is "similar" to the erythrocyte-like ring cell in *Diodon holacanthus*.

As noted, our findings suggest that the secretory granulocyte in buffalofish is not an erythrocyte, but is an advanced stage of a cell that fits Jakowska's (1956, p. 534–535) description of a neutrophil. It is felt that the difference between this cell, the "pseudo-eosinophil or special leucocyte" of Jordan and Speidel, and the secretory granulocyte of Jordan is most likely only nomenclatorial. This discussion is presented to give our interpretation of the nature of the secretory granulocyte in buffalofishes in light of the interpretations of previous authors regarding the status of this cell.

ACKNOWLEDGMENTS

The study was possible only through the help of Mr L. F. Miller, Lakeland, Minnesota, and Mr Milton Sorensen, Bay City, Wisconsin, both commercial fishermen, who allowed us access to their operations and donated most specimens used in this investigation. Mr Robert Strand, Minnesota Conservation Department, provided us with specimens of *Ictiobus cyprinellus* from Waterville, Minnesota, in April 1969. Professor William D. Schmid, Zoology Department, University of Minnesota, prepared the photographs shown in the figures and offered consultation on statistical procedures.

REFERENCES

DIXON, W. J., AND F. J. MASSEY, JR. 1957. Introduction to statistical analysis. 2nd ed. McGraw-Hill Book Co., Inc., New York, N.Y. 488 p.

DOWNEY, H. 1909. The lymphatic tissue of the kidney of *Polyodon spathula*. Folia Haematol. 8: 415–466 + 2 p. fig.

GARDNER, G. R., AND P. P. YEVICH. 1969. Studies on the blood morphology of three estuarine cyprinodontiform fishes. J. Fish. Res. Bd. Canada 26: 433–447.

JAKOWSKA, S. 1956. Morphologie et nomenclature des cellules du sang des téléostéens. Rev. Hematol. 11: 519–539.

JORDAN, H. E. 1938. Comparative hematology, p. 703–862. *In* H. Downey [ed.] Handbook of hematology. Vol. 2. Paul B. Hoeber, Inc., New York, N.Y.

JORDAN, H. E., AND C. C. SPEIDEL. 1924. Studies on lymphocytes II. The origin, function, and fate of the lymphocytes in fishes. J. Morphol. 38: 529–549.

LARSEN, H. N., AND S. F. SNIESZKO. 1961. Comparison of various methods of determination of hemoglobin in trout blood. Progressive Fish-Culturist 23: 8–17.

MCKNIGHT, I. M. 1966. A hematological study on the mountain whitefish, *Prosopium williamsoni*. J. Fish. Res. Bd. Canada 23: 45–64.

SAUNDERS, D. C. 1966. Differential blood cell counts of 121 species of marine fishes of Puerto Rico. Trans. Am. Microscop. Soc. 85: 427–449.

SMITH, C. G., W. M. LEWIS, AND H. M. KAPLAN. 1952. A comparative morphologic and physiologic study of fish blood. Progressive Fish-Culturist 14: 169–172.

WINTROBE, M. M. 1961. Clinical hematology. 5th ed. Lea and Febiger, Philadelphia. 1186 p.

Theory of the Exploitation of Tidal Energy and Its Application to the Bay of Fundy

G. GODIN

Marine Sciences Branch
Department of Energy, Mines and Resources of Canada
Ottawa, Ont.

GODIN, G. 1969. Theory of the exploitation of tidal energy and its application to the Bay of Fundy. J. Fish. Res. Bd. Canada 26: 2887–2957.

Considerable progress has been made in the understanding of the concepts underlying the exploitation of tidal energy during the last 20 years; this progress has culminated in the actual construction of a tidal plant at the mouth of the Rance River near St. Malo, France. Since the Bay of Fundy is one of the largest reservoirs of tidal energy in the world, the theory of exploitation of tidal energy has been reviewed with a view to its application to the Bay of Fundy.

The rate of change of the energy contained in an oscillating mass of water in a basin on a rotating earth can be written out using the equations of hydrodynamics. The concept of power transfer arises immediately, which enables one to follow the transit of power from one part of the basin to another. This makes it possible to establish a balance of the power present in the basin.

Only the potential energy present in the tide can be profitably exploited, and it is obtained by enclosing part of the basin by a dam in which some turbines and pumps are imbedded, as well as some complementary sluices. The emptying and filling of the enclosed part of the basin through the turbines during the fall and rise of the sea leads to the production of energy. The upper bounds of the energy available in this way can be easily established and it can also be readily shown that the use of pumps increases the amount of energy available. The actual amount of energy drawn from the reservoir is limited by the smaller range of the tide inside the reservoir and the efficiency of the turbines. The timing and duration of the various operations involved in the operation of a tidal plant, pumping, generating power, opening or closing the sluices, waiting for a head to develop, can be studied quantitatively.

For this purpose the type and number of fundamental operations are carefully studied and accurate definitions are given of them, permitting calculations on a number of possible sequences of operations up to 25 tidal periods. The number of possible sequences is very large and it is not possible to study all of these sequences individually.

Under some circumstances a given sequence of operations for the actual times of starting and stopping the turbines, starting and stopping the pumps, opening and closing the sluices, waiting for a head, and the changes of level inside the reservoir can be calculated with the help of the calculus of variations. For instance, these quantities yield to systematic calculation if the plant is operated with the purpose of producing the maximum amount of energy. The calculus of variations, however, cannot help directly when other modes of operation are considered, such as operating the plant in such a way as to supply power only during peak demand.

The response of the basin to the oscillating ocean will be altered after the construction of the reservoir needed for the operation of the tidal plant. This modification may be important when the plant draws considerable amounts of energy from the tide.

Printed in Canada (J1408)

With the help of the concepts developed it becomes an easy task to make a balance sheet for the tidal power present in the Bay of Fundy, restricting ourselves to M_2, the main lunar semidiurnal constituent that is representative of average conditions. Many sites in the Bay of Fundy are found to be suitable for the generation of energy; some involve relatively simple engineering and yield modest amounts of energy such as the Digby site; others, such as the Minas Channel site, could yield very considerable amounts of energy but the engineering difficulties associated with their construction might prove prohibitive.

Received March 11, 1969

LIST OF SYMBOLS, ABBREVIATIONS, AND UNITS

a	Inverse pumping: water is pumped into the reservoir
b	Direct pumping: water is pumped out of the reservoir
C	Chézy's coefficient
D	Depth of water
E	Energy produced
$\underline{F}$	Force of friction exerted on an element of fluid
f	Friction coefficient $= g\|v\|/C^2D$
g	Acceleration due to gravity $= 9.8$ m/sec^2
h	Height of the surface of the sea above an arbitrary datum, usually the level of the lowest low water
h_0	Amplitude of the vertical tidal oscillation
h_0'	Amplitude of the tidal oscillation inside the reservoir
H	Head of water between the reservoir and the sea
H_m	Minimum head under which a turbine may generate power
k	Friction parameter (dimensionless) $= g/C^2$
m	Semiminor axis of the ellipse drawn by the tidal stream
M	Semimajor axis of the ellipse drawn by the tidal stream
n	Number of turbines in action at a given instant
n_0	Number of turbines installed in the plant
N	Power generated by a turbine
N_0	Maximum power output of a turbine
p	Pressure
$p(t)$	Value of the power generated
$P(t)$	Total value of the power generated
$\underline{P}_a$	Alternating part of the power transfer vector
$\underline{P}_p$	Pulsating part of the power transfer vector
q	Average discharge through a turbine
q'	Actual discharge through a turbine
$\bar{q}$	Value of the discharge through a turbine when the turbine performs at peak efficiency
q_m	Minimum discharge for which a turbine may generate power
Q	Discharge out of the plant
s	Area of the vertical cross section
$S(z)$	Horizontal area of the reservoir at a level z
t	Time
T	Duration of a tidal period
$\underline{T}$	Tidal force exerted on an element of fluid
$\underline{v} = (u,v,w)$	The velocity vector with its x, y, z components pointing towards the east, the north and downwards
V	Volume of water contained in the reservoir between low and high water
V_0	Maximum discharge through the sluices for a given head H
z	Level inside the reservoir

0	Wait: the level is kept constant inside the reservoir
1	Turbines on while the reservoir is being emptied
2	Turbines on while the reservoir is being filled
3	Contact: the level of the reservoir follows the level of the sea
α	Inclination of the semimajor axis of the tidal stream ellipse with respect to the east
β	Difference between the phase of the tide in the basin and the phase of the tide in the sea just outside the basin
ζ	Efficiency coefficient of a pump
η	Efficiency coefficient of a turbine
λ	Ratio of the number of turbines in operation to the number of turbines installed
μ	Phase of the tidal stream vector
ν	Phase of the vertical tidal oscillation
ρ	Density of sea water
σ	Frequency of the tidal oscillation; for M_2, $\sigma = 28.9°/hr$
Ω	Angular of the velocity of the earth's rotation $= .729 \times 10^{-4}$ sec^{-1} at the equator
$\underline{\nabla}$	Grad operator
m	Meter
km	Kilometer
kw	Kilowatt
kj	Kilojoule

GENERAL THEORY OF THE EXPLOITATION OF TIDAL ENERGY

Energy Contained in an Oscillating Basin

BASIC EQUATIONS

The equations of hydrodynamics that describe the motion of a mass of water in an oceanic basin are

$$\frac{d\underline{v}}{dt} + 2\Omega \times \underline{v} = -\frac{1}{\rho}\underline{\nabla}p + \underline{G} + \underline{T} - \underline{F} \tag{1}$$

$$\underline{\nabla}\cdot\underline{v} = 0 \tag{2}$$

if we assume that the fluid is incompressible and that its density ρ is constant.

The components (x, y, z) point toward east, north, and downwards, respectively.

$\underline{v} = (u, v, w)$ is the velocity vector, $[v] = m/sec$

Ω = angular velocity vector of the earth's rotation. In practice we take $\Omega = (0, 0, \Omega)$ where $\Omega = .729 \times 10^{-4} \sin \varphi$ sec^{-1}, φ being the mean latitude of the sea.

ρ = density of the fluid, $[\rho] =$ tons sec^2/m^4

p = pressure, $[p] =$ tons/m^2

$\underline{G}$ = acceleration due to gravity. $\underline{G} = (0, 0, g)$ and $g = 9.8$ m/sec^2

$\underline{T}$ = tidal force per unit mass exerted on an element of the fluid. $[T] =$ m/sec^2

$\underline{F}$ = force per unit mass exerted by the friction on an element of fluid. We assume the quadratic law of friction.

$$\underline{F} = \frac{g\,\underline{v}\,v}{C^2 D}$$

where C is the Chézy coefficient. $[C] = m^{\frac{1}{2}}/sec$

D = the depth of the fluid at a given point. $[D] =$ meters

To evaluate the rate of change of the energy in an element of the fluid we take the dot product of $\underline{v}$ with equation 1 and using equation 2 obtain

$$\underline{\nabla}\cdot p\underline{v} = -\frac{d}{dt}\left(\tfrac{1}{2}|\underline{v}|^2\rho + \rho gz\right) + \rho\underline{v}\cdot(\underline{T} - \underline{F}). \tag{3}$$

By making use of the divergence theorem in taking the volume integral of equation 3 over the volume element of the fluid bounded by the surface S, we get

$$\int dS\, p\, v_n = \int dx dy dz\left[\frac{d}{dt}\left(\tfrac{1}{2}|\underline{v}|^2\rho + \rho gz\right) - \rho\underline{v}\cdot(\underline{T} - \underline{F})\right]. \tag{4}$$

v_n is the component of velocity perpendicular to the boundary surface S at a given point and pointing inward.

We see that the rate of work done by the pressure forces over the surface bounding a given volume of fluid equals the total rate of change of the kinetic and potential energy inside the fluid plus the work done by the tidal and frictional forces.

We may consider the quantity $p\underline{v}$, often referred to as energy flux density, as a *power transfer vector* that affects the potential and kinetic energy of an element of fluid contained in a given volume.

Equation 4 can be written more explicitly for the case in which the vertical acceleration of the fluid particles can be neglected. This is precisely the case of tidal motion (Schönfeld, 1956). Then by replacing the third component of equation 1 with the hydrostatic equation, equations 1 and 2 can be written as

$$\frac{d\underline{v}}{dt} + 2\Omega\times\underline{v} = -g\underline{\nabla}h - \frac{g|\underline{v}|\underline{v}}{C^2D} + \underline{T} \tag{5}$$

and

$$\underline{\nabla}\cdot D\underline{v} + \frac{\partial h}{\partial t} = 0 \tag{6}$$

in which all the vectors may be considered as two dimensional with the exception of $\underline{\Omega}$. h is the perturbation height that measures the displacement of the surface of the fluid from its equilibrium position.

We assume that the motion is periodic with the period $\frac{2\pi}{\sigma}$. This implies that $\frac{d}{dt} \rightarrow \frac{\partial}{\partial t}$ since periodic motion can only occur under some restrictions, if we retain the convective operator $u\frac{\partial}{\partial x} + v\frac{\partial}{\partial y}$.

The two-dimensional vectors can be represented by complex numbers and written as

$$h = h_1 e^{i\sigma t} + h_2 e^{-i\sigma t} \tag{7}$$

$$\underline{v} = u + iv = v_1 e^{i\sigma t} + v_2 e^{-i\sigma t} \tag{8}$$

where

$$h_1 = h_2^* = \tfrac{1}{2} h_0 e^{i\nu}$$

$$v_1 = \tfrac{1}{2}(M + m)\, e^{i(\alpha+\mu)}$$

$$v_2 = \tfrac{1}{2}(M - m) e^{i(\alpha-\mu)}.$$

h_0 is the amplitude, in meters, of the vertical oscillation. ν and μ are the phases of h and $\underline{v}$ measured from some arbitrary time origin (in tidal practice, phase lags are used and they are measured from the meridian transit of the "astre fictif" corresponding to the chosen tidal constituent, over Greenwich). M and m are the semimajor and semiminor axes of the ellipse drawn by the tidal stream vector during one tidal period. α is the inclination of the major axis with respect to the chosen x direction. h_0, M, m, α, μ, and ν are real quantities.

We note

$$v_1 \neq v_2^*$$

in contrast to

$$h_1 = h_2^*.$$

In this notation, $2\Omega \times v$ may be represented by

$$2i\Omega\ (u + iv) = 2i\Omega(v_1 e^{i\sigma t} + v_2 e^{-i\sigma t}).$$

The dot product $a \cdot b$ becomes $\frac{1}{2}(a^* b + a b^*)$ in the new notation. $e^{i\sigma t}$ and $e^{-i\sigma t}$ are linearly independent and they behave like orthogonal basic vectors. Thus by taking their components in equations 5 and 6:

$$[i(\sigma + 2\Omega) + f]\, v_1 + g\nabla + h_1 = T_1 \tag{9a}$$

$$[i(-\sigma + 2\Omega) + f]\, v_2 + g\nabla + h_2 = T_2 \tag{9b}$$

$$\nabla_-(Dv_1) + \nabla_+(Dv_2^*) + 2i\sigma h_1 = 0$$

and

$$\nabla_-(Dv_2) + \nabla_+(Dv_1^*) - 2i\sigma h_2 = 0 \tag{10}$$

where

$$f = \frac{g|\underline{v}|}{C^2 D}$$

and

$$\nabla_\pm = \frac{\partial}{\partial x} \pm \frac{\partial}{\partial y}.$$

Naturally we have also written $\underline{T} = T_1 e^{i\sigma t} + T_2 e^{-i\sigma t}$ since the response of the basin must have the same oscillatory character as T.

To obtain an expression analogous to equation 3, we multiply the complex conjugate of equation 9*a* by $\rho D v_1$, equation 9*b* by $\rho D v_2^*$, and the first form of equation 10 by $\rho g h_1^*$. By adding and rearranging we obtain:

$$\nabla_- P_1 + \nabla_+ P_2^* = \tfrac{1}{2} i\sigma\rho \, [D(M^2 + m^2) - h_0^2 g] + 2i\Omega D \, \rho M m + \rho D(v_1 T_1^* + v_2^* T_2) - \tfrac{1}{2} f D \rho \, (M^2 + m^2) \qquad (11)$$

in which the quantities

$$P_1 = \rho g D h_1^* v_1 \qquad P_2 = \rho g D h_2^* v_2 \qquad (12)$$

have been introduced and which are related to the power transfer vector

$$\underline{P} = \rho g D h \, \underline{v}$$

mentioned previously, integrated over the vertical since the motion is assumed uniform throughout the vertical.

Equation 11 is certainly more explicit than 3 since each of its terms admits of a physical interpretation. At first sight, we note that $\nabla_- P_1 + \nabla_+ P_2^*$ is the counterpart of $\underline{\nabla} \cdot p\underline{v}$, and $\rho i\sigma \tfrac{1}{2}(D(M^2 + m^2) - h_0^2 g)$ reflects $\dfrac{d}{dt} \, (\tfrac{1}{2} |\underline{v}| \, 2\rho + \rho g z)$ and

$$D(v_1 T_1^* + v_2^* T_2) - \tfrac{1}{2} f D \rho \, (M^2 + m^2)$$

corresponds to $\rho \underline{v} \cdot (\underline{T} - \underline{F})$. The change in rotational energy introduced by the Coriolis acceleration $2i\Omega\rho D M m$ has no counterpart in equation 3, yet the term does not vanish as long as the current is rotational ($m \neq 0$). It would have been absent, had we taken the dot product of equation 5 with $\underline{v}$, as was done for equation 1.

Before investigating equation 12 further, let us examine the components of the power transfer vector P_1 and P_2.

POWER TRANSFER VECTOR $\underline{P}$

If, at a given point (x, y, z) of the basin, the velocity is $\underline{v}$, the rate of work done by the pressure across a narrow vertical section perpendicular to the velocity vector is

$$\int_0^{D+h} \rho g z \, \underline{v} \, dz = \tfrac{1}{2} \, \rho g \underline{v} (D^2 + 2Dh + h^2) \qquad (13)$$

and if as before $\underline{v}$ does not vary vertically. If $\underline{v}$ and h oscillate with the same period, the average value of $\underline{v}D^2$ and $\underline{v}h^2$ over such a period is 0, whereas the average value of $\underline{v}h$ may be distinct from 0 over the same interval if $\underline{v}$ and h are not 90° out of phase. The net rate of transfer of power will therefore take place across the section through the term $\rho g \underline{v} D h$ in equation 13. We note that this term is formally identical to the quantity P introduced in equation 11.

As stated already, part of P may have a 0 average over a period whereas another part may have a nonzero average. Equation 11 indicates explicitly the terms to which the alternating and constant parts of P correspond in terms

of kinetic and potential energy (inductance and capacitance in electrical usage) and of the Coriolis acceleration (gyro reactance).

$\underline{P}$ can be expressed then as $\underline{P} = \rho g D h \underline{v}$ in terms of the quantities h_1, h_2, v_1, and v_2 or

$$\begin{aligned}\underline{P} &= \rho g D h \underline{v} = \rho g D (h_1 e^{i\sigma t} + h_2 e^{-i\sigma t})\,(v_1 e^{i\sigma t} + v_2 e^{-i\sigma t}) \\ &= \rho g D\,[(h_2 v_1 + h_1 v_2)\,(1 + \cos 2(\sigma t + \nu) + i(h_2 v_1 - h_1 v_2)\sin 2(\sigma t + \nu)] \\ &= (P_1 + P_2)\,(1 + \cos 2(\sigma t + \nu)) + i(P_1 - P_2)\sin 2(\sigma t + \nu). \qquad (14)\end{aligned}$$

The nonoscillating part of $\underline{P}$ is

$$P_1 + P_2 \qquad (15)$$

and its oscillating part is

$$(P_1 + P_2)\cos 2(\sigma t + \nu) + i(P_1 - P_2)\sin 2(\sigma t + \nu). \qquad (16)$$

The function $1 + \cos 2(\sigma t + \nu)$ behaves like a pulse with average value 1 over a period, so that the power transfer vector may be written in terms of pulsating power transfer and alternating power transfer:

$$\underline{P} = \underline{P}_p(1 + \cos 2(\sigma t + \nu) + \underline{P}_a \sin 2(\sigma t + \nu) \qquad (17)$$

where

$$\underline{P}_p = P_1 + P_2$$
$$\underline{P}_a = i(P_1 - P_2).$$

By equating real and imaginary parts, equation 11 yields:

$$\underline{\nabla} \cdot \underline{P}_p = -\tfrac{1}{2} f D(M^2 + m^2)\rho + \rho g D(v_1 T_1^* + v_2^* T_1)_R \qquad (18)$$

and

$$\underline{\nabla} \cdot \underline{P}_a = \tfrac{1}{2}\sigma D(M^2 + m^2)\rho - \tfrac{1}{2}\sigma g h_0^2 + 2\Omega D M m \rho + \rho g D(v_1 T_1^* + v_2^* T_1)_I \qquad (19)$$

since

$$P_1 + P_2^* = P_{p_x} - iP_{a_x} \text{ and } -i(P_1 - P_2^*) = P_{p_y} - iP_{a_y}$$

then

$$(P_{p_x}, P_{p_y}) \text{ and } (P_{a_x}, P_{a_y})$$

are the components in the x and y directions of the pulsating and oscillating power transfer vectors $\underline{P}_p$ and $\underline{P}_a$.

A volume integral of equations 18 and 19 with a volume element $dxdydz$, taking account of our restrictive assumptions, and using the divergence theorem, yields

$$\int_1 dx\, P_{p_y} - \int_2 dx\, P_{p_y} = \int dx \int dy\,[-\tfrac{1}{2}\rho f D\,(M^2 + m^2) + \rho g D(v_1 T^*_1 + v_2^* T_2)_R] \qquad (20)$$

and

$$\int_1 dx\, P_{a_y} - \int_2 dx\, P_{a_y} = -\int dx \int dy$$
$$[\tfrac{1}{2}\rho\sigma D\,(M^2 + m^2) - \tfrac{1}{2}\rho\sigma g h_0^2 + 2\Omega D\rho M m + \rho g D(v_1 T_1^* + v_2^* T_2)_1]. \qquad (21)$$

1 and 2 label the two vertical surfaces that delineate the volume of water considered.

Equation 20 gives the amount of tidal power lost over the basin, the loss being caused by friction and retardation of the sun or of the moon. In the latter instance, the loss may actually be a gain depending on the phase of the moon or of the sun with respect to the phase of the tide in the basin (Taylor, 1919).

Equation 21 measures the amplitude of the power that is oscillating in the volume considered. The net change of energy is 0 over a period but the actual amount of energy present at a given moment may be considerable.

If tidal current observations over the basin and coastal observations of the tide are available, it is possible to draw relatively accurate cotidal charts for a given tidal constituent. This can be done by smoothing away the unevenness of the coastal observations and checking the consistency of the whole of the observations using the integrated form of the equation of continuity (equation 6). The dynamical equations do not normally check out as well on account of the need for determining the gradients in h quite accurately, as well as the need for a fair estimate of the Chézy coefficient C.

As a matter of fact, C may be obtained from equation 20 since all the other quantities are given by observations. Having obtained C in this way, it is quite evident that the checking of equations 5 and 6 is no longer absolute since equation 20 is derived from them.

COMPARISON BETWEEN HYDRAULIC AND TIDAL POWER AND SOME ORDERS OF MAGNITUDE

The potential energy contained in a column of water of horizontal section S and height D amounts to $\frac{1}{2}\rho g S D^2$. If this water is now allowed through some turbines, assuming no loss, the power generated by the turbines amounts initially to

$$P = \frac{d}{dt}\,(\tfrac{1}{2}\rho g S D^2) = \rho g S D \cdot \frac{dD}{dt} = \rho g D Q \qquad (22)$$

Q being the discharge through the turbines, in m^3/sec.

In a fall the water is continuously replenished and the height D is not allowed to change. Therefore the power produced by a fall of water of height D and of discharge Q amounts to $\rho g D Q$ kw. If the height and discharge are kept constant over a finite interval of time T, the total energy released during this interval amounts to

$$E = \rho g D Q T \text{ kj}. \qquad (23)$$

In the previous paragraph an expression analogous to equation 22 was found for the power transferred across a section by a tidal oscillation. To

make some comparisons between the magnitudes of the two types of power using some concrete examples, we have selected Niagara Falls and Minas Channel in the Bay of Fundy.

For Niagara Falls

$$D = 55 \text{ m} \qquad Q = 6 \times 10^3 \text{ m}^3/\text{sec}$$

which gives

$$P_N = \rho g D Q = 3{\cdot}3 \times 10^6 \text{ kw}.$$

The vertical amplitude of the M_2 tidal oscillation in Minas Channel amounts to 4.3 m. The semimajor axis of the M_2 tidal stream has a length of 2.1 m/sec.

There is a phase difference of 68° between the horizontal and the vertical oscillation. The channel has a vertical section of 4.8×10^5 m^2 so that the amplitude of the pulsative and alternative power transfers are

$$P_p = 21.3 \times 10^6 \cos 68° = 7.9 \times 10^6 \text{ kw}$$

$$P_a = 21.3 \times 10^6 \times \sin 68° = 19.8 \times 10^6 \text{ kw}.$$

P_p is lost in Cobequid Bay mainly through friction. Both P_p *and* P_a may be used at the site of Minas Channel to generate energy.

In the examples studied, the amounts of power available are therefore of comparable magnitude although physical structures such as Niagara Falls and Minas Channel are rather rare.

Exploitation of Tidal Energy

Some practical schemes of exploitation

The energy in a tided ocean exists mainly as kinetic and potential energy, so the question arises immediately as to which form of energy is more suitable for exploitation. In other words, should one try to put the tidal streams to work or the vertical tide. In fact, the choice is very easy to make. For 1 ton of water moving at a speed of v m/sec at an elevation of z m above the reference level, its kinetic and potential energy are respectively $\frac{1}{2}v^2$ and gz kj. If we take $v = 2$ m/sec, a relatively large value for a tidal stream, and $z = 5$ m, a relatively small value for a vertical tide especially in the Bay of Fundy, the two types of energy amount to 2 kj and 49 kj, respectively, a ratio of 25:1. To exploit the kinetic energy, one must use a device analogous to a wind mill (Remenieras and Smagghe, 1956) totally immersed in the water and firmly anchored at the bottom; the surface of the propeller must amount to many square meters to obtain a reasonable power output. The practical use of such a device accompanied by the promise of an unavoidably small power output certainly does not make the exploitation of tidal streams very promising. So one must turn towards the vertical tide.

The practical way of exploiting tidal energy (Maynard, 1919; Davey, 1923) consists in enclosing part of the tided basin, which we shall call the *basin* (or the *reservoir*), and in generating energy with the help of hydroelectric turbines by filling the basin when the level inside it is lower than outside or by emptying it for the opposite situation. We call the portion of the tided basin that is in communication with the ocean, the *sea*.

The amount of energy generated over a tidal period depends on the range of the tide outside the basin and on the storage capacity of the basin between low and high water. As we have already stated in the previous paragraph, the alternating part of the tidal energy may be used for this purpose as well as the pulsating part.

The bare scheme of exploitation just described may be modified in an indefinite number of ways to fit the type of turbines used in the system and the configuration of the part of the basin serving as a reservoir.

Energy may be generated only while the tide is falling. This cannot be avoided if the turbines can only generate in one direction of flow or if their capacity is so small that the reduction in the range of the tide inside the basin has reached a point where more energy may be generated by opening the sluices from low to high water to build an appreciable head during the emptying of the basin between high and low water. This applies especially for shallow water tides that rise rapidly and then fall less rapidly. Also, on account of the usual vertical convergence of the sides of the reservoir, more energy is obtained, for the same initial head, by emptying it than by filling it.

Two basins may be exploited concurrently. One basin is kept at a level higher than that of the sea and energy is generated while it is being emptied. The other basin is kept at a level lower than that of the sea and energy is generated while it is being filled. In this fashion energy may be generated from the tide almost continuously using a simple type of turbine that can generate energy only for one direction of flow. The two reservoirs need not be in the immediate vicinity of each other. Then the time difference between the occurrence of high and low water at the mouth of the two reservoirs makes even easier the continuous overlap of their energy production.

In the scheme mentioned there is no communication between the basins. In fact, for some geographical configurations, turbines may be installed between the two reservoirs. If this is feasible, the turbines are installed between the two basins to exploit the difference in level. The two basins are in communication with the sea through sluices only.

To conclude we must state that all the schemes involving more than a single basin were conceived in the older days when continuous power production was considered essential. In fact these schemes invariably lead to a smaller energy output and to an inefficient utilization of the tidal energy. Nowadays they tend to be disregarded in favour of the single basin in direct communication with the sea.

AMOUNT OF ENERGY GENERATED BY THE SUDDEN EMPTYING OR FILLING OF A BASIN AT LOW OR HIGH WATER

To evaluate the maximum energy that can be obtained from the basic scheme of exploitation just mentioned, we consider the situation in which the energy is drawn all at once by emptying or filling the basin suddenly at low or high water. This mode of exploitation does not make sense physically but it helps in fixing the upper bounds of the energy actually available. In practice the amount of energy obtained will always be less than the amount calculated in this way.

The horizontal surface area $S(z)$ of the storage basin normally varies with the depth of water z. The potential energy stored in the basin after it has been filled to a height $2h_0$ above the low water level amounts to

$$E_e = \rho g \int_0^{2h_0} S(z) z dz. \tag{24}$$

This represents the amount of energy that would be collected if the basin were suddenly emptied at low water.

If the basin is then closed while the tide is rising, the energy obtained by filling it up suddenly at high water amounts to

$$E_f = \rho g \int_0^{2h_0} S(z) \ (2h_0 - z) dz. \tag{25}$$

The total amount of energy drawn over one tidal period is

$$E = E_e + E_f = \rho g 2h_0 V \tag{26}$$

where

$$V \doteq \int_0^{2h_0} S(z) dz,$$

the storage capacity of the basin between low and high water.

Equation 26 indicates that the energy that may be drawn from the basin over one tidal period is directly proportional to the range of the tide $2h_0$ and to the storage capacity of the basin between low and high water. If the basin had a constant surface area over the range of the tide, the total amount of energy generated would be

$$E = \rho g S_0 (2h_0)^2$$

S_0 being the constant surface area of the basin.

In general we may always write

$$S(z) = S_0 + f(z) \qquad f(z) \geq 0$$

S_0 being the section of the basin at low water, so that the energy generated depends at least on the square of the range if not on a higher power. Therefore, for two basins of the same storage capacity, if the ratio of the range of the tide at their mouths is 2:1, the ratios of the amounts of energy generated are at least in the ratio 4:1. *Hence the interest in locating tidal plants in areas where the tide has a large range.*

Now we look at the energy available from Cobequid Bay if a dam were installed across Minas Channel (see Fig. 8). The surface of the reservoir amounts to about 8.5×10^8 m^2 and we take it to be a constant over the range of the tide. The range is 10 m and the period of the M_2 tide is 12.4 hr. For the basin under consideration, we therefore have

$$E = 8.5 \times 10^{11} \text{ kj.}$$

We recall that the amount of energy that would be supplied by the pulsating part of the power transfer vector is

$$E_p = P_p \times T = 1.5 \times 10^{11} \text{ kj}$$

so that

$$E_p < E.$$

It is evident, therefore, that for such an exploitation we have to draw some energy from the alternating part of the power transfer vector since some of the energy that is normally returned to the sea over the next half period will be retained in the bay. In turn this implies that the tidal regime of the Bay of Fundy will be modified by the installation of the tidal power plant. This point will be discussed further.

We have yet to show that the sudden emptying or filling of the basin represents the maximum energy that can be drawn from the basin. Any other type of exploitation stretching over a finite amount of time will yield less energy. This can be seen with the help of some qualitative reasoning.

Suppose that we start emptying the basin for a head H less than $2h_0$, then we will be able to draw energy till the level of the basin coincides with that of the sea. The sea level will go to zero during the course of the exploitation and it will reach some new level $h_2 = z_2$ when both the basin and the sea are level. The energy effectively drawn from the basin will be less than the potential energy of the mass of water contained in 1 and 2 (Fig. 1), 1 representing the volume of water shed by the basin while the sea was going down, and 2 the volume shed while the sea was rising. This volume is evidently less than the volume considered at the beginning of this paragraph.

ADVANTAGE OF PUMPING

The amount of energy given by equation 26 is the maximum amount of energy that may be obtained by the simple emptying and filling of the basin during one tidal period. This amount may be increased if the technique of exploitation is complicated by the additional operation of pumping water into the basin at high water or out of the basin at low water. The energy spent by the pumping operation will be more than compensated by the energy gained from the larger vertical trajectories of the added masses of water (Gibrat, 1966). The law of conservation of energy is not violated by this process, the extra energy gained being drawn from the energy present in the sea.

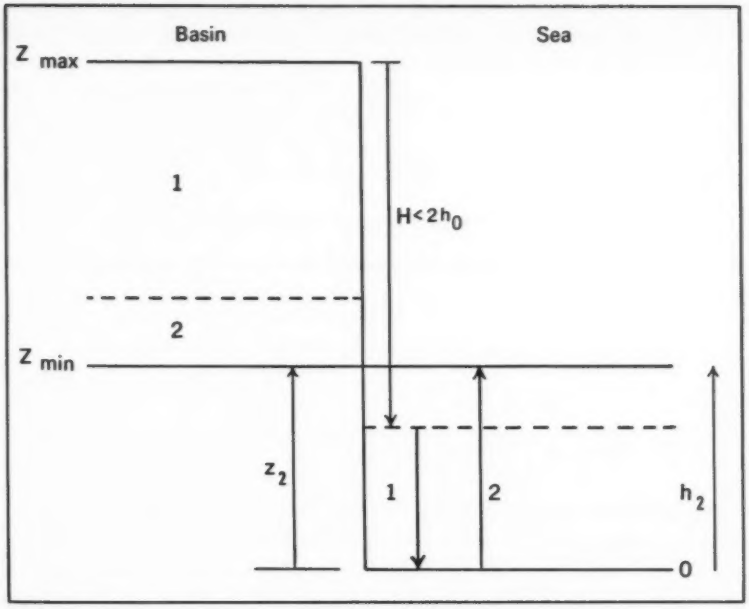

FIG. 1. Oscillations of the levels of the basin and of the sea during one tidal period. 1 indicates the volume of water involved while the tide is falling, 2 the volume involved while the tide is rising. The range of the oscillation in the basin is smaller than in the sea.

The technique of exploitation consists now in the following operations:

(1) At low water, water is pumped *out* of the basin so that its level is lowered to $-h_1$. The energy *spent* to accomplish this amounts to

$$E_{p_1} = \rho g \int_0^{-h_1} S(z) z dz. \tag{27}$$

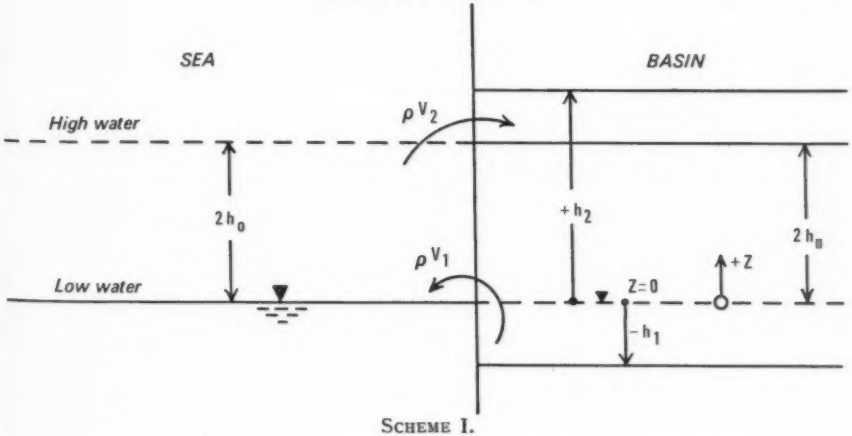

SCHEME I.

(2) At high water, the basin is filled suddenly to a level $2h_0$. The energy *gained* by this operation amounts to

$$E_f = \rho g \int_{-h_1}^{2h_0} (2h_0 - z) S(z) dz. \tag{28}$$

(3) At high water, water is pumped into the basin to a level h_2. The energy *spent* in doing this is

$$E_{p_2} = \rho g \int_{2h_0}^{h_2} (z - 2h_0) S(z) dz. \tag{29}$$

(4) At low water, the basin is emptied at once. The energy *gained* is

$$E_e = \rho g \int_0^{h_2} S(z) z dz. \tag{30}$$

The total energy gained from the sequence of operations is

$$\begin{aligned} E &= -E_{p_1} + E_f - E_{p_2} + E_e \\ &= \rho g \left[-\int_0^{-h_1} S(z) dz + \int_{-h_1}^{2h_0} (2h_0 - z) S(z) dz - \int_{2h_0}^{h_2} (z - 2h_0) S(z) dz + \int_0^{h2} S(z) z dz \right] \\ &= \rho g \left[\int_{-h_1}^{h_2} S(z) z dz + \int_{-h_1}^{h_2} (2h_0 - z) S(z) dz \right] \\ &= \rho g 2h_0 \int_{-h_1}^{h_2} S(z) dz \\ &= \rho g 2h_0 (V + V_1 + V_2) \end{aligned} \tag{31}$$

so that

$$E = \rho g 2h_0 (V + V_1 + V_2)$$

where

V = the storage capacity of the basin between $z = 0$ and $z = 2h_0$
V_1 = the storage capacity of the basin between $z = 0$ and $z = -h_1$
V_2 = the storage capacity of the basin between $z = 2h_0$ and $z = h_2$

The energy gained has therefore been increased by an amount proportional to the volumes of water pumped at high and low water in spite of the energy spent in carrying out the pumping. This at least is what the algebra says. But the process has to be visualized closer physically to ascertain that we are not dealing with a paradox.

Let us consider what happens to a mass of water ρV_2 that is pumped into the basin at high water. Its elevation above the reference level is h_2. When the basin is emptied at low water, it travels through a vertical distance h_2 and it does work to the amount of $\rho g V_2 h_2$. However, it was necessary to expend the amount of energy $\rho g V_2 (h_2 - 2h_0)$ to raise it to h_2 from the level $2h_0$ at high water. The net gain of energy is $\rho g V_2 2h_0$, which coincides with the third term of equation 31.

Energy is gained by this process in spite of the work expended on account of the larger trajectory travelled by V_2 during the emptying of the basin. This extra energy is by necessity supplied by the ocean.

In a practical exploitation the extra energy gain implied by pumping is limited by the efficiency of the pumps and by the time lost in pumping since

pumping takes a finite amount of time and the level outside the basin varies continuously. If we denote by a prime the energy obtained or expended in a practical exploitation, we always have

$$E_{p_1'} > E_{p_1},\ E_{p_2'} > E_{p_2},\ E_f' < E_f,\ \text{and}\ E_e' < E_e$$

so that the total energy gain in a practical exploitation is

$$E' = E_f' + E_e' - E_{p_1}' - E_{p_2}' < E_f + E_e - E_{p_1} - E_{p_2} \gtrless E_f' + E_e'. \tag{32}$$

The first inequality is certain, the second inequality will be used to determine if pumping actually leads to a gain of energy over the straightforward operation.

Thus, in spite of its theoretical attractiveness, the use of pumping will be limited by practical considerations.

Practical Limitations to the Amounts of Energy Actually Available

Smaller range of the tide inside the reservoir

The very presence of turbines between the reservoir and the sea limits in many ways the amount of energy that may be extracted from the tide. First, the vertical cross section of the reservoir at the dam site is effectively reduced from the value it had before the construction of the plant. To obtain the same range of tide as before, inside the reservoir, higher velocities of flow through the turbines are necessary. These higher velocities are limited by the value of the effective head at the dam site, the maximum flow that the structure of the turbines can endure, and the flow that must be maintained inside the turbines to obtain the optimum conditions of exploitation. The net result of all this is that the range of the tide inside the reservoir is reduced to a value $2h_0'$, smaller than the range $2h_0$ that prevailed before the construction of the dam.

Since the turbines obstruct the flow in and out of the reservoir, it is evident that the more turbines are installed and the larger their admittance, the larger will be the range of the oscillation in the reservoir and therefore the larger the upper bound of the energy available from the reservoir. Reasons of economics, structural strength, and electrical engineering limit the number of turbines to a finite number.

The range of the oscillation inside the basin is therefore reduced on account of the finite time taken for the extraction of the energy and the reduction of the effective cross section of the reservoir at the dam site.

Figure 2 shows the superposition of the tidal oscillation in the sea (which is taken to be sinusoidal throughout the paper unless stated otherwise) and the fluctuation in level of the reservoir for the case of ideal exploitation. In this example, fluctuations of level occur during a practical cycle of exploitation when the reservoir is emptied or filled.

The actual range of the tide inside the reservoir is $2h_0' < 2h_0$. The area shaded indicates the time interval during which energy is effectively generated. The head of water H over the turbines is less than $2h_0$ but it may exceed $2h_0'$

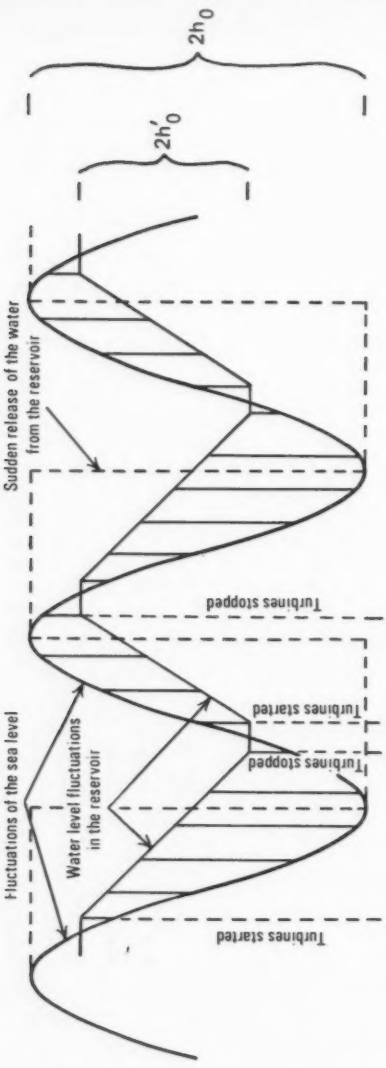

FIG. 2. Fluctuations in the levels of the basin and of the sea on a time scale. The broken lines represent the fluctuations in the level of the basin for the hypothetical case in which the basin is emptied or filled suddenly at low or high water. The solid lines delineate the real fluctuations of the basin level. The instants when energy production is started or stopped are indicated on the horizontal scale.

at times. It varies from 0 at the instant the reservoir is cut off from the sea to a maximum value near high or low water. Its average value $\overline{H}$ must have the same magnitude as h_0 or less.

The energy gained by emptying or filling the reservoir through the turbines over a tidal period amounts to

$$E = \int_{t_1}^{t_2} \rho g\, Q(t)\, H\, dt + \int_{t_3}^{t_4} \rho g\, Q(t)\, H\, dt \qquad (33)$$

t_1, t_2, t_3, and t_4 indicating the times at which the turbines are turned on or off. QH is essentially a positive quantity when energy is generated.

For the sake of simplicity, although this should not be done in practice, one can assume the surface of the reservoir to be a constant S_0 over the range of the tide. Also, we note that the conservation of mass gives

$$Q = S(z) \frac{dz}{dt} \tag{34}$$

z denoting the level of the reservoir.

Thus equation 33 becomes

$$E = \rho g S_0 2 \int_0^{2h_0'} H dz \simeq \rho g S_0 2\overline{H}\ 2h_0' < \rho g S_0 2\overline{H}\ 2h_0 \leq \rho g S_0 (2h_0)^2,$$

which confirms the conclusion that had been reached qualitatively previously.

CHOICE, TIMING, AND DURATION OF THE OPERATIONS

In the practical scheme of operation depicted in Fig. 2, energy must start being drawn soon after the sluices have been closed after high water and not at the next low water as the ideal scheme might suggest. The instant at which the turbines are started is of fundamental importance, and many conflicting factors affect this decision.

The turbines cannot be put in operation till a minimum head difference is established between the reservoir and the sea since ordinary turbines need a minimum head before energy can be produced. The starting time must therefore occur when the minimum head is established or sometime later.[1]

The power generated is a function of QH and an early start implies a small head H and initially a low yield of energy. Under such conditions the head cannot increase rapidly since the level of the reservoir is lowering. Increasing the discharge Q would worsen the head situation, and decreasing Q would improve the head but it might not improve the energy output significantly. A late start, closer to the next low water, implies a good head H, initially. In this instance the power yield is further improved by the need of a large discharge factor, Q, to drain the reservoir as rapidly as possible and to generate as much energy as possible for the next half cycle.

The alternatives are then a large burst of power over a short interval of time or a prolonged production of energy at low power. A starting time can be chosen for a preset lowering of the level by $2h_0'$ over a half tidal period that will yield the maximum energy. This in turn will affect the amount of energy available for the next half period, but qualitative reasoning cannot go further in determining the ideal starting time. The quantity of energy produced is not necessarily the best criterion for assessment of the success of the exploitation since the regularity of the output and the demand for the energy must also be considered. If the peak demand, for instance, occurs close to the time

[1]There are some exceptions to this statement. See subsection "Starting the Turbines", p. 2927.

of low water, a late start is obviously appropriate but the turbine output does not depend linearly on QH; as a matter of fact, a turbine becomes inefficient past a maximum flow for a given head. For a given head, the turbine gives the most power at a set discharge rate but it produces less power more efficiently at other discharge rates.

Some quantitative criteria must be devised for setting the appropriate starting and stopping times. The same applies to the head and the discharge which must be maintained during the exploitation.

If pumping is possible and profitable, it is certain that the turbines must be used as orifices as soon as, or before, the minimum head has been reached and that all the available sluices must be opened to lower the level of the reservoir as quickly as possible. Once the sea and the reservoir are level, the sluices are closed and the pumps are started. The instant at which the pumps must be stopped, the duration of the interval of waiting before starting the turbines over the next half period are not obvious either. The amount of water pumped will depend on the actual cost of pumping, the speed with which it can be performed, and whether the gain of energy that it entails is desirable. The instant at which the pumps are stopped in conjunction with the time at which the turbines are started, the high level reached by the reservoir all determine the amount of energy that will be gained over the next half period. It is evident that pumping when there is a large demand on power is absurd, that pumping prior to a time of low demand is equally absurd. But there are other times when the value of pumping is not that clear cut.

We come to realize at this point that exploiting a tidal plant is a very complicated matter and that some quantitative techniques must be developed to face this problem. The following sections describe this quantitative approach. In the first section we survey the possible sequences of operations that are necessary for the exploitation of a tidal plant. In the second section the calculus of variations is used to derive the optimum times and levels for given sequences of operations, using some basic criteria for exploitation.

Sequences of Operations

Elementary operations and cycles

In the practical exploitation of tidal energy, one must be concerned with the sequences of operations: pumping, waiting for a head to develop between the reservoir and the sea, and generation of energy. In order to make a systematic review of these operations, develop a notation, introduce the concept of elementary cycles, and denumerate the number of possible sequences that may be constructed from the elementary cycles (Gibrat, 1953, 1956a, b; Caseau, 1962), let us start by defining some statements:

(1) An operation is defined over a half tidal period (if the tide is not perfectly sinusoidal, a half period means the time interval between high and low water, or low and high water).

(2) A sequence of operations may start at high or low water.

(3) A single symbol can be used to denote more than one operation when one operation automatically implies another operation. The notation used, as long as it is properly defined, will be unequivocal.

The symbols used for these elementary operations are the following:

Elementary operations

0: Wait — Sluices closed, turbines shut, and as a consequence, the level inside the reservoir is held constant *at least* over a half tidal period. No energy is produced during this operation. 0 may be initiated at high or low water.

1: Turbines on while the reservoir is being emptied. Physically this operation indicates a short interval of waiting after high water followed by opening the turbines, for a flow out of the basin; the turbines are kept going *over part* of the next half period. Operation 1 can start only at high water. Energy is produced during 1.

2: Turbines on while the reservoir is being filled. This operation represents a short interval of waiting after low water, followed by opening the turbines; the flow is into the basin. The turbines are kept going over part of the next half period. 2 can start only at low water. Energy is produced.

3: Contact — The sluices are opened, the turbines act as orifices, and the level of the reservoir follows closely the fluctuations of the level of the sea. No energy is produced. 3 indicates the *end* of a sequence of operations and it may start at high or low water.

(*a*) *Inverse pumping* — Water is pumped into the reservoir in order to raise its level. (*a*) can start only at high water and it *cannot* extend over a half period. It must therefore be followed by another operation over the same half period. Energy is spent during this operation.

(*b*) *Direct pumping* — Water is pumped out of the basin in order to depress its level. (*b*) can start only at low water and it cannot extend over a half period. It must be followed by another operation over the same half period. Energy is spent during the operation.

These elementary operations are depicted in Fig. 3. The fluctuations in the level of the sea and of the reservoir are indicated by solid and broken lines respectively.

Weak and strong operations

A weak operation cannot extend over a half tidal period. A strong operation may stretch over a half period. (*a*) and (*b*) are *weak* operations; 0, 1, 2, 3, are *strong* operations. (*a*) may be followed by 0 or 1; (*b*) may be followed by 0 or 2.

Elementary cycles

A complete sequence of operations can be defined only over an interval of time of at least one complete tidal period. A sequence of operations defined over an interval of *one tidal period* is called an *elementary cycle*; any longer sequences of operations may be built out of these elementary cycles.

An elementary cycle must consist of at least two elementary operations and it is denoted by the couple (x, y), x denoting the operation performed during the first half of the period and y referring to the second half. x and y

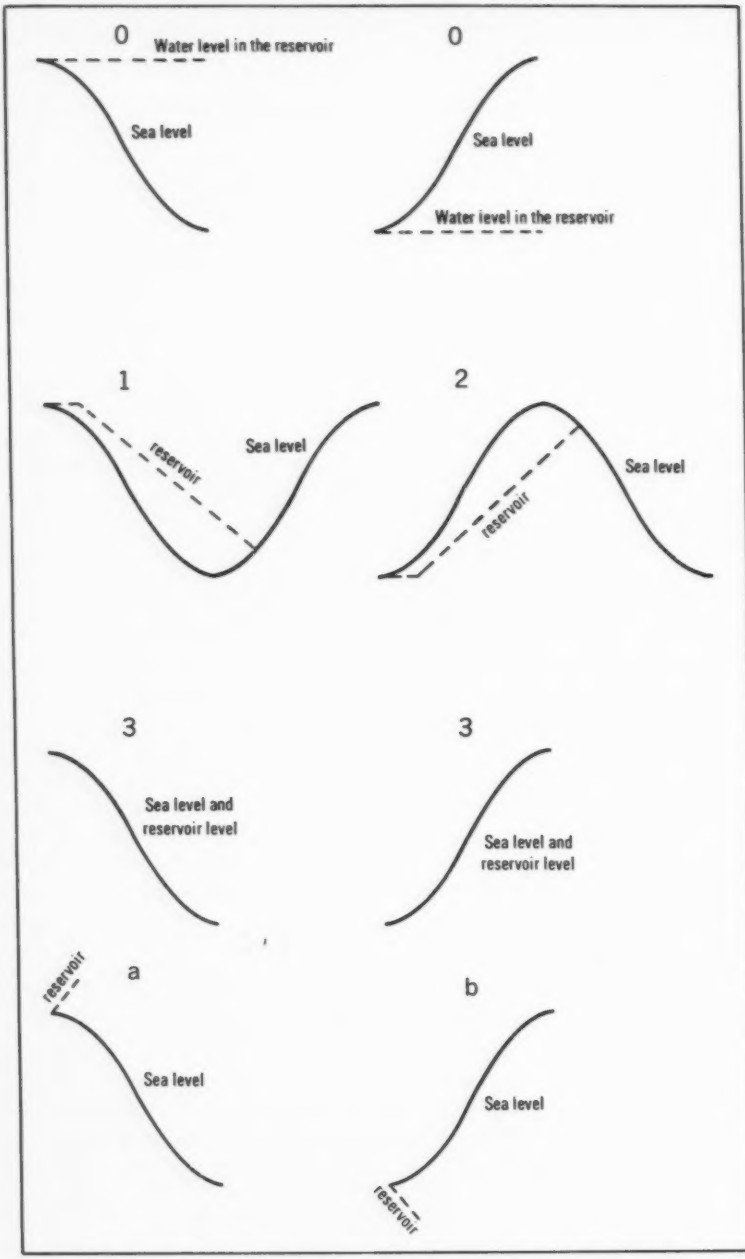

FIG. 3. Elementary operations used for the exploitation of tidal energy. They are on a horizontal time scale and the fluctuations of the basin level are indicated by the broken lines.

may consist of a double symbol such as $a1$ or $b0$ if the cycle starts with a weak operation. For instance we may have ($a1$, $b0$), (1, 2), etc. *By considering only the elementary cycles that make physical sense,* we exclude any sequence of operations that implies a waste of energy that cannot be recuperated in the subsequent cycles. We may call such wasteful operations absurd, impossible, or negative in the sense of Gibrat. For instance ($a1$, $a0$) represents an absurd elementary cycle in which energy is wasted. We exclude such elementary cycles although their importance has been studied by Gibrat (1966).

An admissible elementary cycle may belong to any of the following three types:

(1) *Wait cycles* which themselves may be subdivided into two subtypes: (*a*) *Absolute wait — no* energy whatsoever is produced during the whole tidal period. Example: ($a0$,0) and ($b0$,0). (*b*) *Relative wait* — energy is generated during the first half of the period but the cycle ends on a wait operation. Example: ($a1$, $b0$) and ($b2$, $a0$).

(2) *Productive cycles* — Energy is generated during the two half periods. Example: ($a1$, $b2$), ($b2$, $a1$), (1, 2), and (2, 1).

(3) *Terminal cycles* — These cycles indicate the end of a sequence of operations and end the 3 operation. Example: ($a1$, 3), (2, 3), and (3, 3).

Table 1 gives a list of all the acceptable elementary cycles together with the elementary cycles by which they may be followed. The table shows as well the variations in the level of the reservoir implied by the given elementary cycle.

We note that the diagrams in the table, for high and low water, are the reflection of each other around the horizontal axis. Therefore, from now on we will consider only the sequences of operations that start at high water.

No sequence of operations starting at high water can begin with the elementary cycles (0, 2) or (0, $b2$). On the other hand any relative wait operation must be followed by either (0, 2) or (0, $b2$). The same rule applies for (0, 1) and (0, $a1$) for sequences starting at low water.

DENUMERATION OF THE POSSIBLE SEQUENCES OF OPERATIONS

The notation developed in the previous paragraph and the diagrams shown in Fig. 3 and Table 1 suffice to describe completely any elementary cycle of operation and no further diagrams of this sort are required.

When it comes to sequences of operations, these consist of the permissible juxtapositions of the elementary cycles listed in Table 1. *A juxtaposition of 1, 2, 3, etc., elementary cycles will be called a 1, 2, 3, etc., period sequence.* We wish, however to establish a distinction between an *extended* and a *nonextended* n period sequence.

An extended n period sequence contains $(n + 1)$ *elementary cycles, the last of which is* (3, 3).

A nonextended n period sequence contains n elementary cycles, the last of which is either (1, 3) *or* ($a1$, 3).

TABLE 1.

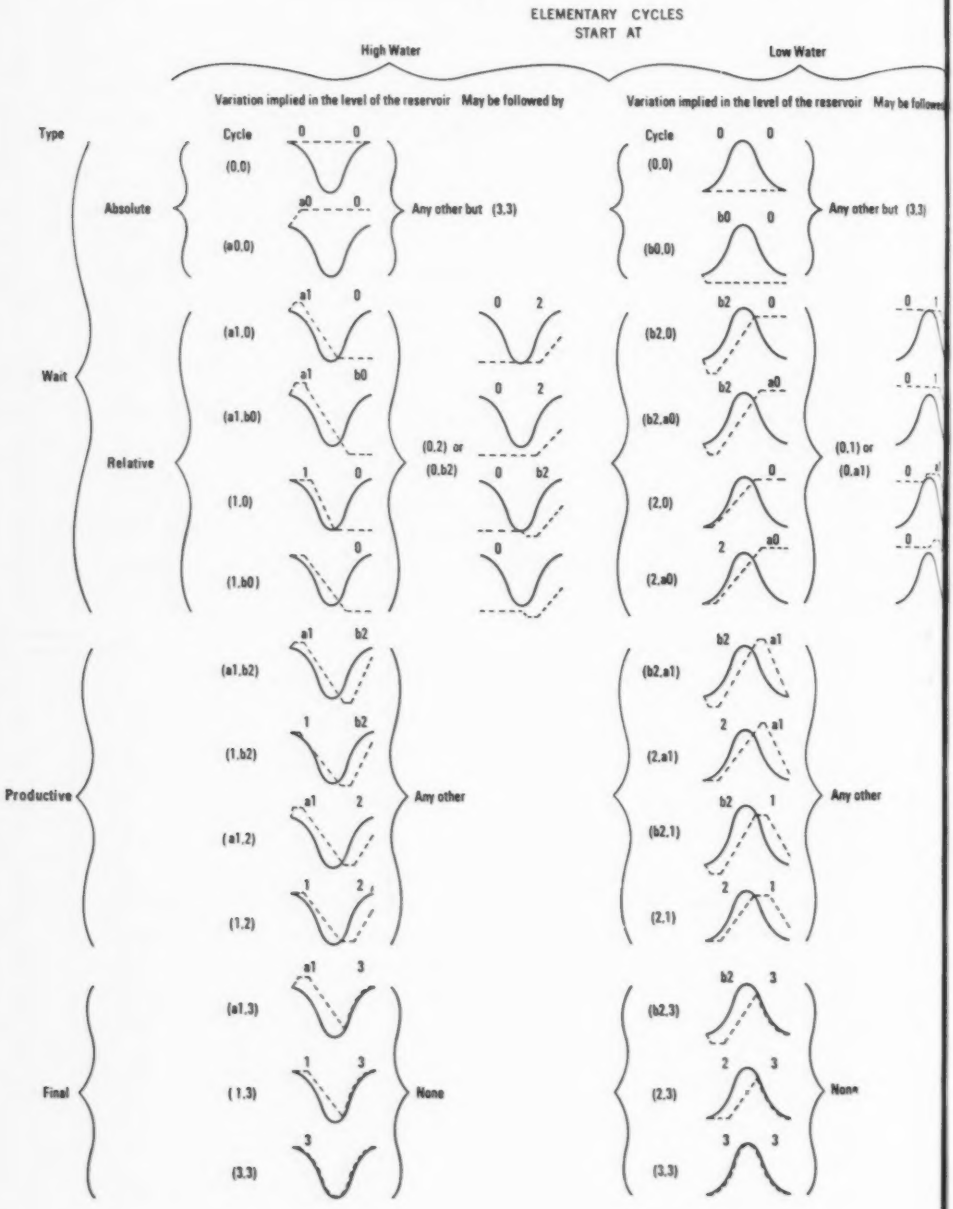
ELEMENTARY CYCLES START AT
High Water
Low Water
Variation implied in the level of the reservoir
May be followed by
Type
Cycle
Absolute
Relative
Wait
Productive
Final
(0.0)
(a0.0)
(b0.0)
(a1.0)
(a1.b0)
(1.0)
(1.b0)
(b2.0)
(b2.a0)
(2.0)
(2.a0)
(a1.b2)
(1.b2)
(a1.2)
(1.2)
(b2.a1)
(2.a1)
(b2.1)
(2.1)
(a1.3)
(1.3)
(3.3)
(b2.3)
(2.3)
Any other but (3.3)
(0.2) or (0.b2)
(0.1) or (0.a1)
Any other
None

Essentially an extended n period sequence covers n periods but its last operation in the nth elementary cycle is prolonged slightly into the $(n + 1)$ period.

For instance (1, 2) (3, 3) is an extended 1 period sequence, in which the operation 2 persists for a little while in the 2nd period.

We note incidentally that *in an extended sequence, the cycle that precedes the final cycle (3, 3) cannot be an absolute wait cycle.*

To study the possible types of sequences and their number, we have to make even more compact our notation of the elementary cycles, by considering only their character.

We denote by: P, a productive elementary cycle; W, an absolute wait cycle; $w \cdot p$, a relative wait cycle followed by its specific productive cycle; F, the final cycle of a nonextended sequence; f, the final cycle of an extended sequence.

As seen in Table 1 there are four possible productive cycles, two absolute wait cycles, eight possible combinations of a relative wait cycle followed by its specific productive cycle, two final cycles of a nonextended sequence, and one final cycle of an extended sequence.

A nonextended n period sequence may be represented by the symbol,

$$(\{\mathrm{P}^r, \mathrm{W}^s, (w \cdot p)^t\}, \mathrm{F}) \tag{35}$$

in which the brackets denote all the possible sequences that may be built out of r productive cycles, s absolute wait cycles, and t relative wait cycles followed by their specific productive cycles; the parentheses denote a specific sequence.

For example, equation 35 means for $n = 3$:

$$(w,p,\mathrm{F}),\ (\mathrm{P},\mathrm{W},\mathrm{F}),\ (\mathrm{W},\mathrm{P},\mathrm{F}),\ (\mathrm{W},\mathrm{W},\mathrm{F}),\ (\mathrm{P},\mathrm{P},\mathrm{F}).$$

In an n period nonextended sequence

$$r + s + 2t = n - 1$$

so that

$$t = \tfrac{1}{2}(n - 1 - r - s).$$

Within the same notation, all the possible extended n period sequences will have the form:

$$(\{\mathrm{P}^r, \mathrm{W}^s, (w \cdot p)^t\}, \mathrm{P}, f) \tag{36a}$$

or

$$(\{\mathrm{P}^r, \mathrm{W}^s, (w \cdot p)^t\}, w \cdot p, f) \tag{36b}$$

where in equations 36a and b

$t = \tfrac{1}{2}(n - 1 - r - s)$ and $t = \tfrac{1}{2}(n - 2 - r - s)$ respectively.

In the case of equations 35 and 36*a*, if $n - 1$ is even, $r + s$ is even, $n - 1$ is odd, $r + s$ is odd. The reverse holds for equation 36*b*.

Equations 35 and 36 represent in the most general way all the possible sequences. Some specific subgroups of these sequences are those that contain:

(1) only productive cycles, (P^{n-1}, F), (P^n, f)

(2) only absolute wait cycles, (W^{n-1}, F)

(3) only relative wait cycles, $((w \cdot p)^{\frac{1}{2}(n-1)}, F)$, n odd; $((w \cdot p)^{\frac{1}{2}n}, f)$, n even

and then the mixed sequences that contain:

(1) productive and absolute wait cycles, $(\{P^r, W^s\}, F)$ and $(\{P^r, W^s\}, P, f)$ and $r + s = n - 1$, $r + s = n - 1$

(2) productive and relative wait cycles, $(\{P^r, (w \cdot p)^t\}, F)$, $(\{P^r, (w \cdot p)^t\}, w \cdot p, f)$ with $r + 2t = n - 1$.

There is no difficulty in listing the possible sequences for $n = 1, 2, 3$ in this new notation. Doing this will give us a chance to look at the actual sequences of operations:

$n = 1$ period

(*a*) Nonextended (F) $\begin{cases} (a1, 3) \\ (1, 3) \end{cases}$

(*b*) Extended (P,*f*) $\begin{cases} ((a1, b2), (3, 3)) \\ ((1, b2), (3,3)) \\ ((a1, 2), (3, 3)) \\ ((1, 2), (3, 3)) \end{cases}$

$n = 2$ periods

(*a*) Nonextended (P,F) $\begin{cases} ((a1,b2),(a1,3)),((a1,b2),(1,3)) \\ ((1,b2),(a1,3)),((1,b2),(1,3)) \\ ((a1,2),(a1,3)),((a1,2),(1,3)) \\ ((1,2),(a1,3)),((1,2),(1,3)) \end{cases}$

(W,F) $\begin{cases} ((0,0),(a1,3)),((0,0),(1,3)) \\ ((a0,0),(a1,3)),((a0,0),(1,3)) \end{cases}$

(*b*) Extended (from now on we keep only the symbolic representation)

(P,P,*f*)
(W,P,*f*)
(*w*,*p*,*f*)

$n = 3$ periods

(*a*) Nonextended

(P,P,F)
(P,W,F)
(W,P,F)
(W,W,F)
(*w*,*p*,F)

(*b*) Extended

(P,P,P,*f*)
(P,W,P,*f*)
(W,P,P,*f*)
(W,W,P,*f*)
(*w*,*p*,P,*f*)

(P,*w*,*p*,*f*)
(W,*w*,*p*,*f*)

The number of possible sequences in the cases considered is:

$n = 1$	(*a*) 2	(*b*) 4
$n = 2$	(*a*) $8+4=12$	(*b*) $16+8+8=32$
$n = 3$	(*a*) $32+32+8+16=88$	(*b*) $64+64+16+32=176$
		$32+16 = 48$
		224

(*a*) and (*b*) refer to the nonextended and extended sequences.

To generalize these results we compute the number of possible sequences that can be built out of r productive cycles, s absolute wait cycles, and t relative wait cycles followed by their specific wait cycles.

We denote by [ ] enclosing a sequence or a subsequence the number of such possible sequences so that in particular, [P] = 4; [W] = 2; [*wp*] = 8; [F] = 2; [*f*] = 1.

The number of distinct possible sequences of the type (P^r, W^s, $(w\cdot p)^t$) is therefore

$$\frac{[P]^r\,[W]^s\,[w\cdot p]^t\,(r+s+t)!}{r!\,s!\,t!} \tag{37}$$

which simply is the number of permutations of $r + s + t$ objects, r, s, and t of them belonging to the same type.

In equations 35 and 36*a*

$$t = \tfrac{1}{2}(n-1-r-s)$$

and in equation 36*b*

$$t = \tfrac{1}{2}(n-2-r-s).$$

We denote $r + s$ by k so that $s = k - r$.

Then the number of possible sequences containing an even or odd number of elementary cycles of the type P,W and $w\cdot p$ is

$$N_e = \sum_{\substack{k=0\\ \text{even}}}^{e} \frac{(\tfrac{1}{2}(e+k))!\,[w\cdot p]^{\frac{1}{2}(e-k)}}{(\tfrac{1}{2}(e-k))!} \sum_{r=0}^{k} \frac{[P]^r\,[W]^{k-r}}{r!\,(k-r)!} \tag{38}$$

and

$$N_o = \sum_{\substack{k=1 \\ \text{odd}}}^{o} \frac{(\frac{1}{2}(o+k))!\,[w\cdot p]^{\frac{1}{2}(o-k)}}{(\frac{1}{2}(o-k))!} \sum_{r=0}^{k} \frac{[P]^r\,[W]^{k-r}}{r!(k-r)!} \tag{39}$$

where e and o stand for $n-1$ depending on whether it is even or odd.

It follows that

$$[(\{P^r, W^s, (w\cdot p)^t\}, F)] = N_{n-1}\,[F],$$

$$[(\{P^r, W^s, (w\cdot p)^t\}, P, f)] = N_{n-1}\,[P]\,[f] \qquad \text{and}$$

$$[(\{P^r, W^s, (w\cdot p)^t\}, w\cdot p, f)] = N_{n-2}\,[w\cdot p]\,[f]$$

so that the number of possible nonextended n period sequences is

$$N_{n-1}\,[F]$$

and the number of extended n period sequences is

$$N_{n-1}\,[P]\,[f] + N_{n-2}\,[w\cdot p]\,[f].$$

We may check these formulas for the particular cases of $n = 1, 2, 3$.

$n = 1$ (*a*) $N_0[F] = [F] = 2$

(*b*) $N_0[P]\,[f] = [P]\,[f] = 4$

$n = 2$ (*a*) $N_1[F] = 6 \times 2 = 12$

(*b*) $N_1[P]\,[f] + N_0[w\cdot p]\,[f] = 6 \times 4 \times 1 + 1 \times 8 \times 1$
$= 24 + 8 = 32$

$n = 3$ (*a*) $N_2[F] = 44 \times 2 = 88$

(*b*) $N_2[P]\,[f] + N_1[w\cdot p]\,[f] = 44 \times 4 \times 1 + 6 \times 8 \times 1$
$= 176 + 48 = 224$

Table 2 gives the number of possible sequences of operations for $n = 1$ to $n = 25$. $n = 25$ spans about 2 weeks of time for a semidiurnal tide, which is the approximate time lapse between spring and neap tide. The number of possibilities increases rapidly with n and for each specific sequence there is a combination of starting and ending times that yield the maximum energy. For a given n, one of all the sequences will yield the maximum amount of energy; this very sequence with its appropriate starting and ending times will be called the *optimum sequence* if the maximum energy output is the goal of exploitation (which is not always the case).

A systematic evaluation of the maximum energy yielded by each one of the sequences is not possible even with the fastest computer; intuition must be used to pick those sequences that seem likely to lead to an optimum of exploitation.

TABLE 2. Number of possible nonextended and extended sequences of operation.

$n-1$	Nonextended sequences $2N_{n-1}$	Extended sequences $4N_{n-1}+8N_{n-2}$
0	2	4
1	12	32
2	88	224
3	624	1600
4	4448	11392
5	31680	81152
6	225664	578048
7	1.607×10^{6}	4.118×10^{6}
8	1.145×10^{7}	2.933×10^{7}
9	8.156×10^{7}	2.089×10^{8}
10	5.809×10^{8}	1.488×10^{9}
11	4.138×10^{9}	1.060×10^{10}
12	2.948×10^{10}	7.551×10^{10}
13	2.099×10^{11}	5.378×10^{11}
14	1.496×10^{12}	3.831×10^{12}
15	1.065×10^{13}	2.729×10^{13}
16	7.588×10^{13}	1.944×10^{14}
17	5.405×10^{14}	1.385×10^{15}
18	3.850×10^{15}	9.863×10^{15}
19	2.743×10^{16}	7.025×10^{16}
20	1.954×10^{17}	5.004×10^{17}
21	1.392×10^{18}	3.565×10^{18}
22	9.912×10^{18}	2.539×10^{19}
23	7.061×10^{19}	1.809×10^{20}
24	5.029×10^{20}	1.288×10^{21}

TURBINES AND THE OPERATION OF THE TIDAL PLANT

TURBINES

One cannot avoid the discussion of the means for the transformation of tidal energy into electricity, namely the turbine. Originally, the turbine was designed to work in conventional hydroelectric plants where the conditions were such that it operated under nearly constant head and discharge. The turbine can be designed so that it works at maximum efficiency over a narrow range of head and discharge.

A turbine that can transform tidal energy has to function under quite different conditions. In a tidal basin, the head varies between at most ±15 m and the flow reverses itself about every 6 hr. Such a turbine must be developed from the conventional turbine, a task that will require considerable engineering skill (Casacci and Kammerlocher, 1956; Chevalier, 1956; Kammerlocher and Duclos, 1956; Dubois, 1962). The new turbine, if it has to be referred to the standard classification of turbines, would be a low head and large discharge

turbine of the reaction type (Kovalev, 1965). It must have a large diameter to be able to produce an adequate amount of energy.

Whatever the ultimate tidal turbine will be, we know that the wide fluctuations in range and discharge that are inherent to tidal energy will leave the turbine inefficient over a fair domain of the tidal oscillation. As far as it is feasible, it should be operated within the region where it is most efficient and where it can output the maximum power. Also, during the exploitation of tidal energy, the turbine has to be started and stopped at least once during one tidal period. The way this operation is performed may have a significant bearing on the amount of energy produced. The initial amount of power generated is also significant.

The overall range of energy for many tidal periods will depend mainly on the performance characteristics of the turbine installed, on the storage capacity of the basin and on the shape and amplitude of the tidal oscillation. To look into this, the problem must be defined quantitatively. Using the now standard notation of Gibrat (Gibrat, 1953; Gauthier, 1962), we denote the elevation of the sea above a zero reference level by

$$h(t). \tag{40a}$$

In most of what follows, $h(t)$ will be considered as a simple sinusoidal oscillation:

$$h(t) = h_0(1 + \sin\sigma t). \tag{40b}$$

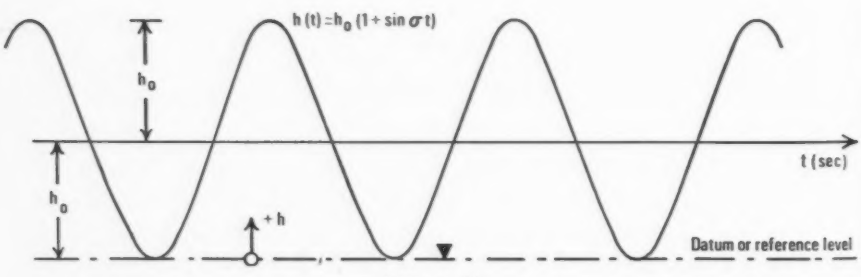

SCHEME II.

The power N produced by the turbine depends on the discharge q' through it and on the head H under which it operates. Thus

$$N = N(q', H). \tag{41}$$

The level of the basin above the same reference level is denoted by

$$z(t) \tag{42}$$

so that

$$H = z - h. \tag{43}$$

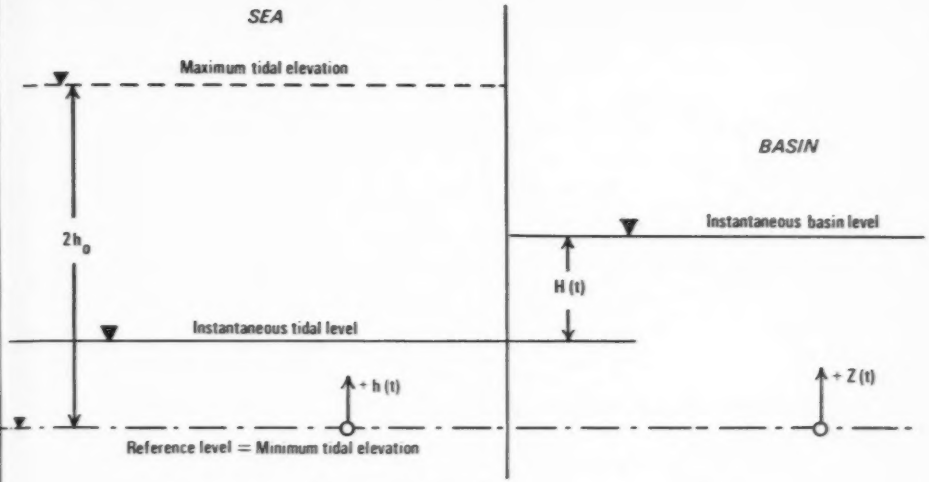

SCHEME III.

There will be a certain number, n_0, of turbines installed in the plant; they might not all be in operation at the same time and we denote by n the number of turbines in operation at a given time and by

$$\lambda = n/n_0 \tag{44}$$

the ratio of the number of turbines in operation to their total number.

The outflow from the basin being divided by n_0 turbines, it is convenient to divide the area $S(z)$ of the basin at a given height z by the number of turbines n_0 to obtain the area of the basin drained by one turbine:

$$s(z) = S(z)/n_0. \tag{45}$$

The outflow from the basin may also be increased by some sluices that contribute V m³/sec so that the outflow of the sluices per turbine is

$$v = V/n_0 \tag{46}$$

and if the maximum outflow of the sluices for a given head H is V_0, the specific maximum sluice outflow per turbine is

$$v_0 = V_0/n_0. \tag{47}$$

Finally

$$\mu = v/v_0 = V/V_0 \tag{48}$$

is the ratio of the actual discharge of the sluices to their maximum possible discharge.

The total discharge of the basin is

$$Q = nq' + V = n_0 q + V \tag{49}$$

where, in the second expression, the discharge through the n turbines has been assigned and spread to the n_0 turbines present, whether they be in action or not. Naturally if all the turbines are in action, $q = q'$, which is the case when the plant is in full production. Otherwise $q' = q/(n/n_0) = q/\lambda$. Dividing equation 49 by n_0 to obtain the specific discharge of the basin for one turbine and using the equation of continuity $Q = -S\ dz/dt$, we get

$$q = -s\ dz/dt - \mu v_0. \tag{50}$$

The conventional way of representing the characteristics of the power output of a turbine is by a family of lines on a q', H diagram. The lines may be conceived as the projection of the $N(q', H)$ surface on the q', H plane. Since the efficiency of the turbine is less than 100%, we may write

$$N = \eta q' H \tag{51}$$

where $0 \leq \eta < 1$, $q'H$ being the power generated by an ideal turbine of perfect efficiency.

In the q', H diagram, the lines

$$\partial N/\partial q' = 0 \tag{52}$$

and

$$\partial \eta/\partial q' = 0 < n - q'\partial N/\partial q' = 0 \tag{53}$$

are respectively the lines of maximum power output and of maximum efficiency, and delineate an area within which the turbine is normally expected to perform. Also, the line

$$N = 0, \tag{54}$$

which is the minimum head for which the turbine can generate energy, and the line

$$N = N_0$$

where N_0 is the maximum power that can be extracted in practice from the turbine for a given q' and H, mark the upper and lower limits of the region within which the turbine can normally operate. Equations 52 and 53 meet at (H_m, q'_m), H_m being the lowest head for which the turbine can generate power for the minimum discharge q'_m (Fig. 4).

The performance of the pumps must also be considered. Some turbines may act as pumps; if this is the case it implies a considerable saving in the installation of the plant. Otherwise pumps have to be installed separately. The electrical power that they draw to pump q' m^3/sec may be represented by

$$P = \zeta q' H \qquad \zeta > 1 \tag{55}$$

for a given head H. The closeness of ζ to 1 and the opportunity of pumping will decide on the profitability of the installation of pumps.

A conventional turbine may generate power normally for a given direction of flow. In the exploitation of tidal energy, it seems preferable to use a turbine

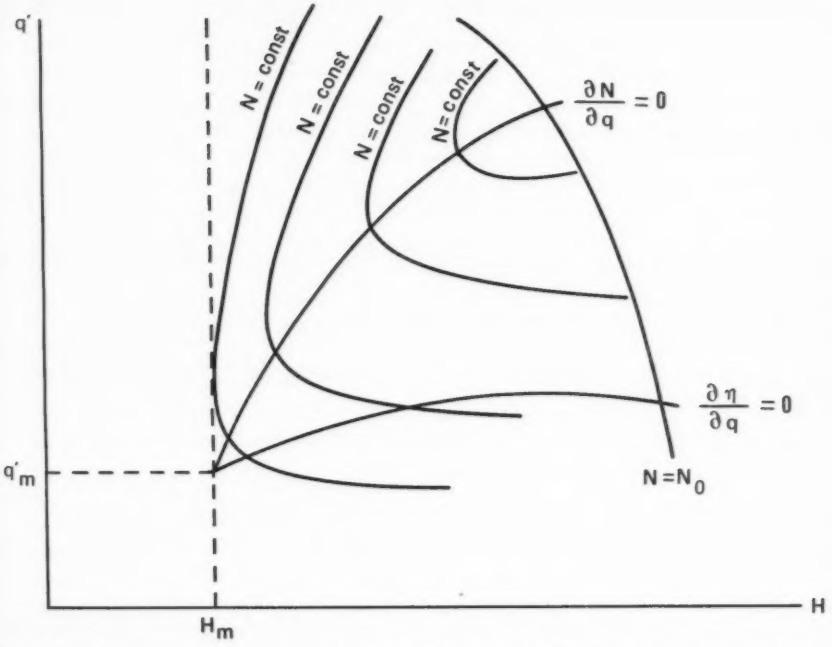

FIG. 4. Projection of the energy surface $N(q', H)$ on the q', H plane. Some important parametric lines are shown as well.

that can generate power for flows in and out of the basin. In that case Fig. 4 has to be extended for negative values of q' and H.

In practice, as already stated, the power drawn from emptying the basin is always larger than the power generated by filling it. Considerations of economy might lead to the choice of unidirectional turbines. On the other hand, turbines that can generate for the two directions of flow allow the generation of power over longer intervals of time and will make the tidal plant more flexible.

In the course of the exploitation of power we have to answer one or all of the following questions under the following conditions of operation: (1) When should the turbines be started? (2) When should they be stopped? (3) When should the sluices be opened? (4) How should the turbines be started? (5) What is the influence of the demand fluctuations on the operation of the plant? (6) Should pumping be used and if so when should it be started? (7) What must be done when the maximum power output of the turbine is reached?

Semiquantitative answers to these questions may be obtained with the help of the calculus of variation (Gibrat, 1953, 1954, 1955, 1956a, and b; Gauthier, 1962).

CALCULUS OF VARIATION

Given an explicit function F that depends not only on an independent variable t but also on one or more indeterminate functions $z_1(t)$, $z_2(t)$, etc., and their derivatives $z_1'(t)$, $z_2'(t)$, etc. The problem of the calculus of variation is to determine the functions $z_1(t)$, $z_2(t)$, etc., so that the integral

$$I = \int_{t_0}^{t_1} F(t, z_1(t), z_1'(t), z_2(t), z_2'(t), \ldots)dt \tag{56}$$

is stationary. t_0 and t_1 are not fixed end points and they have to be determined from the same prerequisite.

A necessary but not sufficient condition for I to be a maximum is that for a slight change δz_1 and $\delta z_1'$ in z_1 and z_1', δz_2 and $\delta z_2'$, etc., δt_0 and δt_1 in t_0 and t_1, the first order variation δI of I vanishes. The analytical expression of this statement is

$$\begin{aligned}\delta I &= \int_{t_0+\delta t_0}^{t_1+\delta t_1} F(t, \delta z_1 + \delta z_1, z_1' + \delta z_1', z_2 + \delta z_2, z_2' + \\ &\quad \delta z_2', \ldots)dt - \int_{t_0}^{t_1} F(t, z_1, z_1', z_2, z_2', \ldots)dt \\ &= \left[\int_{t_0+\delta t_0}^{t_0} + \int_{t_1}^{t_1+\delta t_1}\right](F(t, z_1 + \delta z_1, z_1' + \delta z_1', z_2 + \delta z_2, z_2' + \\ &\quad \delta z_2', \ldots)dt + \int_{t_0}^{t_1} F(t_1, z_1 + \bar{\delta} z_1, z_1' + \bar{\delta} z_1', z_2 + \bar{\delta} z_2, z_2' + \bar{\delta} z_2', \ldots) \\ &\quad dt - \int_{t_0}^{t_1} F(t, z_1, z_1', z_2, z_2', \ldots)dt = 0.\end{aligned} \tag{57}$$

In this expression we have to make a distinction between the arbitrary variation $\bar{\delta} z_1$ and $\bar{\delta} z_1'$ in z_1 and z_1' and the extra variation induced in them by the variation of the end point δt so that

$$\delta z_1 = \bar{\delta} z_1 + z_1' \delta t$$

and

$$\delta z_1' = \bar{\delta} z_1' + z_1' \delta t \text{ etc.}$$

To a first order, equation 57 becomes

$$\delta I = F(t, z_1, z_1', z_2, z_2', \ldots)\,\delta t\Big|_{t_0}^{t_1} + \frac{\partial F}{\partial z_1'}\,\bar{\delta} z_1\Big|_{t_0}^{t_1} +$$

$$\frac{\partial F}{\partial z_2'}\,\bar{\delta} z_2'\Big|_{t_0}^{t_1} + \int_{t_0}^{t_1}\left[\left[\frac{\partial F}{\partial z_1} - \frac{d}{dt}\,\frac{\partial F}{\partial z_1'}\right]\delta z_1 +\right.$$

$$\left.\left[\frac{\partial F}{\partial z_2} - \frac{d}{dt}\,\frac{\partial F}{\partial z_2'}\right]\bar{\delta} z_2 + \ldots\right]dt.$$

A way to satisfy this condition is to require that

$$\frac{\partial F}{\partial z_1} - \frac{d}{dt}\,\frac{\partial F}{\partial z_1'} = 0 \qquad \frac{\partial F}{\partial z_2} - \frac{d}{dt}\,\frac{\partial F}{\partial z_2'} = 0 \text{ etc.} \tag{58}$$

and

$$(F - z_1' \frac{\partial F}{\partial z_1'} - z_2' \frac{\partial F}{\partial z_2'} - \dots)\,\delta t + \frac{\partial F}{\partial z_1'}\,\delta z_1 + \frac{\partial F}{\partial z_2'}\,\delta z_2 + \dots |_{t_0}^{t_1} = 0. \quad (59)$$

Equations 58 are known as the Euler equations whereas equation 59 represents the extra boundary conditions often known as the conditions of transversality that have to be satisfied by the function at the end points. If equations 58 and 59 are satisfied it implies that I has a stationary value. To insure that the stationary value is a maximum, one must check if $\delta^2 I < 0$. This is seldom verified in practice because of the analytic complications. The function I may effectively have many maxima for various choices of the z_i's, some of these may be smaller than the minima; the largest of the maxima may be called an optimum.

Under such conditions, the search for an optimum is obviously not straightforward but still the imposition of stationarity may be of some use in discovering the rules for the operation of a tidal plant.

OPERATION FOR MAXIMUM ENERGY OUTPUT

Operating a tidal plant to obtain the maximum possible energy output is somewhat naive since the energy produced might not always be needed in the network. On the other hand, tidal energy must be considered as wild energy, that is to say, an energy that makes itself available at times of its own choosing, in spite of its periodicity (which is lunar whereas the periodicity of human activities is solar). So it is perhaps sensible to use all the energy it may supply and try rather to control the more controllable sources of energy of the network. The extra tidal energy could be used to pump water in auxiliary basins (not necessarily close to the plant), which would yield energy when needed.

So, for the moment, we work with the hypothesis that the plant is operated in such a way that we extract the maximum possible amount of energy from the tide.

In this instance, the quantity to be maximized over a sequence of operations is

$$n\mathrm{N}(q', \mathrm{H}) \quad (60)$$

which may be expressed more explicitly as

$$\lambda \mathrm{N}(q/\lambda, \mathrm{H}) = \lambda \mathrm{N}\left[\frac{1}{\lambda}\,(-s\,\frac{\mathrm{d}z}{\mathrm{d}t} - \mu v_0),\ z - h\right]. \quad (61)$$

It is therefore necessary that

$$\mathrm{I} = \int_{t_0}^{t_1} \lambda \mathrm{N}(q/\lambda, \mathrm{H})\mathrm{d}t \quad (62)$$

be stationary. t_0 and t_1 indicate the instants at which the sequence of operation is started and stopped.

Taking λ, μ, and z as our arbitrary functions, we need according to equations 58 and 59

$$N - \frac{q}{\lambda} \frac{\partial N}{\partial(q/\lambda)} = 0 \tag{63}$$

$$\frac{\partial(\lambda N)}{\partial(q/\lambda)} \cdot \frac{v_0}{\lambda} = 0 \tag{64}$$

$$\frac{\partial(\lambda N)}{\partial H} - \frac{\mu}{\lambda} \frac{\partial v_0}{\partial H} \frac{\partial(\lambda N)}{\partial(q/\lambda)} + \frac{s}{\lambda} \frac{d}{dt}\left[\frac{\partial(\lambda N)}{\partial(q/\lambda)}\right] = 0 \tag{65}$$

and

$$[\lambda N - \frac{(q + \mu v_0)}{\lambda} [\partial(\lambda N/\partial q/\lambda]]\delta t - \frac{s}{\lambda} [\partial(\lambda N)/\partial q/\lambda]\delta z|_{t_0}^{t_1} = 0. \tag{66}$$

The latter part of equation 66 is automatically satisfied since $\delta z = 0$ initially, as the initial level of the basin may not be arbitrarily varied. At t, the turbines must operate at 0 power output with $(H, q) = (H_m, q_m)$.

Starting the operations — One either starts by a pumping operation or by a wait operation followed by the generation of power. If one starts by pumping, the initial condition to be satisfied is $H = 0$. The sluices are closed ($\mu = 0$) and all the pumps are at work ($\lambda = 1$). The condition of transversality (equation 66) becomes (writing P for N as energy is now expended)

$$(P - q\partial P/\partial q)\delta t - s(\partial P/\partial q)\delta z \,|_{t_0} = 0 \tag{67}$$

which gives

$$\delta z/\delta t = \frac{P + sz'\partial P/\partial q}{s\,\partial P/\partial q} \tag{68}$$

using equation 50. z' is the rate of change of the level of the reservoir after the pumps have been started; it is determined by equation 68 and $\delta z/\delta t$ is a variational quantity. For $H_{,} = 0$, the transversal must follow the tide, i.e. $\delta z = (dh/dt)\,\delta t$. We are now in a position to calculate the initial change of head $dH/dt = dh/dt - dz/dt$ which from equation 68 amounts to

$$dH/dt = \frac{P}{s\partial P/\partial q}. \tag{69}$$

If we start immediately with the turbines without pumping there is no a priori condition on the initial head but the condition of transversality must be satisfied for a fixed initial level $z_0(\rightarrow \delta z = 0)$. Assuming that all the turbines are in operation ($\lambda = 1$) and the sluices being closed by necessity ($\mu = 0$) the condition of transversality yields

$$\delta I = [N - q\,\partial N/\partial q]\delta T \,|_{t_0} = 0 \tag{70}$$

which is satisfied for $\partial\eta/\partial q = 0$, i.e. the turbines when turned on must be performing at *peak efficiency*. Graphically this means that the extremal path must start on the curve $\partial\eta/\partial q = 0$ in Fig. 4; this then determines a single value for q.

Physically, condition 70 indicates that if $\partial\eta/\partial q < 0$ and $\delta I > 0$ it is advantageous to keep on waiting before starting the operations. If $\partial\eta/\partial q > 0$ and $\delta I < 0$ the operations should have started. So the turbines must therefore be started for $\partial\eta/\partial q = 0$. The same reasoning can be used to demonstrate that the pumps must be stopped when performing at their peak efficiency.

Ending the operations — After an n period sequence of operations, the exploitation is brought to an end. The last profitable operation must be a turbine operation; it would not make any sense to do anything else. The sluices must be kept closed in this last cycle as all the water available must be exploited, the extremal path staying everywhere below the curve $\partial N/\partial q = 0$. The final condition is that the turbines must be stopped at the point (q_m, H_m) in the qH diagram or the minimum head and discharge for which the turbine can still generate power. The transversality condition at that instant becomes

$$[N - q\partial N/\partial q]\delta t - s(\partial N/\partial q)\ \delta z\ |^{t_1} = 0 \tag{71}$$

at (q_m, H_m), $\partial N/\partial q$, and $N = 0$ so that equation 71 is automatically satisfied. The fact that the extremal path must necessarily end at (q, H) is discussed extensively by Gibrat (1953).

Transitions — The transitions in power operation will be of several kinds depending on the power, pumping, and sluicing cycles. We must be able to relate the heads and times for which pumping is ended and the turbines are started. After this sequence, the level of the reservoir will have to be depressed or raised as rapidly as possible to get the most energy from the next cycle. This implies that the sluices (if present) must be put in operation at the end of the cycle. We must know the condition for which the sluices are to be opened. Finally, once the turbines are turned off, a pumping or a wait operation is initiated.

For the first type of transition, from pumping to power generation, we assume that the minimum energy has been spent in pumping and that the maximum energy will be gained from the operation of the turbines. Let us consider the gain of energy obtained by pumping a little bit longer and starting the turbines earlier. If we write the efficiency of the pump as ζ, the loss of energy from the pump and the gain in energy from the turbines are

$$(\zeta\bar{q}H\Delta t)_0 \text{ and } (\eta\bar{q}H\Delta t)_1$$

respectively, $\bar{q}$ indicating the value of the discharge on the curve of peak efficiency $\partial\zeta/\partial q = 0$ or $\partial\eta/\partial q = 0$ if we label by 0 and 1 the instant at which the pumps are stopped and the turbines started. The extra water pumped at 0 must be utilized at 1 in order that

$$(\bar{q}\Delta t)_0 = (\bar{q}\Delta t)_1. \tag{72}$$

The net gain in energy is

$$\delta I = -(\zeta H)_0 + (\eta H)_1 \tag{73}$$

and being on an extremal path, $\delta I = 0$ so that

$$(\zeta H)_0 = (\eta H)_1 \tag{74}$$

or

$$(P/\bar{q})_0 = (N/\bar{q})_1 \tag{75}$$

which is the condition to be satisfied in a transition from a pumping to a turbine operation. Equation 75 allows the linking of the various portions of the extremal trajectory, which are separated by wait operations.

The reverse situation in which the a turbine operation is followed by a pump operation is easier to consider. If the sluices are open the turbines must be stopped when the head reaches the minimum value consistent with a positive generation of power. The sluices are then closed and the pumps are started when the head reaches the value 0.

The next problem to investigate is to find the time at which the sluices must be opened when the turbines are in operation. In the case when the sluices are opened, all the turbines are in operation ($\lambda = 1$, $q' = q$) and μ should have some value lying between 0 and 1. Equations 64 and 65 become

$$(\partial N/\partial q)v_0 = 0 \tag{76}$$

$$\partial N/\partial H - \mu(\partial v_0/\partial H)\,(\partial N/\partial q) + s\frac{d}{dt}\,(\partial N/\partial q) = 0. \tag{77}$$

The transversal conditions do not come in as we are in the middle of a sequence of operations. Equation 76 may be satisfied if $v_0 = 0$, i.e. if the sluices are closed at all times, or if $\partial N/\partial q = 0$. The second alternative implies

$$\partial N/\partial H = 0. \tag{78}$$

It is not possible to satisfy equation 78 along with $\partial N/\partial q = 0$ during the whole of the operations. Therefore equations 76 and 77 do not seem to admit of any solution for a continuous variation of μ.

Normally the operations should be carried out in such a way that $\partial N/\partial q > 0$ for which the power output of the turbine increases with an increase in discharge when following the extremal path; it is physically evident that the sluices should be kept closed ($\mu = 0$) so that the discharge through the turbines may be effectively increased. Equations 76 and 77 reduce then to

$$\partial N/\partial H = -s\frac{d}{dt}\,\partial N/\partial q \tag{79}$$

which may be effectively satisfied as long as $\partial N/\partial q \neq 0$.

If $\partial N/\partial q < 0$, the power output diminishes with an increase in discharge. This is an undesirable situation as the water stored is actually misused. The way to correct it is to open the sluices ($\mu = 1$) to reduce the discharge through

the turbines, if this cannot be managed with the turbines themselves, and thus avoid diminishing their energy output.

Operating at $\partial N/\partial q = 0$, i.e. at maximum power output, is not possible for any extended interval of time according to equations 76 and 77. So when the extremal path in the qH diagram reaches the curve $\partial N/\partial q = 0$, the sluices must be opened at once to dispose of the excess water. The turbines eventually stop generating power when the head reaches the minimum value for the given discharge and they may be used as sluices to lower or raise the level as rapidly as possible till the levels of the reservoir and of the sea are equal. Then a wait operation is required.

Increasing gradually the number of turbines in operation when a power generating operation is started — After having considered the coarse features of the operations we can now examine the finer points as to whether it is better to start the turbines one by one or all at once to gain the maximum energy output. This involves investigating the variation of λ between 0 and 1 when $\mu = 0$ since the sluices must be closed at the beginning of power generation. It turns out that to a first order, the energy change is the same for both procedures. In practice the first alternative is preferable since the change in discharge in or out of the plant is more gradual and less likely to upset the navigation in the vicinity of the tidal plant.

If we denote by t_0 and t_a the starting time and the time when all the turbines are in action, by z_0 and z_a the level of the reservoir at these instants, the energy produced during the time interval (t_0, t_a) amounts to

$$I = \int_{t_0}^{t_1} \lambda N \, dt = \int_{t_0}^{t_1} - \frac{s}{\lambda} \frac{\partial(\lambda N) dz}{\partial q' \, dt} \, dt$$

$$= \int_{z_0}^{z_a} - \frac{s}{\lambda} \frac{\partial(\lambda N)}{\partial q'} \, dz \qquad (80)$$

since we operate at $\partial\eta/\partial q' = 0$ and $q = -sz'$ for $\mu = 0$. The first order variation in the energy for changes δz and δt in z and t is, according to equation 66

$$\delta I = [\lambda N - q'\partial(\lambda N)/\partial q']\delta t - \frac{s}{\lambda}[\partial(\lambda N)/\partial q']\delta z = - \frac{s}{\lambda}[\partial(\lambda N)/\partial q']\delta z \qquad (81)$$

for the same conditions. The total change of energy for a lowering of level from z_0 to z_a amounts to

$$I = \int_{z_0}^{z_a} - \frac{s}{\lambda} [\partial(\lambda N)/\partial q'] dz \qquad (82)$$

which is identical to equation 81 to a first order. The gain in energy is the same either way.

We may go back and evaluate the time it takes to put all the turbines in operation.

The basic equations for $\mu = 0$ are

$$N - \frac{q'}{\lambda} \frac{\partial N}{\partial (q'/\lambda)} = 0 \tag{83}$$

$$\frac{\partial(\lambda N)}{\partial H} + \frac{s}{\lambda} \frac{d}{dt} \frac{\partial(\lambda N)}{\partial (q'/\lambda)} = 0 \tag{84}$$

and

$$\lambda N - \frac{q'}{\lambda} \frac{\partial(\lambda N)}{\partial (q'/\lambda)} \delta t \Big|_{t_0} = 0. \tag{85}$$

Initially each turbine must perform at peak efficiency so that $q'/\lambda = \bar{q}$. Equation 83 is then automatically satisfied. Equation 57 becomes

$$\lambda = -s \frac{\dfrac{d}{dt}(N/\bar{q})}{(\partial N/\partial H)}. \tag{86}$$

When all the turbines are in operation, $\lambda = 1$ so that equation 86 gives us an expression to evaluate Δt, the time taken to put them all into operation:

$$\Delta t \simeq \frac{-s}{(\partial N/\partial H)} \Delta\left(\frac{(N)}{\bar{q}}\right). \tag{87}$$

s is assumed to be constant and the change in level at the beginning of the operations is taken to be small. Δt is of the order of 5–25 min for the Neyrpic turbines according to Gauthier (Gauthier, 1962).

The same formula may be interpreted in an identical way for the gradual stoppage of the turbines.

Limitation of the maximum power output of the turbines — In practice the power output of a turbine cannot exceed a predetermined maximum value $N = N_0$. However, it may happen that the path of the extremal leads directly to this maximum value; the question arises as to what is to be done when the maximum permissible value is reached in order to still obtain the maximum possible energy output.

The restriction of $N \leq N_0$ implies that the extremal path will follow the curve $N = N_0$ in the qH diagram entering it at some point A and leaving it at some other point B (not illustrated). The point A is determined from the Euler equations, the point B is to be determined.

When this situation prevails $\lambda = 1$ and $\mu = 0$, as we are generating power and are still away from the situation in which the sluices have to be opened because the head is nearing its minimum acceptable value.

Equations 63 to 66 reduce to

$$\frac{\partial N}{\partial H} + s \frac{d}{dt}\left(\frac{\partial N}{\partial q}\right) = 0. \tag{88}$$

The transversality conditions do not have to be considered as we are in the middle of a sequence.

The change of energy over the path AB amounts to

$$\delta I = \int_A^B \left(\frac{\partial N}{\partial H} + s \frac{d}{dt} \frac{\partial N}{\partial q} \right) \delta z \, dt \tag{89}$$

since the Euler equation is not satisfied for the individual points of that part of the extremal path. The condition to be satisfied over the same portion of the path is

$$N_0 - N = 0 \tag{90}$$

which implies

$$\left(\frac{\partial N}{\partial H} - \frac{\partial N}{\partial q} \frac{\partial s}{\partial z} z' \right) \delta z - s \frac{\partial N}{\partial q} z' = 0 \tag{91}$$

which may be rewritten as

$$\{N\} \delta z = \frac{d}{dt} \left(s \frac{\partial N}{\partial q} \delta z \right) \tag{92}$$

$\{N\}$ denoting the variational derivative of N shown on the left-hand side of equation 88. To obtain an extremum, we must have $\delta I = 0$ which implies from equation 92 that

$$\int_A^B d \left(s \frac{\partial N}{\partial q} \delta z \right) = 0$$

or

$$s \frac{\partial N}{\partial q} \delta z \Big|_A = s \frac{\partial N}{\partial q} \delta z \Big|_B . \tag{93}$$

This happens to be a rather inconvenient expression on account of the δz's.

If we introduce the new variable

$$u \equiv s \frac{\partial N}{\partial q} \delta z \tag{94}$$

and note that

$$\frac{du}{u} = \frac{\{N\}}{s \dfrac{\partial N}{\partial q}} dt \tag{95}$$

equation 93 becomes

$$u_A = u_B$$

and the integrated form of equation 95 yields

$$\log (u_A/u_B) = \int_A^B \frac{\{N\}}{s\dfrac{\partial N}{\partial q}}\, dt \tag{96}$$

or using equation 93

$$\int_A^B \frac{\{N\}}{s\dfrac{\partial N}{\partial q}}\, dt = 0 \tag{97}$$

which determines the point B implicitly. Some portions of the path AB may be covered twice by the extremal path.

OPERATING FOR MAXIMUM PROFITS

The value p of the power generated by the tidal plant varies with the time of day

$$p = p(t). \tag{98}$$

It also depends on the amount of power generated by the plant as the initial kilowatts of output are usually more expensive, so that

$$p = p(t, nN). \tag{99}$$

The total value of the power generated by the plant at a given instant of time may then be written as

$$P(t, nN) = \int_0^{nN} p(t, x)dx. \tag{100}$$

If we want to operate the plant for maximum profit, we must maximize the integral

$$I = \int_{t_0}^{t_1} P(t, nN)dt. \tag{101}$$

It is the task of the economist to determine the form of the functions p and P; however, we assume that p varies discontinuously when intervals of peak demands are met. We also assume

$$\partial p/\partial(nN) \leq 0 \tag{102}$$

namely that the value of power decreases or stays steady as the power output is increased. Assuming that all the turbines are in operation ($n = n_0$) and that the sluices are closed, the maximization of equation 101 leads to the requirement that

$$n_0 p\,(\partial N/\partial H) + s\frac{d}{dt}\,(p\partial N/\partial q) = 0 \tag{103}$$

and

$$[\int_0^{nN} p\, dx - pn_0 q(\partial N/\partial q)]\delta t - pS(\partial N/\partial q)\delta z\Big|_{t_0}^{t_1} = 0 \tag{104}$$

which are the generalizations of equations 74, 65, and 66 with $\lambda = 1$, $\mu = 0$. Here again $\delta z = 0$.

Starting the turbines — The initial condition to be satisfied at t_0 is

$$\int_0^{n_0 N} p\,dx - p n_0 q\,(\partial N/\partial q) = 0. \tag{105}$$

We note from Gibrat (1956a, b) that

$$\int_0^{n_0 N} p\,dx = p n_0 N - \int_0^{n_0 N} x\,dp$$

and

$$n_0(N - q(\partial N/\partial q)) = - n_0 q^2 H\,(\partial \eta/\partial q)$$

the first relation having been obtained from partial integration, and the second from the definition of the efficiency coefficient.

Equation 105 takes the form

$$\partial \eta/\partial q = - (1/\eta_0 q^2 H p) \int_0^{n_0 N} x\,dp = - (1/\eta_0 q^2 H p) \int_0^{n_0 N} x\,(\partial p/\partial x)\,dx \geq 0 \tag{106}$$

from equation 102, since x (the dummy symbol for power) is an essentially positive quantity.

If $\partial p/\partial(nN) = 0$, the starting condition is identical to the conditions on p. 2920, otherwise the turbines have to be started for

$$\partial \eta/\partial q > 0. \tag{107}$$

Equation 107 means that the turbines have to be started at a performance below their peak efficiency so that less power is produced for a given head, whenever the price of power decreases with increased output.

Looking at the original form equation 104, the boundary condition requires

$$\frac{1}{p} \int_0^{nN} p\,dx = nq\ \partial N/\partial q.$$

If $\partial \eta/\partial q = 0$, $N/q = \partial N/\partial q$ and in that case the boundary condition would become

$$\frac{1}{p} \int_0^{nN} p\,dx = nN$$

which can only be satisfied if $p = p_0$ a constant. For $\partial p/\partial(nN) < 0$, the left-hand side is always greater than nN, so that the turbines must be started for $\partial \eta/\partial q > 0$. The exact value of $\partial \eta/\partial q$ for which the operation has to be started is given by equation 106.

Discontinuous changes in the value of power — Supposing that we are in the course of power production and that the value of power is suddenly increased on account of the occurrence of a peak in demand, the Euler equation 103 has to be satisfied throughout the sequence of operations.

At the instant of the change in value of p, equation 103 may be written as

$$d(p\partial N/\partial q) = 0 \tag{108}$$

since $dt = 0$ and we assume that n_0, p, and $\partial N/\partial H$ have finite values. If p goes from p_1 to p_2 at that instant, the head cannot change its value but more water will be passed through the turbines to meet the increased power requirement (so long as we are operating with $\partial N/\partial q < 0$). Equation 108 may be rewritten as

$$p_1(\partial N/\partial q)_{q_1,H_1} = p_2(\partial N/\partial q)_{q_2,H_1}. \tag{109}$$

Equation 109 is sometimes called the condition for the refraction of the extremal: it is analogous to the bending of a light path when the rays enter a medium with a different index of refraction. In the q, H diagram, the refraction of the extremal may be represented as in Fig. 5. Similarly, Fig. 5 shows the refraction of the extremal path $z(t)$ in the z, t, diagram.

Other modes of exploitation — We may conceive of other modes of exploitation besides those of maximum energy production and of maximum profit. The plant may be operated so that it supplies energy only during times of peak demand or during times of relatively high demand. The calculus of variation does not apply to these modes of exploitation, the time of starting and ending the energy production being determined only by the occurrence of the threshold demand. The problem is now to organize the flow of water in and out of the basin so that the requirements of power production on sufficient demand are met.

In Fig. 6 we have illustrated the operation of a tidal plant that generates power only during times of peak demand. The broken line is the oscillating sea. The horizontal bars indicate the times of peak demand. The fluctuations in the level of the basin are indicated by the full lines.

Pumping, using the energy of the network, is carried out whenever power is not generated till a maximum or minimum level is reached in the basin. The change in level of the basin while energy is generated must be quite rapid. This implies the installation of powerful turbines with large output. Similarly the pumping must be effected by pumps of large capacity.

In the example considered, for the power installed, we note that energy could not be produced during the peak demands no. 5 and 6 and that they were not adequately met for, no. 4. It is evident that such a mode of operation is warranted only if the value of the power at peak demand vastly exceeds that of the off peak power. This situation is not likely in a well-integrated network. In the latter instance, the value of p is independent of time and

$$p = p(nN)$$

only. Then equation 103 becomes identical to 74 whereas 104 remains unchanged. The turbines are started for $\partial\eta/\partial q > 0$ but the extremal will never be refracted.

SEMIEMPIRICAL APPROACH OF VOYER AND PENEL

Equations 103 or 74 imply the actual calculation of the extremal paths. These paths will depend on the surface $S(z)$ of the basin for the various values

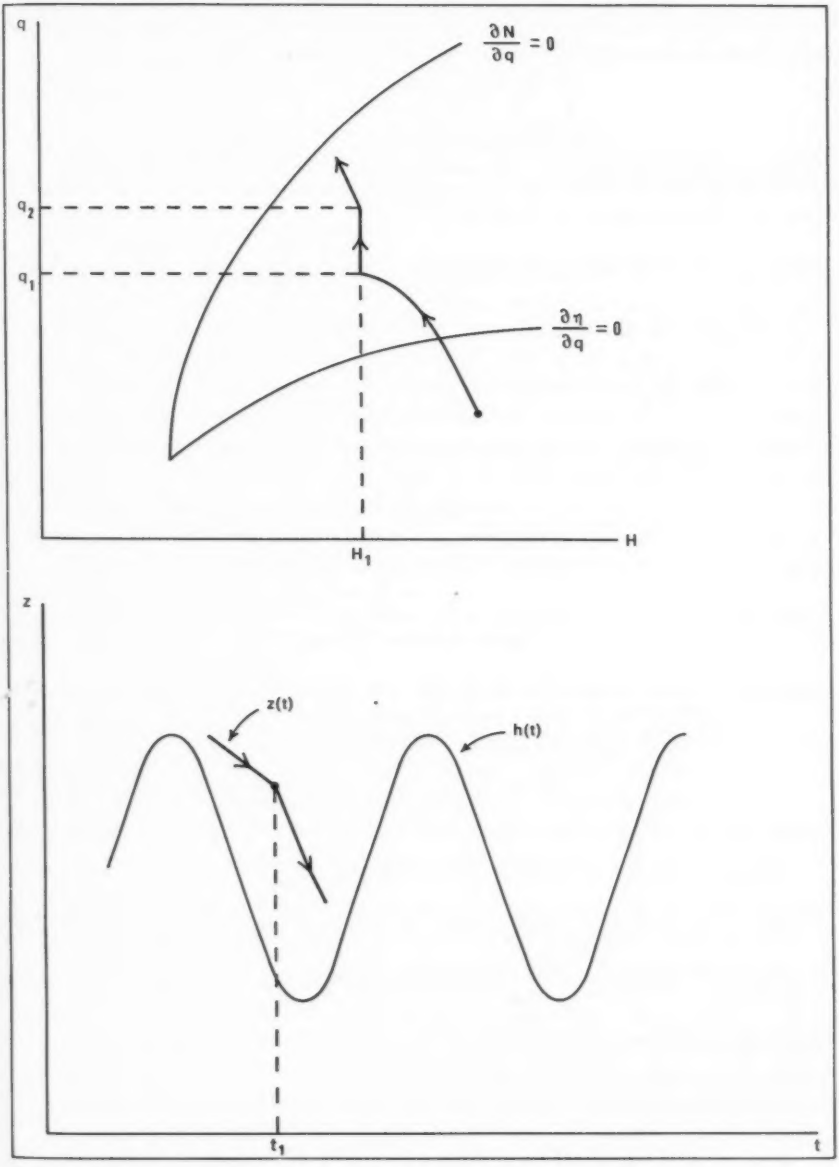

FIG. 5. So-called diffraction of the extremal induced by a sudden change in the value of the power at an instant t_1 shown in a q, H and in a z, t diagram.

TABLE 3. Résumé of the results of the calculus of variation for the operation of a tidal plant.

Physical relations for a single turbine: $H = z - h$; for the reservoir: $H = z - h$

$$q = -s\frac{dz}{dt} - \mu v_0 \qquad Q = nq' + V = n_0 q + V$$

RESULTS OF THE CALCULUS OF VARIATION

Maximum energy output:

Quantity to be maximized: $I = \int_{t_0}^{t_1} \lambda N \, dt$

Euler equations and boundary conditions implied: $N - \frac{q}{\lambda}\frac{\partial N}{\partial (q/\lambda)} = 0 \quad \frac{\partial (\lambda N)}{\partial (q/\lambda)} \cdot \frac{v_0}{\lambda} = 0$

$$\frac{\partial (\lambda N)}{\partial H} - \frac{\mu}{\lambda}\frac{v_0}{H}\frac{\partial (\lambda N)}{\partial (q/\lambda)} + \frac{s}{\lambda}\frac{d}{dt}\frac{\partial (\lambda N)}{\partial (q/\lambda)} = 0$$

$$\left[N - \frac{(q + \mu v_0)}{\lambda}\frac{\partial (\lambda N)}{\partial (q/\lambda)}\right]\delta t - \frac{s}{\lambda}\left[\frac{\partial (\lambda N)}{\partial (q/\lambda)}\right]\delta z \Bigg|_{t_0}^{t_1} = 0$$

Condition for starting the operations: (1) Pump: $H = 0$ initial $\frac{dH}{dt} = \frac{P}{s\frac{\partial P}{\partial q}}$

(2) Turbine: The extremal path in the qH diagram starts on the curve $\partial n/\partial q = 0$

initial $\frac{dz_0}{dt} = -\frac{q_0}{s(z_0)}$

Ending the operations: Final condition on the turbine $(q', H) = (q'_m, H_m)$. The extremal path in the qH diagram lies under the curve $\partial N/\partial q = 0$ and terminates at (q'_m, H_m)

Transitions: (1) Pump to turbine: Pumping stops at t_0, turbines start at t_1. Condition for transition $(P/\bar{q})_0 = (N/\bar{q})_1$

(2) Sluices closed to open: The sluices are opened fully when the extremal path in the qH diagram reaches the curve $\partial N/\partial q = 0$

(3) Turbines to pump: Turbines alone for $\partial N/\partial q > 0$, turbines with sluices at $\partial N/\partial q = 0$, turbines stopped at minimum head, sluices closed, and pumps started at $H = 0$.

Gradual turning on of the turbines at the start of a power generating operation: $\lambda = 0 \rightarrow 1$. The time taken to turn on all the turbines $\Delta t \simeq \frac{-s}{(\partial N/\partial H)}\Delta\left(\frac{N}{\bar{q}}\right)$

The limitation $N \leq N_0$ on the power output of the turbines: For $N < N_0$, the extremal path given by Euler's equation is followed. For $N = N_0$, the path follows the curve $N = N_0$ from A to B leaving the curve $N = N_0$ when the condition $\int_A^B \frac{\left\{\frac{N}{\bar{q}}\right\}}{s\,(\partial N/\partial q)}\,dt = 0$ is satisfied.

Operating for Maximum Profits:

Quantity to be maximized: $I = \int_{t_0}^{t_1} P(t, nN)\,dt$

Euler equation and boundary condition for sluices closed and all the turbines in operation:

$$n_0 p\frac{\partial N}{\partial H} + S\frac{d}{dt}\left(p\frac{\partial N}{\partial q}\right) = 0 \qquad \left[\int_0^{nN} p\,dx - pn_0 q\frac{\partial N}{\partial q}\right]\delta t - pS\frac{\partial N}{\partial q}\delta z \Bigg|_{t_0}^{t_1} = 0$$

Starting the turbines: The extremal path starts below the curve $\partial \eta/\partial q = 0$ if $\partial p/\partial (nN) < 0$

Refraction of the extremal path caused by a discontinous change in price:

$$p_1(\partial N/\partial q)_{q_1, H_1} = p_2(\partial N/\partial q)_{q_2, H_1}$$

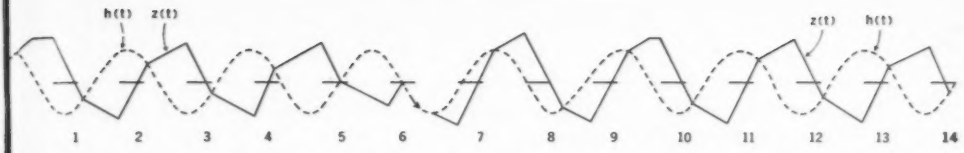

g. 6. An attempt at the exploitation of a tidal plant with the purpose of producing energy only during intervals eak demand. The solid line represents the level of the basin and the broken line is the sinusoidal oscillation of level of the sea. The intervals of peak demand are indicated by segments on the time scale and they have been numbered.

of z, on the tide $h(t)$, on the discharge capacity of the sluices V(H), and finally on the power characteristics of the turbines and of the pumps. Essentially, one needs a series of graphs giving lines of $\partial N/\partial H = \text{const}$ and $\partial N/\partial q = \text{const}$, in addition to the useful lines $\partial N/\partial q = 0$, $\partial \eta/\partial q = 0$, and $N = N_0$ on a q, H diagram. In particular, one needs to calculate the differences between the various $\partial N/\partial q$'s to evaluate successfully the extremal paths. It is evident that a particular type of turbine and a specific basin must be considered to carry out such calculations. The type of turbine considered in France was the Neyrpic bulb type. In that particular instance, it turned out that the differences in the $\partial N/\partial q$'s could not be calculated with too much accuracy.

Gibrat (1954) had noted that N, for the Neyrpic turbine, could be approximately represented by the function

$$N = a[(H - H_m)q - f(q)] \tag{110}$$

H_m being the minimum depth for which the turbine can generate power, a, a constant, and $f(q)$, a function depending on q only and measuring essentially the decrease in efficiency of the turbine with respect to a perfectly efficient turbine.

For such a representation, the line $\partial N/\partial q = 0$ becomes

$$H - H_m - \frac{df}{dq} = 0$$

so that

$$\frac{df}{dq} = H - H_m$$

on $\partial N/\partial q = 0$.
At $H = H_m$

$$\frac{df}{dq} = 0 \text{ or } f(q_m) = \text{const}$$

and since $N(q_m, H_m) = 0$, it follows

$$f(q_m) = 0. \tag{111}$$

On the other hand, the line $\eta = \eta_{max}$ ($d\eta/\partial q = 0$) is given by the line on which $f(q) = 0$, namely the line $q = q_m$. In this algebraic model, therefore, the line of peak efficiency is given by the horizontal line $q = q_m$ in the q, H diagram. For the type of turbine considered, the actual line of peak efficiency is only approximately horizontal.

Euler equation 74 with 110 becomes

$$naq + Sa(\dot{H} - \frac{d}{dt}\frac{df}{dq}) = 0 \tag{112}$$

or, using equation 50 with $\mu = 0$ and equation 43

$$\frac{d}{dt}(H - z) = \frac{d}{dt}\frac{df}{dq}$$

which means that

$$\Delta(H - z) = \Delta h = \Delta\left(\frac{df}{dq}\right) \tag{113}$$

over an interval of time Δt.

Within the algebraic representation of $N(q, H)$, Euler's equation simply means that a change Δh in the tide during the time Δt must cause an equal change $\Delta(df/dq)$ over the same time interval. This situation is shown in Fig. 7.

If the value of the power p is independent of t and nN, the operations will be started on $\partial\eta/\partial q = 0$. The level of the basin is z_0 and the height of the tide is $h(t_0)$. With an interval of time Δt, later, the change in the height of the tide is $h_1 = h(t_0 + \Delta t) - h(t_0)$ and, according to equation 113, it should equal $\Delta(df/dq)$. Since $df/dq = 0$ on $\partial\eta/\partial q = 0$, it follows that

$$\Delta(df/dq)_{t_1} = df/dq \mid_{t_0 + \Delta t}$$

so that

$$\Delta h_1 = df/dq \mid_{t_1}.$$

As a consequence of this, taking a distance Δh_1 from the vertical raised at H_m to $\partial N/\partial q = 0$, will give the discharge q_1 for which Euler's equation is satisfied. Similarly the knowledge of Δt gives the head H_1 since the water discharge is $\Delta t\ (q_0 + q_1)$ which determines z_1.

In this way, the second point on the extremal is found without the need of either calculating or knowing the lines of $\partial N/\partial q = \text{const}$ and $\partial N/\partial H = \text{const}$. The approximate amount of energy produced during this interval is $\Delta t \cdot N((q_0 + q_1), (H_0 + H_1))$, which can be gradually accumulated to give the amount of energy produced during the cycle.

The final condition for the end of the operations requires that the head equal H_m, the minimum head for which energy can be generated. This condition is imposed by the turbine and not by the calculus of variations that simply requires that the turbines be started or stopped on or near the line $\partial\eta/\partial q = 0$.

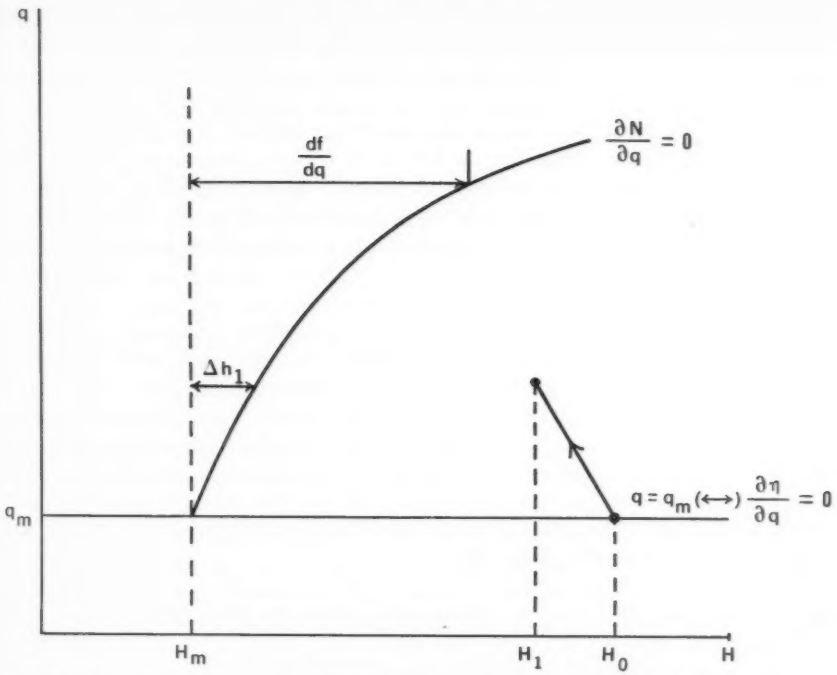

FIG. 7. Method for tracing of the extremal path when the function N may be represented analytically by $N = a\,[(H - H_m)q - f(q)]$.

The choice of the initial time for starting the operations is proven right or wrong depending on whether or not the extremal meets the point (q_m, H_m) at the end of the operations.

The application of the calculus of variation would then be a very simple matter if the power output characteristics of the turbine were given by equation 110.

This is not quite the case, so one could attempt to satisfy Euler's equation 74 or 110 using the actual $N(q, H)$ by trial and error, in an effort to keep away from the lines $\partial N/\partial q = \text{const}$ and $\partial N/\partial H = \text{const}$. One might ascertain the probable path of the extremal in the q, H diagram. We know for certain that the longer it takes to fill or empty the basin, the smaller will be the energy obtained.

If the tide is small (neap tide) there will be a small volume of water converted into energy and since the turbines start approximately on $\partial\eta/\partial q = 0$ it will be convenient to attempt to extract the energy at peak efficiency to exploit best the amount of water available even if the discharge is not large at any time. On the q, H diagram, this means that the path of the extremal should lie close to $\partial\eta/\partial q = 0$ over a good part of the cycle.

If the tide is large (spring tide), the volume of water to be handled will be at its maximum and exploiting it at peak efficiency would make the exploitation unduly long. It is therefore advantageous to increase the discharge so that the energy is generated at near its maximum value for the given value of q, H. In this instance, this means that the path of the extremal should leave $\partial\eta/\partial q = 0$ and move close to $\partial N/\partial q = 0$ over a good part of the cycle.

For a given initial time, various trajectories can be tried using the criterion just mentioned till a maximum of energy output is obtained. Then one can check if in the final cycle, the extremal falls on q_m, H_m. If this is not so, another initial time must be tried. This method naturally takes more time but the actual $N(q, H)$ function would be used.

Voyer and Penel (1956) suggest a compromise that exploits the graphical convenience of the algebraic representation $N(q, H)$ and the confidence that is gained by using the actual $N(q, H)$ of the turbine.

They propose simply to use the algebraic method on the actual $N(q, H)$ surface of the turbine, Δh being measured between the vertical $H = H_m$ and $\partial N/\partial q = 0$ with the departure taking place on the actual curve $\partial\eta/\partial q = 0$. The calculations are thus greatly accelerated and for the turbine considered, the discrepancies between the pure empirical approach and the technique they propose are of the order of 1%.

Reaction on the Energy Available of the Exploitation of the Tidal Motion

The tide in a basin that is suitable for its exploitation consists normally of the cooscillation of the water in the basin with the oscillations of the ocean with which it is in contact; the latter are caused directly by the tide-generating forces. The tide in the basin is therefore a response phenomenon and this response depends fundamentally on the depth and width configuration of the basin, the frequency of the oscillation being that of the ocean.

Any artificial construction in the basin will automatically alter this configuration. If the part of the basin that is enclosed is small with respect to the dimensions of the cooscillating basin, the effect on the response of the basin will be drastically altered and the tide at the gate of the tidal plant might be significantly different from what it was before its construction. This is a very peculiar and very fundamental feature of tidal energy and this fact makes it very different from the conventional hydraulic energy.

The alteration in the tidal response may go in any direction: the tide may be enhanced after the construction of the tidal plant or it may be diminished. In a rectangular basin of constant depth open at one end to the ocean, the tide will be enhanced or reduced by the construction of a plant at its head, depending on whether its length and depth are such that it is longer or smaller than the one-quarter wave length of the resonant configuration. In the case of the Bay of Fundy the length of the bay is less than the resonant length for the M_2 (lunar semidiurnal) tidal oscillation so that the complete closure of Minas Basin would reduce the tide just outside by over 15% (Yuen, MS,

1967). In the Chausey project in France, the expected reduction is of the order of 20% (Gibrat, 1966). By exploiting the tide in Passamaquoddy Bay in the Bay of Fundy, the amplitude would be slightly increased at the head of the Bay of Fundy for the simple reason that less energy would be diverted into the Passamaquoddy and therefore more energy would reach the head (McLellan, 1958).

In the actual exploitation of the tide in Minas Basin, the lowering in the head would be less than 15% since some water would be allowed to pass in and out of the basin, thus compensating partly for the shortening of the Bay of Fundy.

In any case, the reaction of the construction of the tidal plant on the tide must always be carefully studied before a closer assessment of the feasibility of the project is undertaken. Modest plants will affect the tide slightly but ambitious and costly projects might alter the key source of their contemplated energy. This investigation is naturally within the reach oi contemporary hydrodynamics and the Hansen numerical method is particularly suitable for it (Hansen, 1956).

Modification of the Tide in a Rectangular Basin

The simple model of a rectangular basin whose open end is in contact with the ocean and in which a tidal plant is installed across a given section near the head, yields some valuable information on the modification of the tidal regime.

The basin of constant depth D has length L, and the dam in which the turbines are housed lies at $L_1 < L$, measured from the entrance of the basin. The basin is considered narrow enough so that the motion is significant along it and not across. The equations to be solved, neglecting friction, are

$$\partial u/\partial t = - g\partial h/\partial x \tag{114}$$

$$\partial h/\partial t = - D\partial u/\partial x \tag{115}$$

x being the coordinate along the length of the basin, h and u the tidal amplitude and the mean velocity of the tidal current. These equations have the general solution:

$$h = h_0 \cos K(x\text{–}L) \cos\sigma t + A \cos (Kx + \sigma t - \delta) + B \cos (Kx - \sigma t - \epsilon) \tag{116}$$

$$u = (g/D)^{\frac{1}{2}}[h_0 \sin K(x\text{–}L) \sin\sigma t - A \cos (Kx + \sigma t - \delta) + B \cos (Kx - \sigma t - \epsilon)] \tag{117}$$

where $K = (\sigma^2/gD)^{\frac{1}{2}}$, for a harmonic oscillation of frequency σ.

The first term of equations 116 and 117 represents the standing wave that would prevail in the basin before the installation of the tidal plant. The two following terms represent the progressive waves that are generated by the presence and the operation of the tidal plant. A, B, δ, and ϵ are arbitrary constants that are to be determined from the boundary conditions.

We assume that the level of the reservoir located from L_1 to L varies according to the law

$$h_r = h_1 \cos(\sigma t - \beta) \tag{118}$$

h_1 being the amplitude and β the phase retardation of the oscillation in the reservoir behind the tide in the sea. h_1 and β are quantities predetermined by the exploitation considered and by the pumps and turbines installed. Equation 118 is far from representing the actual variation in the level of the reservoir as seen for instance in Fig. 2 but it has the advantage of analytic simplicity. Without pumps h_1 cannot be larger than $h_0 \cos K\Delta$ where $\Delta = L_1 - L$, the amplitude of the tide at the dam site before the installation of the plant.

If the dam were opaque,

$$u(L_1) = 0 \text{ and } \beta \text{ is indeterminate since } h_1 = 0.$$

If the dam did not exist,

$$u(L_1) = (g/D)^{\frac{1}{2}} h_0 \sin K\Delta \sin\sigma t \text{ and } \beta = 0.$$

In any actual exploitation

$$0 < hu(L_1) < (g/D)^{\frac{1}{2}} h_0 \sin K\Delta \sin\sigma t.$$

The upper limit can be expected only if the pumps are used extensively.

Taking as positive a current in the direction of increasing x (moving towards the head of the basin), the conservation of water in the reservoir requires that

$$S\, dh_r/dt = su$$

where S is the surface of the reservoir and s the cross-section of the basin at the dam site, so that

$$u(L_1) = -(S/s)\, \sigma h_1 \sin(\sigma t - \beta). \tag{119}$$

The arbitrary constants are now determined by applying the boundary conditions at $x = 0$ and $x = L_1$.

At $x = 0$, the mouth of the basin, we assume that the influence of the tidal plant on the tide is negligible so that

$$A \cos(\sigma t - \delta) + B \cos(\sigma t - \epsilon) = 0$$

which implies

$$A \cos\delta + B \cos\epsilon = 0. \tag{120}$$

$$A \sin\delta + B \sin\epsilon = 0. \tag{121}$$

For equations 120 and 121 to have a solution, we need

$$\cos\delta \sin\epsilon + \sin\delta \cos\epsilon = \sin(\delta + \epsilon) = 0$$

which implies

$$\delta + \epsilon = \pi$$

or

$$\delta = \tfrac{1}{2}\pi + r \qquad \epsilon = \tfrac{1}{2}\pi - r \tag{122}$$

r to be subsequently determined from the further boundary condition at $x = L_1$.

A consequence of equation 122 is that

$$A = B$$

Equations 116 and 117 can now be written as

$$h = h_0 \cos K(x - L) \cos\sigma t + 2A \sin Kx \cos(\sigma t - r) \tag{123}$$

$$u = (g/D)^{\frac{1}{2}} [h_0 \sin K(x - L) \sin\sigma t - 2A \cos Kx \sin(\sigma t - r)]. \tag{124}$$

The boundary condition (equation 119) at $x = L_1$

$$(g/D)^{\frac{1}{2}} [h_0 \sin K\Delta \sin\sigma t - 2A \cos KL_1 \sin(\sigma t - r)] = -(S/s)\,\sigma h_1 \sin(\sigma t - \beta)$$

or

$$h_0 \sin K\Delta \sin\sigma t - 2A \cos KL_1 \sin(\sigma t - r) = -R \sin(\sigma t - \beta) \tag{125}$$

where

$$R = (S/s)\sigma h_1 (D/g)^{\frac{1}{2}}.$$

We note

$$0 < R < h_0 \sin K\Delta \tag{126}$$

provided the pumps are not used too extensively.

The equating of the coefficients of $\cos\sigma t$ and $\sin\sigma t$ in equation 125 gives

$$A \sin r = \frac{R \sin\beta}{2 \cos KL_1} \tag{127}$$

$$A \cos r = \frac{h_0 \sin K\Delta + R \cos\beta}{2 \cos KL_1} \tag{128}$$

which may be solved as

$$A = \frac{1}{2 \cos KL_1} \sqrt{h_0^2 \sin^2 K\Delta + 2R \cos\beta\, h_0 \sin K\Delta + R^2} \tag{129}$$

$$\tan r = \frac{R \sin\beta}{h_0 \sin K\Delta + R \cos\beta}. \tag{130}$$

NEAR ZERO FLOW AT THE DAM SITE

This hypothesis holds when the flow at the dam site is much reduced compared with the flow that prevailed there before. We may then handle R as a first order quantity compared with $h_0 \sin K\Delta$. We may use equations 127 and 128 directly to obtain

$$A \simeq \frac{h_0 \sin K\Delta + R \cos\beta}{2 \cos KL_1} \tag{131}$$

and

$$r \simeq \frac{R \sin\beta}{h_0 \sin K\Delta}. \tag{132}$$

To a first order in R, the modified elevation at the dam site is

$$h(L_1) = h_0 \cos\sigma t \frac{\cos KL}{\cos KL_1} + R \tan KL_1 \cos(\sigma t - \beta). \tag{133}$$

The first term represents the amplitude of the tide at the dam site if it were *opaque*. If $KL < \frac{1}{2}\pi$, this quantity will be smaller than the value it had before the construction of the dam. If both KL and KL_1 are $> \frac{1}{2}\pi$ (L and L_1 being longer than one-quarter wave length for the constituent considered), the quantity will be larger than before.

The second term represents the modification in the amplitude of the tide due to the slight but net flow at the dam site:

$$h' = R \tan KL_1.$$

For $KL_1 < \frac{1}{2}\pi$ $\quad h' > 0$

$KL_1 > \frac{1}{2}\pi$ $\quad h' < 0.$

This term therefore counteracts up to a point the decrease or increase in the amplitude in the tide brought about by the construction of the dam (making it slightly transparent).

The energy generated during one tidal period amounts to

$$\begin{aligned} E &= \rho g \int_0^T su(L_1)(h_r - h)dt \\ &= -\rho g S\sigma h_1 \int_0^T \sin(\sigma t - \beta)(h_1\cos(\sigma t - \beta) - h(L_1))dt \\ &= \rho g S h_1 \sigma \int_0^T h_0 \frac{\cos KL}{\cos KL_1} \cos\sigma t \sin(\sigma t - \beta)\, dt \\ &= -\rho g S h_1 h_0 \frac{\cos KL}{\cos KL_1} \pi \sin\beta \end{aligned} \tag{134}$$

since $\sigma = 2\pi/T$. The minus sign indicates that energy is drawn from the tide.

The value of β which maximizes equation 134 is

$$\beta = \tfrac{1}{2}\pi \tag{135}$$

which approximates very closely to the phase of the ideal operation shown in Fig. 2.

The maximum energy obtainable is therefore

$$E_{max} = \rho g S \pi h_1 h_0 \frac{\cos KL}{\cos KL_1}. \tag{136}$$

It is the same as if the reservoir were closed, with $\beta = \frac{1}{2}\pi$. If we compare this expression with the energy obtained from the ideal exploitation of the plant, we get, using equation 26

$$E_{max}/E = \frac{\pi}{4} \frac{h_1}{h_0} \frac{\cos KL}{\cos^2 K\Delta \cos KL_1} \tag{137}$$

since in our present notation the h_0 of equation 26 stands for $h_0 \cos K\Delta$, the amplitude of the tide at the dam site before its construction.

For a reservoir of small dimensions relative to the basin, $\cos K\Delta \simeq 1$ while $\cos KL/\cos KL_1 \lesseqgtr 1$ depending on whether KL and KL_1 are $\lesseqgtr \frac{1}{2}\pi$. Therefore

$$E_{max}/E < \frac{\pi}{4} \frac{h_1}{h_0} \text{ for KL and } KL_1 < \tfrac{1}{2}\pi \tag{138}$$

and

$$E_{max}/E > \frac{\pi}{4} \frac{h_1}{h_0} \text{ for KL and } KL_1 > \tfrac{1}{2}\pi.$$

In practice, h_1 can barely reach the value of h_0. However, the energy obtained from a practical exploitation could exceed the theoretical energy E given by equation 26 if the length of the basin exceeds one-quarter wave length, equation 26 having been obtained ignoring the reaction of the tidal oscillation to the presence of the tidal plant, whereas in this paragraph we take this fact into consideration. The second alternative simply indicates that the original tidal oscillation in the rectangular sea would be amplified by the effective shortening of the sea to a length closer to one-quarter wave length, theoretically the resonant length.

Disadvantages of Tidal Energy

The exploitation of tidal energy presents many difficulties that are not encountered in the exploitation of hydraulic energy.

First, the power available is intermittent and when it is available, it varies rapidly. The human need for power is also intermittent but it follows the solar cycles whereas the tide (where it is of importance) essentially follows the periods of the moon. As stated already, this forces us to consider the tide as a wild form of energy and its exploitation in a fashion suitable to human needs leads to many problems.

The exploitation of a conventional hydroelectric plant is simple compared with that of a tidal plant. Water is drawn from a reservoir of large capacity at a rate sufficient to meet the demand and to keep the level of the reservoir

almost steady. Fluctuations in the rainfall are damped out by the large capacity of the reservoir and their cumulative effects take months before they are felt. In a tidal plant, the turbines are turned on and off and an ill-timed operation might affect the production of energy for many subsequent cycles. The number of possible sequences of operations has been studied and calculated in a previous section and it is simply staggering. Even at that, not only is the number of possible sequences extremely large but within a given sequence, the timing of each individual operation requires special considerations and we have to bring the calculus of variations to our aid.

Normally the installation of a conventional hydroelectric plant is welcomed by the local population as it often regulates the flow of rivers, dissipates the danger of floods, and may even be beneficial for the purpose of irrigation. In contrast, the installation of a tidal plant implies complications in the navigation in and around the plant, possibly adverse effects on the fish population and its migrations, and it may even cause an adverse modification of the tide that it purports to exploit.

When it comes to the tool used for the exploitation of tidal energy, one turns almost automatically towards the conventional hydroelectric turbines; as they are, none of them are actually suitable for the exploitation of tidal energy since they are normally devised to generate power for steady flows in a given direction over a very narrow range of flow and head. Tidal motion implies rapid and continuous changes in the head and in the direction of flow. Only very recently has any attention been paid to the design of a suitable turbine (Schwob, 1956; Wilson, 1965; Kammerlocher and Duclos, 1956).

Finally, the medium normally used in a conventional hydroelectric plant is fresh water whereas the medium for a tidal plant is sea water. Sea water is notoriously corrosive and conductive. Since normally turbines are made up of various combinations of alloys for reasons of strength and rigidity, electrolytic effects may lead to unexpected corrosion on alloys that, individually, are corrosionproof in sea water.

It is easy to understand, after these considerations, why tidal energy was not actually exploited until very recently (Gibrat, 1966) although this prospect has preoccupied many scientists and engineers for a very long period of time (Davey, 1923; Fichot, 1923).

The only positive thing that may be said on behalf of tidal energy is that it is clean energy compared with nuclear or thermal energy.

TIDAL ENERGY IN THE BAY OF FUNDY

Characteristics of the Tide in the Bay of Fundy

The semidiurnal vertical tidal oscillation is large all over the Bay of Fundy. If we restrict ourselves to M_2, the main lunar semidiurnal constituent, which represents as well the mean amplitude of the vertical oscillation, the amplitude of M_2 exceeds already 2 m in the vicinity of Grand Manan Island and it increases to more than 5.5 m at Burncoat Head, at the head of Cobequid Bay (Fig. 8 and 9).

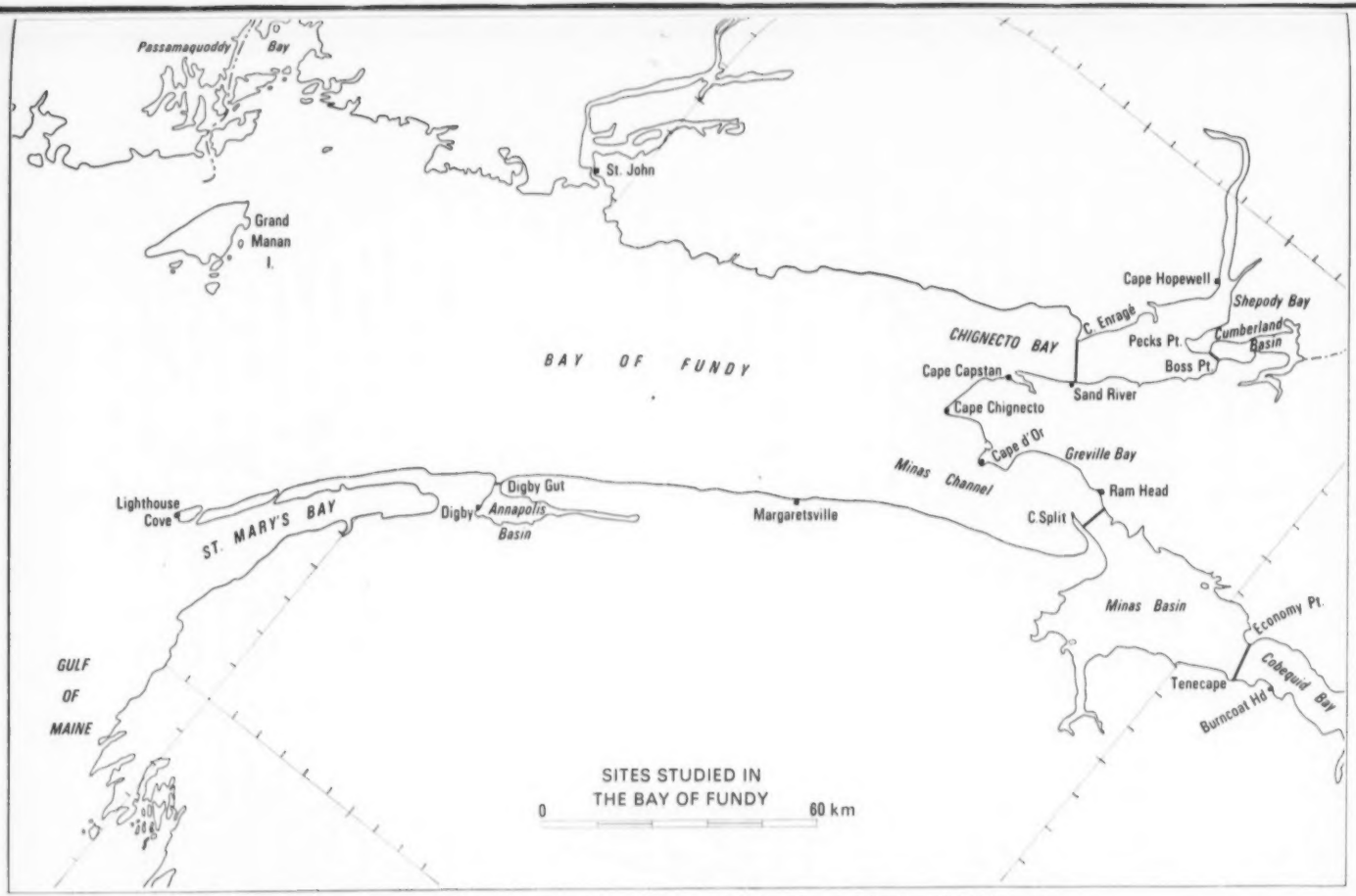

FIG. 8. Some sites in the Bay of Fundy favourable for the exploitation of tidal energy.

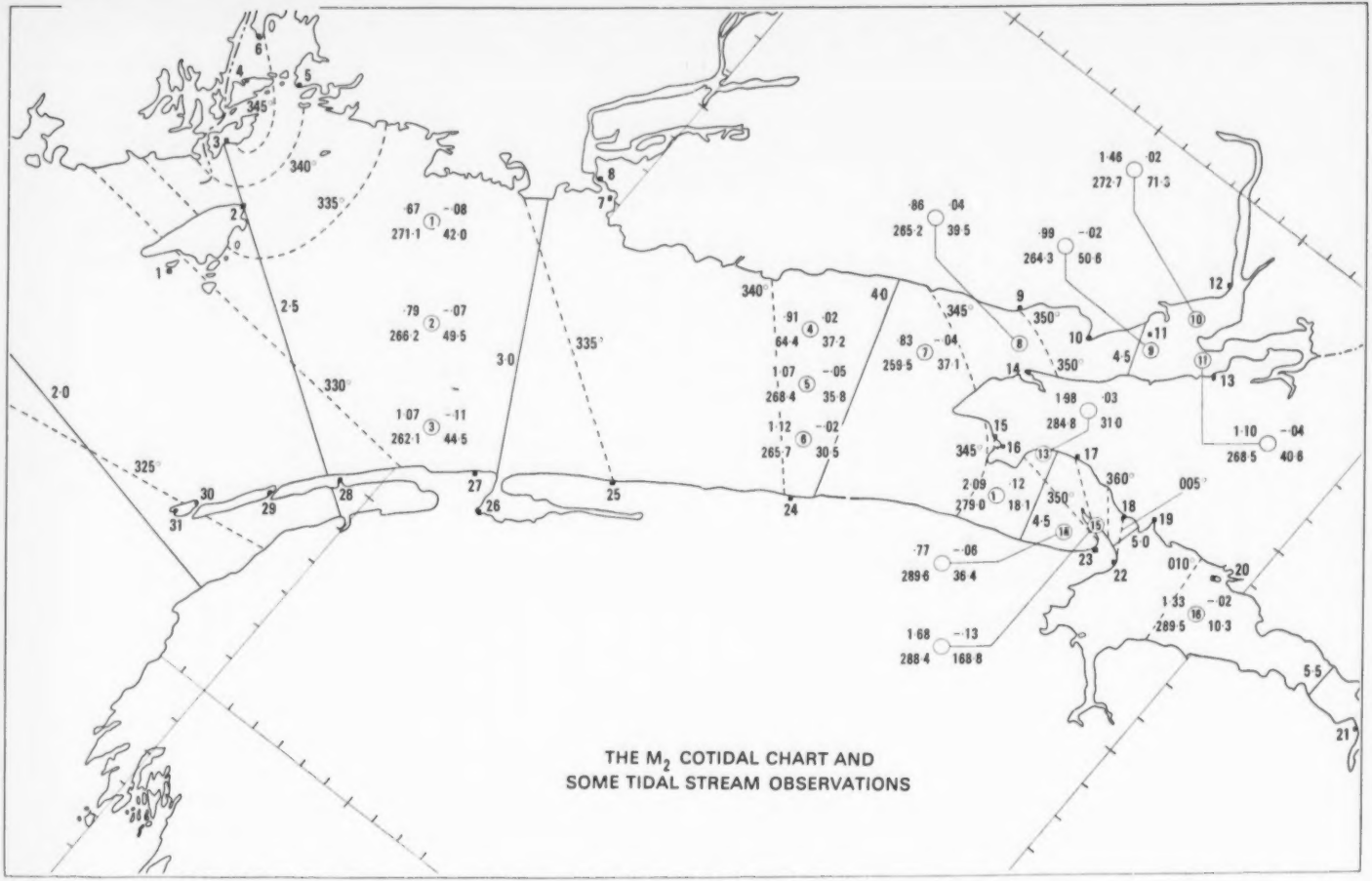

FIG. 9. Cotidal chart for M_2 in the Bay of Fundy. The points indicated by a number in a square are the coastal stations mentioned in Table 4. The stations indicated by a circled number are the stations occupied during the 1965 Bedford Institute of Oceanography current survey. The cotidal lines are labelled in degrees; the coamplitude lines are labelled in meters. The four quantities plotted over the current station give from left to right and from top to bottom the semimajor and semiminor axes of the stream ellipse in meters/second, the phase of the stream in degrees, and the inclination of the major axis with

Another feature peculiar to the Bay of Fundy is the size of N_2, the semidiurnal constituent associated with the variable distance of the moon from the earth (lunar apogee and perigee). It is everywhere larger than S_2, the main solar semidiurnal constituent, and its amplitude varies from .5 m near Grand Manan to over 1 m at Burncoat Head. S_2 itself varies from .4 to .8 m over the same area.

The diurnal constituents increase but slightly over the body of the Bay of Fundy and they are much smaller than the semidiurnal constituents; the largest of them, K_1 and O_1, have an amplitude of the order of .15 m over the bay.

With these circumstances, the variation between neap and spring tide is not the most important variation in the sea level but rather the occurrence of spring tide at perigee and of neap tide at apogee. The mean amplitude of the tide is given by M_2 and the mean equinox spring tide at perigee and the solstices neap tide at apogee are $M_2 + N_2 + S_2$ $(+ K_2)$ and $M_2 - N_2 - S_2$ $(- K_2)$ respectively. K_2 interferes with S_2 over an interval of 6 months and it is related to the equinox and the solstices. It is left in parentheses because it cannot be separated from S_2 from short series of observations and this happens to be the case for most of the stations around the Bay of Fundy.

The time interval between two successive lunar perigees is one anomalistic month or 27.55 days whereas the time interval between two successive spring or neap tides is $\frac{1}{2}$ synodic month or 14.76 days. The overlap of spring tide with lunar perigee (or neap tide with lunar apogee) will occur at intervals of about 7 months.

The smallness of the diurnal constituents leads to a small diurnal inequality that, when it is marked, is due rather to the interference of the semidiurnal constituents.

The semidiurnal tidal streams run nearly one-quarter period ahead of the vertical tide over the body of the Bay of Fundy, thus indicating that the oscillation in this basin approximates closely to a standing wave oscillation. The streams are nearly rectilinear and when they are rotating they tend to rotate clockwise. Their magnitude is of the order of .8 m/sec near Grand Manan and they increase steadily towards the head of the Bay. In constricted areas such as Minas Channel they reach a velocity of 3 m/sec.

The diurnal streams are small and seldom exceed .05 m/sec.

Table 4 lists the value of the main tidal constituents of the vertical tide for a few stations around the Bay of Fundy. Some of the observations are very old and they extended over intervals of less than 3 months; the values given cannot be considered as accurate. However, since it is all that is available, we have used the data on M_2 to draw a cotidal chart for this constituent (Fig. 9); it gives lines of equal amplitude and phase lags. The stations are indicated by a squared number in the figure, which corresponds to the number given in Table 4. On account of the scanty information available, there are many possibilities in the drawing of the cotidal lines. As a consequence, we have kept them as straight and schematic as possible.

FIG. 9. Cotidal chart for M_2 in the Bay of Fundy. The points indicated by a number in a square are the coastal stations mentioned in Table 4. The stations indicated by a circled number are the stations occupied during the 1965 Bedford Institute of Oceanography current survey. The cotidal lines are labelled in degrees; the coamplitude lines are labelled in meters. The four quantities plotted over the current station give from left to right and from top to bottom the principal current ellipse, the direction of the greatest current, the phase of the greatest current and the ratio of the minor to the major axis.

TABLE 4. The main constituents of the tide for some coastal stations around the Bay of Fundy.

Name	Lat N	Long W	M_2		N_2		S_2		K_2		K_1	
			h_0 m	$\lvert v\rvert$ °	h_0 m	$\lvert v\rvert$ °	h_0 m	$\lvert v\rvert$ °	h_0 m	$\lvert v\rvert$ °	h_0 m	$\lvert v\rvert$ °
1. Littlewood Is.	44°36′	66°48′	2.01	328	.26	317	.42	026	.11	026	.12	116
2. North Head	44 46	66 45	2.51	339	.49	312	.39	015	.11	015	.14	131
3. Welsh Pool	44 53	66 57	2.60	344	.46	317	.37	018	.10	018	.15	136
4. Fairhaven	44 58	67 01	2.68	346	.59	316	.45	018	.12	024	.13	142
5. Letite Harbour	45 03	66 52	2.54	340	.60	312	.45	013	.12	013	.12	136
6. Port St. Andrews	45 04	67 03	2.72	349	.62	318	.44	022	.12	022	.16	144
7. Partridge Is.	45 14	66 03	3.08	337	.60	308	.51	009	.14	009	.16	131
8. St. John	45 15	66 04	3.03	342	.62	314	.50	016	.14	016	.16	134
9. Herring Cove	45 35	64 58	4.15	351	.79	322	.66	026	.18	026	.19	138
10. Cape Enragé	45 36	64 46	4.27	352	.81	323	.69	027	.19	027	.20	129
11. Grindstone Is.	45 44	64 38	4.57	353	.86	324	.73	028	.20	028	.20	134
12. Cape Hopewell	45 52	64 35	4.85	354	.91	325	.78	029	.21	029	.13	137
13. Joggins Wharf	45 41	66 28	4.88	351	.77	321	.72	031	.20	031	.16	134
14. Cape Capstan	45 28	66 51	4.13	347	.78	318	.66	022	.18	022	.19	134
15. West Advocate	45 21	64 49	4.09	342	.88	311	.68	026	.18	026	.18	122
16. Advocate	45 20	64 47	4.21	343	.85	317	.72	026	.20	026	.18	135
17. Port Greville	45 40	64 56	4.61	356	.86	324	.69	037	.19	037	.17	136
18. Cape Sharp	45 22	64 23	4.80	005	.91	345	.72	056	.20	056	.16	140
19. Parrsboro	45 22	64 20	5.05	005	.85	337	.75	049	.20	049	.19	143
20. Five Is.	45 23	64 08	5.30	011	.98	345	.79	053	.21	053	.22	155
21. Burncoat Head	45 19	63 49	5.64	014	1.10	351	.83	059	.23	059	.14	154
22. Cape Blomidon	45 16	64 21	5.03	004	1.00	336	.73	044	.20	044	.16	150
23. Scott's Bay	45 19	64 26	4.66	349	.96	321	.67	032	.18	032	.16	138
24. Margaretsville	45 03	65 04	3.93	344	.72	316	.68	009	.22	009	.16	123
25. Parker's Cove	44 50	65 32	3.26	335	.70	310	.51	007	.14	007	.20	135
26. Digby	44 38	65 45	3.11	337	.58	309	.55	005	.15	005	.19	132
27. Deep Cove	44 40	65 50	2.97	334	.60	314	.44	006	.12	006	.16	129
28. Sandy Cove	44 30	66 06	2.54	333	.54	307	.45	005	.12	005	.17	132
29. Tiverton	44 24	66 13	2.33	324	.52	291	.41	359	.11	359	.16	123
30. Westport	44 16	66 21	2.20	325	.51	294	.30	357	.08	357	.14	130
31. Light House Cove	44 15	66 24	2.15	325	.45	297	.34	357	.09	357	.16	124

The stations indicated by circled numbers over the body of the bay are the main stations occupied during the current survey carried out in 1965 by the Bedford Institute of Oceanography under the direction of Mr C. J. Langford.

The four numbers plotted around each station give respectively from left to right and top to bottom M, m, in m/sec, $|\mu|$, and α. α is measured from a horizontal axis running towards the east. The current data for stations 1, 2, and 3 are not representative of the current across the whole vertical section as most of them were taken at a depth of 13 m whereas the average depth across the whole vertical section is about 68 m. It is probable that the average phase of the M_2 stream across the section is smaller than the value of 266.4° indicated by the observations. The abnormal phase at station 5 may perhaps be attributed to the asymmetrical configuration of the basin in that part of the bay. The data for station 14 were obtained from a single 15-day analysis and they are not satisfactory. As we will see below, they fail to satisfy the equations of continuity and the energy relationships. The value of the data at station 14 is problematic on account of the ambiguity of the clock time used at that station (Godin, MS, 1968). From the cotidal chart (Fig. 9), we note that the vertical tide progresses quite rapidly in the bay (30° of phase $\simeq$ 1 hr or 5° of phase $\simeq$ 10 min of time), the crest of high water travels from Light House Cove to Cape Chignecto in less than 40 min. There is some evidence that it is strongly refracted around Cape Split with a delay of about half an hour between its entrance in Minas Channel and its exit into Minas Basin. The progress of the M_2 tide is much more rapid in the northern arm of the bay, Chignecto Bay, if we chose to believe the coastal and current observations. The increase in range from the mouth to the head of the bay is far from dramatic, the ranges being in the ratio of 2:6 between Burncoat Head and Light House Cove; the response to the M_2 tide in that part of the bay to the oceanic oscillation cannot be attributed to resonance. The amplification of the M_2 tidal signal occurs in fact in the Gulf of Maine (Rao, 1968).

At the mouth of the bay, the tidal streams occur later in the northern part of the bay as the tidal wave emerges from the Gulf of Maine in a northward direction. In the centre of the bay, the later streams are found in its middle portion. Further ahead the wave progresses more slowly in Minas Channel than in Chignecto Bay.

The larger ranges of the vertical tide and the strongest tidal streams are found in the southern part of the Bay of Fundy, in Minas Channel, and the largest concentration of tidal energy is found between Cape Split and Ram Head at the head of Minas Channel.

Power Transfer Vector

It is possible to use the data on M_2 to evaluate the values of the power transfer vector across various sections of the bay. We restrict ourselves to M_2 since it represents the mean tide and therefore stands for average conditions; the use of the mean spring tide or the mean spring tide at apogee would yield

larger values and yield a rosier picture of the power potential of the Bay of Fundy, but it would not be representative of average conditions.

From our definitions 12 and 17, the pulsating and alternating power transfer vectors are given by

$$\underline{P}_p = \tfrac{1}{2}h_0\rho g\mathrm{D}e^{i\alpha}\,[\mathrm{M}\cos(\mu - \nu) + im\sin(\mu - \nu)] \tag{139}$$

and

$$\underline{P}_a = \tfrac{1}{2}h_0\rho g\mathrm{D}e^{i\alpha}\,[-\mathrm{M}\sin(\mu - \nu) + im\cos(\mu - \nu)]. \tag{140}$$

α stands for the inclination of the major tidal stream axis with respect to the east. We do not incorporate it in our calculations since we use the axis of the current ellipse itself as our frame of reference in our drawing of the power vectors (Fig. 10).

In the conventional tidal practice, μ and ν are negative phase lags measured from the Greenwich transit of the astre fictif appropriate to the constituent considered. We therefore have $\mu - \nu = |\nu| - |\mu|$ in practice.

P_p and P_a have the dimensions of kw/m. Since we wish to know the total power transfer across a given section, we multiply P by the width of the section over which the current observations have been carried out. P then has the dimensions of kw and it gives the total power transferred across a given section.

Table 5 lists the value of the power transfer vector for each of the stations occupied by the 1965 Atlantic Oceanographic Laboratory current survey and Fig. 10 shows the same vectors depicted graphically. Not all of the values given can be considered as accurate but their values must represent a fair estimate of the amounts of power transferred especially across the sections manned by stations occupied more than 15 days.

The alternating and pulsating power vectors are nearly in opposite directions since the streams are nearly 90° out of phase with the vertical tide. In spite of the appearance, the alternating power vector flows in and out of the bay as its value oscillates between positive and negative values during one tidal period. The amount of alternating power is much larger than the amount of pulsating power, especially in Chignecto Bay. The alternating power is restituted to the ocean after each tidal cycle.

On the other hand, the pulsating power transfer vector flows steadily in the same direction and, as we note, it points everywhere towards the head of the bay. The value shows its average value over one tidal period. It is linked with the loss of tidal energy caused by friction (if we neglect the effect of the gravitational forces). We see that the loss due to friction is much less in Chignecto Bay than in Minas Channel. We must therefore have a nearly standing oscillation in Chignecto Bay while the tide has more the character of a travelling wave in Minas Channel, which itself is induced by the increased effect of friction in that area.

In the older studies of tidal energy, such as the one by McLellan (1958), only the pulsating part of the power transfer vector was considered as useable in

TABLE 5. The power transfer vector for the M_2 constituent at the sites occupied during the 1965 Bedford Institute of Oceanography current survey of the Bay of Fundy

TABLE 5. The power transfer vector for the M_2 constituent at the sites occupied during the 1965 Bedford Institute of Oceanography current survey of the Bay of Fundy.

Station	α Inclination of the major axis w.r.t. east (*degrees*)	h_0 Amplitude of the vertical tide (*m*)	$\mu-\nu$ Phase difference between the vertical and horizontal tide (*degrees*)	M Semimajor axis (*m/sec*)	*m* Semiminor axis (*m/sec*)	D Mean depth of the section (*m*)	W Width of the section (10^3 *m*)	$\underline{P}_p$ Pulsating power transfer vector (10^6 *kw*)	$\lvert\underline{P}_p\rvert$ (10^6 *kw*)	$\underline{P}_a$ Alternating power transfer vector (10^6 *kw*)	$\lvert\underline{P}_a\rvert$ (10^6 *kw*)
1	42.0	2.83	63	.67	−.08	86	19.84	(7.2,−1.6)	7.4	(−14.1,−.9)	14.1
2	49.5	2.83	66	.79	−.07	113	23.81	(12.2,−2.5)	12.5	(−27.0,−1.4)	27.0
3	44.5	2.83	69	1.07	−.11	82	19.84	(8.6,−2.3)	8.9	(−22.6,−.9)	22.6
4	37.2	3.66	77	.91	.02	38	16.15	(2.3,.2)	2.3	(−9.8,.1)	9.8
5	36.4	3.69	69	.97	.01	51	16.15	(5.2,.2)	5.2	(−13.5,.1)	13.5
6	30.5	3.75	75	1.12	−.02	46	16.15	(3.9,−.3)	3.9	(−14.7,−.1)	14.7
7	37.1	3.90	84	.83	−.04	37	24.87	(1.5,−.6)	1.6	(14.3,−.1)	14.3
8	39.5	4.11	83	.86	.04	29	13.72	(.8,.3)	.9	(7.0,.0)	7.0
9	50.6	4.60	89	.99	−.01	9	12.25	(.0,.0)	.0	(−2.5,.0)	2.5
10	71.3	4.82	80	1.46	.02	9	4.57	(.3,.0)	.3	(−1.4,.0)	1.4
11	40.6	4.88	82	1.16	−.04	15	3.48	(.2,−.1)	.2	(−1.4,.0)	1.4
12	18.1	4.27	68	2.09	.12	32	15.00	(7.9,1.1)	8.0	(−19.5,.5)	19.5
13	31.0	4.42	67	1.53	..03	18	20.85	(4.9,.2)	4.9	(−11.6,.1)	11.6
14	36.4	4.60	57	.77	−.06	35	9.51	(3.2,−.3)	3.1	(−4.8,−.3)	4.8
15	11.2	4.79	70	1.68	−.12	51	6.04	(4.2,−.8)	4.3	(−11.5,−.3)	11.5
16	10.3	5.27	81	1.33	−.03	13	15.73	(1.1,−.1)	1.1	(−6.8,−.1)	6.8

Power losses

Section	$(\Delta P_a)_y$ $\times 10^6$ kw	$(\Delta P_p)_y$ $\times 10^6$ kw
(1) (2) (3) → (4) (5) (6)	−63.7+38.0=−25.7	28.0−11.4=16.6
(4) (5) (6) → (8) (12)	−38.0+26.5=−11.5	11.4−8.7=2.7
(8) → (9)	− 4.5	.8
(12) → (15)	− 8.0	3.7
(15) → (16	− 4.7	3.1

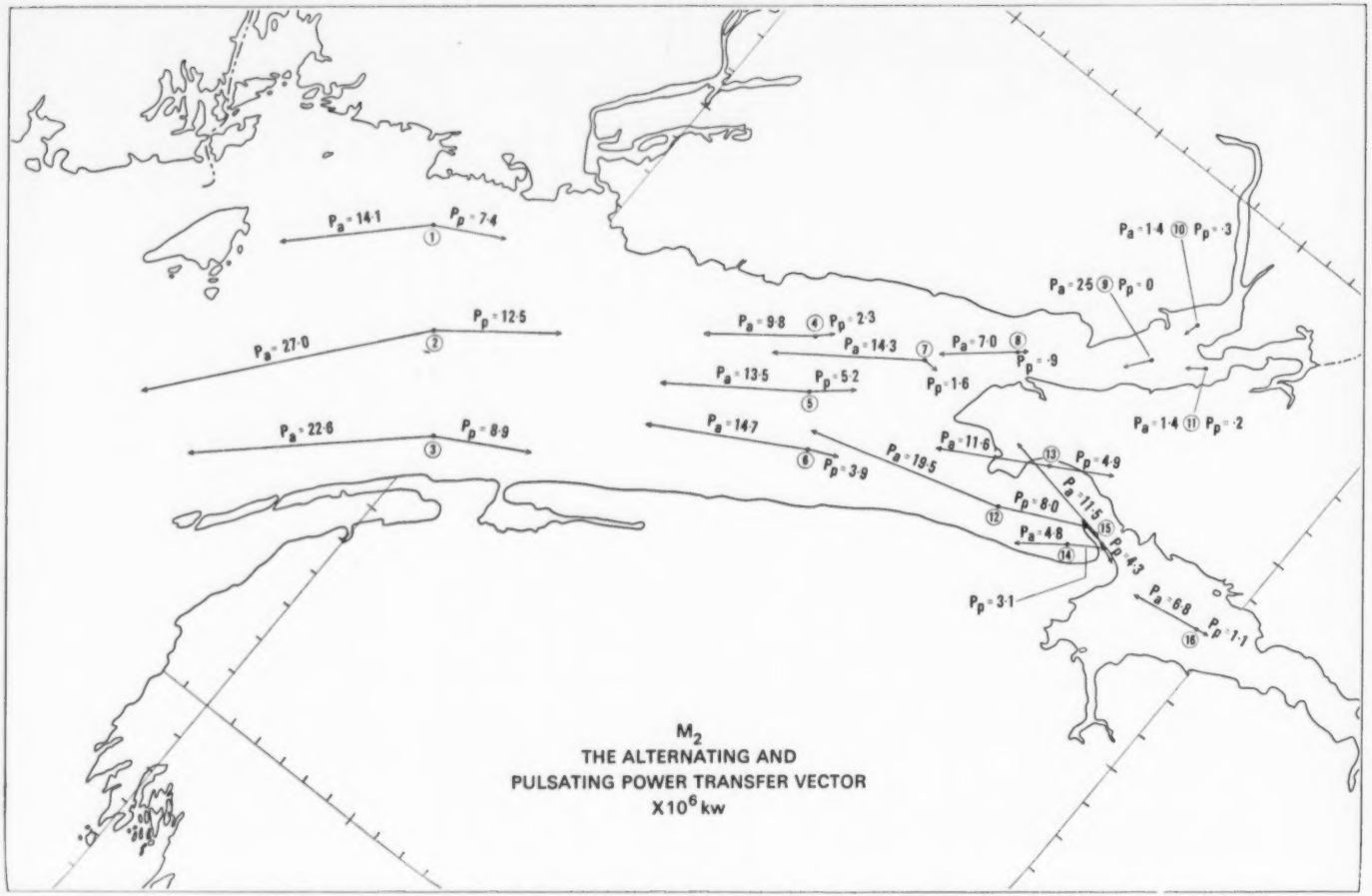

Fig. 10. Alternating and pulsating power transfer vectors over the Bay of Fundy in millions of kilowatts.

the exploitation of tidal energy. In fact both the pulsating and alternating parts of the power are available for such an exploitation. Table 5 shows that the pulsating power transferred across the section defined by stations 1, 2, and 3 amounts to 28.0×10^6 kw which compares with the value of 30.0×10^6 kw quoted by McLellan in his paper in which he used some very old data on current observations. The amount of alternating power that crossed this section is 63.7×10^6 kw. If the phases of the streams in the lower layers of this section are less than 266° as we suspect, the amount of pulsating power should in fact be larger than the figure quoted and the pulsating power should be less.

The power at the junction of Minas Channel and Chignecto Bay is split into two very unequal parts: 19.5×10^6 and 8.0×10^6 kw of alternating and pulsating power enter Minas Channel whereas 7.0 and $.9 \times 10^6$ kw of alternating and pulsating power enter Chignecto Bay. There are obviously very large losses due to friction in Minas Channel, indicated by the large gradients in the pulsating power vector across various sections in that area.

Equation of Continuity and the Power Relationships

As mentioned in a previous section, a check can be obtained on the data available by verifying if it satisfies the equation of continuity (equation 6) and the power relationships (equations 20 and 21).

When it comes to the continuity, it is preferable to use equation 6 integrated over a closed domain. It takes the approximate form

$$(Ms)_2 - (Ms)_1 = S\partial h/\partial t. \tag{141}$$

1 and 2 are two vertical sections perpendicular to the length of the bay; s is the area of the cross section; and S is the surface area between the two sections. We assume that the major axis of the ellipse M is exactly perpendicular to s, which is nearly the case. We write

$$M = \overline{M} \cos(\sigma t - |\mu|) \tag{142}$$

$\overline{M}$ being the average amplitude of M over the section and μ is its average phase. Similarly we write

$$h = h_0 \cos(\sigma t - |\nu|) \tag{143}$$

h_0 being the average amplitude of the vertical tide between the two sections. Then equation 141 becomes

$$(\overline{M}s \cos |\mu|)_2 - (\overline{M}s \cos |\mu|)_1 = S\sigma h_0 \sin |\nu| \tag{144}$$

$$(\overline{M}s \sin |\mu|)_2 - (\overline{M}s \sin |\mu|)_1 = S\sigma h_0 \cos |\nu|. \tag{145}$$

Table 6 shows the test of equations 144 and 145 for the various current stations occupied during the 1965 survey.

Continuity is approximately verified between stations 4, 5, and 6 to 8, 12, 8–9. It is coarsely verified between stations 1, 2, 3 to 4, 5, 6, 12–15, 15–16. It fails between stations 9–10, 11.

TABLE 6. A check on the equation of continuity for the M_2 constituent over the Bay of Fundy.

Vol.	S Area of the horizontal section ($10^9 m^2$)	h_0 Amplitude of the vertical tide (m)	$\lvert\nu\rvert$ ($degrees$)	$-\sigma h_0 S \sin\lvert\nu\rvert$ ($10^5 m^2/sec$)	$(\Sigma\overline{M}s\cos\mu)_2-(\Sigma\overline{M}s\cos\mu)_1$ ($10^5 m^2/sec$)	$\sigma h_0 S\cos\nu$ ($10^3 m^3/sec$)	$(\Sigma\overline{M}s\sin\mu)_2-(\Sigma\overline{M}s\sin\mu)_1$ ($10^5 m^2/sec$)
(1)(2)(3) to (3)(4)(5)	4.51	3.2	336	8.28	2.19	18.6	28.3
(4)(5)(6) to (8)(12)	1.62	4.0	344	2.50	2.66	8.69	8.49
(12) to (15)	.46	4.8	350	.50	.10	3.15	4.98
(15) to (16)	.49	5.2	005	−.31	−.77	3.54	2.40
(8) to (9)	40	4.3	352	.33	.18	2.38	2.33
(9) to (10)(11)	.10	4.6	354	.06	.12	.62	.05

Basic data

Station:	1	2	3	4	5	6	8	9	10	11	12	15	16	Units
$\overline{M}$	.67	.79	1.07	.91	1.07	1.12	.86	.99	1.46	1.16	2.09	1.68	1.33	m/sec
s	17.05	26.99	16.32	6.20	8.21	7.38	4.01	1.12	.42	.38	4.80	3.09	2.01	$\times 10^5 m^2$
μ	271.1	266.2	262.1	264.4	268.4	265.7	265.2	264.3	272.7	268.5	279.0	288.5	289.5	Degrees
$\overline{M}s\cos\mu$	.22	−1.41	−2.39	−.55	−.22	−.62	−.29	−.11	.03	−.02	1.56	1.66	.89	$\times 10^5 m^2/sec$
$\overline{M}s\sin\mu$	−11.41	−21.32	−17.44	−5.61	−7.96	−8.26	−3.43	−1.10	−.61	−.44	−9.91	−4.91	−2.52	$\times 10^5 m^2/sec$

The inaccuracy of the fit between stations 1, 2, 3 to 4, 5, 6 may be attributed to an inaccurate determination of the phase of the tidal stream. Between stations 12 and 15, the observations are probably correct, but the strong refraction occurring around Cape Split may make our rough approximation to the integral of equation 6 invalid.

The power relationships discussed previously take the form

$$\Delta P_a = S\,[\tfrac{1}{2}\rho\sigma D\,(M^2 + m^2) - \tfrac{1}{2}\sigma\rho g h_0^2 + 2\Omega D\rho\, Mm] \tag{146}$$

$$\Delta P_p = S\,\tfrac{1}{2}\,\rho f D\,(M^2 + m^2). \tag{147}$$

In equation 146, all the quantities are known from observations whereas f is not known in equation 147. We can therefore have a direct check on equation 146, and 147 can be used to evaluate the dimensionless friction parameter:

$$k = g/C^2 = fD/\,|v| \simeq \frac{2\Delta P_p}{M\,(M^2 + m^2)\,S}. \tag{148}$$

Table 7 shows a check on the data using ΔP_a and an estimate of k derived from ΔP_p. The section between stations 1, 2, 3 and 4, 5, 6 once again shows that all is not well with the data in that area. The value for k in particular is much too large. Stations 4, 5, 6 to 8, 12 and 8–9 reflect their consistency with respect to continuity.

Sites Favourable for the Exploitation of Tidal Energy in the Bay of Fundy

Equation 141 gives what we consider to be the upper bound to the energy that may be drawn from a basin that may store a volume $[S_0 \cdot 2h_0]$ of sea water. We assume that the use of pumps will not succeed in practice to increase the range $2h_0$ of the tide appreciably. We also use the hypothesis that in an actual exploitation of the tide, we can utilize 30% of the available energy.

Before studying various storage basins in the Bay of Fundy we must be more specific about the range $2h_0$ of the tide since it always varies.

In the Bay of Fundy, the average range varies between the mean equinoctial spring tide at perigee and the solstitial neap tide at apogee. We therefore write $2h_0$ as

$$2h_0 \pm \epsilon \tag{149}$$

$2h_0$ being the mean range due to M_2 whereas ϵ is the additional range contributed by $N_2 + S_2 + K_2$. Since the energy generated varies with the square of this quantity for a basin with vertical walls, we have to consider the average value of the square of equation 149. Assuming that the range varies evenly between the extremes given by equation 149, its average square value amounts to

$$\overline{(2h_0)^2} = (1/2\epsilon) \int_{2h_0-\epsilon}^{2h_0+\epsilon} x^2 dx = (2h_0)^2 + (\tfrac{1}{3})\,\epsilon^2. \tag{150}$$

TABLE 7. A check on the power relationships for the M_2 constituent in the Bay of Fundy.

Vol.	$\bar{h}_0$ (m)	$\overline{M}$ (m/sec)	$\overline{m}$ (m/sec)	S ($\times 10^9 m^2$)	$\overline{D}$ (m)	A $\frac{1}{2}\rho\sigma\overline{D}(M^2+m^2)$ (10^{-4} tons/sec^3)	B $-\frac{1}{2}\rho\sigma\bar{h}_0^2$ (10^{-4} tons/sec^3)	C $2\rho\Omega\overline{D}Mm$ (10^{-4} tons/sec^3)	(A+B+C)S (10^6 kw)	ΔP_a (10^6 kw)	ΔP_p (10^6 kw)	$k=g/C^2$ (10^{-3})
(1)(2)(3) to (4)(5)(6)	3.50	.94	−.06	4.51	69.5	43.5	− 84.7	−4.0	−20.8	−25.7	16.6	8.8
(4)(5)(6) to (8)(12)	3.96	1.26	.03	1.62	37.84	42.4	−108.5	1.5	−10.5	−11.5	2.7	1.7
(8) to (9)	4.3	.93	.01	.40	19.7	12.0	−127.9	.2	− 4.6	− 4.5	.8	5.0
(12) to (15)	4.8	2.94	0	.35	41.63	62.5	−159.3	0	− 4.41	− 8.0	3.7	6.8
(15) to (16)	5.2	1.51	−.07	.49	32.03	51.6	−187.0	3.5	− 5.2	− 4.7	3.1	3.7

$\sigma = 1.4 \times 10^{-4}$ sec^{-1} $\Omega = 1.03 \times 10^{-4}$ sec^{-1}

Thus the average energy output expected over one tidal period from a storage basin of surface section S_0 amounts to, in a practical exploitation,

$$E = 30\% \text{ of } \rho g S_0 [(2h_0)^2 + \tfrac{1}{3} \epsilon^2]. \tag{151}$$

In the Bay of Fundy, especially near the head, the walls of the proposed storage basins are far from being vertical. As a consequence we have used equation 151 taking as S_0 the area of the basin that is covered at low water. It follows that our estimates of E in Table 7 are underestimates.

A tidal cycle lasts on the average 12.4 hr and we can calculate the mean power output in kilowatts from equation 151 by dividing E by that time interval evaluated in seconds.

As a criterion of the efficiency of the utilization of the dam area, we have used the number of kilowatts output per square meter of dam. The French school (Gibrat, 1966) uses the dam width divided by the energy output per year. Since the depth varies widely in the sites studied in the Bay of Fundy, this criterion is too coarse for our purpose, still we have retained the latter criterion for purposes of comparison.

Since there are about 705 tides per year, the energy output per year is given by

$$E_y = 30\% \text{ of } \rho g S_0 (2h_0)^2 \text{ or } \frac{9.81 \times 705 \times .30}{3600} S_0 (2h_0)^2$$
$$\simeq .6 S_0 (2h_0)^2 \text{ kw-hr.} \tag{152}$$

The French school uses the mean spring range at equinox for $2h_0$ rather than our mean range, which leads to higher estimates of the power output.

Figure 8 shows the sites that we have considered in the Bay of Fundy for the exploitation of tidal energy. Table 8 lists the most important parameters pertaining to these sites. They are: 1. the Digby Gut; 2. Minas Channel; 3. Cobequid Bay; 4. Cumberland Basin; and 5. Chignecto Bay. We have also included some data on the Rance (adapted for the purpose of this study). We have excluded Passamaquoddy Bay from our considerations since it has already been extensively studied (International Joint Commission, 1961).

We have also excluded St. John Harbour. Although it happens to be a favourable site, the disruption to navigation in and out of the harbour caused by the operation of a tidal plant would be difficult to control. Finally we have excluded Shepody Bay and the Petitcodiac since this site is very unfavourable compared to the others.

Table 8 shows that Minas Channel comes first for power output with a mean output of nearly 6×10^6 kw. Digby yields the smallest amount of power.

If one disregards the power output to consider the amount of power generated per square meter of dam (the larger this quantity, the more profitable the construction and the smaller its relative costs), once again Minas Channel comes first whereas the sites of Digby, Cumberland, and Chignecto yield about a third of the power output of the Minas project for the same dam area.

TABLE 8. Tidal power output parameters for some sites in the Bay of Fundy.

Site	Basin	Dam	Dam width W (*km*)	Dam area *s* ($10^6 m^2$)	Mean amplitude of the tide M_2 (*m*)	Additional amplitude at equinox spring tide at perigee $S_2+K_2+N_2$ (*m*)	Mean square range $\overline{(2h_0^2)}$ (m^2)	Area of storage S_0 ($10^7 m^2$)	Energy output per tidal period E (10^6 *kj*)	No. of square meter of dam P/*s* (*kw*/m^2)	Mean sprint range at equinox $2h_0$ $M_2+S_2+K_2$ (*m*)	Energy output per year ($.6S_0(2h_0)^2$)	Ratio of energy output per year to dam width ($.6S_0$ $(2h_0)^2$/W)
Digby	Annapolis	Head of Digby Gut	.8	2.1	3.11	1.28	40.9	5.8	6,978	7.44	7.5	1,959	2.5
Minas	Minas Basin	Between Cape Split and Ram Head	6.2	28.0	5.03	1.94	106.2	85.0	265,660	21.25	11.3	65,129	11.1
Cobequid	Cobequid Bay	Between Economy Point and Tenecape	8.8	10.0	5.64	2.13	133.3	12.0	45,775	10.25	13.2	12,542	1.4
Cumberland	Cumberland Basin	Between Pecks Point and Bass Point	2.6	2.8	4.88	1.68	99.0	2.7	7,797	6.23	11.4	2,106	.8
Chignecto	Shepody Bay and Cumberland Basin	Between Cape Enragé and Sand R.	9.1	23.0	4.27	1.68	76.7	30.0	67,701	6.59	10.2	19,098	2.1
Rance			.725									1,729	2.4

When it comes to the size of the dam, Digby would require a dam barely .8 km long whereas the Chignecto site would require over 9 km of dam, quite an engineering task.

With the experience gained in the Rance project (Gibrat, 1966), it is evident that the Digby site could be exploited at any time and that its power output would be of the same order as that of the Rance, that is to say, relatively modest. The hindrance to navigation of the plant will be of importance since Digby is one of the few good harbours on the southern shore of the Bay of Fundy. But a lock could certainly be constructed to accommodate the ships in and out of the Annapolis basin. On the other hand, the Annapolis River brings in a fair amount of sediments. With the lessened tidal flushing after the construction of the plant, the zone of flocculation and precipitation that seems to lie in the vicinity of Goat Island would be brought closer to the mouth of the basin. The reduced range of the tide on the other hand will increase the area of land on the shore that would not be reached by high water. This might be of interest to the property owners around the basin.

The Minas Channel site lies at the other extreme of the scale. The power output of such a plant would be very large and of great commercial value. It is highly efficient from the point of view of dam utilization. But it is not certain if the construction of a tidal plant at this site is within the reach of contemporary engineering techniques. Large currents of the order of 3 m/sec prevail already in the strait and during the construction of the dam they will increase even more. Immense masses of water move across the strait during a short time interval. The depth at some points of the section exceeds 80 m and therefore the construction of a dam over 6 km long under such conditions is difficult to conceive. Finally, on account of the amount of energy drawn from the tide, the tidal regime would be modified unfavourably (Yuen, MS, 1967).

More modest projects with outputs still exceeding 10^6 kw could be achieved at the Chignecto and Cobequid sites.

The Cobequid project is particularly attractive. It would require a long dam of the order of 9 km but the depths are nowhere great and most likely do not exceed 20 m. The masses of sea water involved are not as great as for Minas Channel and this project is certainly within the grasp of contemporary engineering. Once again the problem of sediments in Cobequid Bay has to be studied carefully. After the lessening of the tidal range inside the storage basin, immense areas of mud flats could be utilized for salt grass cultivation or other useful purposes.

The least attractive location studied is the Cumberland site. It would yield an amount of power similar to the output of Digby but the dam would have to be over 3.5 km long to achieve the same purpose. The increase in range at the mouth of the basin compared with Digby is offset by the small storage capacity of the basin.

To conclude, we see that there are three sites in the Bay of Fundy which would be highly favourable for the exploitation of tidal energy; (1) Digby:

small power output, no major engineering difficulties; (2) Cobequid: moderate power output, moderate engineering difficulties; (3) Minas Channel: large power output, perhaps disproportionate engineering difficulties.

To make a closer study of these sites we would need to consider specific types of turbines that could be utilized in the plant. Their number, their flow characteristics, their efficiency under various heads, and their power output will determine the range of the oscillation within the reservoir, the power actually generated by the plant, and the economic feasibility of the project.

ACKNOWLEDGMENTS

Dr P. Leblond of the Institute of Oceanography of the University of British Columbia has read and criticized the manuscript. Dr N. J. Campbell, Mr F. G. Barber, and Mr K. B. Yuen of the Division of Oceanographic Research of the Department of Energy, Mines and Resources of Canada have provided editorial comments. Mr M. Isabelle of the same organization has drawn the diagrams. The coastal tidal data were supplied by the Tides and Water Levels Section and the current data by the Atlantic Oceanographic Laboratory, both of the Department of Energy, Mines and Resources of Canada. Valuable information has also been supplied by Mr F. Lawton of the Atlantic Development Corporation. This paper was written while the author was located at the Institute of Oceanography of the University of British Columbia.

REFERENCES

Bedford Institute of Oceanography. MS, 1966. Bay of Fundy, data report, tidal and current survey 1965. Data Series 66-2-D.

Casacci, S. X., and L. Kammerlocher. 1956. Analyse du fonctionnement des groupes axiaux de grandes dimensions. La Houille Blanche 17: 153–162.

Caseau, M. 1962. Classification des cycles d'une usine marémotrice. La Houille Blanche 17: 276–283.

Chevalier, J. 1956. Comparaison entre les rendements industriels et modèles pour le fonctionnement en turbinage inversé des groupes bulbes de Cambeyrac et Saint-Malo, p. 141–152. *In* Les énergies de la mer. Comp. Rend. Quatrièmes J. Hydraulique Vol. 1. Société Hydrotechnique de France. 1956. La Houille Blanche, Grenoble.

Davey, N. 1923. Studies in tidal power. Constable, London. 255 p.

Dubois, R. 1962. Les essais du groupe marémoteur expérimental de Saint-Malo. La Houille Blanche 17: 131–140.

Fichot, E. 1923. Les Marées et leur utilisation industrielle. Gauthier-Villars, Paris. 255 p.

Gauthier, M. 1962. Éléments nouveaux dans le calcul des cycles des usines marémotrices. La Houille Blanche 17: 269–275.

Gibrat, R. 1953. L'énergie des marées. Bull. Soc. Française Électriciens 3: 283–332.

1954. Premiers critères de comparaison des diverses turbo-machines au point de vue des usines marémotrices. La Houille Blanche 9: 64–74.

1955. Exploitation des usines marémotrices compte tenu des limitations imposées aux vitesses de variations des débits. La Houille Blanche 10: 275–282.

1956a. Cycles d'utilisation de l'énergie marémotrice, p. 488–502. *In* Les énergies de la mer. Compt. Rend. Quatrièmes J. Hydraulique Vol. 2. Société Hydrotechnique de France 1956. La Houille Blanche, Grenoble.

1956b. L'exploitation d'une usine marémotrice en régime d'économie de charbon, p. 503–510. *In* Les énergies de la mer. Compt. Rend. Quatrièmes J. Hydraulique Vol. 2. Société Hydrotechnique de France 1956. La Houille Blanche, Grenoble.

1966. L'énergie des marées. Presses Universitaires de France, Paris. 219 p.

Godin, G. MS, 1968. The 1965 current survey of the Bay of Fundy — A new analysis of the data and an interpretation of the results. Marine Sciences Branch, Dept. Energy, Mines Resources, MS Rept Ser. 8. 97 p.

HANSEN, W. 1956. Theoriezur Errechnung des Wasserstandes und der Stromungen in Randmeeren nebst Anwendungen. Tellus 8: 287–300.

INTERNATIONAL JOINT COMMISSION. 1961. Report of the International Joint Commission United States and Canada on the International Tidal Power Project, Washington–Ottawa. Rept. Intern. Joint Comm. Docket 72, Invest. Intern Passamaquoddy Eng. Fish Bd., April 1961. 271 p.

KAMMERLOCHER, L., AND J. DUCLOS. 1956. Évaluation constructive des groupes de la Rance, p. 511–521. *In* Les énergies de la mer. Compt. Rend. Quatrièmes J. Hydraulique Vol. 2. Société Hydrotechnique de France 1956. La Houille Blanche, Grenoble.

KOVALEV, N. N. 1965. [Hydroturbines.] (In Russian; Israel Program Sci. Transl., Jerusalem.) 687 p.

MAYNARD, E. 1919. Études sur l'utilisation des marées pour la production de la force motrice. Rev. Gén. Électricité 4: 653–697.

MCLELLAN, H. J. 1958. Energy considerations in the Bay of Fundy system. J. Fish. Res. Bd. Canada 15: 115–134.

RAO, D. B. 1968. Natural oscillations of the Bay of Fundy. J. Fish. Res. Bd. Canada 25: 1097–1114.

REMENIERAS, G., AND P. SMAGGHE. 1956. Sur la possibilité d'utiliser l'énergie des courants marins au moyen de machines analogues aux aérogénérateurs, p. 532–539. *In* Les énergies de la mer. Compt. Rend. Quatrièmes J. Hydraulique Vol. 2. Société Hydrotechnique de France. La Houille Blanche, Grenoble.

SCHÖNFELD, J. C. 1956. Circulation de l'énergie dans les mers littorales, p. 157–165. *In* Les énergies de la mer. Compt. Rend. Quatrièmes J. Hydraulique Vol. 1. Société Hydrotechnique de France 1956. La Houille Blanche, Grenoble.

SCHWOB, L. 1956. La turbine à admission constante et à vitesse variable dans l'utilisation de l'énergie des marées, p. 522–531, 540–541. *In* Les énergies de la mer. Compt. Rend. Quatrièmes J. Hydraulique Vol. 2. Société Hydrotechnique de France 1956. La Houille Blanche, Grenoble.

TAYLOR, G. I. 1919. Tidal friction in the Irish Sea. Phil. Trans. Roy. Soc. 220A: 1–31.

1920. Tidal friction and the secular acceleration of the moon. Monthly Notices Roy. Astronomical Soc. 80: 308–309.

VOYER, M., AND M. PENEL. 1956. Les calculs de la production d'une usine marémotrice, p. 472–487. *In* Les énergies de la mer. Compt. Rend. Quatrièmes J. Hydraulique Vol. 2. Société Hydrotechnique de France 1956. La Houille Blanche, Grenoble.

WILSON, E. M. 1965. The Solway Firth tidal power project. Water Power 7: 431–439.

YUEN, K. B. MS, 1967. The effect of tidal barriers upon the M_2 tide in the Bay of Fundy. Marine Sciences Branch, Dept. Energy, Mines Resources, MS Rept Ser. 5. 53 p.

Some Salinity-Induced Changes in Growth, Pigments, and Cyclohexanetetrol Content of *Monochrysis lutheri*[1]

J. S. CRAIGIE

National Research Council of Canada
Atlantic Regional Laboratory, Halifax, N.S.

CRAIGIE, J. S. 1969. Some salinity-induced changes in growth, pigments, and cyclohexanetetrol content of *Monochrysis lutheri*. J. Fish. Res. Bd. Canada 26: 2959–2967.

Growth rates of *Monochrysis lutheri* Droop increased with light intensity in seawater medium (SWM), whereas cells grown at either low NaCl (0.013 M) or high NaCl (1.02 M) showed reduced growth at higher light intensities with an optimal intensity near 0.05 g cal/cm² per min.

Chlorophyll and total carotenoids usually declined with increasing light intensity except in cells maintained on a high salt regime, when the carotenoid content remained high at all light intensities.

The concentration of intracellular cyclohexanetetrol in SWM cells was approximately 0.3 M and was dependent upon the osmotic properties of the medium. Added NaCl, mannitol, sucrose, but not glycerol, caused accumulation of the cyclitol, whereas dilution of the medium caused its expulsion from the cells. Addition of 0.5 moles/liter of NaCl to SWM cells caused an 80–90% increase in cyclitol concentration within 4 hr; dilution of the medium reduced the cyclitol to the new steady state level within 10 min.

Received July 11, 1969

INTRODUCTION

THE CONCEPT of salinity as an ecological determinant both for algae (Braarud, 1951; Provasoli, 1958; Biebl, 1962) and for higher plants (Boyko, 1966) seems well established. The effects of desiccation, salinity extremes, and ionic balance were examined in several seaweeds (Munda, 1963; Ogata and Matsui, 1965; Chapman, 1966) and phytoplankton species (Provasoli et al., 1954; Droop, 1958; McLachlan, 1961), but our general knowledge remains meagre concerning the physiological processes of algae adapting to altered salinities.

Experiments with *Chlorella pyrenoidosa* show that the addition of magnesium sulfate, ammonia, nitrate, or phosphate enhances photosynthetic fixation of $^{14}CO_2$, and directs the carbon flow into amino acids rather than into sugar phosphates (Holm-Hansen et al., 1959). Somewhat similar experiences were reported for the dark fixation of carbon dioxide by spinach homogenates in the presence or absence of NaCl, and for three marine plants (Joshi et al., 1962). Photoassimilated $^{14}CO_2$ accumulates in the sugar phosphates of NaCl-treated spinach homogenates (Gee et al., 1965) giving a labelling pattern reminiscent of plants living in an increasingly saline environment (Joshi, 1967).

[1]Issued as NRCC No. 11047.

Printed in Canada (J1524)

The intracellular glycerol content of fully adapted *Dunaliella tertiolecta* was shown to depend upon the salinity of the medium (Craigie and McLachlan, 1964). More recently, Kauss (1967) demonstrated a similar osmotic role for isofloridoside in *Ochromonas malhamensis* and observed that the galactosyl glycerol content of *Porphyra perforata* may be elevated by increased salinity (Kauss, 1968). These observations are consistent with the report of increased sucrose synthesis in *C. pyrenoidosa* induced by low water potentials (Hiller and Greenway, 1968).

The following data describe some steady-state and short-term responses of the tide pool flagellate, *Monochrysis lutheri* Droop, to altered salinities. Such an euryhaline organism naturally encounters marked changes in external osmotic potential and, therefore, was chosen for these studies.

MATERIALS AND METHODS

Monochrysis was maintained routinely on a modified seawater medium, SWM-1 (McLachlan, 1964), contained in suitable Erlenmeyer flasks. The experimental media were prepared either by partial substitution of the sea water with glass-distilled water or by adding to SWM-1 the appropriate quantities of solute. Cells ultimately grown near their salinity extremes were first adapted by culturing at intermediate salt concentrations. Temperature was controlled at 20–22 C, and continuous illumination usually was obtained from cool-white fluorescent lamps.

Cells grown under various light intensities were obtained from a continuous culture apparatus equipped with a quartz iodine lamp and a $CuSO_4$ filter (Eppley and Coatsworth, 1966). Light intensities for the growth experiments are given in g cal/cm² per min and were measured with a selenium photocell calibrated against a spectral radiometer. The sea water used for these experiments had a salinity of 33.5‰.

All media were autoclaved, and periodic microscopic examination showed that bacterial contamination of the cultures was negligible. Cell growth was determined by Coulter counting. Adjustments of the cell concentration were made with filtered sea water, or with 50% sea water when cells grown in low salinity were counted.

Preliminary experiments showed that no cyclohexanetetrol was synthesized in darkness, and that the loss of cyclitol from cells placed in hypotonic medium was unaffected by light or darkness. Accordingly, all the kinetic experiments were conducted in cool-white fluorescent light (2200 ft-c, Weston Model 756 light meter) at 22 C with 100 ml of culture in 250-ml Erlenmeyer flasks. Sea water of 30.9‰ was used in these experiments. Additional $NaHCO_3$ (0.3 mmoles) was added to each flask including the controls at time zero.

Pigment analyses were performed on centrifuged 90% acetone extracts of the cells by a standard procedure (Strickland and Parsons, 1965, p. 185).

Initially, 25-ml cell-samples were collected by gentle filtration on Whatman GF/C filters. Analyses of these samples occasionally gave erratic replication, which was attributed to cellular damage caused by the glass-fiber filters. Such errors were eliminated when cells were concentrated by centrifugation. Supernatant culture medium was removed by suction and the cell pellet was extracted with hot 50% ethanol. An internal standard of either erythritol or xylitol was added. Each batch of extract was desalted with Permutit Q (H^+) and Dowex 2 × 8 carbonate ion-exchange resins. A portion of the neutral fraction was dried in vacuo prior to derivative formation.

Silyl derivatives were prepared in pyridine solution (Sweeley et al., 1963) when erythritol was the internal standard. Samples were analyzed on a Loenco gas chromatograph equipped with dual-flame ionization detectors and matched 6-ft × ¼-inch stainless steel columns containing 3% SE-30 liquid phase on silanized 60- to 80-mesh Chromosorb W. A temperature of 165 C with a helium flow rate of 70 ml/min resulted in good separations. Calibration with crystalline erythritol and 1,4/2,5-cyclohexanetetrol (Ramanathan et al., 1966) gave an area-ratio slope factor (Sawardeker et al., 1965) of 1.06 for the cyclitol derivative. A prolonged tailing of the solvent peak

under these conditions eventually led to the use of fully acetylated derivatives (Sawardeker et al., 1965). Separation of the acetates was achieved on a 3-ft × ⅛-inch stainless steel column of 5% ECNSS-M liquid phase on Gas Chrom Q operated at 195 C with a nitrogen flow of 70 ml/min. Reagents from the acetylation reaction were removed by evaporation before the sample was redissolved in $CHCl_3$ for chromatography. With xylitol as the internal standard, an area-ratio slope factor of 1.00 was obtained for cyclohexanetetrol on a dual flame ionization, F and M Model 700 gas chromatograph. All measurements cited are the averages of triplicate analyses.

RESULTS AND DISCUSSION

Table 1 provides a comparison of growth rates and 1,4/2,5-cyclohexanetetrol concentration for *Monochrysis* grown under three salinities and several light intensities. Previous work (Droop, 1958; McLachlan, 1961) showed that a distinct salinity optimum does not exist for this organism although it may favour salinities somewhat less than sea water. Both extremes of salinity

TABLE 1. Influence of salinity on the mean generation time and cyclohexanetetrol content of *Monochrysis* grown at various light intensities.

Light intensity (*g cal/cm² per min*)	0.013 M Na+		0.46 M Na+		1.02 M Na+	
	Mean generation time (*hr*)	Tetrol (*nmole/10⁶ cells*)	Mean generation time (*hr*)	Tetrol (*nmole/10⁶ cells*)	Mean generation time (*hr*)	Tetrol (*nmole/10⁶ cells*)
0.012	69.8	–	–	–	–	–
0.025	31.3	0[a]	25.1	7.7	–	–
0.036	–	–	–	–	33.8	–
0.050	18.0	–	21.5	–	33.8	39
0.100	26.3	0	18.1	11.2	41.0	36
0.200	38.0[b]	0	14.9	13.3	67.2	27

[a]Limit of detection was approximately 0.05 nmole/10⁶ cells.
[b]After 3 days at high light intensities cell division ceased.

used in the present study resulted in decreased growth rates upon increasing the light levels. The optimal light intensity for low salt grown cells is about 0.05 g cal/cm² per min. Under moderate light intensities, constant growth rates could be maintained at all salinities by the periodic addition of fresh medium. On the other hand, cells grown on 0.013 M Na+ medium at high light intensity (0.2 g cal/cm² per min) stopped dividing after 3–4 days, although they remained motile and would resume cell division 3–4 days after reducing the light level to 0.05 g cal/cm² per min. This unusual response was not observed at the higher salinities. The minimum mean generation time of 14.9 hr observed for cells grown in sea water is in good agreement with existing data (Antia and Kalmakoff, MS, 1965).

Cells from the low-salinity medium contained no detectable cyclohexanetetrol, although at the higher salinities the cyclitol concentration is correlated with increased cell division rates.

Pigment fluctuations in cells grown under various light and salinity regimes are presented in Fig. 1, 2, and 3. In all cases, the chlorophylls showed a decline as light intensity increased. At the lowest salinity, the total carotenoids were reduced by 45% between 0.025 and 0.2 g cal/cm² per min, but at higher salinities this drop was attenuated so that at 1.02 M Na^+, very little change occurred in the concentration of total carotenoids.

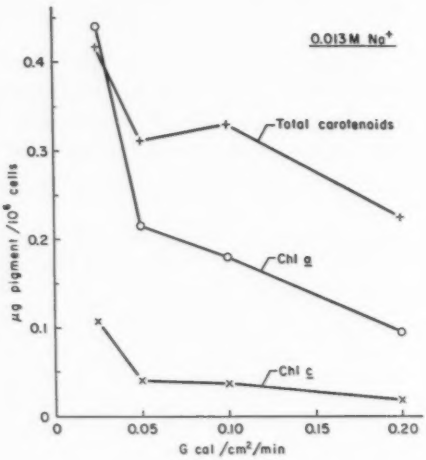

FIG. 1. Relationship between pigment concentrations and light intensity at low salinity (0.013 M Na^+). Carotenoid concentrations are in milli specific plant units.

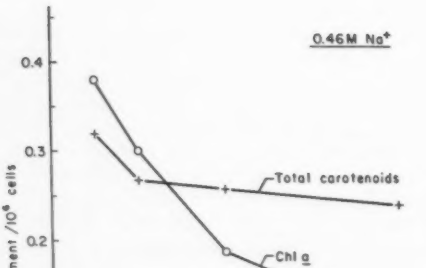

FIG. 2. Relationship between pigment concentration and light intensity on sea water medium (0.46 M Na^+). Carotenoids are in milli specific plant units.

The steady state levels of cyclohexanetetrol in young cultures grown at seven salinities are presented in Fig. 4. The cellular cyclitol content increased in an approximately linear manner until 1 M NaCl was reached. Beyond this value, the injurious effects of salinity become evident in the much reduced

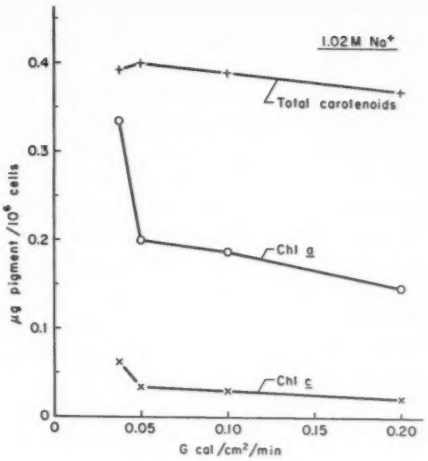

FIG. 3. Relationship between pigment concentration and light intensity at high salinity (1.02 M Na+). Carotenoids are in milli specific plant units.

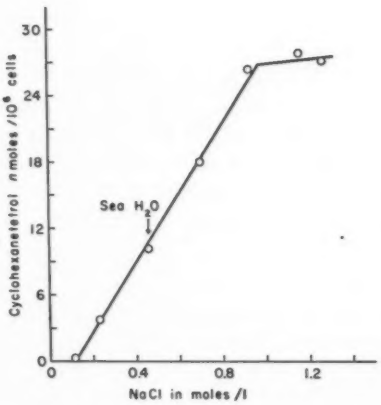

FIG. 4. Cyclohexanetetrol content of cells adapted to media of various salinities. Cells including those grown at 0.7 M Na+ were harvested after 4 days of growth, and those at higher salinities were collected after 9 days. All cultures were growing at the time of harvest.

growth rates and motility, and the inability of the cells to further increase their cyclitol content. It was observed that cell growth rates were progressively suppressed by salt levels above that of sea water although the cultures could be maintained indefinitely at all salinities shown.

A common hazard encountered by tide pool organisms is the rapid dilution of their environments by freshwater runoff or rainfall. Figure 5 shows the cyclitol content of *Monochrysis* grown in sea water 3.5 and 6 hr after being diluted with glass-distilled water. The cells rapidly adjusted to their new osmotic milieu by reducing their free cyclitol concentration. In separate experiments it was observed that abruptly diluted *Monochrysis* cells began to show swollen and distorted organnelles in 20–25% sea water and extensive lysis in 15% sea water. These seawater concentrations approximately correspond to those at which the internal cyclitol concentration becomes negligible.

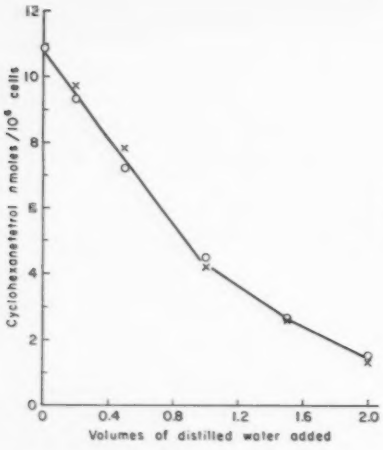

FIG. 5. Effects of reduced salinity on the intracellular cyclohexanetetrol content of a seawater grown culture at 3.5 (O) and 6 (X) hr after the addition of distilled water.

The rapidity with which the organism responds to altered salinities is strikingly illustrated by Fig. 6. The reduction in cyclitol concentration after dilution of cells grown in SWM-1 with one volume of distilled water is completed within 10 min. The adjustment of cells grown in SWM-1 to the addition of NaCl (0.5 moles/liter) is less rapid and requires about 4 hr in the presence of excess bicarbonate and light for the cyclitol to reach the new levels. A lag of 10–20 min followed by an abrupt synthesis of cyclitol was observed in three experiments. No cyclitol was synthesized by cells placed in darkness.

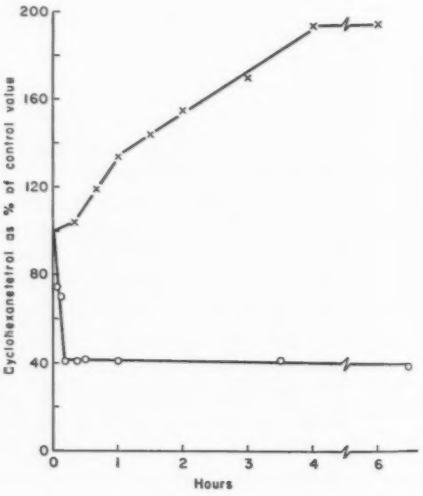

FIG. 6. Rate of formation or disappearance of cyclohexanetetrol in seawater grown cells when 0.5 moles NaCl/liter (X), or an equal volume of distilled water (O) was added at time 0. The data are presented for a constant cell number in both cases.

The rapid decline of intracellular cyclitol during dilution of the medium suggests that it is removed by release into the medium rather than by cellular catabolism. This conclusion was verified by subjecting $^{14}CO_2$-labelled cells grown in SWM-1 to dilution either with filtered sea water or with distilled water. In both cases the medium was clarified by centrifugation and the non-ionic materials were recovered from ion-exchange resins and separated by paper chromatography in *n*-butanol–acetic acid–water (4:1:2.2 v/v). Cells diluted with sea water released very little radioactive cyclitol into the medium, whereas cells diluted with distilled water released a strongly radioactive component corresponding to authentic cyclohexanetetrol.

In order to establish the general osmotic nature of these responses, compounds other than salt were tested for their effects on cyclitol production. On an osmolar basis, both mannitol and sucrose were equal in their effect to added NaCl (Table 2). The cells must be capable of discriminating against

TABLE 2. Effect of various solutes on cyclohexanetetrol production in *Monochrysis* after 4.5 hr of photosynthesis. Control was grown on SWM-1.

Solute added	Mole/liter	Cyclohexanetetrol	
		nmole/10^6 cells	As % of control
None	–	10.9	100
NaCl	0.25	16.8	154
KBr	0.25	12.3	113
Glycerol	0.50	10.2	94
Mannitol	0.50	16.4	150
Sucrose	0.50	16.3	150

both Na^+ and Cl^- although the operation of an efficient sodium pump (Eppley and Cyrus, 1960) cannot be excluded. The relatively small effect of KBr may be due to a high permeability of K^+ or the generally deleterious effects of elevated K^+ levels, or both (Provasoli, 1958; Yamamoto and Okamoto, 1967; J. McLachlan, personal communication). Glycerol caused no impairment as judged by cellular motility, and as it caused no increase in cyclitol concentration, it must have ready access to the intracellular spaces.

Previous workers investigating osmotic properties of algae have concentrated on the influence of inorganic ions (Guillard, 1962; Munda, 1963) and seem to have given little consideration to the auxiliary role that organic solutes may play. It is well known that animal cells employ a variety of organic (usually nitrogenous) compounds as osmoregulators (Potts, 1968), and it now appears that certain freshwater and marine algae may employ their secondary photosynthetic products in an analogous manner. Yamamoto and Ogamoto (1967) recently proposed that unknown osmotically active substances, other than Na^+ and K^+ salts, may be extruded when their halophilic *Chlamydomonas* was bathed in hypotonic medium. Candidates for such osmoregulatory functions

may include glycerol in marine chlamydomonads (Craigie et al., 1967), galactosylglycerols in *Ochromonas* (Kauss, 1967) and *Porphyra* (Kauss, 1968; Craigie and McLachlan, unpublished), and cyclohexanetetrol in *Monochrysis*.

Assuming that the corpuscular shaped *Monochrysis* approximates a right circular cylinder ($r = 3\ \mu$; $a = 2\ \mu$), and that one-third of the cellular volume is occupied by organelles, a solute volume of about 37 μ^3 appears reasonable. A cell grown on SWM-1 under moderate light intensity and containing about 11×10^{-15} moles of cyclohexanetetrol (Table 2) is therefore approximately 0.3 M in cyclitol. In other words, 6–7 atm of the intracellular osmotic pressure of *Monochrysis* grown in sea water may be accounted for by this solute.

Among the pertinent questions already raised (Yamamoto, 1967) are those concerning functions of the cell-wall membranes in osmoregulation. A second group of problems arises from a consideration of the regulatory mechanisms whereby a physical phenomenon such as increased external osmotic pressure influences the accumulation of the appropriate osmoregulator. Observations bearing on the latter topic will constitute a future report.

ACKNOWLEDGMENTS

This research was initiated while the author visited the Institute of Marine Resources, Scripps Institute of Oceanography, in 1967–68. Financial support by the National Research Council of Canada and the U.S. Atomic Energy Commission (Contract No. AT(11-1) GEN 10, P.A. 20) are gratefully acknowledged. It is a pleasure to record the many courtesies extended to me, and the discussions with the staff of the Institute of Marine Resources especially Drs R. W. Eppley, J. D. H. Strickland, and P. M. Williams.

REFERENCES

ANTIA, N. J., AND J. KALMAKOFF. MS, 1965. Growth rates and cell yields from axenic mass culture of fourteen species of marine phytoplankters. Fish. Res. Bd. Canada, MS Rept. 203. 24 p.

BIEBL, R. 1962. Seaweeds, p. 799–815. *In* R. A. Lewin [ed.] Physiology and biochemistry of algae. Academic Press, Inc., New York.

BOYKO, H. 1966. Salinity and aridity, new approaches to old problems. Dr. W. Junk Publishers, The Hague, The Netherlands. viii + 408 p.

BRAARUD, T. 1951. Salinity as an ecological factor in marine phytoplankton. Physiol. Plantarum 4: 28–34.

CHAPMAN, V. J. 1966. The physiological ecology of some New Zealand seaweeds, p. 29–54. *In* E. G. Young and J. L. McLachlan [ed.] Proc. V Intern. Seaweed Symp. Pergamon Press, Oxford, England.

CRAIGIE, J. S., AND J. MCLACHLAN. 1964. Glycerol as a photosynthetic product in *Dunaliella tertiolecta* Butcher. Canadian J. Botany 42: 777–778.

CRAIGIE, J. S., J. MCLACHLAN, R. G. ACKMAN, AND C. S. TOCHER. 1967. Photosynthesis in algae III. Distribution of soluble carbohydrates and dimethyl-β-propiothetin in marine unicellular Chlorophyceae and Prasinophyceae. Canadian J. Botany 45: 1327–1334.

DROOP, M. R. 1958. Optimum relative and actual ionic concentrations for growth of some euryhaline algae. Verhandl. Intern. Ver. Theoret. Angew. Limnol. 13: 722–730.

EPPLEY, R. W., AND J. L. COATSWORTH. 1966. Culture of the marine phytoplankter *Dunaliella tertiolecta*, with light–dark cycles. Arch. Mikrobiol. 55: 66–80.

EPPLEY, R. W., AND C. C. CYRUS. 1960. Cation regulation and survival of the red alga, *Porphyra perforata*, in diluted and concentrated sea water. Biol. Bull. 118: 55–65.

GEE, R., G. JOSHI, R. F. BILS, AND P. SALTMAN. 1965. Light and dark $C^{14}O_2$ fixation by spinach leaf systems. Plant Physiol. 40: 89–96.

GUILLARD, R. R. L. 1962. Salt and osmotic balance, p. 529–540. *In* R. A. Lewin [ed.] Physiology and biochemistry of algae. Academic Press, Inc., New York.

HILLER, R. G., AND H. GREENWAY. 1968. Effects of low water potentials on some aspects of carbohydrate metabolism in *Chlorella pyrenoidosa*. Planta 78: 49–59.

HOLM-HANSEN, O., K. NISHIDA, V. MOSES, AND M. CALVIN. 1959. Effects of mineral salts on short-term incorporation of carbon dioxide in *Chlorella*. J. Exptl. Botany 10: 109–124.

JOSHI, G. V. 1967. Studies in photosynthesis in marine plants of Bombay, p. 256–264. *In* V. Krishnamurthy [ed.] Proc. Seminar Sea, Salt & Plants. Catholic Press, Ranchi, India.

JOSHI, G., T. DOLAN, R. GEE, AND P. SALTMAN. 1962. Sodium chloride effect on dark fixation of CO_2 by marine and terrestrial plants. Plant Physiol. 37: 446–449.

KAUSS, H. 1967. Metabolism of isofloridoside (O-α-D-galactopyranosyl-(1→1)-glycerol) and osmotic balance in the fresh water alga *Ochromonas*. Nature 214: 1129–1130.
1968. α-Galaktosylglyzeride und Osmoregulation in Rotalgen. Z. Pflanzenphysiol. 58: 428–433.

MCLACHLAN, J. 1961. The effect of salinity on growth and chlorophyll content in representative classes of unicellular marine algae. Canadian J. Microbiol. 7: 399–406.
1964. Some considerations of the growth of marine algae in artificial media. Canadian J. Microbiol. 10: 769–782.

MUNDA, I. 1963. Water and electrolyte exchange in the brown algae *Ascophyllum nodosum* (L.) LeJol., *Fucus vesiculosus* L. and *Fucus ceranoides* L. Botan. Marina 6: 158–188.

OGATA, E., AND T. MATSUI. 1965. Photosynthesis in several marine plants of Japan as affected by salinity, drying and *p*H, with attention to their growth habitats. Botan. Marina 8: 199–217.

POTTS, W. T. W. 1968. Osmotic and ionic regulation. Ann. Rev. Physiol. 30: 73–104.

PROVASOLI, L. 1958. Nutrition and ecology of protozoa and algae. Ann. Rev. Microbiol. 12: 279–308.

PROVASOLI, L., J. J. A. MCLAUGHLIN, AND I. J. PINTNER. 1954. Relative and limiting concentrations of major mineral constituents for the growth of algal flagellates. Trans. N.Y. Acad. Sci., Ser. II, 16: 412–417.

RAMANATHAN, J. D., J. S. CRAIGIE, J. MCLACHLAN, D. G. SMITH, AND A. G. MCINNES. 1966. The occurrence of D-(+)-14/25-cyclohexanetetrol in *Monochrysis lutheri* Droop. Tetrahedron Letters 14: 1527–1531.

SAWARDEKER, J. S., J. H. SLONEKER, AND A. JEANES. 1965. Quantitative determination of monosaccharides as their alditol acetates by gas liquid chromatography. Anal. Chem. 37: 1602–1604.

STRICKLAND, J. D. H., AND T. R. PARSONS. 1965. A manual of sea water analysis. 2nd ed. Bull. Fish. Res. Bd. Canada 125. 203 p.

SWEELEY, C. C., R. BENTLEY, M. MAKITA, AND W. W. WELLS. 1963. Gas-liquid chromatography of trimethylsilyl derivatives of sugars and related substances. J. Am. Chem. Soc. 85: 2497–2507.

YAMAMOTO, M. 1967. Osmotic regulation in a halophilic strain of *Chlamydomonas* II. Effects of sulfhydryl reagents. Z. Allgem. Mikrobiol. 7: 267–277.

YAMAMOTO, M., AND H. OKAMOTO. 1967. Osmotic regulation in a halophilic *Chlamydomonas* cell. I General feature of the response to the change in osmotic pressure. Z. Allgem. Mikrobiol. 7: 143–150.

Chemical Composition of Shrimp Flesh (*Parapenaeus* spp.) and its Nutritive Value

TEOFIL DABROWSKI, EDWARD KOLAKOWSKI, AND BARBARA KARNICKA

Sea Fisheries Institute, Gdynia
Department of Commercial Fish Technology
Szczecin, Poland

DABROWSKI, TEOFIL, EDWARD KOLAKOWSKI, AND BARBARA KARNICKA. 1969. Chemical composition of shrimp flesh (*Parapenaeus* spp.) and its nutritive value. J. Fish. Res. Bd. Canada 26: 2969–2974.

The chemical composition and yield of edible shrimp (*Parapenaeus* spp.) were determined. Shrimp of 15.5–23.4 cm and mean weight of 37.3 g yielded from 47.2 to 55.1% of flesh (mean 51.3%). Average composition of flesh was: water 76.74%, fat 0.91%, ash 1.71%, total phosphorus 0.49%, and total protein 22.07%, the last being made up of 76.5% pure protein. Shrimp flesh protein contained a large amount of arginine, histidine, and proline, but not so much threonine, methionine, valine, lysine, and tryptophane. Amine nitrogen constituted 39.5% of the total nonprotein nitrogen. Its composition was mainly of the following free amino acids: glycine, arginine, proline, and alanine. In contrast to the flesh of fish, that of shrimps contained a considerable amount of free methionine.

Received September 23, 1968

INTRODUCTION

DESPITE the need to make good use of shrimps, they have not been thoroughly investigated, from either the chemical or industrial point of view, as has been done for fish. This situation was due to factors such as variety of shrimp species and specific catching and processing methods. Earlier investigations (Jones, 1926; Lanham and Lemon, 1938; Varela, 1955) have shown the high nutritive and caloric value of shrimps as compared with other crustaceans and lean fish. In the bibliography on shellfish by Börgstrom (1962), the papers on shrimps are limited and throw only fragmentary light on the subject. The present authors undertook a thorough examination of chemical composition and nutritive value of certain shrimps that are, among others, the subject of great interest to the Polish fish industry.

This paper reports the yield and chemical composition of edible shrimp (*Parapenaeus* spp.) flesh, especially the composition of free amino acids chemically bound in proteins.

MATERIALS AND METHODS

Shrimps (*Parapenaeus* spp.) (Fig. 1) were caught on the fishing grounds of Georges Bank, in square 1444, frozen immediately in a plate contact freezer to –18 C, and brought to the laboratory.

MORPHOMETRIC ANALYSIS

After partial thawing of the frozen shrimp blocks (in open air at 20 C), undamaged individuals were put to morphometric tests such as full length measuring (distance between be-

Printed in Canada (J1225)

ginning of the rostrum and end of the "caudal plates"), total weight, weight of the cephalothorax and armature, and yield of edible meat.

Preparation of Samples

For chemical analysis, 47 shrimps were selected, representing equally all length groups from 15.5 to 23.4 cm. Meat from the shrimp necks was put through a mincer with 1.5-mm diam sieves, ground until a uniform mass was obtained, and sampled for chemical analysis immediately.

Chemical Methods

Water content was estimated by drying at 105 C to a constant weight. Total nitrogen and nonprotein nitrogen (after extraction with 10% trichloroacetic acid) were determined by the Kjeldahl method, using the macro-type Parnas–Wagner apparatus for ammonia distillation. Protein nitrogen was calculated by difference. Amino nitrogen was determined by the Pope–Stevens (1939) method. Phosphorus fractions were determined by the Schmidt–Thannhauser (1945) method. Individual fractions were digested in concentrated sulphuric acid with hydrogen peroxide solution as catalytic agent, then the PO_4^{3-} groups were determined by the Scheel method (Struszynski, 1952) using a Pulfrich photometer red filter of 726 mμ.

Quantitative and Qualitative Analysis of Amino Acids

Free amino acids were extracted (Jones, 1955), then separated and designated as described by Awapara (1948), with modifications (Kolakowski and Dabrowski, 1967). Protein-bound amino acids in the tissue sediment were determined after free amino acid extraction. The precipitate remaining on the funnel was dried at 37 C under reduced pressure, and crushed in a mortar to obtain a fine meal. A sample of this meal, equivalent to 100 mg of protein, was weighed out into a 10-ml test tube and 10 ml of 6 N HCl (acid hydrolysis) or 10 ml saturated solution of $Ba(OH)_2$ (alkali hydrolysis) was added and hydrolyzed (Block et al., 1960).

Free and bound amino acid separation was carried out by the combined method of chromatography and low-voltage electrophoresis (Podeszewski, 1962) with modified conditions, using in the first run ascending chromatography in *n*-butanol:formic acid:H_2O (75:15:10, respectively) for about 32 hr (2 × 16 hr); then perpendicularly to the first run, using electrophoresis in an acetate buffer of *p*H 1.9 (H_2O:CH_3COOH:HCOOH at 16:3:1 vol respectively) for about 2.5 hr (300 v, 1.0–1.6 ma/cm of Whatman No. 3 filter paper).

After electrophoresis, the chromatoelectropherograms were dried at room temperature, sprayed with 0.25% acetone solution of ninhydrin with addition of water and acetic acid (Bode, 1955), and developed in a darkroom at room temperature for 24 hr.

Quantitative amino acid determination was made by the Fischer and Dorfel method (1953), using calibration curves made on the English standard solutions ("Shandon" — Standard Solution for Paper Chromatography).

RESULTS

Morphometric Analysis

Preliminary morphometric analysis of some scores of shrimps ranging in length from 15.5 to 23.4 cm, and weight from 17.1 to 65.0 g gave the following averages: weight, 37.3 g; edible meat, 51.3%; cephalothorax, 37.9%; armature, 8.6%. The yield of edible meat ranged from 47.2 to 55.1%. Bigger individuals generally had higher percentage meat yields.

Chemical Analysis

The elementary chemical composition of shrimp meat was as follows:

Water	Fat	Ash	Crude protein	Phosphorus *mg/100 g*		
				Total	Acid-sol.	Acid-insol.
76.74%	0.9%	1.71%	22.07%	490	266	224

The distribution of N in *Parapenaeus* spp. meat (in g N/100 g of fresh meat) was: total N, crude protein, 3.532; nonprotein N, 2.701; protein N, 0.831; amino acid N, 0.328.

Free and Bound Amino Acids

The composition of free and bound amino acids of the shrimp meat (Table 1 and Fig. 2) included at least 20 amino acids. The amount of glutamine was not determined, but we presume from Fig. 2A that it might be considerable. Of the 18 main amino acids, glutamic acid, arginine, aspartic acid, leucine, and isoleucine accounted for about 51.6 g/100 g of protein.

Table 1. Composition of free and bound amino acids of shrimp (*Parapenaeus* spp.) meat.

No.	Amino acid	Amino acids	
		Free, mg/100 g of fresh meat	Bound, g/100 g of pure protein
1.	Cystine + cysteine	Traces	1.37
2.	Lysine	58.00	8.76
3.	Arginine	290.79	12.87
4.	Histidine	–[a]	3.07
5.	Glutamine	?[b]	–
6.	Aspartic acid	66.81	10.90
7.	Serine	68.80	3.35
8.	Glycine	311.25	3.65
9.	Threonine	44.43	3.63
10.	Glutamic acid	18.89	14.15
11.	α-Alanine	107.82	5.60
12.	Proline	133.21	3.99
13.	Tyrosine	15.20	3.95
14.	α-Aminobutyric acid	Traces	–
15.	Methionine	22.47	2.36
16.	Tryptophane	Traces	0.98
17.	Valine	41.62	3.39
18.	Phenylalanine	20.03	4.05
19.	Leucine + isoleucine	88.31	13.67
X_3	Oxyproline	Traces	–
20.	Taurine	160.03	–

[a]Does not appear.
[b]No estimations were performed.

DISCUSSION

The physical and chemical investigations carried out show that, in comparison with other sea and freshwater crustaceans and fish of the cod family, meat of *Parapenaeus* spp. shrimps has high nutritive value (Table 2).

The total protein, fat, and phosphorus content in shrimp meat dry mass is higher than in the sea and freshwater crustaceans listed in Table 2, and also

TABLE 2. Comparison of chemical composition and yield of edible shrimp (*Parapenaeus* spp.) product with some species of sea and freshwater crustaceans and the fish of cod family.

Species	Yield of edible product (%)	Dry residue (%)	Contents in dry mass (%)					Source
			Crude protein	True (pure) protein	Fat	Ash	Phospho-rus	
Sea crustaceans								
Prawn	–	24.74	94.00	70.67	1.27	6.73	–	Konosu et al. (1958)
Lobster	–	–	95.25	62.38	1.46	8.10	–	"
Blue crab	–	19.85	86.61	61.44	0.52	7.99	–	"
Shrimp	51.3	23.26	94.89	72.57	3.90	7.35	2.10	Data of this paper
Freshwater crustaceans								
Crayfish (*Astacus leptodactylus*)	15.47	16.78	85.96	70.68	3.52	7.09	–	Dabrowski et al. (1966a)
American crayfish (*Orconectes limosus*)	24.18	19.41	88.72	73.47	–	–	1.52	Dabrowski et al. (1966b)
Cod family fish								
Cod (*Gadus callarias*)	19.60	60[a]	92.34	–	1.66	6.07	–	Kordyl (1959)
Baltic cod (*Gadus callarias*)	38.9[b]	–	92.35	–	1.53	5.61	1.11	Taarland et al. (1958)
	18.02							

[a]Gutted and headed cod.
[b]Fillets of cod with skin.

FIG. 1. Shrimps (*Parapenaeus* spp.), from above and from the side.

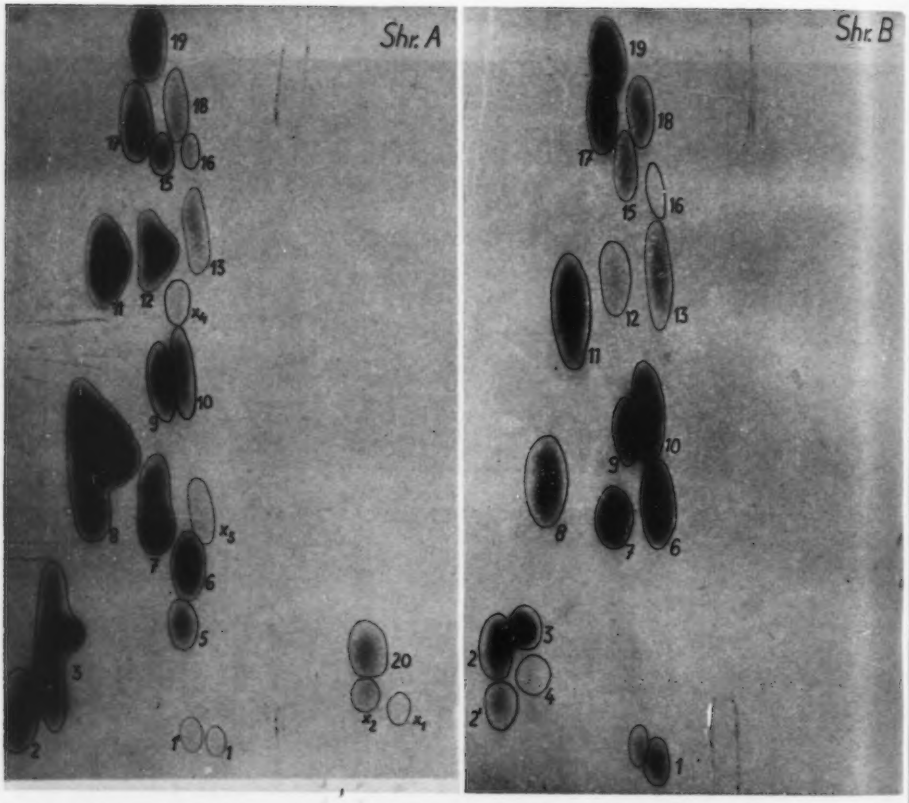

FIG. 2. Chromatoelectropherograms of free (A) and of acid protein hydrolyzate (B) amino acids of shrimp (*Parapenaeus* spp.) fresh meat. Samples plotted: A — 10 μliters (2×5 μliters) equal to 25 mg of fresh tissue. B — 5 μliters of protein acid hydrolyzate equal to 0.25 mg of protein. Estimations: 1′, 1 — cystine + cysteine; 2′, 2 — lysine; 3 — arginine; 4 — histidine; 5 — glutamine; 6 — aspartic acid; 7 — serine; 8 — glycine; 9 — threonine; 10 — glutamic acid; 11 — α-alanine; 12 — proline; 13 — tyrosine; 14 — α-aminobutyric acid; 15 — methionine; 16 — tryptophane; 17 — valine; 18 — phenylalanine; 19 — leucine + isoleucine; 20 — taurine; X_3 — oxyproline; X_1, X_2, and X_4 — unidentified compounds.

than in cod; the amount of pure protein is also higher and is exceeded only by the American freshwater crayfish (*Orconectes limosus*).

The meat of shrimp *Parapenaeus* spp. has a higher dry weight than that of blue crab, and lower than that of the prawn. The amount of ash in shrimp is higher by about 27.7% than that of the cod. Shrimp *Parapenaeus* spp., because of its comparatively small cephalothorax, gives a fairly high meat yield, twice as high as that of freshwater crustaceans and approaching that of cod.

In comparison with fish (Connell and Howgate, 1959; Braekkan and Boge, 1962) and also other sea crustaceans (Kōnosū et al., 1958), shrimp protein contains a higher level of arginine and histidine, but a slightly lower level of threonine, serine, methionine, and tryptophane. This was partly confirmed by Beach et al. (1943). Our investigations show that in comparison with such other sea crustaceans as prawn, lobster, blue crab, and fish, shrimp protein is lower in lysine and valine, but higher in proline. The remaining amino acid levels are similar to those of other sea shrimp and fish. *Parapenaeus* spp. meat contains, like other shrimps (Campbell, 1934–35; Dabrowski et al., 1966a, b; Kōnosū et al., 1958) a high level of nonprotein nitrogen (about 23.5%), in relation to total nitrogen, which places them, in this respect, close to bony and cartillaginous fishes.

The amino nitrogen accounted for about 39.5% of the total nonprotein nitrogen. The difference between amino nitrogen determined by Pope–Stevens method (1939) and the total nitrogen content of the individual free amino acids shows that some amino nitrogen appears in the form of peptides and other chemical links.

Glycine, arginine, proline, and α-alanine account for 65% of the total free amino acids. The taurine level is half that found in fish (Jones, 1955). Free glutamine and the compound X_4 (Kolakowski and Dabrowski, 1967) also appear in large amounts in shrimps but were not quantitatively determined. We were unable to confirm the presence of free histidine, however.

De Almeida (1954) and Ranke (1959) state that free cysteine and cystine do not appear in shrimps. According to our determinations, it has been possible to demonstrate their presence. They appear only in trace amounts, however, similar to tryptophane, α-aminobutyric acid, oxyproline, and also α-alanine.

REFERENCES

AWAPARA, J. 1948. Application of paper chromatography to the estimation of free amino acids in tissues. Arch. Biochem. 19: 172–173.

BEACH, E. F., B. MUNKS, AND A. ROBINSON. 1943. The amino acid composition of animal tissue protein. J. Biol. Chem. 148: 431–439.

BLOCK, R. J. 1960. Amino acid analysis of protein hydrolisates, p. 6–7. *In* P. Alexander and R. J. Block [ed.] A laboratory manual of analytical methods of protein chemistry, Vol. 2. Pergamon Press, London.

BODE, F. 1955. Eine Vereinfachung und Verbesserung der Methode zur quantitativen Bestimmung von Aminosäuren und Peptiden mittels des Ninhydrin-Kupferkomplexes. Biochem. Z. 326: 433–435.

BÖRGSTROM, G. 1962. Shellfish protein — nutritive aspects, p. 115–147. *In* Fish as food, Part II. Academic Press, Inc., New York and London.

BRAEKKAN, O. R., AND G. BOGE. 1962. Rept. Technol. Res. Norwegian Fish. Ind. 4: 7–19.

CAMPBELL, J. 1934–35. The non-protein nitrogen constituents of fish and lobster muscle. J. Fish. Res. Bd. Canada 1: 179–189.

CONNELL, J. J., AND P. F. HOWGATE. 1959. The amino acid composition of some British food fishes. J. Sci. Food Agr. 10: 241–244.

DABROWSKI, T., E. KOLAKOWSKI, AND E. SOKOLOWSKI. 1966a. Zusammensetzung und Nährwert des Krebsfleisches von Astacus leptodactylus. Z. Lebensm. Untersuch.-Forsch. 129: 337–344.

DABROWSKI, T., E. KOLAKOWSKI, H. WAWRESZUK, AND CZ. CHOROSZUCHA. 1966b. Studies on chemical composition of American crayfish (*Orconectes limosus*) meat as related to its nutritive value. J. Fish. Res. Bd. Canada 23: 1653–1662.

DE ALMEIDA, M. E. W. 1954. Aminoàcidos livros con camarões variacões decorridas durante a decomposicao. Rev. Inst. Adolfo Lutz 15: 158–167.

FISCHER, F. G., AND H. DÖRFEL. 1953. Zur quantitativen Auswertung der Papierchromatogramme von Eiweiss-Hydrolysaten. Biochem. Z. 324: 544–566.

JONES, D. B. 1926. The nutritional value of oysters and other seafoods. Am. J. Public Health 16: 1177–1182.

JONES, N. R. 1955. The free amino-acids of fish. I. — Taurine in the skeletal muscle of codling (*Gadus callarias*). J. Sci. Food Agr. 6: 3–8.

LANHAM, W. B., AND J. M. LEMON. 1938. Nutritive value for growth of some proteins of fishery products. Food Res. 3: 549–553.

KOLAKOWSKI, E., AND T. DABROWSKI. 1967. Untersuchungen über die Veränderungen der Stickstoffsubstanz im Gewebe des Ostseeherings (*Clupea harengus membras* L.) bei verschiedenen Lagerungsbedingungen. 1. Mitt. Die qualitativen Veränderungen der freien Aminosäuren. Die Nahrung 11: 493–500.

KŌNOSŪ, S., S. KATORI, T. AKIYAMA, AND T. MORI. 1958. Amino acid composition of crustacean muscle proteins. Bull. Japan. Soc. Sci. Fish. 24: 300–304.

KORDYL, E. 1959. Przetwórstwo dorsza, p. 84–93. [Processing of cod.] *In* Dorsz baltycki, GTN, Gdańsk. (English summary.)

PODESZEWSKI, Z. 1962. Chromatoelektroforeza aminokwasów. [Chromatoelectroforetic separation of amino acids.] Roczniki Panstwowego Zakladu Hig. 13: 71–75. (English summary.)

POPE, C. G., AND M. F. STEVENS. 1939. Determination of amino nitrogen using a copper method. Biochem. J. 33: 1070–1076.

RANKE, B. 1959. Über die nicht-eiweissgebundenen Aminosäurebestande von Fischen, Mollusken und Krebsen. Arch. Fischereiwiss. 10: 193–198.

SCHMIDT, G., AND S. J. THANNHÄUSER. 1945. A method for the determination of DNA, RNA and phosphoproteins in animal tissues. J. Biol. Chem. 161: 88–92.

STRUSZYNSKI, M. 1952. Analiza ilościowa i techniczna. Vol. II. 275 p. PWT, Warszawa.

TAARLAND, T., E. MATHIESEN, O. OVSTHUS, AND O. R. BRAEKKAN. 1958. Naeringsverdi og vitaminer i norsk fisk og fiskevarer. Tidsskr. Hermetikind. 44: 405–412.

VARELA, G. 1955. Sobre el valor biológico nutritivo de las proteinas del abadejo ahumado y del camarón. Anales Bromatol. Madrid 7: 127–140.

Hypertrophy of the Interrenal Tissue in Sexually Maturing Sockeye Salmon (*Oncorhynchus nerka*) and the Effect of Gonadectomy

J. R. McBride and A. P. van Overbeeke[1]

Fisheries Research Board of Canada
Vancouver Laboratory, Vancouver 8, B.C.

McBride, J. R., and A. P. van Overbeeke. 1969. Hypertrophy of the interrenal tissue in sexually maturing sockeye salmon (*Oncorhynchus nerka*) and the effect of gonadectomy. J. Fish. Res. Bd. Canada 26: 2975–2985.

Sockeye salmon (*Oncorhynchus nerka*) develop marked hypertrophy of the interrenal tissue during the period of sexual maturation and spawning. No differences were found between fish held in captivity and those that matured in their natural habitat. Feeding appeared to have an inhibitory effect, but did not prevent the hypertrophy. Gonadectomy of sexually mature fish resulted in a rapid involution of the hyperplastic interrenal tissue. On the other hand, gonadectomy, when performed in an early stage of sexual maturity, prevented the development of interrenal hypertrophy. The interrenal hyperplasia was not accompanied by apparent changes in the ACTH cells of the pituitary gland. Gonadectomy, however, led to increased affinity of these cells for lead-hematoxylin, but this effect did not take place until after interrenal involution had commenced. The results are discussed and it is concluded that the hypertrophy of the interrenal at this time is caused by gonadal hormones, which may act directly on the adrenal homologue without mediation by the pituitary gland.

Received July 29, 1969

INTRODUCTION

Despite a number of studies on the interrenal tissue of Pacific salmon (genus *Oncorhynchus*) during the period of sexual maturation and spawning, the physiological role of the adrenocortical homologue at this stage is not clearly understood. Robertson and his co-workers reported progressive hypertrophy of the interrenal cells during sexual maturation and a concomitant increase in the plasma concentration of 17-OH-corticosteroids (Robertson and Wexler, 1957, 1959; Hane and Robertson, 1959; Robertson et al., 1961a, b; Hane et al., 1966). A similar observation concerning the plasma-corticosteroids was made by Idler et al. (1959) and Schmidt and Idler (1962). Robertson suggested that hyperadrenocorticism is the main cause of degenerative tissue changes taking place in these fish and indeed, that it may be related to the postspawning death of Pacific salmon (Robertson and Wexler, 1959; Robertson et al., 1961a, b).

---

[1]Present address (A.P.O.): Department of Biological Sciences, Simon Fraser University, Burnaby 2, B.C.

Printed in Canada (J1546)

Idler and Truscott (1963) concluded from their study on clearance of injected hormones that the elevated corticosteroid level found in mature and reproducing sockeye salmon may be the result of impaired hormone metabolism rather than of excessive hormone production. Fagerlund's investigations (1967) on the other hand, indicate that in this species the plasma concentration of cortisol remains low, when the fish are in resting conditions, but that various forms of stress induce an increased level of this hormone. Histological examination has shown that sockeye salmon (*Oncorhynchus nerka*) develop extensive hyperplasia of the interrenal tissue during sexual maturation, both in their natural environment and under laboratory conditions (van Overbeeke, unpublished results).

The lack of uniformity in these findings seemed to warrant a further investigation of the relation between sexual maturation and interrenal function. Furthermore, conclusive evidence for a causal relationship between corticosteroid production and degenerative alterations in these fish, is lacking. In previous studies we reported that feeding has an inhibitory effect on the development of many of the degenerative tissue changes in sockeye salmon (McBride, 1967). Gonadectomy had an even more striking effect. In maturing fish this operation was followed by a re-appearance of the silvery condition, characteristic of immature "sea-green" fish (McBride et al., 1963; McBride and van Overbeeke, 1969).

The observations prompted an investigation of the effects of feeding and gonadectomy on the activity of the interrenal tissue. The present communimunication describes the results of this study with regard to the histological characteristics of the interrenal tissue and the corticotrophic cells in the pituitary gland. The changes in the dynamics of corticosteroid secretion will be reported separately (E. M. Donaldson and U. H. M. Fagerlund, unpublished results).

METHODS AND MATERIALS

Fish

The fish used in this study were adult migratory sockeye salmon, captured in June 1968 at the entrance to Great Central Lake, Vancouver Island, B.C., while they were on their way to the spawning grounds. Methods of capture and transportation to the Vancouver Laboratory have been described (McBride et al., 1963). Also, general culture procedures, details concerning the diet as well as the method used in inducing the fish to resume feeding while in captivity and the technique for bilateral gonadectomy were reported previously (McBride et al., 1963; McBride, 1967). All fish were held in aquaria under conditions of the natural photoperiod; the temperature of the water ranged from a high of 13 C (in September) to a low of 6 C (in November).

Of the fish held in captivity, 56 were killed at various intervals after their arrival in the laboratory to examine the condition of the interrenal tissue during sexual development and spawning. Forty-six of these were starved (groups 1, 2, 5, and 7); the remaining 10 (group 6) were fed and they were killed when, judging by their external characteristics, they were sexually mature. To compare the data with those of fish existing under natural conditions, an additional 24 fish were collected (groups 3, 4, and 8). These last fish had undergone maturation in their natural habitat, but were transported to the laboratory and killed 4–8 days later.[2] To study the effect

[2]Since these fish had to be used for additional physiological experiments the sampling of tissues could not be done at the site of collection.

of gonadectomy, 20 fish collected in June were held till maturity and then bilaterally gonadectomized. Samples of these fish were killed at various intervals after the operation (groups 9, 10, and 11). A total of 100 fish were used in these investigations.

To complement the results concerning the effect of gonadectomy of mature fish, we have included pertinent data from a study carried out in previous years (1966, 1967) where sockeye were gonadectomized in July, while they were still sexually immature (group 12). These fish were killed at various intervals between September and January. Further details are presented in Table 1.

TABLE 1. Effect of feeding on gonad development of sockeye salmon held in captivity compared with fish from their natural habitat.

Group	Date of sampling	No. fish	Experimental conditions	Gonad development[a]
1	June 27	8 ♂		0.78±0.23
			Captive, unfed	
		4 ♀		3.43±0.18
2	Aug. 29	6 ♂		3.86±2.24
			Captive, unfed	
		6 ♀		12.29±2.48
3	Sept. 4	6 ♂		3.89±2.55
			Controls from wild	
		4 ♀		11.15±3.61
4	Oct. 1	6 ♂		3.34±0.71
			Controls from wild	
		6 ♀		14.63±2.98
5	Oct. 6	5 ♂		2.34±0.53
			Captive, unfed	
		6 ♀		23.36±2.95
6	Oct. 24	6 ♂		2.60±0.46
			Captive, fed	
		4 ♀		22.93±5.17
7	Nov. 1	4 ♂		
			Captive, unfed	Completed spawning[b]
		7 ♀		
8	Nov. 6	1 ♂		
			Controls from wild	Completed spawning[b]
		1 ♀		
9	Oct. 22	6 ♂		
			Captive; gonadectomized[c] Oct. 7	
		3 ♀		
10	Nov. 12	2 ♀	Captive; gonadectomized[c] Oct. 7	
11	Dec. 1	4 ♂		
			Captive; gonadectomized[c] Oct. 7	
		5 ♀		
12[d]	Sept. 13–Jan. 10	6 ♂		
			Captive, fed; gonadectomized	
		4 ♀	July	

[a]Expressed in weight of gonad as percentage of total body weight (mean ± SD).
[b]Approximately 1 week before date of sampling.
[c]Fish were not fed until after gonadectomy.
[d]Data of experiment, carried out in 1967; see text.

Histological Techniques

Fish were killed by severing the spinal cord, just caudal to the head. The pituitary gland and samples of the head kidney, containing the interrenal tissue, were excised and fixed in Bouin–Hollande–Sublimate. Sagittal sections, 5 μ thick, of the pituitary gland were cut serially and stained either with Masson's trichrome method (including Ponceau de xylidine) (Culling, 1957) or with lead-hematoxylin (MacConaill, 1947). Transversal sections, 5 μ thick, of the interrenal tissue were stained with Masson's trichrome method.

Microscopic examination of the interrenal tissue and the corticotrophic cells in the pituitary gland focused on cytoplasmic granulation and prominence of nuclei and nucleoli. In addition, the mean diameter of the interrenal cell nuclei, for each fish, was determined by measuring a total of 200 nuclei, selecting 50 nuclei at random from each of four separate areas.

RESULTS

Interrenal Tissue

CHANGES ACCOMPANYING SEXUAL MATURATION

In sexually immature fish, captured in June just after they had entered the river (group 1), the interrenal tissue consisted of large groups of closely packed small cells (Fig. 1, 2). The cytoplasm of these cells was finely granulated. Their nuclei were usually spherical with a mean diameter of 6.13 ± 0.31 μ and contained inconspicuous nucleoli. In all specimens, however, a few small cell groups, ranging from 2 or 3 to approximately 20 cells, were found in which the cells were slightly hypertrophied and had larger nuclei with prominent, centrally located nucleoli. The tissue was poorly vascularised. Fish killed at the end of August and showing advanced gonad maturation (group 2) exhibited striking changes in the interrenal tissue. Groups of hypertrophied cells were larger and much more abundant than in the immature fish. Also many of the cells were arranged in narrow columns (Fig. 3). A significant increase in mean nuclear size was evident (7.00 ± 0.14 μ). Virtually all of the nuclei showed prominent nucleoli. In fully mature fish, killed during early October (group 5), the hypertrophy had progressed further and included practically all of the cells (Fig. 4, 5), but there was no further increase in the mean diameter of the nuclei (7.19 ± 0.16 μ). The columns of cells were separated by sinusoids filled with erythrocytes. In a few fish small hemorrhages were found occasionally.

The tissue in fish that had completed spawning and that were killed the first week of November (group 7) did not differ appreciably from that in the mature fish. In all specimens, however, hemorrhages were present and pyknosis of the nuclei was also more frequently observed in spent fish. Another sign of beginning cytolysis was vacuolization of the cytoplasm, which had affected many cells.

Fish, held under the same conditions, but which were fed (group 6), showed similar changes in their interrenals, but the hypertrophy was less pronounced. Indeed, even at sexual maturity, there were still many groups of small cells. Although the mean nuclear diameter of the interrenal tissue ($6.94 \pm 0.24\mu$) was significantly larger than that of the immature fish, it was significantly smaller than that of the comparable mature, but unfed fish (group 5).

Examination of sockeye that underwent gonad maturation in their natural habitat (groups 3 and 4), showed that the changes occurring in the interrenal tissue are the same as noted in the laboratory fish. The nuclear diameter in these "wild" sexually maturing fish was, however, significantly lower (6.81 ± 0.08 and 6.94 ± 0.11 μ, respectively) than in the fish held in captivity (7.19 ± 0.16 μ). Spent fish (groups 7 and 8) on the other hand, showed no differences in this respect. The mean nuclear diameters of the various groups discussed above are presented in Fig. 13. No differences between males and females were seen in any of the groups.

EFFECT OF GONADECTOMY

In both sexes, gonadectomy of sexually mature fish led to a gradual involution of the interrenal tissue (Fig. 14). This process apparently started at the level of the nuclei. Two weeks after the operation (group 9), many nuclei had small, inconspicuous nucleoli, and the mean nuclear diameter was reduced (6.86 ± 0.32 μ). The effects were more pronounced in fish killed 5 weeks after gonadectomy (group 10); the mean nuclear diameter was further reduced to 6.57 ± 0.09 μ, and also a reduction in cell size was evident. In fish killed 8 weeks after the operation (group 11) the mean nuclear diameter was 6.03 ± 0.21 μ and the tissue in general resembled that of the sexually immature salmon (group 1) (Fig. 6, 7). In fish gonadectomized while sexually immature and killed from 2 to 6 months later (group 12) the interrenal tissue had undergone no apparent changes; the mean nuclear diameter was 5.78 ± 0.14 μ.

ACTH CELLS

The ACTH cells in the pituitary gland of the sockeye salmon can be readily identified in the pars distalis. They are located in its rostral part and form a palisadelike epithelium, which separates this part from the neurohypophysis. In addition, it penetrates between the rostral and the proximal pars distalis. The finely granulated cytoplasm stains distinctly orange–brown with Masson's trichrome method. The granules also have a strong affinity for lead-hematoxylin, which gives them a blue–black colour. This last dye, however, is not entirely specific since it is also a nuclear stain and stains, moreover, the secretory granules in part of the cells of the pars intermedia.

Generally, the layer of corticotrophic cells in the fish examined in the present study had the appearance of a pseudostratified epithelium. The individual cells were prismatic and the basal location of the nuclei accentuated their polarity. The shape of the nuclei was variable, from oval to spherical, often showing indentations. The nucleoli were mostly located near the nuclear membrane and were usually inconspicuous. The degree of granulation appeared to vary. This variability concerned the relative abundance of secretory granules within the cells of any one single pituitary gland, but more pronounced were differences between fish belonging to the same experimental group. Comparison of fish of groups 1, 2, 5, and 7 revealed that during sexual maturation and spawning only minor changes in the corticotrophic cells took place. In all fish, the histological structure of these cells suggested a moderate to low activity

(Fig. 8, 9, 10). In none of them did we find any depleted cells. No mitotic figures were seen; neither were there indications that these cells may divide amitotically.

Mature and spent sockeye differed from the immature fish in that they contained some isolated cells and groups of cells, very similar to the corticotrophs, but more deeply stained and lying in the adjacent part of the neurohypophysis. In the spent fish some of the corticotrophs showed occasional pyknosis of the nucleus and loss of granulation. No differences in the corticotrophs were seen between fed and unfed sockeye or between fish from the wild and fish held in the laboratory.

Although removal of the gonads had a slow but distinct effect on the cytoplasmic granulation of the corticotrophs, it did not affect the size or shape of either the nuclei or the nucleoli. Two weeks after the operation (group 9), the granulation had undergone no apparent change, but in the second sample, killed 5 weeks after gonadectomy (group 10), the granulation was much heavier than in unoperated mature fish (Fig. 11, 12). By the 8th week (group 11), the granulation was somewhat reduced, as compared to that in fish of group 10, but still heavier than in any of the earlier samples.

DISCUSSION

The results show that in sockeye salmon of both sexes from Great Central Lake, gonad maturation and spawning is accompanied by extensive hyperplasia of the interrenal tissue. These observations confirm those for both chinook and sockeye salmon from the Sacramento River system, reported in the pioneer study by Robertson and Wexler (1959). Comparison of our data with those described by Robertson and Wexler indicate that in the sockeye of Great Central Lake the degree of hyperplasia is apparently not so marked, and that the degenerative changes occurring at the time of spawning (hemorrhages, pyknosis, vacuolization of the cytoplasm, and cytolysis) are also less pronounced. Only in mature salmon, kept in the laboratory beyond the normal time of reproduction, or in specimens held from 2 to 3 months after spawning,

FIG. 1. Interrenal tissue of a sexually immature sockeye salmon killed in June. The compact interrenal cells border on a branch of a cardinal vein (V). Note the poor vascularization of the tissue. Masson's trichrome. ×125.

FIG. 2. Higher magnification of interrenal cells shown in Fig. 1. Cell nuclei are uniform in size and with few exceptions the nucleoli are inconspicuous. The cytoplasm appears finely granulated. Masson's trichrome. ×500.

FIG. 3. Interrenal tissue of a sexually maturing sockeye killed in August. The interrenal cells are hypertrophied, but compact groups of small cells are still present (lower right). Many small blood vessels traverse the tissue. Compare with Fig. 1. Masson's trichrome. ×125.

FIG. 4. Interrenal tissue of a sexually mature sockeye killed in early October, showing widespread hypertrophy of the cells. Compare with Fig. 1 and 3. Masson's trichrome. ×125.

FIG. 5. Higher magnification of the interrenal cells shown in Fig. 4. Note the marked hypertrophy of the cortical tissue; also, the presence of prominent nucleoli. Compare with Fig. 2. Masson's trichrome. ×500.

FIG. 6. Fish gonadectomized when sexually mature (October) and killed after 8 weeks. The interrenal tissue consists of compact groups of small cells. Compare with Fig. 1 and 4. Masson's trichrome. ×125.

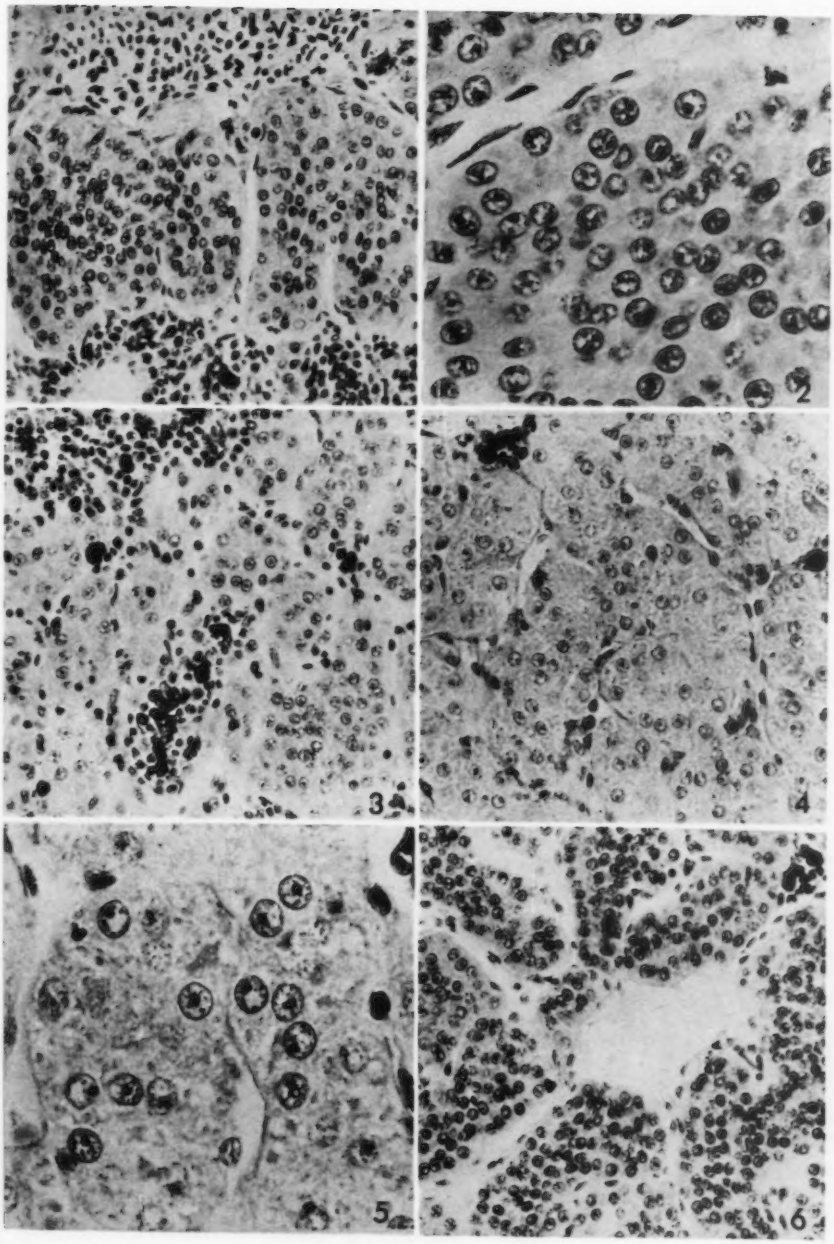

McBride and van Overbeeke — J. Fish. Res. Bd. Canada

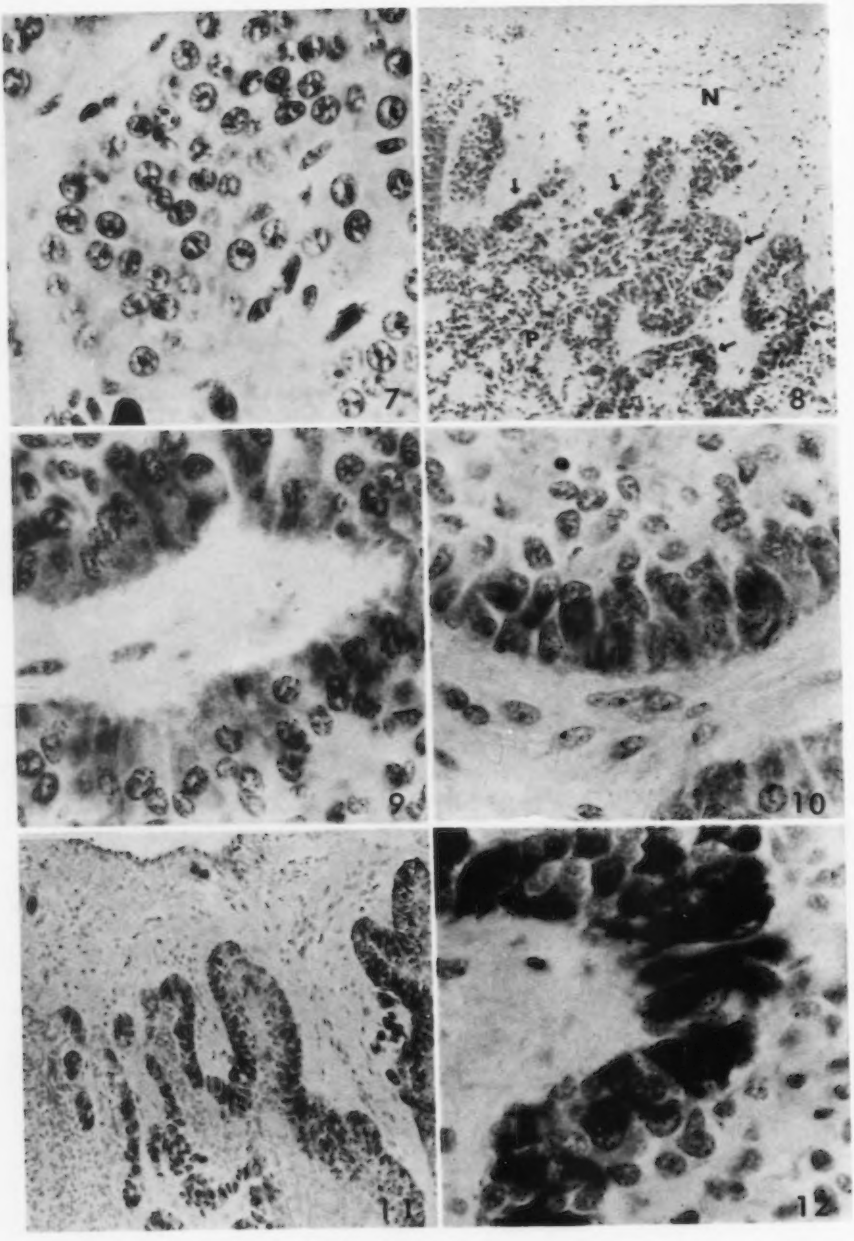

McBride and van Overbeeke — J. Fish. Res. Bd. Canada

as well as in diseased fish, could widespread degeneration of the adrenocortical homologue be found (van Overbeeke and McBride, unpublished observations).

No essential differences were noted between fish in their natural environment and those that underwent maturation in captivity. The degree of nuclear hypertrophy was slightly lower in two samples of wild fish (groups 3 and 4), but this may be ascribed to the fact that in these groups gonad development was less advanced than in the captive fish killed at the same time (groups 2 and 5) (Table 1).

In an attempt to analyse the various factors that might initiate the adrenal hypertrophy, Robertson and Wexler (1959) concluded, on the basis of a comparative study of Pacific salmon and rainbow trout, that starvation is probably not a major causal factor. The results of the present study lead to the same conclusion. The interrenal hyperplasia in fish that had been feeding actively for several months (group 6) was not markedly different from that in comparable mature nonfeeders (group 5). Judged by its effect on the nuclear diameter, however, feeding seems to limit somewhat the development of hyperadrenocorticism.

A striking effect on the interrenal tissue was evident after gonadectomy. Indeed, in both sexes, removal of the gonads in sexually mature sockeye brought about a gradual loss of the hyperplasia, and 8 weeks after the operation the condition of this tissue was virtually the same as that in sexually immature sockeye. In this connection the effects of gonadectomy, performed in an early stage of sexual maturation are of interest. In such fish (group 12) interrenal hyperplasia was totally prevented. The conclusion from these findings is that the development of interrenal hypertrophy is directly related to gonad maturation. The question arises how to further specify this effect of the gonads. It is well known that gonad formation in Pacific salmon normally takes place under conditions of starvation and is accompanied by excessive depletion of body tissues. It is possible that the over-all metabolic activities involved, per se, place unusual demands on the production of corticosteroids, but the hormonal regulation of this process remains to be elucidated. As Robertson and Wexler (1959) pointed out, it is not likely that the change in body me-

←

FIG. 7. Higher magnification of the interrenal tissue shown in Fig. 6. The tissue is similar to that of the sexually immature fish (Fig. 2). Masson's trichrome. ×500.

FIG. 8. Midsagittal section of the pituitary of a sexually immature sockeye killed in June showing the layer of ACTH cells (arrows) that separates the neurohypophysis (N) from the pars distalis (P). Lead-hematoxylin. ×125.

FIG. 9. Higher magnification of area shown in Fig. 8. Note that the ACTH cells are only lightly stained by lead-hematoxylin. Lead-hematoxylin. ×500.

FIG. 10. ACTH cells of a sexually mature sockeye, killed in October. Note that the appearance of these cells is the same as those of an immature fish, as shown in Fig. 9. Lead-hematoxylin. ×500.

FIG. 11. Midsagittal section of the pituitary gland of a sockeye gonadectomized when sexually mature and killed 5 weeks later. Note strong affinity of the ACTH cells for lead-hematoxylin. Compare with Fig. 8. Lead-hematoxylin. ×125.

FIG. 12. Higher magnification of ACTH cells, shown in Fig. 11. Compare with Fig. 9 and 10. Lead-hematoxylin. ×500.

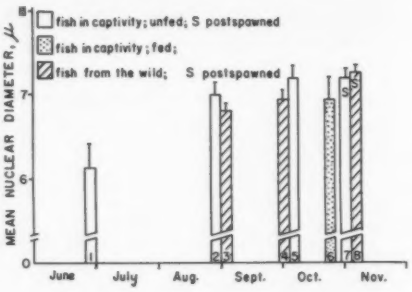

FIG. 13. Development of nuclear hypertrophy in interrenal cells of sockeye salmon during sexual maturation. The numbers in the columns refer to the groups of fish, listed in Table. 1.

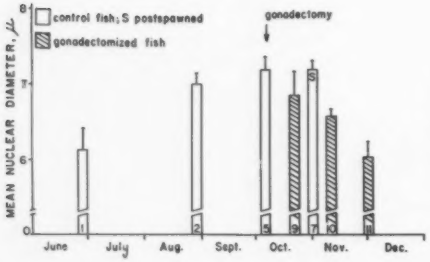

FIG. 14. Effect of gonadectomy on the nuclear hypertrophy in the interrenal cells of sexually mature sockeye salmon. The numbers in the columns refer to the groups of fish, listed in Table 1.

tabolism that occurs during gonad development is the only stimulus inciting hyperadrenocorticism. In their studies, hyperplasia was observed to commence while the gonads were still small and body reserves abundant, and the same can be said of the sockeye used in the present study. The fact that feeding does not substantially reduce the hyperplasia, tends to support the above opinion. Hane et al. (1966) suggested the possibility that it is the gonadal hormones that exert an influence on the interrenal. It has been demonstrated that in rats, estrogen induces and maintains extensive hypertrophy of the adrenal cortex (Bernstein and Biskind, 1957; Bernstein, 1958, 1964). Also, in both sexes removal of the gonads results in decreased production in vitro of corticosterone and this defect can be reversed by treatment with estradiol and testosterone (Kitay et al., 1965, 1966). In humans, estrogens may cause a marked elevation in the level of plasma 17-OH corticosteroids (Wallace et al., 1957). Direct support for a similar role of gonadal steroids in salmon comes from a recent study on the effect of 11-ketotestosterone and estradiol on gonadectomized sockeye salmon. These fish develop changes in the interrenal tissue, which are similar to those taking place during normal sexual maturation (McBride, in preparation). The morphological changes, moreover, are accompanied by an increase in plasma levels of cortisol (Fagerlund and Donaldson, 1969).

In sockeye salmon, the corticotrophic cells in the pituitary gland have been identified on the basis of their morphological characteristics (van Overbeeke and McBride, 1967), on the basis of changes correlate with those in the interrenal tissue induced by the corticosteroid blocking agent metopirone

(Fagerlund et al., 1968), and on the basis of their immunohistochemical response to antibodies against mammalian ACTH (McKeown and van Overbeeke, 1969). In various studies of corticotrophs in teleost fishes, changes in cytomorphological features, such as size and shape of the cells, nuclear diameter, position and size of nucleoli, degree of granulation, stainability (in particular the affinity for lead-hematoxylin), vacuolization of the cytoplasm etc., have been interpreted as changes in physiological activity of these cells. Using this type of analysis several workers have demonstrated that changes of the teleost interrenal function may induce alterations in the corticotrophic cells (Ball and Olivereau, 1966; Hanke et al., 1967; Fagerlund et al., 1968; Mattheij, 1968). Admittedly, these results were obtained after pharmacological interference with the interrenal function and, therefore, they do not necessarily indicate that under physiological conditions a change in activity of the interrenal tissue should be reflected in the structure of the corticotrophic cells. Yet, it seems surprising that the marked hyperadrenocorticism in maturing sockeye salmon is not accompanied by clear changes in the corticotrophs. This may suggest that the gonadal effect on the interrenal is not, or only partly, mediated by the pituitary gland. The effect of gonadectomy seems to support this. Although the increased granulation, noted in the corticotrophs after the operation, indicates that the release of ACTH (relative to its production) is reduced, this effect is minor as compared to the marked involution that the interrenal undergoes. Furthermore, the fact that no response of these cells could be seen in fish killed 2 weeks after gonadectomy, in which interrenal involution had commenced, indicates that the changes in the corticotrophs are secondary to those in the interrenal tissue. Thus, this sequence indicates that the gonadal hormones exert their effect directly on the interrenal. Such an effect has been shown to exist in mammals. Kitay et al. (1965, 1966) demonstrated that the stimulatory effect of testosterone on the adrenal cortex in male rats is not mediated by the pituitary gland or by changes in ACTH secretion, although such an effect of estradiol in females is at least in part due to a direct influence of this hormone on the adrenal cortex.

ACKNOWLEDGMENTS

The authors are indebted to the Department of Fisheries and Forestry of Canada, Vancouver, B.C., for making available the fish used in this study. We thank Dr B. M. Bary, Department of Zoology, University of British Columbia, for his assistance in the collection of the marine zooplankton. The skilled technical assistance of Mr Jack Baker, Department of Fisheries and Forestry of Canada in trapping the fish and Miss Karen Forgeron in the preparation of the histological material is gratefully acknowledged.

REFERENCES

BALL, J. N., AND M. OLIVEREAU. 1966. Identification of ACTH cells in the pituitary of two teleosts, *Poecilia latipinna* and *Anguilla anguilla*: Correlated change in the interrenal and in the pars distalis resulting from administration of metopirone (SU 4885). Gen. Comp. Endocrinol. 6: 5–18.

BERNSTEIN, D. E. 1958. Autotransplantation of the adrenal of the rat to the portal circulation: Effect of administration of sex hormones. Endocrinology 63: 765–767.

1964. Autotransplantation of the adrenal to the portal circulation: Further evidence for the dependency of adrenal hypertrophy on estrogen. Endocrinology 74: 661–663.

BERNSTEIN, D. E., AND G. R. BISKIND. 1957. Autotransplantation of the adrenal of the rat to the portal circulation: Induced adrenal hypertrophy and its prevention by oophorectomy. Endocrinology 60: 575–577.

CULLING, C. F. A. 1957. Handbook of histopathological technique. Butterworth & Co. Limited, London, England. 446 p.

FAGERLUND, U. H. M. 1967. Plasma cortisol concentration in relation to stress in adult sockeye salmon during the freshwater stage of their life cycle. Gen. Comp. Endocrinol. 8: 197–207.

FAGERLUND, U. H. M., AND E. M. DONALDSON. 1969. The effect of androgens on the distribution and secretion of cortisol in gonadectomized male sockeye salmon (*Oncorhynchus nerka*). Gen. Comp. Endocrinol. 12: 438–448.

FAGERLUND, U. H. M., J. R. MCBRIDE, AND E. M. DONALDSON. 1968. Effects of metopirone on pituitary–interrenal function in two teleosts, sockeye salmon (*Oncorhynchus nerka*) and rainbow trout (*Salmo gairdneri*). J. Fish. Res. Bd. Canada 25: 1465–1474.

HANE, S., AND O. H. ROBERTSON. 1959. Changes in plasma 17-hydroxycorticosteroids accompanying sexual maturation and spawning of the Pacific salmon (*Oncorhynchus tshawytscha*) and rainbow trout (*Salmo gairdneri*). Proc. Natl. Acad. Sci. 45: 886–893.

HANE, S., O. H. ROBERTSON, B. C. WEXLER, AND M. A. KRUPP. 1966. Adrenocortical response to stress and ACTH in Pacific salmon (*Oncorhynchus tshawytscha*) and steelhead trout (*Salmo gairdnerii*) at successive stages in the sexual cycle. Endocrinology 78: 791–800.

HANKE, W., K. BERGERHOFF, AND D. K. O. CHAN. 1967. Histological observations on pituitary ACTH cells, adrenal cortex, and the corpuscles of Stannius of the European eel (*Anguilla anguilla* L.). Gen. Comp. Endocrinol. 9: 64–75.

IDLER, D. R., A. P. RONALD, AND P. J. SCHMIDT. 1959. Biochemical studies on sockeye salmon during spawning migration. VII. Steroid hormones in plasma. Canadian J. Biochem. Physiol. 37: 1227–1238.

IDLER, D. R., AND B. TRUSCOTT (with the collaboration of H. C. Freeman, V. Chang, P. J. Schmidt, and A. P. Ronald). 1963. *In vivo* metabolism of steroid hormones by sockeye salmon. A. Impaired hormone clearance in mature and spawned Pacific salmon (*O. nerka*). B. Precursors of 11-ketotestosterone. Canadian J. Biochem. Biophys. 41: 875–887.

KITAY, J. I., M. D. COYNE, R. NELSON, AND W. NEWSOM. 1966. Relation of the testis to adrenal enzyme activity and adrenal corticosterone production in the rat. Endocrinology 78: 1061–1066.

KITAY, J. I., M. D. COYNE, W. NEWSOM, AND R. NELSON. 1965. Relation of the ovary to adrenal corticosterone production and adrenal enzyme activity in the rat. Endocrinology 77: 902–908.

MACCONAILL, M. A. 1947. Staining of the central nervous system with lead-hematoxylin. J. Anat. 81: 371–372.

MATTHEIJ, J. A. M. 1968. The ACTH cells in the adenohypophysis of the Mexican cave fish *Anoptichthys jordani*, as identified by metopirone (SU 4885) treatment. Z. Zellforsch. Mikroskop. Anat. Abt. Histochem. 92: 588–595.

MCBRIDE, J. R. 1967. Effects of feeding on the thyroid, kidney, and pancreas in sexually ripening adult sockeye salmon (*Oncorhynchus nerka*). J. Fish. Res. Bd. Canada 24: 67–76.

MCBRIDE, J. R., U. H. M. FAGERLUND, M. SMITH, AND N. TOMLINSON. 1963. Resumption of feeding by and survival of adult sockeye salmon (*Oncorhynchus nerka*) following advanced gonad development. J. Fish. Res. Bd. Canada 20: 95–100.

MCKEOWN, B. A., AND A. P. VAN OVERBEEKE. 1969. Immunohistochemical localization of ACTH and prolactin in the pituitary gland of adult migratory sockeye salmon (*Oncorhynchus nerka*). J. Fish. Res. Bd. Canada 26: 1837–1846.

VAN OVERBEEKE, A. P., AND J. R. MCBRIDE. 1967. The pituitary gland of the sockeye (*Oncorhynchus nerka*) during sexual maturation and spawning. J. Fish. Res. Bd. Canada 24: 1791–1810.

ROBERTSON, O. H., M. A. KRUPP, C. B. FAVOUR, S. HANE, AND S. F. THOMAS. 1961a. Physiological changes occurring in the blood of the Pacific salmon (*Oncorhynchus tshawytscha*) accompanying sexual maturation and spawning. Endocrinology 68: 733–746.

ROBERTSON, O. H., M. A. KRUPP, S. F. THOMAS, C. B. FAVOUR, S. HANE, AND B. C. WEXLER. 1961b. Hyperadrenocorticism in spawning migratory and non-migratory rainbow trout (*Salmo gairdnerii*): Comparison with Pacific salmon (Genus *Oncorhynchus*). Gen. Comp. Endocrinol. 1: 473–484.

ROBERTSON, O. H., AND B. WEXLER. 1957. Pituitary degeneration and adrenal tissue hyperplasia in spawning Pacific salmon. Science 125: 1295–1296.

1959. Hyperplasia of the adrenal cortical tissue in Pacific salmon (Genus *Oncorhynchus*) and rainbow trout (*Salmo gairdnerii*) accompanying sexual maturation and spawning. Endocrinology 65: 225–238.

SCHMIDT, P. J., AND D. R. IDLER. 1962. Steroid hormones in the plasma of salmon at various states of maturation. Gen. Comp. Endocrinol. 2: 204–214.

WALLACE, E. Z., H. J. SILVERBERG, AND A. C. CARTER. 1957. Effect of ethinyl estradiol on plasma 17-hydroxycorticosteroids, ACTH responsiveness and hydrocortisone clearance in man. Proc. Soc. Exptl. Biol. Med. 95: 805–808.

Revision of the Genus *Salmincola* Wilson, 1915 (Copepoda: Lernaeopodidae)

Z. KABATA

Fisheries Research Board of Canada
Biological Station, Nanaimo, B.C.

KABATA, Z. 1969. Revision of the genus *Salmincola* Wilson, 1915 (Copepoda: Lernaeopodidae). J. Fish. Res. Bd. Canada 26: 2987–3041.

The morphology of the genus *Salmincola* is reviewed and its relationship to the genus *Achtheres* examined. Four species of *Achtheres* are transferred to *Salmincola*: *A. coregonorum*, *A. extensus*, *A. strigatus*, and *A. corpulentus*. The taxonomy of the genus is based on new and more reliable criteria, mainly on the details of the appendages. The structure of the second antenna and of the maxilliped, as well as the type of the bulla, are regarded as best recognition marks. All species of *Salmincola* are redescribed with these criteria in mind and the genus is recognized as having 15 species. A key to the species is given.

The genus is divided into two subgenera. Subgenus *Salmincola* (*Salmincola*) is parasitic mainly on Salmonidae and is distinguished by the well-developed claw of the maxilliped. Subgenus *Salmincola* (*Brevibrachia*) is parasitic exclusively on Coregonidae and is distinguished by the vestigial claw of the maxilliped.

Species of *Salmincola* fall into one of three categories: circumpolar, continental, and bicontinental. The first category comprises five species: *S. carpionis*, *S. edwardsii* (parasites of *Salvelinus*), *S. thymalli* (parasite of *Thymallus*), *S. extensus*, and *S. extumescens* (parasites of the coregonids). The continental species are subdivided into Palearctic and Nearctic. There are seven Palearctic species: *S. coregonorum*, *S. stellatus*, *S. lotae*, *S. cottidarum*, *S. nordmanni*, *S. strigatus*, and *S. jaculicus*. Only one Nearctic species is known, *S. siscowet*. Two species are bicontinental: *S. salmoneus* has a distribution straddling the Atlantic Ocean and *S. californiensis* is a Pacific species, found in North America and Asia.

Received July 18, 1969

INTRODUCTION

IT IS IMPORTANT to know the identity of the investigated animal. Unfortunately, when one deals with the parasitic copepods, this basic prerequisite is not always fulfilled. Many species of these parasites have been vaguely known for about a century and a half, without being adequately described. Early biologists had neither the technical means nor sufficiently precise knowledge of morphology to determine accurately the taxonomic status of the parasites they described. More recent workers seldom have the time or opportunity to unravel the skein of taxonomic intricacies, sometimes very tangled.

Prior to the investigation of the biology of *Salmincola* and its effects on the host, I thought it prudent to reexamine the status of the species within the genus. It soon became obvious that the taxonomy of *Salmincola* is in a deplorable condition. A thorough review seemed advisable. This paper is an attempt at such a revision.

Printed in Canada (J1530)

In view of the inadequate quality of the earlier work, I attempted to reexamine and redescribe each species of *Salmincola* from specimens. Whenever possible, the type material was examined. The original descriptions were always consulted, but I did not rely upon them or upon any subsequent descriptions for the fine structural details. Specimens of only two species were unobtainable. In their case little could be done except to leave them as they were originally defined and reserve judgment on their validity.

Examination of all available species involved the study of both entire specimens and their dissected appendages. The methods used were the same as those outlined in an earlier work (Kabata, 1968). To avoid repetitions, the morphology of *Salmincola* is discussed in general terms before the individual species are described. The type species, *S. salmoneus* (L.), is dealt with more fully, the descriptions of others being concentrated more on differences between them and *S. salmoneus*. Each description is followed by a brief discussion. In one instance only, three species are discussed together.

After the key to the species of *Salmincola* a brief account of the host affinities and distribution of various species is presented.

COMMENTS ON THE GENUS *SALMINCOLA*

Lernaeopodid copepods parasitic on freshwater fishes were known before the time of Linnaeus. The first description of a lernaeopodid was that by Gissler (1751), who gave a brief account and several rough drawings of a "lax lusen" (salmon louse), known today as *Salmincola salmoneus* (L.). It is the type species of its genus. Linnaeus (1758) gave it its specific name and placed it in the genus *Lernaea*. Blainville (1822) transferred it to *Lernaeopoda*. There it remained until Wilson (1915) established the genus *Salmincola* for the freshwater species of *Lernaeopoda*.

Nordmann (1832) described two more closely related genera of freshwater lernaeopodids. They are *Achtheres*, with the type species *A. percarum* Nordmann, 1832, and *Basanistes*, with the type species *B. huchonis* (Schrank, 1786). At that time all the other species were still in Blainville's *Lernaeopoda* and played no part in the taxonomic considerations of either *Achtheres* or *Basanistes*. The differences between these two genera are quite clear. *Basanistes* is distinguished by prominent protuberances on the cephalothorax and trunk of its various species, protuberances that are absent from *Achtheres*. Similar differences exist between *Basanistes* and *Salmincola*, the latter also being devoid of conspicuous swellings. These general differences, however, proved insufficient to prevent some confusion. For example, *Basanistes salmonea* Milne Edwards, 1840, was eventually identified as *Salmincola edwardsii* (Olsson, 1869) and *Basanistes coregoni* Neresheimer, 1909, was later transferred, incorrectly, to the genus *Achtheres*, although it clearly belongs to *Salmincola*.

Since *Achtheres* and *Lernaeopoda* (later *Salmincola*) could not be told apart by these gross morphological features, the confusion between them was much greater. Wilson's (1915) definitions of *Salmincola* and *Achtheres* did little to eliminate the difficulties. His attempt to introduce into generic diagnoses

the characteristic features of the appendages proved to be of limited value because of the contemporary lack of knowledge of these appendages.

One of the features to which considerable importance was attached, and which is still being mentioned as a good discriminant between *Achtheres* and *Salmincola*, is the presence or absence of the external segmentation of the trunk. According to Wilson (1915), the trunk of *Achtheres* is more or less clearly segmented, particularly on its ventral surface, whereas *Salmincola* shows no traces of trunk segmentation. Nordmann (1832) also suggested that *Achtheres* can be distinguished by its segmented trunk. The lernaeopodid trunk consists of four segments. Longitudinal muscles, both dorsal and ventral, run the entire length of the trunk, breaking into four parts and inserting into the lower surface of the cuticle at positions corresponding with the old segmental boundaries. When contracted, these muscles buckle the cuticle between the points of insertion and produce transverse grooves coinciding with the vanished boundaries. Relaxation of trunk musculature causes disappearance of these markings. Thus, in the past, many specimens were classified as *Achtheres* or *Salmincola* in accordance with the condition of their trunk musculature at the moment of fixation. Another character that caused a lot of misunderstanding and confusion was the abdomen, the part of the posterior end of the trunk mentioned by Wilson (1915) as present in *Achtheres*. In some of his drawings Wilson showed this part clearly delimited from the rest of the trunk by a sharp border. It is unfortunate that Wilson's methods of illustration included the drawing of firm dividing lines, where no such lines existed in the specimens. I have been unable to find any division marking off the posterior part of the trunk in *Achtheres* as a definite abdomen. Indeed, no known lernaeopodid genus can be said to have any trace of abdomen, save perhaps a slight elevation of the perianal area. As regards the genital process, which was also considered as being characteristic of *Salmincola* and absent in *Achtheres*, it is now known to disappear with age and, therefore, cannot safely be used for taxonomic purposes.

It is clear from the foregoing that a revision of *Salmincola* must include also a reexamination of *Achtheres* and must draw a definite border between these two genera. In the course of this work I have found that the two genera are well distinguished by the differences summarized below.

Salmincola	*Achtheres*
Posterior extremity of trunk rounded, not protruding far beyond points of attachment of egg sacs.	Posterior extremity of trunk conical or pointed, protruding well beyond points of attachment of egg sacs.
First antenna usually with obscure segmentation and with apical armament usually damaged or absent, seldom intact.	First antenna distinctly three-segmented, apical armament usually intact.
Upper lip roughly triangular, with unarmed margins.	Upper lip armed on the tip with many setules, though sometimes short and very fine.

Salmincola	*Achtheres*
Mandible armed with primary teeth only.	Mandibular teeth include one secondary tooth, second from the tip.
First maxilla with greatly reduced exopod (often a mere spinule).	First maxilla with well-developed exopod, equipped with two spines.
Subchela of maxilliped with poorly developed armature, often with reduced claw, seldom with spinulation. Palp usually well developed.	Subchela of maxilliped with well-developed armature and claw. Palp reduced to a single spine, accompanied by a slightly inflated spinulated pad.

One could add to the above differences also the genital process, already mentioned as being a feature of *Salmincola*, as well as the fact that in *Achtheres* the prominent second antennae are usually folded across the anterior margin of the cephalothorax, whereas in *Salmincola* they point outwards. Neither feature, however, is invariable. The genital process is completely absent in older individuals of *Salmincola*. *Achtheres* is found, however rarely, with its second antennae pointing straight up from their bases. Consequently, these features should not be used as a basis for discrimination. The list of differences given above suffices, in any case, for this discrimination to be quite clear. On their basis, the definition of *Salmincola* can now be amended as follows:

Lernaeopodidae — Body divided into cephalothorax and trunk. Cephalothorax short, inclined ventrally to long axis of trunk. No posterior processes or abdomen. Genital process sometimes present. Posterior extremity of trunk evenly rounded, not protruding far beyond points of attachment of egg sacs. First antennae peglike, short, usually with obscure segmentation. Dentiferous margin of mandible armed with primary teeth diminishing in size towards the base of appendage. Tip of upper lip unarmed. First maxilla with three papillae and greatly reduced exopod. Second maxilla fused only at tip, where it is attached to bulla of various shapes. Maxilliped well developed but with tendency towards reduction of armature of subchela. Claw sometimes greatly reduced. Palp usually well developed.

Application of this new definition to the species now in the genus *Achtheres* and their comparison with the type species of that genus shows that four of them belong properly to *Salmincola*. In this category are *Achtheres coregonorum* (Kessler, 1868), *Achtheres extensus* (Kessler, 1868), *Achtheres corpulentus* Kellicott, 1882,[1] and *Achtheres strigatus* Markevich, 1936. Left in the genus *Achtheres* are: *A. percarum* Nordmann, 1832 (type), *A. ambloplitis* Kellicott, 1880, *A. lacae* Krøyer, 1863, *A. micropteri* Wright, 1882, and *A. pimelodi* Krøyer, 1863. This regrouping of *Salmincola* and *Achtheres* on purely morphological grounds draws also a neat dividing line between species with radically different host affiliations. The species now included in *Salmincola* parasitize fishes belonging to Salmonidae and related families (with the exception of two species only). The five species of *Achtheres* have hosts of different orders, being parasitic on the percoid and siluroid fishes.

The confusion surrounding the taxonomy of *Salmincola* did not spare its generic name. In the frequent changes of generic status the older species

[1]More will be said about this species in the discussion of *Salmincola extumescens*, p. 3014.

of the genus acquired a long and involved history, reflected in their synonymies. One of the consequences of this confusion was the recent proposal (Yamaguti, 1963) that the name *Salmincola* be abandoned in favour of Lamarck's (1816) *Entomoda*. The proposal is untenable and I wish to deal with it at some length to prevent any further confusion, which an unnecessary change of the generic name would create.

As constituted originally, the genus *Entomoda* Lamarck, 1816, consisted of four species, listed in the following order: *E. salmonea*, *E. cornuta*, *E. gobina*, and *E. radiata*. Yamaguti (1963) contends that by mentioning *E. salmonea* (= *Salmincola salmoneus*) as the first of these species, Lamarck implied its position as the type species of *Entomoda*. According to the rules of zoological nomenclature (Stoll et al., 1961), Article 67, the fact of being mentioned first in the list does not constitute a designation as the type species. In the case of *Entomoda* a subsequent designation of type species was validly made, in accordance with the Article 69 of these rules, by Fowler (1913, p. 475). In his synonymy of the genus *Chondracanthus*, Fowler states the following: "*Entomoda* Lamarck, An. San. Verteb., III, 1818, p. 68. Type *Lernaea cornuta* Müller, second species." The species so designated is a chondracanthid, now in the genus *Acanthochondria*. Neither *Salmincola* nor any other lernaeopodid can, therefore, be included in *Entomoda*, if the old name is to be retained at all. The name *Salmincola* is valid.

Having redefined the genus *Salmincola* and redrawn its limits where they lacked clarity, I propose now to deal with intrageneric divisions and the criteria on which they should be based. All past descriptions of *Salmincola* species disregarded the existence of individual morphological variations. No account was taken of the possible influences exerted on the morphology by factors such as differences in the host species or in the location on the host. The fact that the morphology might vary to some extent from one part to another of the distribution range of the species was never considered in relation to *Salmincola*. All these omissions added considerably to difficulties in understanding valid interspecific differences in the genus.

The characters used as specific discriminants fall into two categories: gross morphological features such as configuration or proportions of the body and finer features, the structural details of the appendages. The former were commonly used in the past and are responsible for much of the current taxonomic difficulties. Most of them are greatly variable. Some, as already mentioned in connection with the segmentation of the trunk, depend on the condition of the musculature at the time of fixation. For example, the length of the so-called "arms," the second maxillae, is directly dependent on the degree of contraction of their longitudinal muscles. The same applies in part to the shape of the trunk, which, in addition, can be greatly affected by several other factors. In the genus *Salmincola* there is only one species that can be said to have distinctive shape of the trunk. This species is *S. nordmanni* (Kessler, 1868), which has each lateral margin of the trunk equipped with three permanent swellings.

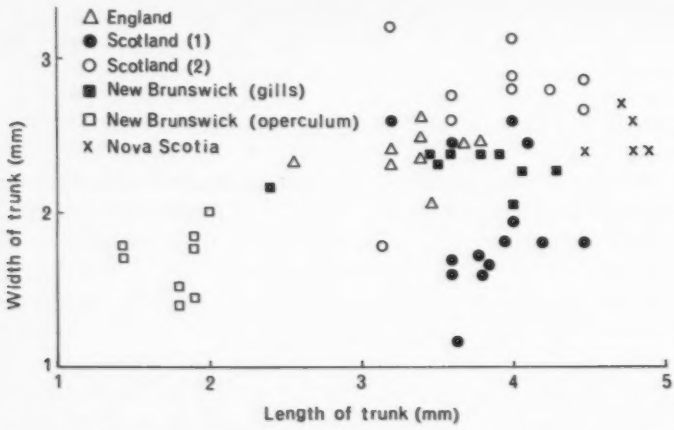

FIG. 1. Proportions of trunk of *Salmincola salmoneus* from different samples.

A modest illustration of these variations is shown in Fig. 1, where the length of the trunk of *S. salmoneus* is plotted against its width. Samples of the parasite come from various localities, some quite far apart. The trunks of specimens from the sample Scotland (1) are much more slender than those of specimens from the sample Scotland (2), both collected in rivers of northeast Scotland. The sample from England (south of England, river Exe) contains specimens with trunks of intermediate proportions. Striking differences are evident between the specimens collected in the sample from New Brunswick (operculum) and the sample from Nova Scotia. The New Brunswick specimens are small and very squat, their trunks about as long as they are broad. The effect these differences have on the general appearance of the parasite is shown in Fig. 2–4. The small specimen from the New Brunswick smolt (Fig. 3) looks sufficiently different from the specimen shown in Fig. 2 to tempt its identification as a different species. The morphology of their appendages, however, leaves no room for doubt. They are both *S. salmoneus*, living on the same host fish, *Salmo salar*, in different localities and attached to different parts of the fish. The particularly large bulla of the specimen in Fig. 3 is probably due to its attachment to the inner surface of the operculum, a site less accommodating than the soft tissues of the gill filaments.

Another characteristic commonly used in the past as a specific discriminant is the shape of the cephalothorax in its dorsal aspect. Here, too, the differences between the individual specimens are great. In using this feature as a possible clue to the identity of the specimen, one should consider the *type* rather than the exact *shape*. For example, Fig. 6 differs in shape from Fig. 7, though both represent the same type of cephalothorax and both are distinguishable from Fig. 32, 45, and 46 that show the outline of the cephalothorax of *S. carpionis*. The range of variations of this character is shown in Fig. 68–71, representing outlines of cephalothoraces of some specimens of *S. californiensis*, and by Fig.

171–173 showing *S. edwardsii*. Like that of the trunk, the shape of the cephalothorax is moulded by contractions of the many strong muscles, which operate the antennae and mouth parts and which insert at various points on the inner surface of its dorsal wall. Superimposed on the inherent individual variations, these influences can introduce many considerable differences in shape.

It is clearly safer to base the diagnosis of the species on characteristics that are more constant. Although such features as the proportions of the trunk and the outline of the cephalothorax might provide useful corroborating evidence, it is the structure of the appendages on which the diagnosis should depend.

The examination of the appendages is not without its difficulties. Most investigators were satisfied with observing and drawing them in situ. Since only infrequently the same appendage was observed twice from the same angle, no clear idea has emerged of the structure of individual appendages. Consequently, we have no basis for a comparative study of the appendages. For example, a superficial look at Fig. 179 and Fig. 18 makes one think they represent very different structures, whereas in fact they show different views of quite similar structures, both being second antennae. The appendages are very small and it is difficult to dissect and prepare them for observation without causing damage. Handling results in the appearance of spurious features that have not always been recognized. It must also be remembered that the appendages, in addition to showing individual variations, might also differ in specimens from different geographical areas and can be affected by the position of the parasite on its host. They also might be, and often are, abnormally developed. At least one species of *Salmincola* (*S. bicauliculata*, p. 3006) was based on an abnormality. The appendages are subject to wear with age. They sustain minor injuries capable of affecting their appearance. Appreciation of all these influences on the structure of the appendages can be gained only through careful study of a long series of specimens.

I will now discuss the structure and relative merits of various appendages as diagnostic features.

The first antenna — The diagnosis of many species of *Salmincola* makes use of the first antenna as a characteristic feature. It is described as short and peglike, either with obscure segmentation or consisting of two, sometimes three, segments. Its apical armature is referred to as absent or comprising two to several setae. For anybody trying to identify *Salmincola*, these descriptions are of little help. I have established that specimens of the same species differ in the structure of their first antenna to the point where this appendage loses its value as a diagnostic feature. Unless the specimen is quite young (preferably before the ovigerous stage), the first antenna is usually badly worn at the tip. Its segmentation is seldom clear, sometimes the same specimen having first antennae that appear to consist of different numbers of segments. Similarly, the apical armature might differ in the number of its components.

The intact first antenna of the type species (Fig. 15 and 16) is described here to show the structure that is probably the same throughout the genus.

I do not recommend its use for taxonomic purposes and will refrain from mentioning it in subsequent descriptions. The segmentation of the appendage is obscure, its basal part slightly inflated. On the dorsomedial wall of the basal part there is a small tubercular outgrowth, homologous with a larger seta carried at this place by the first antennae of other lernaeopodid genera. The tubercle is usually difficult to detect, though it is invariably present. The apex of the first antenna is crowned by six processes, typical in position and appearance. They, too, have their homologues in other lernaeopodid genera. In Fig. 16 these processes are numbered in accordance with the practice adopted in my earlier publications on Lernaeopodidae (Kabata, 1963, 1964). The most prominent is seta 4 on the medial side of the apex. It is long, blunt, and robust. In the centre is seta 5, which in most lernaeopodids splits at the base into two unequal branches but in *Salmincola* shows no such division. Seta 6 is in a lateral position. It is the longest and most slender element of the apical armature, in *Salmincola* being rather less elongated than in other genera. The remaining three structures were described as "tubercles" in other Lernaeopodidae, though in *Salmincola* they are too long to fit this name. Tubercle 1 is present at the base of seta 4, whereas tubercle 2 is associated usually with the base of seta 5. Tubercle 3 is normally at some distance from the base of seta 6. In most of the specimens examined, not more than three or four of these processes could be found, those most commonly present being setae 4 and 5. Stubs of setae were often present. By analogy with most genera of Lernaeopodidae (with some notable exceptions), I expect most species of *Salmincola* to have a very similar armature of the first antenna, when undamaged. Why the tip of the first antenna should be so extensively and commonly damaged in *Salmincola*, whereas in the closely related *Achtheres* it is seldom found in disarray, is a question still to be answered.

The second antenna — Although this appendage, the most misrepresented one of *Salmincola*, is relatively large, it is also very mobile and might become fixed in widely differing attitudes. Its general appearance is thereby greatly affected.

The second antenna is attached to the anterolateral corner of the cephalothorax. Its base is oval in cross section, with the long diameter in the dorsoventral plane. The base of the antenna is hinged so that it is capable of being swung inwards to meet its opposite member near the center of the anterior margin of the head. It is seldom, however, that one sees in it this position. The sympod consists of two segments, though one can seldom see the segmentation very clearly. The distal segment of the sympod (Fig. 18) has on its lateral wall a spiny pad, often raised above the surface. This elevation is sometimes pronounced, though it varies from species to species and from specimen to specimen. A good example of it is shown in Fig. 179. The distal segment of the sympod is followed by two rami: the exopod and the endopod. The exopod is one-segmented. Its tip (Fig. 19) and part of its dorsal wall are covered with crowded small spines in some species, though in others they might be bare. On the lateral part of the tip are two structures referred to as "papillae,"

though in some species they appear more as spines. Their true nature is uncertain. The exopod is roughly bulbous and its shape varies to some extent from one specimen to another. It appears to be capable of some rotation and movement in relation to the sympod; it certainly has musculature that might be capable of producing such movements. The endopod is two-segmented. The proximal segment is short and cylindrical and carries a spiny pad resembling that of the distal segment of the sympod. The pad is ventral but can be displaced by rotation of the sympod or by the pressure of a coverslip. The distal segment (Fig. 20–22) is quite complicated. It also is capable of rotation and other movements, which add to the difficulty of the observer. Dissection and separate mounting are often necessary to display its structure in full. When the second antenna is in situ, the distal segment of its endopod is often turned so as to face in lateral direction, as shown in Fig. 18. It appears in this position in the close-up in Fig. 20. Some difficulties might be experienced in trying to relate this view to the lateral aspect of the same segment (Fig. 21 and 22). The most dominant part of the segment's armature in most species is a hook (1), which arises from the dorsal side of the tip and curves ventrally, often projecting beyond the ventral wall. On the medial side of its base is a short but robust spine (2) and on its lateral side a tubercular swelling (3). The prominence of this tubercle varies from species to species and often within the species. In *S. salmoneus* it is usually quite noticeable. On the ventrolateral side of the swelling is the opening of a duct, often projecting in a nipple-like fashion. The duct itself can be traced in some specimens for some distance through the segment. The ventral side of the segment differs from species to species. In all instances, however, it carries a prominent process (4) from the lateral side of which arises another and smaller one, process 5. The relative sizes and positions of these processes provide the most useful taxonomic evidence. The identification of *Salmincola* cannot be made definite without examination of the endopod of the second antenna.

The mandible and first maxilla — The mandible cannot be used as a safe diagnostic feature. Although some small differences between species can be found, the detection of these differences calls for considerable familiarity with the genus. The same is largely true for the first maxilla. Only one species, *S. lotae*, has a maxilla that distinguishes it from its congeners. Both mandible and first maxilla should be examined, however, to provide supporting evidence for identification.

The second maxilla and the bulla — Often referred to as an "arm," the second maxilla has no value as a diagnostic feature. The bulla, the attachment organ, on the other hand, provides a lot of useful information on the identity of the species. It must be stressed again that it is the *type*, not the precise *shape* of the bulla that is taxonomically useful. Several types of bulla occur in the genus, sometimes more than one species having bullae of the same type. The representative types of bulla are illustrated in Fig. 8 and 9 (*S. salmoneus*), 33 (*S. carpionis*), 93 (*S. thymalli*), 117 (*S. extensus*), 149 (*S. extumescens*), 174 (*S. edwardsii*), 199 (*S. coregonorum*), and 239 (*S. stellatus*).

The maxilliped — The *Salmincola* maxilliped is similar to that of other lernaeopodid genera. It consists of a main body of uncertain segmentation and a terminal subchela, opposable against the medial margin of the body (Fig. 24). The fine structural details of the maxilliped make it, besides the second antenna, another excellent appendage for identification of the species. The characteristic features are grouped at the tip of the subchela and at the midlength of the medial margin, where the maxilliped palp is attached. The type of the palp provides a very good distinguishing feature for most species, in spite of its considerable variability within each species. The tip of the subchela and the nature of the terminal claw also serve as good identifying characters. The genus divides into two groups, according to the size of the claw. In view of other differences, fairly consistently distinguishing the species with the large claw from those with the reduced claw, it appeared useful to subdivide the genus into two subgenera, *Salmincola* (*Salmincola*) and *Salmincola* (*Brevibrachia*).

DESCRIPTIONS OF SPECIES

Subgenus ***Salmincola*** (***Salmincola***) subgen.n.

The species of this subgenus are equipped with well-developed claws at the tips of their maxillipeds. The ventral regions of the endopods of their second antennae have only one spiny pad, on the basal segment. No spinulation occurs on the distal segment of that ramus. In addition to the salmonid fishes, the members of this genus occur also on *Thymallus* and its allies, as well as on fishes completely unrelated to the salmonoids (Gadidae and Cottidae).

Salmincola salmoneus (L.)

(Fig. 2–30)

Synonyms — Lax-lusen Gissler, 1751; *Lernaea salmonea* L., 1758; *Schisturus salmoneus* (L.); Oken, 1816; *Entomoda salmonea* (L.); Lamarck, 1816; *Lernaeopoda salmonea* (L.); Blainville, 1822; *Salmincola salmonea* (L.); Wilson, 1915; *Salmincola gordoni* Gurney, 1933.

Material examined — (1) numerous females, *Salmo salar*, gills, northeast Scotland, 1963; (2) 10 females, same host and locality, 1964; (3) 8 females, same host, river Exe, England, 1965; (4) 12 females, same host, gills, off Cape Breton Island, Nova Scotia, 1956; (5) 8 females, same host, gills (adult), Salmon River, New Brunswick, 1966; (6) 9 females, same host (smolt), gills and operculum, same locality, 1966; (7) 10 females, same host, Tay estuary, Scotland, 1937, USNM 85513; (8) 2 females, same host, Cornwall, undated, USNM 74354; (9) 5 females, same host, gills, England, undated, USNM 39608; (10) 3 females, same host, gills, Banffshire, Scotland, 1884, USNM 8339 (part of Canon Norman's collection); (11) 2 females, "sea trout," gills, Isle of Man, 1965; (labelled as *S. gordoni*) (12) 2 females, trout and grayling, gills and gill chamber, River Rye, Yorkshire, England, 1933 (Gurney's paratypes).

Description of the female — Variations in the general appearance of *S. salmoneus* are illustrated in Fig. 2–4, and in the outline of its cephalothorax in Fig. 6 and 7. In young specimens, the posterior extremity of the trunk (Fig. 10) carries a genital process (*gp*), which is usually delimited from the trunk by a marked circular line (Fig. 11 and 12). Some specimens are found to carry parts of spermatophores (Fig. 12, *sp*) still protruding from the end of the genital process.

The second antenna (Fig. 18–22) is distinguished by the nature of the ventral processes of the endopod's distal segment. Process 4 is conical, smooth, and usually protrudes ventrally. The smaller process 5 most commonly arises from the lateral wall of process 4. The nipple of

the duct orifice on tubercle 3 is quite prominent and usually easy to observe (Fig. 21 and 22). The exopod (Fig. 19) has a part of its tip covered by small, though densely packed, denticles much smaller than the two papillae (Fig. 19, *x*).

The mandible (Fig. 17) has seven teeth of roughly the same shape and gradually diminishing in size towards the base of the appendage.

The first maxilla (Fig. 23) is distinguished by the fairly long papillae and their setae. The ventral papilla is slightly shorter than the other two. The exopod is present halfway down on the lateral wall of the appendage. It is in the shape of a setule, mounted on a small swelling protruding from the wall.

The second maxilla (Fig. 2–4) usually expands only slightly at its tip, where it is linked with the manubrium of the bulla (Fig. 8 and 9). The bulla is very typical of the species. Its upper surface, i.e., the surface that is not attached to the host (Fig. 9), appears almost oviform in outline, its wide end somewhat flattened or even slightly concave. The manubrium is short and arises near the wider end of the bulla. The upper surface is slightly convex and passes imperceptibly into the manubrium. Seen in lateral view (Fig. 8), the lower surface, i.e., the one applied to the tissues of the host, is flat or even concave. The bulla adheres to the surface of the host's epithelium and does not embed in it deeply. A thin epithelial film covers its outer surface.

The maxilliped (Fig. 24–30) is distinguished by its palp. The claw of the subchela (Fig. 25) is strong and well developed. At its base, the tip of the subchela carries also a small tubercular papilla (Fig. 25, *aux*). This is the structure that in other lernaeopodids often has a spinelike character and has been referred to as the "auxiliary spine." The subchela also carries a ventral setule some distance from its junction with the body of the appendage (Fig. 24, *a*). The palp (*p*) of young specimens appears as shown in Fig. 26. It is quite prominent and bears at its tip three structures. The largest of them is a central tubercle (2), often tapering and with a finely pointed tip. (In Fig. 26 this structure is tilted away from the observer and appears smaller than it is.) On the ventral side of tubercle 2 is another and usually smaller tubercle (1), whereas on its dorsal side is a small and slender protuberance (3), sometimes with an inflated base. This protuberance is often missing. Figures 27 and 28 show two views of the same palp from an older specimen. In these older specimens the tip of the palp is often worn and damaged. Figure 29 shows a palp in which tubercle 1 is much reduced. In Fig. 30 only tubercle 2 remains at the tip of the palp, the other two structures presumably having been worn away. The entire maxilliped varies in size from one specimen to another, commonly extending nearly to the level of the anterior margin of the cephalothorax (Fig. 5).

In view of their variability, the sizes of the specimens will be largely disregarded. To obtain a rough idea of the general size of the species, the trunk length will be quoted in all subsequent descriptions. The trunk length of the examined specimens of *S. salmoneus* varied from 1.48 to 4.88 mm.

Comments — As the oldest species of its genus, *S. salmoneus* has undergone many changes in its generic status. The history of the species is, however, almost free of complications at the species level. The synonymy of *S. salmoneus* includes only one other species name, *S. gordoni* Gurney, 1933. The specimens on which Gurney (1933) based this species lived on hosts other than *Salmo salar*, the common host of *S. salmoneus*. This fact in itself could be sufficient to account for the slight difference between them and the parasites of the salmon. The only difference was the "very much larger" cephalothorax of *S. gordoni*. The comparison of Gurney's drawing of *S. salmoneus* (Gurney, 1933, fig. 1984, p. 349) with that of *S. gordoni* (Gurney, 1933, fig. 2010, p. 358) is at variance with this statement. The relative sizes of the cephalothoraces in these specimens certainly do not warrant separation in different taxa. Gurney's fig. 2012 (1933, p. 358) can be compared with Fig. 5 of this review. The differences are well within the range of variability of the species. Gurney stated: "The two species are, however,

very close in other respects and it is possible that this species should be regarded as a subspecies, or even as the parent form, of *S. salmonea*." It is not clear what Gurney meant by "parent form," but certainly no justification can be found for the continued existence of *S. gordoni*. I propose, therefore, that it be relegated to synonymy with *S. salmoneus*.

Salmincola carpionis (Krøyer, 1837)

(Fig. 31–52)

Synonyms — *Lernaeopoda carpionis* Krøyer, 1837; *Lernaeopoda gibber* Wilson, 1908; *Salmincola gibber* (Wilson, 1908); Wilson, 1915; *Salmincola salvelini* Richardson, 1938; *Salmincola smirnovi* Markevich, 1940.

Material examined — (labelled as *S. carpionis*) (1) 3 females, host unknown, Iceland, undated collections of Copenhagen University; (2) 5 females, host unknown, Greenland, undated, collections of Copenhagen University (both these samples constitute a part of Krøyer's type material); (3) 8 females, *Salmo carpio* (= *Salvelinus alpinus*), gills, undated, collections of Copenhagen University; (4) 4 females, migratory char, Hrutafjordara, Iceland, 1947, USNM 85514; (labelled as *S. siscowet*) (5) 3 females, *Salvelinus alipes* (= *S. alpinus alipes*), Etah, Greenland, 1913–1917, USNM 49767; (labelled as *S. oquassa*) (6) 12 females, *Salvelinus malma*, Alitak Bay, Alaska, 1903, USNM 56633; (labelled as *S. gibber*) (7) numerous females, same host, Attu, Alaska, 1906, USNM 38583 (this sample was part of the type material of *S. gibber*); (8) 3 females, same host, gills, Bering Is., 1885, USNM 13686; (9) 6 females, same host and locality, USNM 38591; (10) 10 females, *Salvelinus alpinus alipes*, roof of mouth and tongue, Cairn Lake, Baffin Land, 1922, USNM 56552; (11) 12 females, same host and habitat, Kanochickolak Lake, Baffin Land, 1922, USNM 56553; (labelled as *S. smirnovi*) (12) 5 females, *Salvelinus taimyricus*, mouth, Lake Taimyr, USSR, 1948; collection of Zoological Institute, Leningrad; (13) 5 females, *S. leucomaenis*, mouth, South Sakhalin, 1949, collection of Zoological Institute, Leningrad; (labelled as *S. salvelini*) (14) 2 females, *S. fontinalis*, mouth, Gaspé, Quebec (part of type material of *S. salvelini*, collection of Dr L. R. Richardson).

Description of the female — In its general appearance (Fig. 31, 43, 44) this species bears some resemblance to *S. salmoneus*. The main difference between them is the presence in *S. carpionis* of a necklike, narrow part of the trunk, where it links with the cephalothorax. This necklike impression is very seldom encountered in *S. salmoneus*. Another difference between these two species is the outline of the cephalothorax. In *S. carpionis* it is roughly oviform (Fig. 32, 45, 46), usually with slightly flattened wider end. This type of cephalothorax outline does not occur in *S. salmoneus*.

The second antenna (Fig. 35–38, 47, 48) has few and large spines on the spiny pad of the sympod (Fig. 37) and of the basal segment of the endopod. All the salient features of the endopod structure are essentially the same as in *S. salmoneus*. The only possible difference is in the greater swelling of the ventral region, from which the ventral processes 4 and 5 appear to arise separately (Fig. 35, 36, 47). The tip of the exopod (Fig. 38, 48) is distinguished by the absence of spinulation. Only the two exopod papillae (Fig. 38, *x*) can be found near the tip, unequal in size and usually distinctly papilliform. In some specimens minute specks were observed on the surface of the tip. It was not possible to determine whether they were anything more than particles of extraneous matter attached to it.

The mandible (Fig. 49) has seven teeth of fairly uniform size, with the exception of the most proximal, which is smaller than the others. One of the specimens examined had only six teeth on the dentiferous margin of the mandible.

The first maxilla (Fig. 39, 50) is distinguished by the squat, almost spherical papillae, which contrast with the cylindrical structures of the first maxilla of the type species. The basal swelling of the exopod is fairly prominent, but the setule on its apex is very small.

The second maxilla (Fig. 31, 43, 44) is moderately inflated at the tip, the tips of both maxillae forming a small collar around the base of the manubrium of the bulla (Fig. 33, *m*). The bulla itself can be described as an inverted mushroom, buried in the tissues of the host in such a way that its convex surface is deeper than the concave. Figure 33 shows the bulla in its most common form, exposing the concave surface to the observer. The lateral view (Fig. 34) shows that in some of the specimens the disc of the bulla can become distorted and crumpled. The definitive shape of the disc is influenced by conditions at the site of attachment. Other views of the bulla are shown in Fig. 43, 44.

The maxilliped (Fig. 42) shows indistinct signs of being subdivided into two. The distal half tapers distally and connects with the subchela. The claw of the subchela (Fig. 40, 52) is fairly short and curved, often with the diameter irregularly decreasing towards the tip. The auxiliary papilla (*aux*) in some specimens is pointed (Fig. 40), whereas in others (Fig. 52) it has a blunt tip. A distinguishing characteristic of the species is the small size of the maxilliped palp, generally resembling a broad-based tubercle of quite irregular shape. In some specimens (Fig. 41) this tubercle has near its base a small digitiform outgrowth, absent in most maxillipeds. The tip is sharply pointed in most specimens (Fig. 51). A characteristic drooping posture is recognizable in most maxilliped palps.

The dimensions of *S. carpionis* differ widely from one locality to another. The specimens from Greenland and Iceland measure from 4.00 to 5.60 mm in trunk length, whereas the trunk length of those from the island of Sakhalin is only from 3.80 to 4.00 mm. The specimens from the Asian mainland (Lake Taimyr, USSR) have trunks from 5.80 to 7.68 mm long. Such differences proved to be common in most species with a circumpolar distribution.

Comments — The first description of *S. carpionis* was in Danish. It was accompanied by small and very generalized illustrations (Krøyer, 1837, 1863). The name of the type host, *Salmo carpio*, was subsequently altered to *Salvelinus alpinus*. The original description remained rather inaccessible to most workers and the change in the name of the original host also added to the difficulty and tended to divert attention when subsequent finds were being identified. Under the circumstances, it is quite understandable that most records identified as *S. carpionis* were produced by Danish authors. All these records come from either Iceland or Greenland (Wesenberg-Lund, 1895; Stephensen, 1912, 1940; Hansen, 1923). Wesenberg-Lund's record was made under the name *Lernaeopoda alpina*. It is now accepted that the specific name *alpina* is a synonym of *S. edwardsii*. Stephensen (1943), however, was able to identify Wesenberg-Lund's material as *S. carpionis*. With the exception of the original description (Krøyer, 1837), no descriptions or illustrations of *S. carpionis* can be found in the literature under its correct name.

Workers other than Danish were obviously handicapped when dealing with *Salmincola* parasitic on *Salvelinus*. Unable to relate his find to the old Greenland record, Wilson (1908) described a parasite from *Salvelinus malma* taken in Alaska as a new species, *Lernaeopoda gibber*. Figure 43 shows one of Wilson's specimens and its similarity to the original *S. carpionis* (Fig. 31). All other features (cephalothorax outline, Fig. 45; second antenna, Fig. 47, 48) support the view that these specimens are morphologically indistinguishable. The same is true of later synonyms, *S. salvelini* Richardson, 1938, and *S. smirnovi* Markevich, 1940. It must be pointed out, however, that without reference to specimens it would have been impossible to establish the single identity of these animals. The descriptions produced by various authors could

not be used for comparative purposes. It is also interesting that all these parasites are parasitic on species of the genus *Salvelinus* and that all show preference for attachment to parts other than gills.

It should be noted that Krøyer (1837) mentioned in his original description a "variety" of *S. carpionis* occurring on a stickleback, *Gasterosteus aculeatus*, in Greenland. No *Salmincola* has ever been found on this fish and one must suspect that a labelling mistake was responsible for this record. Krøyer's type material contained two small specimens of *S. edwardsii*, a species also parasitic on *Salvelinus*. A drawing resembling *S. edwardsii* was published by Krøyer as representing the parasite of the stickleback.

Salmincola californiensis (Dana, 1853)

(Fig. 53–80)

Synonyms — *Achtheres carpenteri* Packard, 1874; *Lernaeopoda californiensis* Dana, 1852; *Lernaeopoda beani* Wilson, 1908; *Lernaeopoda falculata* Wilson, 1908; *Salmincola carpenteri* (Packard, 1874) Wilson, 1915; *Salmincola beani* (Wilson, 1908), Wilson, 1915; *Salmincola falculata* (Wilson, 1908), Wilson, 1915; ? *Salmincola lata* Markevich, 1940; *Salmincola yamame* Hoshina and Suenaga, 1954.

Material examined — (labelled as *S. californiensis*) (1) 5 females, *Oncorhynchus nerka*, gills, Big Fayette Lake, Idaho, 1914, USNM 43563; (2) 8 females, *Salmo gairdneri*, gills, Waddell Creek, California, 1937, USNM 69909; (3) 5 females, *Salmo clarkii*, Yellowstone Lake, undated, USNM 54084; (labelled as *S. carpenteri*) (4) 1 female, "salmon," Battle Creek, Colorado, undated, USNM 43569; (5) 12 females, *Salmo mykiss*,[2] Yellowstone Park, Wyoming, 1923, USNM 59790; (6) 5 females, *Salmo gairdneri*, gills, Deschutes River, Oregon, USNM 69775; (labelled as *S. beani*) (7) numerous females, same host and habitat, Sisson, California, USNM 38605 and 39538; (8) 14 females, *Oncorhynchus tshawytscha*, gills, Battle Creek, California, undated, USNM 38584 and 38585; (9) 5 females, same host and habitat, Baird, California, 1908, USNM 39541; (10) numerous females, same host and habitat, McCloud River, California, 1881, USNM 40104 (these specimens constitute type material of *S. beani*, no holotype specimen was selected); (11) numerous specimens, "trout," gills and fins, Columbia River watershed, 1909, USNM 59812; (labelled as *S. falculata*) (12) 4 females, *Oncorhynchus nerka*, gills, Baker Lake, Washington, 1902, USNM 38586 (these specimens constituted type material of *S. falculata*); (13) 2 females, "trout," gills, Fork Feather River, California, 1898, USNM 38588; (14) 2 females, "trout," operculum, Hot Creek, Cassel, California, 1898, USNM 38589; (15) numerous females, Heart Lake, Wyoming, *Salmo gairdneri*, mouth, 1898, USNM 39620; (16) numerous females, *O. tshawytscha*, gills, McKenzie River, Oregon, 1912, USNM 44575; (17) 10 females, *O. nerka*, British Columbia, undated, USNM 49739; (18) 3 females, same host, skin, Lake Owikeno, British Columbia, undated, USNM 60457; (19) 6 females, *Salmo clarkii*, locality uncertain, undated, USNM 65459; (20) numerous females, *O. nerka*, gills, McKenzie River, Oregon, undated, USNM 69882; (21) 10 females, same host, Lake Washington, undated, USNM 69889; (22) numerous females, *Salmo gairdneri*, gills, Santa Cruz Co., California, 1937, USNM 79008; (23) 4 females, same host and habitat, Mt. Shasta, California, 1968; (24) 5 females, *O. nerka*, operculum, Cultus Lake, British Columbia, 1963; (25) numerous females, *O. nerka*, Issaquah Creek, Washington, 1968; (26) numerous females, *O. tshawytscha*, gills, Little White Salmon River, Washington, 1968; (27) 12 females, same host and habitat, Nason Creek, Washington, 1968; (labelled as *S. yamame*) (28) 2 females, *Oncorhynchus masou*, gill cavity, Gumma Prefecture, Japan, 1965; (labelled as *S. edwardsii*) (29) numerous

[2]This specific name is not applied at present to any salmonid species in North America. The host in this instance must have been one of the local *Salmo* species.

females, *Salmo gairdneri*, Mt. Shasta, California, 1949, USNM 90379; (30) numerous females, same host, Eel River, California, 1949, USNM 90380.

Description of the female — The outline of the cephalothorax varies from a narrow, with slight posterior expansion (Fig. 71), to a broad and fairly short type (Fig. 69). Figures 68 and 70 show intermediate stages between these two. The trunk is characteristic enough to make the species quite easy to recognize from its general appearance (Fig. 53–61). It is rather short and orbicular. In some specimens the dorsum of the trunk is distinguished by a middorsal raised welt (Fig. 56), in others a transverse welt might be seen (Fig. 58). The posterior extremity of the trunk is marked by oblique lines at the points of attachment of the egg sacs (Fig. 53). Anal area is often raised slightly above the surface of the trunk and in many specimens a minute genital process is noticeable.

The second antenna (Fig. 62–66) has several distinctive features. The spiny pads of the sympod and the first segment of the endopod are armed with very large and robust spines. In some views of the endopod (Fig. 64) they project well beyond the margin of the appendage. The distal segment of the endopod resembles those of *S. salmoneus* and *S. carpionis*. Tubercle 3 varies in size, as can be seen in Fig. 63 and 64. In some specimens the ventral processes 4 and 5 arise from a fairly distinct swelling, which alters, to some extent, the appearance of the ventral region of this segment. The exopod is bulbous and distinguished by its armature. The tip of the exopod (Fig. 65) is covered by a cluster of very strong and large spines, almost as large as the two exopod papillae (Fig. 65, *x*). In some specimens the exopod has a slightly bilobed appearance due to the presence of a small indentation of the apex. The exopod papillae are occasionally found with grossly inflated bases, which give them a very unusual appearance (Fig. 66). The spines vary in size but they are always very conspicuous and larger than in any other species in the subgenus.

The mandible has six teeth, on rare occasions only five. The mandibles from different specimens vary in the size of the two smallest, proximal teeth. In some specimens (Fig. 73) these teeth are much smaller than the four distal teeth, in others (Fig. 72) the discrepancy in size is less marked.

The first maxilla (Fig. 74–76) shows a wide range of variations, manifest mainly in the extent of development of the three papillae. The most common structure of this appendage is shown in Fig. 74, in which the maxilla has a reduced ventral papilla and a fairly large central papilla. In some specimens the dorsal papilla is not fully developed (Fig. 75), being reduced to about half its usual size. In others (Fig. 76) all three papillae might be similarly reduced, so that wide spaces open between their bases. The lateral swelling of the exopod is barely noticeable, but its setule is fairly large.

The second maxilla produces hardly any terminal inflations. The bulla (Fig. 53, 55, 61, 67) resembles the type described for *S. carpionis*. The disc might be almost regularly circular or might be indented in its posterior margin (Fig. 67). It is embedded in the tissues of the fish.

The maxilliped (Fig. 77) is distinguished by the prominence of its palp, which is robust and squat. On its apex (Fig. 78, 79) it usually carries two outgrowths, often tipped with small protrusions. These two outgrowths, marked 1 and 2 in Fig. 78 and 79, differ in size, outgrowth 2 being the smaller. In Fig. 78 the palp is inclined towards the observer so that its full length is not obvious. It is also slightly rotated around its long axis, causing the two outgrowths to overlap (compare with Fig. 79). Some palps have as many as three smaller outgrowths, resembling outgrowth 3 in Fig. 78. It is difficult to determine whether these structures represent true morphological features or are merely flaps of damaged cuticle. The claw of the maxilliped (Fig. 80) is sharply curved and its diameter decreases rather unevenly towards its tip. The auxiliary papilla is fairly long, cylindrical, and with a minute terminal extension.

Regardless of their origin and earlier synonymy, the specimens of this species had trunk lengths between 1.60 and 2.80 mm.

Comments — As evident from the list of synonyms, *S. californiensis* presented a considerable taxonomic problem. The type material of this species is no longer extant and its original description consists of a brief general outline and two sketchy drawings, which fit almost all members of the genus. Even

the identity of the type host cannot be established beyond the fact that it was a salmon of the genus *Oncorhynchus*. It is not surprising therefore, that with the passing of time more species were described from *Oncorhynchus* and *Salmo* of western North America. The examination of specimens of all these species revealed no significant morphological differences among them. All of them share the same shape of body, the same type of bulla, the same details of the second antenna, and the same type of maxilliped palp. It is now clear that the Pacific salmons and trouts carry only one species of *Salmincola*. In view of this fact it is reasonable to apply to it the oldest name used for the parasite of these fishes. In spite of the inability to examine the type material of this species, I decided, therefore, to use for it the name *Salmincola californiensis* (Dana, 1853), relegating all the other names to synonymy. *Salmincola californiensis* occurs also on the Asian side of the Pacific, recognized there under the names *S. yamame* and *S. falculata*.

Salmincola thymalli (Kessler, 1868)

(Fig. 92–113)

Synonyms — *Lernaeopoda thymalli* Kessler, 1868; *Lernaeopoda clavigera* Olsson, 1872; *Salmincola baicalensis* Messjatsev, 1926.

Material examined — (1) 2 females, *Thymallus thymallus*, gills, river Pechora, USSR, 1959, collection of Zoological Institute, Leningrad; (2) 3 females, *Salmo alpinus* (= *Salvelinus alpinus*), gills, Jemtland, Sweden, undated, USNM 19999; (3) 1 female, *Thymallus vulgaris*, gills, Jemtland, Sweden, undated, USNM 43564; (4) 6 females, *Prosopium* sp., Keewatin, Nueltin Lake, Alaska, 1947, USNM 86170; (5) 17 females, *Thymallus signifer*, same locality and date, USNM 86173; (6) 4 females, same host, locality and date, USNM 86172; (7) 13 females, same host, locality and date, USNM 86171; (8) 2 females, *T. vulgaris*, gills, Finland (part of Olsson's type material of *Lernaeopoda clavigera*), USNM 3209; (9) 2 females (part of same material), British Museum, London, 1911.11.8.48432-433.

Description of the female — The general appearance of *S. thymalli* (Fig. 92–94) is distinguished by a fairly elongate cephalothorax (Fig. 95). The maxillipeds are relatively small and do not protrude close to the anterior margin of the cephalothorax (Fig. 96). The trunk varies from elongate oval to almost orbicular, barely longer than broad. A feature peculiar to the preserved specimens of *S. thymalli* is the tendency of the maxilliped to be extended, as illustrated in Fig. 109.

The second antenna (Fig. 97–104), although showing considerable variability from one region to another, has many distinguishing features. The distal segment of the endopod is dominated by hook 1. Spine 2 is robust and has a slightly inflated base (Fig. 99, 100). In specimens from the Palearctic (Fig. 104), tubercle 3 is large and has a very prominent duct orifice. In Nearctic specimens (Fig. 97, 98) this tubercle is smaller and its duct orifice is not detectable. The ventral processes (4 and 5) provide a clear distinction between the Palearctic and Nearctic parasites. In the former (Fig. 104), process 5 arises from the side of a large and smooth process 4 whereas in the latter (Fig. 97–100) processes 4 and 5 arise side by side on a small swelling. Process 4 of the Nearctic specimens is unique in the crenation of its surface. In some views it resembles a pine cone. The character and extent of crenation varies from specimen to specimen (cf. Fig. 99, 100). Also variable is the armament of the exopod. In the Palearctic specimens the denticulation consists of very small and scattered spinules that make the papillae (*x*) appear very promiment (Fig. 102). In the Nearctic specimens this ramus is either similar (Fig. 103) to that of the Palearctic one or armed with fewer but much larger spinules (Fig. 101) that dwarf the papillae(*x*).

The mandible (Fig. 106) normally has seven teeth, though on one occasion a mandible with only six teeth was found (Fig. 105). In the latter there was a small denticle in front of the distal

normal tooth. This denticle appeared to be a remnant of a normal tooth, which had broken. In another specimen, a typical angular fracture line was found at the tip of the mandible. It is probable that subsequent to such fracture the use of the mandible has a filing effect, which restores a smooth, rounded contour to this part of the appendage. The three posterior teeth are usually smaller than the other four but there is no abrupt transition in their size from the large to the small teeth.

The first maxilla (Fig. 107) is different in proportions from those of most other species. Relative to the body of the maxilla, the dorsal and medial papillae are much larger than is usual for the genus. The ventral papilla is much smaller than the other two. The exopod has no swelling at the base of the setule.

The second maxilla often produces a marked inflation around the base of the bulla (Fig. 92–94). The bulla is very characteristically clavate (no other *Salmincola* has such a bulla) and is usually fairly long. In some specimens, however (Fig. 94), it can be unusually short.

The maxilliped (Fig. 108–113) provides some of the most distinguishing features of this species. It is short and squat, perching on a large and inflated base. The palp is long (Fig. 108, 111, 112) and slender and carries on its apex one or two small denticles. Some distance from the apex is another single denticle of about the same size. Since the maxilliped is exposed to wear, some palps are damaged. Some rather short palps (Fig. 109, *bp*), on closer examination, proved to be broken (Fig. 113). The subchela has a strong, though slender claw, strongly curved in its distal half (Fig. 110). The diameter of the claw is often irregular, the auxiliary papilla long. The ventral surface of the subchela carries near its base the usual short seta.

The trunk length of *S. thymalli* varies from 1.80 to 2.40 mm.

Comments — The distribution of *S. thymalli* is circumpolar. In view of the wide distribution range, some differences in morphology between populations from widely separated localities are not surprising. Some morphological differences, however, have no regional significance. For example, the armature of the exopod of the second antenna in the Nearctic Region can be either similar to, or quite different from, that found in the Palearctic Region. Other differences between specimens from these two regions appear to be more constant. I was unable to find any Old World specimens with crenation of the ventral process (4) of the endopod of the second antenna, whereas the New World specimens invariably had these processes distinctly crenated. It is tempting to speculate on the possibility of incipient speciation caused by geographical separation of these populations. The basic similarities are, however, much more compelling and at this stage no subdivision of *S. thymalli* should be contemplated.

Salmincola coregonorum (Kessler, 1868) n.comb.

(Fig. 197–206)

Synonyms — *Lernaeopoda coregonorum* Kessler, 1868; *Basanistes coregoni* Neresheimer, 1909; *Achtheres pseudobasanistes* Zandt, 1935; *Achtheres coregonorum* (Kessler, 1868), Markevich, 1937.

Material examined — Two immature females, *Coregonus lavaretus*, gills, Lake Onega, USSR, 1934, collection of Zoological Institute, Leningrad.

Description of the female — The general appearance of the specimens examined (Fig. 197, 198) cannot be considered as representative of the species, since they are still immature. This is particularly true of their trunks. Markevich (1956) gives 2.9–3.1 mm as the length of the trunk of adult females. These two specimens are only 2.60 mm in trunk length. The earlier de-

scriptions (Kessler, 1868; Markevich, 1956) create an impression that this species resembles *S. thymalli*.

The second antenna is shown in Fig. 200, 201. The armament of the endopod is similar to those of *S. salmoneus*, *S. carpionis*, and the Palearctic specimens of *S. thymalli*. Tubercle 3 is large, its duct orifice prominent (Fig. 200). The surface of the ventral process 4 is smooth. The exopod differs from those of most species in appearing soft and lobate (Fig. 201). Careful observation shows that it is armed with rather sparse but relatively large spines, about the size of the two papillae (*x*). In Fig. 201 most of these spines appear to have been lost and leave behind them marks similar to the scars present on the spiny pads of the endopod and the sympod. One of the spines still present in Fig. 201 is marked *y*. The spiny pads are also equipped with sturdy spines and are considerably inflated.

The mandible (Fig. 202) has seven teeth, the proximal three being much smaller than the rest.

The first maxilla (Fig. 203) has all three papillae well developed. The ventral papilla, often reduced in many species, here appears to be only slightly smaller than the other two. The setule of the exopod is very small and the swelling on which it is located is hardly noticeable.

The second maxilla shows scarcely any inflation at the tip (Fig. 197, 198). The bulla is asymmetrical (Fig. 199). Markevich (1956) described it as being "almost club-shaped." This shape is apparent in the view shown in the right half of Fig. 199. Rotating the bulla, one notices that one side of the club is sliced off and somewhat concave, as in the left half of Fig. 199. The original description (Kessler, 1868) shows a similar bulla, though the text of that description refers to it as simply "club-shaped."

The maxilliped (Fig. 204–206) is almost a replica of that of *S. thymalli*. In particular, its palp (Fig. 205) is equally long and prominent. It differs from the maxilliped palp of *S. thymalli* only in having a relatively larger subterminal spine. In *S. coregonorum* it is more like a flat, articulated process and extends to the tip of the palp. The claw (Fig. 206) of the subchela is strongly curved and the auxiliary papilla small and almost conical.

Comments — The type of the bulla is one of the unique features of *S. coregonorum*. It is the only species in which the bulla bears any resemblance to that of the type species. However, whereas the flat surface of the bulla of *S. salmoneus* is invariably on the ventral side, in this species it is usually lateral.

The armament of the maxilliped suggests that *S. coregonorum* is closely related to *S. thymalli*. This similarity extends to other morphological features. Since *S. coregonorum* is much more restricted in distribution and much less common than *S. thymalli*, it is possible that *S. coregonorum* derives from *S. thymalli*. It should be noted that *S. coregonorum* is the only species of its subgenus to live on *Coregonus*.

Salmincola edwardsii (Olsson, 1869)

(Fig. 165–196)

Synonyms — *Lernaeopoda salmonea* Mayor, 1824; *Basanistes salmonea* Milne Edwards, 1840; *Lernaeopoda edwardsii* Olsson, 1869; *Lernaeopoda fontinalis* Smith, 1874; *Lernaeopoda alpina* Olsson, 1877; *Lernaeopoda arcturi* Miers, 1877; *Lernaeopoda bicauliculata* Wilson, 1908; *Salmincola arcturi* (Miers, 1877), Wilson, 1915; *Salmincola bicauliculata* (Wilson, 1908), Wilson, 1915; *Salmincola oquassa* Wilson, 1915; *Salmincola mattheyi* Dedie, 1940; *Salmincola exsanguinata* Sandeman and Pippy, 1967.

Material examined — (labelled as *S. edwardsii*) (1) 9 females, *Salvelinus lepechini*, fins, Lake Onega, USSR, 1934, collection of Zoological Institute, Leningrad; (2) 3 females, *Salvelinus* sp., Lake Taimyr, USSR, 1943, collection of Zoological Institute, Leningrad; (3) 15 females, *Salvelinus malma spectabilis*, fins and gill chamber, Yellow Bay, Pacific coast USA, 1941, USNM

90924; (4) 8 females, *Salvelinus fontinalis*, gills, Caledonia, New York, undated, USNM 39587; (5) numerous females, same host, Wild Rose, Wisconsin, undated, USNM 43574; (6) 1 female, same host, Adirondacks, USA, undated, USNM 49708; (7) numerous females, same host, Hudson, Wisconsin, 1916, USNM 49738; (8) numerous females, same host, Mirror Lake, New Hampshire, undated, USNM 49742; (9) 20 females, same host, Smithtown, New York, 1917, USNM 49781; (10) 2 females, same host, Hudson, Wisconsin, 1916, USNM 49789; (11) 2 females, same host, Smithtown, New York, undated, USNM 53493; (12) 4 females, same host, Montana, USNM 53521; (13) 10 females, same host, Smithtown, New York, undated, USNM 54092; (14) 8 females, same host, Whitefish Lake, British Columbia, 1940, USNM 60488; (15) 10 females, same host, Caledonia, New York, undated, USNM 74344; (16) numerous females, "Aurora trout," gills, Ontario, undated, USNM 59771; (labelled as *S. oquassa*) (17) 5 females, *Salvelinus oquassa* (= *Salvelinus alpinus*), operculum, Rangeley Lake, Maine, 1884, USNM 39604; (18) 1 female, same host and locality, USNM 43578 (these two samples constitute paratypes and the holotype respectively of *S. oquassa*); (19) 2 females, same host and locality, USNM 74343; (labelled as *S. bicauliculata*) (20) 3 females, *Salvelinus malma*, Bering Island, undated, USNM 38594 (this was type material of *S. bicauliculata*, holotype was not designated); (21) 1 female, host unknown, Bering Island, 1882–1883, USNM 8453; (22) 1 female, *Salvelinus malma*, Pemberton River, British Columbia, undated, USNM 60456; (labelled as *S. arcturi*) (23) 4 females, *Salmo arcturi* (= *Salvelinus alpinus*), Floeberg Beach, Ellsmere Island, Canadian Arctic, undated (from type material in British Museum, London); (labelled as *S. exsanquinata*) (24) 6 females, *Salvelinus fontinalis*, Newfoundland, 1964, collection of Mr J. Pippy.

Description of the female — There are few features of taxonomic value in the general appearance of *S. edwardsii* (Fig. 165–169), the appearance of individual specimens being largely dependent on the state of preservation and the condition at the time of fixation. Figure 166 shows a specimen from the type material of *S. oquassa*. Figure 167 comes from the type material of *S. bicauliculata*. One of the more distinctive features is the length of the cephalothorax, though this feature is also greatly variable (Fig. 171–173). The maxilliped often extends nearly as far as the anterior margin of the cephalothorax (Fig. 170). The shape of the trunk is roughly oval, with rounded margins and usually convex dorsum.

The second antenna (Fig. 176–184) distinguishes *S. edwardsii* from all other species of *Salmincola*. Even under low magnification (Fig. 176), its rami show very definite characteristics. The spiny pads of the endopod and sympod (Fig. 179, *en* 1, *s*) are much inflated. Their spines are long, slender and prominent (Fig. 184). The distal segment of the endopod has all the usual armature but the relative proportions of its components are very distinctive. At variance with other species, in which the predominent component of this armature is hook 1, the endopod of *S. edwardsii* is dominated by ventral process 4. This is illustrated in Fig. 178, 180, 181. Ventral process 5 is always present. Usually one finds it in its normal place at the base of process 4, though in one antenna it was found near the tip of this process (Fig. 180). The size of process 4 varies from rather modest (Fig. 177, 182) to almost gigantic (Fig. 178, 181). Even the smallest process 4 observed, however, is larger than the hook 1. In some specimens the surface of this process is marked with dark spots of unknown nature (Fig. 178, 182). The proportions of process 4 and hook 1 suggested to one of the early investigators (Smith, 1874) the appearance of pincers. Tubercle 3 is noticeable in some specimens (Fig. 178) but in others it seems to be absent (Fig. 177, 180, 181). The exopod (Fig. 183) is often somewhat bulbous at the tip and sometimes gives the impression of being subdivided into two lobes. Its spinulation consists of strong and prominent, though usually rather scattered, spines, which are often in two groups with a smooth area between them. The papillae (*x*) are of about the same size as the largest of the spines.

The mandible (Fig. 185, 186) has either six or seven teeth. In all specimens the distal four teeth are uniformly large, the proximal two or three are much smaller. The difference in size between the large and small teeth is not constant. In some mandibles (Fig. 185) the small teeth are relatively larger than in others (Fig. 186). Occasionally mandibles occur with only one small tooth.

The first maxilla (Fig. 187, 188) also has a wide range of morphological variations. The usual structure of this appendage is shown in Fig. 187. The three papillae are of about the same

size and their apical setae are short. The exopod is relatively prominent, its basal swelling being well distinguishable and the seta only slightly smaller than those of the three papillae. One specimen from the northern USSR had a maxilla with greatly reduced dorsal and ventral papillae (Fig. 188), in some others reduction was observed in the dorsal papilla only. The prominence of the exopod appears to be quite constant.

The second maxilla is devoid of terminal inflation. The bulla (Fig. 174) has a short manubrium and a roughly rounded disc, sometimes with a slightly convex distal surface. In some specimens the posterior margin of the disc is indented, giving it the appearance of a "hoof" (Markevich, 1956).

The maxilliped (Fig. 189–196) is also distinctive. Its short and robust body carries on its medial margin a prominent palp (Fig. 189, *p*). The distal half of the palp is shown in detail in Fig. 190. It is tipped with three complicated processes, two of them usually arising from a common base. Some changes caused in the tip of the palp by the wear and damage are shown in Fig. 191, where the three processes are still recognizable, and in Fig. 192, where damage has been more extensive. In spite of these changes, however, the palp remains very prominent and bears some resemblance to that of *S. salmoneus*. The subchela is another distinctive part of the maxilliped (Fig. 193–196). The region of the auxiliary papilla and the dorsal side along the base of the claw are equipped with varying numbers of small spines. They were first observed by Markevich (1956) who saw them in some specimens, though not in all and considered them difficult to notice. They are particularly difficult to see when the appendage is in situ and the dorsal side of the subchela is away from the observer. The ventral view of the tip of the subchela and the claw is shown in Fig. 193. The same claw is shown from the dorsal side in Fig. 194. It is best to study this part of the maxilliped dissected away and with the aid of interference phase illumination. The tip of the subchela, like the palp, is subject to wear and one can expect the spines to be less numerous in old specimens. Their numbers differ also in specimens from different geographical regions. More often than not, they are absent from the North American specimens. Even there, however, some specimens still have them (Fig. 195, 196). In some of the Nearctic specimens (Fig. 195) the claw is less curved than in the specimens from the Old World. The claws of the latter usually have a pronounced flexure in the proximal part.

The trunk length and, consequently, the size of the specimens also differ from one area to another. The Palearctic specimens measure from 2.96 to 3.00 mm in trunk length. The trunks of the Nearctic specimens are only between 1.60 and 2.00 mm long. This means that the American *S. edwardsii* reaches only half the size of the same species in the Old World.

Comments — The differences in the size of the Nearctic and Palearctic specimens are not sufficient to call for their separation into two species. Apart from this difference, the populations of *S. edwardsii* from these two regions differ only in the spinulation at the base of the claw of the subchela, the American specimens being less spinous. The general appearance, the type of the bulla, and, most of all, the unique structure of the second antenna, are all similar and provide strong links between them.

The long synonymy of *S. edwardsii* can be largely attributed to the inadequacy of early descriptions. Olsson (1869) gave no illustrations. The authors of subsequent synonyms were all in some doubt about the relationship between species they described and *S. edwardsii*. Miers (1877), describing *S. arcturi*, suggested that a better knowledge of *S. edwardsii* might result in relegation of *S. arcturi* to synonymy with it. The lack of information about the details of morphology resulted in Wilson's (1915) description of *S. oquassa*. The history of *S. bicauliculata* is particularly interesting. Wilson (1908) had three specimens in his type material. One of them had a bulla with an unusual, double manubrium (Fig. 175). I found this bulla severed from the parasite and floating

in the vial. The second specimen had no bulla. The third (Fig. 167) had a bulla with a normal, single manubrium. The specimens in two other vials were damaged and had no bullae. In all morphological details these specimens corresponded with the typical *S. edwardsii*. It seems fair to suppose that the double manubrium is an abnormality that can occur during the early stages of the parasite's attachment. At that stage the bulla is still soft and a vigorous pull can rip the two components of the manubrium apart. This abnormality was also found in other species of *Salmincola* (e.g., *S. jaculicus*, Fig. 130).

The specimens of *S. exsanguinata* that I examined also bear all the morphological features, particularly the second antenna, that link it with the European specimens of *S. edwardsii*. The authors of this species (Sandeman and Pippy, 1967) depended on the comparison of their material with descriptions and drawings rather than with specimens of *S. edwardsii*. Since most of these descriptions are much too generalized for comparative purposes, their mistake was not surprising.

I have not been able to obtain any material of *S. mattheyi*. However, reference to the original description (Dedie, 1940, p. 15), particularly to fig. 9 and 10, shows that the second antenna of this parasite is identical with that of *S. edwardsii*. As corroborating evidence, the host of *S. mattheyi* is *Salvelinus alpinus*, the common host of *S. edwardsii*.

Salmincola siscowet (Smith, 1874)

(Fig. 207–224)

Synonym — *Lernaeopoda siscowet* Smith, 1874.

Material studied — (1) 4 females, *Salmo siscowet* (= *Salvelinus namaycush siscowet*), Lake Superior, undated, USNM 39577 (according to Wilson (1915) these specimens are labelled in Smith's handwriting and are to be considered as type material of the species); (2) 15 females, same host, fins, Lake Commandant, Quebec, Canada, 1930, USNM 60487; (3) 2 females, same host, fins and skin, Lake Belair, USA, 1944, USNM 79583; (4) 2 females, same host, gills, Lake Superior, 1906, USNM 74348.

Description of the female — The general appearance of *S. siscowet* (Fig. 207, 208) is characterized by a dorsal prominence of the cephalothorax, more noticeable than in most other species. The cephalothorax tends to be elongated (Fig. 210, 211). The trunk is fairly long and forms a quite distinct, necklike narrowing anteriorly. The "arms" are usually longer than the trunk.

The second antenna (Fig. 212–214) is very distinctive. The spiny pads of the sympod and the endopod are inflated and resemble those of *S. edwardsii* both in shape and in type of spinulation. The distal segment of the endopod (Fig. 212, 213) is particularly characteristic. The ventral side of the segment is grossly inflated and the position of hook 1 has been thereby apparently displaced. The auxiliary spine 2 and tubercle 3 have normal shape and position, though tubercle 3 is absent in some specimens. Ventral processes 4 and 5 are in the form of small conical protuberances near the apex of a very large swelling (Fig. 213). This swelling is the best recognition mark of *S. siscowet*. The exopod (Fig. 214) is not unlike that of *S. edwardsii*. The two papillae (*x*) are easily noticeable and the spinulation is scattered and sparse.

The mandible (Fig. 215) has either six or seven teeth. As in *S. edwardsii*, the four distal teeth are large and uniform, whereas the proximal two or three are much smaller. These smaller teeth appear crowded together and in some mandibles overlap one another. They are often found enclosed in the space between the tip of the cutting blade and the first large tooth.

The first maxilla (Fig. 216–219) is fairly short and stocky. Its ventral papilla is almost completely reduced, so that only the apical seta remains in its usual position (Fig. 216). The structure of the exopod varies. Most commonly it is the usual small, rather blunt setule, on the tip of a very small swelling. One of the specimens examined, however, had two separate structures in this position (Fig. 217). Another (Fig. 218) had a single structure with traces of incipient subdivision, shown in detail in Fig. 219. The true nature of these unusual features is difficult to assess without more material to study.

The second maxilla (Fig. 207) does not inflate noticeably at the tip. The bulla (Fig. 209) is of the mushroom type, though in some specimens its margin is notched, as often happens in the bullae of this type. The rim of the disc is swollen and often curls inwards.

The maxilliped (Fig. 220–224) is also distinctive. It has a prominent palp (Fig. 220, *p*). The details of the palp are shown in Fig. 221 and the effects of wear are illustrated in Fig. 222. In some specimens only one or two processes can be found at the tip of the palp. Another feature shared by *S. siscowet* with *S. edwardsii* is the spinulation at the base of the claw of the subchela (Fig. 223). It can be seen from both the ventral and the dorsal sides (Fig. 224), though it does not extend far along the dorsal side. The spiny area seems to have an uneven surface, one or two swellings being sometimes observed, as in Fig. 223. Another unusual feature of the subchela is the presence of a dent along its inner margin (shaded in Fig. 220). It is this dent that abuts on the palp when the subchela is retracted. A dent of this kind was not seen in other species and requires further examination.

The trunk length of *S. siscowet* varies from 3.49 to 4.31 mm.

Comments — It is probable that *S. siscowet* is closely related to, perhaps derived from, *S. edwardsii*. Modifications in the ventral part of the second antenna's endopod and the spinulation of the subchela link these two species and set them apart from all the others. Also, their hosts are closely related. The differences between them are, however, sufficient to recognize these two parasites as belonging to different species.

Salmincola lotae (Olsson, 1877)

(Fig. 81–91)

Synonym — *Lernaeopoda lotae* Olsson, 1877.

Material examined — (1) One female, *Lota lota*, Lake Onega, USSR, 1932, collection of Zoological Institute, Leningrad; (2) two females, same host, Ostersund, Sweden, undated, British Museum, London, 1911.1.8.48382-384 (part of type material of the species).

Description of the female — The general appearance of *S. lotae* (Fig. 81) gives an impression of slenderness. The cephalothorax has a slender, oviform outline (Fig. 82), expanding only slightly posteriorly. The "arms" are also long and slender and the same is true of the trunk, which is evenly rounded posteriorly and only moderately narrowed in its anterior part.

The second antenna (Fig. 83–85) has the spiny pads of the sympod and endopod much less prominent than in some other species. The pad of the sympod is armed with few very long spines. One usually finds also a few scars, where the spines were broken off. Similar scars occur on the corresponding pad of *S. californiensis* (Fig. 62). The pad on the endopod appears to have much shorter spines. Not enough observations were made to determine the length of spines with accuracy. The endopod (Fig. 83) has a robust hook 1, very broad at the base. The lower half of the auxiliary spine 2 seems almost triangular, due to the width of its base. The ventral processes 4 and 5 are short and unarmed. Tubercle 3 is fairly large and has a well-developed nipple of the duct orifice. The exopod (Fig. 84, 85) is slender and tapers to its tip where the two papillae (*x*) can be seen clearly. The inflated bases of the papillae give, in some views, a bifid appearance to the ramus. The exopod tilts to the lateral side in all specimens examined.

The upper lip (Fig. 86) has a structure normal for the genus.

The mandible (Fig. 87) has seven teeth. In contrast to some species described earlier, these teeth cannot easily be divided into distal and proximal groups. They are much more uniform in structure and only gradually decrease in size proximally. The proximal tooth is overlapped by the ventral cutting blade.

The first maxilla (Fig. 88) is very distinctive. It has a squat, almost square body, unlike that of the maxilla of any other *Salmincola* species. The ventral papilla is almost completely reduced, its long seta projecting outwards. All three papillae have long setae. Perhaps in some maxillae the ventral papilla might be less reduced. The short seta of the exopod is mounted on quite a prominent swelling. Although only one specimen was examined in close detail, earlier authors (Markevich, 1956, fig. 119) observed a similar character of the first maxilla.

The second maxilla has no swelling at the tip, at the base of the bulla (Fig. 81). The latter is very distinctive. It has a slender, rather short manubrium and a flat disc with a very wide diameter. The disc is sometimes distorted, but its general circular outline and its flatness are always recognizable.

The maxilliped (Fig. 89–91) is also distinctive. It is short and robust and has a small palp. The palp (Fig. 90), in spite of its small size, shows some subdivisions. One outgrowth appears near the base and another at the tip of the terminal part. In view of the earlier observations on the maxilliped palp, these observations cannot be considered as definitive. The size and position of the palp, however, are good distinguishing features of *S. lotae*. The claw of the subchela (Fig. 91) is relatively short and not strongly curved. Its base is very broad. The claw tapers abruptly to the tip. The auxiliary papilla is long and cylindrical.

The trunk length of *S. lotae* is about 5 mm, the diameter of the bulla 2.60 mm.

Comments — *Salmincola lotae* is probably closest to *S. carpionis*, from which it differs in the type of the bulla and the shape of the first maxilla. Its distribution is limited to a small area in the Palearctic. The North American species of *Lota* have not been reported as yet as carrying this parasite.

Salmincola cottidarum Messjatzeff, 1926

(Fig. 225–238)

Material examined — Three females, one ovigerous and all with males attached, *Cottus kessleri*, gill chamber, Lake Baykal (off Listvenichnoye), USSR, 1949, from the collections of Dr E. A. Koryakov.

Description of the female — The general appearance of this small species (Fig. 225, 226) bears some resemblance to *S. edwardsii*. The poor condition of the specimens examined made more exact comparisons impossible. The specimens were damaged, their bullae missing and their second maxillae badly contracted (Fig. 225). The cephalothorax is elongated, the second antennae more prominent than usual. Below the bases of the second maxillae a shallow constriction separates the cephalothorax from the trunk, which is short and orbicular. The egg sacs (Fig. 225) are short and compact, the eggs large.

The details of the second antenna (Fig. 227–230) show unexpected variety. In some specimens the second antenna is distinguished from that of all other species of *Salmincola* by the position of the endopod (Fig. 227, *en*). This ramus is pressed into the distal half of the sympod in such a manner that it assumes an oblique position, tilting away from the head of the parasite, with hook 1 turned laterally. In such antennae the exopod becomes the prominent feature. Some of the previous observers (Koryakov, 1959, fig. 2) noted a similar position of the endopod. In other specimens of this species the endopod is in its more usual, erect position. Such specimens were described originally by Messjatzeff (1926). In the material examined during this work both types were present. It is interesting to note that "deflected" endopods also differ from the "erect" endopods in very distinctive details. In the former (Fig. 230) the ventral process 4 is in the form of a very prominent swelling, affecting the appearance of the entire segment. The swelling is armed with relatively large, though scattered, spines. Process 5 arises from its lateral wall and is papilliform,

with a blunt tip. The ventral region of the distal segment of the erect endopod (Fig. 228, 229) is quite different. In this type of endopod the ventral processes 4 and 5 are of more or less the same size, both arising from a prominent swelling and the area being devoid of any spinulation. Both types occur with similar exopods, which are bulbous at the tip and covered by scattered spines resembling those of the endopod. The two exopod papillae are easy to see.

The mandible (Fig. 231) has six teeth, of which the proximal two (in one mandible the proximal three) are much smaller than the distal teeth.

The first maxilla (Fig. 232, 233) also shows considerable structural variability. One of the specimens had a first maxilla of the usual type (Fig. 233), with a reduced ventral papilla and very small exopod. The maxilla of the other specimen is shown in Fig. 232. It has no dorsal papilla. The area where it is present in the maxillae of other species curves in a pronounced convexity. The ventral papilla is small and the central papilla is very large, with a short seta. The exopod is conspicuously large, particularly in ventral view (right half of Fig. 232). Both types of maxilla are covered by a particularly thick cuticle in the distal half of their dorsal surfaces. The heavy cuticle ends in a clearly demarcated line and appears to be finely sculptured in delicate parallel ridges. The original description of *S. cottidarum* (Messjatzeff, 1926) shows the first maxilla with all three papillae present, though the dorsal one is rather smaller than the central. The exopod is clearly noticeable. In a later description (Koryakov, 1959), the maxilla is shown as having a very large central papilla, the ventral and the dorsal being equally reduced. The exopod is small.

According to earlier descriptions, the second maxilla is short and forms no terminal inflations. Its bulla is mushroom-shaped and varies in size.

The maxilliped (Fig. 234–238) is characterised by the small size of its palp. In general appearance (Fig. 235, 236), the palp resembles that of *S. lotae*. It is a soft, papilliform structure, with different numbers of poorly defined outgrowths. Very distinctive also is the tip of the subchela (Fig. 237). Near the base of the small and relatively weak claw, the subchela carries, in addition to the usual auxiliary papilla, a bulbous swelling (Fig. 237, *w*) from which three digitiform outgrowths extend distally. On the dorsal side of the same area (Fig. 238) there are two pectinate flaps with serrated margins and some small denticles on the surface. These are not known from any other species of *Salmincola*.

The trunk length of *S. cottidarum* is from 1.2 to 1.8 mm.

Comments — The most puzzling feature of *S. cottidarum* is the lack of uniformity in the structure of the endopod of its second antenna. The differences shown by this ramus are unparalleled within the genus. These differences were found in the material examined and confirmed the observations of earlier authors. One is tempted to speculate on the possible existence of not one but two species of *Salmincola* parasitic on the cottid fishes in Lake Baykal. These fishes are the dominant group in the fauna of the lake and are in the process of a very vigorous speciation. Perhaps the differences in the structure of the second antenna are also indicative of an incipient speciation. This speculation can be substantiated only on the basis of much more extensive studies.

Salmincola stellatus Markevich, 1936

(Fig. 239, 242)

I was unable to procure any specimens of this species. The illustrations and descriptions are based on the original reference (Markevich, 1936).

Description of the female — The general appearance of *S. stellatus* is shown in Fig. 239. The characteristic details are the posterior expansion of the cephalothorax and the distinct waistlike constriction in the anterior part of the trunk.

The appendages cannot be described in detail, since the original illustrations do not lend themselves readily to comparisons. The unique feature of the species is a hornlike projection (Fig. 242, ?) in the basal area of the endopod of the second antenna. As far as can be judged from Fig. 242, the distal segment of the endopod has all the usual components of the apical armature. The exopod appears to be devoid of spines, but the two papillae are very prominent.

The second maxilla (Fig. 239) produces no terminal inflations. The bulla is very distinctive, its disc being stellate and providing the clue to the specific name of the parasite.

The trunk length is between 3.0 and 3.9 mm.

Comments — The validity of this species is firmly supported by the type of the bulla and the presence of the peculiar horn on the endopod of the second antenna. Even if the latter proves to be an error of interpretation, the type of the bulla is distinctive enough to ensure the status of an independent species for *S. stellatus*.

Subgenus ***Salmincola* (*Brevibrachia*)** subgen.n.

Grouped in this subgenus are species characterized by the possession of greatly reduced claws in their maxillipeds. All of them parasitize mainly fishes belonging to the family Coregonidae. I include here five species. It must be pointed out, however, that I am not completely statisfied with the validity of all these species. The differences among them are small, and the material available for examination was rather limited. Three of these species (*S. nordmanni*, *S. extensus*, and *S. jacuticus*) differ from one another mainly in the shape of the trunk. This kind of difference does not offer a satisfactory discriminant in taxonomy. For reasons that will become obvious as the species are described, I decided to retain the taxonomic status of these species, with strong reservations. Detailed study of more abundant data is necessary to clarify definitively the taxonomy of some of these species.

Salmincola nordmanni (Kessler, 1868)

(Fig. 137–148, 247)

Synonyms — *Basanistes nordmanni* Kessler, 1868; *Lernaeopoda tuberculata* Gadd, 1908.

Material examined — Six females, *Stenodus leucichthys*, gills and gill chamber, River Pechora, USSR, 1960, from the collection of Dr O. N. Bauer.

Description of the female — The general appearance of *S. nordmanni* (Fig. 137–139), like that of other species of this subgenus, is characterized by the prominence of its maxillipeds. The cephalothorax (Fig. 140) is medium length with wider posterior part. The most characteristic part of the species is the trunk. Unlike any other species of its genus, the trunk of *S. nordmanni* has three distinct lateral swellings (Fig. 138, 139).

The second antenna is distinguished by the broad base of its endopod (Fig. 142). The dorsal side of the distal segment is pitted with small crypts (Fig. 141, 142). The armament of the distal segment is distinguished by the size of tubercle 3 (Fig. 141) and by the appearance of ventral processes 4 and 5. Process 4 is hardly distinguishable at the tip of a prominent swelling covered with coarse spinulation. Process 5 is often a small and slender outgrowth not much larger than the spines covering process 4 (Fig. 141). The exopod (Fig. 143) is covered by densely crowded spines, spreading over much of the distal half of the ramus. The two papillae (Fig. 143, *x*) are usually quite prominent.

The mandible is robust and has seven teeth (Fig. 144). The teeth diminish in size gradually towards the proximal end. The two proximal teeth are often overlapped by the ventral cutting blade.

The first maxilla (Fig. 145) has fairly long and cylindrical papillae, with the exception of the reduced ventral papilla, less than half the size of the other two. The terminal setae are short. The exopod is small but easy to observe.

The second maxilla (Fig. 137, 138) has slight terminal inflations but does not form a large collar around the base of the manubrium. In one specimen (Fig. 138), the base of the manubrium was split into two separate parts. The bulla is subspherical.

The maxilliped (Fig. 146–148) is very robust and its body appears to consist of two parts (Fig. 146). The palp (Fig. 148) is very small and in some specimens escapes detection. It is a minute cylinder with a fine projection at its tip. The subchela appears to be devoid of the usual small seta near the base. The place in which this seta is normally located is easily found (Fig. 146, z) but in spite of careful observation from all angles, I was unable to see the seta itself. If present, it must be much smaller than in all other species. Similarly, the claw of the subchela (Fig. 147) is greatly reduced, showing under low magnification as a minute denticle at the tip of the subchela. The auxiliary papilla is present, though also very small.

The trunk length of specimens examined varied from 3.08 to 5.00 mm.

Comments — See *S. jacuticus*, p. 3013.

Salmincola extensus (Kessler, 1868) n.comb.

(Fig. 114–128, 245)

Synonyms — *Lernaeopoda extensa* Kessler, 1868; *Lernaeopoda coregoni* Smith, 1874; *Lernaeopoda maraenae* Olsson, 1877; *Achtheres coregoni* Baumann, 1911; *Achtheres extensus* (Kessler, 1868), Markevich, 1937; *Salmincola wisconsiniensis* Tidd and Bangham, 1945.

Material examined — (Labelled as *Achtheres extensus*) (1) 12 females, *Coregonus lavaretus*, fins, Lake Onega, USSR, 1932, collection of Zoological Institute, Leningrad; (2) 4 females, *Coregonus sardinella*, fins, River Pechora, USSR, 1959, collection of Zool. Institute, Leningrad; (labelled as *Lernaeopoda coregoni*) (3) 2 females, *Coregonus albus*, undated, Michigan, USNM 39575; (labelled as *S. wisconsiniensis*, holotype) (4) 1 female, *Leucichthys artedi clemensi*, Trout Lake, Wisconsin, 1944, USNM 169497; (5) 1 female, paratype, same host and locality, partly dissected on a slide, loaned by Dr G. Hoffman.

Description of the female — The general appearance of *S. extensus* (Fig. 114, 115) is characterized by the great length of its cephalothorax (Fig. 118, 119), which is very slender in its anterior half. The trunk is slender and gradually increases in width towards its posterior extremity. The dorsal surface of the trunk is pitted with two rows of depressions marking the points of attachment of the dorsoventral musculature. The posterior end of the trunk (Fig. 116) has on its ventral side two slits rimmed with heavy cuticle. These are the orifices of the oviducts. The anal orifice is also raised above the surface in a weltlike longitudinal swelling.

The second antenna (Fig. 120, 121) closely resembles that of other species in the subgenus. The basal segment of the endopod has a heavily spinulated pad. The distal segment (Fig. 120) is characterized by the large size of tubercle 3 and by a spiny swelling in the position of ventral process 4. Process 5 arises from the lateral side of the swelling. The apex of the exopod (Fig. 121) is covered by strong spines, scattered but numerous. The papillae (*x*) are slightly larger than the individual spines.

The mandible (Fig. 122) has seven teeth. The terminal four teeth are much larger than the basal three. In Fig. 122 the tip of the mandible is slightly deflected from the horizontal plane, so that the terminal tooth is not seen in its true shape.

The first maxilla (Fig. 123) is small. Its exopod is in the form of a small swelling with a hardly visible setule at the tip. The ventral papilla is much reduced and the central is the largest of the three.

The second maxilla produces a small collar around the base of the manubrium (Fig. 117) and in some specimens almost completely covers this part of the bulla. The bulla is subspherical, though in some specimens it is more flattened and disclike.

The maxilliped (Fig. 124–127) resembles that of the preceding species. It is characterized by the small size of its palp (Fig. 124, *p*) which, however, is relatively larger than that of *S. nordmanni*. The palp forms a small tubercle with a pointed outgrowth at the apex (Fig. 127). The claw of the subchela (Fig. 126) is greatly reduced. It forms a small, curving denticle with an auxiliary papilla near its base. The important distinguishing feature of this species is the presence of a small, transverse group of denticles (Fig. 125) near the tip of the subchela. Although difficult to see when the appendage is in situ, they can be easily detected in interference illumination and in a suitably tilted position of the subchela.

The trunk length of *S. extensus* varies from 4.20 to 4.72 mm.

Comments — See *S. jaculicus*, p. 3013.

Salmincola jaculicus Markevich and Bauer, 1950

(Fig. 129–136, 246)

Material examined — Four females, *Coregonus cylindratus*, pectoral fins, River Vitim (tributary of Lena), USSR, undated, collection of Zoological Institute, Leningrad.

Description of the female — The general appearance of this species (Fig. 129) is characterized by its broad, short trunk. The outline of the cephalothorax (Fig. 128) is of the same type as that of the other species in the subgenus, though rather shorter and broader.

The second antenna (Fig. 132, 133) differs from that of *S. extensus* in having fewer and relatively larger spinules both on the endopod and exopod. Its tubercle 3 is relatively smaller than in the preceding species.

The mandible (Fig. 134) of all specimens examined has only five teeth. The proximal tooth is much smaller than the remaining four, being also partly overlapped by the ventral cutting blade.

The first maxilla (Fig. 135) shows a tendency towards reduction in its dorsal and ventral papillae, although not all maxillae have these papillae reduced to the same extent.

The second maxilla (Fig. 129) is inflated terminally around the base of the manubrium. The bulla is of the same type as those of the previous two species (Fig. 131). One of the specimens had a bulla with a double manubrium (Fig. 130), similar to that on which the description of *S. bicauliculata* was based (cf. p. 3006).

The maxilliped provides no features of taxonomic interest. It closely resembles that of *S. extensus*. The tip of its subchela (Fig. 136) has a transverse group of denticles, similar to, but relatively larger than, those of *S. extensus*.

The trunk length of *S. jaculicus* is between 1.80 and 2.00 mm.

Comments — These comments include questions raised by the descriptions of *S. nordmanni*, *S. extensus*, and *S. jaculicus*.

The most important differences between these three species of *Salmincola* are the proportions of the body, and the shape of the trunk. The differences among their trunks are illustrated in Fig. 245–247. All of these features belong to the category that was earlier in this paper defined as unreliable, and are not recommended as bases for taxonomic decisions. The differences among the structural details of the appendages are such that they can be accommodated within the intraspecific range of variations. Of the three species, *S. nordmanni* is fairly easily distinguished from the other two. It was originally placed in the genus *Basanistes* by Kessler (1868) who considered its trunk as being more

in keeping with those of other *Basanistes* than of the members of the present genus *Salmincola*. *Salmincola nordmanni* alone among *Salmincola* has lateral swellings on the margins of its trunk. It must be stressed that the swellings are in this instance permanent features and are not merely a result of the muscular contractions. Similar outlines of the lateral margins of the trunk can be produced by such contractions, but they cannot be either constant or common, as they are in *S. nordmanni*. Another distinction between it and the two other species is the apparent absence of denticles from the tip of the subchela. The scarcity of the material available did not allow me to determine how definite this difference is. In all, the differences between *S. nordmanni* and the other two suggest that it is a valid species.

The positions of *S. extensus* and *S. jacuticus* are less certain, their differences being restricted to the size and proportions. The only other morphological difference detected was the number of mandibular teeth, seven in *S. extensus* and only five in *S. jacuticus*. Here also more observations are required, since in some species of *Salmincola* the number of teeth is not invariable. It is significant that both these species possess denticles on the tip of the subchela. I am inclined to suppose that *S. jacuticus* is only a local variety of *S. extensus*. Markevich (1956) stressed the existence of similarity between *S. jacuticus* and *S. extensus* but had to place it in a separate taxon, because *S. extensus* was then believed to belong to a different genus.

As regards *S. wisconsiniensis*, its original description (Tidd and Bangham, 1945) stressed its elongated shape and in particular the length of its cephalothorax. Having examined the type material of this species, I was unable to confirm the existence of this feature. Figure 119 shows the outline of the cephalothorax of the holotype specimen of *S. wisconsiniensis*. Comparison with that of a typical *S. extensus* (Fig. 118) shows the difference between them to be negligible. There were no other significant morphological differences. Spinulation of the subchela was present in both species. Consequently, the existence of *S. wisconsiniensis* is untenable.

Salmincola extumescens (Gadd, 1901)

(Fig. 149–164)

Synonyms — *Lernaeopoda extumescens* Gadd, 1901; *Lernaeopoda inermis* Wilson, 1911; *Salmincola inermis* (Wilson, 1911), Wilson, 1915; *Salmincola omuli* Messjatzeff, 1926.

Material examined — (Labelled as *S. extumescens*) (1) 1 female, *Coregonus lavaretus*, gill chamber, Lake Onega, USSR, 1932, collection of Zoological Institute, Leningrad; (2) 1 female, same host, Lake Ladoga, USSR, 1947, collection of Zoological Institute, Leningrad; (3) 1 female, *Coregonus autumnalis*, Lake Taimyr, USSR, 1948, collection of Zoological Institute, Leningrad; (4) 3 females, *Coregonus* sp., gills, Nueltin Lake, Canada, 1947, USNM 86197; (labelled as *S. inermis*) (5) 1 female, *Coregonus* sp., Yukon, Alaska, undated, USNM 6113; (6) numerous females, *Leucichthys harengus*, gill cavity, Saginaw Bay, Michigan, 1910, USNM 42278; (7) 1 female, same host, Knife River, Michigan, undated, USNM 42283 (this specimen is the holotype of *S. inermis*); (8) 1 female, same host, Lake Huron, USNM 42284 (paratype of *S. inermis*); (9) 1 female, same host, Lake Superior, undated, USNM 42285 (paratype); (10) 5 females, same host, gill chamber, Lake Superior, undated, USNM 49775; (11) 2 females, same host, gill cavity, Lake Michigan,

undated, USNM 49787; (12) 1 female, *Coregonus* sp., Fort George, Canada, undated, USNM 60468; (13) numerous females, *Leucichthys harengus*, gill chamber, Saginaw Bay, Michigan, undated, USNM 69907; (14) numerous females, same host and locality, undated, USNM 74373; (labelled as *S. omuli*) (15) 1 female, *Coregonus lavaretus*, Lake Baykal, USSR, undated, USNM 62773.

Description of the female — The general appearance of *S. extumescens* is distinguished (Fig. 149, 150) by the curving line of its dorsum, the fairly long cephalothorax (Fig. 156) and, when present, the shape of the egg sacs. Unlike those of any other species of the genus, these sacs curve and tend to lie along the sides of the trunk, as in Fig. 150, or even to cross in front of the trunk. The posterior end of the trunk bears some resemblance to that of *S. extensus* but the orifices of the oviducts form slits on the surface of the trunk which are much more oblique than in that species (Fig. 152).

The second antenna (Fig. 153–155, 157) clearly distinguishes this species from all the other species of the subgenus, since its endopod lacks a spinulated swelling in the ventral region of the distal segment. That segment (Fig. 153–155) has a very large tubercle 3. The structure of ventral processes 4 and 5 is rather variable, particularly the size of process 4. In Fig. 155 it is slightly larger than process 5, but in Fig. 154 it is several times larger. Intermediate size relationship is shown in Fig. 153. The exopod (Fig. 157) is profusely spinulated. In some specimens its two papillae (*x*) have strongly inflated bases.

The mandible (Fig. 158, 159) has either seven or eight teeth, though the former number is much more common. As in the related species, the two or three proximal teeth are much smaller and the first tooth is sometimes overlapped by the ventral cutting blade.

The first maxilla (Fig. 160) has a reduced ventral papilla. In some specimens it is difficult to see, particularly when the maxilla tilts away from the horizontal. The other two papillae are of about the same size. (The seta of the dorsal papilla in Fig. 160 is tilted towards the observer and appears foreshortened.) The exopod is in the form of a small, conical swelling. Its terminal setule is seldom obvious.

The second maxilla (Fig. 149–151) does not form any terminal swelling, but tapers towards the manubrium of the bulla (Fig. 151). The manubrium is fairly long (Fig. 149) and the disc of the bulla is a flat, circular structure of very wide diameter. In some specimens this diameter exceeds half of the trunk length. In preserved specimens some bullae are damaged so that the disc inflates, its two surfaces separating. In others, the disc is flat and thin.

The maxilliped (Fig. 161–164) is covered by particularly heavy cuticle. Its division into two parts is rather less evident than in the other species of the subgenus. The palp (Fig. 161, *p*) is very small, soft, and papilliform (Fig. 163), usually pointed at the tip. In some specimens it shows some signs of subdivision by a transverse constriction. The claw of the subchela (Fig. 162) is reduced to a small hook, though it is more prominent than in the other species of the subgenus. The auxiliary papilla is very small.

The trunk length of the Palearctic specimens varies from 4.82 to 5.90 mm, the disc diameter of the bulla is between 2.90 and 4.56 mm. For the Nearctic specimens the corresponding figures are: trunk length 3.73–4.65 mm, disc diameter 3.07–3.82 mm.

Comments — The absence of the denticles on the tip of the subchela, and of the spinulation of the distal segment of the endopod of the second antenna, make this species readily identifiable. The gross morphology is also distinctive enough, the curving egg sacs and the wide disc of the bulla being easily noticed clues to the identity of *S. extumescens*.

In connection with *S. extumescens*, it is necessary to discuss the taxonomic status of *Achtheres corpulentus* Kellicott. Known since 1880, this parasite was many times recorded on the coregonid fishes in the Great Lakes area. With one exception, however, all these records come from the end of the 19th century. The original description (Kellicott, 1880) under the name of "herring

gill-sucker" is rather superficial. The following points can be accepted: the bulla is a wide, flat disc with a long manubrium, the egg sacs are upturned and lie along the sides of the trunk. The trunk itself has a characteristically convex dorsum. All these features fit exactly the description of *S. extumescens*. Wilson (1915) quotes many records of *A. corpulentus* but all of them are prior to 1900. It is interesting to note that with the description of *S. extumescens* in 1901 and its redescription (Wilson, 1911), all records of *A. corpulentus* ceased. From that time on *S. inermis* (= *S. extumescens*) begins to appear in the literature as a parasite of the hosts of *A. corpulentus* in the Great Lakes. One is tempted to assume that *A. corpulentus* and *S. extumescens* are identical. The situation is complicated somewhat by the record of the occurrence of these two species together (Mueller, 1937) on the gills of *Leucichthys artedi* in Lake Ontario. An earlier report from the same lake (Pritchard, 1931) mentions only *Salmincola inermis*. No type material of *A. corpulentus* is extant. According to Mueller (personal communication), the specimens he identified as *A. corpulentus* are also no longer available. Under the circumstances, *A. corpulentus* must be considered as species inquirenda. Should it be proved that it is identical with *S. extumescens*, its name would have to be adopted as chronologically prior to that given to the species by Gadd (1901).

Salmincola strigatus (Markevich, 1936) n.comb.

(Fig. 240, 243, 244)

Synonym — *Achtheres strigatus* Markevich, 1936.

No specimens of this species were available for examination. This description is, therefore, based on the original description of the species. Only those features that could be used for diagnostic purposes are considered.

Description of the female — The original decision to place it in the genus *Achtheres* was in part due to the apparent segmentation marks on the trunk, as illustrated in Fig. 240. The inadvisibility of the use of this characteristic in the taxonomy of Lernaeopodidae has been discussed already. Unlike *S. nordmanni*, *S. strigatus* has indentations in the outline of the lateral margins of the trunk caused by muscular contractions. The same is true of the dorsal transverse markings. The posterior extremity of the trunk shows clearly that the species belongs to the genus *Salmincola*.

The second antenna (Fig. 243), as far as can be judged from the original illustration, possesses a spinulated swelling in the position of the ventral process 4. This places it in relationship with *S. nordmanni*, *S. extensus*, and *S. jacuticus*. No known species of *Achtheres* has this kind of structure. Sparse spinulation is present on the tip of the exopod.

The shape of the bulla is of great importance in determining the separate identity of this species. Markevich (1956) describes it as follows: "The organ of attachment has a short stalk and somewhat resembles the shape of a hoof." This rather irregular shape can be seen also in Fig. 240. Departing radically from the radially symmetrical structures of the bullae in the subgenus, it strongly suggests that the species is valid.

Of the other appendages only the maxilliped (Fig. 244) can be seen as having any diagnostic value. The presence of a reduced claw of the subchela places it in the subgenus *Brevibrachia*. Unfortunately, it cannot be determined whether any spinulation is present at the tip of the subchela.

The trunk length of *S. strigatus* is 2.8 mm (Markevich, 1956).

SPECIES INQUIRENDAE

Salmincola heintzi (Neresheimer, 1909)

Synonym — Lernaeopoda heintzi Neresheimer, 1909.

The original description of this species, based on examination of six specimens, is inadequate for definite identification. The general appearance (Neresheimer, 1909, fig. 6) resembles that of *S. edwardsii*. The identity of the host, a member of the genus *Salvelinus*, also suggests that Neresheimer dealt with *S. edwardsii*. However, the description involved only the bulla, other structures not being mentioned. Consequently, there is no basis for comparisons.

The type specimens of *S. heintzi* were destroyed in Munich during the second world war (H. H. Reichenbach-Klinke, personal communication). It is doubtful, therefore, if the identity of this species can ever be established.

Salmincola lata Markevich, 1940

(Fig. 241)

Earlier, I placed this species tentatively in the synonymy of *S. californiensis*. The only illustration known is that by Markevich (1940), showing its general appearance (Fig. 241). It fits well with the drawings of *S. californiensis* (Fig. 53–61). No records of *S. lata* have been made subsequent to the original description. The recorded type host is *Oncorhynchus keta*, from the fins of which the type specimens were collected in 1886. If these specimens are still available in the USSR, their identity can now be definitely established.

KEY TO THE SPECIES OF *SALMINCOLA*

1 Maxilliped with normally developed claw (about $\frac{1}{3}$–$\frac{1}{4}$ length of rest of subchela) 2
Maxilliped with greatly reduced claw 10

2 Length of maxilliped palp between $\frac{1}{3}$ and $\frac{1}{2}$ length of subchela (exclusive of claw) and more than twice palp's diameter at base 3
Length of maxilliped palp not greater than $\frac{1}{3}$ length of subchela (exclusive of claw) and equal to or slightly greater than palps's diameter 4

3 Bulla long, clavate ..... *S. thymalli*
Bulla of irregular shape, one side flat or slightly concave ..... *S. coregonorum*

4 Ventral side of basal segment of endopod of second antenna with large, smooth, tapering outgrowth; bulla stellate ..... *S. stellatus*
Ventral side of basal segment of endopod of second antenna with spiny pad; bulla not stellate 5

5 Ventral side of terminal segment of endopod of second antenna with one process as large as, or larger than, dorsal hook and another much smaller process ..... *S. edwardsii*
Ventral side of terminal segment of endopod of second antenna with very large semispherical swelling tipped by two small, conical processes ..... *S. siscowet*
Ventral side of terminal segment of endopod of second antenna with two processes, often arising from common base and either equal or subequal in size 6

6 Bulla ovate, with one side flat or somewhat concave ..... *S. salmoneus*
Bulla not ovate 7

7 Length of first maxilla (exclusive of terminal papillae) only slightly greater than its width ..... *S. lotae*
Length of first maxilla (exclusive of terminal papillae) at least twice its width 8

8 Tip of subchela of maxilliped denticulated near base of claw.....*S. cottidarum*
Tip of subchela of maxilliped not denticulated near base of claw.....9
9 Tip of exopod of second antenna with many large spines.....*S. californiensis*
Tip of exopod of second antenna unarmed save for two papillae.....*S. carpionis*
10 Terminal segment of endopod of second antenna without large denticulated process.....*S. extumescens*
Terminal segment of endopod of second antenna with large denticulated process.....11
11 Bulla irregular, its disc hoof-shaped.....*S. strigatus*
Bulla more or less spherical, with short manubrium.....12
12 Subchela of maxilliped without denticles at base of claw; trunk with three swellings on each lateral margin.....*S. nordmanni*
Subchela of maxilliped with denticles at base of claw; trunk with smooth lateral margins.....*S. extensus* and *S. jaculicus*

DISTRIBUTION AND HOST AFFILIATION OF *SALMINCOLA*

The reduction of the genus *Salmincola* to 15 species, as well as introducing more reliable criteria to the taxonomy of this genus, allows one to draw broad outlines of its distribution range and its host affiliations. I refrain deliberately from the use of the term "specificity." We know as yet too little about the biology of *Salmincola* to speak of its specificity in the strict sense.

The literature concerning *Salmincola* is replete with misleading records and poorly identified host fishes. This is not surprising. Correct identification of *Salmincola* was hardly possible while its taxonomy was in disorder. The taxonomy of its host fishes was in no better shape. It is more profitable, therefore, to discuss *Salmincola* in broad terms, always keeping in mind the existence of a wide margin of variability, very characteristic of this genus. Adaptability and pliability must be expected. The host fishes of *Salmincola* are an active and vigorous group from the point of view of evolution. They are on the move, and so is *Salmincola*.

The distribution of the individual species of *Salmincola* is summarized graphically in Fig. 248. As regards the type of their distribution, they fall within one of three categories: circumpolar, continental, and bicontinental. The second and third categories can be further subdivided, as shown in the table below:

Category	*Distribution*	*No. species*
Circumpolar	Circumpolar	5
Continental	Palearctic	7
Continental	Nearctic	1
Bicontinental	Atlantic	1
Bicontinental	Pacific	1

The species classified as Palearctic are exclusive to the Old World and those as Nearctic to the New World. Those described as bicontinental have a distribution that straddles an ocean. The Atlantic species occurs along both European and American shores of the Atlantic, whereas the Pacific species lives in the American and Asian coastal areas.

A third of all species of *Salmincola* are circumpolar, both subgenera being represented among them. Two of these species are parasitic on the genus *Salvelinus*. Both species can be found on various populations of *Salvelinus*, often in the same locality or even on the same fish. These species are *S. carpionis* and *S. edwardsii*, clearly distinguishable from each other and differing to some extent in their preferred habitat on the host. *Salmincola carpionis* occurs more often on the fins and within the buccal and branchial cavities. *Salmincola edwardsii* is more common on the gills. Some degree of habitat overlap is, however, quite common. The third circumpolar species is *S. thymalli*, a parasite of the genus *Thymallus*. Also an easily distinguishable species, it is sometimes found on fishes other than *Thymallus*. The remaining two species in this category are *S. extensus* and *S. extumescens*, both parasitic on various species of *Coregonus* and related fishes.

Eight species are in the continental category. Seven of them are Palearctic and only one Nearctic. At least some of them seem to be related to, or even derived from, the circumpolar species. Thus, *S. siscowet* might be derived from *S. edwardsii*. Some characteristics of *S. cottidarum* are also reminiscent of *S. edwardsii*, though a direct relationship is more difficult to propose in this instance. *Salmincola coregonorum* is probably a descendant of *S. thymalli*, *S. lotae* could be derived from *S. carpionis*, and *S. jacuticus* is almost certainly an offshoot of *S. extensus*, if, indeed, not its synonym.

The host affiliations of the continental species cannot be easily summarized. Some of them are parasitic on the hosts of their presumed parent species or related fishes. *Salmincola siscowet* parasitizes a species of *Salvelinus*, as does *S. edwardsii*. The members of the subgenus *Brevibrachia* are parasitic on the coregonid fishes, but so also is *S. coregonorum*, the only member of the subgenus *Salmincola*, possibly derived from *S. thymalli*. Two species became adapted to parasitism on nonsalmonid fishes. *Salmincola lotae* is parasitic on a gadid and *S. cottidarum* on several cottid species. This departure from association with the group of hosts normal for the genus is not unique. *Salmincola* gave rise to other genera of Lernaeopodidae parasitic on freshwater fishes other than salmonids. A good example of this is the genus *Achtheres*, closely related to *Salmincola* but living on the percoid and siluroid fishes.

The continental species usually have a very restricted distribution. Probably the most widespread among them is *S. coregonorum*, occurring in many European localities in a disconnected manner. Others are less widely dispersed. *Salmincola siscowet* is known only from the Great Lakes of North America, *S. stellatus* from the Far East, *S. lotae* and *S. nordmanni* from northern Europe, and *S. strigatus* and *S. jacuticus* from Siberia. Whether this can be taken as indicative of the more recent origin of these species, is difficult to say. This suggestion is at least possible.

The bicontinental species occur in the coastal areas of two continents bordering upon the same ocean. The type species, *S. salmoneus*, occurs mainly on *Salmo salar* in Europe and in the eastern areas of North America, spreading as far as the distribution of the host species. The other bicontinental species

is *S. californiensis*. Parasitic mainly on the species of *Oncorhynchus*, *S. californiensis* inhabits the Pacific rim, being found in all areas colonized by *Oncorhynchus*.

I hope that this new appreciation of the genus *Salmincola* will prove useful to those interested in the problems of phylogeny of the salmonid fishes. Only a better knowledge of their phylogeny can explain the much greater abundance of species of *Salmincola* in the Old World (14 out of 15) than in the New World (8 out of 15).

ACKNOWLEDGMENTS

I wish to thank all those colleagues, scattered over the world, who went out of their way to provide me with specimens and literature, as well as those who gave me the benefit of their views. It is my pleasant duty to acknowledge assistance from the following (mentioned in alphabetical order of their countries); Dr L. R. Richardson (Australia); Dr L. Margolis and Mr J. H. C. Pippy (Canada); Dr Torben Wolff (Denmark); Dr C. R. Kennedy, Dr J. D. Slinn, and Mr W. A. Smith (Great Britain); Dr L. B. Holthuis (Holland); Dr S. Kamegai and Dr T. Hoshina (Japan); Dr Roy Oleröd (Sweden); Dr R. Cressey, Dr J. F. Mueller, Dr J. H. Wales, Dr R. R. Rucker, Dr G. Hoffman, and Mr E. E. Arnold (USA); and Dr O. N. Bauer, Dr A. V. Gusev and Dr E. A. Koryakov (USSR).

REFERENCES

BLAINVILLE, H. M. D. DE. 1822. Mémoire sur les Lernées (*Lernaea*, Linn.). J. Phys. Chim. Hist. Nat. 95: 372–380, 437–447.

DEDIE, O. 1940. Étude de *Salmincola mattheyi* n. sp., copépode parasite de l'omble-chevalier (*Salmo salvelinus* L.). Rev. Suisse Zool. 47: 1–63.

FOWLER, H. W. 1913. The Crustacea of New Jersey. Rept. New Jersey Museum 1911: 29–650.

GADD, P. 1901. Nagra förut oberskrifna, parasitisk lefvante copepoder. Medd. Soc. Fauna Flora Fennica 27: 98–100, 181–182.

GISSLER, N. 1751. Ron om laxens natur och fiskande i de norrlandska alfvarna. Kgl. Svenska Vetenskapsakad. Handl. 12: 171–190.

GURNEY, R. 1933. British freshwater Copepoda. Vol. 3. Ray Soc., London. p. i–xxix, 1–384.

HANSEN, H. J. 1923. Crustacea Copepoda, II. Copepoda parasita and hemiparasita. Danish Ingolf Expedition 3(7): 1–92.

KABATA, Z. 1963 *Clavella* (Copepoda) parasitic on British Gadidae: one species or several? Crustaceana 5: 64–74.

1964. Revision of the genus *Charopinus* Krøyer, 1863 (Copepoda: Lernaeopodidae). Videnskabelige Medd. Dansk Naturhist. Foren. 127: 85–112.

1968. Some Chondracanthidae (Copepoda) from fishes of British Columbia. J. Fish. Res. Bd. Canada 25: 321–345.

KELLICOTT, D. S. 1880. On certain Crustacea parasitic on fishes from the Great Lakes. Proc. Am. Soc. Microscopists 1: 53–57.

KESSLER, K. 1868. [Contributions to knowledge of Lake Onega and its region.] Suppl. Proc. First Congress Russian Naturalists, St. Petersbourg. 143 p. (In Russian.)

KORYAKOV, E. A. 1959. [Neo-endemic parasite from the Baykal found in the basin of Lena.] Trudy Soveshch. Ikhtiologicheskoi Komis. (Trudy Soveshch. Bol. Rybn.) 9: 168–173. (In Russian.)

KRØYER, H. 1837. Om snyltekrebsene, isaer med hensyn til den danske fauna, III. Formbeskrivelser. Naturhist. Tidsskr. 1: 252–304.

1863. Bidrag til kundskab om snyltekrebsene. Naturhist. Tidsskr., Ser. 3, 2: 75–423.

LAMARCK, G. B. P. DE. 1816. Histoire naturelle des animaux sans vertèbres. Vol. 3. Deterville and Verdiere, Paris. 568 p.

LINNAEUS, C. A. 1758. Systema Naturae. 10th ed. p. 655.

MARKEVICH, A. P. 1936. [New representatives of the family Lernaeopodidae (Copepoda parasitica).] Zbirnyk Prats' Zoologichnoho Muzeyu Akad. Nauk Ukr. SSR 17: 103–105. (In Ukrainian.)

1940. [New species of parasitic copepods.] Dopovidi Akad. Nauk Ukr. RSR 11: 11–16. (In Ukrainian, German text p. 17–21.)

1956. [Parasitic Copepoda of fishes of the USSR.] Kiev Akad. Nauk Ukr. SSR. 259 p. (In Russian.)

MESSJATZEFF, I. I. 1926. Parasitische Copepoden aus dem Baikal-See. Arch. Naturgeschichte 92A: 120–134.

MIERS, E. J. 1877. Report on the Crustacea collected by the naturalists of the Arctic Expedition in 1875–1876. Ann. Mag. Nat. Hist. (Ser. 4) 20: 52–66, 96–110.

MUELLER, J. F. 1937. Parasitism and diseases in fishes of the Lake Ontario watershed, p. 211–225. *In* A biological survey of the Lake Ontario watershed. Ann. Rept. New York State Conserv. Dept. 29 (Suppl.)

NERESHEIMER, E. 1909. Studien über süsswasser Lernäpodiden. Ber. Kgl. Bayerischen Biol. Versuchsta. 2: 1–9.

NORDMANN, A. VON. 1832. Erster Beitrag zur Naturgeschichte der Lernäen. Mikrograph. Beitr. Naturgeschichte Wirbellosen Thiere 2: 49–150.

OLSSON, P. 1869. Prodromus faunae copepodorum parasitantium Scandinaviae. Acta Univ. Lundensis 1868: 1–49.

PRITCHARD, A. L. 1931. Taxonomic and life history studies on the ciscoes of Lake Ontario. Univ. Toronto Studies, Biol. Ser. 35, Publ. Ont. Fish. Res. Lab. 41: 1–78.

SANDEMAN, I. M., AND J. H. C. PIPPY. 1967. Parasites of freshwater fishes (Salmonidae and Coregonidae) of insular Newfoundland. J. Fish. Res. Bd. Canada 24: 1911–1943.

SMITH, S. I. 1874. The crustacean parasites of the fresh-water fishes of the United States. Rept. U.S. Comm. Fish Fish. 1872–1873: 661–665.

STEPHENSEN, K. 1912. Report on the Malacostraca, Pycnogonida and some Entomostraca collected by the Denmark-Expedition to North-East Greenland. Zool. East Greenland 45: 501–630.

1940. Parasitic and semiparasitic Copopeda. Zool. Iceland 3(34): 1–24.

1943. Marine Ostracoda, parasitic and semiparasitic Copepoda and Cirripedia. Zool. East Greenland 121(9): 1–24.

STOLL, N. R. ET AL. [ed. comm.] 1961. International code of zoological nomenclature adopted by the XV International Congress of Zoology, London. Intern. Trust Zool. Nomenclature, London. 176 p.

TIDD, W. M., AND BANGHAM, R. V. 1945. A copepod parasite of the cisco from Trout Lake, Wisconsin. Ohio J. Sci. 45: 82–84.

WESENBERG-LUND, C. 1895. Fersk och saltvandsentomostraca. Zool. East Greenland 19: 133–143.

WILSON, C. B. 1908. North American parasitic copepods. A list of those found upon the fishes of the Pacific coast, with description of new genera and species. Proc. U.S. Natl. Museum 35: 431–481.

1911. North American parasitic copepods. Description of new genera and species. Proc. U.S. Natl. Museum 39: 625–634.

1915. North American parasitic copepods belonging to the Lernaeopodidae, with a revision of the entire family. Proc. U.S. Natl. Museum 47: 565–729.

YAMAGUTI, S. 1963. Parasitic Copepoda and Branchiura of fishes. Interscience, New York, London, and Sydney. 1104 p.

(FIGURES 2–248 *follow*)

LIST OF ABBREVIATIONS

a — ventral seta of maxilliped subchela
aux — auxiliary papilla of maxilliped subchela
bp — broken palp of maxilliped
en — endopod
en 1 — basal segment of endopod
en 2 — terminal segment of endopod
es — egg sac
ex — exopod
gp — genital process
m — manubrium
mxp — maxilliped
mx 2 — second maxilla
p — palp of maxilliped
s — spiny pad of sympod of second antenna
sp — spermatophore
w — swelling on subchela of maxilliped
x — papilla of exopod of second antenna
y — spine of exopod of second antenna
z — location of ventral seta on subchela of maxilliped

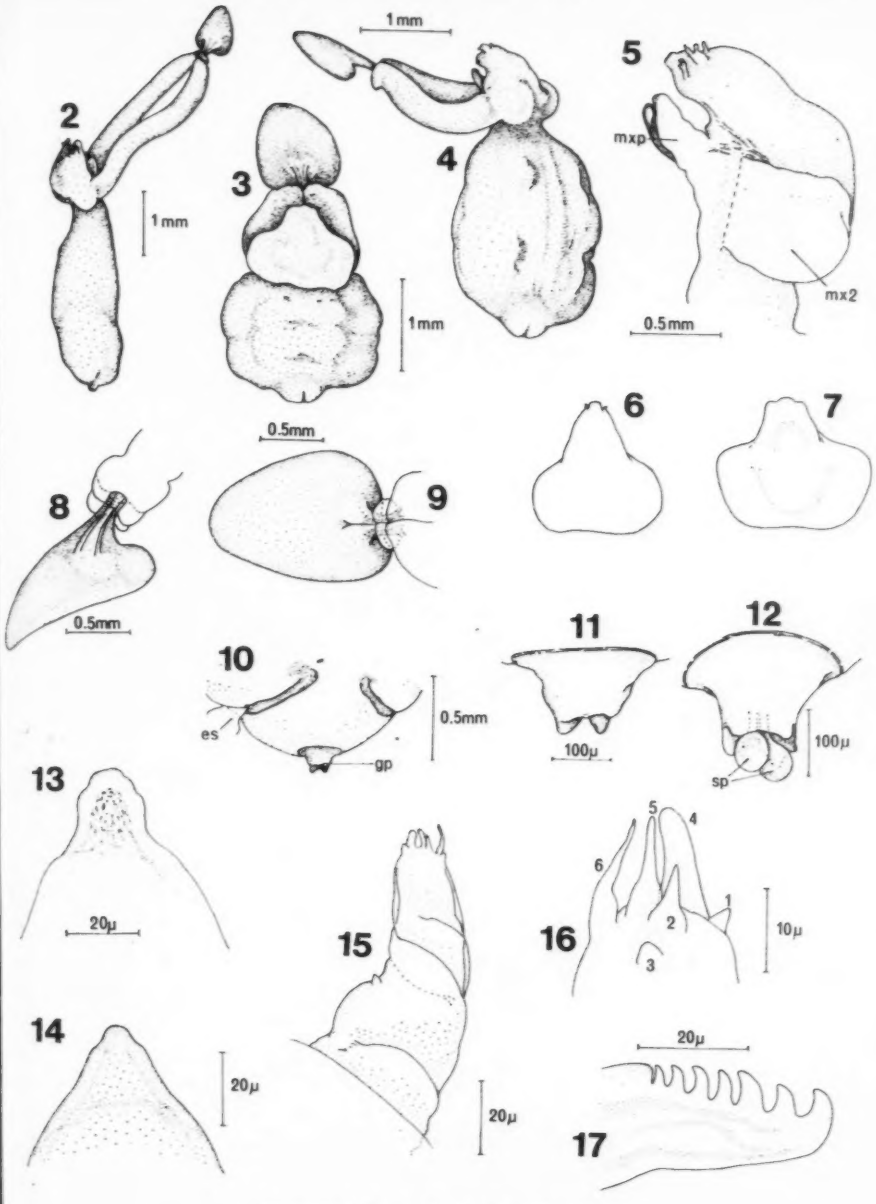

FIGURES 2–17. ***Salmincola salmoneus.***

Fig. 2. Female from North-East Scotland, entire, lateral; Fig. 3. Female from a smolt in New Brunswick, entire, dorsal; Fig. 4. Female from adult salmon in New Brunswick, entire, dorsolateral; Fig. 5. Cephalothorax, lateral; Fig. 6 and 7. Outlines of cephalothorax, diagrams; Fig. 8. Bulla, lateral; Fig. 9. Same, dorsal; Fig. 10. Posterior extremity of trunk, ventral; Fig. 11 and 12. Genital process, ventral; Fig. 13 and 14. Tip of upper lip, dorsal; Fig. 15. First antenna, entire, dorsal; Fig. 16. Same, tip, dorsal; Fig. 17. Mandible, distal part, lateral.

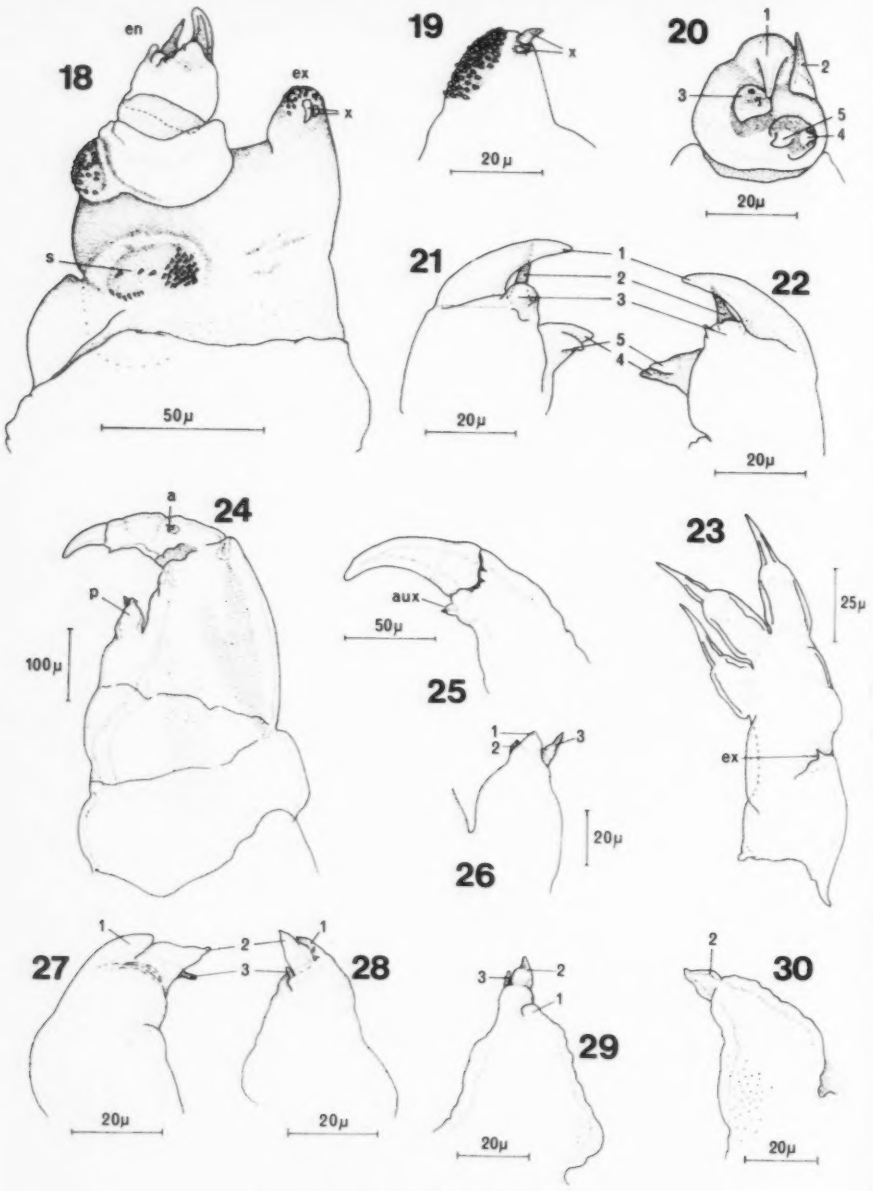

FIGURES 18–30. ***Salmincola salmoneus.***

Fig. 18. Second antenna, entire, lateral; Fig. 19. Same, exopod, dorsolateral; Fig. 20. Same, endopod, ventral; Fig. 21 and 22. Same, lateral; Fig. 23. First maxilla, lateral; Fig. 24. Maxilliped, entire, ventral; Fig. 25. Same, claw, ventral; Fig. 26–30. Same, palp.

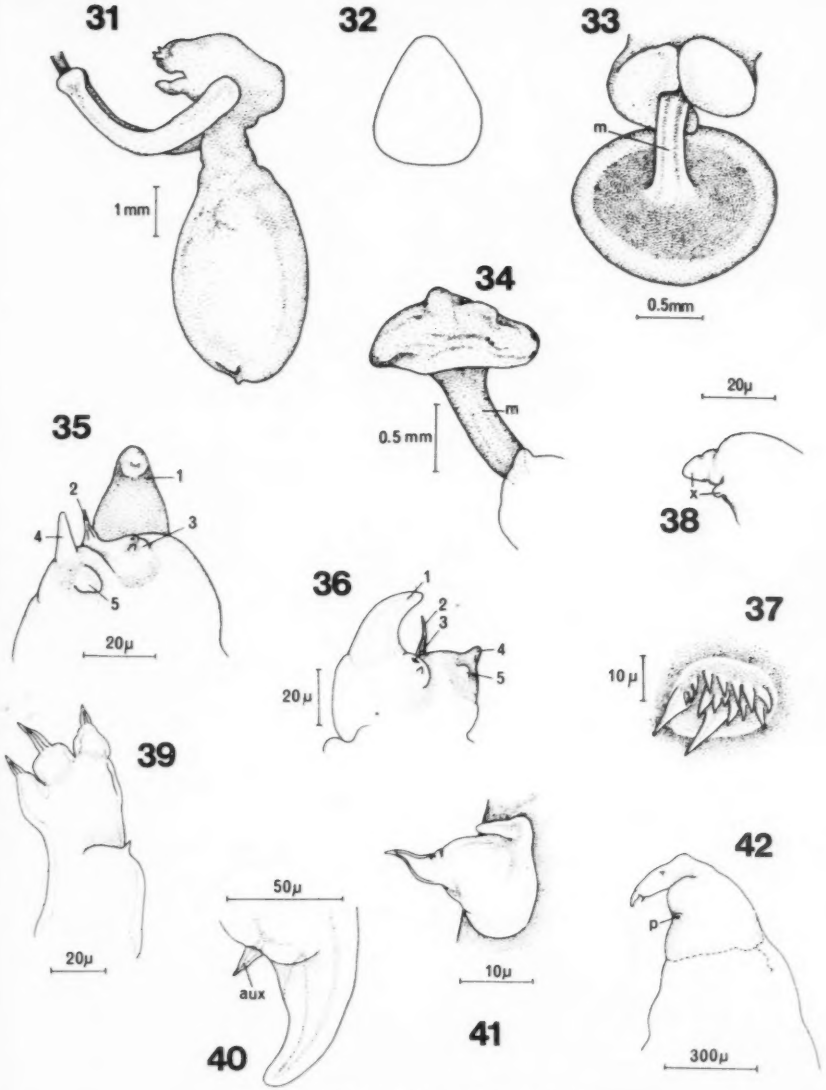

FIGURES 31–42. ***Salmincola carpionis.***

Fig. 31. Female, entire, lateral; Fig. 32. Cephalothorax outline; Fig. 33. Bulla, concave surface; Fig. 34. Same, lateral; Fig. 35. Second antenna, tip of endopod, ventral; Fig. 36. Same, lateral; Fig. 37. Same, spiny pad of sympod; Fig. 38. Same, tip of exopod, dorsal; Fig. 39. First maxilla, lateral; Fig. 40. Maxilliped, claw, ventral; Fig. 41. Maxilliped, palp, ventral; Fig. 42. Maxilliped, entire, ventral.

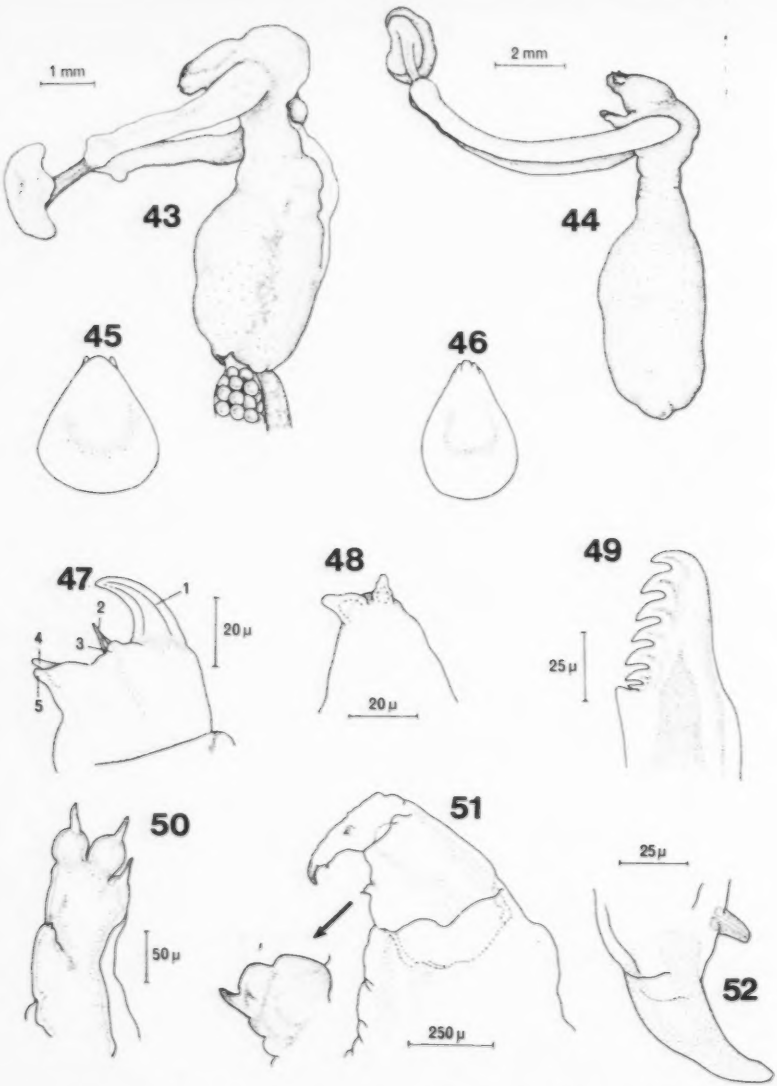

FIGURES 43–52. ***Salmincola carpionis.*** (Names after captions refer to the synonyms under which specimens were known previously.)

Fig. 43. Female, entire, lateral (*gibber*); Fig. 44. Same (*smirnovi*); Fig. 45. Cephalothorax outline (*gibber*); Fig. 46. Same (*smirnovi*); Fig. 47. Second antenna, tip of endopod, lateral (*smirnovi*); Fig. 48. Same, tip of exopod, lateral (*smirnovi*); Fig. 49. Mandible, distal part, lateral (*smirnovi*); Fig. 50. First maxilla, lateral (*smirnovi*); Fig. 51. Maxilliped, entire, ventral, arrow points to enlarged view of palp (*smirnovi*); Fig. 52. Same, tip of subchela, ventral (*smirnovi*).

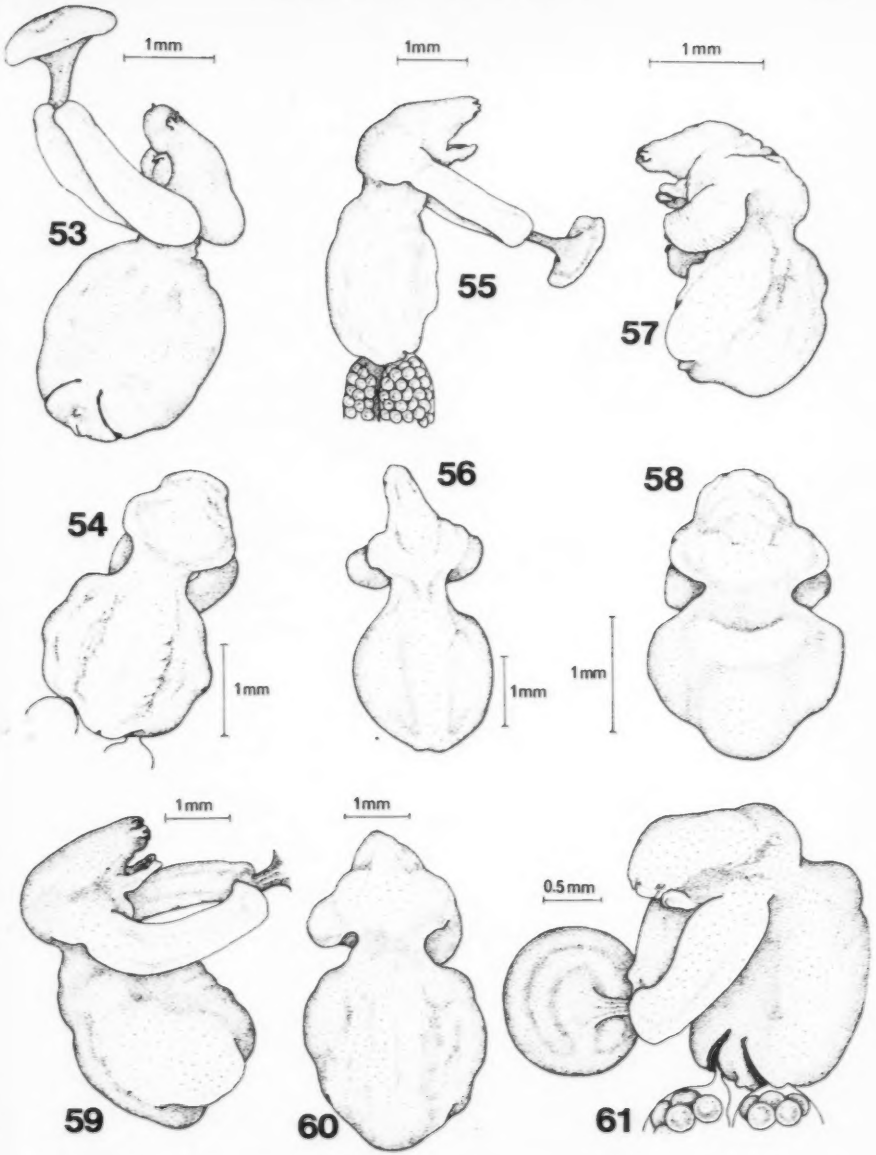

FIGURES 53–61. ***Salmincola californiensis.*** (Names after captions refer to synonyms under which specimens were known previously.)
Fig. 53. Female, entire, ventrolateral (*californiensis*); Fig. 54. Same, dorsal (*californiensis*); Fig. 55. Same, lateral (*beani*); Fig. 56. Same, dorsal (*beani*); Fig. 57. Same, lateral (*carpenteri*); Fig. 58. Same, dorsal (*carpenteri*); Fig. 59. Same, lateral (*falculata*); Fig. 60. Same, dorsal (*falculata*); Fig. 61. Same, ventrolateral (*yamame*).

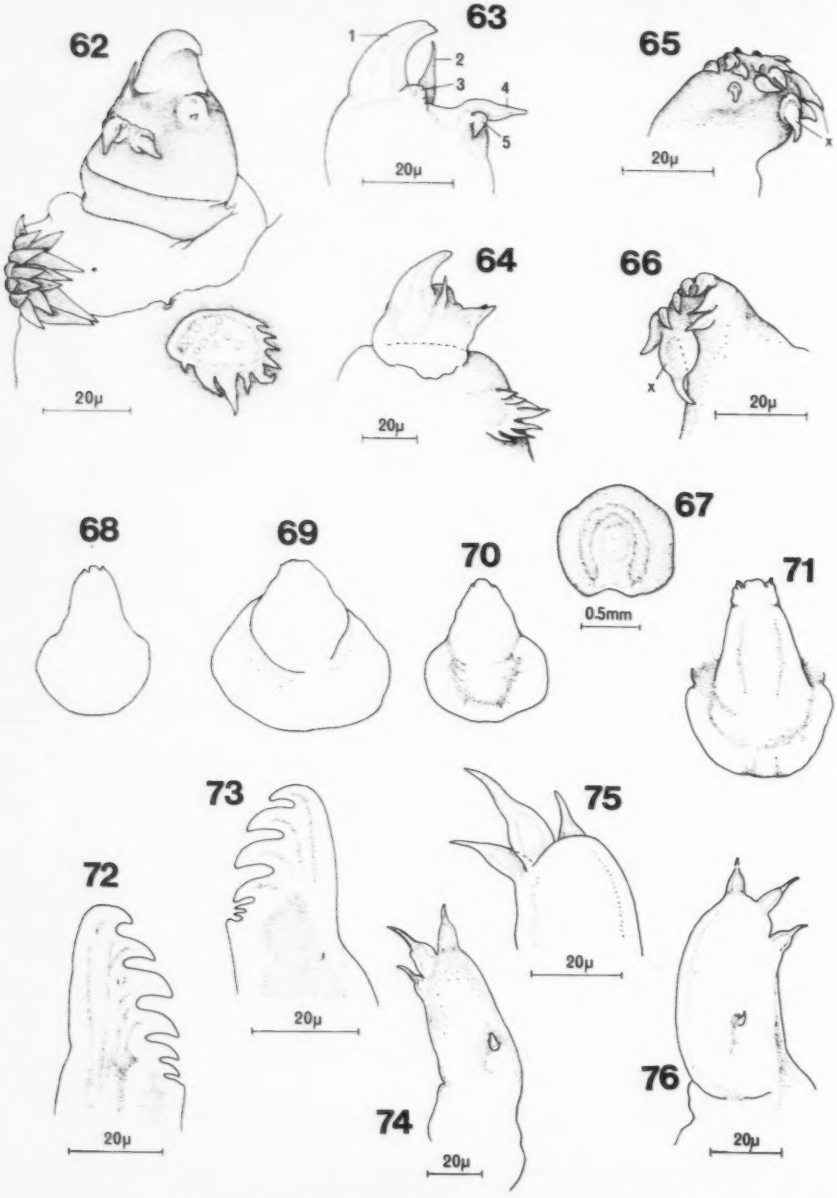

FIGURES 62–76. ***Salmincola californiensis.*** (Names after captions refer to synonyms under which specimens were known previously.)

Fig. 62. Second antenna, endopod and part of sympod (*californiensis*); Fig. 63. Same, tip of endopod, lateral (*californiensis*); Fig. 64. Same (*beani*); Fig. 65. Same, expod (*californiensis*); Fig. 66. Same (*falculata*); Fig. 67. Bulla, distal surface (*beani*); Fig. 68 and 69. Cephalothorax outline (*californiensis*); Fig. 70. Same (*carpenteri*); Fig. 71. Same (*beani*); Fig. 72. Mandible, distal part, lateral (*californiensis*); Fig. 73. Same (*carpenteri*); Fig. 74. First maxilla, lateral (*californiensis*); Fig. 75. Same, distal part with abnormally developed dorsal papilla (*falculata*); Fig. 76. Same, entire, with underdeveloped papillae (*falculata*).

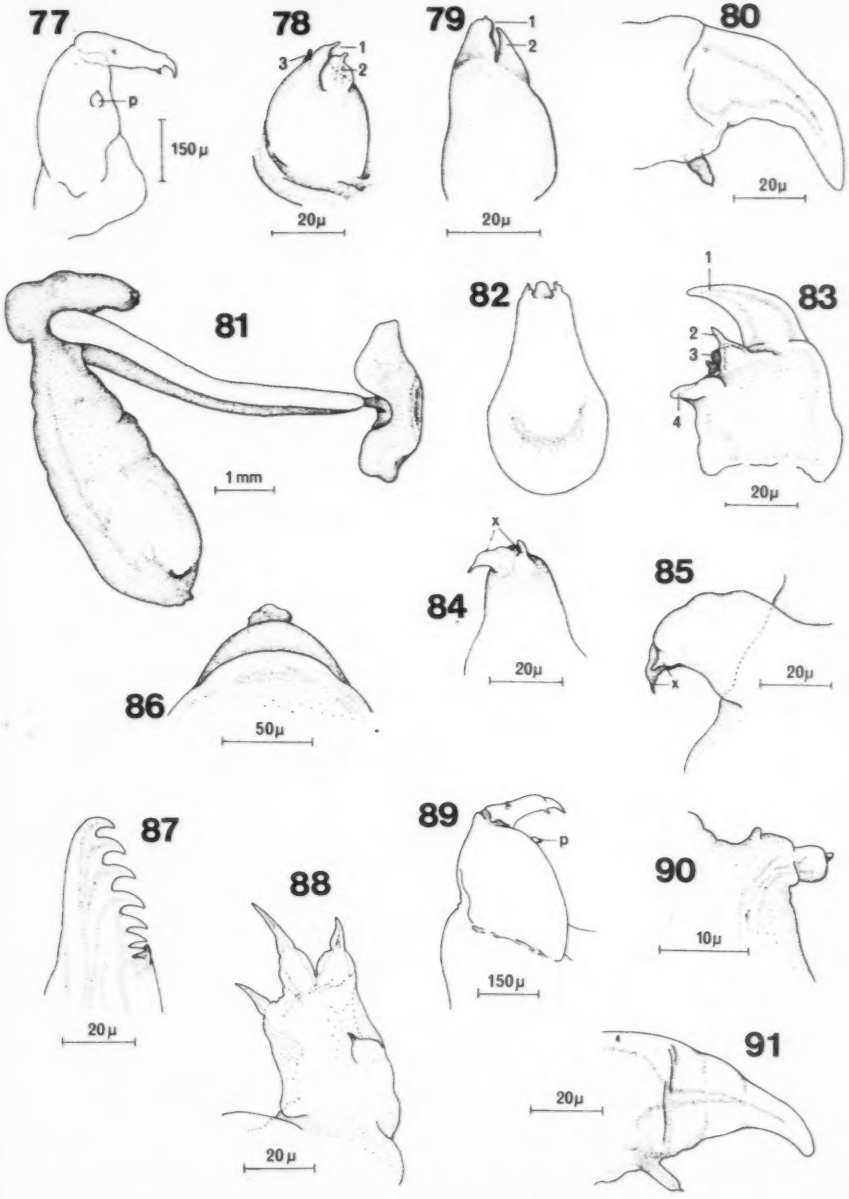

FIGURES 77–80. ***Salmincola californiensis.***

Fig. 77. Maxilliped, entire, ventral; Fig. 78. Same, palp, ventral; Fig. 79. Same; Fig. 80. Maxilliped, tip of subchela, ventral.

FIGURES 81–91. ***Salmincola lotae.***

Fig. 81. Entire, lateral; Fig. 82. Cephalothorax outline; Fig. 83. Second antenna, tip of endopod, lateral; Fig. 84. Same, exopod, lateral; Fig. 85. Same, dorsal; Fig. 86. Upper lip, dorsal; Fig. 87. Mandible, distal part, lateral; Fig. 88. First maxilla, entire, lateral; Fig. 89. Maxilliped, entire, ventral; Fig. 90. Same, palp, ventral; Fig. 91. Same, tip of subchela, ventral.

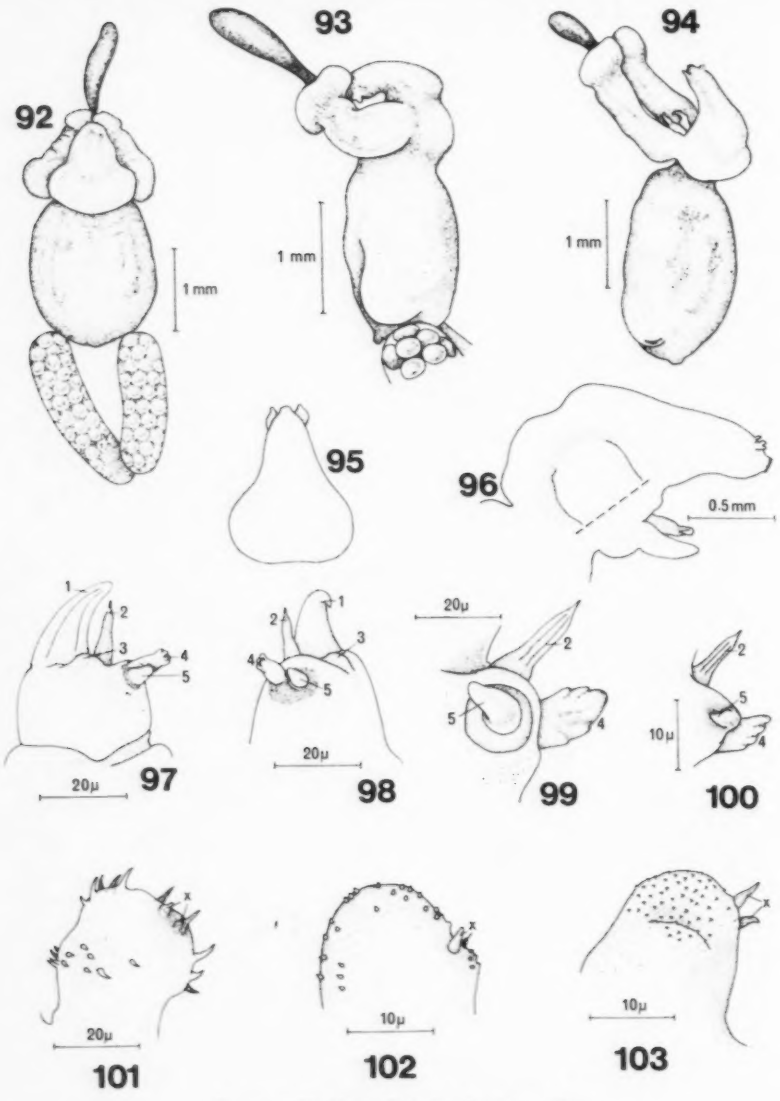

FIGURES 92–103. ***Salmincola thymalli.***

Fig. 92. Female, entire, dorsal; Fig. 93. Same, lateral; Fig. 94. Same, dorsolateral; Fig. 95. Cephalothorax outline; Fig. 96. Cephalothorax, lateral; Fig. 97. Second antenna, tip of endopod, lateral; Fig. 98. Same, ventral; Fig. 99 and 100. Same, details of armament; Fig. 101–103. Same, exopod.

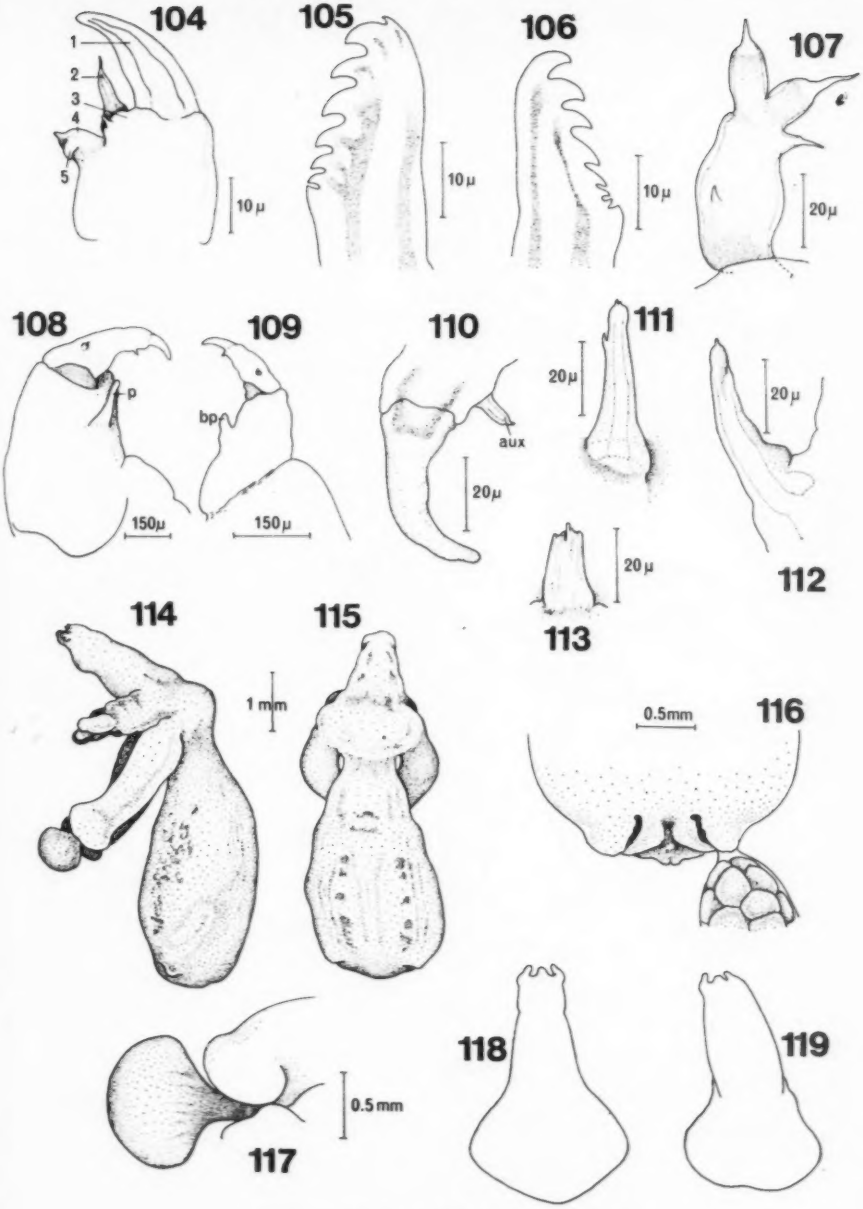

FIGURES 104–113. ***Salmincola thymalli.***
Fig. 104. Second antenna, tip of endopod, lateral; Fig. 105 and 106. Mandible, distal part, lateral; Fig. 107. First maxilla, lateral; Fig. 108. Maxilliped, ventral; Fig. 109. Same, ventrolateral; Fig. 110. Same, tip of subchela, ventral; Fig. 111. Palp, entire, ventral; Fig. 112. Same, lateral; Fig. 113. Same, broken.

FIGURES 114–119. ***Salmincola extensus.*** (Name after caption refers to synonym under which specimen was known previously.)
Fig. 114. Entire, lateral; Fig. 115. Same, dorsal.; Fig. 116. Posterior end of trunk; Fig. 117. Bulla; Fig. 118. Cephalothorax outline; Fig. 119. Same (*wisconsiniensis*).

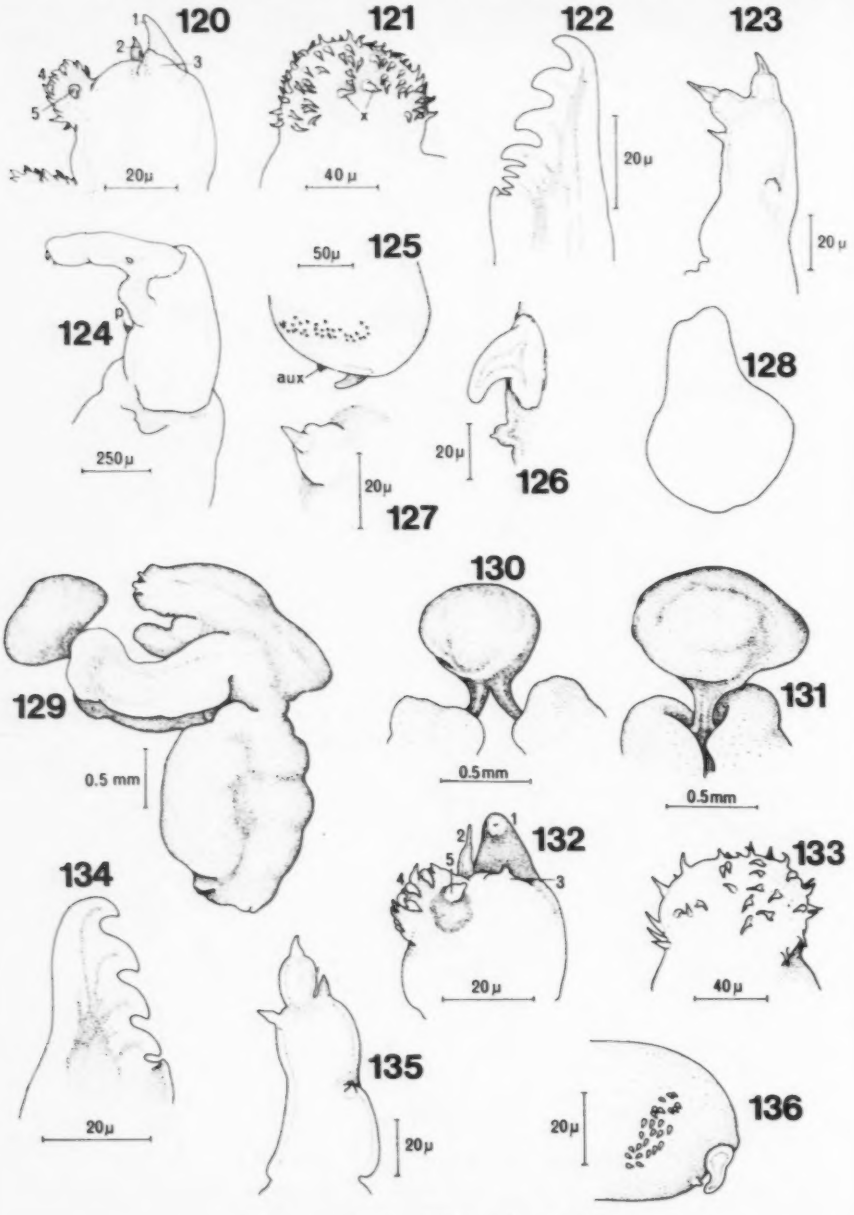

FIGURES 120–127. ***Salmincola extensus.***
Fig. 120. Second antenna, tip of endopod, ventrolateral; Fig. 121. Same, exopod; Fig. 122. Mandible, distal part, lateral; Fig. 123. First maxilla, lateral; Fig. 124. Maxilliped, entire, ventral; Fig. 125. Same, tip of subchela; Fig. 126. Same, claw; Fig. 127. Same, palp.

FIGURES 128–136. ***Salmincola jacuticus.***
Fig. 128. Cephalothorax outline; Fig. 129. Entire, lateral; Fig. 130. Bulla with abnormal manubrium; Fig. 131. Bulla with normal manubrium; Fig. 132. Second antenna, tip of endopod, ventral; Fig. 133. Same, exopod; Fig. 134. Mandible, distal half, lateral; Fig. 135. First maxilla with abnormal papillae; Fig. 136. Maxilliped, tip of subchela.

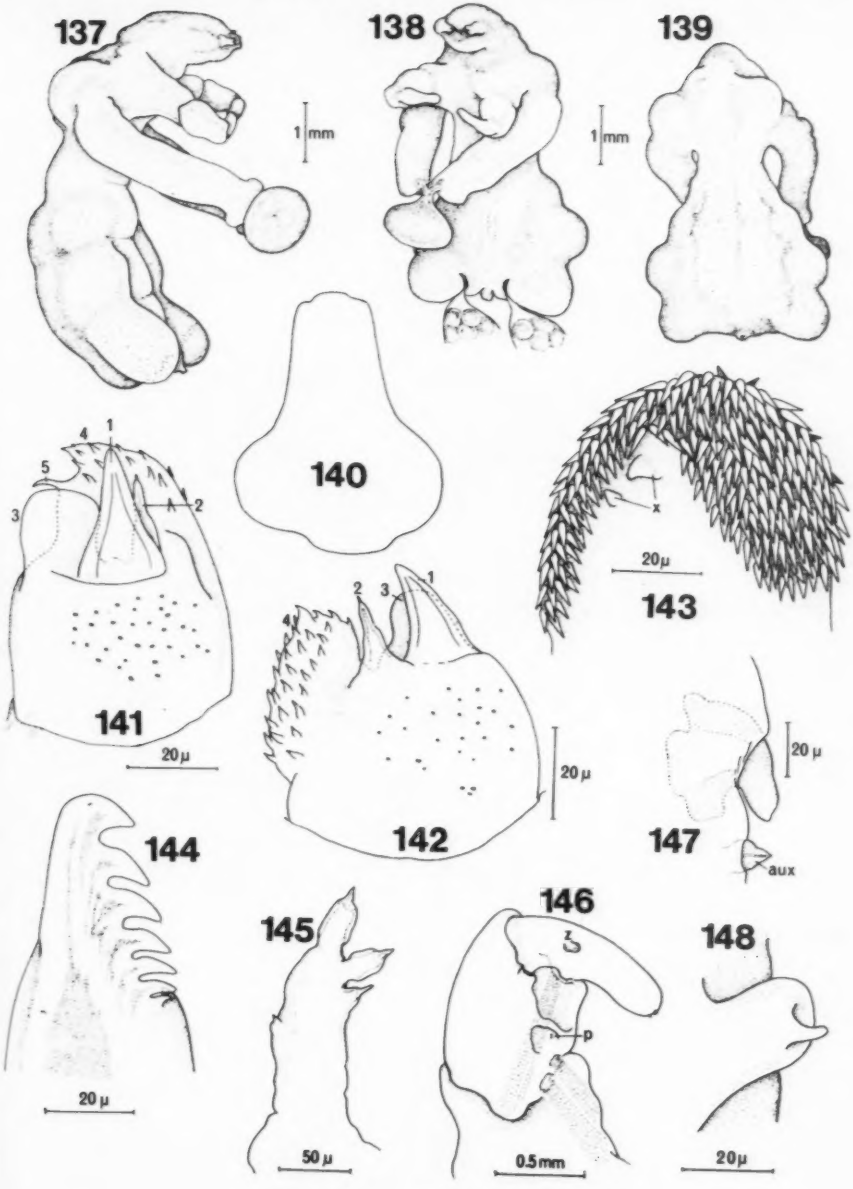

FIGURES 137–148. ***Salmincola nordmanni.***

Fig. 137. Female, entire, lateral; Fig. 138. Same, ventral; Fig. 139. Same, dorsal; Fig. 140. Cephalothorax outline; Fig. 141. Second antenna, tip of endopod, dorsal; Fig. 142. Same, dorsolateral; Fig. 143. Same, exopod; Fig. 144. Mandible, distal half, lateral; Fig. 145. First maxilla, entire, lateral; Fig. 146. Maxilliped, entire, ventral; Fig. 147. Same, claw, ventral; Fig. 148. Same, palp, ventral.

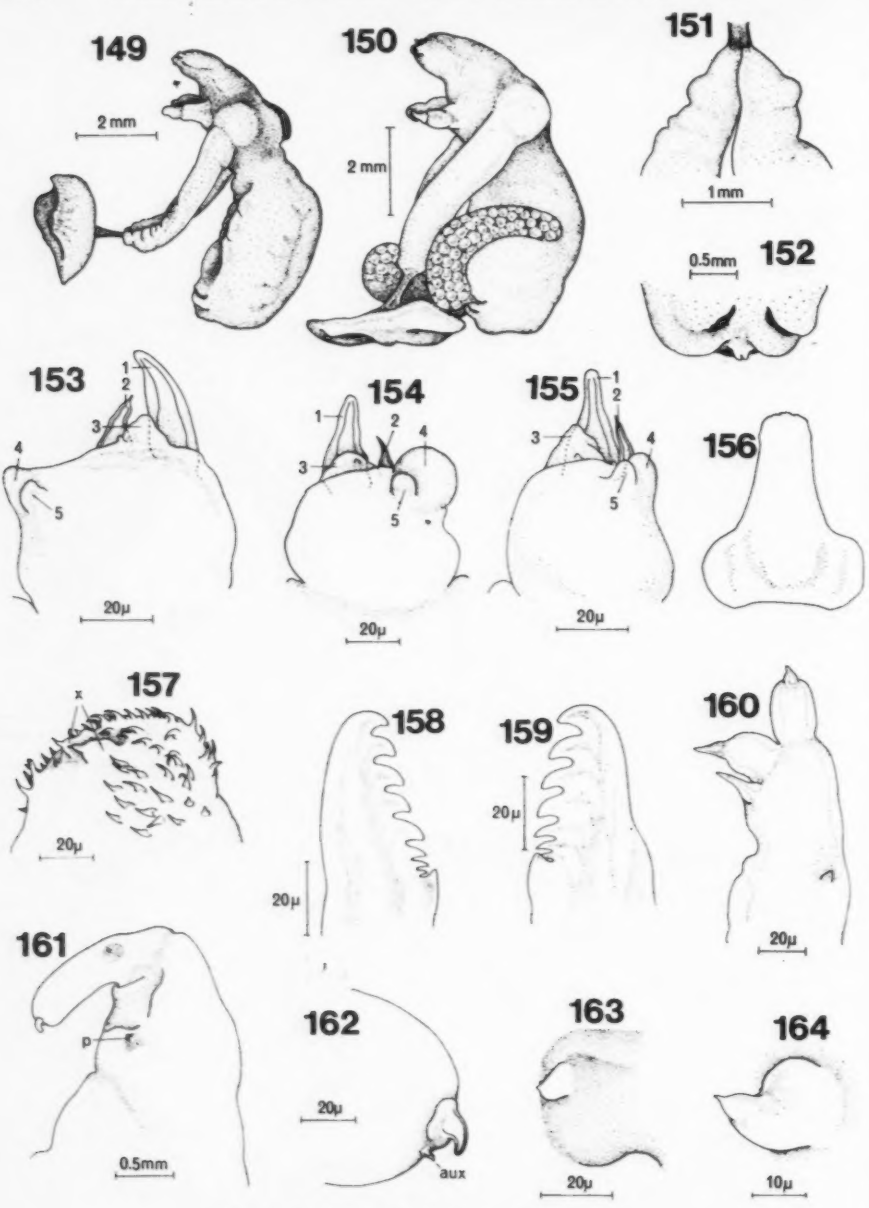

FIGURES 149–164. ***Salmincola extumescens.***

Fig. 149. Female, entire, lateral; Fig. 150. Same; Fig. 151. Tips of second maxillae; Fig. 152. Posterior end of trunk, ventral; Fig. 153–155. Second antenna, tip of endopod, ventral; Fig. 156. Cephalothorax outline; Fig. 157. Second antenna, exopod; Fig. 158 and 159. Mandible, distal half, lateral; Fig. 160. First maxilla, lateral; Fig. 161. Maxilliped, entire, ventral; Fig. 162. Same, tip of subchela, ventral; Fig. 163 and 164. Same, palp, ventral.

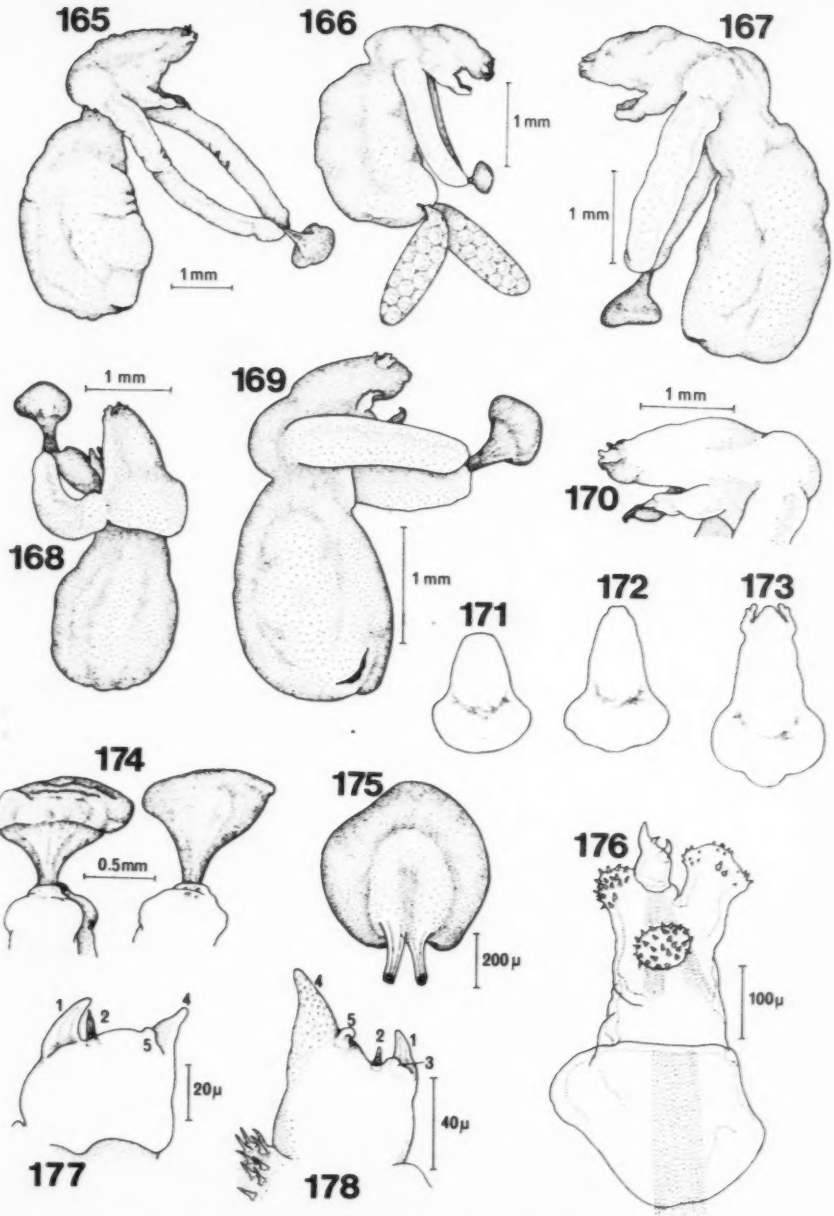

FIGURES 165–178. ***Salmincola edwardsii.*** (Names after captions refer to synonyms under which specimens were known previously.)
Fig. 165. Female, entire, lateral, from northern Europe (*edwardsii*); Fig. 166. Same (*oquassa*); Fig. 167. Same (*bicauliculata*); Fig. 168. Same, dorsal, from North America (*edwardsii*); Fig. 169. Same, lateral (*edwardsii*); Fig. 170. Cephalothorax, lateral; Fig. 171–173. Cephalothorax outlines; Fig. 174. Bulla, lateral; Fig. 175. Same, dorsal (*bicauliculata*); Fig. 176. Second antenna, entire, lateral; Fig. 177 and 178. Same, tip of endopod, lateral.

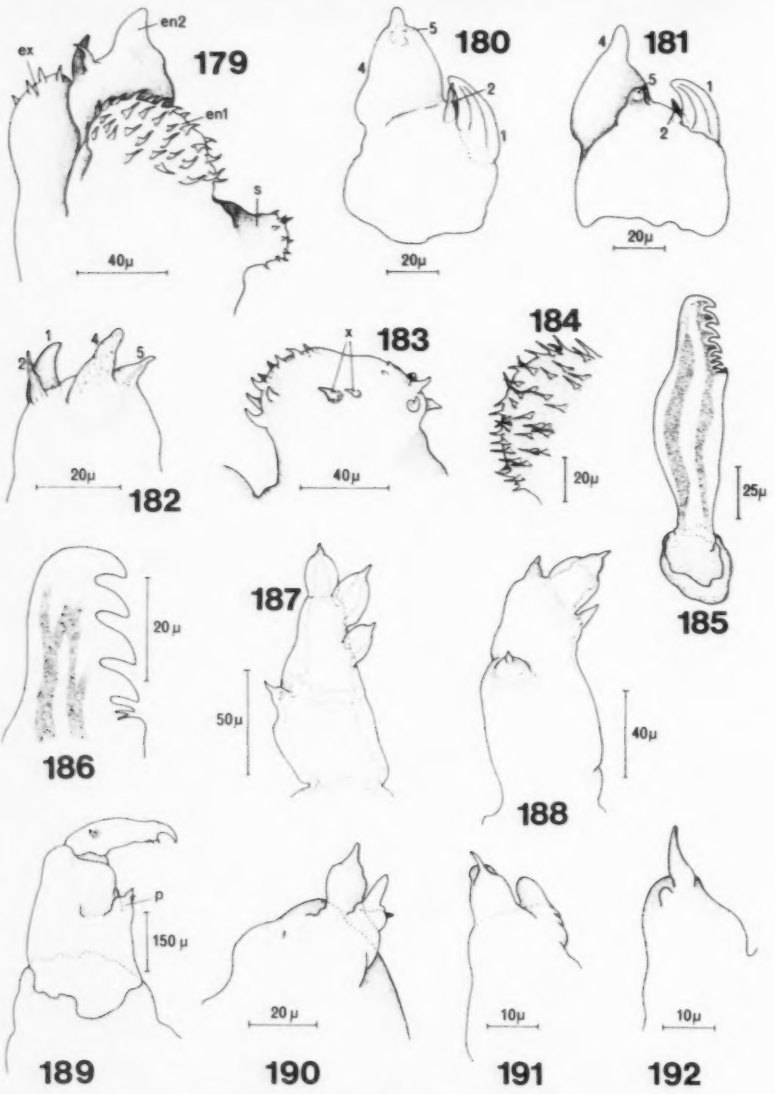

FIGURES 179–192. ***Salmincola edwardsii.***

Fig. 179. Second antenna, distal half, ventral; Fig. 180. Same, tip of endopod, medial; Fig. 181. Same, lateral; Fig. 182. Same, medial; Fig. 183. Same, exopod; Fig. 184. Same, details of spiny pad of endopod; Fig. 185. Mandible, entire, lateral; Fig. 186. Same, distal part, lateral; Fig. 187. First maxilla, lateral; Fig. 188. Same, with abnormal papillae; Fig. 189. Maxilliped, entire, ventral; Fig. 190–192. Same, palp, ventral.

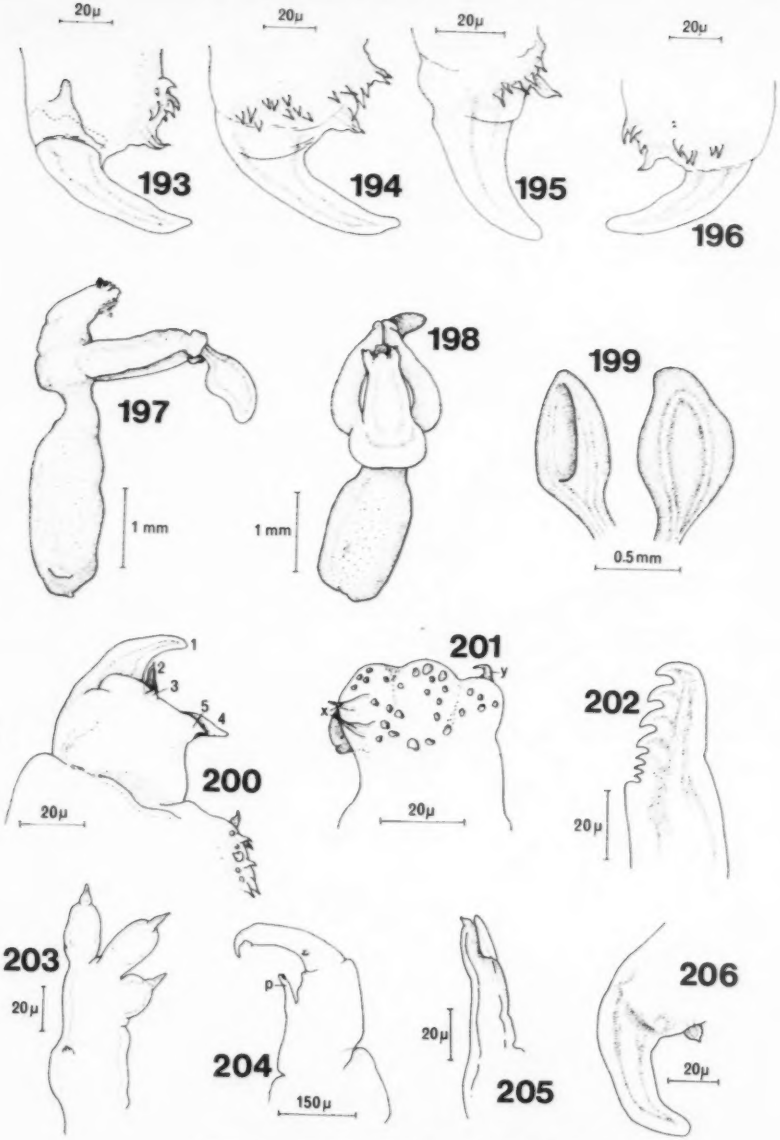

FIGURES 193–196. ***Salmincola edwardsii.***

Fig. 193. Maxilliped, tip of subchela, ventral; Fig. 194–196. Same, dorsal.

FIGURES 197–206. ***Salmincola coregonorum.***

Fig. 197. Female, entire, lateral; Fig. 198. Same, dorsal; Fig. 199. Bulla; Fig. 200. Second antenna, tip of endopod, lateral; Fig. 201. Same, exopod; Fig. 202. Mandible, distal part, lateral; Fig. 203. First maxilla, lateral; Fig. 204. Maxilliped, entire, ventral; Fig. 205. Same, palp, ventral, Fig. 206. Same, tip of subchela, ventral.

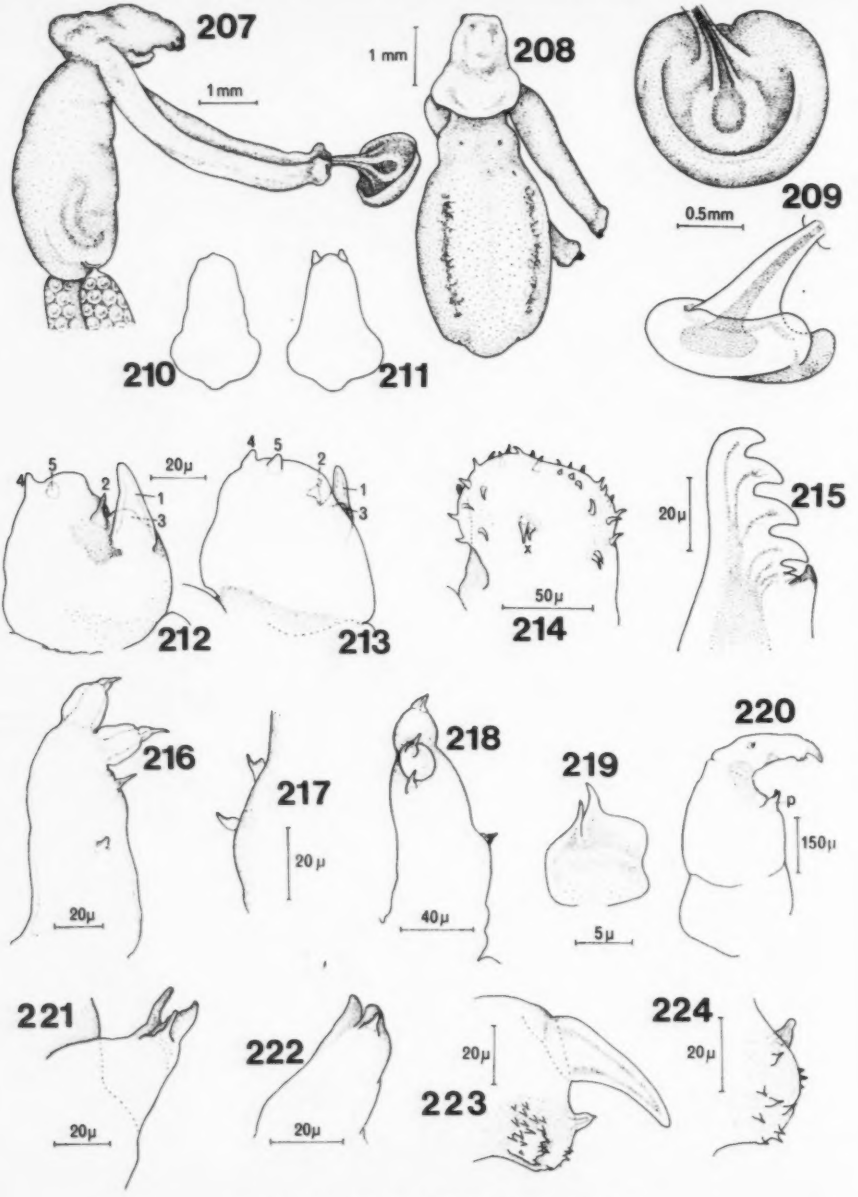

FIGURES 207–224. ***Salmincola siscowet.***

Fig. 207. Female, entire, lateral; Fig. 208. Same, dorsal; Fig. 209. Bulla; Fig. 210 and 211. Cephalothorax outline; Fig. 212. Second antenna, tip of endopod, dorsomedial; Fig. 213. Same, ventrolateral; Fig. 214. Same, exopod; Fig. 215. Mandible, distal part, lateral; Fig. 216. First maxilla, entire, lateral; Fig. 217. Same, lateral side with abnormal exopod; Fig. 218. Same, ventral; Fig. 219. Same, abnormal exopod; Fig. 220. Maxilliped, entire, ventral; Fig. 221 and 222. Same, palp, ventral; Fig. 223. Same, tip of subchela, ventral; Fig. 224. Same, base of claw, dorsal.

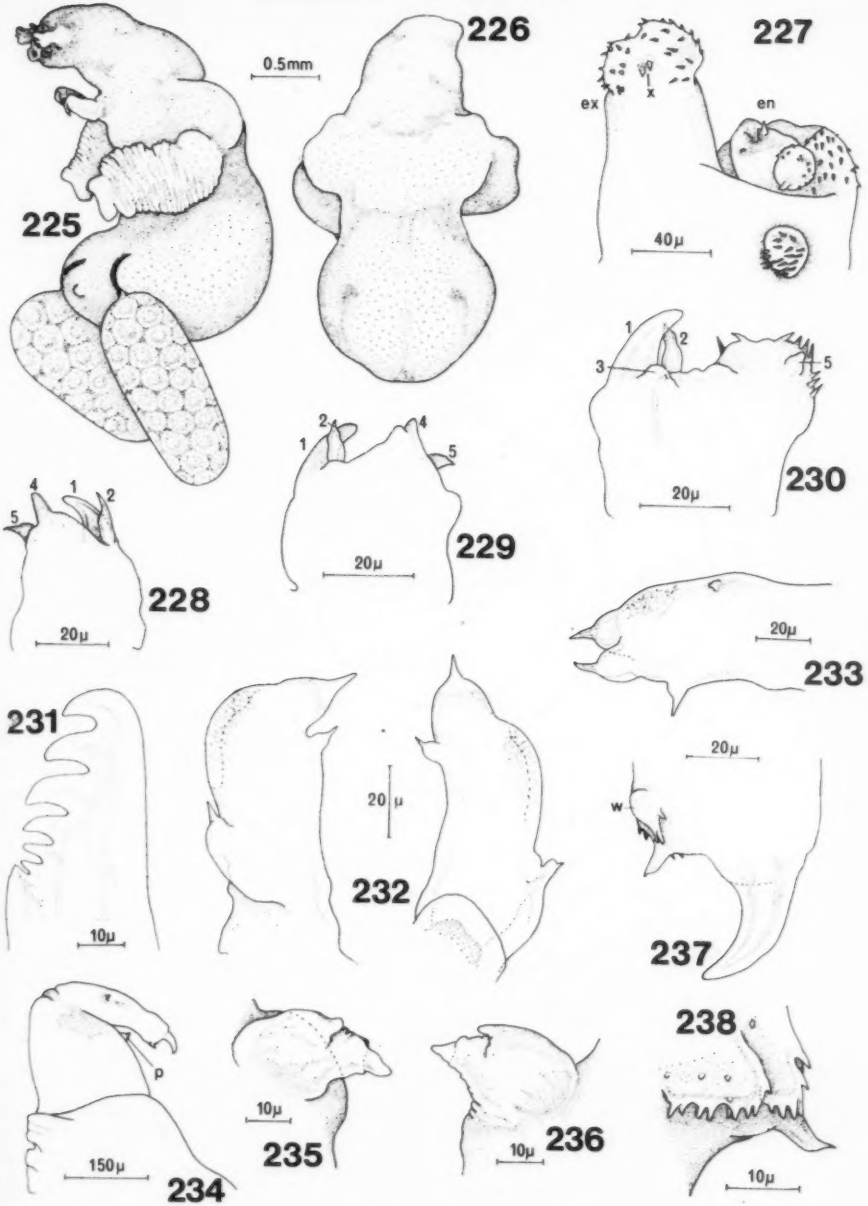

FIGURES 225–238. ***Salmincola cottidarum.***

Fig. 225. Female, entire, ventrolateral; Fig. 226. Same, dorsal; Fig. 227. Second antenna, distal part, lateral; Fig. 228. Same, tip of endopod, ventromedial; Fig. 229. Same, medial; Fig. 230. Same, lateral; Fig. 231. Mandible, distal part, lateral; Fig. 232. First maxilla, lateral and ventral; Fig. 233. Same, ventrolateral; Fig. 234. Maxilliped, entire, ventral; Fig. 235 and 236. Same, palp, ventral; Fig. 237. Same, tip of subchela, ventral; Fig. 238. Same, detail of base of claw, dorsal.

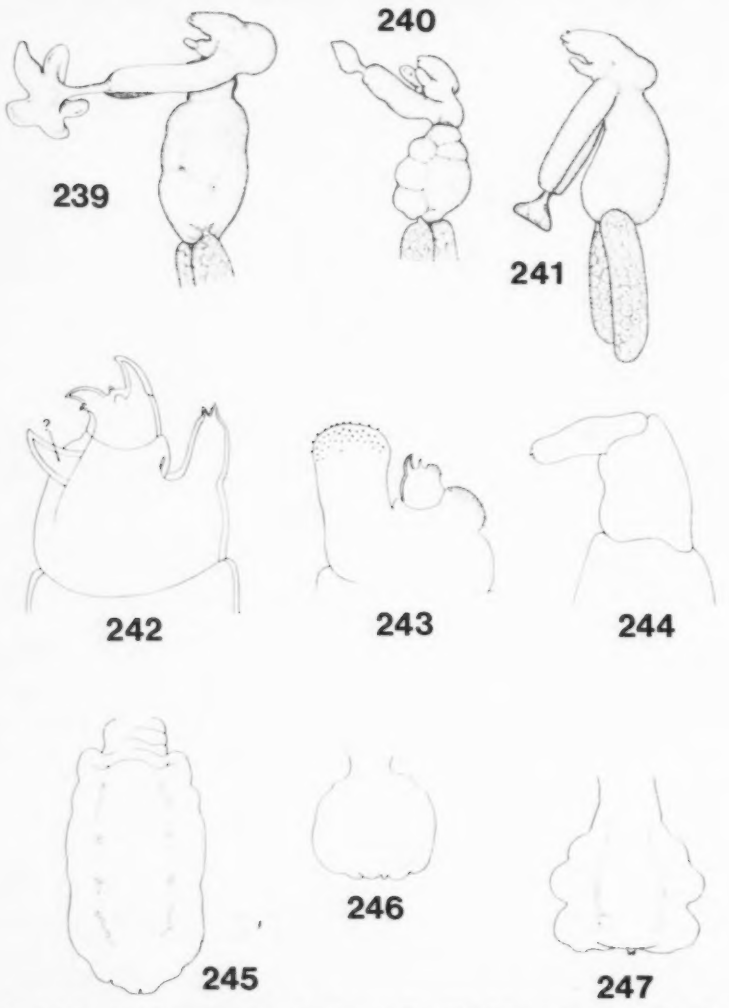

FIG. 239. *Salmincola stellatus*, female, entire, lateral. FIG. 240. *Salmincola strigatus*, female, entire, lateral. FIG. 241. *Salmincola latus*, female, entire, lateral. FIG. 242. *Salmincola stellatus*, second antenna, entire, lateral. FIG. 243. *Salmincola strigatus*, second antenna, distal half. FIG. 244. Same, maxilliped, ventral. FIG. 245. *Salmincola extensus*, trunk, dorsal. FIG. 246. *Salmincola jacuticus*, trunk, dorsal. FIG. 247. *Salmincola nordmanni*, trunk, dorsal. (Fig. 239–244 from Markevich, 1956.)

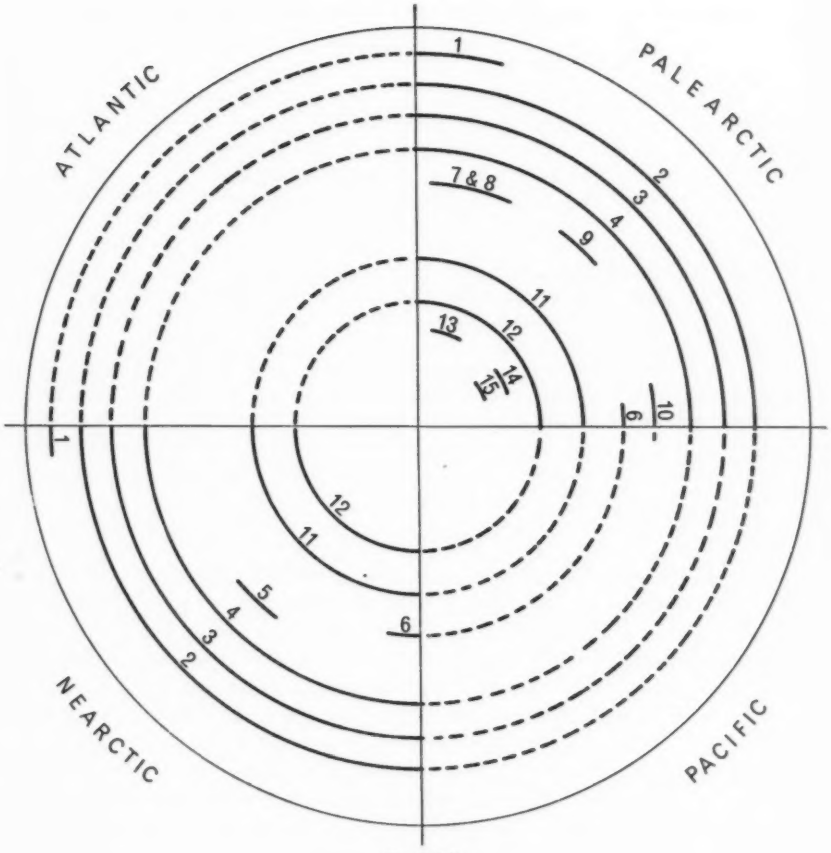

FIG. 248. Diagram of distribution ranges of individual species of *Salmincola*: 1 = *S. salmoneus*; 2 = *S. carpionis*; 3 = *S. edwardsii*; 4 = *S. thymalli*; 5 = *S. siscowet*; 6 = *S. californiensis*; 7 = *S. coregonorum*; 8 = *S. lotae*; 9 = *S. cottidarum*; 10 = *S. stellatus*; 11 = *S. extumescens*; 12 = *S. extensus*; 13 = *S. nordmanni*; 14 = *S. strigatus*; 15 = *S. jaculicus*.

Chondracanthus narium sp.n. (Copepoda: Chondracanthidae), a Parasite of Nasal Cavities of *Ophiodon elongatus* (Pisces: Teleostei) in British Columbia

Z. KABATA

Fisheries Research Board of Canada
Biological Station, Nanaimo, B.C.

KABATA, Z. 1969. *Chondracanthus narium* sp.n. (Copepoda: Chondracanthidae), a parasite of nasal cavities of *Ophiodon elongatus* (Pisces: Teleostei) in British Columbia. J. Fish. Res. Bd. Canada 26: 3043–3047.

The male and the female of *Chondracanthus narium* sp.n. (Copepoda: Chondracanthidae), living in the nasal cavities of *Ophiodon elongatus* Girard, 1854, off the coast of British Columbia are described and illustrated. The parasite differs from all other species of *Chondracanthus* by the structure of its trunk, particularly by the absence of the posterior processes.

Received July 28, 1969

INTRODUCTION

THE NASAL CAVITIES of teleost fishes have not been extensively searched for the presence of copepod parasites. The earliest known record of a copepod occurring in the nose of its host was that of *Bomolochus solae* Claus, 1864. Occurring quite frequently in the nasal cavities of several fishes belonging to the family Gadidae, this parasite on occasions shares its hosts with another and closely related species, *Bomolochus confusus* Stock, 1953.

Smirnova et al. (1964) listed six species of copepods from the nostrils of fishes. Five of them belong to Ergasilidae and are, therefore, related to the two bomolochids. The sixth is an unidentified larval lernaeocerid.

Kabata (1965) recorded a caligoid copepod, *Caligus fortis* Kabata, 1965, from the nose of *Carangoides emburyi*, a teleost from the west coast of Australia. Among the elasmobranchs, *Scyllium canicula* in British waters was found to harbour a lernaeopodid parasite, *Lernaeopoda globosa* Leigh-Sharpe, 1918, in the olfactory groove.

No copepod of the family Chondracanthidae has been known to use the nose of its host as its site of predilection. The discovery of a chondracanthid in the nasal cavities of *Ophiodon elongatus* in the coastal waters of British Columbia is, therefore, of particular interest. The description of this chondracanthid is given below.

Printed in Canada (J1545)

Chondracanthus narium sp.n.

(Fig. 1–23)

Record of specimens — Two females, one ovigerous and both with males attached were found by Mr A. Sekerak on May 31, 1969. The ovigerous specimen becomes the holotype of the species and is stored in the National Museum in Ottawa, Catalogue No. NMC 15055. Since the original discovery another specimen was found in the same host near the type locality.

Host — *Ophiodon elongatus* Girard, 1854.

Habitat — Nasal cavities.

Locality — Dolphin Beach, north of Nanaimo, east coast of Vancouver Island.

Description of the female — General appearance of this parasite (Fig. 1–3) is very characteristic. The body of the female can be divided into three regions. The anterior region is the cephalothorax, irregularly quadrangular, with rounded corners and devoid of any outgrowths. The two pairs of antennae are situated at its anterior margin whereas its ventral surface carries posteriorly the buccal opening and associated appendages (Fig. 1). The middle region has a complicated shape. Immediately behind the cephalothorax there is a narrow necklike part indistinctly divided into two by a slight annular constriction (Fig. 1). The anterior half of that part bears on its ventral side the first pair of thoracic legs. A small conical protuberance is present on the dorsum of the posterior half (Fig. 3). Behind the neck, the middle region extends broadly in two pairs of digitiform outgrowths that impart to it a winged appearance. Two conical protuberances are present on the dorsum of this region: one large protuberance is situated at the level between the two pairs of lateral outgrowths, the other and much smaller one at the posterior limit of the region (Fig. 2, 3). The ventral side of the region carries the second pair of thoracic legs at the level of the anterior pair of lateral outgrowths. The posterior limit of the middle region is marked by a constriction, behind which the trunk expands broadly into its posterior region. This region is roughly quadrangular, widest anteriorly and tapering towards the posterior extremity (Fig. 2). The posterior margin is gently rounded. In the place usually occupied in the genus *Chondracanthus* by the posterior processes of the trunk there are small and indistinct swellings (*p?*, Fig. 1) and between them is situated the genital–abdominal region (Fig. 4). A small but distinct caudal furca is present in front of a fairly large anal cleft. The egg sacs (Fig. 2) are curved in circles, both in fresh and in preserved specimens.

The sizes of the specimens examined were 6.92 and 7.60 mm.

The first antenna (Fig. 5, 6) consists of two parts, a longer and thicker proximal and a cylindrical and shorter distal one. The ventral side of the proximal part has in it a dent (shaded in Fig. 6) into which fits the hook of the second antenna, when in situ. There are three small papillae on the anterior margin of the proximal part (*p*, Fig. 6). The armature of the distal part could not be studied in detail, but at least three unarmed setae were seen along its length. The apical armature (Fig. 5) appears to consist of eight short setae, with a ninth in subapical position.

The second antenna (Fig. 7) is uniramous, its exopod being completely suppressed. The endopod is a short, strong hook. Along the concave margin of the hook there is a small opening that appears to be leading to a narrow duct and is marked with a query in Fig. 7. Another query marks the position of a shallow crypt in the ventral wall of the proximal part of the hook.

The mandible (Fig. 9) is of the usual chondracanthid structure and shows no characteristic features. The mandibular palp (Fig. 8) is armed with a terminal papilla carrying a short, blunt seta. Similar, though smaller structure is present on the medial side of that papilla, slightly towards the ventral surface.

The maxilla (Fig. 10) has a claw of the usual type. There are from 8 to 10 teeth along the dorsal margin of the claw. The basal seta (*bs*) is short and the tip of the auxiliary spine (*aux*) is denticulated (Fig. 11).

The maxilliped (Fig. 12) has a long and narrow strip of denticles along its tip. The claw is curved. Near its tip there are two teeth, opposite each other.

The thoracic legs are bilobed and their shape is common to the genus. The details of their armature were not investigated. Neither was a detailed study made of the caudal furca.

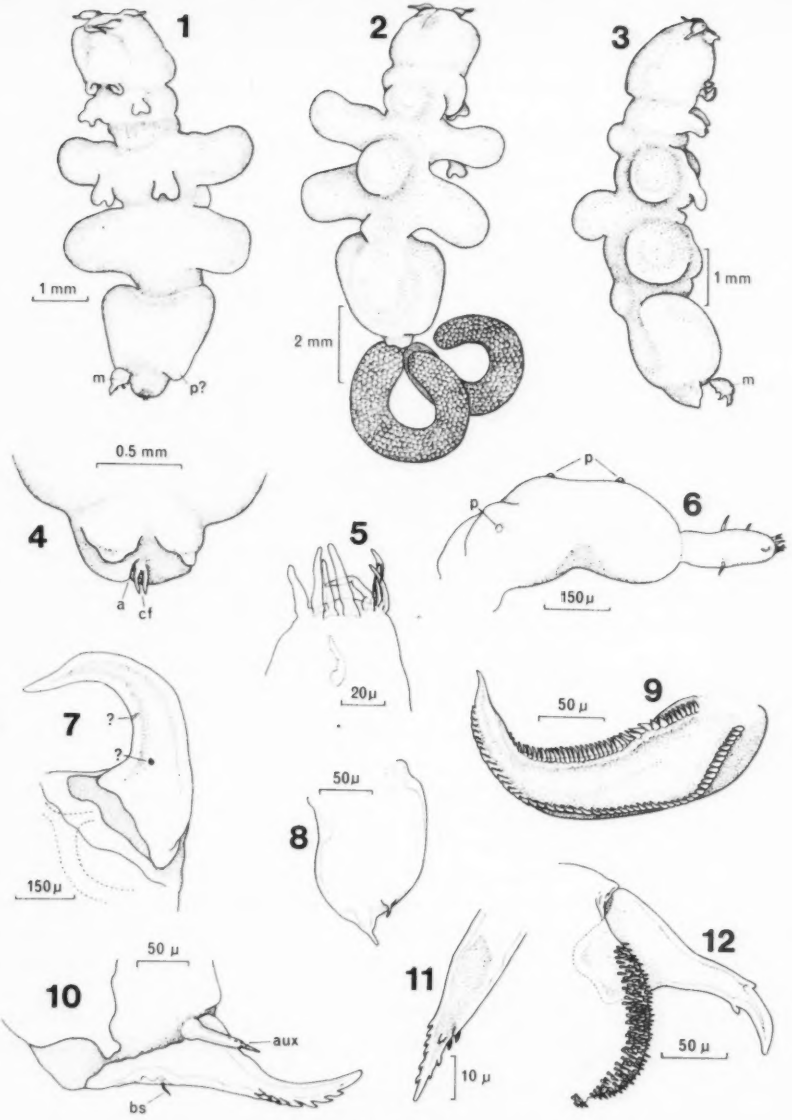

FIGURES 1–12. ***Chondracanthus narium,*** female.

Fig. 1. Entire, ventral; Fig. 2. Same, dorsal; Fig. 3. Same, lateral; Fig. 4. Posterior extremity, ventral; Fig. 5. First antenna, tip; Fig. 6. Same, entire, ventral; Fig. 7. Second antenna, ventral; Fig. 8. Mandibular palp, ventral; Fig. 9. Mandible, distal part; Fig. 10. Maxillary claw, dorsal; Fig. 11. Maxillary claw, tip of auxiliary spine; Fig. 12. Maxilliped, tip. *a* = anus; *aux* = auxiliary spine; *bs* = basal seta; *cf* = caudal furca; *m* = male; *p* = papilla.

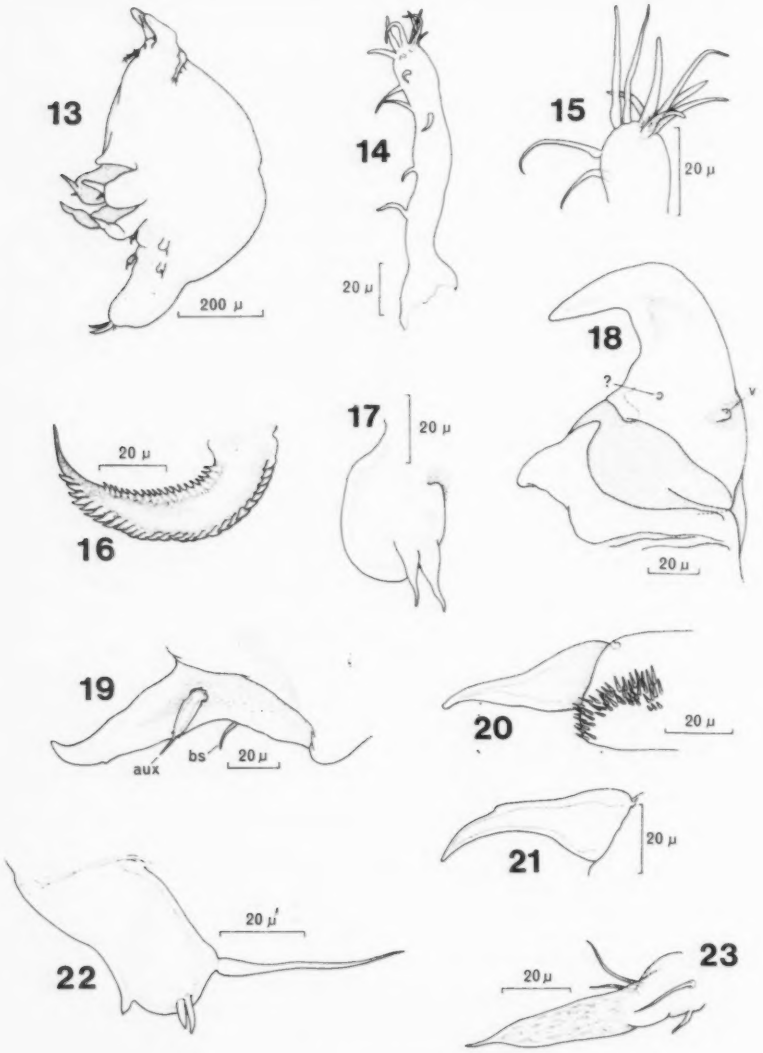

FIGURES 13–23. ***Chondracanthus narium,*** male.

Fig. 13. Entire, lateral; Fig. 14. First antenna, entire; Fig. 15. same, tip; Fig. 16. Mandible, distal part; Fig. 17. Mandibular palp; Fig. 18. Second antenna, ventral; Fig. 19. Maxillary claw, dorsal; Fig. 20. Maxilliped, tip, posterior; Fig. 21. Maxilliped claw, ventral; Fig. 22. First thoracic leg, ventral; Fig. 23. Caudal lamina, dorsal. *aux* = auxiliary spine; *bs* = basal seta; *v* = location of vanished exopod.

Description of the male — In its general appearance (Fig. 13) the male of this species bears general resemblance to other males of *Chondracanthus*. Its anterior part is round in outline (in dorsal aspect), flat ventrally and has a curved dorsum; its posterior part is cylindrical and tapers towards the extremity. There are two pairs of thoracic legs. The length of the males examined was 680 μ.

The first antenna (Fig. 14, 15) is cylindrical, with rounded tip and obscure segmentation. The details of its armature are uncertain, about six setae having been observed along the anterior margin of the appendage. The apical armature (Fig. 15) consists of eight terminal and two subterminal setae.

The second antenna (Fig. 18) is uniramous, only a small pit (*v*, Fig. 18) remaining in the place where the exopod is located, when present. A small depression(?) is found on the ventral surface of the hook, near its base. The hook is short, sturdy and strongly curved.

The mandible (Fig. 16) resembles that of the female. The mandibular palp (Fig. 17), however, differs from that of the female in the length and nature of the two apical structures. They are much longer and cannot be subdivided into papillae and setae. (This makes it possible that the corresponding structure of the female is not a true seta.)

The maxilla (Fig. 19) carries no teeth on its claw. (One slight swelling was detected near the end of the claw, but it was impossible to determine whether it was a tooth.) A basal seta (*bs*) and auxiliary spine (*aux*) are present.

The maxilliped (Fig. 20, 21) has a curved claw. Unlike that of the female, the claw has no teeth, though a slight swelling is present in the place where the female has one of the teeth (Fig.21). The spinulation near the tip of the distal segment (Fig. 20) is less abundant than that of the female.

The thoracic legs (Fig. 22) appear to be all of the same structure. They are biramous, the endopod being represented by a small, pointed lobe medial to the apex of the leg. (In Fig. 22 the leg is tilted towards the observer so that its tip is foreshortened and the two apical setae seem to be subapical.) On the lateral margin, at the point marking the base of the exopod, there is a long, robust seta.

The laminae of the caudal furca (Fig. 23) taper distally to a fine point. Their distal halves have finely corrugated surfaces. Four setae are present near to or at the bases of the laminae.

Discussion — The structure of its cephalothorax and of its mouth parts places this parasite in the genus *Chondracanthus*. Its trunk distinguishes it from all other species of the genus. The trunk of *Chondracanthus* varies from species to species in the number, shape, size, and arrangement of outgrowths. Whatever differences might exist between the trunks of different species, they all have one feature in common. Every *Chondracanthus* has a trunk equipped with a pair of posterior processes, often quite long and never vestigial, one process on each side of the genital–abdominal region. *Chondracanthus narium* has no such processes unless one accepts the small swellings (*p?*, Fig. 1) as being their vestiges. This feature alone suffices to place the present species in a distinct taxon. The general structure of the trunk, i.e., the number and arrangement of outgrowths, also distinguishes it from its congeners.

ACKNOWLEDGMENTS

I wish to thank Mr A. Sekerak for making available to me the specimens of this new species.

REFERENCES

KABATA, Z. 1965. Copepoda parasitic on Australian fishes. IV. Genus *Caligus* (Caligidae). Ann. Mag. Nat. Hist. Ser. 13, 8: 109–126.

SMIRNOVA, T. S., YU. A. STRELKOV, V. A. TIMOFEEV, AND S. S. SHULMAN. 1964. [Nasal cavities of Teleostei fishes as a site of dwelling for parasites.] Zool. Zh. 42: 1649–1658. (In Russian.)

Lactate Dehydrogenase Isozymes in Longnose and Blacknose Dace (*Rhinichthys cataractae* and *R. atratulus*) and Their Hybrid

J. W. CLAYTON

Fisheries Research Board of Canada
Freshwater Institute, Winnipeg, Man.

AND

J. H. GEE

Department of Zoology
University of Manitoba, Winnipeg, Man.

CLAYTON, J. W., AND J. H. GEE. 1969. Lactate dehydrogenase isozymes in longnose and blacknose dace (*Rhinichthys cataractae* and *R. atratulus*) and their hybrid. J. Fish. Res. Bd. Canada 26: 3049–3053.

Electrophoresis of tissue extracts of both longnose and blacknose dace reveals five isozymes corresponding to tetramers of heart and muscle type subunits. The species are readily distinguished by the greater electrophoretic mobility of longnose dace isozymes that contain heart type subunits. The F_1 hybrid displays the multiple band pattern expected in a fish able to produce two kinds of heart subunit. In addition a variant type of muscle lactate dehydrogenase has been detected in the longnose dace.

Received May 5, 1969

INTRODUCTION

THE ELECTROPHORESIS OF TISSUE EXTRACTS coupled with the staining of the resulting separated proteins for specific enzymes may in principle lead to the visualization of the effects of a small number of specific genes. The electrophoresis of lactate dehydrogenase (LDH) is a convenient example of such a procedure. We have applied this technique to the examination of a number of blacknose and longnose dace and their hybrids with a view to distinguishing between hybrids and the parental species.

Lactate dehydrogenase in birds and mammals has been shown to exist in the catalytically active form as a tetramer of four polypeptide chains. In these groups of animals electrophoresis of tissue extracts, followed by the appropriate visualization procedure, usually reveals five isozyme bands corresponding to the five possible tetramer combinations of two kinds of subunits. The evidence supporting these conclusions was presented initially by Apella and Markert (1961) and has been summarized by Kaplan (1964). The latter report also relates the catalytic properties of the isozymes to the subunit composition of tetramer isozymes in specific tissues. Thus the usually more

Printed in Canada (J1470)

negatively charged heart (H) subunits are found to be concentrated in aerobic tissues whereas the less highly charged muscle (M) subunits are concentrated largely in relatively anaerobic skeletal muscles.

The occurrence of the five possible HM tetramers in fishes is not as common as in other higher vertebrates. Frequently either only the homopolymer H_4 and M_4 tetramer isozymes or these two plus the H_2M_2 heteropolymer isozyme are all that are observed (Markert and Faulhaber, 1965; Odense et al., 1966). In fact it would appear that there is such a range of lactate dehydrogenase isozyme types in fishes that few generalizations can be made (Markert and Whitt, 1968). Thus while the present investigation was undertaken with the object of distinguishing possible hybrids of two sympatric species, which spawn at similar times of the year in the same parts of the stream, the precise pattern of LDH isozymes to be expected in longnose and blacknose dace was unknown.

MATERIALS AND METHODS

The fish utilized in this study consisted of longnose and blacknose dace collected from the Mink River in June and October 1968, together with individuals of each species and their interspecific hybrids that were reared in the laboratory. These laboratory-reared fish were offspring from parents collected in June 1967 from the Mink and Valley rivers, both of which originate in the Duck Mountains (Manitoba) and flow into Dauphin Lake. Interspecific hybridization was accomplished in the laboratory by stripping eggs from females and fertilizing them with milt from males of the opposite species. The hybrids examined were progeny of five pairs of parents of each reciprocal cross. Matings within each species were carried out in a similar way. Three matings of longnose and five of blacknose dace provided individuals of each species for examination.

Wild fishes kept in the laboratory prior to examination and laboratory-reared fishes were held in tanks at room temperature and fed Tetramin flakes and frozen brine shrimp. Laboratory-reared fishes in the early stages of life were fed Tetramin paste. Tissue extracts were prepared for electrophoresis from laboratory-reared fishes at an age of 20 months and from wild fishes aged 2 years or older.

Chemicals and Reagents

The chemicals and reagents used in this study were generally of the best available commercial grade and were used without additional purification.

Tissue Preparation

Tissues were removed from frozen fish and then homogenized with distilled water in a Teflon and glass tissue grinder. The ratio of tissue to water was 1:3 for skeletal muscle and 1:2 for other tissues. The extracts were centrifuged at 25,000 *g* and 2 C. The clear supernatant was drawn off for electrophoresis.

Electrophoresis

Starch-gel electrophoresis was performed at 3 C using the micro technique of Tsuyuki et al. (1966). The starch and electrode buffers were 2.00 and 40.0 mM in citric acid respectively. Both were adjusted to *p*H 8.00 at 22 C with tris (hydroxymethyl) amino methane.

Lactate dehydrogenase was visualized by staining at room temperature with a solution containing the following ingredients: 72 mg nicotinamide adenine dinucleotide, 40 mg Nitro BT,[1] 2.4 mg phenazine methosulphate, 6 ml of 2.0 M lactic acid adjusted to *p*H 7.0 with NaOH, and 94 ml of 0.150 M diethanolamine adjusted to *p*H 9.0 with HCl.

---

[1]Nitro BT, Dajac Laboratories, Philadelphia [2, 2′-di-*p*-nitrophenyl-5, 5′-diphenyl-3′-(3,3′-dimethoxy-4,4′-biphenylene)-ditetrazolium chloride].

When the isozyme bands were sufficiently stained, the starch strips were washed with distilled water then soaked in a solution of methanol, acetic acid, and water, 5:1:5 by volume. The latter treatment shrinks the gel slightly and toughens it.

RESULTS AND DISCUSSION

All of the lactate dehydrogenase (LDH) isozyme types encountered are shown in Fig. 1, 2, and 3. It may be seen (Fig. 1) that the anodal bands stain more intensely in heart tissue whereas the cathodal bands stain more intensely in muscle tissue. The homogenates of whole fish heads show an intermediate intensity of staining. It is significant that no additional bands migrating more rapidly toward the anode than heart type LDH appear in the dace head. This is in contrast to virtually all salmonids, which have an additional set of LDH isozymes in eye and brain tissues that are more anodal than heart isozymes (Morrison and Wright, 1966; Klose et al., 1968; J. W. Clayton, unpublished observations).

The appearance of five isozymes in the dace, although similar to the situation in birds and mammals (Kaplan, 1964), is not the rule in fishes. Of 30 species of fishes, Markert and Faulhaber (1965) found only 3 which produced all five possible HM tetramers. Also, although the dace heart extract produced anodal bands that stain more intensely than the cathodal bands as do most birds and mammals, Markert and Faulhaber (1966) found 10 out of 30 fish species with reversed heart–muscle LDH mobility.

The M_3H isozymes of the hybrid (Fig. 2) are a doublet as expected for a diploid organism heterozygous for the H LDH subunit gene. The succeeding isozymes also show multiplet bands but they are too faint to be seen clearly on this photograph (Fig. 2). The hybrid should display 15 bands corresponding to the possible tetramers of the common muscle LDH subunit and the two kinds of heart subunit characteristic of each pure species, as shown in Table 1. However, Fig. 2 shows that some of these, for example H_4^b and H_3^1M are likely to be of such similar electrophoretic mobility as to be indistinguishable under the present conditions. Therefore, the total count of isozyme bands in hybrid fish is likely to always be less than the theoretical total of 15.

Another feature apparent in Fig. 2 is the splitting into a doublet of the band corresponding to the H_2M_2 isozyme in both of the pure species. This would appear to be evidence for nonequivalance of two forms of this isozyme. This is not altogether unexpected since a little reflection will show that an H_2M_2 tetramer could exist in either symmetrical or asymmetric forms. The concept of electrophoretically distinguishable conformers of malate dehydrogenase has been expressed by Kitto et al. (1966a, b) but a similar behaviour of LDH has apparently not been observed.

The variant longnose dace is presumably heterozygous for the normal M LDH subunit and a variant M′LDH subunit of lower mobility (Fig. 3). The hybrid pattern, with the expected gross multiplicity of bands, indicative of heterozygosity at both the H and M LDH subunit loci, was displayed by two fish. The theoretical total of isozymes to be expected is 35 but because of

TABLE 1. Subunit composition of lactate dehydrogenase isozymes in longnose-blacknose hybrid dace.

⊖	
M_4	M = the common type of dace muscle LDH subunit
M_3H^b M_3H^l	H^b = the blacknose dace heart LDH subunit
$M_2H_2^b$ $M_2H^bH^l$ $M_2H_2^l$	H^l = the longnose dace heart LDH subunit
MH_3^b $MH_2^bH^l$ $MH^bH_2^l$ MH_3^l	
H_4^b $H_3^bH^l$ $H_2^bH_2^l$ $H^bH_3^l$	
H_4^l	⊕

identical mobilities of several isozymes and the faintness of others the total number observable is less than the maximum. The important point, the multiplicity of M_4 bands in the hybrid, is however, quite apparent. Since the LDH isozyme pattern of the actual parents of the various hybrid progenies were not determined, the nature of the heritability of the variant M LDH in longnose dace is not conclusively proven. On the other hand the presence of multiple isozymes corresponding to heterozygosity in the H LDH locus in all the hybrids examined is suggestive of a diploid organism with two genes at the H LDH locus that are codominant. These views are in accord with those of Ohno et al. (1967) and Bender and Ohno (1968) who suggest that cyprinid fishes with chromosome counts of about 50 are diploid. Although the chromosomes of the particular species of dace we have utilized have not been determined, the longnose dace of British Columbia coastal streams were found to have approximately 52 chromosomes (J. D. McPhail, personal communication).

The numbers of fish with each LDH isozyme pattern are presented in Table 2. The expected occurrence of the M′M′ homozygous genotype shown

TABLE 2. Occurrence of phenotypes of dace lactate dehydrogenase.

Species:	Longnose		Blacknose	Hybrid	
	Normal muscle type	Variant muscle type		Normal muscle type	Variant muscle type
Wild fish	8	5	13		
Laboratory-reared	1	2	9	27	2
Total	9	7	22	27	2

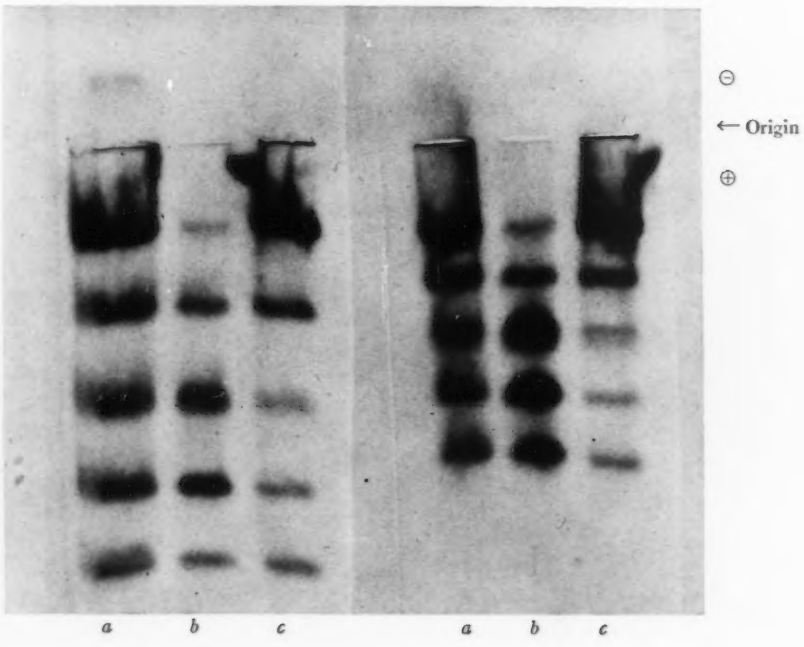

FIG. 1. Electropherograms of LDH isozymes in various tissues from assumed homozygous types of longnose and blacknose dace. *a* = head; *b* = heart; *c* = muscle.

Clayton and Gee — J. Fish. Res. Bd. Canada

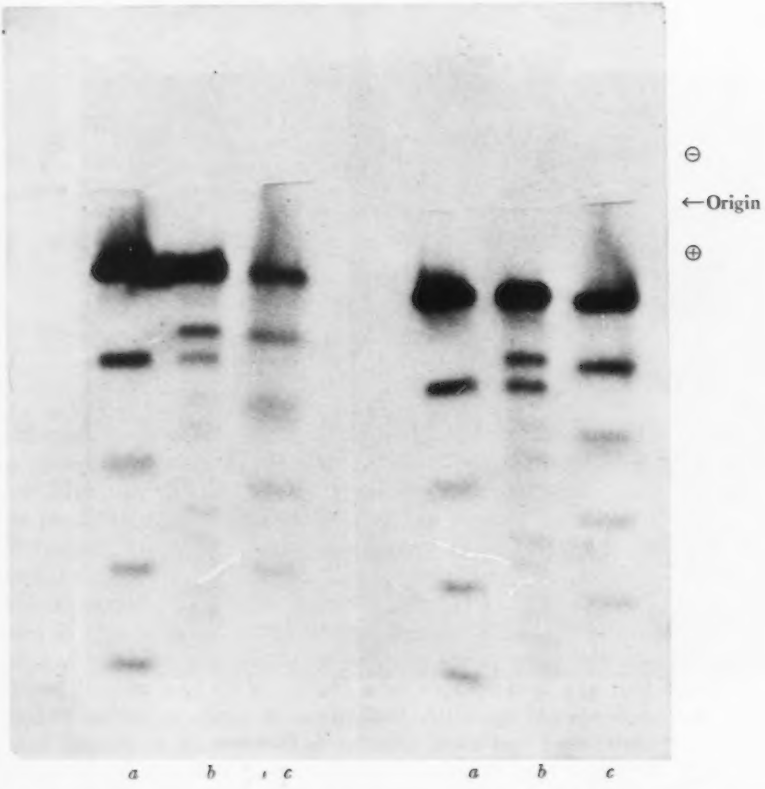

FIG. 2. Electropherograms of LHD isozymes in skeletal muscle from assumed homozygous types of longnose dace, blacknose dace, and their hybrid. *a* = longnose; *b* = hybrid; *c* = blacknose.

Clayton and Gee — J. Fish. Res. Bd. Canada

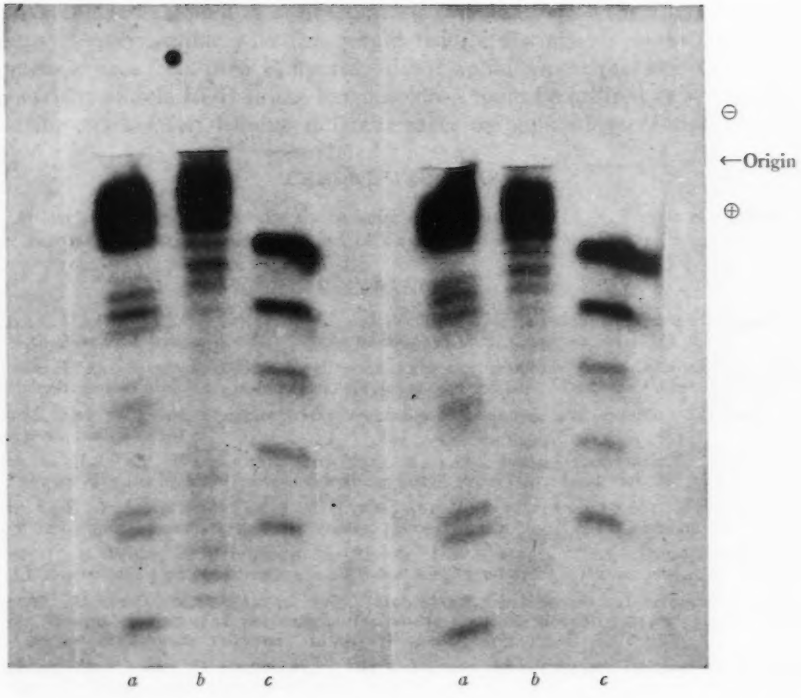

FIG. 3. Electropherograms of LDH isozymes in skeletal muscle from longnose dace, blacknose dace, and their hybrid. *a* = longnose dace with variant M LDH; *b* = hybrid dace with variant M LDH; *c* = blacknose dace.

Clayton and Gee — J. Fish. Res. Bd. Canada

below was calculated according to the Hardy Weinberg law[2] using the observed values of the MM and MM′ genotypes. That no M′M′ phenotype was observed is not surprising since it is likely to occur at a frequency of 1 fish in 21 and only 16 fish were examined.

	MM	MM′	M′M′
Observed	9	7	0
Calculated	–	–	1 in 21

We conclude from this study that an examination of the LDH isozyme pattern of questionable wild fish would readily distinguish either blacknose or longnose dace from their F_1 hybrid. Also it would appear that the occurrence of a variant muscle LDH in the longnose dace could be utilized as a naturally occurring marker for defining different races or populations of this species.

ACKNOWLEDGMENTS

It is a pleasure to acknowledge the technical assistance of Mr D. N. Tretiak of the Freshwater Institute, Fisheries Research Board of Canada, Winnipeg, Man.

REFERENCES

APPELLA, E., AND C. L. MARKERT. 1961. Dissociation of lactate dehydrogenase into subunits with guanidine hydrochloride. Biochem. Biophys. Res. Commun. 6: 171–176.

BENDER, K., AND S. OHNO. 1968. Duplication of the autosomally inherited 6-phosphogluconate dehydrogenase gene locus in tetraploid species of cyprinid fish. Biochem. Genet. 2: 101–107.

KAPLAN, N. O. 1964. Lactate dehydrogenases — structure and function. Brookhaven Symp. Biol. 17: 131–153.

KITTO, G. B., P. M. WASSARMAN, AND N. O. KAPLAN. 1966a. Enzymatically active conformers of mitochondrial malate dehydrogenase. Proc. Nat. Acad. Sci. 56: 578–585.

KITTO, G. B., P. M. WASSARMAN, J. MICHJEDA, AND N. O. KAPLAN. 1966b. Multiple forms of mitochondrial malate dehydrogenases. Biochem. Biophys. Res. Commun. 22: 75–81.

KLOSE, J., U. WOLF, H. HITZEROTH, H. RITTER, AND S. OHNO. 1968. Duplication of the LDH gene loci by polyploidization in the fish order Clupeiformes. Humangenetik 5: 190–196.

MANWELL, C., AND C. M. A. BAKER. 1969. Hybrid proteins, heterosis and the origin of species I. Unusual variation of polychaete *Hyalinoecia* "nothing dehydrogenases" and of quail *Coturnix* erythrocyte enzymes. Comp. Biochem. Physiol. 28: 1007–1028.

MARKERT, C. L., AND I. FAULHABER. 1965. Lactate dehydrogenase isozyme patterns of fish. J. Exptl. Zool. 159: 319–332.

MARKERT, C. L., AND G. S. WHITT. 1968. Molecular varieties of isozymes. Experientia 24: 977–991.

MORRISON, W. J., AND J. E. WRIGHT. 1966. Genetic analysis of three lactate dehydrogenase isozyme systems in trout: evidence for linkage of genes coding sub units A and B′. J. Exptl. Zool. 163: 259–270.

ODENSE, P. H., T. M. ALLEN, AND T. C. LEUNG. 1966. Multiple forms of lactate dehydrogenase and aspartate aminotransferase in herring (*Clupea harengus harengus* L.) Canadian J. Biochem. 44: 1319–1326.

OHNO, S., J. MURAMOTO, L. CHRISTIAN, AND N. B. ATKIN. 1967. Diploid tetraploid relationship among Old-World members of the fish family Cyprinidae. Chromosoma (Berlin) 23: 1–9.

TSUYUKI, H., E. ROBERTS, R. H. KERR, AND A. P. RONALD. 1966. Micro starch gel electrophoresis. J. Fish. Res. Bd. Canada 23: 929–933.

[2]We are aware that very recently (see Manwell and Baker, 1969) credit has been given to W. E. Castle for prior discovery of the algebra of population genetics. We use "Hardy Weinberg law" because it is most familiar at present.

Tetrachloro-*o*-benzoquinone as a Component in Bleached Kraft Chlorination Effluent Toxic to Young Salmon

B. S. Das and S. G. Reid

Ontario Research Foundation
Sheridan Park, Ont.

AND

J. L. Betts and K. Patrick

Fraser Companies Limited
Edmundston, N.B.

Das, B. S., S. G. Reid, J. L. Betts, and K. Patrick. 1969. Tetrachloro-*o*-benzoquinone as a component in bleached kraft chlorination effluent toxic to young salmon. J. Fish. Res. Bd. Canada 26: 3055–3067.

Evidence is given that tetrachloro-*o*-benzoquinone is involved in the toxicity of bleached kraft chlorination effluent (BKCE) to young Atlantic salmon, *Salmo salar*. The main experimental support was isolation of tetrachlorocatechol from whole BKCE and from a BKCE fraction toxic to salmon, after reduction of both with sodium borohydride. Tetrachloro-*o*-benzoquinone was shown to be toxic to salmon at low concentrations. Instability of the toxic component in BKCE and substantial loss of toxicity upon treatment of BKCE with sulfur dioxide agreed with the properties of tetrachloro-*o*-benzoquinone in water solution.

Received May 30, 1969

INTRODUCTION

The objective of the work reported here was to determine the cause of the toxicity of bleached kraft chlorination effluent (BKCE) to aquatic life, salmon in particular, by isolating and identifying the substances involved.

Walden (1965), Howard and Walden (1965), Servizi et al. (MS, 1966), and Sprague and McLeese (1968a) have all reported on the lethal thresholds of bleached kraft mill effluent for salmon. Betts and Wilson (1966) reported on the same subject, showed that BKCE was the main contributor of toxicity to the mill effluent, and evolved a number of empirical treatments that reduced the toxicity. The most effective treatment devised by Betts and Wilson involved treating BKCE with small quantities of sulfur dioxide.

To date, no chemical investigation of the toxic substance(s) in BKCE has been reported in the literature. Such a study was undertaken on the assumption that knowledge of the toxic substance(s) would lead to optimum

Printed in Canada (J1491)

control of empirical detoxifying treatments, and possibly indicate new commercially feasible approaches to the problem.

A brief review of current ideas (Sarkanen, 1962; Dence, 1963) on the mechanism of the chlorination of lignin indicates that one or more of the following general reactions may occur during the aqueous acidic chlorination of lignin (Fig. 1, I): (*a*) substitution of chlorine into the guaiacyl nucleus; (*b*) electrophilic aromatic displacement of the side chain by chlorine; (*c*) cleavage of the methoxyl group; (*d*) substitution of chlorine into the aliphatic side chain; and (*e*) oxidation of the aliphatic and aromatic portions of the lignin structure to water soluble fragments. The classes of lignin fragmentation products of low molecular weight speculated as being present in BKCE, regardless of toxicity, are aliphatic chloro carbonyl/carboxylic acids (II), chloroguaiacols (III), chlorocatechols (IV), chloro-*o*-benzoquinones (V), and chloromuconic acids (VI).

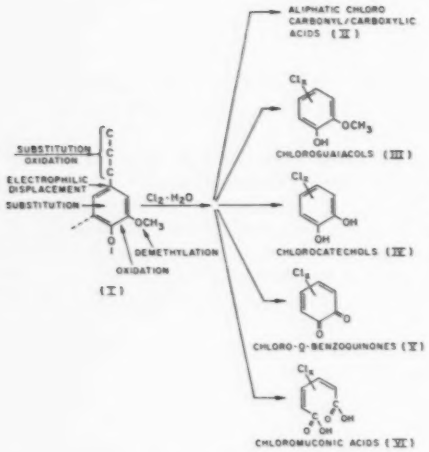

FIG. 1. Formation of lignin degradation products in BKCE during the aqueous chlorination of a kraft softwood lignin fragment. Clx denotes chlorine substituent(s) on unspecified position(s).

MATERIALS AND GENERAL METHODS

The first stage chlorination effluent (BKCE) was obtained from a kraft bleachery in which the pulp was treated with the following chemicals in succession: chlorine, sodium hydroxide, hypochlorite, chlorine dioxide, sodium hydroxide, and chlorine dioxide. The wood used in the operation was a mixture of spruce and fir, with the former species predominating, and the pulp was cooked to a permanganate number of approximately 16 prior to bleaching. The BKCE was light yellow in color, had a *p*H less than 2.0, and contained less than 0.01% solids, of which a substantial portion was ligneous materials. Also present in the BKCE was a considerable amount of hydrochloric acid formed during chlorination of the unbleached pulp.

The procedures used for handling samples and testing them for salmon toxicity have been described by Betts and Wilson (1966).

All reductions of BKCE volume were carried out on a vacuum rotary evaporator at a bath temperature of 35–40 C unless otherwise stated. The melting points were determined on a Fisher-Johns melting point apparatus and are uncorrected. The elementary analyses were carried out by Dr C. Daessle of Organic Microanalyses, Montreal, and by Schwarzkopf Microanalytical

Laboratory, New York. Analytical and preparative thin-layer chromatography (TLC) were carried out on glass plates coated with silica gel G (Merck & Co., Darmstadt, Germany). Whatman No. 1 paper was used in descending paper chromatography. Qualitative gas–liquid chromatography (GLC) was carried out with a Varian Aerograph model 1200 gas chromatograph equipped with flame ionisation detector. Ultraviolet spectra were recorded with a Cary model 14 using 1-cm cells. The infrared spectra were obtained in KBr pellets and in $CHCl_3$ solution on a Perkin-Elmer model 237 spectrophotometer. Nuclear magnetic resonance (NMR) spectra were measured using 60 Mcycle/sec (Varian A-60 spectrometer) and 100 Mcycle/sec (JEOL C-100H spectrometer) instruments. The mass spectra were taken on a Hitachi Perkin-Elmer RMU6D mass spectrometer by Morgan and Schaffer Corporation, Montreal, with an ionisation potential of 10 ev and an inlet temperature of 40 C for direct introduction of sample.

To secure substantial amounts of material suitable for elucidation of structure of toxic substances, initial work was directed towards isolation of "cleaned up" toxic fractions from large volumes of dilute BKCE, with the different fractions produced being evaluated for toxicity to salmon by bioassay tests.

The initial approach gave a number of problems, stemming mainly from the wide variations in toxicity of BKCE between batches and from the fugitive nature of the toxic compounds. The procedures used, though mild, were lengthy, taking 2 weeks in many instances, and in this space of time even the control sample of BKCE had often lost much of its toxicity. This reduction in toxicity with time made the interpretation of the results very difficult. However, of the procedures investigated, toxicity was detected most often in a chloroform acetone extract of BKCE, and it was considered logical to investigate this fraction in the hope of gaining information on structure pertinent to toxicity.

SOLVENT FRACTIONATION OF BKCE AND ANALYSIS OF THE FRACTIONS

Dilute BKCE (100 liters) was processed by methods described in Scheme I: 2.79 g of ether insoluble, chloroform acetone soluble extract and 3.36 g of ether soluble, choroform acetone soluble extract were isolated. Both the fractions were dissolved in H_2O and filtered, and the filtrate passed through a cation exchange resin (Rexyn H^+) and freeze-dried. The freeze-dried residues were then dried over KOH under vacuum for 48 hr at 25 C. Yield: 1.8 g crude ether insoluble, chloroform acetone soluble extract (Fraction A), and 2.1 g crude ether soluble, chloroform acetone soluble extract (Fraction B).

Fraction A — Very hygroscopic, dark brown powder; failed to crystallize; failed to resolve by chromatography; soluble in H_2O, ethanol, methanol, acetone, dimethyl sulfoxide (DMSO), acetic acid; no color reaction with $FeCl_3$; λ_{max} 215 mμ, $E^{\%}_{1\ cm}$ 203 (0.0032% in ethanol); ν_{max} (KBr) 3500–3300 (broad and strong), 3000–2900 (very weak and broad shoulder), 1775 (strong), 1730 (strong), 1625 (strong), 835–825 cm^{-1} (strong); NMR data (acetone-d_6); no absorption attributable to aliphatic, phenyl, phenolic, and carboxylic OH proton. Found: % C, 38.13; H, 3.45; O, 33.34; Cl, 24.66; ash, 0.00.

Fraction B — Very hygroscopic, dark brown syrup; failed to crystallize; chromatographic characteristics, solubility, color reaction, and UV, IR, and NMR data same as for Fraction A. Found: % C, 39.10; H, 3.20; O, 32.30; Cl, 25.10; ash, 0.00.

DISTILLATION AND ANALYSIS OF DILUTE BKCE

Dilute BKCE (20 liters) was distilled in N_2 at 85–90 C for 6 hr, and the distillate (500 ml) collected in 500 ml of 1% solution of 2,4-dinitrophenyl hydrazine in 0.5 N HCl. The orange precipitate formed during the collection of the distillate was collected by filtration, washed first with 0.5 N HCl, then washed free of chloride with water, and dried. The crude product, 55 mg, was separated by TLC with benzene–methanol (95:5 v/v) as eluent into the following two fractions.

Fraction I — Yield, 5 mg (0.25 ppm of BKCE); yellow powder; mp 168–170 C; not identified.

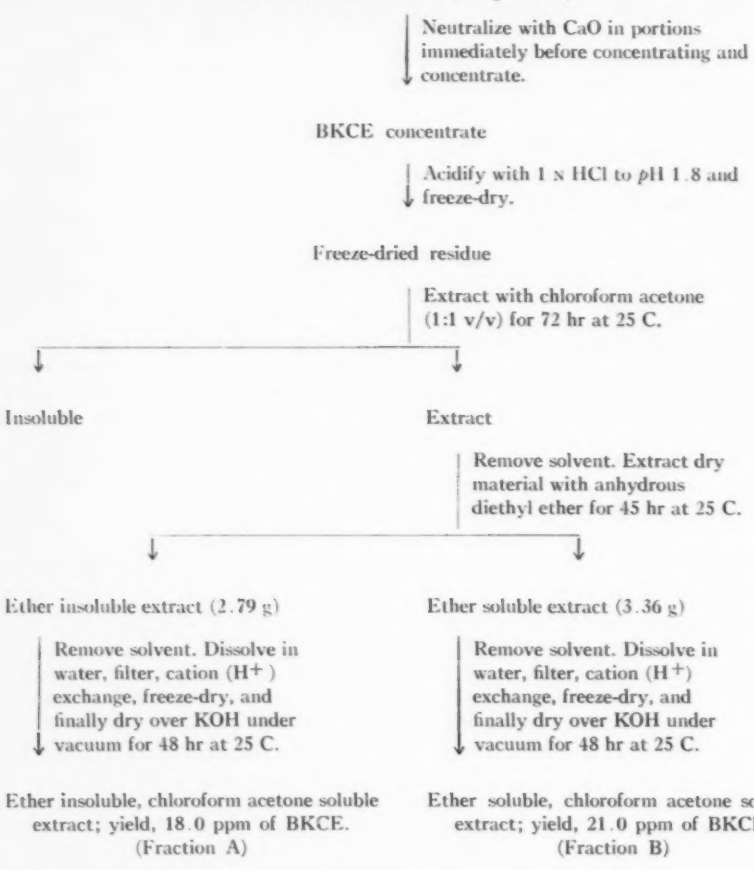
100 liters of dilute BKCE (pH 1.8)
Neutralize with CaO in portions immediately before concentrating and concentrate.
BKCE concentrate
Acidify with 1 N HCl to pH 1.8 and freeze-dry.
Freeze-dried residue
Extract with chloroform acetone (1:1 v/v) for 72 hr at 25 C.
Insoluble
Extract
Remove solvent. Extract dry material with anhydrous diethyl ether for 45 hr at 25 C.
Ether insoluble extract (2.79 g)
Ether soluble extract (3.36 g)
Remove solvent. Dissolve in water, filter, cation (H+) exchange, freeze-dry, and finally dry over KOH under vacuum for 48 hr at 25 C.
Remove solvent. Dissolve in water, filter, cation (H+) exchange, freeze-dry, and finally dry over KOH under vacuum for 48 hr at 25 C.
Ether insoluble, chloroform acetone soluble extract; yield, 18.0 ppm of BKCE. (Fraction A)
Ether soluble, chloroform acetone soluble extract; yield, 21.0 ppm of BKCE. (Fraction B)

SCHEME I. Isolation of fractions A and B from dilute BKCE.

Fraction II — Yield, 33 mg (1.65 ppm of BKCE); yellow powder; mp 315 C, mixed mp with an authentic sample of glyoxal bis-2,4-dinitrophenyl hydrazone was not depressed. Found: % C, 40.31; O, 31.0; N, 27.13; Calculated for $C_{14}H_{10}N_8O_8$: % C, 40.19; O, 30.62; N, 26.79.

In a qualitative study, a distillation similar to the above was carried out with 2 liters of dilute BKCE in N_2 at 65–70 C and the volatiles trapped in 10 ml of 0.5 N HCl. The trap solution was analyzed by GLC using a 5-ft × ⅛-inch glass column packed with 3% silicone SE-30 on 60–80 mesh DMCS-treated and acid-washed Chromosorb W (column temperature was 25 C and flow rate of nitrogen used as carrier gas was 20 ml/min), and only chloroform was detected. Similar detection of chloroform was also made in the distillate from an alkaline BKCE (pH 8.5). In another study, the distillation residue from the alkaline BKCE was freeze-dried and analyzed, and oxalic acid was detected by colorometric spot test by heating with diphenylamine (Feigl, 1966, p. 457). No formic acid or formaldehyde were detected in the above distillation experiments.

REDUCTION OF THE BKCE WITH SODIUM BOROHYDRIDE

Qualitative Study

Dilute BKCE (2 liters, *p*H 1.8) was treated with 5 g $NaBH_4$ at 25 C. After about 8 hr of reaction, when the color of the solution had changed from yellow to pink and the *p*H had gone up to 8.5, the solution was filtered. The filtrate was acidified with dilute HCl to *p*H 1.8, and then extracted with ether. The syrupy, crude ether extract was analyzed by TLC in the following two solvent systems. Solvent system A (ethanol–ammonia (25%)–water (100:16:12v/v)) gave a violet red round spot near the solvent front, visible without spray. Solvent system B (toluene–ethyl formate–formic acid (50:40:10 v/v)) gave six close spots of different colors with one intense dark grey spot, all visible without spray; these spots turned green with $FeCl_3$ and then red with Na_2CO_3 spray. In solvent system A, samples of pure catechol, 4-chloro-, 4,5-dichloro-, and tetrachlorocatechol showed similar violet red spots at the same position as observed with the crude extract. Also, in the solvent system B, the above catechols had the same R_f value as the intense spot observed with the extract. The catechols also showed a similar color change on $FeCl_3$ + Na_2CO_3 spray.

In another experiment, a $NaBH_4$ reduction of the BKCE was carried out at 70 C maintaining the *p*H at 9.5, the reaction mixture processed, and the crude ether extract analyzed by TLC as before. In solvent system B, six close spots of different colors with two intense spots were visible without spray, one of the intense spots corresponding to the dark grey spot observed earlier, and the other, a deep violet spot, near the starting line of the chromatogram. This new violet spot had a R_f corresponding to that of chloranilic acid (Scheme II, VII).

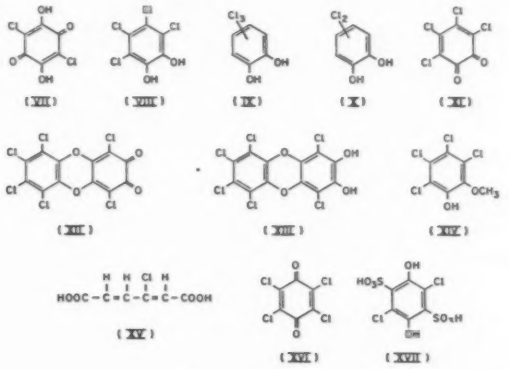

Scheme II.

Quantitative Study

BKCE (75 liters) was concentrated to 1/50 of its volume (1.5 liters), and the insoluble ligneous material removed by filtration. To the clear yellow concentrate was slowly added 30 g $NaBH_4$ at 25 C over a period of 4 hr with vigorous stirring. After the reaction had continued for another 18 hr, the resulting pink solution (*p*H 8.5), which contained a substantial amount of black precipitate, was acidified with 1 N HCl to *p*H 1.8 and filtered, and the yellow filtrate continuously extracted with diethyl ether (800 ml) in a liquid–liquid extractor for 24 hr. The ethereal solution of the extract was concentrated to about 100 ml, when most of the boric acid crystallized. The ether solution was then filtered, and dried over anhydrous Na_2SO_4; the ether was removed by evaporation, and the crude ether extract finally dried in vacuum over $CaCl_2$ at 25 C. Yield: 2.36 g brown syrup (31 ppm of BKCE).

The above extract (2.30 g dissolved in 5 ml ethanol) was subjected to TLC using 22 silica gel G plates (20 × 30 cm) and solvent system B as eluent. One fraction (Fraction C), containing the major component, was purified by repeated TLC and isolated as a brown syrup. Fraction C still showed some tailing when the purity was checked by TLC. Yield was 155 mg (2.12 ppm of BKCE); TLC R_f value in solvent system B was the same as for pure 4-chloro-, 4,5-dichloro-, and tetrachloro-catechol; paper chromatographic R_f value in benzene–acetic acid–water (1:1:2 v/v) was the same as for tetracholorocatechol; IR spectrum was identical to that observed with tetrachlorocatechol except that resolution was poorer and there was an extra peak (ν_{max} at 1725–1710 cm^{-1}), thought to be due to traces of formic acid from TLC eluent; UV spectral data indicated λ_{max} 292 mμ, $E^{1\%}_{1\ cm}$ 34 (0.002% in ethanol), whereas UV spectral data of tetrachlorocatechol (Table 1) indicated λ_{max} 297 mμ, ϵ_{max} 6448 (ethanol); NMR data (DMSO-d_6) indicated no

TABLE 1. Ultraviolet light absorption of lignin and lignin model compounds.

Compound	λ_{max}, mμ (ϵ_{max})	Solvent
Catechol	280(2,750)	Ethanol
	218(6,073)	
Tetrachlorocatechol	297(6,448)	"
5-Carboxy vanillic acid	312(2,650)	"
	265(5,300)	
	225(2,200)	
Protocatechunic aldehyde	315(7,763)	"
	280(8,338)	
	235(11,788)	
	215(13,225)	
β-Chloromuconic acid	265(1,722)	"
p-Benzoquinone	296(425)	"
	242(17,700)	
Tetrachloro-p-benzoquinone	292(23,800)	Chloroform
	282(21,400)	
Tetrachloro-o-benzoquinone	215(22,960)	Ethanol
Lignosulfonic acid	280	"
Chlorolignin (chlorination in CCl_4)[a]	266	"
Fractions A and B (Fig. 2)	215	"

[a]From Brauns and Brauns (1960, p. 283–285).

absorption; mass spectral data indicated a complex mixture in which three parent peaks were observed at masses 246, 212, and 178. At mass 246, the observed distribution ratios of the parent peak (P) to the isotopic peaks (P+2, P+4, P+6, and P+8) and also the observed ratio of the parent peak to P+1 indicated four chorine and six carbon atoms, respectively, which agreed with tetrachlorocatechol structure (Scheme II, VIII). At masses 212 and 178, the observed 212/214/216/218 ratios and the 178/180/182 ratios agreed well with trichlorocatechol (IX) and dichlorocatechol structure (X), respectively. Fraction C gave the following elementary analysis: % C, 45.8; H, 4.84; Cl, 27.6; O (by difference), 21.76.

Fraction C (100 mg) was further purified by TLC as described, and a chromatographically pure fraction (Fraction C-1) containing the major component (Fig. 2) was isolated as a black powder. Yield was 81 mg (1.8 ppm of BKCE); mp was 95–105 C (tetrachlorocatechol trihydrate melts at 94 C, and tetrachlorocatechol monohydrate at 180–184 C); IR spectrum was identical to that of pure tetrachlorocatechol; UV spectrum (water, pH 9.0) was identical to that of tetrachlorocatechol (λ_{max} 308 mμ, ϵ_{max} 2835; λ_{max} 266 mμ, ϵ_{max} 4252; λ_{max} 225 mμ, ϵ_{max} 24,450); NMR

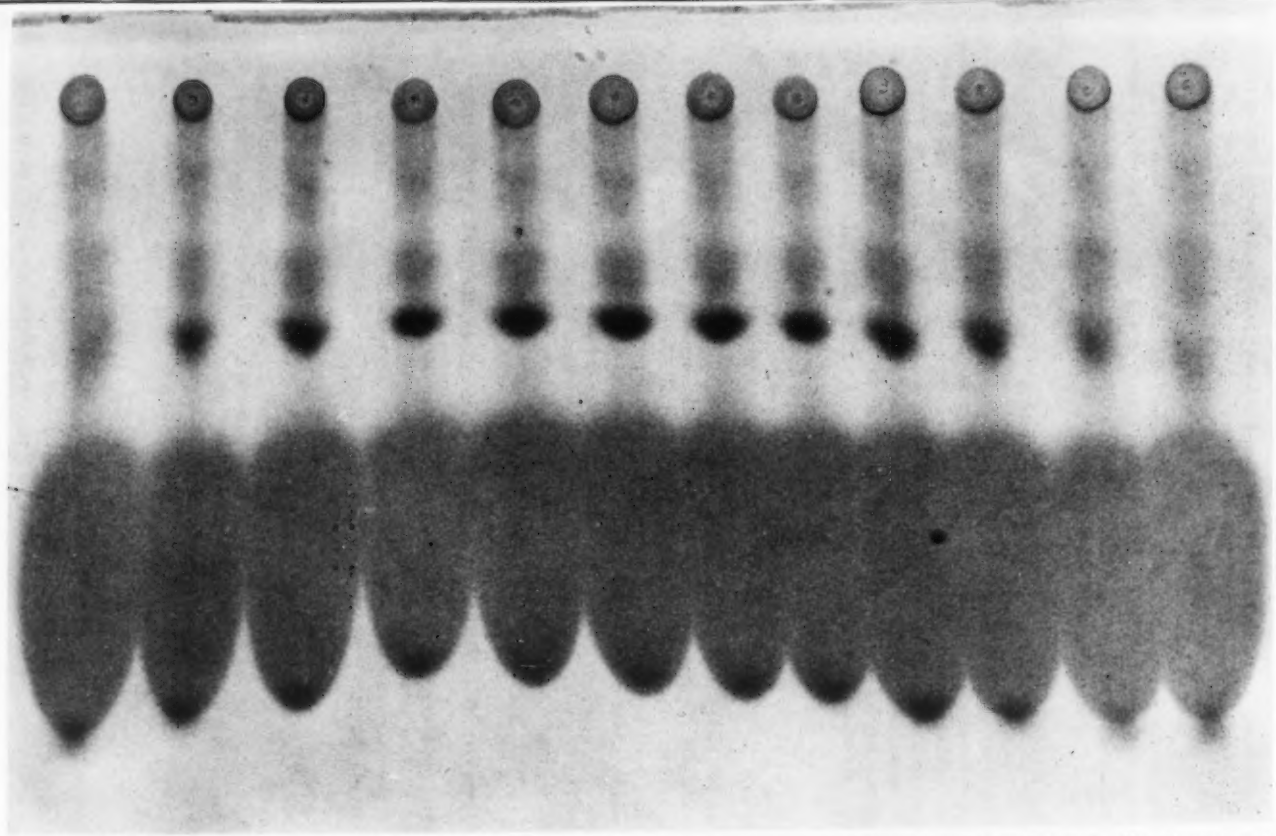

FIG. 2. A typical thin-layer chromatogram of Fraction C isolated from crude ether extract of BKCE reduced with $NaBH_4$. The intense spot, containing the major component, represents Fraction C-I. Adsorbent: Silica gel G. Solvent: tolune–ethyl formate–formic acid (50:40:10 v/v). Visible without spray.

spectral data (DMSO-d_6) indicated no proton absorption, with an identical observation for tetrachlorocatechol; mass spectral data indicated that the distribution ratios of the parent peak to the isotopic peaks, the ratio of the parent peak to P+1, and the fragmentation pattern were consistent with the structure of tetrachlorocatechol. Found: % C, 28.80; H, 1.48; Cl, 53.09, O (by difference), 16.63. Calculated for tetrachlorocatechol monohydrate, $C_6Cl_4(OH)_2 \cdot 1H_2O$: % C, 27.06; H, 1.50; Cl, 53.88; O, 18.04.

Reaction of Fraction C-1 in DMSO with acetic anhydride at 0 C gave a crystalline diacetate derivative (ethanol), mp 192 C (diacetate of tetrachlorocatechol melts at 190 C). Found: % C, 36.51; H, 2.16; Cl, 41.83; O (by difference), 19.50. Calculated for tetrachlorocatechol diacetate, C_6Cl_4 $(OCOCH_3)_2$: % C, 36.14; H, 1.80; Cl, 42.77; O (by difference), 19.29.

ISOLATION OF TOXIC FRACTION FROM BKCE BY ETHYL ACETATE EXTRACTION

BKCE (30 liters) was reduced in volume (4 liters) at 25 C under diminished pressure and the concentrate extracted with ethyl acetate (3 × 1500 ml) in a separatory funnel in as short a time as possible (6 days). Yield of dried extract was 0.90 g. An aqueous solution of one-half of the above extract (0.45 g), and the mother liquor from the extraction (both equivalent to 15 liters of dilute BKCE) were evaluated for toxicity to salmon by 96-hr bioassays (Table 2, tests 15 and 16, respectively). The other half of the extract (0.45 g) was reduced with $NaBH_4$, and tetrachlorocatechol (Scheme II, VIII) was detected in the reduction product by the TLC and spectral methods already described.

AQUEOUS CHLORINATION OF CATECHOL AND BIOASSAY EVALUATION OF THE CHLORINATED SOLUTION FOR TOXICITY

Chlorine gas was passed into a solution of recrystallized catechol (4.50 g) in water (1800 ml) at 25 C, until a clear yellow–orange color persisted, and then the excess Cl_2 was removed by passage of N_2. The chlorinated solution failed to show the typical TLC spots of catechol and chlorocatechols in either solvent system A or B (there was only a streak near the starting line) and the yellow–orange color was an indication of the formation of chloro-*o*-benzoquinones. Also, the typical color reaction of catechol and chlorocatechols with $FeCl_3$ + Na_2CO_3 was negative with the chlorinated solution. Aliquots of the chlorinated solution were adjusted to 30 ppm and 60 ppm concentration with water, and then evaluated for toxicity to salmon by 96-hr bioassay before and after SO_2 treatment (Table 2, test 13, 13*a*, 14, and 14*a*).

BIOASSAY EVALUATION OF BKCE MODEL COMPOUNDS FOR TOXICITY

Samples of pure monochloropyruvic acid, trichloropyruvic acid, monochloro-, dichloro-, and trichloro-acetic acid, and trichloroacetaldehyde (chloral) were evaluated by 96-hr bioassay tests and found nontoxic to salmon up to 100 ppm concentration. Monochloropyruvic acid was prepared according to Garino (1922) and the other compounds were commercially available.

Chloranilic acid (Scheme II, VII) and β-chloromuconic acid (XV) were also evaluated as nontoxic in 96-hr bioassay tests at 20 ppm concentration (Table 2, tests 1 and 2, respectively). Results of the bioassay toxicity tests of 4-chlorocatechol, 4,5-dichlorocatechol, 3,5-dichlorocatechol, tetrachlorocatechol, and tetrachloro-*o*-benzoquinone before and after treatment with SO_2 (tests 3 through tests 12*c*) are recorded in Table 2.

4-Chloro- and 4,5-dichloro-catechol were prepared according to Willstatter and Muller (1911), β-chloromuconic acid was prepared according to Braddon and Dence (1968), and the other compounds were commercially available.

DISCUSSION

In the UV spectra of Fractions A and B the absence of any absorption maximum except the one observed at λ_{max} 215 mμ clearly rules out the presence

TABLE 2. Mortality rates for young salmon[a] in 96 hr continuous-flow bioassay tests of BKCE extract fractions and model compounds.[b]

Test	Compound	Concentration (*ppm*)		Mortality (% at time shown)
		Without SO_2	With SO_2	
1	Chloranilic acid	20	—	0 (96 hr)
2	β-Chloromuconic acid	"	—	0 (96)
3	4-Chlorocatechol	"	—	100 (1)
4	4-Chlorocatechol	"	40	100 (2)
5	3,5-Dichlorocatechol	"	—	100 (3)
6	3,5-Dichlorocatechol	"	40	100 (2)
7	4,5-Dichlorocatechol	"	—	100 (1)
8	4,5-Dichlorocatechol	"	40	100 (2)
9	Tetrachlorocatechol	"	—	100 (1)
10	"	"	40	100 (1)
10*a*	"	"	60	100 (1)
11	Tetrachloro-*o*-benzoquinone	3	—	100 (10)
11*a*	"	10	—	100 (3)
11*b*	"	20	—	100 (1)
12	"	"	40	100 (17)
12*a*	"	"	60	80 (14)
12*b*	"	10	40	0 (96)
12*c*	"	3	20	0 (96)
13	Aqueous solution of chloro-*o*-benzoquinones	30	—	90 (96)
13*a*	"	60	—	100 (96)
14	"	30	60	0 (96)
14*a*	"	60	120	0 (96)
15	Ethyl acetate extract of BKCE[c]	75[d]	—	100 (3.5)
16	BKCE mother liquor after ethyl acetate extraction[c]	75[d]	—	30 (55)

[a]Ten fish tested in each test.

[b]Mortalities in parallel tests with 75% BKCE were 100% in 10 hr or less (in 1 hr in tests 15 and 16).

[c]Same BKCE used for extraction and control.

[d]Percentage.

of any guaiacol (Fig. 1, III), catechol (IV), or muconic acid (VI) structures in the fractions. This was also substantiated by IR and NMR studies. Furthermore, the fractions gave a negative $FeCl_3$ test, demonstrating that any phenolic structures (III, IV) are absent in the fractions. The UV absorption maximum at 215 mμ is assigned to chromophores from *o*-benzoquinones (V) or keto-carboxylic acids (II), and the presence of the same structural units can be inferred from the IR spectra of the fractions (1775 cm^{-1}, carboxylic acid C=O, probably shifted to higher frequency because of electron withdrawing chlorine substituents; 1730 cm^{-1}, ketone or quinone C=O; 1625 cm^{-1}, carboxylic acid OH; 3500–3300 cm^{-1}, carboxylic acid OH). The NMR spectrum failed to show any proton absorption whether aliphatic, phenyl, phenolic, or carboxylic OH. This indicates that structures present in the fractions are highly chlorine

substituted. Additional evidence of the high chlorine substitution is furnished by the IR spectral studies, which showed no strong absorption due to C—H frequency (the weak shoulder band observed at 3000–2900 cm^{-1} is normally very intense for C—H stretching). The strong peak at ν_{max} 835–825 cm^{-1} is attributable to C—Cl stretching, probably shifted from the normal 750–700 cm^{-1} position because of high chlorine substitution. In fact, such a shift in highly chlorinated complex molecules is known (Bellamy, 1964, p. 331).

The structural information gained from the above investigation indicates that the BKCE extract fractions have nonbenzenoid structure, contain carbonyl/carboxyl functional group(s), and are highly substituted by chlorine. Compounds containing such structures visualised as being present are aliphatic chlorocarbonyl/carboxylic acids (II) or nonbenzenoid chloro-*o*-benzoquinones (V).

The fact that fresh BKCE slowly loses its toxicity with time suggests that the toxic substances undergo some sort of chemical transformation, such as decomposition, condensation, or polymerisation, to nontoxic products. In analysis of the effluent for decomposition products, glyoxal and chloroform were identified, and oxalic acid detected in the effluent. This furnished indirect evidence of the presence of structures of class II in the BKCE, since the most likely source of chloroform, glyoxal, and oxalic acid in the effluent is hydrolysis of compounds such as dichloro- and trichloro- derivatives of pyruvic acid and acetaldehyde. However, when a number of compounds belonging to class II, viz. monochloro- and trichloro-pyruvic acid, trichloroacetaldehyde, monochloro-, dichloro-, and trichloro-acetic acid were evaluated for toxicity to salmon, none of them was found toxic in 96-hr bioassays even up to 100 ppm concentration. This is strong evidence that the above aliphatic chlorocarbonyl/carboxyl compounds (II), which are normally considered to be extremely toxic, are not responsible for the toxicity of BKCE to salmon. It also suggests that BKCE contains toxic substances specific to salmon. This belief is substantiated by Sprague and McLeese (1968b) who reported that such effluent apparently contained different toxic materials for lobster larvae and small salmon.

Another class of chlorocarbonyl compound which might still contribute to the toxicity in BKCE is the nonbenzenoid chloro-*o*-benzoquinone (V). Such *o*-quinones can originate in the effluent by chlorination, demethylation, and oxidation of the guaiacyl propane unit (I) present in the residual lignin of the unbleached pulp, through intermediate formation of chlorocatechols (IV) via chloroguaiacols (III). Further oxidation of structure V can also lead to the formation of chloromuconic acids (VI) by rupture of the quinoid structure.

The presence of either a structure of class VI or the intermediates of classes III and IV in the effluent is ruled out because of the lack of their characteristic UV absorption maxima. As is apparent from Table 1, structures containing guaiacyl or catechol nuclei as normally present in lignin or its degradation products can be easily identified by UV studies, e.g., catechol (280 mμ), tetrachlorocatechol (297 mμ), 5-carboxy vanillic acid (265 mμ), protocatechunic aldehyde (280 mμ), and lignosulfonic acid (280 mμ). Even a chlorolignin (pre-

pared under nonaqueous chlorination conditions to keep the demethylation of the guaiacyl unit (I) to a minimum) is also known to absorb at λ_{max} 266 mμ (Brauns and Brauns, 1960, p. 283–285). Similarly, UV characteristics can be used to identify structures containing unsaturation chromophores as present in muconic acid, e.g., β-chloromuconic acid (265 mμ). Also, a *p*-benzoquinoid structure, the presence of which in BKCE is highly unlikely, is identifiable by UV studies, e.g., *p*-benzoquinone (242 mμ) and tetrachloro-*p*-benzoquinone (292, 282 mμ).

The *o*-quinone structure as present in tetrachloro-*o*-benzoquinone shows a UV absorption maximum at 215 mμ only. This is significant because identical absorption was observed with the BKCE extract fractions. This finding along with other observations made earlier in connection with BKCE justified a search for the presence of any *o*-benzoquinone structures (V) in the effluent.

It is known that *o*-benzoquinones, because of their highly reactive nature, are very unstable and undergo rapid transformation in aqueous solution. It is, therefore, apparent that isolation of such compounds from a dilute aqueous BKCE would be extremely difficult, unless processed rapidly under mild conditions (Adler and Magnusson, 1959). Also, the fate of the *o*-quinones when undergoing transformation is not definitely known. It is generally believed that self condensation reactions take place leading to largely undefined complex products, which probably bear a structural resemblance to humic acid. However, if the complex structure from the above transformation still retains the *o*-benzoquinoid unit, there is a chance that reduction of this structure will result in the formation of catechols. In fact, after qualitative reduction of BKCE with $NaBH_4$, the presence of a mixture of chlorocatechols (Fig. 1, IV) and chloranilic acid (Scheme II, VII) was detected by TLC. Confirmation for the conjecture of the presence of the *o*-benzoquinoid structure in the effluent is furnished by the identification of a mixture of chlorocatechols (IV) in a crude major fraction (Fraction C). Evidence that tetrachloro-*o*-benzoquinone (XI) or its quinoidal structure was present as the major component was obtained by further purifying the crude Fraction C by TLC to Fraction C-I (yield, 1.8 ppm of BKCE) and identifying the fraction as pure tetrachlorocatechol (VIII) by chromatographic, chemical, IR, UV, NMR, and mass spectral analyses, and by preparation of a diacetate derivative.

An *o*-benzoquinoidal structure is defined here as a stable complex molecule derived from the parent *o*-benzoquinone and still retaining the *o*-quinoid nucleus. In BKCE, one such possible complex is a stable hexachlororthoquinopyrocatechol ether (XII) formed by self condensation of tetrachloro-*o*-benzoquinone (XI) in the presence of water. This supposition is supported by the work of Jackson and McLaurin (1906, 1907) who reported the isolation of the highly acid stable ether (XII) by reacting the quinone (XI) with water, its decomposition to chloranilic acid (VII) by alkali, and its conversion to a mixture of hexachlorodihydroxypyrocatechin ether (XIII) and tetrachlorocatechol (VIII) by sodium amalgam reduction. Since the conversion of structure XI to structure VII by alkali treatment (Braddon and Dence, 1968) and the

reduction of structure XI to structure VIII is known, it seems plausible that the tetrachlorocatechol (VIII) and chloranilic acid (VII) detected in the alkaline borohydride reduction of BKCE can originate from both quinone (XI) and its *o*-benzoquinoidal ether (XII). In any event, the parent compound in BKCE is considered to be the tetrachloro-*o*-benzoquinone (XI).

The formation of tetrachloro-*o*-benzoquinone (XI) in BKCE is consistent with the current concept (Sarkanen, 1962; Dence, 1963) of the mechanism of chlorination of lignin. Because of the highly condensed structure of the residual lignin in unbleached kraft pulp, it is likely that only the guaiacyl propane end units are involved in forming the fully substituted quinone. The end groups of spruce lignin have been shown by Dence and Sarkanen (1960) to participate in nonaqueous chlorination with formation of tetrachloroguaiacol (XIV), though under more severe conditions than commercial first stage chlorination (glacial acetic acid, 100–110 C, 50 min).

Having produced evidence of the presence of tetrachloro-*o*-benzoquinone (XI) in the BKCE, the next step was the evaluation of its toxicity to salmon by bioassays both before and after treatment with SO_2. The toxicity of BKCE is known to be reduced by treatment with SO_2 (Betts and Wilson, 1966). Study of the toxicity of tetrachloro-*o*-benzoquinone (XI) and a number of model compounds before and after SO_2 treatment (Table 2) indicated that the tetrachloro-*o*-benzoquinone (XI) and all the chlorocatechols tested are extremely toxic to salmon (tests 3, 5, 7, 9, 11, 11*a*, and 11*b*). (It should be noted that Servizi et al. (MS, 1968) reported similar toxicities of 4,5-dichloro- and tetrachloro-catechol to salmon). It is also evident from the table that after treatment with SO_2, all of the chlorocatechols still remain extremely toxic (tests 4, 6, 8, 10, and 10*a*), whereas the quinone (XI) is rendered less toxic or nontoxic upon addition of SO_2 (tests 12, 12*a*, 12*b*, and 12*c*). In test 11, all of the fish died in 10 hr at 3 ppm concentration of the quinone (XI), whereas the same solution after treatment with 20 ppm SO_2 had no toxicity (test 12*c*). Similar results were obtained at 10 ppm concentration of the quinone (XI) and 40 ppm SO_2 (tests 11*a* and 12*b*). The fact that tetrachloro-*o*-benzoquinone (XI) is toxic at low concentrations and is rendered nontoxic by treatment with SO_2 in the same way as BKCE gives good support to the argument that it is present in the effluent as a toxic component. It is also of interest to note that chloro-*o*-benzoquinones, prepared in aqueous solution by chlorination of catechol at 25 C, and initially toxic to fish (tests 13 and 13*a*), lose their toxicity when treated with SO_2 (tests 14 and 14*a*).

Having provided chemical evidence for the presence of tetrachloro-*o*-benzoquinone (XI) as a toxic component in BKCE, and having demonstrated that loss of toxicity of BKCE upon SO_2 treatment is consistent with the presence of tetrachloro-*o*-benzoquinone, the next step was direct examination of toxic BKCE. For this purpose fresh toxic BKCE was concentrated under mild conditions and extracted with ethyl acetate. By bioassay tests, most of the toxicity was shown to be in the ethyl acetate extract (Table 2, test 15); and,

upon reduction of this extract with $NaBH_4$, tetrachlorocatechol (VIII) was formed, indicating the presence of tetrachloro-*o*-benzoquinone.

The finding of tetrachloro-*o*-benzoquinone (XI) as a toxic ingredient in BKCE is also consistent with most of the results observed by Betts and Wilson (1966) in their effluent detoxification studies. For instance, effective detoxification by treatment with NaOH is attributable to the nucleophilic displacement of chlorine in structure XI (Braddon and Dence, 1968) with the resulting formation of nontoxic chloranilic acid (VII) (Table 2, test 1). Failure to detoxify the effluent with reducing agents such as ascorbic acid or sodium sulfide is ascribed to the reduction of toxic quinone to tetrachlorocatechol (VIII), another toxic substance (Table 2, test 9). Since SO_2 treatment renders the effluent nontoxic, a plausible hypothesis is that both reduction and sulfonation of quinone are involved. This conjecture is supported by the fact that tetrachloro-*p*-benzoquinone (XVI) undergoes simultaneous reduction and sulfonation when treated with dilute aqueous acid bisulfite to 2,5-dichloro-3,6-disulfohydroquinone (XVII) (Huntress, 1948). However, final proof of this supposition would require a detailed study of the reaction of the tetrachloro-*o*-benzoquinone (XI) with SO_2, which is beyond the scope of the present investigation.

Prolonged aeration of BKCE probably converts the toxic quinone (XI) to nontoxic humus substances. Failure to detoxify BKCE by oxidizing agents such as ClO_2, H_2O_2, and O_3 (Betts and Wilson, 1966) is explained by resistance of the quinone (XI) to oxidation under the conditions employed to presumably nontoxic tetrachloromuconic acid (c.f. Table 2, β-chloromuconic acid (XV), nontoxic, test 2).

Chlorine dioxide is known to attack aromatic nuclei containing free phenolic groups rapidly, converting these to quinones and cyclic peroxides; and with aromatic nuclei having etherified phenolic groups, demethylation and subsequent oxidation to quinones occur at a slow rate. However, unlike chlorination, substitution of the aromatic nuclei and electrophilic displacement of the side chain of lignin by chlorine is not feasible during bleaching with ClO_2. In hypochlorite bleaching, HOCl is known to react as a chlorine substituting agent and can cause electrophilic displacement in the same way as molecular chlorine. Hypochlorite also attacks aromatic nuclei with free phenolic groups rapidly, but unlike aqueous chlorination, the etherified units in lignin are quite unreactive. From the above, it is evident that neither ClO_2 nor hypochlorite bleaching fulfils the conditions postulated for the formation of tetrachloro-*o*-benzoquinone (XI) from lignin, namely substitution–sidechain displacement–demethylation–oxidation. This possibly explains why effluents from bleaching of kraft pulp by ClO_2 or by hypochlorite are nontoxic to salmon as observed by Betts and Wilson (1966).

At this time the amount of tetrachloro-*o*-benzoquinone formed in BKCE during the first stage chlorination of kraft pulp, and the contribution of the quinone and related orthoquinoidal compounds to the total toxicity of BKCE are not known. The concentrations of the quinone and orthoquinoidal compounds cannot be derived stoichiometrically from the amount of tetrachloro-

catechol isolated after reduction of BKCE and this aspect of the problem will be the subject of future research.

ACKNOWLEDGMENTS

The authors wish to thank Fraser Companies, Limited, and the Ontario Research Foundation for permission to publish the results of the investigations; Mr G. G. Wilson of Fraser Companies, Limited, for assistance in the direction of the toxicity investigations; Mr D. E. Routledge of Fraser Companies, Limited, for his contributions to the experimental work in the chlorination of catechol and the toxicity evaluation of the compounds so formed; and Mr G. P. Tam of the Ontario Research Foundation for his assistance in the chemical aspects of the work.

REFERENCES

ADLER, E., AND R. MAGNUSSON. 1959. Periodate oxidation of phenols. I. Monoethers of pyrocatechol and hydroquinone. Acta Chem. Scand. 13: 505–519.

BELLAMY, L. J. 1964. The infrared spectra of complex molecules. Chapter 19. Halogen compounds. John Wiley and Sons, New York, N.Y.

BETTS, J. L., AND G. G. WILSON. 1966. New methods for reducing the toxicity of kraft mill bleachery wastes to young salmon. J. Fish. Res. Bd. Canada 23: 813–824.

BRADDON, S. A., AND C. W. DENCE. 1968. Structure and reactivity of chlorolignin. I. Alkaline hydrolysis of chlorine-substituted lignin model compounds. Tappi 51: 249–256.

BRAUNS, F. E., AND D. A. BRAUNS. 1960. The chemistry of lignin: supplement volume. Chapter XI. The halogenation of lignin. Academic Press, New York, N.Y.

DENCE, C. W. 1963. Chlorination, p. 40–66. *In* W. H. Rapson [ed.] Bleaching of pulp. Tappi Monograph 27. Chap. 4. Tappi, New York, N.Y.

DENCE, C. W., AND K. V. SARKANEN. 1960. A proposed mechanism for the acidic chlorination of softwood lignin. Tappi 43: 87–96.

FEIGL, F. 1966. Spot tests in organic analysis. Chapter 5. No. 45. Oxalic acid, test no. (2). Elsevier Publishing Company, Amsterdam, the Netherlands.

GARINO, M. 1922. Trihalogenated pyruvines. Gazz. Chim. Ital. 52(II): 207–220. (Chem. Abst. 17: 1624–1625 (1923).)

HOWARD, T. E., AND C. C. WALDEN. 1965. Pollution and toxicity characteristics of kraft pulp mill effluents. Tappi 48: 136–141.

HUNTRESS, E. H. 1948. Organic chlorine compounds. Chapter XI. Serial Number 3:4978, 2,3,5,6-tetrachlorobenzoquinone-1,4. John Wiley and Sons, New York, N.Y.

JACKSON, C. L., AND R. D. MCLAURIN. 1906. On certain derivatives of tetrachlororthobenzoquinone. Am. Chem. J. 37: 7–19.
1907. Some derivatives of tetrachlororthobenzoquinone. Am. Chem. J. 38: 127–175.

SARKANEN, K. V. 1962. The chemistry of delignification in pulp bleaching, p. 219–231. *In* Proceedings of the wood chemistry symposium (1961, Montreal). Butterworths, London, England.

SERVIZI, J. A., R. W. GORDON, AND D. W. MARTENS. MS, 1968. Toxicity of two chlorinated catechols, possible components of kraft pulp mill bleach waste. Intern. Pacific Salmon Fish. Comm., New Westminster, B.C., Progr. Rept. 17. 43 p.

SERVIZI, J. A., E. T. STONE, AND R. W. GORDON. MS, 1966. Toxicity and treatment of kraft pulp bleach plant waste. Intern. Pacific Salmon Fish. Comm., New Westminster, B.C., Progr. Rept. 13. 34 p.

SPRAGUE, J. B., AND D. W. MCLEESE. 1968a. Toxicity of kraft pulp mill effluent for larval and adult lobster, and juvenile salmon. Water Res. 2: 753–760.
1968b. Different toxic mechanisms in kraft pulp mill effluent for two aquatic animals. Water Res. 2: 761–765.

WALDEN, C. C. 1965. Water pollution and the kraft pulp mill industry. Western Fish. 34: 36–37, 38–40; 71: 18–20.

WILLSTATTER, R., AND H. E. MULLER. 1911. Über Chlorderivate des Brenzcatechins und des o-Chinons. Ber. Deut. Chem. Ges. 44: 2182–2184.

A Formulation of the von Bertalanffy Growth Curve when the Growth Rate is Roughly Constant

WILLIAM KNIGHT

Fisheries Research Board of Canada
Biological Station, St. Andrews, N.B., and The University of New Brunswick
Fredericton, N.B.

KNIGHT, WILLIAM. 1969. A formulation of the von Bertalanffy growth curve when the growth rate is roughly constant. J. Fish. Res. Bd. Canada 26: 3069–3072.

The author contends that the parameters of any growth curve should be a direct description of the graphical appearance of the data. For growth that is even approximately linear this is not true of the von Bertalanffy curve in its usual form (von Bertalanffy, Human Biol. 10: 181–213, 1938). On the above grounds, an alternate form of the von Bertalanffy curve for use in such instances is proposed.

Received June 6, 1969

INTRODUCTION

THE SIMPLEST and statistically most pleasant growth curve is the straight line. This being so, it follows from the law of fundamental cantankerousness of the universe that growth data, whose growth curve is almost a straight line but just sufficiently nonlinear that a straight line will not suffice, will appear. What is then wanted is a small correction term that can be attached to the straight line formula, altering it from

$$\text{size at age} = \text{initial size} + \text{growth rate} \times \text{age} \tag{1}$$

to

$$\text{size at age} = \text{initial size} + \text{growth rate} \times \text{age} + \text{correction.} \tag{2}$$

The mathematician will automatically suggest a quadratic correction; if a straight line will not work, try a parabola. But the student of growth will probably prefer a correction whose extrapolation is not actually silly (the parabola, of course, may extrapolate to negative sizes at old ages), and commonly selects an exponential correction factor, thus being led to the von Bertalanffy (1938) curve. This is usually a proper and reasonable curve to use under the circumstances. Unfortunately it is not a solution to the problem posed; as usually written, the von Bertalanffy curve does not have the algebraic form of a straight line plus a correction term. However, the von Bertalanffy curve can be so formulated, and it is the purpose of this report to do so.

If two formulations give the same growth curve, what difference does it make? The author's answer arises from certain preconceptions upon which the reader will have to make his own judgement: Although many growth curves, the von Bertalanffy among them, have been proposed upon physio-

Printed in Canada (J1498)

logical grounds, these grounds do not seem to be generally accepted. Perhaps at some future time, growth curves will have a generally accepted physiological basis; until then, our immediate need is growth curves that are a good summary of the data, and a growth curve must be evaluated as an empirical description of data in hand rather than from physiological theory.

From the point of view of empirical description it is good if the parameters of the formulation of the growth curve are easily interpreted in terms of the data, in particular the parameters should relate easily to the age–size scatter plot. In the standard form of the von Bertalanffy curve,

$$\text{length at age } t = L_t = L_\infty(1 - \exp(-K(t - t_0))), \tag{3}$$

this is not so when the growth is nearly linear. (When the growth is markedly nonlinear, the standard form is to be preferred to the one to be proposed.) L_∞ has the dimension of length but is away outside the observed length range; a size intercept might be preferable to the age intercept, t_0, given; K as a compound interest rate is of little interest in nearly linear growth, and its interpretation as a nonlinearity index is not often made. Worst of all, although this is called a growth curve, no symbol in equation 3 has the dimensions of growth, length per unit time!

THE ALTERNATE FORM

The alternate formulation,

$$L_t = A + B(t - \bar{t}) + B(1 - K(t - \bar{t}) - \exp(-K(t - \bar{t})))/K \tag{4a}$$

$$= A + B(1 - \exp(-K(t - \bar{t})))/K \tag{4b}$$

where $\bar{t}$ is the average age, has the desired properties. (This formulation can be used for other choices of $\bar{t}$ than the average age, in particular the midrange might be useful.) The first two terms of equation 4*a* are a straight line; the third is a correction term that is small for t near to $\bar{t}$. Moreover equations 4*a* and 4*b* describe the same growth curve as the standard form 3, the relation being:

$$\begin{aligned} L_\infty &= A + B/K \\ t_0 &= \bar{t} - \log_e(1 + KA/B)/K \\ B &= KL_\infty(\exp(-K(\bar{t} - t_0)) \\ A &= L_\infty(1 - \exp(-K(\bar{t} - t_0))). \end{aligned} \tag{5}$$

K is the same in both formulations. In equation 4 it plays the role of a nonlinearity parameter; however, a better measure of nonlinearity is the dimensionless number $K\Delta$, where Δ is the half age span over which growth has been observed. (For example, if the youngest and oldest ages observed are 1 and 6 years, $\Delta = 2\frac{1}{2}$). See the discussion of equations 9–11 for more detail on this point. The centering of the description at the average age makes no sense if the von Bertalanffy curve is thought of as a physiological verity, much sense if thought of as a summary of a set of growth data.

In passing, it is noted that if t_0 is about zero, as sometimes happens, this crude description can be made:
Since

$$\text{rate of growth at age } t_0 = KL_\infty, \tag{6}$$

the growth curve is roughly a line passing through the origin with slope (growth rate) KL_∞ and nonlinear to the extent of $K\Delta$.

METHODS OF FITTING

Given a set of growth data, how does one fit equation 4? One method is to fit the usual form 3 using the reader's favourite method (e.g., Walford, 1946; Allen, 1966), and then convert the parameters using the relations equation 5. Another possibility will be described shortly.

The remainder of this report describes a method of fitting equation 4 using a parabolic approximation. As equation 4 is intended for use when the nonlinearity is small, one might hope that the parabolic and exponential correction would yield about the same curve, and this is indeed the case. The fitting of a parabola,

$$L_t = a + b(t - \bar{t}) + c(t - \bar{t})^2 \tag{7}$$

is not hard and is described in many statistical handbooks. The parabola, once fitted, can be converted to form 4 of the von Bertalanffy by

$$\begin{aligned} A &= a \\ B &= b \\ K &= -2c/b. \end{aligned} \tag{8}$$

A rather better approximation is this. Take Δ as the half age span about $\bar{t}$, that is all observed ages lie within $\bar{t} \pm \Delta$. Take

$$\begin{aligned} U &= \sqrt{3}K\Delta/4 \\ K' &= 2 \log_e((1 + U)/(1 - U))/(\sqrt{3}\Delta) \\ A' &= a \\ B' &= b(K/K')\ (1 - U^2), \end{aligned} \tag{9}$$

where K is taken from equation 8, A′, B′, and C′ are primed to distinguish them from the quantities in equation 8, and U is an artificial quantity for computation only. Provided $K\Delta < \frac{1}{2}$ the error of the approximation of the von Bertalanffy by the parabola, in the age range, $\bar{t} \pm \Delta$, is at most 0.83% of the length range spanned by the growth curve over the age range $\bar{t} \pm \Delta$. This is partial justification for using $K\Delta$ as a measure of nonlinearity. As further justification, we notice that in the parabolic case the relative error,

$$\frac{\text{maximum difference between parabola and line}}{\text{length range}}, \tag{10}$$

over the age range, $\bar{t} \pm \Delta$, is approximately

$$c\Delta^2/2b\Delta = -K\Delta. \tag{11}$$

The derivation of equations 8 and 9 follows: 8 merely equates the exponential to the first three terms of its Taylor series about $\bar{t}$. Equation 9 defines that exponential that coincides with the parabola at the three points, $\bar{t}, \bar{t} \pm \sqrt{3}/4\Delta$. The error bound is adapted from the standard error bound for polynomial interpolation (e.g., Macon, 1963, p. 96–97).

AN EXAMPLE

Solely as an illustration, Table 1 shows a parabola that has been fitted to a set of cod length figures (Graham, 1933) and converted to a von Bertalanffy curve using equations 8 and 9. In addition, K. R. Allen has been kind enough to fit the von Bertalanffy curve directly using his method (Allen, 1966). This is shown in the last column.

TABLE 1. Approximate fit of a von Bertalanffy growth curve.

Parabola: $L_t = 61.031+14.114(t-3.5)-1.268(t-3.5)^2$
Equation 8: $L_t = 61.031+14.114[1-\exp(-.180(t-3.5))]/.180$
Equation 9: $L_t = 61.031+13.756[1-\exp(-.182(t-3.5))]/.182$
Direct[a]: $L_t = 61.007+13.730[1-\exp(-.181(t-3.5))]/.181$

Age (*years*)	Length				
	Actual (*cm*)	Parabola	Eq. 8	Eq. 9	Direct
1	18	17.82	16.47	17.48	17.60
2	36	37.01	36.73	37.31	37.35
3	55	53.66	53.65	53.83	53.82
4	68	67.77	67.78	67.61	67.57
5	78	79.35	79.58	79.08	79.04
6	89	88.39	89.44	88.66	88.62
Residual sum of squares		5.09	7.46	4.80	4.78

[a]The author thanks K. R. Allen for these coefficients.

REFERENCES

ALLEN, K. RADWAY. 1966. A method of fitting growth curves of the von Bertalanffy type to observed data. J. Fish. Res. Bd. Canada 23: 163–179.

BERTALANFFY, LUDWIG VON. 1938. A quantitative theory of organic growth (inquiries on growth laws. II). Human Biol. 10: 181–213.

GRAHAM, MICHAEL. 1933. Report on the North Sea cod. Fish. Invest. London (Ser. 2) 13: 1–160.

KNIGHT, WILLIAM. 1968. Asymptotic growth: an example of nonsense disguised as mathematics. J. Fish. Res. Bd. Canada 25: 1303–1307.

MACON, NATHANIEL. 1963. Numerical analysis. John Wiley & Sons, Inc., New York.

WALFORD, LIONEL A. 1946. A new graphic method of describing the growth of animals. Biol. Bull. 90: 141–147.

NOTES

Derivation of Average Lengths of Different Age-Groups in Fishes

V. G. JHINGRAN AND A. V. NATARAJAN

Central Inland Fisheries Research Institute
Barrackpore, West Bengal, India

JHINGRAN, V. G., AND A. V. NATARAJAN. 1969. Derivation of average lengths of different age-groups in fishes. J. Fish. Res. Bd. Canada 26: 3073–3076.

Fishes in general show much growth variation between years from environmental influences, food availability, and stock density, and this variation is especially more pronounced in the tropics. Average growth rate and average length at age of constituent age-groups of fish stocks, under the circumstances, appear more appropriate especially for yield computations. By the method elaborated in this note, the modal values of sizes of constituent age-groups (derived from Petersen's method of length-frequency analysis) as obtained each month for all months over a number of years (9 years, in the present case, covering the period 1957–65) are simultaneously plotted and this results in as many oblique rows as there are age-groups. Regression lines corresponding to the oblique rows of scatters of modal plots are statistically derived and used to read off the average lengths at ages. The slopes of the lines represent the average growth rates for the size ranges delimited by regression lines.

Received February 3, 1969

THE AGES OF FISHES are commonly determined by fishery workers by studying length-frequency distributions, and release and recovery of marked fish as well as from the markings on the hard parts like scales, otoliths, opercula, vertebrae, fin rays, etc.

The length-frequency distribution method, also known as Petersen's method of age determination, presupposes that the individuals pertaining to each age-group in a population of a species of fish form a "normal" distribution. This method works successfully only when the duration of spawning is restricted. In such a case the modes of the polymodal length-frequency distribution represent separate age-groups. When the length frequencies are plotted at periodic intervals the growth progression of constituent age-groups can be traced from the shifted modal locations. The numerous inflexions, especially for very short class intervals, in the cumulative percentage distribution curves linearly transformed on probability paper, as advocated by Harding (1949) and Cassie (1954) and as applied by Pantulu (1961) are as subjective to interpretation as modal locations themselves (Jhingran and Jena, 1964).

Printed in Canada (J1357)

It is observed in many species of fish of Lake Chilka (India) that their growth varies rather inconsistently between years — perhaps from environmental influences, food availability, and stock density. There is, in fact, a necessity to evolve a method that will provide average growth rates and average lengths at different ages over a period of years and will, at the same time, discount errors of random sampling. It was, therefore, considered that if the modal values of sizes of the constituent age-groups as obtained each month, for all months over a number of years, are simultaneously shown on a graph, the plots would necessarily lend themselves into as many oblique rows as there are age-groups in the population of the fish under study. These oblique rows represent scatters of modal plots of monthly growth variations between years and are statistically accessible to derive regression equations. Since the same modal value can occur more than once at the same point on the scatter diagram (this is because the points do not represent the individual measurements of the variables as is usual in such diagrams but only modal values derived on the basis of common class intervals into which the length frequency has been grouped) the relevant frequency of their occurrence has been shown by numbers in the graph placed close to the points concerned (Fig. 1, 2). These frequencies enter into computation of the regression line. The regression lines are used to derive the average length at age for the constituent age-groups and the regression coefficients of these lines represent the average growth rates

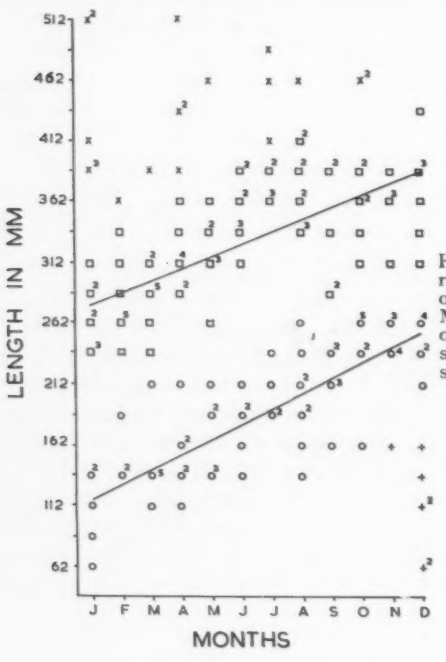

FIG. 1. Regression lines showing average rates of growth and average lengths at ages of *Hilsa ilisha* during the period 1957–65. Modal locations of sizes of different months of different years pertaining to each regression line were marked off by using different signs and the numbers indicate frequency of occurrence of the modes.

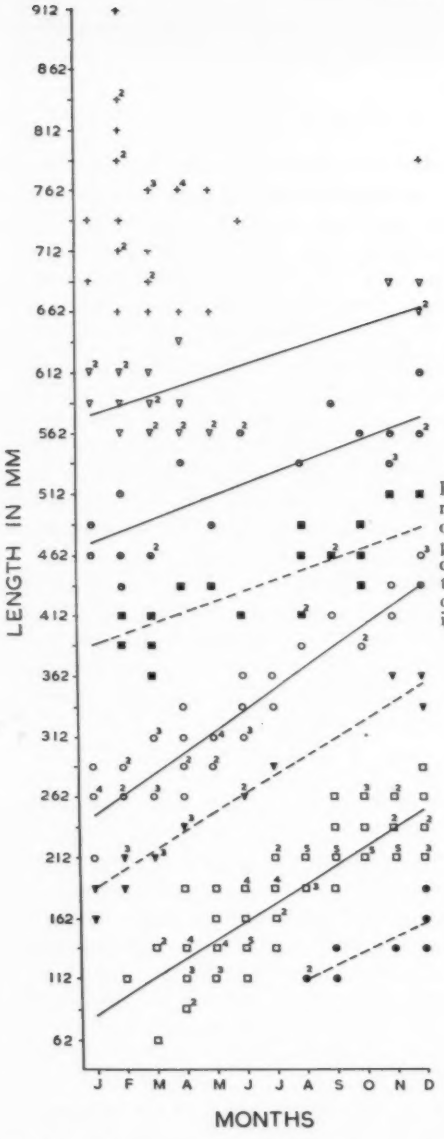

FIG. 2. Regression lines showing average rates of growth and average lengths at ages of *Eleutheronema tetradactylum* during the period 1957–65. Modal locations of sizes of different months of different years pertaining to each regression line were marked off by using different signs and the numbers indicate the frequency of occurrence of the modes.

of the size ranges delimited by regression lines. The advantages of this method are that it: (1) facilitates derivation of average length and average growth rate at different ages over a period of years and these are best suited for yield estimations; (2) dispenses with the pooling of length-frequency statistics of corresponding months or quarters of various years; (3) provides a method by

which length-frequency statistics of many years can be simultaneously analysed; and (4) tends to nullify the positive and negative errors of random sampling, as the size of the sample increases.

The disadvantages in this method of analysis are that it: (1) does not reflect the seasonal growth variations, but in the "seasonless" tropics variations in seasonal growth in capture fishery waters like Chilka Lake are not so pronounced; and (2) does not permit tracing the average growth rate beyond the initial 2–4 years, a disadvantage applicable to Petersen's method of age determination for tropical fish in general. This mode of analysis has been attempted here in two species of fish of Chilka Lake, namely, *Hilsa ilisha*, in which breeding takes place from August to October with a peak in September, and *Eleutheronema tetradactylum*, in which breeding has two peaks — one around March and the other around August. The duration of observations in respect of these two fishes covers the period 1957–65. In *H. ilisha*, the growth progression is confined to a single brood; in *E. tetradactylum*, it pertains to two broods (Fig. 1, 2). The modal values plotted in Fig. 1 and 2 are actual modes. The length-frequency distributions in the above two species are normal or nearly normal for the constituent age-groups and there was no necessity for any dissection of polymodal curves by methods adopted by Buchanan-Wollaston and Hodgson (1929), Harding (1949), and Cassie (1954).

Hilsa ilisha attains an average length of 217 mm in year I and 357 mm in year II (Fig. 1). In *E. tetradactylum*, one of the broods (represented by broken line in Fig. 2) reaches an average size of 217 mm in year I and 404 mm in year II. The other brood (unbroken line in Fig. 2) reaches an average size of 189 mm in year I and 369 mm in year II. Subsequently, separate identity of broods is not distinguishable. With mixed broods (unbroken line) the fish reaches an average size of 537 mm in year III and 632 mm in year IV.

The average growth rates represented by slopes (or regression coefficients) of regression lines (Fig. 1, 2) pertain only to the size ranges delimited by these lines. Since modal values have been plotted from January to December in all cases without adjustment to breeding period the regression lines do not *exactly* cover each of the age groups in full. This does not prevent directly reading the average lengths at various ages from the regression lines; only the average growth rates for age-groups will have to be computed from average lengths at ages.

REFERENCES

BUCHANAN-WOLLASTON, H. J., AND W. C. HODGSON 1929. A new method of treating frequency curves in fishery statistics, with some results. J. Conseil Conseil Perm. Intern. Exploration Mer 4: 207.

CASSIE, R. M. 1954. Some uses of probability paper in the analysis of size frequency distributions. Australian J. Marine Freshwater Res. 5: 513–522.

HARDING, J. P. 1949. The use of probability paper for the graphical analysis of polymodal frequency distributions. J. Marine Biol. Assoc. U.K. 28: 141–153.

JHINGRAN, V. G., AND S. JENA. 1964. Recovery of a tagged mullet, *Liza troschelli* (Bleeker), about a year after tagging in Chilka Lake, India. Sci. Cult. 30: 464–466.

PANTULU, V. R. 1961. Determination of age and growth of *Mystus gulio* (Ham.) by the use of pectoral spines, with observations on its biology and fishery in the Hooghly estuary. Proc. Natl. Inst. Sci. India 27: 198–225.

Evaluation of Lamprey Larvicides in the Big Garlic River and Saux Head Lake[1]

PATRICK J. MANION

Bureau of Commercial Fisheries
Biological Station, Marquette, Michigan 49855, USA

MANION, PATRICK J. 1969. Evaluation of lamprey larvicides in the Big Garlic River and Saux Head Lake. J. Fish. Res. Bd. Canada 26: 3077–3082.

Bayluscide (5,2′-dichloro-4′-nitrosalicylanilide) and TFM (3-trifluoromethyl-4-nitrophenol) were evaluated as selective larvicides for control of the sea lamprey, *Petromyzon marinus*, in the Big Garlic River and Saux Head Lake in Marquette County, Michigan. Population estimates and movement of ammocetes were determined from the recapture of marked ammocetes released before chemical treatment. In 1966 the estimated population of 3136 ammocetes off the stream mouth in Saux Head Lake was reduced 89% by treatment with granular Bayluscide; this percentage was supported by a population estimate of 120 ammocetes in 1967, an indicated reduction of 96% from 1966. Post-marking movement of ammocetes was greater upstream than downstream.

Received May 21, 1969

THE SELECTIVE LARVICIDE TFM (3-trifluoromethyl-4-nitrophenol) has been used to control the sea lamprey, *Petromyzon marinus*, in the upper Great Lakes since 1958 (Applegate et al., 1961). The larvicide has successfully reduced the populations of lampreys in tributary streams, but application in estuaries and lakes is too difficult and costly. TFM dissipates rapidly and becomes diluted below the lethal concentration for lampreys when it enters a lake from a stream (Applegate et al., 1961).

Bayluscide[2] (5,2′-dichloro-4′-nitrosalicylanilide) is extremely toxic to larval lampreys, and is sometimes used as a synergist with TFM to lower the cost of treatments in streams tributary to the Great Lakes (Howell et al., 1964). Newton and Fetterolf (1967), who experimented with a formulation of 5% Bayluscide adhered to sand granules (300–600 μ) as a molluscicide to control swimmers' itch (schistosome cercarial dermatitis), found that the active ingredient remains in the bottom 6 inches of water. In a granular form, it is well suited as a "bottom toxicant" for control of the sea lamprey in estuaries and lakes. The granules sink rapidly and release little active ingredient until they reach the bottom.

The present study gives data on the first chemical treatments with 5% Bayluscide granules as a lamprey larvicide in inshore waters of Saux Head Lake (Marquette County, Michigan) and on the effectiveness of TFM in the Big Garlic River, a tributary to the lake.

---

[1]Contribution No. 398, U.S. Bureau of Commercial Fisheries, Great Lakes Fishery Laboratory, Ann Arbor, Michigan 48107.

[2]Registered trade mark of Farbenfabriken Bayer AG, Leverkusen, West Germany. Mention of commercial products does not imply endorsement.

Printed in Canada (J1481)

Study area — Saux Head Lake has a surface area of 138 acres and an average depth of 10 ft. The west shoreline is of wind-swept sand, the east shoreline is mostly of rock and hard-packed sand, and the north and south shorelines are of sand and mud. The bottom is mud and silt; aquatic vegetation grows throughout the lake. The lake drains into Lake Superior through a channel $\frac{1}{4}$ mile long.

The Big Garlic River flows into the south end of Saux Head Lake. The study area extended from the lake $1\frac{1}{2}$ miles upstream to a concrete dam that was a barrier to upstream migration of fish (McLain and Manion, 1967). The river varied from 10 to 30 ft wide and averaged 2 ft deep. Water flow fluctuated between 15 and 25 ft^3/sec during chemical treatments.

The river and lake were divided into three study areas (Fig. 1). Area 1 extended from the dam to 150 ft above Saux Head Lake; area 2 extended from

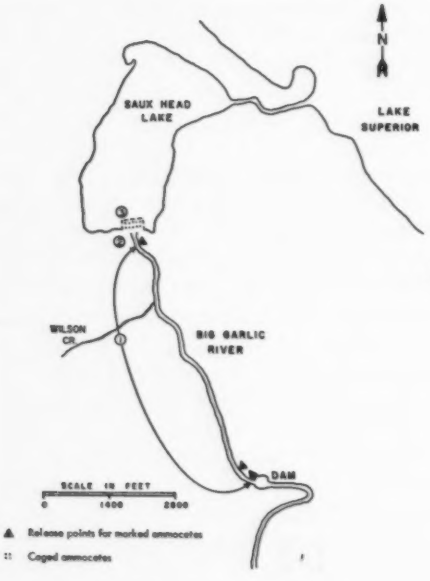

FIG. 1. Big Garlic River and Saux Head Lake. Numbers indicate study areas.

150 ft above Saux Head Lake to the mouth of the river; and area 3 encompassed 150 ft on each side of the mouth of the river and 200 ft into the lake. The maximum water depth in area 3 was 10 ft.

Materials and methods — The Big Garlic River was treated with TFM in 1965 and 1966 and with a mixture of TFM and Bayluscide as a synergist in 1967 (Table 1). On the basis of pretreatment bioassays, the concentration of the larvicide in the Big Garlic River was well above that needed to destroy larval lampreys. The methods of bioassay and treatment of a stream with TFM were described by Applegate et al. (1961), and the methods of treatment with a mixture of TFM and Bayluscide were described by Howell et al. (1964). TFM was introduced at the dam in area 1 by a fuel-pump feeder (Anderson, 1962).

TABLE 1. Details on the chemical treatments of the Big Garlic River, 1965–67.

Item	Date of chemical treatment		
	Sept. 29, 1965	Sept. 20, 1966	July 7, 1967
Water temp (*C*)	4	10	12
Phenolphthalein alkalinity (*ppm as* $CaCO_3$)	0	0	0
Total alkalinity (*ppm as* $CaCO_3$)	49	56	42
Conductivity ($\mu mhos/cm^3$ *at 18 C*)	109	113	92
Discharge at mouth (ft^3/sec)	18	15	25
Avg concentration of TFM (*ppm*)	6.0	9.0	3.8[a]
Period of exposure (*hr*)	8	7	8

[a]Concentration included 1% Bayluscide.

The alluvial fan and adjacent areas in Saux Head Lake (area 3) were also treated in each of the 3 years. In 1965 the treatment was with 36 lb active ingredient of TFM for 1 hr. The larvicide was applied with a back-pack hand pump from a 14-ft boat. In 1966 and 1967, a formulation of 5% granular Bayluscide was used. The bioassay and application methods for granular Bayluscide were developed by personnel of the Hammond Bay laboratory, U.S. Bureau of Commercial Fisheries (Great Lakes Fishery Commission, 1967). To obtain the maximum synergistic action, the granular Bayluscide was applied in Saux Head Lake 2 hr before the TFM in the river reached the lake. The granules were broadcast at 109 lb (5.5 lb active ingredient) per acre with a power blower from a 14-ft boat. A hand-cranked spreader was used to apply the granules in shallow water along the beach.

Before each treatment ammocetes collected with an electric shocker from other streams tributary to Lake Superior were marked and released at various points in the Big Garlic River and the alluvial fan, to aid in the estimation of lamprey populations and the evaluation of the effectiveness of the treatment. The ammocetes were anesthetized in a 75 ppm solution of M.S. 222 (tricaine methanesulfonate) and marked on the head or body with an injection of cadmium sulfide (yellow) and brilliant orange[2] dyes. The marking procedure has been described by Wigley (1952). A combination of dyes and different locations on the body permitted the separation of each marked group.

An estimate of marking mortality for ammocetes was obtained in 1965 when 50 each of marked and unmarked ammocetes were placed in a cage in the Big Garlic River and held 2 weeks. All unmarked and 49 (98%) marked ammocetes survived. No correction was made for mortality of marked ammocetes in the present study.

Before the chemical treatment in 1966, American brook lamprey, *Lampetra lamottei*, ammocetes were placed in 10 live cages, which were distributed on the bottom of the alluvial fan of Saux Head Lake; the cages were removed 24 hr after the treatment. The lower half of each cage was made of galvanized metal and filled with sand. The upper half of the cages was made of ¼-inch mesh screen.

Ammocetes were collected in the river and lake with dipnets during the chemical treatments and were preserved in 5% formalin. All unmarked lampreys collected were sea lampreys.

Populations of sea lamprey ammocetes were estimated by the formula $N = \frac{nT}{t}$ where N equals the total population, T the total number of ammocetes marked originally, n the number (marked and unmarked) in the sample, and t the number of marked ammocetes in the sample.

[2]Obtained as samples from Mr John F. LesVeaux, Niagara Chemical Company, Middleport, New York.

1965 Treatment — The Big Garlic River and Saux Head Lake were treated with TFM on September 29, 1965. Eighty-four (42%) of 200 American brook lamprey ammocetes marked and released in area 1 on May 20 (4 months before the treatment) were recaptured (Table 2) — 40 of 100 ammocetes released randomly in the river between the dam and a point ½ mile downstream and 44 of 100 released in a 6-ft square area ½ mile below the dam.

TABLE 2. Number of marked lampreys released before chemical treatments and number of lampreys (marked and unmarked) recaptured during chemical treatments of the Big Garlic River and Saux Head Lake, 1965–67. (See Fig. 1 for location of the areas.)

Year and area	Marked lampreys: No. released	No. and area of capture: 1	2	3	Total recaptured	% recaptured	Unmarked sea lampreys	Total in collection
				1965				
1	200	84	0	0	84	42	106	190
2	0	0	0	0	0	0	10	10
3	0	0	0	0	0	0	448	448
Total	200	84	0	0	84	42	564	648
				1966				
1	100	51	0	0	51	51	433	484
2	223	0	68	3	71	32	98	169
3	394	1	26	73	100	25	481	581
Total	717	52	94	76	222	31	1012	1234
				1967				
1	100	30	0	0	30	30	786	816
2	100	0	24	1	25	25	9	34
3	94	0	1	11	12	13	2	14
Total	294	30	25	12	67	23	797	864

Of the 564 unmarked ammocetes taken throughout the study area during the chemical treatment, 448 were from the alluvial fan in Saux Head Lake. During the chemical treatment, ammocetes were observed swimming from the river into the lake and in the vicinity of the alluvial fan and adjacent waters.

The estimate of population in area 1 was 452 ammocetes. Most of the larvae (69%) collected in area 1 were from a population of known-age ammocetes established above the dam on the Big Garlic River[4] in 1960. The known-age lampreys, which were separated easily from other ammocetes by length,

[4]The study of the known-age population is a part of the sea lamprey program conducted by the U.S. Bureau of Commercial Fisheries under contract with the Great Lakes Fishery Commission. This study is the reason the stream was treated annually.

migrated downstream into area 1. Marked ammocetes were not released in areas 2 and 3 in 1965; therefore, the numbers of ammocetes were not estimated.

1966 Treatment — On September 20, 1966, the Big Garlic River was treated with TFM and Saux Head Lake with granular Bayluscide. A total of 1234 ammocetes was collected during the treatment; 222 were marked (Table 2). Fifty-one (51%) of 100 American brook lampreys marked and released in area 1 from the dam to a point ½ mile downstream and 100 (25%) of 394 marked and released in area 3 in the alluvial fan on August 9 (about 6 weeks before the treatment) were recaptured, and 71 (32%) of 223 released in area 2, 50 yards above the lake in the estuary on September 19 (the day before the treatment) were recaptured.

The success of the treatment of the alluvial fan in Saux Head Lake with granular Bayluscide was estimated from the mortality of ammocetes that were in 10 cages in the lake during the chemical treatment. Of the 223 larvae placed in the cages, 198 died; reduction of the population of larvae, therefore, was estimated at 89%. Estimates of populations of ammocetes before chemical treatment for areas 1, 2, and 3 were 949, 554, and 3136, respectively. All but 10% of the ammocetes recovered in area 1 were from the known-age population above the study area. The ammocetes in area 2 were mostly age-group I from Wilson Creek, a small tributary of the Big Garlic River that was only partially treated, and some that probably moved into the river from area 3 after the treatment in 1965. The larvae in area 3 were largely lampreys from an apparently unsuccessful treatment of the alluvial fan in 1965.

1967 Treatment — The Big Garlic River was treated with a mixture of TFM and Bayluscide and Saux Head Lake was treated with granular Bayluscide on July 7, 1967. A total of 864 ammocetes (67 marked) was collected during the chemical treatment (Table 2). Marked sea lampreys (294) were released on June 22 (2 weeks before the treatment) in the same areas as the brook lampreys in 1966. Of the 100 marked ammocetes released in each of areas 1 and 2 and of the 94 marked larvae released in area 3 in 1967, 30 (30%), 25 (25%), and 12 (13%) were recaptured, respectively.

Population estimates for ammocetes were 2720 in area 1, 142 in area 2, and 120 in area 3. Most (98%) of the ammocetes in area 1 were from the known-age population above the dam. The population estimate for area 3 indicated a decline of 96% from 1966 and thus supports the estimated 89% reduction determined in 1966 from the mortality of larvae in cages.

Movement of ammocetes — Movement of marked ammocetes among areas was common. American brook lampreys released in 1965 at a point ½ mile below the dam were distributed between the dam and a point 100 ft below the point of release indicating larger movement upstream, than downstream.

In 1966, as in 1965, more marked American brook lampreys moved upstream than downstream. Of those released in area 3, 26 (7)% were recovered in area 2, and one in area 1, 2 miles upstream. Only three (1%) of the ammocetes released in area 2 were recaptured downstream in area 3.

In 1967, one (1%) of the sea lampreys released in area 3 was recovered 30 yards upstream in area 2 and one (1%) released in area 2 was found in area 3. Movement of American brook lampreys marked in 1965 and 1966 was greater than that of sea lampreys marked in 1967.

Ammocetes in the lake and those drifting from the river appear to remain on the alluvial fan within the influence of the river.

Mortality of fish — Mortality of fishes from the granular Bayluscide was confined to small species: mottled sculpin, *Cottus bairdi*; logperch, *Percina caprodes*; and black bullheads, *Ictalurus melas*. Few fish were killed in the experiment conducted by Newton and Fetterolf (1967) to control swimmers' itch. The mortality of fishes from TFM was minimal.

Evaluation of lamprey larvicides — On the basis of pretreatment bioassays, all of the lamprey larvae should have been killed during the chemical treatment of the Big Garlic River. Even though the river was treated for longer periods and at concentrations above those needed to insure eradication of all sea lampreys, some ammocetes survived the treatments in 1965 and 1966. One ammocete marked and released in area 1 before the chemical treatment in 1965 was collected in area 1 during the 1966 treatment. Fifteen marked ammocetes released before the treatment in 1966 were recaptured throughout the study areas during the treatment in 1967; four released in area 1 were recaptured in area 1, two released in area 2 were recaptured in area 3, and nine released in area 3 were recaptured in area 2. I believe the lampreys in area 1 probably escaped into fresh water and evaded lethal doses of TFM. Ammocetes in areas 2 and 3 may have moved into the untreated water in Saux Head Lake and later migrated back into the stream.

Granular Bayluscide applied in the lake to synergize with TFM from the stream treatment was considerably more effective than TFM alone in destroying sea lampreys.

Acknowledgments — Bureau personnel from the Marquette Biological Station and the Hammond Bay Biological Station conducted the chemical treatments. This study was part of a program conducted by the Bureau of Commercial Fisheries under contract with the Great Lakes Fishery Commission.

REFERENCES

ANDERSON, G. A. 1962. Three portable feeders for metering chemical into streams for control of the sea lamprey. Progressive Fish-Culturist 24: 190–192.

APPLEGATE, V. C., J. H. HOWELL, J. W. MOFFETT, B. G. H. JOHNSON, AND M. A. SMITH. 1961. Use of 3-trifluoromethyl-4-nitrophenol as a selective sea lamprey larvicide. Great Lakes Fish. Comm. Tech. Rept. 1. 35 p.

GREAT LAKES FISHERY COMMISSION. 1967. Annual report for the year 1966. 37 p.

HOWELL, J. H., E. L. KING, JR., A. J. SMITH, AND L. H. HANSON. 1964. Synergism of 5,2′-dichloro-4′-nitro-salicylanilide and 3-trifluoromethyl-4-nitrophenol in a selective lamprey larvicide. Great Lakes Fish. Comm. Tech. Rept. 8. 21 p.

MCLAIN, A. L., AND P. J. MANION. 1967. An all-season trap for downstream-migrating fish and other aquatic organisms. Progressive Fish-Culturist 29: 114–117.

NEWTON, M. E., AND C. M. FETTEROLF, JR. 1967. Experimental use of Bayluscide for control of swimmers' itch. State of Michigan, Water Resources Comm. Dept. Conservation. 11 p.

WIGLEY, R. L. 1952. A method of marking larval lampreys. Copeia 1952: 203–204.

A Device to Detect Magnetized Wire Tags in Migrating Adult Coho Salmon

JOSEPH T. DURKIN, WESLEY J. EBEL, AND JIM ROSS SMITH

Bureau of Commercial Fisheries
Biological Laboratory, Seattle, Washington 98102, USA

DURKIN, JOSEPH T., WESLEY J. EBEL, AND JIM ROSS SMITH. 1969. A device to detect magnetized wire tags in migrating adult coho salmon. J. Fish. Res. Bd. Canada 26: 3083–3088.

A device that can be used for rapid detection and separation of migrating adult coho salmon marked as juveniles with magnetized wire tags was tested in November and December 1967 at the Minter Creek Hatchery of the Washington Department of Fisheries. About two-thirds of the test fish in the holding pond entered the structure; the device correctly separated 89% of the fish with tags and 99% of the untagged fish. Placement of this equipment in streams, fish ladders at dams, and in hatcheries, would facilitate removal of tagged specimens from the general population of fish.

Received June 23, 1969

RECENTLY we had need to detect magnetized wire tags imbedded in the snouts of Pacific salmon (genus *Oncorhynchus*) and steelhead trout (*Salmo gairdneri*) migrating upstream to spawn in the Columbia River. A system, or device, that would detect and separate tagged from untagged fish would be beneficial in evaluating our experiments on transportation of juvenile fish past hazardous areas. The effect of transport on the ability of adult fish to return to their native streams or hatcheries could also be studied.

The magnetized wire tag, developed by Jefferts et al. (1963) is small (1 × 0.25 mm), easily inserted, has a high retention rate, and does not alter appearance of the fish. The usual method of detection in adult salmon is to pass the snout manually through a detector unit (Bergman et al., 1968). This method is satisfactory for examining sport and commercially caught fish but not large numbers of migrants. To overcome delay, we developed a system that could be used in a fish ladder for rapid detection and separation.

In the summer of 1967, a preliminary study was made near Bonneville Dam at the Fisheries-Engineering Research Laboratory operated by the U.S. Bureau of Commercial Fisheries to determine if the detector unit should be placed in a fish ladder below or above the surface of the water. The tagged fish (adult steelhead trout and chinook salmon (*O. tshawytscha*)) moved past the underwater detector too slowly to induce sufficient current when they broke the magnetic field; this approach was abandoned. The detector proved satisfactory, however, when taken out of the water and used in a fish ladder where the fish jumped over a false weir and slid down a chute past the detector. This movement was rapid enough to induce sufficient current for detection.

Printed in Canada (J1511)

Because the preliminary study was encouraging, a small fish ladder (including a tag detector and fish separator) was assembled and tested at the Minter Creek Hatchery of the Washington Department of Fisheries near Purdy. The tests were run in November and December 1967 when adult coho salmon (*O. kisutch*) were available, some of which had been tagged as juveniles. This report describes the operation of the device and its effectiveness in automatically detecting and separating fish.

Description of detection and separation system — The structure (Fig. 1) was placed in the adult holding pond (Fig. 2) of the hatchery in November. The first step of the fish ladder (3 × 20 ft) was about 6 inches above the water. Each of the three remaining steps was about 1 ft high, bringing the water level in the final pool to about 3 ft above the pond. A "V" channel for passage of water and fish was deeply cut in the first three steps but made less angular in the final one (Fig. 3). This design conserved water and kept the fish centered in the ladder.

The expected size of the fish predetermined several of the dimensions (mean fork length of coho salmon was about 26 inches). An important dimension was the inside diameter (10 inches) of the detection coil, which was satisfactory for the salmon tested but not for larger fish, such as chinook salmon.

The water (from a reservoir formed by a low dam at the upper end of the holding pond) was piped through an 8-inch pipe and upwelled at the last and highest step. The flow ranged from 1 to 1¼ ft³/sec.

In operation, a salmon entered the fish ladder, passed over the last step and onto a chute, and slid downward through the detector coil onto the separator board (Fig. 4). Fish without magnetized tags were shunted back into the adult holding pond. When a tagged fish passed through the tubular detector unit and interrupted the magnetic field, a signal was transmitted to a solenoid that activated the separator through a compressed air unit; this action tilted the separator clockwise about 90° and shunted the fish into a separate holding area.[1] An audio signal from the detector activated the separator in 0.3 sec.

Test procedure — Adult coho salmon that returned to the main hatchery pond were checked with a portable detector to determine if they had been tagged as juveniles. Those with magnetized tags (eight males) were marked with a yellow plastic spaghetti tag in the left dorsal musculature with a high-speed tagging gun (Thorson, 1967) and released into a picketed enclosure just below the fish ladder.

On each day of testing, 26 or more untagged males were marked with a red spaghetti tag containing a magnetized wire tag. These newly tagged fish were then placed in the holding pond with those previously tagged as juveniles. Finally, 30 or more untagged females were placed in the holding pond with the other tagged fish.

After a test group — about half were males with tags and the other half females without tags — had been assembled, the water was turned on in the fish ladder and the fish were allowed to enter the structure. As a salmon passed over the end of the fish ladder onto the chute and through the detector unit, the audio response of the detector and the direction of separation were noted, as well as the time and color of the tag. When the fish ceased moving, the test was terminated; the water was released from the structure, and the remaining salmon were returned to the main hatchery pond.

The 11 tests made lasted 3–5½ hr; the average was 4½ hr. The total number of salmon in the holding pond and the number that entered the detection device are shown in Table 1.

Effectiveness of tag detector and fish separator — The numbers of tagged coho salmon that were separated from the untagged fish and the numbers

[1]The installation and operating mechanism of the separator was provided by the Technical Research Company, 13535 Monster Road South, Seattle, Wash., USA.

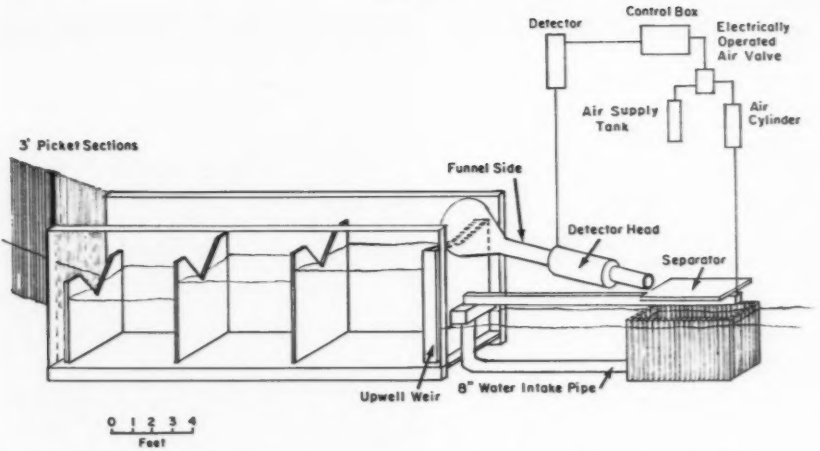

FIG. 1. Structure at Minter Creek Hatchery for separating coho salmon bearing magnetized wire tags from untagged fish.

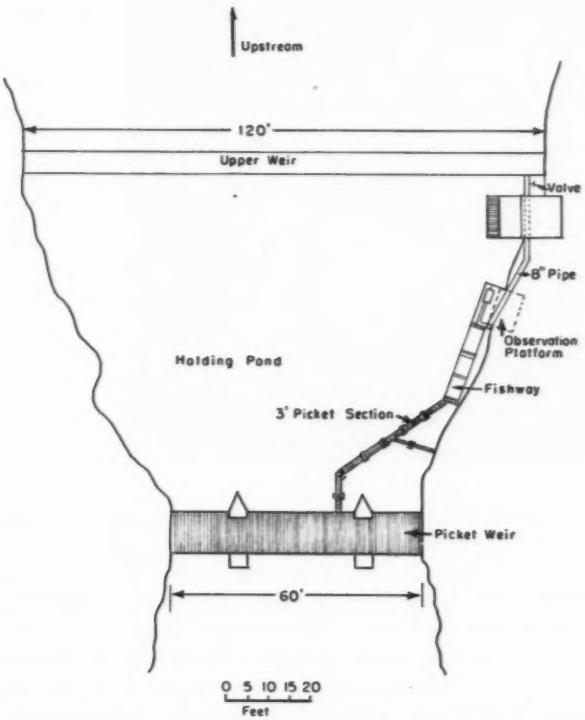

FIG. 2. Location of detection and separation system in the holding pond of Minter Creek Hatchery.

FIG. 3. Front view of fish ladder in holding pond at Minter Creek Hatchery.

FIG. 4. Looking down into chute of detector and separator units.

of untagged fish that correctly passed through the detection device are shown in Table 2. Of the tagged coho salmon, 89% (272 of 304 fish) were correctly separated by the detection device; 99% (329 of 333 fish) of the untagged fish correctly passed through the device. The eight salmon tagged as juveniles were all correctly separated.

The numbers of tags not detected by the device (30 of 304 tags) was larger than expected. Later studies showed that two factors probably accounted for nearly all of the 30 failures to detect tags: (1) some of the tagged fish passed the detector unit too slowly to break the magnetic field; and (2) some tags

TABLE 1. Numbers of tagged and untagged coho salmon in holding pond and numbers that entered detection device.

Date	No. of fish in holding pond			No. of fish that entered detection device		
	Total	Tagged	Untagged	Total	Tagged	Untagged
Nov. 30	57	26	31	40	18	22
Dec. 1	59	26	33	50	24	26
2	75	36	39	66	34	32
3	100	50	50	91	45	46
3	60	30	30	49	22	27
4	100	50	50	78	37	41
5	89	49	40	62	32	30
6	101	51	50	56	29	27
7	81	42	39	55	26	29
8	120	54	66	69	30	39
12	100	42	58	21	7	14
Total	942	456	486	637	304	333

TABLE 2. Numbers of tagged coho salmon correctly separated from the untagged fish by detection device and numbers of untagged coho salmon that correctly passed through detection device.

Date	Tagged fish				Untagged fish		
	Total no.	No. correctly separated	Tags detected but fish not separated	Tags not detected	Total	No. correctly passed	No. separated into tagged group
Nov. 30	18	14	1	3	22	21	1
Dec. 1	24	21	0	3	26	25	1
2	34	30	0	4	32	32	0
3	45	38	0	7	46	46	0
3	22	21	0	1	27	27	0
4	37	36	0	1	41	41	0
5	32	28	0	4	30	30	0
6	29	27	0	2	27	27	0
7	26	25	0	1	29	28	1
8	30	27	0	3	39	38	1
12	7	5	1	1	14	14	0
Total	304	272	2	30	333	329	4

were not magnetized. The slow movement through the magnetic field was partially caused by a faulty lining in the entrance tube of the detector. The failure of some of the tags to be magnetized was probably caused by passing of the magnet over the tags at an incorrect angle. After we had carefully magnetized some of the undetected tags, the fish were successfully separated by the detection device.

Four untagged fish were classified as tagged. This error was probably caused by imperfect mounting of the detection coil. We later found that tags were falsely detected if the coil moved while the fish was inside it.

Conclusion — We conclude that this device, with some improvements, will detect most (90–95%) adult coho salmon bearing magnetized wire tags, and separate them from the untagged fish. Placement of the device in streams, fish ladders at dams, and in hatcheries would facilitate removal of tagged specimens from the general population of fish.

Acknowledgments — Superintendent Arthur Gallaghan and Director C. R. Ellis of the Division of Hatcheries, Washington Department of Fisheries, arranged for the use of Minter Creek Hatchery; David Misitano assisted in collecting data, and Winston Farr designed the fishway; Vernon Orn and Nikla Salmella designed and assembled the detector and separator unit.

REFERENCES

BERGMAN, PETER K., K. P. JEFFERTS, HUGH F. FISCUS, AND ROBERT C. HAGER. 1968. A preliminary evaluation of an implanted, coded wire fish tag. Washington Dept. Fish., Fish. Res. Papers 3: 63–84.

JEFFERTS, K. B., P. K. BERGMAN, AND H. F. FISCUS. 1963. A coded wire identification system for macroorganisms. Nature 198: 460–462.

THORSON, KENNETH N. 1967. A new high-speed tagging device. Calif. Fish Game 53: 289–292.

Extension of Range for *Manayunkia aestuarina* (Polychaeta: Sabellidae) to British Columbia

WILLIAM J. LIGHT

Department of Biological Sciences
Simon Fraser University, Burnaby 2, B.C.

LIGHT, WILLIAM J. 1969. Extension of range for *Manayunkia aestuarina* (Polychaeta: Sabellidae) to British Columbia. J. Fish. Res. Bd. Canada 26: 3088–3091.

The brackish water polychaetous annelid *Manayunkia aestuarina* (Bourne) is newly recorded for North America and constitutes the second species of the genus known to occur on this continent. Its range is extended from the British Isles, the Baltic and North Sea areas, and the Barents Sea (Kola Fjord).

Received June 9, 1969

MANY INDIVIDUALS of the minute European sabellid *Manayunkia aestuarina* (Bourne, 1883) were taken from the exposed mud flats at the head of Indian Arm Inlet near Vancouver, B.C. (49°28′N, 122°53′W), in March 1969. They were collected in samples of surface mud, which were allowed to settle in shallow dishes overnight, permitting the animals to reconstruct their tubes

Printed in Canada (J1499)

and burrows. This procedure rendered the organisms readily visible and proved to be more successful than sifting the mud through various-sized sieves.

The specimens have been deposited at the Department of Invertebrate Zoology, California Academy of Sciences, and the Allan Hancock Foundation, University of Southern California.

Manayunkia aestuarina (Bourne, 1883)

(Fig. 1–4)

Synonymy — Haplobranchus aestuarinus Bourne, 1883; *Haplobranchus balticus* Karling, 1934; *Manayunkia polaris* Zenkewitsch, 1935.

This species is widely spread from England and Ireland, throughout the Baltic and North Seas, and as far north as the Barents Sea. It is found in brackish and marine waters with a muddy substratum and ranges from the high intertidal to a depth of over 20 m. It has been found in salinities ranging from less than 5 to over 50‰, but, although it has been shown to withstand changes from salt to completely fresh water, apparently does not naturally occur in areas that are

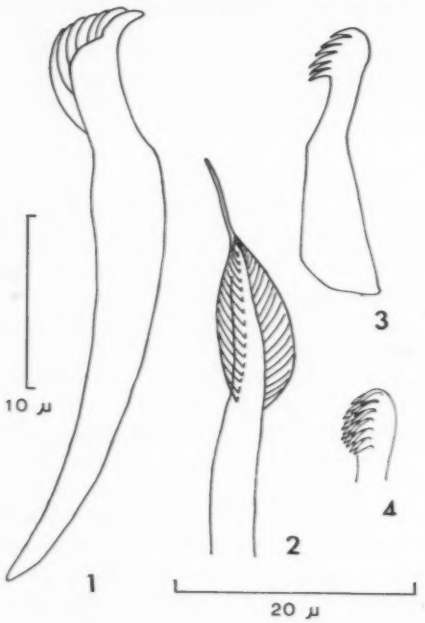

FIGURES 1–4.

Manayunkia aestuarina (Bourne).

Fig. 1: Thoracic neuropodial uncinus; Fig. 2: Thoracic spatulate seta of notopodium; Fig. 3: Abdominal notopodial uncinus in left lateral view; Fig. 4: Abdominal uncinus in latero-frontal aspect.

completely isolated from a marine influence (Schütz, 1965). The Indian Arm examples come from an area of fluctuating salinity (<5‰ at the time of collection). The salinity becomes especially low during the spring because of the heavy snow meltwater entering the fjord from the nearby Indian River. The specimens were found in association with the phyllodocid, *Eteone longa* (Fabricius, 1870), and an ampharetid, *Amphicteis* sp.

The animals conform in every respect with the descriptions given for *M. aestuarina* (Bourne, 1883; Banse, 1956; Schütz, 1965): a well-developed peristomial collar with 2 prominent eyespots, 8 thoracic and 3 abdominal segments; the blood in living animals tinged a faint green due to the

pigment, chlorocruorin; 8 branchial tentacles in addition to 2 ventral blood-bearing filaments in every specimen examined; the abdominal segments with 10–16 multidentate dorsal uncini on each side (Fig. 3, 4) although the usual number is 14, then 12–13, and 10 as one progresses toward the pygidium; uncinal teeth borne 5–6 per row, each uncinus with about 4 such rows (Fig. 4); 3–4 limbate capillaries, 2–3 spatulate setae (Fig. 2), and 4–5 long-stemmed uncini (Fig. 1) on each side of every thoracic segment, excluding the first. The specialized condition of the sixth setiger seen in *Manayunkia speciosa* (see below) has not been reported for *M. aestuarina*, and is not found on any of the present specimens, although that somite is somewhat elongated in some individuals.

The greenish hue of the blood is difficult to discern and is not as obvious as one is led to believe from the literature. It is noteworth that Nusbaum (1901) denied the presence of green blood in *Dybowscella baicalensis*, which he had earlier that same year described as a new genus and species (but see Zenkewitsch, 1935; Hartman, 1951; Banse, 1956). The number of branchial tentacles would certainly seem to be a valid diagnostic criterion for *M. aestuarina*, as asserted by Banse, by virtue of its constancy regardless of the environment or geographical province from which the specimens may come (however, see Holmquist, 1967).

The tubes are simple structures of mud and mucous ranging from 2 to 5 mm in length. They may protrude as much as 2 mm above the level of the muddy substrate, and are either grey or conspicuously orange in color.

The animals were found both in and out of their tubes when examined alive, and many were seen to exhibit the same creeping behaviour as described by Schütz (1965). However, Lewis (1968) states that a closely related fabriciine, *Fabricia sabella* (Ehrenberg, 1836), was seen to crawl about the surface of the mud, pygidium foremost, when removed from its tube, but that *M. aestuarina* failed to exhibit any such behaviour. He did not, however, specify either the age of his specimens or the conditions under which they were observed.

This remarkable range extension probably represents inadequate collecting rather than a recent introduction into this area. The population was found some 12 miles up Indian Arm Inlet where the probability for any artificial introduction would be exceedingly remote, especially in view of the absence of any pelagic larval stage. It seems more likely that this form is circumarctic and circumboreal in estuarine conditions, and that future collections will turn up examples from other fjords in western and arctic North America. Indeed, it would not be surprising to find this species in the geologically older sloughs and estuaries of the eastern coast of this continent, as well. In this regard, it is noteworthy that *M. speciosa* Leidy, 1858, has until recently been known only from the Great Lakes region and from the Schuylkill River, Pennsylvania (type locality). In 1963, however, it was recovered in Sacramento County, California, and in 1964 it was found in Klamath County, Oregon (Hazel, 1966). Holmquist (1967) collected the species in several northern Alaskan lakes from 1961 to 1964, where it must have been occurring naturally and without any assistance by man or his agents. The extremely small size of these organisms (2–5 mm for both North American species) precludes their being readily taken, since they easily pass through most sieves.

Acknowledgments — I wish to express my thanks to Dr Norine Haven, Department of Biological Sciences at Simon Fraser University, who chartered the boat from which the collections were made, and to Dr William C. Austin of the same institution, who read the manuscript and under whose grant (NRC 721-020) this study was partially supported. I am especially indebted to Dr Karl Banse, Department of Oceanography, University of Washington, for criticising the manuscript and for his invaluable comments and advice.

REFERENCES

BANSE, K. 1956. Beiträge zur Kenntnis der Gattungen *Fabricia*, *Manayunkia* und *Fabriciola* (Sabellidae, Polychaeta). Zool. Jahrb. (Systematik) 84: 415–438.

BOURNE, A. G. 1883. On *Haplobranchus*, a new genus of capitobranchiate annelids. Quart. J. Microscop. Sci. 23: 168–176.

HARTMAN, O. 1951. Fabriciinae in the Pacific. Pacific Sci. 2: 3–58.

HAZEL, C. R. 1966. A note on the freshwater polychaete, *Manayunkia speciosa* Leidy, from California and Oregon. Ohio J. Sci. 66: 533–535.

HOLMQUIST, C. 1967. *Manayunkia speciosa* Leidy — a fresh-water polychaete found in northern Alaska. Hydrobiologia 29: 297–304.

KARLING, T. 1934. *Haplobranchus balticus* n.sp. eine neue sedentäre Polychäte aus dem Finnischen Meerbusen. Mem. Soc. Fauna Flora Fennica 10: 242–245.

LEWIS, D. B. 1968. Feeding and tube-building in the Fabriciinae (Annelida, Polychaeta). Proc. Linnean Soc. London 179: 37–49.

NUSBAUM, J. 1901. Noch ein Wort über *Dybowscella baicalensis* mihi und einige andere Süsswasserpolychaeten. Biol. Centralbl. 21: 27–273.

SCHÜTZ, L. 1965. Über Verbreitung, Ökologie und Biologie des Brackwasserpolychaeten *Manayunkia aestuarina* (Bourne), inbesondere an den Küsten Schleswig-Holsteins. Faunistiche Mitt. Norddeut. 2: 225–234.

ZENKEWITSCH, L. A. 1935. Über das Vorkommen der Brackwasser-Polychaete *Manayunkia* (*M. polaris* n.sp.) an der Murmanküste. Zool. Anz. 109: 195–203.

Pugheadedness in Landlocked Atlantic Salmon (*Salmo salar*)

WILLIAM C. LEGGETT[1]

Department of Biology
University of Waterloo, Waterloo, Ont.

LEGGETT, WILLIAM C. 1969. Pugheadedness in landlocked Atlantic salmon (*Salmo salar*). J. Fish. Res. Bd. Canada 26: 3091–3093.

A mature, male, pugheaded, landlocked Atlantic salmon (*Salmo salar* Linn.) was collected from Gambo Pond, Newfoundland, in 1964. Analysis of age, growth, and spawning histories for this specimen, relative to other members of the population, indicated that the pugheaded condition did not affect its ability to compete successfully.

Received February 20, 1969

THE OCCURRENCE OF pugheadedness in teleost fishes is widespread both taxonomically and geographically (Gudger, 1929; Dawson, 1964, 1966). The earliest known record of pugheadedness dates to 1554 (Gudger, 1928). Although the exact causes of pugheadedness in fish are not presently known, available

[1]Present address: Essex Marine Laboratory, Essex, Connecticut 06426, USA, and McGill University, Montreal 2, Que.

Printed in Canada (J1385)

evidence suggests that germinal defects, perhaps augmented by endocrine disturbances, are important contributing factors. Adverse environmental conditions, especially oxygen deficiency in the microenvironment of early developmental stages may also contribute to the development of this abnormal phenotype (Gudger, 1929, 1930; Schapperclaus, 1954; Mansuetti, 1958, 1960). Genetic factors may also be involved (Gudger, 1930; Mansuetti, 1960).

Characteristically, pugheaded fish exhibit a pronounced shortening of the upper jaw resulting in a steep forehead. The eyes are generally exopthalmic, interorbital width is frequently increased, and the head is occasionally deeper than normal. The degree of pugheadedness may vary from extreme to near normal (Isaacson, 1965).

On June 23, 1964, a male, pugheaded, landlocked Atlantic salmon (*Salmo salar* Linn.) was collected at Gambo Pond, Newfoundland (48°40′N, 54°25′W) (Fig. 1). It was the only pugheaded specimen in a total of 1126 landlocked salmon collected by the author from two Newfoundland lakes during the summers of 1963 and 1964. This is believed to be the first reported instance of pugheadedness in landlocked Atlantic salmon.

The specimen measured 58.0 cm fork length and weighed 900 g. Its age, determined by scale reading (validated for landlocked salmon by Havey, 1959), was 7 years, and it had spawned at least twice.

Only 52 (9.1%) of 475 landlocked salmon sampled at Gambo Pond in 1964 were 7 or more years of age; the maximum age was 10 years. Student's *t*-tests indicated that the pugheaded salmon was not statistically different in mean length or weight from other members of its age-group, although it was longer than 97% of its age class (38 fish). However, its coefficient of condition ($100{,}000 \times W\ (g)/L^3\ (cm)$) at 0.69 was noticeably less than that of 103 normal fish (1.13 ± 0.04).

Previous reports describing pugheadedness in fish species have dealt primarily with descriptions of the specimens, and have related observed abnormalities to the normal phenotypic condition. The effects of this malformation on the ability of individual fish to compete successfully have seldom been documented. Cheek (1965) indicated that the fork length of a single juvenile American shad (*Alosa sapidissima*), collected in a sample of 25 young-of-the-year fish, was 12 mm less than the mean for the sample. Isaacson (1965) reported the size range of 14 embryo black perch (*Embiotoca jacksoni*) to be greater than ranges encountered in 245 normal broods. These findings suggest that the pugheaded condition may affect the competitive ability of individual fish at a very early age. Mansuetti (1960) determined the growth history of an adult pugheaded striped bass (*Roccus saxatilis*) by back calculation from the scales and compared its growth with extensive age and growth data for normal striped bass. He found that this specimen was smaller at each comparable age, markedly so beyond 2 years of age, suggesting that the deformity prevented the fish from attaining optimum growth.

The longevity, spawning history, and growth record of the pugheaded Atlantic salmon, described above, relative to normal members of its popu-

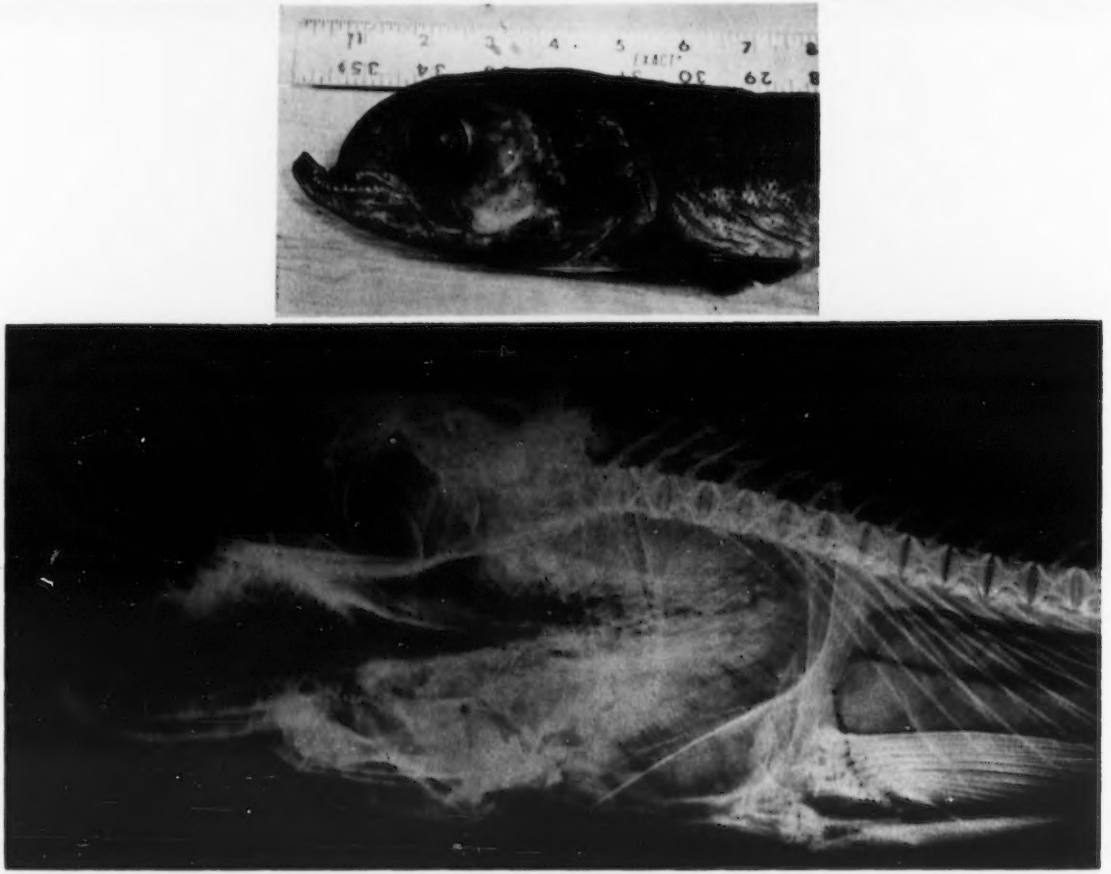

FIG. 1. Adult, pugheaded, landlocked Atlantic salmon.

Leggett — J. Fish. Res. Bd. Canada

lation suggest that the pugheaded condition did not seriously affect its ability to compete. The only indication that any hardship may have resulted from the deformity comes from the observed reduction in its length–weight relationship.

Inter- and intra-specific competition at Gambo Pond are not intense. Food is abundant throughout the growing season, and severe environmental conditions do not appear to be important limiting factors on the population (Leggett and Power, 1969). This may explain the apparent competitive success of this deformed specimen.

These findings suggest that environmental factors may be important in determining the fate of pugheaded specimens. There is a need for more detailed information on the apparent competitive success of these malformed specimens, as determined by comparisons with normal members of the population. Data on the degree of inter- and intra-specific competition and the relative harshness of the environment are also important. Such information, when available, will greatly facilitate the study of the influence of environment on abnormal members of fish populations, and may aid in analyses of their frequency of occurrence and geographical distribution.

REFERENCES

CHEEK, RANDALL P. 1965. Pugheadedness in an American shad. Trans. Am. Fish. Soc. 94: 97.

DAWSON, C. E. 1964. A bibliography of anomalies of fishes. Gulf Res. Rept. 1: 308–399.
1966. A bibliography of anomalies of fishes. Supplement 1. Gulf Res. Rept. 2: 169–176.

GUDGER, E. W. 1928. Guillaum Rondelet's pugheaded carp. Nat. Hist. 28: 102–104.
1929. An adult pugheaded brown trout, *Salmo fario*, with notes on other pugheaded salmonids. Bull. Am. Museum Nat. Hist. 58: 531–559.
1930. Pugheadedness in the striped sea bass, *Roccus lineatus*, and in other related fishes. Bull. Am. Museum Nat. Hist. 61: 1–19.

HAVEY, K. A. 1959. Validity of the scale method for ageing hatchery reared Atlantic salmon. Trans. Am. Fish. Soc. 88: 193–196.

ISAACSON, P. A. 1965. Pugheadedness in the black perch *Embiotoca jacksoni*. Trans. Am. Fish. Soc. 94: 98.

LEGGETT, WILLIAM C., AND G. POWER. 1969. Differences between two populations of landlocked Atlantic salmon (*Salmo salar*) in Newfoundland. J. Fish. Res. Bd. Canada 26: 1585–1596.

MANSUETTI, R. 1958. Eggs, larvae and young of the striped bass, *Roccus saxatilis*. Maryland Dept. Res. Educ. Contrib. 112. 35 p.
1960. An unusually large pugheaded striped bass, *Roccus saxatilis*, from Chesapeake Bay, Maryland. Chesapeake Sci. 1: 111–113.

SCHAPPERCLAUS, W. 1954. Fishkrankheiten. 3rd ed. Akad.-Verlag. 12. 708 p.

Oceanic Occurrence of Black Rockfish (*Sebastodes melanops*) in the Central North Pacific

J. R. DUNN

Bureau of Commercial Fisheries
Biological Laboratory, Seattle, Washington 98102, USA

AND

C. R. HITZ

Bureau of Commercial Fisheries
Exploratory Fishing and Gear Research Base, Seattle, Washington 98102, USA

DUNN, J. R., AND C. R. HITZ. 1969. Oceanic occurrence of black rockfish (*Sebastodes melanops*) in the central North Pacific. J. Fish. Res. Bd. Canada 26: 3094–3097.

Adult rockfish of the genus *Sebastodes* are generally considered to be demersal fish of the continental shelf. A pelagic existence has been suggested for the adult forms of certain of the dark rockfishes. A single spent *Sebastodes melanops* was captured in a surface gillnet on February 14, 1969, at 50°00′N, 165°00′W, over 240 nautical miles (445 km) south of the Alaska Peninsula. Depth of water exceeded 2700 fath (4938 m). Other offshore captures of this species are reported and available evidence suggesting a pelagic existence for the black rockfish is examined.

Received July 2, 1969

THE LITERATURE on the distribution of the rockfish of the genus *Sebastodes* generally indicates for most species a demersal existence over the continental shelf (Phillips, 1957; Alverson et al., 1964; Lyubimova, 1963). Certain rockfish, however, are thought to be pelagic (Alverson et al., 1964), especially the dark species (e.g., *S. ciliatus*, *S. entomelas*, *S. flavidus*, and *S. melanops*), which Clemens and Wilby (1961) indicate live primarily near the surface; those rockfish in deep water often have red predominating. This matter of a pelagic habitat is not well documented. A recent oceanic occurrence of an adult black rockfish, *S. melanops* (Girard), in the central North Pacific Ocean, therefore, seems worthy of documentation.

On February 15, 1969, during a salmon research cruise of the RV *George B. Kelez*, a rockfish specimen identified as *S. melanops* was collected by the first author at 50°00′N, 165°00′W. This location is about 240 nautical miles (445 km) south of the Alaska Peninsula. Water depth exceeded 2700 fath (4938 m) and surface water temperature was 3.8 C. The fish, a female, 383 mm long (standard length), was captured in 5¼-inch (133.4 mm) mesh of a surface gillnet (7 m deep). Ovaries were in a spent stage — dark and flaccid (Delacy et al., 1964).

Printed in Canada (J1518)

The specimen followed the description of *S. melanops* given by Phillips (1957); the measurements and ratios showed no appreciable deviation from Phillips' data. The specimen has been deposited in the museum of the College of Fisheries, University of Washington (Cat. no. 200443).

Oceanographic observations at the site of capture indicate the specimen was in the low-velocity (0.25–0.50 knot), eastward-flowing Subarctic Current. Although this fish could have been carried from inshore areas to its location of capture by currents, that travel would have been a long journey. Also, it is possible that this specimen could have swum or followed floating debris or kelp away from shore to its location of capture; this explanation may not apply, however, as other occurrences of *S. melanops* in offshore waters have come to our attention. Although the systematics of *S. ciliatus*, *S. melanops*, and *S. mystinus* may be confusing (J. C. Quast, personal communication), we shall assume that captures of *S. melanops* in a pelagic environment considered here are based on fish that were correctly identified.

Three black rockfish were captured during Canadian high seas salmon investigations (J. I. Manzer, personal communication). A gravid female was caught in a surface gillnet on January 12, 1963, at 45°37′N, 125°04′W (about 48 nautical miles or 89 km from shore), and two gravid females were captured on surface longlines on January 13, 1964, at 51°N, 135°W, about 150 nautical miles (278 km) from land (water depth 1900 fath or 3475 m). Purse seine sampling for salmon by the Fisheries Research Institute, University of Washington (unpublished data), has yielded three black rockfish off the coast of Vancouver Island and one in Clarence Strait in southeast Alaska. Of those collected off Vancouver Island (one in 1966 and two in 1967), one was taken in over 100 fath (183 m) of water, whereas the other two were captured in lesser depths. Rockfish are rarely caught in surface gillnets used by the Bureau of Commercial Fisheries in salmon research on the high seas. Larkins (1964) reported only two *Sebastodes* (species not determined) in 763 gillnet sets in the Gulf of Alaska and central Aleutians during 1955–61. Since then only two other rockfish have been caught in the same general area in 586 sets by the Bureau.

On the other hand, *S. melanops* constitutes a high proportion of the incidental catch in the coastal Washington sport fishery. Buckley (MS, 1967, MS, 1968) reported that this species constituted 44.9% in 1965 and 37.8% in 1966 of the incidental catch by salmon anglers off Neah Bay (from Cape Alava north and inside Juan de Fuca Strait to Sekiu River). From Sekiu River to south of Westport, Washington, black rockfish dominated (42–57%) the incidental sport catch in 1966 (Buckley, MS, 1968). In the summer, schools of surface-feeding black rockfish are commonly seen along the kelp-lined shores of western Juan de Fuca Strait (Frank Haw, personal communication), particularly near Duncan Rock (about 1.5 miles or 2.8 km, north-northwest of Cape Flattery).

Black rockfish also occur in the incidental catch by commercial salmon trollers off coastal Washington. Sampling of the troll catch at Neah Bay,

La Push, and Westport, Washington, in 1965 revealed considerable numbers of *S. melanops* in the troll catch, especially in June through August. Generally speaking, this species occurred in the shallower depths, that is inside the 20–30 fath (37–55 m) contour interval, whereas in deeper water the yellowtail rockfish (*S. flavidus*) replaced *S. melanops* in the catch (Sam Wright, personal communication).

Black rockfish also constitute an important species in the California ocean sport fishery. Miller and Gotshall (1965) reported that this species ranked 12th in numbers and 8th by weight for sport-caught species in areas surveyed from Oregon to Point Arguello, California, and it was the most common incidental species taken on trolling gear north of San Francisco. Generally, black rockfish in northern California are captured by sport anglers trolling for salmon over bottom depths ranging from 10 to 60 fath (18–110 m) with lures fished at depths of 2–10 fath or 3.7–18 m (Daniel Gotshall, personal communication). Miller and Gotshall (1965) considered *S. melanops* as primarily a shallow reef species but noted that it frequented kelp beds and that it was occasionally taken in midwater and by trollers some distance from rock areas.

Phillips (1964) reported that black rockfish dominated the longline commercial fishery for rockfish in northern California prior to 1944, when "balloon"-type trawls replaced longline gear and the canary rockfish (*S. pinniger*) became the dominant species in the catch. The difference in species composition possibly can be attributed to the depth of fishing; longlines used to capture rockfish were generally fished well off the bottom whereas the trawl was used primarily near the bottom (Scofield, 1945, 1947).

In exploratory trawl fishing in the northeastern Pacific Ocean, Alverson et al. (1964) reported that black rockfish were taken in fair quantities in the British Columbia–southeastern Alaska region in depths of 50–99 fath (92–181 m) and that the relative importance of this species declined with depth of fishing. Little trawling, however, was conducted in shallower waters (1–49 fath, i.e., 1.8–90 m) near the surface, particularly off Oregon, Washington, and British Columbia where this species is apparently more abundant than in the more northern waters.

From general information, then, it appears that the black rockfish exists along coastal areas, especially from California to southeastern Alaska, where it is available to trawlers, trollers, and anglers in shallow water. The capture of *S. melanops* offshore by the *George B. Kelez* reported in this paper, along with the Canadian oceanic captures, leads us to believe that this species may, at some stage of its life or in some races, maintain a pelagic existance off the continental shelf over the deeper ocean waters. Since some of these fish were gravid it is also possible that they move offshore during spawning, as Westrheim (MS, 1958) suggested for the Pacific ocean perch, *S. alutus*.

Acknowledgments — We thank Gene DiDonato, Washington State Department of Fisheries, Seattle, Wash., and Michael Dell, Fisheries Research Institute, College of Fisheries, University of Washington, Seattle, Wash., for access to unpublished data.

REFERENCES

ALVERSON, D. L., A. T. PRUTER, AND L. L. RONHOLT. 1964. A study of demersal fish and fisheries of the northeastern Pacific Ocean. H. R. MacMillan Lectures in Fisheries, Inst. Fish., Univ. British Columbia, Vancouver, B.C. 190 p.

BUCKLEY, R. MS, 1967. 1965 bottomfish sport fishery. Wash. Dept. Fish. Suppl. Progr. Rept. Unpublished MS. 40 p.
MS, 1968. 1966 bottomfish sport fishery occurring in Washington marine punch card areas 2 through 12. Wash. Dept. Fish., Suppl. Progr. Rept. Unpublished MS. 41 p.

CLEMENS, W. A., AND G. V. WILBY. 1961. Fishes of the Pacific coast of Canada. 2d ed. Bull. Fish. Res. Bd. Canada 68. 443 p.

DELACY, A. C., C. R. HITZ, AND R. L. DRYFOOS. 1964. Maturation, gestation, and birth of rockfish (*Sebastodes*) from Washington and adjacent waters. Wash. Dept. Fish., Fish. Res. Papers 2: 51–67.

LARKINS, H. A. 1964. Some epipelagic fishes of the North Pacific Ocean. Trans. Am. Fish. Soc. 93: 286–290.

LYUBIMOVA, T. G. 1963. Osnovnye cherty biologii i raspredelenie Tikhookeanskogo morskogo okunya (*Sebastodes alutus* Gilbert) v zalive Alyaska. [Basic aspects of the biology and distribution of Pacific rockfish (*Sebastodes alutus* Gilbert) in the Gulf of Alaska.] Tr. Vses. Nauchn. Issled. Inst. Morsk. Rybn. Khoz. i Okeanogr. 48 (Izv. Tikhookeans. Nauchn. Issled. Inst. Rybn. Khoz. i Okeanogr. 50): 293–303. (Transl. in Soviet fisheries investigations in the northeast Pacific, Part I. p. 308–318. Clearinghouse Fed. Sci. Tech. Inform., Springfield, Va., TT 67–51203.)

MILLER, D. J., AND D. GOTSHALL. 1965. Ocean sportfish catch and effort from Oregon to Point Arguello, California. Calif. Dept. Fish Game, Fish. Bull. 130. 135 p.

PHILLIPS, J. B. 1957. A review of the rockfishes of California (Family Scorpaenidae). Calif. Dept. Fish Game, Fish. Bull. 104. 158 p.
1964. Life history studies on ten species of rockfish (genus *Sebastodes*) Calif. Dept. Fish Game, Fish. Bull. 126. 70 p.

SCOFIELD, W. L. 1945. The "balloon" type otter trawl for rockfishes. Calif. Fish Game 31: 12–15.
1947. Drift and set line fishing gear in California. Calif. Dept. Fish Game, Fish. Bull. 66. 38 p.

WESTRHEIM, S. J. MS, 1958. On the biology of the Pacific Ocean perch, *Sebastodes alutus* (Gilbert). M.S. Thesis. Univ. Washington, Seattle, Wash. 106 p.

Recent Articles on FRB Investigations Published in Other Periodicals

Studies No.

1348. HALLIDAY, R. G. 1969. Rare fishes from the Clyde sea area. J. Nat. Hist. 9: 309–320.

1349. ODENSE, P. H., T. C. LEUNG, W. A. GREEN, AND J. R. DINGLE. 1969. The isolation of cod muscle tropomyosin by heat treatment. Biochim. Biophys. Acta 188: 124–131.

1350. DROZDOWSKI, B., AND R. G. ACKMAN. 1969. Isopropyl alcohol extraction of oil and lipids in the production of fish protein concentrate from herring. J. Am. Oil Chemists' Soc. 46: 371–376.

1351. ACKMAN, R. G., AND S. N. HOOPER. 1969. The "load effect" in open-tubular GLC: relationships among methyl trans-11-octadecenoate and cis isomers with similar retention times. J. Chromatogr. Sci. 7: 549–553.

*1352. IDLER, D. R., AND P. M. JANGAARD. 1969. Cod fishery, p. 129–135. *In* Frank E. Firth [ed.] The encyclopedia of marine resources. Van Nostrand Reinhold Company, New York.

1353. LORING, D. H., AND D. J. G. NOTA. 1969. Mineral dispersal patterns in the Gulf of St. Lawrence. Rev. Geograph. Montr. 23: 289–305.

1354. SCOTT, J. S. 1969. Development of rostellar hooks in *Paricterotaenia paradoxa* (Cestoda: Cyclophyllidea). Canadian J. Zool. 47: 1011–1013.

1355. ANDERSON, G. C., T. R. PARSONS, AND K. STEPHENS. 1969. Nitrate distribution in the subarctic Northeast Pacific Ocean. Deep-Sea Res. 16: 329–334.

Copies of individual reprints, if available, may be obtained from the authors or Board establishments through which the investigations were conducted.

Reprints of these articles are included in an annual volume of "Studies," composed of two parts. These are distributed to a selected mailing list. (Articles numbered 1235 to 1262 appeared in the Studies for 1968, Part 2.)

*Indicates a "Titles only" paper that will not be included in the binding.